Universidade de Aveiro
2014

Departamento de Química

ANA FILIPA MARTINS CLÁUDIO DA SILVA

EXTRAÇÃO DE PRODUTOS DE VALOR ACRESCENTADO A PARTIR DE BIOMASSA UTILIZANDO LÍQUIDOS IÓNICOS

EXTRACTION OF ADDED-VALUE PRODUCTS FROM BIOMASS USING IONIC LIQUIDS

Universidade de Aveiro
2014

Departamento de Química

ANA FILIPA MARTINS CLÁUDIO DA SILVA

EXTRAÇÃO DE PRODUTOS DE VALOR ACRESCENTADO A PARTIR DE BIOMASSA UTILIZANDO LÍQUIDOS IÓNICOS

EXTRACTION OF ADDED-VALUE PRODUCTS FROM BIOMASS USING IONIC LIQUIDS

Tese apresentada à Universidade de Aveiro para cumprimento dos requisitos necessários à obtenção do grau de Doutor em Engenharia Química, realizada sob a orientação científica do Professor Doutor João Araújo Pereira Coutinho, Professor Catedrático do Departamento de Química, CICECO, da Universidade de Aveiro, e coorientação da Doutora Mara Guadalupe Freire Martins, Investigadora Coordenadora do Departamento de Química, CICECO, da Universidade de Aveiro.

Apoio financeiro do POCTI no âmbito do III Quadro Comunitário de Apoio. Cofinanciamento do POPH/FSE.

O doutorando agradece o apoio financeiro da FCT no âmbito do III Quadro Comunitário de Apoio (SFRH/BD/74503/2010).

Dedico este trabalho às 3 meninas lá de casa e a todos os amigos do coração que me apoiaram.

o júri

presidente

Prof. Doutor Jorge Adelino Rodrigues da Costa

Professor Catedrático do Departamento de Educação, Universidade de Aveiro

Prof.ª Doutora Isabel Maria Delgado Jana Marrucho Ferreira

Investigadora Coordenadora do Instituto de Tecnologia Química e Biológica, Universidade Nova de Lisboa

Prof.ª Doutora Mara Guadalupe Freire Martins

Investigadora Coordenadora da Universidade de Aveiro

Prof. Doutor Armando Jorge Domingues Silvestre

Professor Associado com Agregação do Departamento de Química, Universidade de Aveiro

Prof. Doutor Pedro António Palma Madeira

Investigador Auxiliar da Faculdade de Engenharia, Universidade do Porto

Prof. Doutor Jorge Fernando Brandão Pereira

Professor Doutor Assistente da Faculdade de Ciências Farmacêuticas, Universidade Estadual Paulista, Brasil

Prof. Doutor Simão Pedro de Almeida Pinho

Professor adjunto do Instituto Politécnico de Bragança

Prof. Doutora Sónia Patrícia Marques Ventura

Professor Auxiliar Convidada da Universidade de Aveiro

agradecimentos

Como uma tese de doutoramento não se faz sem ajuda de ninguém, felizmente tenho imensas pessoas a quem tenho que agradecer. Em primeiro lugar, um obrigado muito especial de coração aos meus "pais" de investigação que eu muito admiro, Professor João Coutinho e Dra Mara Freire, sem eles este meu percurso não teria sido igual com toda a certeza. Obrigado pela motivação, pelas explicações, pelas oportunidades, pelos sorrisos, pelas chamadas de atenção, pelos convívios e por conseguirem liderar este grupo de forma absolutamente inegualável. Quero também agradecer aos meus muitos irmãos "Path", sim porque somos uma família, por todos os convivíos, amizade, gargalhadas, lágrimas e interajuda, vocês sabem quem são, não arrisco citar nomes sob pena de esquecer alguém... Um obrigado adicional a todos os alunos "Path" que trabalharam comigo por toda a ajuda.

Durante esta minha caminhada tive a sorte de poder conhecer outros "mundos", portanto não posso deixar de agradecer ao grupo do Professsor Tom Welton do Imperial College em Londres e ao grupo do Dr. Robin Rogers na universidade do Alabama, onde felizmente pude trabalhar.

Além dos agradecimentos à "PathFamily", queria agradecer também ao Professor Armando Silvestre e às suas alunas, pela disponibilidade e ajuda que me deram sempre que necessitei. Obrigado também à Engª Ana Caço pela paciência e material disponibilizado.

A nível pessoal não posso deixar de agradecer à minha família adoptiva que sempre me apoiou (Sr. Eduardo, Dª Maria, Otilia, Valter e Tia Belinha), aos meus amigos de Ovar e em especial ao Daniel por toda a ajuda preciosa, paciência que teve comigo e pelos docinhos e salgadinhos que me trazia quando estava a trabalhar.

Por fim e por serem as pessoas do meu sangue e que significam muito para mim, um obrigado ao meu pai e Maria José e às minhas 3 meninas do coração, mãe, mana e sobrinha (a quem dedico esta tese), por todo apoio incondicional e carinho que demonstram diariamente.

palavras-chave Líquidos iónicos, biomassa, compostos de valor acrescentado, compostos fenólicos, alcaloides, aminoácidos, sistemas aquosos bifásicos, extração sólido-líquido, paramêtros solvatocrómicos, hidrótopos.

resumo O principal objetivo desta tese recai sobre a utilização de líquidos iónicos (LIs) como uma nova classe de solventes para a extração de compostos de valor acrescentado a partir da biomassa. Nestes compostos estão incluídos os compostos fenólicos (vanilina e ácidos gálico, siríngico e vanílico), alcaloides (cafeína) e aminoácidos (L-triptofano). O interesse da extração destes compostos naturais está relacionado com as suas excelentes propriedades e consequente interesse para aplicação nas indústrias alimentar, de cosmética e farmacêutica. De forma a desenvolver uma técnica de extração/purificação mais benigna e eficiente do que as habitualmente utilizadas, foram estudados vários sistemas aquosos bifásicos (SABs) constituídos por LIs e sais orgânicos/inorgânicos. Foi também criada uma escala de polaridades para os LIs, através da determinação de parâmetros solvatocrómicos, para se poder avaliar a afinidade de diferentes LIs para compostos de valor acrescentado. Para além do uso de SABs, realizaram-se extrações do tipo sólido-líquido a partir de biomassa e utilizando soluções aquosas de LIs. Neste contexto, otimizou-se a extração da cafeína, quer de sementes de guaraná quer de borras de café, utilizando um planeamento fatorial para o efeito. Mostrou-se ainda que em ambos os tipos de extrações estudados é possível recuperar os compostos de valor acrescentado e reciclar as soluções de LI e sal utilizadas durante o processo extrativo.

Por fim, com o propósito de explorar a recuperação dos compostos de valor acrescentado utilizando técnicas mais simples e sustentáveis, foram determinadas as solubilidades do ácido gálico, vanilina e cafeína em diversas soluções aquosas de LIs e sais. Foi possível demonstrar que os LIs atuam como hidrótropos e, deste modo, pode-se utilizar água como um anti-solvente adequado.

Esta tese descreve a aplicação de LIs no desenvolvimento de processos extrativos mais eficientes e sustentáveis.

keywords Ionic Liquids, biomass, added-value compounds, phenolic compounds, alkaloids, aminoacids, aqueous biphasic systems, solid-liquid extraction, solvatochromic parameters, hydrotropes.

abstract The main purpose of this thesis is to investigate the potential of ionic liquids (ILs) as a new class of extractive solvents for added-value products from biomass. These include phenolic compounds (vanillin, gallic, syringic and vanillic acids), alkaloids (caffeine) and aminoacids (L-tryptophan). The interest on these natural compounds relies on the wide variety of relevant properties shown by those families and further application in the food, cosmetic and pharmaceutical industries.

Aiming at developping more benign and effective extraction/purification techniques than those used, a comprehensive study was conducted using aqueous biphasic systems (ABS) composed of ILs and inorganic/organic salts. In addition, ILs were characterized by a polarity scale, using solvatochromic probes, aiming at providing prior indications on the ILs affinity for particular added-value products. Solid-liquid (S-L) extractions from biomass and using aqueous solution of ILs were also investigated. In particular, and applying and experimental factorial design to optimize the operational conditions, caffeine was extracted from guaraná seeds and spent coffee. With both types of extractions it was found that it is possible to recover the high-value compounds and to recycle the IL and salt solutions.

Finally, aiming at exploring the recovery of added-value compounds from biomass using a simpler and more suistainable technique, the solubility of gallic acid, vanillin and caffeine was studied in aqueous solutions of several ILs and common salts. With the gathered results it was possible to demonstrate that ILs act as hydrotropes and that water can be used as an adequate antisolvent.

This thesis describes the use of ILs towards the development of more effective and sustainable processes.

Contents

Notation

List of Symbols

α	Hydrogen-bond acidity (solvatochromic parameter)
$[Trp]_{IL}$	Concentration of L-tryptophan in the ionic-liquid-rich phase
$[Trp]_{Salt}$	Concentration of L-tryptophan in the salt-rich phase
A, B and *C*	Fitting parameters of th equation proposed by Merchuk et al.
a, *b* and *s*	Solvent-independent coefficients
a_{eff}	Effective contact area between two surface segments
c_{HB}	Hydrogen-bond strength
[Hyd]	Concentration of hydrotrope in aqueous solution
d	Particle diameter
K_H	Hydrotropy constant
K_{Leu}	Partition coefficient of L-Leucine
K_{ow}	Octanol-water partition coefficient
K_{Phe}	Partition coefficient of L-phenylalanine
K_{Trp}	Partition coefficient of L- tryptophan
K_{Tyr}	Partition coefficient of L-tyrosine
K_{val}	Partition coefficient of L-valine
w	Weigth fraction
n_D	Refractive index
*pK*a	Acidic dissociation constant
$pX(\sigma)$	Distribution probability, "σ-profile"
S	Solubility of biomolecules in the presence of hydrotropes
S_0	Solubility of biomolecules in pure water
T	Temperature
w_{IL}	Weight of the ionic-liquid-rich phase
w_{Salt}	Weight of the salt-rich phase
X_M	Weigth fraction composition of the salt in the initial mixture
X_T	Weigth fraction composition of ionic liquid in the top phase
X_T	Weigth fraction composition of salt in the top phase
Y_B	Weigth fraction composition of ionic liquid in the bottom phase
Y_M	Weigth fraction composition of ionic liquid in the initial mixture
β	Hydrogen-bond basicity (solvatochromic parameter)
β_0	Adjusted coefficients for the interception terms
β_i	Adjusted coefficients for the linear terms
β_{ii}	Adjusted coefficients for the quadratic terms
β_{ij}	Adjusted coefficients for the interaction terms
ΔG_{hyd}	Gibbs free energy of hydration
η	Viscosity
π	Dipolarity/polarizability (solvatochromic parameter)
ρ	Density
σ	Standard deviation
σ_{HB}	Threshold for hydrogen-bonding
$\lambda_{max(dye)}$	Wavelength corresponding to maximum absorption

List of Abbreviations

ABS	Aqueous Biphasic System
ATPS	Aqueous Two-Phase System
ATR	Attenuated Total Reflection
CMC	Critical Micelle Concentration
COSMO-RS	Conductor-Like Screening Model for Real Solvents
DLS	Dynamic Light Scattering
DN	Gutmann's Donor Number
EE%	Extraction Efficiency
$E_T(30)$	Reichardt's betaine dye
FDA	Food and Drug Administration
FTIR	Fourier Transform InfraRed
GA	Gallic Acid
GMP	Good Manufacturing Practice
GRAS	Generally Recognized As Safe
HPLC	High Performance Liquid Chromatography
ICP-OES	Inductively Coupled Plasma-Optical Emission Spectrometry
IL	Ionic Liquid
IUPAC	International Union of Pure and Applied Chemistry
LCST	Lower Critical Solution Temperature
Leu	L-Leucine
LLE	Liquid-liquid Eextraction
LSER	Linear Solvation Energy Relationship
NA	Gutmann's Acceptor Number
NMR	Nuclear Magnetic Resonance
PB27	Prussian Blue (pigment blue 27)
PEG	Polyethylene Glycol
PhCs	Phenolic Compounds
Phe	L-Phenylalanine
PILs	Protic Ionic Liquids
POM	Polarized Optical Microscope
PPG	Polypropylene Glycol
$R_{S/L}$	Solid-Liquid Ratio
RSM	Response Surface Methodology
SCG	Spent Coffee Grounds
SEM	Scanning Electron Microscopy
SPE	Solid-Phase Extraction
TD-DFT	Time-Dependent Density Functional Theory
TL	Tie-Line
TLL	Tie-Line Length
Trp	L- Tryptophan
Try	L-Tyrosine
UCST	Upper Critical Solution Temperature
UV-Vis	Ultraviolet-visible
Val	L-Valine
VOCs	Volatile Organic Compounds

List of Cations of ILs

$[EtNH_3]^+$	Ethylammonium
$[(C_2OC_2)mpyr]^+$	1-(2-ethoxyethyl)-1-methylpyrrolidinium
$[1\text{-}C_4\text{-}1\text{-}C_1pip]^+$	1-butyl-1-methylpiperidinium
$[1\text{-}C_4\text{-}1\text{-}C_1py]^+$	1-butyl-1-methylpyrrolidinium
$[1\text{-}C_4\text{-}2\text{-}C_1py]^+$	1-butyl-2-methylpyridinium
$[1\text{-}C_4\text{-}3\text{-}C_1py]^+$ or $[C_4mpy]^+$	1-butyl-3-methylpyridinium
$[1\text{-}C_4\text{-}4\text{-}C_1py]^+$	1-butyl-4-methylpyridinium
$[aC_1im]^+$ or $[amim]^+$	1-allyl-3-methylimidazolium
$[C_{10}C_1im]^+$	1-decyl-3-methylimidazolium
$[C_{12}C_1im]^+$	1-dodecyl-3-methylimidazolium
$[C_{14}C_1im]^+$	1-tetradecyl-3-methylimidazolium
$[C_1C_1im]^+$	Dimethylimidazolium
$[C_1im]^+$	Methylimidazolium
$[C_2im]^+$	Ethylimidazolium
$[C_2mim]^+$ or $[C_2C_1im]^+$	1-ethyl-3-methylimidazolium
$[C_3C_1im]^+$	1-propyl-3-methylimidazolium
$[C_4C_1C_1im]^+$ or $[C_4C_1mim]^+$	1-butyl-2,3-dimethylimidazolium
$[C_4C_1pip]^+$	1-butyl-1-methylpiperidinium
$[C_4C_1pyrr]^+$	1-butyl-1-methylpyrrolidinium
$[C_4mim]^+$or $[C_4C_1im]^+$	1-butyl-3-methylimidazolium
$[C_5C_1im]^+$or $[C_5mim]^+$	1-pentyl-3-methylimidazolium
$[C_5mpyrr]^+$	1-methyl-1-pentylpyrrolidinium
$[C_6mim]^+$ or $[C_6C_1im]^+$	1-hexyl-3-methylimidazolium
$[C_7H_7mim]^+$ or$[C_7H_7C_1im]^+$	1-benzyl-3-methylimidazolium
$[C_7mim]^+$ or $[C_7C_1im]^+$	1-heptyl-3-methylimidazolium
$[C_8mim]^+$ or $[C_8C_1im]^+$	1-octyl-3-methylimidazolium
$[C_8py]^+$	1-octylpyridinium
$[DEA]^+$	Diethanolammonium
$[EA]^+$	Ethanolammonium
$[im]^+$	Imidazolium
$[N_{1112}OH]^+$	Cholinium
$[N_{4444}]^+$	Tetrabutylammonium
$[OHC_2C_1im]^+$	1-hydroxylethyl-3-methylimidazolium
$[P_{4444}]^+$	Tetrabutylphosphonium
$[TEA]^+$	Triethanolammonium

List of Anions of ILs

$[NO_3]^-$	Nitrate
$[(C_2F_5)_3PF_3]^-$	Tris(pentafluoroethyl)trifluorophosphate
$[(C_2H_5O)_2PO_2]^-$	Diethylphosphate
$[(C_4F_9)_2PF_3]^-$	Bis(nonafluorobutyl)trifluorophosphate
$[(C_4H_9O)_2PO_2]^-$	Dibutylphosphate
$[(C_6H_5)CO_2]^-$	Benzoate
$[(CH_3O)_2PO_2]^-$ or $[DMP]^-$	Dimethylphosphate
$[AsF_6]^-$	Hexafluoroarsenate
$[B(C_2O_4)_2]^-$	Bis(oxalate)borate
$[B(CN)_4]^-$	Tetracyanoborate
$[BC_{14}H_8O_6]^-$	Bis(salicylato)borate
$[BC_{24}H_{16}O_4]^-$	Bisbiphenyldiolatoborate
$[BCl_4]^-$	Tetrachlorideborate
$[BF_4]^-$	Tetrafluoroborate
$[C(CN)_3]^-$	Tricyanomethane
$[C(SO_2CF_3)_3]^-$	Tris(trifluoromethylsulfonyl)methide
$[C_{16}H_{34}O_2P]^-$	Bis(2,4,4-trimethylpentyl)phosphinate
$[C_3F_7CO_2]^-$	Heptafluorobutanoate
$[C_3H_7OSO_4]^-$	Methoxyethylsulphate
$[C_4H_9OSO_4]^-$	Ethoxyethylsulphate
$[C_4H_9SO_4]^-$	Butylsulphate
$[C_5OC_1SO_4]^-$	2-(2-methoxyethoxy)ethylsulphate
$[C_6H_4BO_8]^-$	Bis(malonato)borate
$[C_7H_5O_3]^-$	Salicylate
$[C_7H_8SO_3]^-$ or $[TOS]^-$	Toluene-4-sulfonate (tosylate)
$[C_8SO_4]^-$ or $[C8H17SO4]^-$ or $[OctylSO4]^-$	Octylsulphate
$[C_9H_{20}CO_2]^-$	Decanoate
$[CF_3CO_2]^-$	Trifluoroacetate
$[CF_3SO_3]^-$	Tri(fluoromethane)sulfonate
$[CH(CF_3SO_2)_2]^-$	Bis(trifluoromethylsulfonyl)methane
$[CH_3CO_2]^-$	Acetate
$[CH_3SO_3]^-$	Methanesulfonate
$[ClO_4]^-$	Perclorate
$[EtSO_4]^-$ or$[C_2SO_4]^-$ or $[C_2H_5SO_4]^-$	Ethylsulfate
$[FeCl_4]^-$	Tetrachloroferrate
$[HSO_4]^-$	Hydrogensulfate
$[I_3]^-$	Triiodide
$[MeSO_4]^-$ or $[C_1SO_4]^-$ or $[CH_3SO_4]^-$	Methylsulphate
$[N(C_2F_5SO_2)_2]^-$	Bis(pentafluoroethylsulfonyl)imide
$[N(CN)_2]^-$	Dicyanamide
$[N(CN)_3]^-$	Tricyanomethane
$[NO_2]^-$	Nitrite
$[NTf_2]$- or $[N(CF_3SO_2)_2]^-$	Bis(trifluoromethanesulfonyl)imide
$[PF_6]^-$	Hexafluorophosphate
$[PO_2(C_2F_5)_2]^-$	Bis(pentafluoroethyl)phosphinate
$[SbF_6]^-$	Hexafluorostibate
$[SCN]^-$	Thiocyanate

Br^-	Bromide
Cl^-	Chloride
I^-	Iodide

List of Common Salts

$Al_2(SO_4)_3$	Aluminium carbonate
$AlK(SO_4)_2$	Aluminium potassium sulfate
$C_6H_5K_3O_7$	Potassium citrate tribasic
$CaCl_2$	Calcium chloride
K_2CO_3	Potassium carbonate
K_2HPO_4	Potassium phosphate dibasic
K_2SO_4	Potassium sulfate
K_3PO_4	Potassium phosphate tribasic
KCl	Potassium chloride
KH_2PO_4	Potassium phosphate monobasic
KOH	Potassium hydroxide
LiCl	Lithium chloride
$MgSO_4$	Magnesium sulfate
$Na_2C_4H_4O_6$	Sodium tartrate
Na_2CO_3	Sodium carbonate
Na_2HPO_4	Sodium phosphate dibasic
$Na_2S_2O_3$	Sodium thiosulfate
Na_2SO_3	Sodium sulfite
Na_2SO_4	Sodium sulphate
$Na_3C_6H_5O_7$	Trisodium citrate
Na_3PO_4	Sodium phosphate
$NaC_2H_3O_2$	Sodium acetate
$NaC_7H_5O_2$	Sodium benzoate
$NaCH_3CO_2$	Sodium acetate
NaCl	Sodium chloride
NaH_2PO_4	Sodium dihydrogen phosphate
$NaNO_3$	Sodium nitrate
NaSCN	Sodium thiocyanate
NH_4Cl	Ammonium chloride
$(NH_4)_2SO_4$	Ammonium sulfate

List of Figures

List of Tables

1. Introduction

1.1. Scopes and Objectives

The main purpose of this thesis consists on the investigation on the potential of ILs as a new class of extractive solvents for added-value products from biomass. Added-value products from biomass include phenolic compounds, alkaloids and amino acids. The interest on these natural compounds comes from the wide variety of relevant properties shown by those families, namely, among others, their antioxidant, anti-inflammatory, radical scavenger and antimicrobial properties.

Trying to develop more benign extraction/purification techniques than those used nowadays, in this thesis, a study was conducted using aqueous biphasic systems (ABS) composed of ILs and typical inorganic or organic salts. Besides the use of ABS, this thesis also investigates the use of aqueous solution of ILs in solid-liquid extraction processes (from biomass). The added-value molecules investigated include phenolic compounds, such as vanillin, and gallic, syringic and vanillic acids, alkaloids (caffeine) and amino acids (L-tryptophan). These molecules have special relevance in food, wine, dietary and pharmaceutical industries. In both approaches several ILs (different anion/cation combinations) were studied aiming at optimizing the ILs that better perform for the added-value compounds extraction.

In order to gather prior indications on the ILs affinity for particular products, the establishment of an IL polarity scale using solvatochromic probes was also conducted. In particular, the Kamlet-Taft parameters were determined and a novel approach for their predicition was performed applying COSMO-RS (Conductor-Like Screening Model for Real Solvents).

With the goal of achieving an improved characterization of the IL solvating ability, as well as to explore the recovery of added-value products by effective and more sustainable approaches, the solubility of gallic acid, vanillin and caffeine was studied in several aqueous solutions of ILs and more conventional salts. It is here shown that a large variety of ILs act as hydrotropes.

The following information is divided in 3 main parts: i) introduction, ii) extraction/purification using ABS and ILs characterization and iii) solid-liquid extractions (from biomass). Figure 1.1.1 outlines the structure of the following thesis that is divided by published/submitted manuscripts.

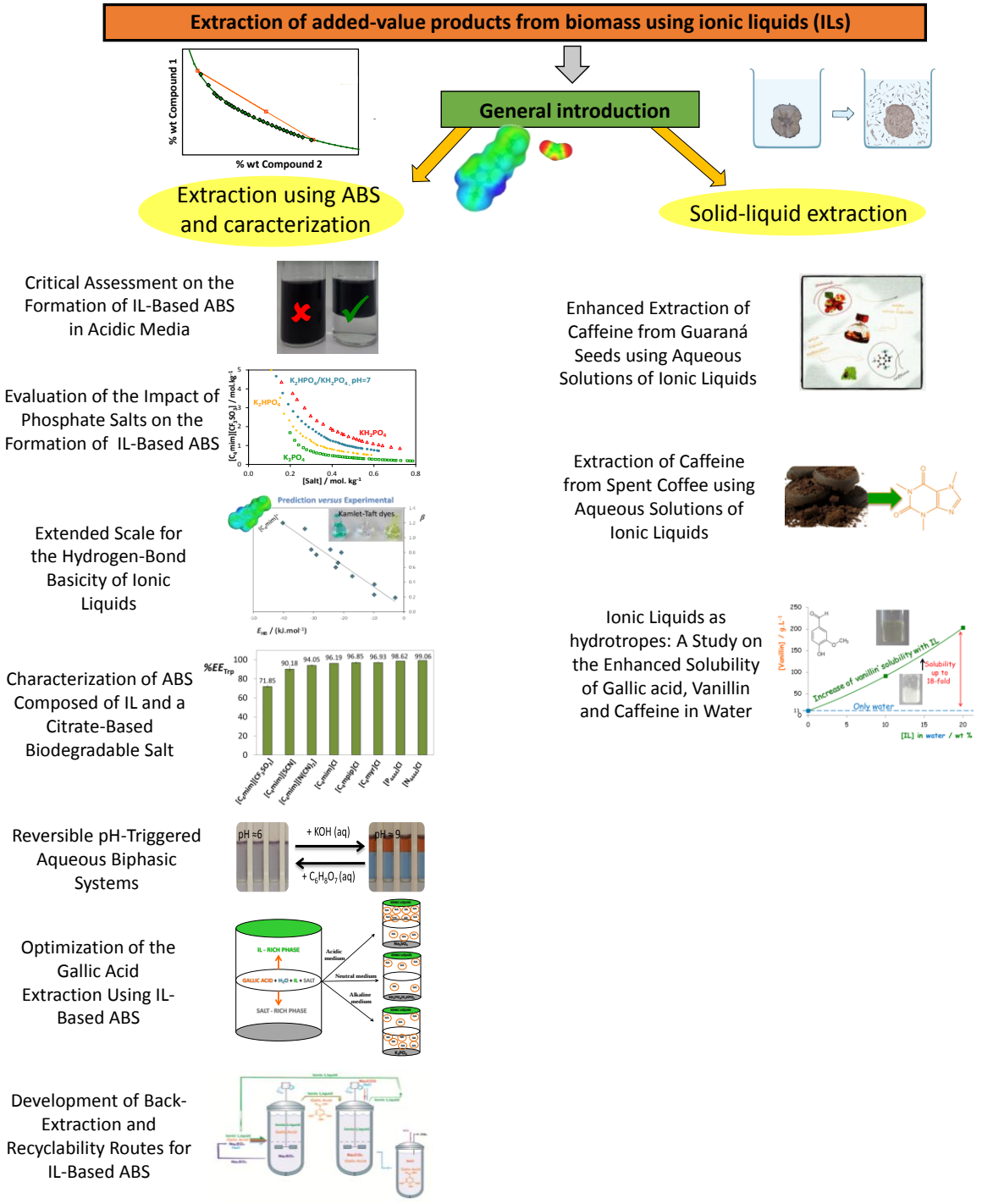

Figure 1.1.1: Illustrative scheme of the thesis main chapters.

The first part of this thesis - **Chapter 1: Introduction -** provides a brief explanation of the main scientific concepts used in this work, such as the common methods used in the extraction of value-added compounds from biomass, the use of ABS and main advantages for extraction/purification purposes, and the main advantages and properties afforded by ILs. In addition, the advantages of ABS using ILs and their applications are also highlighted. Chapters 1.3 to 1.5 are based on the following manuscript: Freire, M. G., Cláudio, A. F. M. Araújo, J. M. M., Coutinho, J. A. P., Marrucho, I. M., Canongia Lopes, J. N., Rebelo, L. P. N., Aqueous biphasic systems: A boost brought about by using ionic liquids, Chem. Soc. Rev., 2012, 41 ,4966-4995.

After the general introduction, in **Chapter 2**, ABS composed of ILs are deeply evaluated, either regarding their formation ability or in the extraction of model biomolecules.

In **Chapter 2.1**: **Critical Assessment of the Formation of Ionic-Liquid-Based Aqueous Biphasic Systems in Acidic Media,** the ability of Na_2SO_4 to induce the formation of IL-ABS is investigated. Ternary phase diagrams, tie-lines, and tie-line lengths for several systems were determined at 298 K and atmospheric pressure. In this chapter it will be shown that, among the ILs studied, only those containing long alkyl side chains at the ions and/or anions with low hydrogen bond basicity are capable of undergoing liquid-liquid demixing in presence of Na_2SO_4 aqueous solutions. The results obtained indicate that, besides the salting-out ability of the inorganic salt, the pH of the aqueous solution plays a crucial role on the formation of IL-based ABS. This chapter is based on the published article: Cláudio, A. F. M.; Ferreira, A. M.; Shahriari, S., Freire, M. G. and Coutinho, J. A. P., A Critical Assessment on the Formation of Ionic-Liquid-Based Aqueous Two-Phase Systems in Acidic Media, J. Phys. Chem. B, 2011, 115, 11145–11153.

In **Chapter 2.2**: **Evaluation of the Impact of Phosphate Salts on the Formation of Ionic-Liquid-based aqueous biphasic systems**, it is addressed the capability of several phosphate-based salts, whose anions can coexist in water depending on the media pH, to promote ABS formation with 1-butyl-3-methylimidazolium-based ILs. The influence of the IL anion in the overall process of liquid-liquid demixing is also ascertained. Novel phase diagrams of ABS composed of several imidazolium-based ILs and three phosphate salts

and a mixture of salts (K_3PO_4, K_2HPO_4, K_2HPO_4 + KH_2PO_4, and KH_2PO_4) were determined by the cloud point titration method at 298 K and atmospheric pressure. The corresponding tie-line compositions, tie-line lengths, and pH values of the coexisting phases were also determined. It was found that the ionic liquids ability to promote ABS is related with the hydrogen-bond basicity of the composing anion - the lower it is the higher the ability of the ionic fluid to undergo liquid-liquid demixing. Moreover, similar patterns on the ILs sequence were observed with the different phosphate salts. The phosphate anion charge plays a determinant role in the formation of ABS. The two-phase formation aptitude (with a similar IL) decreases in the rank: K_3PO_4 > K_2HPO_4 > K_2HPO_4 + KH_2PO_4 > KH_2PO_4. Yet, besides the charge of the phosphate anion, the pH and ionic strength of the aqueous media also influence the phase separation ability. This chapter is based on the following manuscript: Mourão, T.; Cláudio, A. F. M.; Boal-Palheiros, I.; Freire, M. G.; Coutinho, J. A. P., Evaluation of the Impact of Phosphate Salts on the Formation of Ionic-Liquid-Based Aqueous Biphasic Systems, J. Chem. Thermodyn., 2012, 54, 398-405.

Chapter 2.3: Extended Scale for the Hydrogen-Bond Basicity of Ionic Liquids, is based on the published manuscript Cláudio, A. F. M.; Swift, L.; Hallett, J. P., Welton, T., Coutinho J. A. P. and Freire, M. G., ′Extended Scale for the Hydrogen-Bond Basicity of Ionic Liquids, J. Phys. Chem. Chem. Phys, 2014, 16 (14), 6593-6601. Taking in account the extensive research regarding ILs as potential and alternative solvents in many chemical applications, and their effectiveness, recent investigations have attempted to establish polarity scales capable of ranking ILs according to their chemical behaviour. However, some major drawbacks have been found since polarity scales only report relative ranks because they depend on the set of probe dyes used, and they are sensitive to measurement conditions, such as purity levels of the ILs and procedures employed. Due to all these difficulties it is of crucial importance to find alternative and/or predictive methods and to evaluate them as *a priori* approaches able to provide the chemical properties of ILs. In this context, we experimentally determined the Kamlet-Taft solvatochromic parameters for a set of ILs and then evaluated the potential of COSMO-RS, the Conductor-Like Screening Model for Real Solvents, as an alternative tool to estimate the hydrogen-bond basicity of ILs. After demonstrating a linear correlation between the experimental hydrogen-bond basicity

values and the COSMO-RS hydrogen-bonding energies in equimolar cation-anion pairs, an extended scale for the hydrogen-bond accepting ability of IL anions was proposed. This new ranking of the ILs chemical properties opens the possibility to pre-screen appropriate ILs (even those not yet synthesized) for a given task or application, and are of high importance to understand the ILs ability to extract given added-value molecules.

Chapters 2.1 and 2.2 mainly allow the evaluation on the main effects governing the formation of IL-based aqueous biphasic systems. The next chapters are more devoted to the exploitation of IL-based ABS for the extraction and purification of biomolecules, although some phase diagrams and respective formation abilities are also discussed.

In **Chapter 2.4: Characterization of Aqueous Biphasic Systems Composed of Ionic Liquids and a Citrate-Based Biodegradable Salt**, based on the publisded manuscript Passos, H.; Ferreira, A. R.; Cláudio, A. F. M.; Coutinho, J. A. P.; Freire, M. G., Characterization of Aqueous Biphasic Systems Composed of Ionic Liquids and a Citrate-Based Biodegradable Salt, Biochem. Eng. J., 2012, 67, 68-76, a large amount of ILs was evaluated toward their ability to form ABS and their extractive performance in the presence of a biodegradable organic salt: potassium citrate. The ternary phase diagrams, tie-lines, and respective tie-line lengths were determined at 298 K. It is shown that the ILs aptitude to undergo liquid-liquid demixing is mainly controlled by their hydrophobicity. The partitioning of an archetypal amino acid produced by bacteria fermentation, L-tryptophan, was also addressed aiming at exploring the applicability of the proposed systems in the biotechnology field. Single-step extraction efficiencies of L-tryptophan for the IL-rich phase range between 72 % and 99 %.

Chapter 2.5: Reversible pH-Triggered Aqueous Biphasic Systems, demonstrates the striking ability to induce reversible transitions between homogeneous solutions and biphasic systems by a change in the pH of the aqueous media. Their potential application is demonstrated with the selective separation of two textile dyes. Dyes were chosen only as model molecules. Remarkably, the ABS constituted by $[C_4mim]Cl$ (the most hydrophilic IL investigated) is able to completely separate the two dyes for opposite phases with extraction efficiencies of 100% in a single-step procedure. This chapter is based on an article under preparation, namely Ferreira, A. M., Cláudio, A. F. M. Rogers, R. D.,

Coutinho, J. A. P. and Freire, M.G., Reversible pH-Triggered Aqueous Biphasic Systems, (2014).

Aiming at developing more benign and efficient extraction/purification processes for phenolic compounds, **Chapter 2.6: Optimization of the Gallic Acid Extraction using Ionic Liquid-Based Aqueous Biphasic Systems** (based on the manuscript Cláudio, A. F. M.; Ferreira, A. M.; Freire, C. S. R., Silvestre, A. J. D., Freire, M. G. and Coutinho, J. A. P., Optimization of the Gallic Acid Extraction Using Ionic-Liquid-Based Aqueous Two-Phase Systems, Sep. Purif. Technol., 2012, 97, 142–149.) describes the use of ABS composed of IL and inorganic salts (K_3PO_4, K_2HPO_4/KH_2PO_4 and Na_2SO_4) to extract gallic acid. Several combinations of ILs and inorganic salts were studied to understand the influence of the IL structure and of the medium pH through the gallic acid partitioning. It is shown that at low pH values the non-charged form of gallic acid (or other phenolic compounds) preferentially migrates for the IL-rich phase whereas its conjugate base preferentially partitions for the salt-rich phase. These results indicate that IL-based ABS can be the basis of new extraction/purification processes of phenolic compounds from natural matrices.

Chapter 2.7: Development of Back-Extraction and Recyclability Routes for Ionic-Liquid-Based Aqueous Biphasic Systems, according to the published manuscript Cláudio, A. F. M.; Marques, C. F. C.; Boal-Palheiros, I.; Freire, M. G. and Coutinho, J. A. P., Development of back-extraction and recyclability routes for ionic-liquid-based aqueous two-phase systems, Green Chem., 2014, 16, 259–268, describes a novel approach the ILs regeneration, recycling and reuse as phase-forming components of ABS. As a first approach, the phase diagrams of novel ABS composed of imidazolium-based ILs and Na_2CO_3 or Na_2SO_4 were determined and their extraction efficiencies for antioxidants – gallic, syringic and vanillic acid - were evaluated. The most promising IL-ABS were then used in sequential two-step cycles (product extraction/IL recovery) so as to evaluate the efficacy on the ILs recyclability and reusability. Extraction efficiency values ranging between 73% and 99% were obtained in four sequential partitioning experiments involving antioxidants while allowing the 95% of IL regeneration and further reutilization. The remarkable results obtained in this work support the establishment of IL-based ABS

as a sound basis of greener cost-effective strategies with a substantial reduction in the environmental footprint and economical issues.

After, the studies involving extraction steps using aqueous biphasic systems composed of ILs and salts, and where the influence of pH, structure of IL, and type of salt were evaluated, solid-liquid extractions of added value-compounds from biomass were further performed using aqueous solutions of ILs. These studies are included in **Chapter 3**. The possibility of crystallizing added-value biomolecules extracted from biomass (e.g. caffeine, gallic acid and vanillin) was also investigated and making use of the "hydrotropes" concept that also applies to ILs.

Chapter 3.1: Enhanced Extraction of Caffeine from Guaraná Seeds using Aqueous Solutions of Ionic Liquids, addapted from Cláudio, A. F. M.; Ferreira, A. M.; Freire, M. G. and Coutinho, J. A. P., Enhanced Extraction of Caffeine from Guaraná Seeds using Aqueous Solutions of Ionic Liquids, Green Chem., 2013, 15, 2002-2010, demonstrates the use of ionic liquid aqueous solutions to extract a target alkaloid (caffeine) from biomass (guaraná seeds). Several ILs composed of imidazolium or pyrrolidinium cations combined with the chloride, acetate and tosylate anions were investigated. Furthermore, the effect of the cation alkyl side chain length and the presence of functionalized groups were also addressed. Additional conditions such as the IL concentration, the contact time, the solid-liquid ratio and temperature were further optimized by a response surface methodology. Outstanding extraction yields (up to 9 wt % of caffeine *per* guaraná dry weight) were obtained at a moderate temperature and in a short-time. The recyclability and reusability of the IL were also confirmed. It will be shown that aqueous solutions of ILs are superior alternatives for the solid-liquid extraction of caffeine from biomass samples and, as a result, the development of an IL-based process is straightforward envisaged.

Chapter 3.2: Recovery of caffeine from spent coffee using aqueous ionic liquid solutions, is based on an ongoing work with the collaboration of the following authors: Ana M. Ferreira, Hugo Gomes, João A. P. Coutinho and Mara G. Freire. This work envisages the extraction of caffeine from spent coffee grounds (SCG) as a major residue from drinkable coffee. Usually, SCG have no commercial value and are discarded as a solid waste. However, SCG are rich in organic matter, as well as in other compounds, such as

caffeine, tannins and polyphenols. In this chapter, the extraction of caffeine from SCG was performed using aqueous solutions of protic ILs and one aprotic IL, $[C_4mim][CH_3CO_2]$, for comparison purposes. Three protic ILs (PILs) were synthesized, with the goal of replacing the more expensive and less benign imizadolium-based ones used in the previous *Chapter 3.1*. In general, all ILs solutions perform better than pure water for the extraction of caffeine. The extraction yield (up to 3.57 wt %) increases with the number of –OH groups at the IL cation.

Chapter 3.3: Ionic liquids as hydrotropes: A study on the enhanced solubility of gallic acid, vanillin and caffeine in water, is based on a manuscript under preparation, namely Cláudio, A. F. M., Neves, M.C., Freire, M. G. and Coutinho, J. A. P., Ionic liquids as hydrotropes: A study on the enhanced solubility of antioxidants in water (2014). In this work, it is shown, for the first time, that ILs are powerful hydrotropes. Gallic acid and vanillin (both phenolic compounds and antioxidants) and caffeine (alkaloid) were used as model biomolecules in this study. The effects of the hydrotrope structure, concentration, and temperature on the solubility of the biomolecules in aqueous solutions were evaluated. The results reported show that the solubility of the biomolecules studied can increase up to 18-fold using 20 % wt of IL in aqueous media. The solubility mechanism, that is majorly governed by the formation of IL-solute aggregates, is also presented and discussed. These results may have a large impact on explaining the role of ILs in the extraction of biocompounds as well as in designing processes for their recovery from solution.

Finally, in last part of this thesis, general conclusions and future work are presented. The high performance of ILs as alternative extractive solvents is emphasized. As future work, it would be interesting to extend this type of extractions followed by purification to other high-value products, namely from Portuguese agroforestry biomass.

1.2. Methods of Extraction of Biomolecules

General Context

Nowadays, there is a growing request to extract and purify biomolecules for main applications in the food, cosmetic and pharmaceutical industries. In addition, and due to sustainability concerns, it is desired to use sub-products or even wastes aiming their further valorization.

The costs associated with a final product are strongly dependent on the downstream processing and associated techniques. Conventional techniques, namely precipitation, distillation and chromatography typically employed for product recovery and concentration are usually expensive, provide low yields and some can't be applied at a large/industrial scale.[1]

There are two main processes commonly used to extract (bio)compounds from a liquid phase (that usually contains the product of interest and related contaminants) to another: liquid-liquid extraction using organic solvents immiscible with water and aqueous biphasic systems (ABS). ABS consist in two aqueous-rich phases containing polymer/polymer, polymer/salt or salt/salt combinations, which above certain concentrations undergo phase separation.[2] Liquid-liquid extraction processes are usually employed for the purification of biomolecules due to their high effectiveness, high yield, improved purity degree, proper selectivity, technological simplicity and low cost, and also because of a good combination between the recovery and purification steps can be achieved.[3.4] Liquid-liquid extraction is currently applied in many industrial processes, being an ordinary unit operation in several industries, such as in the petrochemical field. However, in some fields, this technique is not the most adequate approach. In the pharmaceutical industry, for instance, the extraction with organic solvents is used in the production and further purification of synthetic antibiotics.[2] For high purification factors, chromatographic methods are further employed. Nevertheless, chromatographic processes have some limitations and are of high cost when used at a large/industrial scale.

For the increase of the separation performance of added-value products using chromatography, it is necessary to use large chromatographic columns or several sequential cycles in smaller columns. The large columns are as robust and reliable as the smaller ones; nevertheless, they require large amounts of resins, buffers and others consumables implying, therefore, a huge cost associated to the purification process and related infra-structures. Furthermore, problems related with the packing in scaled-up processes, hysteresis, edge-effects and resin compression may result in unpredictable fluid distribution and pressure drops.[5] The use of multiple cycles can reduce the initial capital investment but it will increase the operating costs as more equilibration, wash, elution, regeneration and sanitization steps become mandatory.[5] Thus, other alternatives have to be considered in order to increase the manufacturing capacity and to decrease the final cost associated to the added-value products.

Common organic solvents used in liquid-liquid extraction present several disadvantages, such as a high volatility and toxicity and the possibility of denaturating biomolecules, which in turn may influence the quality and purity of these.[4] In addition, even when dealing with the extraction and purification of added-value compounds from biomass, the solvents employed are usually organic, volatile and hazardous.

Currently, industry continually demands the optimization of processes for the separation and purification of biomolecules aiming at finding cost-effective downstream processes, able to provide high yields and high purity levels, and that are simultaneously more environmentally friendly and sustainable.[1] In this context, ABS appear as an alternative technique, with the ability of extraction, purification and concentration in a single-step, are suitable for scale-up, and provide similar recovery yields and purification levels when compared to chromatographic approaches.[6] Moreover, ABS are majorly composed of water and do not use volatile organic compounds (VOCs), being this an advantage compared with liquid-liquid extractions carried out with toxic and flammable compounds.[7-9]

In this thesis, two methods of extraction/purification of added-value compounds were studied, namely solid-liquid extraction from biomass and ABS. Both methods are applied without the use of volatile organic compounds and using ionic liquids instead.

ABS (Aqueous Biphasic Systems)

With the goal of avoiding the use of organic solvents as the extractive phase, several studies have been carried out employing ABS. ABS consist in two aqueous-rich phases containing polymer/polymer, polymer/salt or salt/salt combinations, which above certain concentrations undergo phase separation.[2] The basis of separation of (bio)molecules in a biphasic system results from their equilibration and selective distribution between the two liquid aqueous phases.[13]

The triangular phase diagram depicted in Figure 1.2.1 represents the ternary composition of aqueous biphasic systems. The plotted graph represents only the top tip of the whole triangular diagram, stressing the fact that ABS generally consist of two moderately diluted aqueous solutions.

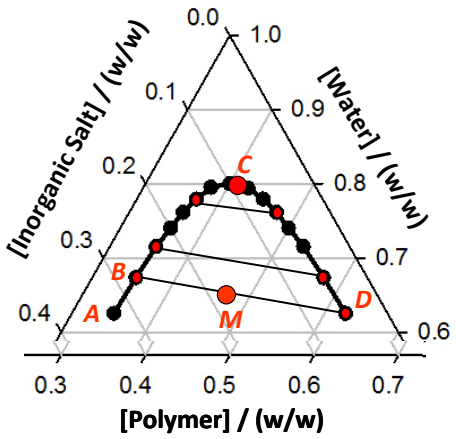

Figure 1.2.1: Triangular phase diagram for a hypothetical system composed of polymer + inorganic salt + water (weight fraction units).

All the mixtures with compositions below the binodal curve (*A*-*B*-*C*-*D*) undergo liquid-liquid demixing, while those above the line fit into the homogeneous and monophasic regions. A given mixture (*M*) under the binodal solubility curve, phase separates and forms two coexisting phases. The compositions of each phase are represented by the points *B* and *D*, which are the end-points (nodes) of a specific tie-line (TL). The tie-line length (TLL) is a numerical indicator of the composition difference between the two phases and is generally used to correlate trends in the partitioning of solutes among the two phases. Mixtures with total compositions along a specific tie-line have different mass or volume ratios of the coexisting phases but the composition of each phase remains the

same. The critical point of the ternary system is Point *C*, where the two binodal nodes meet. Here, the compositions of the coexisting phases become equal and the biphasic system ceases to exist.

In the literature, most of the ABS ternary phase diagrams are depicted in orthogonal representations, so that water concentration is omitted (pure water becomes the origin of the orthogonal axes). In Figure 1.2.2a) it is represented the separation of phases and the migration of target molecules. In Figure 1.2.2b) it is shown the binodal curve, one tie-line and the appearance of two-phases with different initial mixture concentrations along the same tie-line.

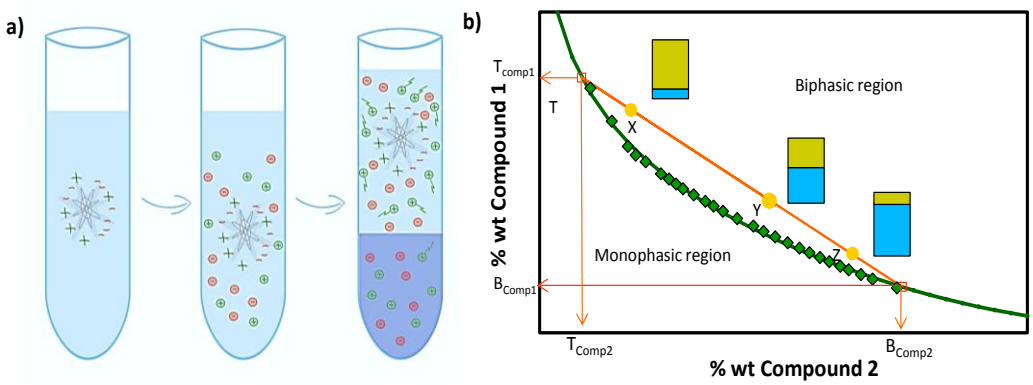

Figure 1.2.2: a) Separation of the two phases and migration of the molecule of interest; **b)** binodal curve, tie-line and the appearance of two-phases with different initial mixture concentrations along the same tie-line.

Proteins, cellular debris, organelles, nucleic acids or even whole cells can suffer permanent damage when exposed to processes involving hazardous organic solvents. Therefore, alternative techniques are required for their purification.[5] In ABS, in general, the coexisting phases are composed of approximately 60-90 % of water, which means that biomolecules are not easily denatured, constituting therefore an important advantage when the goal is to extract biologically active molecules.[13]

Beijerinck[14,15] first discovered the possibility of forming ABS by the end of the 19th century when mixing agar and gelatin or starch and gelatin in aqueous solutions.[16] Some years later, Ostwald and Hertel[17,18] found that starches from different origins and with different fractions of amylose and amylopectin (rice, corn, among others) also form ABS when dissolved in aqueus media. Nevertheless, it was only in 1958 that P.A. Albertsson introduced the potential of ABS for the separation of biologically active molecules and

particles with systems formed by polyethylene glycol (PEG), potassium phosphate and water, or PEG, dextran and water.[21,22] Figure 1.2.3 show the macroscopic aspect of an ABS composed of PEG and an inorganic salt at room temperature.

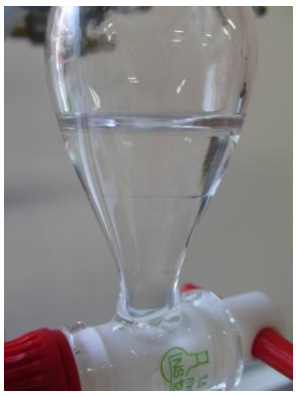

Figure 1.2.3: Macroscopic aspect of an ABS composed of PEG and an inorganic salt.

ABS have several advantages, since they also allow the concentration and partial purification integrated in one single step. Moreover, this technique can be highly selective and easily scaled-up.[23] In addition to the advantageous economic issues and technological simplicity, extractions using ABS can further be considered as an integrated process, in which the insoluble components can be removed while at the same time the target product is purified.[13,23] Hence, this biocompatible technique is gaining increasing importance in biotechnological- and pharamaceutically-related industries. Indeed, ABS have been pointed as an effective method for the purification of different biological products, such as plant and animal cells, microorganisms, virus, RNA, plasmids, proteins and biopharmaceuticals.[16,21-25] This method is largely used at a laboratory scale altough its scale-up was already demonstrated.[13] Indeed, a number of proteins are already purified by ABS at an industrial level.[5]

Figure 1.2.4 reports the number of articles and patents published *per* year concerning ABS or ATPS (aqueous two-phase systems).

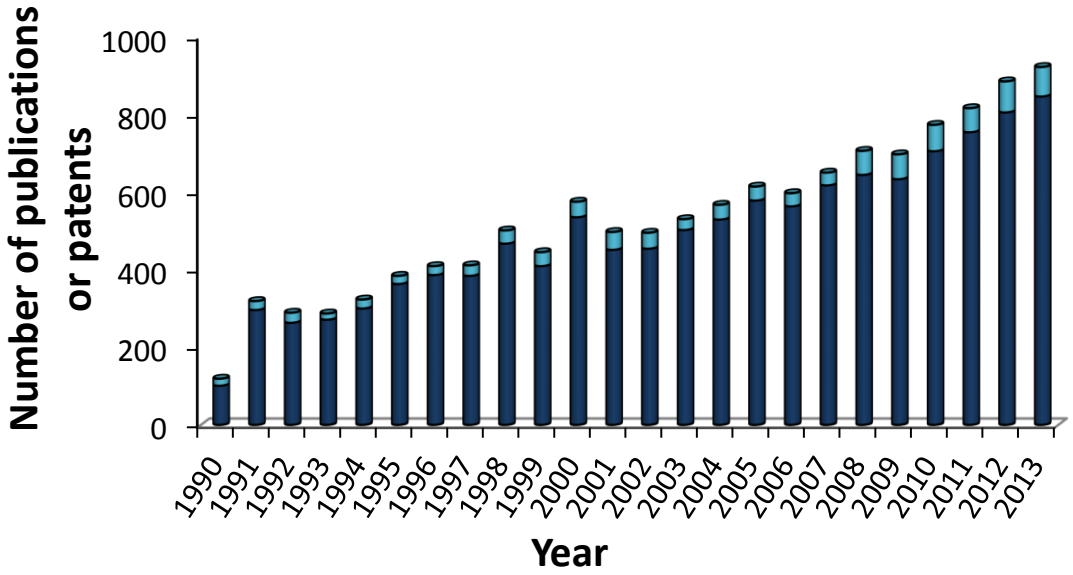

Figure 1.2.4: Number of articles (dark blue) and patents (light blue) published per year concerning ABS or ATPS. Data taken from IsiWeb of Knowledge in 4th May, 2014.

Another important thermodynamic property associated to ABS, and that gives them a significant advantage when compared to the classic oil-water systems, is the low interfacial tension between the two liquid phases.[26,27] For the application in biomolecules separation processes, this small amount of excess Gibbs free energy *per* unit area enables the transfer of bioparticles with a minimum risk of structural alterations in proteins, cells and membranes.[28] The first publication describing interfacial tension results in ABS dates from 1971 by Ryen and Albertsson.[30]

Common ABS are usually formed by polyethylene glycol (PEG) because it easily forms a biphasic system with inorganic salts and other polymers in aqueous solutions.[13] The addition of an inorganic salt to a single polymer-water system leads to the formation of two distinct aqueous phases, where usually the lower phase is rich in the inorganic salt, while the upper phase is rich in the polymer.[31] K_2HPO_4, K_3PO_4, K_2CO_3, KOH, Na_2HPO_4 and Na_2SO_4 are inorganic salts typically employed.[1,24] On the other hand, polymers such as dextran, derivatives of starch,[32] cellulose, polyvinyl alcohol,[33] hydroxypropyl starch (HPS),[34] and ethylhydroxy ethyl cellulose (EHEC)[23] are commonly employed in combination with PEG to form ABS.

The partitioning of a biomolecule in ABS depends on both their intrinsic and extrinsic properties. Intrinsic properties include the biomolecule structure, electrochemical

properties, surface properties and conformational characteristics. Extrinsic properties include type, molecular weight and concentration of the phase forming compounds, temperature, pH, ionic strength, among others[35-37] In the ABS mentioned before, the interactions between a biomolecule and the distinct phases involve hydrogen-bonding, and van der Waals-, dispersive-, and electrostatic-interactions.[24]

Solid-liquid (S-L) Extractions

Solid-liquid extractions allow components to be removed from solids (e.g. biomass) to a solvent as illustrated in Figure 1.2.5. The phases are then separated by centrifugation or filtration where the compounds of interest are dissolved in the liquid phase.[38] This technique is one of the oldest unit operations in the chemical industry. In the food industry, for instance, the process can be used either to obtain important substances or to remove some inconvenient compounds like contaminants or toxins.

The choice of the solvent is carried out taking into consideration its selectivity, capability for dissolving the solute, density, viscosity, surface tension, toxicity, boiling temperature, chemical and thermal stabilities and cost.[38] Obviously, due to the toxicity of some organic solvents, there are some restrictions on their use in the food, cosmetic and pharmaceutical industries. For human consumption, the presence of some solvents, namely acetone, ethanol, ethyl acetate, 1-propanol, 2-propanol and propyl acetate are acceptable in low concentrations, according to good manufacturing practices (GMP).[39] These solvents are classified as Class 3 by the Food and Drug Administration (FDA). On the other hand, solvents such as acetonitrile, chloroform, hexane, methanol, toluene, ethylmethylketone and dichloromethane (Class 2) can also be used; yet, under specific conditions due to their inherent toxicity.[40] Solvents such as benzene, carbon tetrachloride, 1,2-dicloroethane, 1,1-dicloroethane and 1,1,1- trichloroethane, grouped in Class 1, should not be employed at all in manufacturing because of their unacceptable toxicity or their deleterious environmental effects.[39]

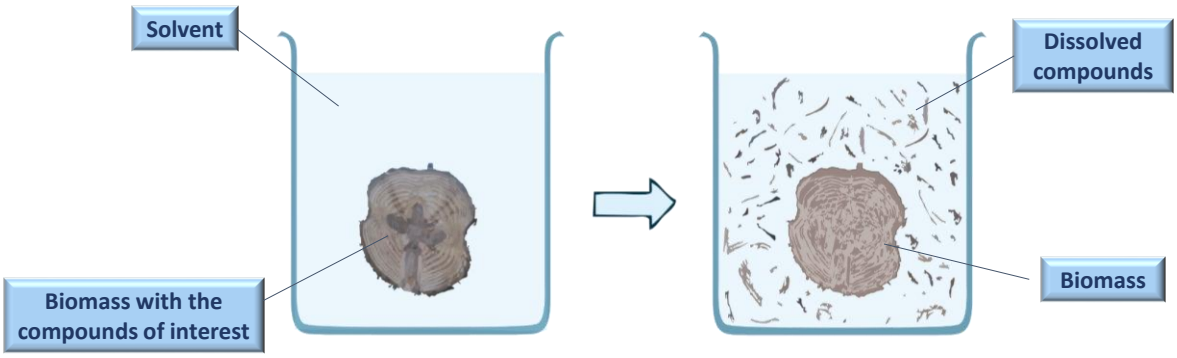

Figure 1.2.5: Schematic solid-liquid extraction.

1.3. Ionic Liquids

General Context

Before the Montreal Protocol,[41] volatile organic compounds (VOCs) were commonly applied as extractive solvents in industrial applications because of their immiscibility with aqueous media.[42] Nevertheless, environmental concerns regarding the use of VOCs has increased in the past few years due to their toxicity, volatility and flammability. Therefore, there is an emergent interest for the research on alternative "greener" solvents for separation processes.[41] In this context, ionic liquids (ILs) appear as potential candidates. ILs are salts that, unlike common salts such as NaCl, are liquid in a wide range of temperatures and with a melting temperature, by general definition, below 373 K (100 ^{o}C).[43-45] They are usually constituted by large organic cations and organic or inorganic anions. The low symmetry, weak intermolecular interactions and a large distribution of charge in the ions are the major reasons behind their low melting temperatures.[46,47]

ILs were firstly reported at the beginning of the 20th century by Paul Walden,[48] when testing new explosive compounds with the aim of replacing nitroglycerin. Walden synthesized ethylammonium nitrate, [$EtNH_3$][NO_3], and found that it has a melting point around 286-287 K (13-14 ^{o}C).[48] In 1934, Charles Graenacher[49] filled the first patent for an industrial application of ILs regarding the preparation of cellulose solutions. Later, during the World War II, ILs were again investigated and new patents were filled[50.51] concerning the application of mixtures of aluminium chloride (III) and 1-ethylpyridinium bromide to the electrodeposition of aluminium. Despite these findings, only in a recent past these compounds have been extensively studied, and as can be seen in Figure 1.3.1 which depicts the increase on the ILs' publications between 1990 and 2013.

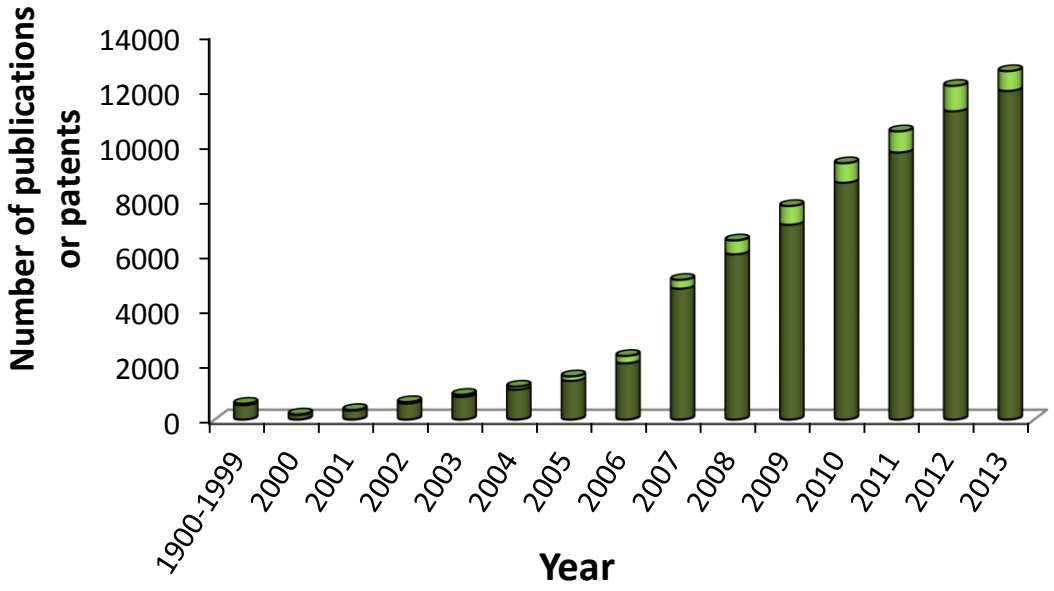

Figure 1.3.1: Number of articles (black green) and patents (light green) published *per* year regarding ILs. Data taken from IsiWeb of Knowledge in 5th May, 2014.

Since the ILs physicochemical properties are strongly dependent on their chemical structure, the possibility of changing their properties through the manipulation of the ions that compose them, represents an important and supplementary advantage. This "tunnability" makes of ILs singular compounds that can be designed with precise conditions for a particular process, as well as to manipulate their extraction capabilities for specific biomolecules.[46,55,68]

Among a large range of ILs that can be synthesized, the most commonly studied are nitrogen-based, namely pyrrolidinium-, imidazolium-, piperidinium-, pyridirium-, and ammonium-based ILs. In Figure 1.3.2 are represented some IL cation structures. The cation can be even more complex with different sizes for the alkyl side chains and additional functionalized groups.[76] In Figure 1.3.2 are depicted some of the main IL anions investigated. These include simple halogenates, such as Cl^- and Br^-, to more complex organic structures, such as tosylate and acetate, to fluorinated ones, namely $[BF_4]^-$, $[PF_6]^-$ and $[NTf_2]^-$.

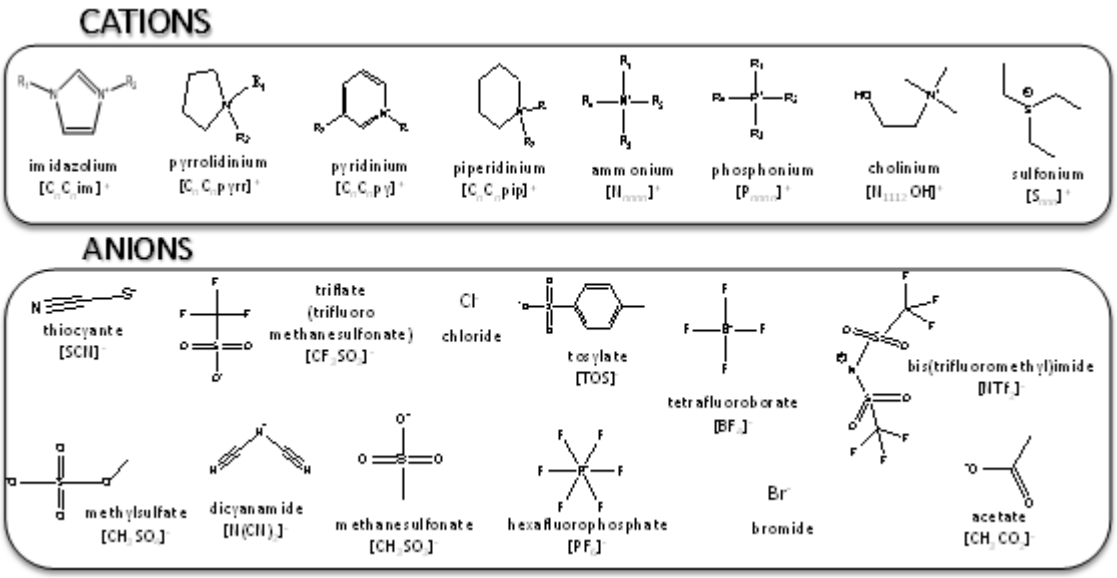

Figure 1.3.2: Chemical strucutures of some IL ions.

In spite of the ILs environmental benefits as "greener" replacements of conventional volatile organic solvents, their toxicity must be also addressed. Several studies[77-82] were conducted to evaluate the toxicity of ILs, combining different anions and cations, as well as changing the alkyl side chain length and the number of alkyl groups at the cation ring. These studies revealed that the ILs toxicity is primordially determined by the cation nature and it is directly correlated with the length of the alkyl side chain and number of alkyl groups. The anion has a less significant influence than the cation, and generally cations with short alkyl chains or hydrophilic ILs present lower toxicity.[79-83]

The ILs aqueous solubility usually decreases with the alkyl chain length increase, which is an advantage since the more toxic ILs (longer alkyl chain lengths) are poorly water soluble at room temperature, minimizing thus the environmental impact of ILs in aquatic streams.[79] Nevertheless, the influence of the cation alkyl chain length in their water solubility was also observed, but it can be considered minor when compared with the IL anion influence.[84]

Due to their ionic nature, ILs present other physical and chemical advantages over more conventional and molecular organic solvents, namely negligible flammability and vapour pressure, high solvation ability for several compounds, high chemical and thermal stabilities [52-57] Apart from these advantages, many organic, organometallic and inorganic compounds can be dissolved in ILs.[58] Due to these features, ILs have been applied in

catalysis,[59] organic synthesis,[53] chemical reactions,[46] multiphase bioprocess operations,[46] electrochemistry,[47] chromatographic separations,[48] mass spectrometry analysis,[63] batteries and in fuel cells research,[64] treatment and/or dissolution of biomass[65-67] and for the separation of biomolecules.[68] Beyond these applications, ILs have also been used in liquid-liquid extractions of metal ions [69,70] and synthetic organic compounds.[71-73]

It was already shown that most ILs do not inactivate enzymes ensuring their structural integrity and enzymatic activity and, therefore, ILs represent a good alternative to the common solvents used in biocatalysis.[4, 54] Furthermore, ILs allow an improved recovery of biomolecules when carrying liquid-liquid extractions while reducing solvent emissions.

Regarding the extraction of added-value compounds from biomass, ILs were already used in the extraction of alkaloids, terpenoids, flavonoids, natural dyes, lipids, among others.[75] However, the field of separation technology is still far from being fully developed or explored. Several examples of extraction are described in a recent review[75] regarding the use of ILs solutions as extractive solvents of value-added compounds from biomass. Examples include the use of ILs in the extraction of essential oils from orange peels, in the extraction of caffeine from guaraná seeds, in the reactive dissolution of star anise seeds towards the isolation of Shikimic acid for the production of Tamiflu, in the sequestration of suberin from cork, in the extraction of lactones, tannins and phenolic compounds from medicinal plants, in the extraction of alkaloids from plants, in the isolation of pharmaceutically active betulin from birch back, in the pretreatment of lignocellulosic biomass, etc.[75] In addition to simpler solid-liquid extractions, microwave-assisted and ultrasound-assisted extractions were also used to improve the extraction yields and to reduce the time of extraction.[75] Based on literature data, IL-based solvents, either as pure ILs, IL aqueous solutions or IL-alcohol mixtures, demonstrated to be enhanced solvents for the extraction of high-value products from biomass.[75] After the extraction, the crucial step still consists on the product recovery and purification, and on the solvents recyclability aiming at developing sustainable technologies. Only few methodologies have already been proposed, including the addition of anti-solvents, back-extraction and adsorption approaches.[75]

Characterization of Ionic Liquids: Solvatochromic Parameters

Since ILs have emerged as promising substitutes for traditional solvents it is crucial to exploit their inherent properties. The knowledge of their physical and chemical properties, such as melting and boiling temperatures, density, viscosity and solvation/polarity properties, in order to define the solvent with adequates better for a specific task, is therefore of high relevance. In summary, the main challenge consists in the selection (and further synthesis) of a "tailored solvent" for a target application. Nevertheless, for that purpose, it is crucial to understand their solvation ability at a molecular level. Among the most important features of an IL to be used as a solvent are the specific interactions occurring between the solvent and the solute which are usually related to the solvent polarity. It has previously been demonstrated that the IL polarity influences its solvation ability, reaction rates, reaction mechanisms, product yields and enzyme activity, among others.[85-90] However,it is difficult to describe the solvents polarity using single solvent parameters, namely dipole moment, relative permittivity and refractive index, and it is further required to define the polarity of ILs by molecular–microscopic solvent-dependent processes aiming at understanding the multitude of possible solute–solvent interactions.[91]

One of the methods often employed to estimate the polarity of ILs consists on the analysis of the UV-Vis spectral band shifts of solvatochromic probes. Specific and nonspecific solute-solvent interactions are reflected in the respective absorbances of a suite of selected dyes.[91-95] A number of empirical solvatochromic parameters has been suggested to quantify the molecular-microscopic solvent properties of ILs.[91-95] For the sake of simplicity only one indicator is frequently used to build the polarity scale and, amongst the various possibilities, the $E_T(30)$ Reichardt's betaine dye has been widely employed.[91] $E_T(30)$ is a measure of the solvent dipolarity/polarizability, though it is also sensitive to the solvents' hydrogen-bond donor ability. On the other hand, a multiparametric approach was proposed by Kamlet, Taft and co-workers[91-95] and consists in the use of a set of solvatochromic probes which allow the assessment of different parameters for the same solvent.[96,97]

The Kamlet-Taft approach,[91-95] in its simple form, is the expression of a Linear Solvation Energy Relationship (LSER), given by the following equation,

$$XYZ = (XYZ)_0 + a\alpha + b\beta + s(\pi^* + d\delta) \qquad \text{eq. 1.3.1}$$

where *XYZ* is the result of a particular solvent-dependent process, $(XYZ)_0$ is the value for the reference system, π^* represents the solvent's dipolarity/polarizability, α is the hydrogen-bond donating ability, β is the hydrogen-bond accepting ability and and δ is a correction term.. The parameters *a*, *b* and *s* represent the solvent-independent coefficients.[91-95]

Different dyes and experimental approaches can result in diverse values of solvatochromic parameters for the same solvent.[91-95] In this context, different empirical techniques only provide unique scales of relative polarity. For instance, two structurally similar probes, *N*,*N*-diethyl-3-nitroaniline and *N*,*N*-diethyl-4-nitroaniline, lead to different values of π^* for the same IL.[98,99] This is a result of the diverse and complex interactions that occur between the solvent and a particular solute, *i.e.*, the polarity scales are always solute-dependent. Published data for α, β and π^* for specific ILs are quite different and mainly depend on the set of solvatochromic dyes employed.[98-101]

For most , and in particular for ionic liquids, the probes dyes depicted in Figure 1.3.3 are the most used.[98]

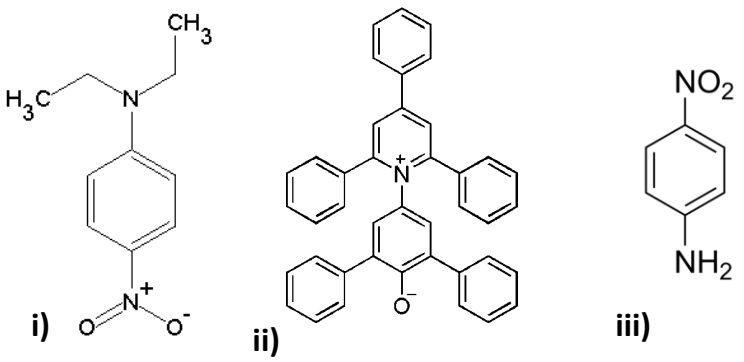

Figure 1.3.3: Probes dyes: i) *N*,*N*-diethyl-4-nitroaniline; ii) Reichard dye; iii) 4-nitroaniline.

The Kamlet-Taft parameters are well established for traditional solvents and are the most accepted polarity scales.[102,103] Nevertheless, for more recent solvents such as ILs, these parameters are still not definitive and are undergoing continuous experimental measurements by several research groups.[98-101] One of the major reasons behind this ongoing research is the sensitivity of the Kamlet-Taft values to impurities.[98,99, 104-106] In ILs, many of these impurities come from their own synthesis. Improvements on the synthetic routes of ILs are also under constant development.[46] Recently, it was demonstrated that water, 1-methylimidazole, 1-chlorobutane and the ions of the salts precursors significantly influence the values of the solvatochromic parameters of ILs.[98,99,107] For instance, for [C_4mim][NTf_2], it was found in literature that 1% of 1-methylimidazole can influence the α, β and π* values by +0.2, +0.25 and -0.18, respectively.[98] In the case of ILs containing 1% of Li[NTf_2], the α and β values may change -0.04 and +0.11, respectively, while π* remains constant.[98] Welton and co-workers[98] also tested the effect of 1% of [C_4mim]Cl and demonstrated that the α and β values show a variation of -0.03 and +0.11, respectively, and without changes on the π* value.[98] Therefore, when stablishing a polarity scale for ILs it is crucial to deal with high purity and non-coulored compounds.

One of the major advantages of ILs over traditional solvents is their lack of vapour pressure at ambient conditions. However, this low volatility doesn't allow their purification by simple distillation. Only volatile impurities can be removed by heating under vacuum. Usually, ILs are also purified by passing them by a column with two layers, the first with acidic alumina and the second with basic alumina, or by washing with other solvents. When ILs are coulored they are typically passed through activated charcoal and then filtered with basic and acidic alumina - Figure 1.3.4.

Figure 1.3.4: Experimental apparatus for decoulorizing ionic liquids.

The solvatochromic parameters are determined by measuring the maximum absorvance wavelength for each sample and applying the following equations:

$$\alpha = 0.0649 \times \left(\frac{28591}{\lambda_{\max R}} \right) - 2.03 - \left(0.72 \times \pi^{*} \right) \qquad \text{eq. 1.3.2}$$

$$\beta = \frac{\left(\Delta\nu_{IL} - \Delta\nu_{cyclohexane} \right) \times 0.76}{\Delta\nu_{DMSO} - \Delta\nu_{cyclohexane}} \qquad \text{eq. 1.3.3}$$

$$\Delta\nu = \nu_{N,N} - \nu_{4N} \qquad \text{eq. 1.3.4}$$

$$\pi^{*} = \frac{\nu_{N,N(IL)} - \nu_{N,N\,cyclohexane}}{\nu_{N,N(DMSO)} - \nu_{N,N\,cyclohexane}} \qquad \text{eq. 1.3.5}$$

where $\lambda_{max(dye)}$ is the wavelength corresponding to maximum absorption and $\nu_{dye}=1/\lambda_{max(dye)} \times 10^{-4}$ kK.

The Kamlet-Taft parameters are obtained as averaged values of a series of selected probes requiring thus a considerable experimental effort to derive the respective values for any new solvent. Still, and despite some divergences found between different authors and probe dyes, it is generally accepted that: (*i*) the dipolarity/polarizability (π*) values are similar amongst several ILs and are higher than those of most molecular solvents (Coulombic interactions as well as dipole and polarizability effects occur in ILs); (*ii*) the hydrogen-bond basicity values cover a large range and are mainly controlled by the IL anion; and (*iii*) the hydrogen-bond acidity values of ILs are comparable to or lower than that of aniline and are mainly determined by the IL cation (although the anion also plays a secondary role).[98-101]

Aiming at overcoming the difficulties encountered with common solvatochromic probes and the establishment of polarity scales in ILs, several attempts have been carried out in order to find suitable alternatives. For instance, Chiappe and Pieraccini[108] studied the formation of an electron donor-acceptor complex between 4,4'-bis(dimethylamino)benzophenone and tetracyanoethene and correlated its visible absorption maximum with the Kamlet-Taft parameters. Wu et al.[109] proposed a spectroscopic method based on the transition energy of spiropyran probes and demonstrated its correlation with the polarity of ILs by means of the $E_T(30)$ values. Lungwitz and co-workers[96,97,110] established that there is a close correlation between α and β. The same research group[96,97,110] proved that β also correlates with the ^{1}H NMR chemical shift of the most acidic proton of the imidazolium cation. In addition, other authors[111] confirmed, for more than 50 organic solvents, a linear correlation between Gutmann's ANs (acceptor number) and the α parameter.[111] However, Schmeisser et al.[112] verified the absence of a good correlation between these two parameters using ILs.

Trying to find another parameter that provides a good correlation with the Kamlet-Taft β parameter, Marcus[113,114] demonstrated, for a vast number of traditional solvents, that the Gutmann's DN (donor number, quantitative value of donating electron pairs by a solvent) presents a close relationship with β.[113,114] Following the Marcus's idea,[113,114] Schmeisser et al.[112] established two kinds of correlations, being the first one for ILs composed of O-donor anions and the second correlation for ILs constituted by N-donor anions. Authors proved that DNs can be measured by ^{23}Na NMR and display a strong dependency with the IL anion.[111] More recently, Hunt and co-workers[115] proposed the use of different computational descriptors for predicting Kamlet-Taft parameters, namely α and β, in ILs.

1.4. ABS with Ionic Liquids

A large part of this thesis is focused on the application of ABS composed of ionic liquids and common salts for the extraction and purification of added-value compounds, such as alkaloids, aminoacids and phenolic compounds. These were used as model compounds to address the potential of ABS for extractions and purifications. Due to the outstanding extraction performance of IL-based, there is a large amount of literature data on this topic. Therefore, in this section, many of these works will be highligted and discussed

based on a previous review manuscript (Freire, M. G., Cláudio, A. F. M., Araújo, J. M. M., Coutinho, J. A. P., Marrucho, I. M., Canongia Lopes, J. N., Rebelo, L. P. N., Aqueous biphasic systems: A boost brought about by using ionic liquids, Chem. Soc. Rev., 2012, 41 (14), 4966-4995).

Conventional polymer-based ABS have been largely used since the 1980's. Neverthless, in 2003, Rogers and co-workers[118] reported the pioneering research pointing to the possible creation of ABS by the addition of inorganic salts (K_3PO_4) to aqueous solutions of ILs ($[C_4C_1im]Cl$ - a hydrophilic ionic liquid). After this initial work[118], three articles were published in 2005; yet, only in 2007, a greater number of manuscripts (12) appeared in the literature. Since 2009 the number of manuscripts has increased rapidly and, more significantly, a large number of both ionic liquids and salting-out agents have been evaluated. These ABS offered new alternatives for the recycling and concentration of ionic liquids from aqueous solutions, for carrying out metathesis reactions, for the formation of new ionic liquids, and for separation approaches.[118] Since then, considerable effort has been directed towards the use of ionic liquids as feasible alternatives to polymeric-rich phases,[44,56,77, 108-171] and more recently, to the salt-rich phases.[172-176]

Due to their ionic nature, ILs present two outstanding properties: negligible volatility and non-flammability.[177-179] These two characteristics have contributed to their common epithet as "green solvents", and as a result, they have been viewed as alternative replacements for the volatile and hazardous organic solvents presently used in a wide range of applications. However, one of the main advantages of IL-based ABS is the ability to tailor their polarities and affinities by the manipulation of the cation/anion design and their combinations. This aspect is indeed a major benefit given the difficulty of overcoming the limited polarity range of polymer-based ABS. Polymer/polymer ABS usually display two hydrophobic phases and the difference in polarities depends essentially on the amount of water in each phase. On the other hand, polymer/salt ABS have a more hydrophobic phase constituted by the polymer and a hydrophilic (and more ionic) phase typically formed by high charge-density salts. By virtue of their tunability, ILs cover the whole hydrophilicity-hydrophobicity range and it's thus possible to tailor the phases' polarities and affinities for given extractions and purifications.

The replacement of polymers by ILs also leads to other benefits, since most of the polymer-based ABS are highly viscous and display slow phase separation – drawbacks generally avoided with ionic-liquid-based ABS. Figure 1.4.1 illustrates the clear appearance of the co-existing phases in a given ABS composed of an IL and an inorganic salt. Chloroanilic acid was added to colour (preferentially) the IL-rich phase.

Figure 1.4.1: Macroscopic appearance of an IL-based ABS.

The physical properties of the co-existing phases at various concentrations and temperatures are indispensable requirements for the design and scale up of IL-based ABS. Density and viscosity measurements of both phases for selected IL-based ABS have been reported.[131,146,180,181] The systems evaluated are made up of inorganic salts and ionic liquids (phosphonium- and imidazolium-based)[131,146,180] and of carbohydrates and ionic liquids.[181] No significant differences in density values between IL-based ABS and typical polymer-based systems have been observed.[131,146,180,181] Nevertheless, phosphonium-based phases are far less viscous (4-11 MPa·s) than typical polymer-rich phases (≈ 40 MPa·s) at close mass fraction compositions.[131] In addition, imidazolium-based ABS present even lower viscosity values than their phosphonium-based counterparts.[181] Even for systems composed of carbohydrates and ILs, the viscosities were found to be similar to those displayed by systems composed of inorganic salts, and substantially lower than those of typical polymer-salt or polymer-polysaccharide ABS.[131] The low viscosity of IL-based ABS thus favours mass transfer during extraction as well as the handling of the phases in scaled-up processes.

Only those ILs miscible with water near room temperature can be considered for the formation of ABS. When dealing with hydrophobic ILs, two phases already exist before the addition of any salt and one of the phases is far from being aqueous rich due to the

low solubility of these compounds in water. Moreover, the number of hydrophobic ILs is limited to few cation/anion combinations, and most of them contain fluorinated ions, which are more expensive, unstable,[182] and less environmentally benign. Nowadays, there are a vast number of hydrophilic ILs to choose from and their environmental impact can be controlled in a more versatile manner. In addition, it is already well accepted that the toxicity of ILs mainly depends on their hydrophobicity.[183-184] In this context, it is useful to mention that most of the hydrophilic ILs used to prepare ABS display lower toxicities.[185]

Aiming at defining general trends in the phase behaviour of IL-based ABS, we have collected a lot of liquid-liquid phase equilibrium data available in the literature[44,56,77, 108-176] and converted the usual reported weight fraction units to molality units to avoid inconsistencies that may result from the varying molecular weights exhibited by ILs and/or the salting-out species used. Below, the influence of the IL chemical structure, the nature of the salting-out species, pH effects, and the influence of temperature on the liquid–liquid demixing phenomenon will be presented and discussed. All phase diagrams were determined at atmospheric pressure and studies on the pressure effect were not found in the literature[44,56,77, 108-176]

Ionic Liquid + Salt + Water Systems

ILs based on the 1-alkyl-3-methylimidazolium cation have received by far the most scrutiny. In this class, $[C_4C_1im]Cl$, $[C_4C_1im]Br$ and $[C_4C_1im][BF_4]$ have been the most investigated. Although $[C_4C_1im][BF_4]$ was one of the most commonly studied fluids in the formation of ABS, it should be stressed that $[BF_4]$-based compounds are not water stable. $[BF_4]$-based ILs suffer hydrolysis in contact with water releasing fluoridric acid, even at room temperature.[182] Although these phase diagrams can be accurately determined due to the short amount of time required to measure them, the user must take into account the fact that these systems are not good candidates for extraction or recycling purposes when longer periods of contact with water are required.

The cornerstone of the formation of ABS comprising ILs and conventional salts is the salting-out effect which is mainly a result of the creation of water-ion complexes that cause the dehydration of the solute and the increase of the surface tension of the cavity

in the aqueous media.[187,188] Freire et al. [187,188] demonstrated the role of ion-specific effects in the solvation phenomena associated to the mixing of ILs in aqueous media. Salting-out inducing ions act mainly through entropic effects resulting from the formation of water-ion complexes whereas salting-in inducing ions directly interact with the hydrophobic moieties of the IL.[187,188] The salting-in/-out effects are thus dominated by the ion-ion *versus* ion-water interactions and not by underlying water-structure modifications, as classically accepted.[187,188] Therefore, the addition of high charge-density salts leads to liquid-liquid demixing due to a preferential hydration of the high charge-density salt over the IL, leading thus to the salting-out (exclusion) of the IL to the IL-rich phase. ILs are generally made up of low-symmetry charge-delocalized ions only capable of weak directional intermolecular interactions (and hence weakly hydrated as compared to the common salting-out inducing salts).

Influence of the Ionic Liquid in IL + Salt + Water Systems

Despite the immense versatility inherent to the cation-anion permutations in ILs, most of the reported phase diagrams of IL-based ABS have made use of imidazolium-based compounds,[119,120,124-127,132,134,143-147,149,150,153,155,157,158,165,168] whereas relatively few studies have used phosphonium-, ammonium- pyridinium-, piperidinium-, or pyrrolidinium-based fluids.[127,135,133,154,164,165,189] The first investigation of the effect of the cation core on the formation of ABS was conducted by Bridges et al.[119] in 2007, where it was evaluated the phase behaviour of imidazolium-, pyridinium-, and quaternary ammonium-, and phosphonium-based chloride salts salted-out by K_3PO_4, K_2HPO_4, K_2CO_3, KOH and $(NH_4)_2SO_4$. Figure 1.3.2 compares the phase behaviours of aqueous solutions of four IL with K_3PO_4 (the strongest salting-out agent evaluated).

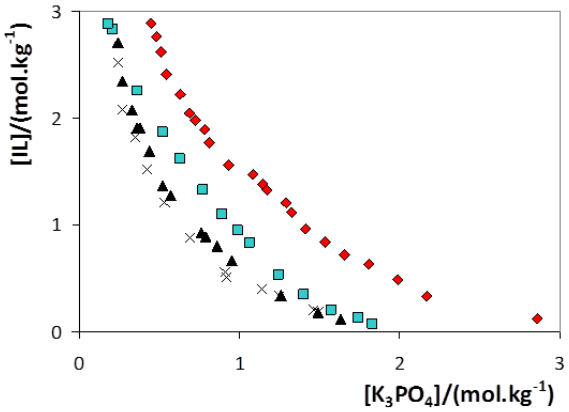

Figure 1.4.2: Ternary phase diagrams for ABS composed of chloride-based ionic liquids + K_3PO_4 at room temperature: ♦ , [C_4C_1im]Cl; ■, [C_4py]Cl; ▲, [N_{4444}]Cl; ×, [P_{4444}]Cl.

The closer to the axis origin a binodal curve is, the higher the IL hydrophobicity (or salting-in behaviour), *i.e.*, the lower the density charge of the IL ions and the higher their ability to phase split. The overall order of the ILs' ability to undergo liquid-liquid demixing in the presence of potassium phosphate concentrated aqueous solutions is as follows: [P_{4444}Cl] > [N_{4444}]Cl > [C_4py]Cl > [C_4C_1im]Cl. The two quaternary salts ([P_{4444}Cl] and [N_{4444}]Cl) have highly shielded charges, located mostly on the heteroatom surrounded by four alkyl chains, thus leading to a higher tendency toward salting-out from aqueous media. The pyridinium-based IL has less shielding compared to that of the quaternary ammonium salt, although the charge is also mostly located on the nitrogen atom. Finally, the imidazolium-based IL has a cation with a charge more evenly dispersed along the entire heterocycle, and a greater ability to interact with water *via* hydrogen-bonding. Similar results for other salting-out agents, like K_2HPO_4 or K_2CO_3, have also been reported.[119] Subsequently, Louros et al.[181] published the ternary phase diagrams of distinct phosphonium-based ILs, also using K_3PO_4 as the salting-out agent, at 298 K. Again, the phosphonium-based ILs are more effective in promoting ABS when compared to their imidazolium-based counterparts with similar anions. The four alkyl chains and non-aromatic character of these compounds are responsible for their lower affinity for water.[181] Indeed, the larger or lower miscibility of phosphonium-based ILs with water mainly depends on the water-anion interactions.[173] In addition, similar results was published by Neves et al.[146] where a large range of ABS composed of imidazolium- and

phosphonium-based ILs with the inorganic salts $Al_2(SO_4)_3$ and $AlK(SO_4)_2$ under acidic media have been compared. Independently of the salt employed and the pH of the aqueous media, the phosphonium-based ILs are always more efficacious in creating ABS.[119, 146,181]

Ventura et al.[157] have assessed the influence of nitrogen-based cyclic ILs (imidazolium-, pyridinium-, pyrrolidinium-, and piperidinium-based) on the formation of ABS. The inorganic salt used consists of a mixture of K_2HPO_4/KH_2PO_4 to control the pH values of the co-existing phases. The influence of the cation core on the formation of IL-based ABS is displayed in Figure 1.4.3.

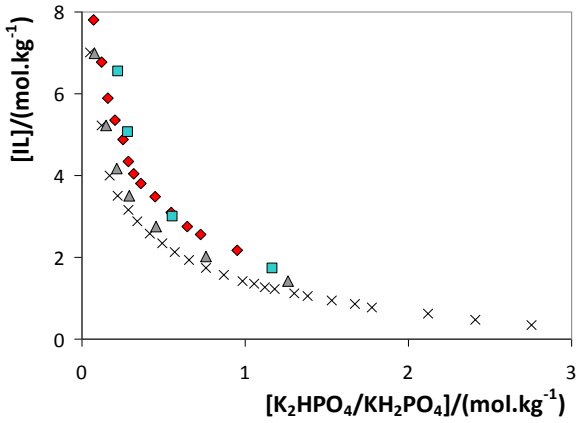

Figure 1.4.3: Ternary phase diagrams for ABS composed of chloride-based ionic liquids + K_2HPO_4/KH_2PO_4 at 298 K: ■, $[C_4C_1pyrr]Cl$; ♦ , $[C_4C_1im]Cl$; ▲, $[C_4C_1pip]Cl$; ×, $[C_4\text{-}3\text{-}C_1py]Cl$.

The formation of ABS with aqueous solutions of K_2HPO_4/KH_2PO_4 for the various families of cations occurs in the following sequence: $[C_4C_1pyrr]Cl$ < $[C_4C_1im]Cl$ < $[C_4C_1pip]Cl$ < $[C_4\text{-}3\text{-}C_1py]Cl$. The authors[157] made use of liquid-liquid equilibria data for binary systems composed of ILs and water to support their results and showed that, albeit the solubility of water in ILs largely depends on the availability of electrons at the aromatic cores for privileged hydrogen-bonding with water, the solubility of ILs in water is mainly ruled by steric and entropic contributions. In this context, the solubility of ILs in water largely depends on their molar volume and closely agrees with the data obtained for the IL-based ABS shown in Figure 1.4.2. Indeed, the aromatic character of ILs has no major influence on their phase behaviour, whereas the size of the cation seems to play a crucial effect. Larger cations such as pyridinium and piperidinium (6-atom heterocyclic compounds) are

better at inducing ABS than the smaller cations imidazolium and pyrrolidinium containing 5-atom rings. In summary, considering the liquid-liquid phase behaviour of ILs and water [189-190], and based on the results regarding the influence of the ionic liquid cation core, it seems that the formation of IL-based ABS are dominated by steric and entropic contributions. The trend shown in Figure 1.3.2, where the ionic liquids' ability follows the order $[P_{4444}]Cl > [N_{4444}]Cl > [C_4py]Cl > [C_4C_1im]Cl$, also closely correlates with the IL molar volume.

Few authors have investigated the effect of the nature of the IL anion through the formation of ABS[124,125,145,155,158] However, only in 2009, Coutinho and co-workers[155] published the first study with a more comprehensive analysis of the anion effect. The experimental phase diagrams shown in Figure 1.3.4 reveal that the ability of ILs to form ABS increases in the order: $[C_4C_1im]Cl < [C_4C_1im][CH_3SO_3] < [C_4C_1im]Br < [C_4C_1im][CF_3CO_2] < [C_4C_1im][N(CN)_2] < [C_4C_1im][HSO_4] < [C_4C_1im][CF_3SO_3]$.

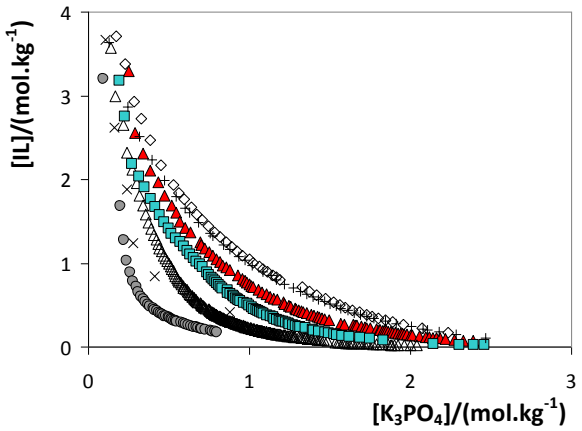

Figure 1.4.4: Ternary phase diagrams for ABS composed of $[C_4mim]$-based ionic liquids + K_3PO_4 at 298 K: ◊, $[C_4C_1im]Cl$; +, $[C_4C_1im][CH_3SO_3]$; ▲, $[C_4C_1im]Br$; ■, $[C_4C_1im][CF_3CO_2]$; ×, $[C_4C_1im][N(CN)_2]$; Δ, $[C_4C_1im][HSO_4]$; ●, $[C_4C_1im][CF_3SO_3]$.

The authors[155] also determined the ternary phase diagrams for $[C_2C_1im]$-based ILs, K_3PO_4, and water at 298 K, and reported the following ABS formation rank: $[C_2C_1im][CH_3SO_3] < [C_2C_1im][CH_3CO_2] < [C_2C_1im]Cl < [C_2C_1im]Br < [C_2C_1im][C_1SO_4] < [C_2C_1im][C_2SO_4] < [C_2C_1im][CF_3SO_3]$. The ABS studied reflect the competition between the salting-out ions and the IL ions for the formation of hydration complexes, or in other words, their relative hydrogen-bond acceptor capacities. The authors[155] showed, for the first time, that the

ability of an IL anion to produce an ABS closely follows the decrease in their hydrogen-bond accepting strength or electron pair donation ability. Anions with lower hydrogen bond basicity values (usually quantified using polarity scales obtained with different solvatochromic probes) present lower abilities to form coordinative bonds and create hydration complexes, therefore easily undergoing salting-out by conventional salts.[155] Nevertheless, this phenomenon had not been previously observed when evaluating the effect of the ionic liquid cation (where steric contributions play the major role). Anions have a higher aptitude for hydration since they are more polarizable and present a more diffuse valence electronic configuration. Moreover, most ILs anions are characterized by the absence of long alkyl side chains which mainly contribute to steric hindrance (some recent exceptions are alkylsulfonate, alkylsulfate and carboxylate anions).

Additional work, [124,158] has provided new information on the IL anions' ability to form ABS, either by studying new ILs anions or by using different salts. With Na_2SO_4, the ability of the IL for phase splitting at 298 K follows the rank: $[C_4C_1im][CF_3SO_3]$ > $[C_4C_1im][C_8SO_4]$ > $[C_4C_1im][TOS]$ > $[C_4C_1im][SCN]$ > $[C_4C_1im][N(CN)_2]$ > $[C_4C_1im][C_2SO_4]$ > $[C_4C_1im][CF_3CO_2]$ > $[C_4C_1im][C_1SO_4]$ > $[C_4C_1im]Br$. [116] Also with a phosphate buffer solution, the ability of the IL to induce liquid-liquid demixing at 298 K follows a similar order.[158] Therefore, for the ILs investigated, the anions rank is universal and independent of the inorganic salts used. As a result, and despite the salt employed for ABS formation, the ability of ILs with distinct anions to undergo the formation of ABS closely follows their decreased ability to hydrogen-bond with water (hydrogen bond basicity values).[124,155,158]

Several authors[120,124,125,127,132,134,143-145,147,149,150,153,157,158,165] have addressed the influence of the IL cation alkyl chain length on the formation of ABS. However, this trend is limited to imidazolium-based compounds combined with the anions $[CH_3CO_2]^-$, $[BF_4]^-$, Cl^- and Br^-. Most of these works systems used ILs with alkyl chains up to hexyl.[124,125,134,144,147,149,153,165] These works indicate that the longer the cation alkyl side chain length (and thus the IL molar volume) the greater is the ability of the IL to phase separate. An increase in the cation alkyl chain length leads to an increase in the fluid hydrophobicity (an intrinsic result of the aliphatic part extension), and thus to a poorer solubility of the IL in water. In fact, it has been previously shown with liquid–liquid equilibria data for binary systems

constituted by ionic liquids and water[191,192] that the decrease in the ILs' solubility in water with their cation size increase is driven by a decrease in the entropy of solution. For this reason, ILs with longer aliphatic chains require less salt for salting-out and are more easily excluded from the salt-rich phase to the IL-rich phase. On the other hand, the liquid-liquid phase behaviour of ternary systems composed of 1-alkyl-3-methylimidazolium chloride ILs (from methyl to tetradecyl), water, and K_3PO_4 has recently received a more extensive analysis.[132] The IL abilities to form ABS, for instance at 1.0 mol.kg^{-1} of K_3PO_4, follow the order: $[C_1C_1im]Cl$ < $[C_2C_1im]Cl$ < $[C_4C_1im]Cl$ < $[C_{10}C_1im]Cl$ < $[C_8C_1im]Cl$ < $[C_7C_1im]Cl$ < $[C_6C_1im]Cl$ < $[C_{12}C_1im]Cl$ < $[C_{14}C_1im]Cl$. Therefore, it is shown that the increase of the cation alkyl chain length leads to an improved ability to form aqueous biphasic systems if alkyl chain lengths until hexyl are considered. For ILs with longer aliphatic chains, the locus of the homogeneous region increases as the alkyl side chain length increases and agrees well with the initial work of Najdanovic-Visak et al.[145]. The results for longer alkyl side chains show that the ABS formation phenomenon is more complex than initially admitted and that the capacity of the IL to self-aggregate also interferes with phase separation. Self-aggregation does not exist in systems containing ILs with alkyl lengths below hexyl but can occur in aqueous solutions of $[C_{8\text{-}14}C_1im]Cl$ (after the corresponding critical micelle concentration (CMC) values are attained).[193] Still, the authors argued that, if the new trend found for ABS formation above hexyl is dominated by micelle formation, such a trend should continue uninterruptedly up to $[C_{14}C_1im]Cl$ since critical micelle concentrations progressively decrease along the homologous series. [193] Based on these observations, the authors[132] concluded that the complex behaviour of the alkylmethylimidazolium-series is a result of a balance between the two above-mentioned opposite effects: (i) an entropic contribution that decreases the solubility of ILs in water with an increase in the cation alkyl side chain length, and (ii) the inherent aptitude of ILs with longer aliphatic chains to self-aggregate in aqueous media.

Although the effect of the cation alkyl chain length has been largely explored, the effect of the alkyl chain length of the anion has received less attention.[124, 126,145,155] The most complete study was reported by Deive et al. [126], where it was studied the influence of the side chain length of the sulphate anion on ABS formation and their phase behaviour at

298.15 K. In the same line as observed before with cations, ILs with longer aliphatic chains require less inorganic salt to undergo phase splitting. This trend was found to be general and mostly independent of the salt employed (K_3PO_4, K_2CO_3, Na_2CO_3 or $(NH_4)_2SO_4$).[126] Remarkably, the influence of the self-aggregation of ILs with long alkyl chains at the anion is less significant than that observed and discussed before for the IL cation.

The number of alkyl substitutions at the imidazolium core was addressed by Bridges et al.[119], Neves et al.[147], and by Freire et al.[132]. Figure 1.3.4 shows the binodal data for several -based ILs, namely one unsubstituted ([im]Cl), two monosubstituted ([C_1im]Cl and [C_2im]Cl) and one disubstituted ([C_1C_1im]Cl) IL. The unsubstituted and monosubstituted ILs containing systems reveal "atypical" behaviour, and verified for the first time for IL-based ABS, and which is similar to that observed for systems composed of polymers and low molecular weight polysaccharides.[147] The authors[147] pointed out the potential of these novel systems as interesting approaches for product separations since, at a fixed K_3PO_4 concentration, two monophasic and one biphasic regions are present. Although [C_1C_1im]Cl is a structural isomer of [C_2im]Cl, their phase diagrams are quite different. To this end, the alkyl substitution at the imidazolium core seems to have a crucial impact on these low molecular weight ILs.

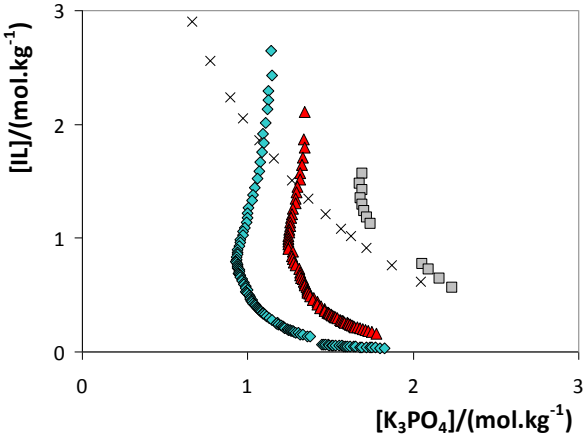

Figure 1.4.5: Ternary phase diagrams for ABS composed of imidazolium-based ILs + K_3PO_4 at 298 K: ■, [im]Cl; ▲, [C_1im]Cl; ♦, [C_2im]Cl; ×, [C_1C_1im]Cl.

Additional data on the number of alkyl substitutions were reported by Bridges et al.[119] and Freire et al.[132] for systems composed of [$C_4C_1C_1$im]Cl and the salts K_3PO_4, K_2HPO_4, K_2CO_3, and KOH. It is well accepted that the substitution of the most acidic hydrogen at C2

by an alkyl group largely reduces the ability of the IL to hydrogen-bond. Nonetheless, the aptitude of this IL to undergo liquid-liquid demixing falls between $[C_4C_1im]Cl$ and $[C_6C_1im]Cl$, behaving like a structural isomer of $[C_5C_1im]Cl$. The authors[132] concluded that these results support the idea that the hydrogen bonding of the IL cation with water is not significant in regards to the phase behaviour of ABS, to the contrary of that for the ILs anions. The researchers proposed that the hydrogen bonding with water is more relevant at the IL-rich phase, whilst the ionic fluid solvation in water is more dependent on the cation size, and, thus, on steric contributions.[132] Similar results were published by Bridges et al.[119] in which small differences were observed for the ABS phase diagrams of $[C_4C_1im]Cl$ and $[C_4C_1C_1im]Cl$ with the inorganic salts K_3PO_4, K_2HPO_4, and K_2CO_3.

Ventura et al.[157] focused on ABS composed of butylmethylpyridinium chloride ILs with the methyl group at the positions C2, C3, and C4, and the mixture of salts K_2HPO_4/KH_2PO_4 (pH=7).The sequence for the increasing ability of phase splitting follows the rank: $[C_4\text{-}2\text{-}C_1py]Cl < [C_4\text{-}3\text{-}C_1py]Cl \approx [C_4\text{-}4\text{-}C_1py]Cl$. The ortho isomer presents a slightly lower ability to undergo liquid-liquid demixing whilst no major differences between the fluid phase behaviour of *meta* and *para* isomers appear. Based on previous results on the mutual solubilities between pyridinium isomers-based ILs and water,[189] the authors called the attention to the weak dependence of the cation to hydrogen-bond with water (at the water-rich phase) and their impact on the ABS formation.[157] Again, these results support the idea that the cation influence on ABS formation is more dependent on the size and steric contributions than on its hydrogen-bonding ability.

The influence of functionalized alkyl side chains at the IL cation has been addressed by the Coutinho group[124,146,147,157] and more recently by Deive et al.[125]. The presence of double bonds, additional aromatic rings, and hydroxyl groups at the side chains of the cation were evaluated. [147] The presence of a hydroxyl group at the longer alkyl side chain of the imidazolium-based IL, $[OHC_2C_1im]Cl$, leads to an evident decrease in the ABS-promoting ability when compared with $[C_2C_1im]Cl$. The presence of a double bound (allyl group) at $[aC_1im]Cl$ also decreases the ability of ABS to form (taking into account that the phase diagram for the analogue $[C_3C_1im]Cl$ should be within $[C_2C_1im]Cl$ and $[C_4C_1im]Cl$). These patterns reflect the introduction of functionalized groups with higher affinity for

water and a higher tendency to hydrogen-bond. Therefore, ILs with functionalized groups enhancing their hydrophilic character are more easily hydrated and are more difficult to separate from aqueous media by the addition of a high charge density salt. Finally, the effect of a benzyl group at $[C_7H_7C_1im]Cl$ does not bring significant changes in the phase diagram behaviour as compared to $[C_7C_1im]Cl$. [132,147] Similar trends on the weak effect of the benzyl group towards the phase diagrams behaviour were found in additional research by Coutinho and co-workers for ABS composed of $[C_7C_1im]Cl$ and $[C_7H_7C_1im]Cl$ and Na_2SO_4,[124] and $[C_7C_1im]Cl$ and $[C_7H_7C_1im]Cl$ and the phosphate buffer solution composed of K_2HPO_4/KH_2PO_4.[157] The data provided by Deive et al.[125] also support this idea for the pair $[C_6C_1im]Cl$ and $[C_7H_7C_1im]Cl$, and the salt Na_2CO_3.

Influence of the Salt in IL + Salt + Water Systems

Amongst the organic salts, one of the most comprehensive studies was reported by Han et al.[135,137], where they found the binodal curves for the phase diagrams constituted by $[C_4C_1im][BF_4]$ + sodium citrate, + sodium tartarate and + sodium acetate, at 298.15 K. The binodal curve trend indicates that the salting-out ability of the sodium-based organic salts follows the order: $Na_3C_6H_5O_7 > Na_2C_4H_4O_6 > NaC_2H_3O_2$. A similar trend has been reported by Shahriari et al.[152] with the same organic salts and one distinct ionic liquid ($[C_4C_1im][CF_3SO_3]$). The increase in the salting-out strength of the salt is a consequence of a decrease in the amount of salt required for the formation of two phases under the same composition of IL. Considering that the salts evaluated share a common cation but different anions, the authors[135] explained the obtained pattern based on the Gibbs free energy of hydration of the constituent ions. Anions with higher valence are better salting-out agents than those with lower one because the latter are more hydrated. Within the organic salts, another work by Han et al.[136] showed that sodium citrate is more effective to induce liquid-liquid demixing as compared to ammonium citrate. The salting-out strength of the salts were explained based on their corresponding Gibbs free energy of hydration ($\triangle G_{hyd}(Na^+)$ = -365 kJ.mol^{-1} and $\triangle G_{hyd}(NH_4^+)$ = -285 kJ.mol^{-1}).[136]

Shahriari et al.[152] published the most complete study on the effect of both inorganic and organic salts toward the liquid-liquid demixing of $[C_4C_1im][CF_3SO_3]$ aqueous mixtures. The results[152] indicate that the salting-out strength of sodium-based salts to induce the

formation of a second aqueous phase follows the rank: $PO_4^{3-} > C_6H_5O_7^{3-} > HPO_4^{2-} \approx CO_3^{2-} > SO_4^{2-} \approx SO_3^{2-} > C_4H_4O_6^{2-} >> H_2PO4^- > OH^- > CH_3CO_2^- \approx HSO_4^- \approx HCO_3^- > Cl^-$. From the collected data[144] it is observed that the salting-out ability in the two series of salts was identical and follows the order: $Mg^{2+} \approx Ni^{2+} \approx Sr^{2+} > Ca^{2+} >> Na^+ > K^+ > Cs^+$.

All published salt effect trends follow the well-known Hofmeister series.[186] This series was initially explained based on the ordering of bulk water and on the ability of the ions to increase or decrease the water structure by a simple hydration phenomenon. Nevertheless, novel mechanisms to explain the salting-in/-out phenomena of ILs have recently been proposed.[187-188] These studies have shown that the salting-out of ILs from aqueous media is driven by an entropic process resulting from the formation of water-ion complexes (causing the dehydration of the solute and the increased surface tension of the cavity). Remarkably, Shahriari et al.[152] used a large compilation of $[C_4C_1im][CF_3SO_3]$–based ABS with conventional salts and found that there is a close correlation between the IL molality necessary for the formation of a given ABS and the molar entropy of hydration of the ions. In addition, the correlation was found to yield a poorer description if the Gibbs free energy of hydration is used.[152]

Influence of the pH in IL + Salt + Water Systems

The use of distinct salts generates different pH values at the co-existing phases of IL-based ABS. The use of ABS with specific pH values (or a limited pH range) can be of crucial importance for extracting vital biomolecules in the biotechnological field, such as proteins. Zafarani-Moattar and Hamzehzadeh[169] demonstrated that a decrease in the pH of the aqueous solution ($[C_4mim]Br$ + potassium citrate-citric acid mixtures) leads to an increase in the area of the monophasic region.[169] Some works[44,141] also shown that ternary phase diagrams of water, $[C_4C_1im]Cl$, and distinct inorganic salts can be readily formed in alkaline aqueous solutions. However, when using acidic or neutral salts, no phase separation has been observed.[141] Thus, both reports[44,141] confirm that besides the salting-in/-out aptitude of the conventional salts, the creation of IL-based ABS largely depends on the pH of the aqueous solutions (that is further related with the inherent speciation of the salts).[195] Yet, later on, other paper[124] provided a critical assessment regarding the formation of IL-based ABS under acidic media. The authors[124] concluded

that, although the Hofmeister series is obeyed and the ability of ILs to create ABS depends on their hydrogen bond basicity values, the pH values of the aqueous solutions are important in determining the number of successful ILs that are capable of undergoing liquid-liquid demixing. When the pH decreases, the number of ILs that are able to suffer phase splitting is largely reduced.

Influence of Temperature in IL + Salt + Water Systems

The influence of temperature on the phase diagram behaviour of IL-based ABS has been assessed by several authors[130,133,134,136,140,145,149,151,154,160-162] for imidazolium-based fluids with the anions $[BF_4]^-$, Br^- and Cl^- combined with distinct salts. The higher the temperature, the higher are the salt and concentrations required for phase separation. Hence, lower temperatures are favourable for the creation of aprotic IL-salt-based ABS. The favourable interactions of hydrophilic ILs with water increase with temperature, enhancing thus their mutual solubilities. Nevertheless, it should be remarked that the intensity of the temperature effect on the phase diagrams depends on the inorganic salt employed.

In typical polymer + inorganic salt systems, an increase in temperature leads to larger immiscibility regions, whilst in polymer-polymer ABS the opposite effect is observed. Moreover, the effect of temperature on the liquid-liquid phase behaviour is more pronounced in polymer-salt-based systems than that verified in IL-based ABS.[151] Although ILs tend to fall into the salting-in regime and can be salted-out by common salts, Sadeghi et al. [151] have observed that water soluble polymers are more easily salted-out by inorganic salts than ILs due to their higher hydrophobic nature, and, thus, the behaviour of their phase diagrams is more dependent on temperature variations.

Ionic Liquid + Amino Acid or Carbohydrate + Water Systems

Some researchers have attempted to find more benign ABS promoters. In this context, amino acids have also been used as phase promoters in the formation of ABS involving hydrophilic ILs.[133,170] Indeed, the substitution of high charge density salts by amino acids (inner charged molecules) can lead to more benign extraction procedures, or less aggressive steps, in the IL recovery from aqueous effluents. Amino acids decrease the

ionic strength of the overall solution and may prevent or minimize the ion exchange between the two phases when compared with the largely explored salt-based ABS. Nevertheless, the number of ILs that are able to form ABS with amino acids is restricted, and only studies with L- Glycine[171], L-Serine[171], L-Proline[129,171] and L-Lysine[129] have been published.

On the other hand, carbohydrates are also a good alternative to common salts. Indeed, the ion exchange among phases can be fully avoided using this type of system whilst falling under the biorefinery concept. The use of carbohydrates to induce IL-based ABS can be visualized as a step towards the usage of a broad spectrum of valuable biocompounds available from biomass. Since carbohydrates are non-toxic and renewable resources, greener processes involving ionic-liquid-based ABS can be immediately envisaged. Some reports regarding this special kind of IL-based ABS have been published.[121-123, 135, 162-164,171] Nevertheless, in the presence of these weaker salting-out agents, the number of ILs that are able to form ABS is limited, and that is the main reason why few ILs have been studied in this context.[121-123, 135, 162-164,171] The proof of principle which demonstrated the ability of carbohydrates to salt-out ILs dates from 2007 and was proposed by Zhang et al.[171].

Ionic Liquid + Polymer + Water Systems

Polymer/polymer ABS usually display two main hydrophobic phases and the difference in polarities mainly depends on the amount of water at each phase. On the other hand, polymer/salt ABS present a hydrophobic phase composed mainly of the polymer and a highly charged and hydrophilic aqueous phase. Therefore, the substitution of a high charge density salt in the second example by an IL will allow for tighter control of the phases' polarities. In addition, further advantages can be associated with the use of ILs in ABS instead of conventional high-melting inorganic salts. Salt crystallization problems can be avoided when employing an IL which melts below room temperature. Even in the case of an IL melting above room temperature, the presence of water will largely prevent its solidification since the saturation levels of ILs in aqueous solutions are usually higher than those observed with common salts. In addition, ILs can optionally be designed to have a

low corrosive character, compared to the highly corrosive aqueous solutions of conventional inorganic salts.

Rebelo and co-workers[174] reported the pioneer work on the salting-in and salting-out effects of ionic liquids through polymers dissolved in aqueous media. Subsequently, other works concerning ABS composed of poly(propylene glycol) (PPG),[175,176] and with PEG)[172,193,194] and ILs have been published.

Ionic Liquid + Inorganic Salt + Polymer + Water Systems

The first example of quaternary systems composed of distinct ILs, one inorganic salt, one polymer, and water was reported in 2010 by Pereira et al.[173]. The goal of this work was to use ILs as additives to control the polarities of the phases of common polymer-inorganic-salt-based ABS. These systems were shown to constitute interesting advances in biotechnological separation processes aiming at replacing the approach of PEG functionalization. [173] Diverse ILs at 5 wt % were added to the systems and their phase behaviours were compared to the ternary system composed of PEG-600 + Na_2SO_4 + water.[173] In some cases, the influence of small amounts of IL was found to be highly helping for tailoring the extraction of model biomolecules.[173] An increase in the cation side alkyl chain length, as well as the presence of more aliphatic chains, reduces the phases' miscibility when compared with the system with no IL. In addition, the presence of a hydroxyl group or a double bond at one of the alkyl chains of the imidazolium cation reduces the ability for phase separation, following their hydrophobicity. However, regarding the cation influence, only $[C_4C_1im]Cl$ and $[C_4C_1C_1im]Cl$ provide a larger immiscibility region when compared with the system with no IL. These results agree well with the work of Rebelo and co-workers[174] for the changes of the fluid phase behaviour of PEG aqueous solutions by the addition of ILs. The authors[174] identified both salting-in and salting-out effects of the IL towards the PEG solubility, while the salting-out was only achieved with imidazolium-based ILs with shorter alkyl chains. Concerning the influence of the IL anion nature, only $[C_4C_1im][HSO_4]$ decreases the demixing locus, whilst $[C_4C_1im]Cl$, $[C_4C_1im][CH_3CO_2]$ and $[C_4C_1im][C_1SO_4]$ increase the ability for phase separation. In summary, the tendency of ILs to induce liquid-liquid demixing closely correlates with that previously shown for ABS of the type IL + inorganic salt + water, and

depends on the hydrogen-bonding ability of the anion.[173] In order to deepen the understanding of the phase behaviour mechanism, the authors determined the partition coefficients of the IL in the PEG-Na_2SO_4-based system. With the exception of the high charge density [im]Cl, the remaining ILs preferentially partition into the PEG-rich phase, while the intensity of their partitioning for the polymeric phase is directly proportional to the salting-in/-out effect they induce regarding their ability to increase (or decrease) the two-phase region.[173]

1.5. Applications of Ionic-Liquid-based ABS

Extractive Approaches

Due to their favourable properties, ABS have been regarded as an economical and efficient downstream processing method, which can be widely used for the recovery and purification of many different solutes.[189-191] The efficient application of ABS for for separation, purification, isolation, or purification of a product, requires the knowledge of the specific mechanism behind the product partitioning between the two aqueous phases. Generally, such mechanisms are complex, commanded mainly by solute–solvent interactions, such as van der Waals, hydrogen-bonding, electrostatic forces and steric and conformational effects. Different net effects of these contributions in each phase allows for the selective partition of the solute into one of the phases.[1] The solute partitioning depends on the properties of the two aqueous phases as well as those of the solute. Achieving successful ABS separation requires the ability to manipulate such phase properties to obtain suitable partition coefficients (and selectivity) for the target solute molecule. Several procedures can be used to manipulate the partition of a target solute, namely: (*i*) controlling the solute affinity for one of the two aqueous phases by using different salts and/or ILs; (*ii*) changing the system composition by manipulating the concentration of salt and/or IL; (*iii*) inserting additional co-solvents, anti-solvents, or amphiphilic structures to the system.

The extractive potential of IL-based ABS for biomolecules was already studied, for instance with testosterone and epitestosterone, alkaloids, antibiotics, bovine serum albumin, insulin, cytochrome C, penicillin G, Y-globulin, L-tryptophan and food colourants,

and where high extraction yields were obtained.[44, 74, 132,147,196-201] The complete extraction and concentration up to 1000-fold were additionally verified with alkaloids and endocrine disruptors.[132,201]

Altough the phase diagrams are usually presented in mol·kg^{-1} units to avoid discrepancies that can result from different molecular weights of the solutes involved in ABS formation, when dealing with extraction purposes, most literature data are presented in terms of weight fraction units, wt %. The extraction results gathered from literature, presented and discussed below, are divided and discussed by three main classes of solutes (those studied in this thesis): alkaloids, amino acids and phenolic compounds.

Alkaloids

The development of methods for alkaloids extraction and further quantitative determination still remains a challenge in doping and drugs control. Nowadays, the two most common methods for sample pre-treatment (containing alkaloids) are liquid-liquid extraction (LLE)[202] and solid-phase extraction (SPE).[203] Although SPE presents good purification and concentration effects, it requires a relatively time-consuming solvent desorption step using traditional volatile organic solvents and pre-treatment processes. LLE also requires the use of toxic volatile organic compounds and the sample recovery is not always adequate. Accordingly, the development of simple and environmentally friendly pre-treatment methods is of great interest.

In 2005, Li et al.[141] suggested a pioneering IL-based ABS ([C_4C_1im]Cl + K_2HPO_4) as a new pre-treatment strategy in the analysis of opium alkaloids from *P. papaveris*. Both phases of the IL-based system are clear and mostly composed of water, facilitating its use for coupling with HPLC (High Performance Liquid Chromatography).

Based on the evidence that no interference with the IL has been observed during the quantification of opium alkaloids using HPLC,[141] Freire and co-workers[132] later showed that the complete extraction of archetypal alkaloids, such as caffeine and nicotine, is possible and can be achieved in a single-step procedure by a proper tailoring of the IL employed in the ABS formulation. The study[132] focused on seventeen different imidazolium-based ILs which yield ABS in the presence of inorganic salt aqueous solutions (water or urine-type samples). Moreover, the presence of a more complex matrix such as

synthetic urine, which includes NaCl and urea, favours the alkaloids partitioning to the IL-rich phase. These results[132] - which can be extended to other bioactive drugs - clearly indicate that new applications of IL-based ABS for analytical purposes can be immediately conceptualized. Compared to conventional LLE and SPE, ABS avoid the use of volatile organic solvents, replacing them with relatively small amounts of recyclable IL solvents in a second aqueous phase.

Aminoacids

The separation of bio-products from bio-reaction media is an important step in biotechnology. Extraction can be applied to first-stage separation or purification processes. Amino acids are a class of useful bio-products for various applications. The conventional separation of amino acids includes ionic exchange, reversed micelle methods,[204] and liquid-membrane extraction processes.[205] Organic solvents are used in the majority of these processes with all their inherent problems, such as high flammability and toxicity to humans and microorganisms. In this context, the partition behaviour of amino acids in ABS is both of academic and practical importance; since amino acid residues determine the surface properties of proteins, further understanding of the driving forces for the partitioning of proteins in a given ABS can be obtained from the study of single amino acids. Furthermore, amino acids are very important bio-products, so their recovery *via* aqueous biphasic extraction from bio-reaction media may represent realistic alternatives to more traditional methods.[206]

IL-based ABS have been successfully applied to the extraction of amino acids.[131,143,147,155,176,181,207] Some of these studies confirmed the potential to control the ABS physicochemical properties by judiciously selecting the IL cations and/or anions, thus enabling the manipulation of the properties of the extraction phases for enhanced product recovery. [143,147,155,181] The extraction aptitude for amino acids of ABS composed of hydrophilic ILs and different salting-out/-in agents, such as inorganic and organic salts, carbohydrates, and PPG 400 was deeply evaluated in literature.[131,143,147,155,176,181,207]

Systematic studies of the extractive potential for amino acids of ABS formed by nineteen hydrophilic imidazolium-based ILs and the inorganic salt K_3PO_4 have been reported in three isolated works.[143,147,155,]The influence of the number of alkyl groups present in the

cation, the cation side alkyl chain length, the presence of double bonds, aromatic rings, and hydroxyl groups on the alkyl side chain, and the influence of a set of different anions, were evaluated. The results demonstrated that the partition coefficient of L-tryptophan (K_{Trp}) in IL-based ABS is considerably higher (up to K_{Trp}=124) than those obtained with conventional PEG-inorganic salt systems (K_{Trp} ≈ 1-7),[208] PEG-polysaccharide systems (K_{Trp} ≈ 1)[209] or with water-immiscible ILs two-phase extractions (K_{Trp} ≈ 0.002-7.8) .[210] Generally, the influence of the imidazolium-based cation on the extraction capacity of ABS is more relevant than the influence of the IL anion.[147,155] The presence of benzyl groups or double bonds in the imidazolium side alkyl chain has been observed to increase the partition coefficients.[147] Regarding the effect of the IL anion on the partition coefficients, it was further found that they closely follow the Hofmeister series.[155]

Louros et al.[181] provided the first report on the evaluation of the extraction capability for amino acids of IL-based ABS with ILs not based on imidazolium cations. In this study,[181] the extraction aptitude for amino acids of the ABS system composed of $[P_{1444}][C_1SO_4]$ and K_3PO_4 was tested using the amino acid L-tryptophan. The values of the partition coefficients obtained (K_{Trp} = 9.00) are larger than those observed with the imidazolium-based IL system with the same anion (K_{Trp} = 4.47),[155] $[C_2C_1im][C_1SO_4]$. In addition, the alkylphosphonium-based ILs are, in general, less dense than water, whereas the imidazolium-based compounds are usually denser than water.[211] This fact can be a plus in product work-up steps for decanting aqueous systems. Furthermore, phosphonium-based fluids have higher thermal stability and no acidic protons, making them more stable under nucleophilic and basic conditions than imidazolium-based ILs.[212]

In the searching for greener salting-out inducing agents, Zafarani-Moattar and Hamzehzadeh[167] have used a citrate-based salt with aqueous solutions of 1-butyl-3-methylimidazolium bromide to form ABS and to extract amino acids. The authors also studied the extraction capability of ABS for five model amino acids: L-Tryptophan (Trp), L-Phenylalanine (Phe), L-Tyrosine (Tyr), L-Leucine (Leu), and L-Valine (Val).[176] Zafarani-Moattar and Hamzehzadeh[176] studied the partition behaviour of amino acids at their isoelectric points, providing an interesting approach to disclosing the effect of their charge and structural/physicochemical properties on the partition coefficient. In general,

the partition coefficients of the amino acids at pH = 6 decrease in the following order: K_{Trp} > K_{Tyr} > K_{Phe} > K_{Leu} > K_{Val}. These results agree with the chemical structure of the amino acids. Trp, Tyr and Phe (aromatic model amino acids) have aromatic π systems that allow them to interact with the aromatic π system in the imidazolium cation. Regarding the aliphatic amino acids, hydrophobicity plays a major role; Leu has a longer hydrocarbon chain (one more $–CH_2$ group) than Val, which makes the smaller amino acid relatively more hydrophilic and originating a smaller affinity towards the hydrophobic IL-rich top phase (K_{Val} < 1). As expected, the affinity of amino acids to the preferred phase rises with the growth of the TLL. The differences in the chemical structure of the amino acids studied allow for the analysis of the effect of the pyrrole ring, -OH and $-CH_2$ groups, and hydrophobicity on their partitioning between the two aqueous phases of ionic-liquid-based ABS. Given that the pyrrole ring and the $–CH_2$ group are hydrophobic, and the –OH group is hydrophilic, it can be concluded that hydrophilic groups decrease, while hydrophobic groups increase, the partitioning of the amino acids into the aqueous IL-rich phase at a given pH.

The authors[176] also found that the solution pH may strongly affect the partitioning of amino acids. The partition coefficient of tryptophan increases in the order: K_{Trp} (pH = 7) > K_{Trp} (pH = 6, the pH close to its isoelectric point) > K_{Trp} (pH = 5). This trend is the result of several factors: (*i*) decreasing the pH leads to an increase of the percentage of phase-forming salt ions with minor valence, diminishing their salting-out power; (*ii*) at lower pH values, the percentage of Trp in its cationic form (more hydrophobic than at its isoelectric point) increases dramatically, which means a lower affinity toward the hydrophobic IL-rich phase; (*iii*) with the increase in the cationic form of Trp, the π···π interactions between the imidazolium cation and the aromatic residue of Trp are weakened, resulting in a decrease in the partitioning of the amino acid to the aqueous IL-rich phase.

Zafarani-Moattar et al.[176] also investigated the partitioning of two essential amino acids, L-tryptophan and L-tyrosine, in $[C_2C_1im]Br$ + PPG-400 aqueous systems. Depending on the TLL, L-tyrosine preferentially migrates either for the polymer-rich phase or the IL-rich phase. On the contrary, L-tryptophan always shows a preferential affinity for the the $[C_2C_1im]Br$-rich phase.[176] Both amino acids have an aromatic π system that makes

possible for them to interact with the imidazolium cation. The preferential migration of L-tryptophan for the imidazolium-rich phase is due to the additional pyrrole ring which further enhance the π···π interactions, while in L-tyrosine the partitioning seems to be governed by the hydrogen-bonding between the –OH group in its side chain and the oxygen atoms contained in the ether groups of the PPG chain. Due to the different behavior displayed by both amino acids the authors further suggested these systems as viable alternatives for the purification of L-tryptophan from its fermentation broth.[176]

Pereira and et al.[173] studied the effect of the addition of various imidazolium-based ILs to conventional PEG/inorganic salt ABS, on the phase behaviour and extraction capability for L-tryptophan. The obtained results[173] indicate that the addition of small amounts of ILs to classical PEG-based ABS could largely control the extraction efficiency of L-tryptophan, which further indicates that the application of ILs as adjuvants to modify the characteristics of the polymer-rich phase could be an interesting alternative to the common approach of PEG functionalization.

Phenolic Compounds

Literature results[124,213,214] indicate that IL-based ABS can be used for the extraction and purification of added-value phenolic compounds, such as vanillin, gallic, vanillic and syringic acids. Despite the variety of applications of phenolic compounds, their recovery and purification by cost-effective and environmental friendly processes is still a major concern.

In a set of imidazolium-based ABS, studied by Cláudio et al.[124], and under all the conditions analysed, vanillin preferentially partitions for the IL-rich phase (partition coefficients larger than 1). The thermodynamic functions of the partitioning process have also been determined based on the temperature dependence of the partition coefficients.[124] The data revealed that the partition of vanillin results from an interplay between enthalpic and entropic contributions where both the IL anion and more complex cations play an essential role.[124]

Both the IL structure and salt nature were evaluated through the extraction of gallic acid using IL-based ABS.[213] For most of the studied systems, the partition coefficients of gallic acid for the IL-rich phase decrease in the following order (according to the employed salt

in the formation of ABS): Na_2SO_4 >> K_2HPO_4/KH_2PO_4 > K_3PO_4.[213] Moroever, both preferentially partitioning for the IL-rich or salt-rich phases was observed.[213] Although K_3PO_4 was the strongest salting-out salt studied by the authors,[213] its efficacy in promoting the migration of the phenolic compound for the more hydrophobic phase (IL-rich) is only marginal. Therefore, the authors pointed out that the pH of the aqueous media plays a major role in the partition behavior observed.[130] Indeed, the authors found that at low acidic pH values, the non-charged form of gallic acid preferentially migrates for the IL-rich phase whereas its conjugate base preferentially partitions to the salt-rich phase.[213] This trend was further supported by the progressive addition of NaOH into a system composed of $[C_4C_1im][CF_3SO_3]$ + Na_2SO_4 aiming at increasing the pH of the aqueous phase. [213]

In literature[215], the use of ILs as additives (at 5 or 10 wt %) in systems composed of PEG and Na_2SO_4 was also investigated for the extraction of vanillic and syringic acids. The addition of 5 wt % of IL leads to extraction efficiencies ranging between 80% and 99%.[215] These data prove the ability of the IL to tune the polarity of the PEG-rich phase and that ILs plays a dominant role in the extraction of phenolic acids in this kind of systems.

1.6. Recovery / Concentration of Hydrophilic Ionic Liquids from Aqueous Solutions

Although IL-based ABS are mostly used in the development and design of extraction processes, their intrinsic nature also provides an effective route for the recovery and/or concentration of hydrophilic ILs from aqueous solutions, as firstly suggested by Gutowski et al.[126]

As the environmental impact of ILs is still an open issue, their removal from water is especially important when dealing with their application on a large scale and in related wastewaters streams. In fact, for the industrial application of these liquids, their recovery and recycling need to be addressed. The potential use of IL-based ABS for the recycling and recovery of hydrophilic ILs has been clearly demonstrated and a summary of the literature regarding this subject is presented in Table 1.6.1.

Table 1.6.1: Ionic-liquid-based ABS reported in the literature for the recycling and recovery of hydrophilic ILs from aqueous solutions.

Ionic Liquid	Salting-out species
$[aC_1im]Cl$	K_2HPO_4[128], K_3PO_4[128], K_2CO_3[128]
$[C_2C_1im][CF_3SO_3]$	$Al_2(SO_4)_3$[146], $AlK(SO_4)_2$[146]
$[C_4C_1im]Cl$	K_3PO_4[118]
$[C_4C_1im][BF_4]$	Na_3PO_4[140], Na_2CO_3[140], Na_2SO_4[140], Na_2HPO_4[140], NaCl[140], sucrose[162,163], glucose[162], xylose[162], fructose[162]
$[C_4C_1im][CF_3SO_3]$	$Al_2(SO_4)_3$[146], $AlK(SO_4)_2$[146], Na_2CO_3[214]
$[C_4C_1im][SCN]$	$Al_2(SO_4)_3$[146]
$[C_4C_1im][tos]$	$Al_2(SO_4)_3$[146]
$[C_4C_1im][N(CN)_2]$	$Al_2(SO_4)_3$[146], Na_2CO_3[214]
$[C_7H_7C_1im][C_2SO_4]$	$Al_2(SO_4)_3$[146]
$[P_{i(444)1}][Tos]$	$Al_2(SO_4)_3$[146]
$[P_{4444}]Br$	$Al_2(SO_4)_3$[146]
$[P_{4444}]Cl$	$Al_2(SO_4)_3$[146]
$[P_{1444}][C_1SO_4]$	$Al_2(SO_4)_3$[146]
$[C_8py][N(CN)_2]$	$Al_2(SO_4)_3$[146], $AlK(SO_4)_2$[146]

Deng and co-workers[128] studied ABS composed of $[aC_1im]Cl$ + salt (K_3PO_4, K_2HPO_4, or K_2CO_3) + water with the aim of recovering the IL from aqueous media. They[128] verified that the recovery efficiency of $[aC_1im]Cl$ increased with the rise of the inorganic salt concentration and that, for the same salt concentration, the recovery efficiencies follow the Hoffmeister series: K_3PO_4 > K_2HPO_4 > K_2CO_3. Li and co-workers[140] also reported that the IL $[C_4C_1im][BF_4]$ can be recovered from aqueous solutions by the addition of distinct "kosmotropic" salts (Na_3PO_4, Na_2CO_3, Na_2SO_4, NaH_2PO_4, or NaCl) aiming at promoting an ABS, and that the maximum recovery efficiency was 98.77 %. These authors[140] also found that a stronger salting-out effect allows for higher recovery efficiency of the IL, and that, for the same amount of salt, the results also agree with the Hofmeister series: Na_3PO_4 > Na_2CO_3 > Na_2SO_4 > NaH_2PO_4 > NaCl.

With the aim of proceeding to more environmentally benign ABS, Neves et al.[146] have recently proposed the use of aluminum-based salts to form ABS for removing and recovering ILs from aqueous media. Aluminum-based salts are actually widely used as coagulants in drinking water treatment processes. Neves et al.[146] studied a large array of ILs (imidazolium-, pyridinium- and phosphonium-based) combined with the inorganic salts

$Al_2(SO_4)_3$ and $AlK(SO_4)_2$. The minimum recovery efficiency found was 96 %, whilst in most of the studied systems recovery efficiencies of 100 % were attained.[146]

In a recent manuscript[214], the regeneration, recycling and reuse of the ILs $[C_4C_1im][CF_3SO_3]$ and $[C_4C_1im][N(CN)_2]$, as phase-forming components of ABS, were also evaluated. The authors[214] proposed a two-step ABS scheme to perform greener IL-recyclable extraction procedures: first the biomolecule of interest is extracted/separated into the IL-rich phase using a Na_2SO_4-based ABS; then, the IL-rich aqueous phase is separated and reused to form a new ABS with Na_2CO_3, where the back-extraction of the compounds of interest is carried out, while regenerating the IL aqueous solution for subsequent reutilization. Extraction efficiency values ranging between 73 % and 99 % were obtained in four sequential partitioning experiments involving gallic acid while allowing the regeneration of 94-95 % of the IL and further reutilization.[214]

All of the studies referred above[128,140,146,214] implemented inorganic salts as salting-out inducing agents, which usually contain highly charged anions (mostly phosphate, sulphate, hydroxide, carbonate, etc.) and which entail further environmental risks given the high concentrations of salt required. The introduction of these types of ions also complicates the recycling, since a small amount of undesirable speciation may occur.[110]

Alternatively, carbohydrates were introduced for the development of sustainable IL-based ABS, since they are non-charged, biodegradable, nontoxic, and a renewable feedstock. Wu and co-workers[162-163] reported that $[aC_1im]Cl$, $[aC_1im]Br$ and $[C_4C_1im][BF_4]$ can be recovered from aqueous solutions by the application of IL + carbohydrates (sucrose, glucose, xylose, fructose) ABS. Although the highest recovery efficiency attained only reached 74 %,[162-163] these studies showed the potential of a more environmentally friendly recovery process which can be further improved by the optimization of a variety of conditions. Nevertheless, we must be aware that on these examples we are adding now a large amount of organic matter to the aqueous medium.

In summary, the ability to control the aqueous miscibility of hydrophilic ILs by implementing salting-out phenomena to induce phase separation is of particular importance for the recovery of ILs from aqueous solutions, overcoming wastewater

contamination issues and further promoting the industrial application of these novel fluids.

1.7. References

1. H. Walter, D.E. Brooks and D. Fisher, Partitioning in Aqueous two-Phase Systems: theory, methods, uses and aplications to Biotechnology, 1985, London Academic Press.
2. B. Zaslavsky, Aqueous Two-Phase Partitioning: Physical Chemistry and Bioanalytical Applications, 1995, Marcel Dekker, New York,
3. A.J. Daugulis, D.B. Axford, B. Ciszek and J.J. Malinowski, Biotechnol Lett, 1994, 16, 637-642.
4. M. Martinez-Aragon, S. Burghoff, E.L.V. Goetheer and A.B. de Haan, Sep. Purif. Technol, 2009, 65, 65-72.
5. P.A.J. Rosa, I.F. Ferreira, A.M. Azevedo and M.R. Aires-Barros, J. Chromatogr. A, 2010, 1217, 2296-2305.
6. P.A.J. Rosa, A.M. Azevedo; S. Sommerfeld, W. Baecker and M.R. Aires-Barros, Biotechnol. Adv. 2011, 29, 559-567.
7. M.D.A. Saldana, C. Zetzl, R.S. Mohamed and G. Brunner, J. Supercrit. Fluids, 2002, 22, 119-127.
8. M.D.A. Saldana, R.S. Mohamed, M.G. Baer and P. Mazzafera, J. Agr. Food Chem., 1999, 47, 3804-3808.
9. M.D.A. Saldana, C. Zetzl, R.S. Mohamed, and G. Brunner, J. Agr. Food Chem., 2002, 50, 4820-4826.
10. S.A.O. Santos, P. Pinto, A.J.D. Silvestre and C.P. Neto, *Ind. Crops Prod.*, 2010, 31, 521-526.
11. C.S.R. Freire, A.J.D. Silvestre, C.P. Neto, J.A.S. Cavaleiro, *Holzforschung*, 2002, 56, 372-379.
12. R.M.A. Domingues, G.D.A. Sousa, C.S.R. Freire, A.J.D. Silvestre and C.P. Neto, *Ind. Crops Prod.*, 2010, 31, 65-70.
13. R. Hatti-Kaul, Aqueous Two-Phase Systems Methods and Protocols, Totowa, New Jersey Humana Press, 2000.
14. M.W. Beijerinck, Zbl. Bakt. II Natur., 1896, 698.
15. M.W. Beijerinck, Kolloid Z. Z. Polym., 1910, 16.
16. P.A. Albertsson, Nature, 1956, 177, 771-774.
17. W. Ostwald and R.H. Hertel, Kolloid-Zeitschrift, 1929, 47, 357-370.
18. W. Ostwald and R.H. Hertel, Kolloid-Zeitschrift, 1929, 47, 258-268.
19. A. Dobry, Bulletin Des Societes Chimiques Belges, 1948, 57, 280-285.
20. A. Dobry and F. Boyerkawenoki, J. Polym. Sci., 1947, 2, 90-100.
21 P.A. Albertsson, Nature, 1958, 182, 709-711.
22. P.A. Albertsson, Biochimica Et Biophysica Acta, 1958, 27, 378-395.
23 R. Gupta, S. Bradoo and R.K. Saxena, Current Sci., 1999, 77, 520-523.
24. P.A. Albertsson, Partitioning of cell particles and macromolecules, 3rd ed. 1986, New York Wiley.
25. P.A. Albertsson and E.J. Nyns, Nature, 1959, 184, 1465-1468.
26. A. Kaul, R.A.M. Pereira, J.A. Asenjo and J.C. Merchuk, Biotechnol. Bioeng., 1995, 48, 246-256.
27. K. Mishima, K. Matsuyama, M. Ezawa, Y. Taruta, S. Takarabe and M. Nagatani, J. Chromatogr. A, 1998, 711, 313-318.
28. A. Venancio, C. Almeida and J.A. Teixeira, J. Chromatogr. A., Biomedical Applications, 1996, 680, 131-136.
29. S.V. Save, V.G. Pangarkar and S.V. Kumar, Biotechnol. Bioeng., 1993, 41, 72-78.
30. J. Ryden and P.A. Albertsson, J. Colloid Interface Sci., 1971, 37, 219-222.
31. J.N. Baskir, T.A. Hatton and U.W. Suter, Biotechnol. Bioeng., 1989, 34, 541-558.

32. P.A. Albertsson, G. Johansson and F. Tjerneld, Separation Processes in Biotechnology 1990, New York Marcel Dekker. 287-327.
33. H. Walter, G. Johansson and D.E. Brooks, Anal. Biochem., 1991, 197, 1-18.
34. F. Tjerneld, S. Berner, A. Cajarville and G. Johansson, Enzyme Microb. Tech, 1986, 8, 417-423.
35. E. Andersson and B. Hahnhagerdal, Enzyme Microb. Tech, 1990, 12, 242-254.
36. H. Walter and G. Johansson, Methods Enzymol. Vol. 228. 1994, London Academic Press.
37. Y. Guan, T.H. Lilley, T.E. Treffry, C.L. Zhou, and P.B. Wilkinson, Enzyme Microb. Tech, 1996, 19, 446-455.
38. A.P.D. Gamse, Liquid - liquid extraction and solid - liquid extraction, 2002, http://www.gunt.de/download/extraction_english.pdf
39. T.M, Takeuchi, C.G. Pereira, M.E.M. Braga, M.R. Maróstica,P.F. Leal and M.A.A Meireles Extracting Bioactive Compounds for Food Products: Theory and Applications, CRC Press 2008, chapter 4.
40. U.S. Food and Drug Administration. Guidance for Industry, http://www.fda.gov/cder/guidance.
41. M. Martínez-Aragon, S. Burghoff, E.L.V. Goetheer and A.B. de Haan, Sep. Purif. Technol., 2009, 65, 65–72.
42. J. Rydberg, C. Musikas, G. R. Choppin, Principles and Practices of Solvent Extraction, 1992, New York, Marcel Dekker, Inc.
43 J.J. Wang, Y.C. Pei, Y. Zhao, and Z.G. Hu, Green Chem., 2005, 7, 196-202.
44. C.Y. He, S.H. Li, H.W. Liu, K. Li, and F. Liu, J. Chromatogr A, 2005, 1082, 143-149.
45. A.E. Visser, R.P. Swatloski, W.M. Reichert, R. Mayton, S. Sheff, A. Wierzbicki, J.H. Davis, and R.D. Rogers, Environ. Sci. Technol., 2002, 36, 2523-2529.
46. P. Wasserscheid and W. Keim, Angew. Chem. Int. Ed., 2000, 39, 3773-3789.
47. N.V. Plechkova and K.R. Seddon, Chem. Soc. Rev., 2008, 37, 123-150.
48. P. Walden, Bulletin de l'Académie Impériale des Sciences de St.-Pétersbourg, 1914, 8, 405-422.
49. C. Graenacher, U.S. Patent 1943176, 1934.
50. F.H. Hurley, U.S. Patent 4446331, 1948.
51. T.P. Wier, Hurley, F.H. U.S. Patent 4446349, 1948.
52. M.J. Earle, J. Esperanca, M.A. Gilea, J.N.C. Lopes, L.P.N. Rebelo, J.W. Magee, K.R. Seddon and J.A. Widegren, Nature, 2006, 439, 831-834.
53. T. Welton, Chem. Rev., 1999, 99, 2071-2083.
54. S. Park and R.J. Kazlauskas, Curr. Opin. Biotechnol., 2003, 14, 432-437.
55. F. van Rantwijk and R.A. Sheldon, Chem. Rev., 2007, 107, 2757-2785.
56. S. Dreyer and U. Kragl, Biotechnol. Bioeng., 2008, 99, 1416-1424.
57. F.Y. Du, X.H. Xiao, X.J. Luo and G.K. Li, Talanta, 2009, 78, 1177-1184.
58. J.D. Holbrey and K.R. Seddon, Clean Technol. Environ. Policy, 1999, 1, 223-236.
59. J. Dupont, R.F. de Souza and P.A.Z. Suarez, Chem. Rev., 2002, 102, 3667-3691.
60. S.G. Cull, J.D. Holbrey, V. Vargas-Mora, K.R. Seddon and G.J. Lye, Biotechnol. Bioeng., 2000, 69, 227-233.
61. F. Zhao, X. Wu, M.K. Wang, Y. Liu, L.X. Gao and S.J. Dong, Anal. Chem., 2004, 76, 4960-4967.
62. J. Ding, T. Welton and D.W. Armstrong, Anal. Chem., 2004, 76, 6819-6822.
63. M. Mank, B. Stahl and G. Boehm, Anal. Chem., 2004, 76, 2938-2950.
64. J.F. Brennecke and E.J. Maginn, Aiche J., 2001, 47, 2384-2389.
65. S.S. Tan and D. R. MacFarlane, Top Curr. Chem., 2010, 290, 311-339.
66. H. Wang, G. Gurau and R. D. Rogers, Chem. Soc. Rev., 2012, 41, 1519-1537.

67. L.C. Tomé, M.G. Freire, L.P.N. Rebelo, A.J.D. Silvestre, C. Pascoal Neto, I.M. Marrucho and C.S. Freire, Green Chem., 2011, 13, 2464-2470.
68. S.P.M. Ventura, C. Neves, M.G. Freire, I.M. Marrucho, J. Oliveira and J.A.P. Coutinho, J. Phys. Chem. B, 2009, 113, 9304-9310.
69. A.E. Visser, R.P. Swatloski, W.M. Reichert, R. Mayton, S. Sheff, A. Wierzbicki, J.H. Davis and R.D. Rogers, Chem. Commun., 2001, 135-136.
70. J.D. Holbrey, A.E. Visser, S.K. Spear, W.M. Reichert, R.P. Swatloski, G.A. Broker and R.D. Rogers, Green Chem., 2003, 5, 129-135.
71. A. Bosmann, L. Datsevich, A. Jess, A. Lauter, C. Schmitz and P. Wasserscheid, Chem. Commun., 2001, 2494-2495.
72. L.C. Branco, J.G. Crespo, C.A.M. Afonso, Angew. Chem. Int. Ed., 2002, 41, 2771-2774.
73. J.G. Huddleston, H.D. Willauer, R.P. Swatloski, A.E. Visser and R.D. Rogers, Chem. Commun., 1998, 1765-1766.
74. H. Zhao, S.Q. Xia and P.S. Ma, J. Chem. Technol. Biotechnol., 2005, 80, 1089-1096.
75 H. Passos, M.G. Freire and J.A.P. Coutinho, Green Chem., DOI: 10.1039/c4gc00236a.
76. S.P.M. Ventura, A.M.M. Gonçalves, F. Gonçalves and J.A.P. Coutinho, Aquat. Toxicol., 2010, 96, 290-297.
77. D.J. Couling, R.J. Bernot, K.M. Docherty, J.K. Dixon and E.J. Maginn, Green Chem., 2006, 8, 82-90.
78. K.M. Docherty and C.F. Kulpa, Green Chem., 2005, 7, 185-189.
79. M.G. Freire, P.J. Carvalho, R.L. Gardas, I.M. Marrucho, L. Santos, and J.A.P. Coutinho, J. Phys. Chem. B, 2008, 112, 1604-1610.
80. M.G. Freire, C. Neves, P.J. Carvalho, R.L. Gardas, A.M. Fernandes, I.M. Marrucho, L. M.N.B.F. Santos and J.A.P. Coutinho, J. Phys. Chem. B, 2007, 111, 13082-13089.
81. J. Ranke, A. Muller, U. Bottin-Weber, F. Stock, S. Stolte, J. Arning, R. Stormann and B. Jastorff, Ecotox. Environ. Safe., 2007, 67, 430-438.
82 K.R. Seddon, A. Stark and M.J. Torres, Pure Appl. Chem., 2000, 72, 2275-2287.
83. M. Petkovic, K.R. Seddon, L.P.N. Rebelo and C.P. Pereira, Chem. Soc. Rev., 2011, 40, 1383-1403.
84. J.G. Huddleston, A.E. Visser, W.M. Reichert, H.D. Willauer, G.A. Broker and R.D. Rogers, Green Chem., 2001, 3, 156-164.
85. D. R. MacFarlane, J. M. Pringle, K. M. Jonansson, S. A. Forsyth and M. Forsyth, Chem. Commun., 2006, 1905-1917.
86. S. V. Dzyba and R. A. Bartsch, Tetrahedron Lett., 2002, 43, 4657-4659.
87. Y. Fukaya, A. Sugimoto and H. Ohno, Biomacromol., 2006, 7, 3295-3297.
88. R.M. Lau, M.J. Sorgedrager, G. Carrea, F.V. Rantwijk, F. Secundo and R. A. Sheldon, Green Chem., 2004, 6, 483-487;
89. L. Crowhurst, R. Falcone, N.L. Lancaste, V.L. Mestre and T. Welton, J. Org. Chem., 2006, 71, 8847-8853;
90. L. Crowhurst, M.L. Lancaster, J.M.P. Arlandis and T. Welton, J. Am. Chem. Soc., 2004, 126, 11549-11555.
91. Reichardt, C., Green Chem., 2005, 7, 339-351.
92. M.J. Kamlet and R. W. Taft, J. Am. Chem. Soc., 1976, 98, 377-383.
93. M.J. Kamlet and R. W. Taft, J. Am. Chem. Soc., 1976, 98, 2886-2894.
94. M.J. Kamlet, J.L. Abboud and R.W. Taft, J. Am. Chem. Soc., 1977, 99, 6027-6038.
95. M.J. Kamlet, J.L. Abboud, M.H. Abraham and R.W. Taft, J. Org. Chem., 1983, 48, 2877-2887.
96. R. Lungwitz and S. Spange, New J. Chem., 2008, 32, 392-394.
97. R. Lungwitz, V. Strehmel and S. Spange, New J. Chem., 2010, 34, 1135-1140.

98. M.A. Ab Rani, A. Brant, L. Crowhurst, A. Dolan, M. Lui, N.H. Hassan, J.P. Hallett, P.A. Hunt, H. Niedermeyer, J.M. Perez-Arlandis, M. Schrems, T. Welton and R. Wilding, Phys. Chem. Chem. Phys., 2011, 13, 16831-16840.
99. L. Crowhurst, P.R. Mawdsley, J.M. Perez-Arlandis, P.A. Salter and T. Welton, Phys. Chem. Chem. Phys., 2003, 5, 2790-2794.
100. C. Chiappe and D. Pieraccini, J. Phys. Org. Chem., 2005, 18, 275-297.
101. C. Chiappe, C. S. Pomelli and S. Rajamani, J. Phys. Chem. B, 2011, 115, 9653-9661.
102. Y. Marcus, Chem. Soc. Rev., 1993, 22, 409-416.
103. S. Spange, E. Vilsmeier, K. Fischer, A. Reuter, S. Prause, Y. Zimmermann Ch. Schmidt, Macromol. Rapid Commun., 2000, 21, 643-659.
104. S.N. Baker, G.A. Baker and F.V. Bright, Green Chem., 2002, 4, 165-169.
105. B.R. Mellein, S.N.V.K. Aki, R.L. Ladewski and J. F. Brennecke, J. Phys. Chem. B, 2007, 111, 131-138;
106. S. Trivedi, N.I. Malek, K. Behera and S. Pandey, J. Phys. Chem. B, 2010, 114, 8118-8125.
107. P.G. Jessop, D.A. Jessop, D. Fu and P. Lam, Green Chem., 2012, 14, 1245-1259.
108. C. Chiappe and D. Pieraccini, J. Phys. Chem. A, 2006, 110, 4937-4941.
109. Y. Wu, T. Sasaki, K. Kazushi, T. Seo and K. Sakurai, J. Phys. Chem. B, 2008, 112, 7530-7536.
110. R. Lungwitz, M. Friedrich, W. Linert and S. Spange, New J. Chem., 2008, 32, 1493-1499.
111. U. Mayer, V. Gutmann and W. Gerger, Monatsh. Chem., 1975, 106, 1235-1257.
112. M. Schmeisser, P. Illner, R. Puchta, A. Zahl and R. van Eldik, Chem. Eur. J., 2012, 18, 10969-10982.
113. Y. Marcus, J. Solution Chem., 1984, 13, 599-624.
114. Y. Marcus, Chem. Soc. Rev., 1993, 22, 409-416.
115. H. Niedermeyer, C. Ashworth, A. Brandt, T. Welton and P. A. Hunt, Phys. Chem. Chem. Phys., 2013, 15, 11566-11578.
116. A. F. M. Cláudio, L. Swift, J. P. Hallett, T. Welton, J. A. P. Coutinho and Mara G. Freire, J. Phys. Chem. Chem. Phys, 2014, 16, 6593–6601.
117. S. Park and R. Kazlauskas, J. Curr. Opin. Biotechnol., 14, 2003, 432-437.
118. K.E. Gutowski, G.A. Broker, H.D. Willauer, J.G. Huddleston, R.P. Swatloski, J.D. Holbrey, and R.D. Rogers, J. Am. Chem. Soc., 2003, 125, 6632-6633.
119. N.J. Bridges, K.E. Gutowski and R.D. Rogers, Green Chem., 2007, 9, 177-183.
120. Q. Cao, L. Quan, C.Y. He, N. Li, K. Li and F. Liu, Talanta, 2008, 77, 160-165.
121. Y.H. Chen, Y.S. Meng, S.M. Zhang, Y. Zhang, X.W. Liu and J. Yang, J. Chem. Eng. Data, 2010, 55, 3612-3616.
122. Y.H. Chen, Y.G. Wang, Q.Y. Cheng, X.L. Liu and S.J. Zhang, J. Chem. Thermodyn., 2009, 41, 1056-1059.
123. Y.H. Chen and S.J. Zhang, J. Chem. Eng. Data, 2010, 55, 278-282.
124. A.F.M. Claudio, A.M. Ferreira, S. Shahriari, M.G. Freire and J.A.P. Coutinho, J. Phys. Chem. B, 2011, 115, 11145-11153.
125. F.J. Deive, M.A. Rivas, and A. Rodriguez, J. Chem. Thermodyn., 2011, 43, 1153-1158.
126. F.J. Deive, A. Rodriguez, I.M. Marrucho and L.P.N. Rebelo, J. Chem. Thermodyn., 2011, 43, 1565-1572.
127. Y.F. Deng, J. Chen and D.L. Zhang, J. Chem. Eng. Data, 2007, 52, 1332-1335.
128. Y.F. Deng, T. Long, D.L. Zhang, J. Chen and S.C. Gan, J. Chem. Eng. Data, 2009, 54, 2470-2473.
129. M. Dominguez-Perez, L.I.N. Tome, M.G. Freire, I.M. Marrucho, O. Cabeza and J.A.P. Coutinho, Sep. Purif. Technol., 2010, 72, 85-91.
130. Z. Du, Y.L. Yu and J.H. Wang, Chem. Eur. J., 2007, 13, 2130-2137.
131. M.G. Freire, C.L.S. Louros, L.P.N. Rebelo and J.A.P. Coutinho, Green Chem., 2011, 13, 1536-1545.

132. M.G. Freire, C.M.S.S. Neves, J.N.C. Lopes, I.M. Marrucho, J.A.P. Coutinho and L.P.N. Rebelo, J. Phys. Chem. B, 2012, 116, 7660-7668.
133. J. Han, Y. Wang, W.B. Kang, C.X. Li, Y.S. Yan, J.M. Pan and X.Q. Xie, Microchim. Acta, 2010, 169, 15-22.
134. J. Han, Y. Wang, Y.F. Li, C.L. Yu and Y.S. Yan, J. Chem. Eng. Data, 2011, 56, 3679-3687.
135. J. Han, C. Yu, Y. Wang, X. Xie, Y. Yan, G. Yin and W. Guan, Fluid Phase Equilib., 2010, 295, 98-103.
136. J.A. Han, R. Pan, X.Q. Xie, Y. Wang, Y.S. Yan, G.W. Yin and W.X. Guan, J. Chem. Eng. Data, 2010, 55, 3749-3754.
137. J.A. Han, Y. Wang, C.L. Yu, Y.S. Yan and X.Q. Xie, Anal. Bioanal. Chem., 2011, 399, 1295-1304.
138. Y. Jiang, H. Xia, J. Yu, C. Guo and H. Liu, Chem. Eng. J., 2009, 147, 22-26.
139. Y.Y. Jiang, H.S. Xia, C. Guo, I. Mahmood and H.Z. Liu, Ind. Eng. Chem. Res., 2007, 46, 6303-6312.
140. C.X. Li, J. Han, Y. Wang, Y.S. Yan, J.M. Pan, X.H. Xu and Z.L. Zhang, J. Chem. Eng. Data, 2010, 55, 1087-1092.
141. S.H. Li, C.Y. He, H.W. Liu, K. Li and F. Liu, J. Chromatogr. B, 2005, 826, 58-62.
142. S.H. Li, C.Y. He, H.W. Liu, K.A. Li and F. Liu, Chin. Chem. Lett., 2005, 16, 1074-1076.
143. Z.Y. Li, Y.C. Pei, L. Liu and J.J. Wang, J. Chem. Thermodyn, 2010, 42, 932-937.
144. Y. Lu, W. Lu, W. Wang, Q. Guo and Y. Yang, Talanta, 2011, 85, 1621-1626.
145. V. Najdanovic-Visak, J.N.C. Lopes, Z.P. Visak, J. Trindade and L.P.N. Rebelo, Int. J. Mol. Sci., 2007, 8, 736-748.
146. C.M.S.S. Neves, M.G. Freire and J.A.P. Coutinho, RSC Advances, 2012, 2, 10882-10890.
147. C.M.S.S. Neves, S.P.M. Ventura, M.G. Freire, I.M. Marrucho and J.A.P. Coutinho, J. Phys. Chem. B, 2009, 113, 5194-5199.
148. Y.C. Pei, Z.Y. Li, L. Liu, J.J. Wang and H.Y. Wang, Sci. China Chem., 2010, 53, 1554-1560.
149. Y.C. Pei, J.J. Wang, L. Liu, K. Wu and Y. Zhao, J. Chem. Eng. Data, 2007, 52, 2026-2031.
150. Y.C. Pei, J.J. Wang, K. Wu, X.P. Xuan and X.J. Lu, Sep. Purif. Technol., 2009, 64, 288-295.
151. R. Sadeghi, R. Golabiazar and H. Shekaari, J. Chem. Thermodynamics, 2010, 42, 441-453.
152. S. Shahriari, C.M.S.S. Neves, M.G. Freire and J.A.P. Coutinho, J. Phys. Chem. B, 2012, 116, 7252–7258.
153. K. Shill, S. Padmanabhan, Q. Xin, J.M. Prausnitz, D.S. Clark and H.W. Blanch, Biotechnol. Bioeng., 2011, 108, 511-520.
154. J.R. Trindade, Z.P. Visak, M. Blesic, I.M. Marrucho, J.A.P. Coutinho, J.N.C. Lopes and L.P.N. Rebelo, J. Phys. Chem. B, 2007, 111, 4737-4741.
155. S.P.M. Ventura, C.M.S.S. Neves, M.G. Freire, I.M. Marrucho, J. Oliveira and J.A.P. Coutinho, J. Phys. Chem. B, 2009, 113, 9304-9310.
156. S.P.M. Ventura, S.G. Sousa, M.G. Freire, L.S. Serafim, A.S. Lima and J.A.P. Coutinho, J. Chromatogr. B, 2011, 879, 2679-2687.
157. S.P.M. Ventura, S.G. Sousa, L.S. Serafim, A.S. Lima, M.G. Freire and J.A.P. Coutinho, J. Chem. Eng. Data, 2011, 56, 4253-4260.
158. S.P.M. Ventura, S.G. Sousa, L.S. Serafim, A.S. Lima, M.G. Freire and J.A.P. Coutinho, J. Chem. Eng. Data, 2012, 57, 507-512.
159. Y. Wang, J.A. Han, X.Q. Xie and C.X. Li, Cent. Eur. J. Chem., 2010, 8, 1185-1191.
160. Y. Wang, X.H. Xu, Y.S. Yan, J. Han and Z.L. Zhang, Thermochim. Acta, 2010, 501, 112-118.
161. X.L. Wei, Z.B. Wei, X.H. Wang, Z.N. Wang, D.Z. Sun, J. Liu and H.H. Zhao, Soft Matter, 2011, 7, 5200-5207.
162. B. Wu, Y.M. Zhang and H.P. Wang, J. Phys. Chem. B, 2008, 112, 6426-6429.
163. B. Wu, Y.M. Zhang and H.P. Wang, J. Chem. Eng. Data, 2008, 53, 983-985.
164. B. Wu, Y.M. Zhang, H.P. Wang and L.L. Yang, J. Phys. Chem. B, 2008, 112, 13163-13165.

165. C. Yu, J. Han, S. Hu, Y. Yan and Y. Li, J. Chem. Eng. Data, 2011, 56, 3577-3584.
166. M.T. Zafarani-Moattar and S. Hamzehzadeh, J. Chem. Eng. Data, 2007, 52, 1686-1692.
167. M.T. Zafarani-Moattar and S. Hamzehzadeh, J. Chem. Eng. Data, 2009, 54, 833-841.
168. M.T. Zafarani-Moattar and S. Hamzehzadeh, J. Chem. Eng. Data, 2010, 55, 1598-1610.
169. M.T. Zafarani-Moattar and S. Hamzehzadeh, Fluid Phase Equilib., 2011, 304, 110-120.
170. J.M. Zhang, Y.Q. Zhang, Y.H. Chen and S.J. Zhang, J. Chem. Eng. Data, 2007, 52, 2488-2490.
171. Y.Q. Zhang, S.J. Zhang, Y.H. Chen and J.M. Zhang, Fluid Phase Equilib., 2007, 257, 173-176.
172. M.G. Freire, J.F.B. Pereira, M. Francisco, H. Rodríguez, L.P.N. Rebelo, R.D. Rogers and J.A.P. Coutinho, Chem. Eur. J., 2012, 18, 1831–1839.
173. J.F.B. Pereira, A.S. Lima, M.G. Freire and J.A.P. Coutinho, Green Chem., 2010, 12, 1661-1669.
174. Z.P. Visak, J.N.C. Lopes and L.P.N. Rebelo, Monatsh. Chem., 2007, 138, 1153-1157.
175. C.Z. Wu, J.J. Wang, Y.C. Pei, H.Y. Wang and Z.Y. Li, J. Chem. Eng. Data, 2010, 55, 5004-5008.
176. M.T. Zafarani-Moattar, S. Hamzehzadeh and S. Nasiri, Biotechnol. Prog., 2012, 28, 146-156.
177. M.J. Earle, J. Esperanca, M.A. Gilea, J.N.C. Lopes, L.P.N. Rebelo, J.W. Magee, K.R. Seddon, and J.A. Widegren, Nature, 2006, 439, 831-834.
178. J.M.S.S. Esperanca, J.N. Canongia Lopes, M. Tariq, L.M.N.B.F. Santos, J.W. Magee and L.P.N. Rebelo, J. Chem. Eng. Data, 2010, 55, 3-12.
179. K.R. Seddon, Nat. Mater., 2003, 2, 363-365.
180. A.F.M. Claudio, M.G. Freire, C.S.R. Freire, A.J.D. Silvestre and J.A.P. Coutinho, Sep. Purif. Technol., 2010, 75, 39-47.
181. C.L.S. Louros, A.F.M. Cláudio, C.M.S.S. Neves, M.G. Freire, I.M. Marrucho, J. Pauly, and J.A.P. Coutinho, Int. J. Mol. Sci., 2010, 11, 1777-1791.
182. M.G. Freire, C.M.S.S. Neves, I.M. Marrucho, J.A.P. Coutinho and A.M. Fernandes, J. Phys. Chem. A, 2010, 114, 3744-3749.
183. K.M. Docherty and C.F. Kulpa, Green Chem., 2005, 7, 185-189.
184. J. Ranke, A. Mueller, U. Bottin-Weber, F. Stock, S. Stolte, J. Arning, R. Stoermann and B. Jastorff, Ecotoxicol. Environ. Saf., 2007, 67, 430-438.
185. http://www.il-eco.uft.uni-bremen.de
186. Hofmeister, F. Arch. Exp. Pathol. Pharmakol. 1888, XXV, 1.
187. M.G. Freire, C.M.S.S. Neves, A.M.S. Silva, L.M.N.B.F. Santos, I.M. Marrucho, L.P.N. Rebelo, J.K. Shah, E.J. Maginn and J.A.P. Coutinho, J. Phys. Chem. B, 2010, 114, 2004-2014.
188. L.I.N. Tome, F.R. Varanda, M.G. Freire, I.M. Marrucho and J.A.P. Coutinho, J. Phys. Chem. B, 2009, 113, 2815-2825.
189. M.G. Freire, C.M.S.S. Neves, K. Shimizu, C.E.S. Bernardes, I.M. Marrucho, J.A.P. Coutinho, J.N. Canongia Lopes and L.P.N. Rebelo, J. Phys. Chem. B, 2010, 114, 15925-15934.
190. M.G. Freire, C.M.S.S. Neves, S.P.M. Ventura, M.J. Pratas, I.M. Marrucho, J. Oliveira, J.A.P. Coutinho and A.M. Fernandes, Fluid Phase Equilib., 2010, 294, 234-240.
191. M.G. Freire, P.J. Carvalho, R.L. Gardas, I.M. Marrucho, L.M.N.B.F. Santos and J.A.P. Coutinho, J. Phys. Chem. B, 2008, 112, 1604-1610.
192. M.G. Freire, C.M.S.S. Neves, P.J. Carvalho, R.L. Gardas, A.M. Fernandes, I.M. Marrucho, L.M.N.B.F. Santos and J.A.P. Coutinho, J. Phys. Chem. B, 2007, 111, 13082-13089.
193. M. Blesic, M.H. Marques, N.V. Plechkova, K.R. Seddon, L.P.N. Rebelo and A. Lopes, Green Chem., 2007, 9, 481-490.
194. J.F.B. Pereira, K.A. Kurnia, O.A.Cojocaru, G. Gurau, L. P. N. Rebelo, R. D. Rogers, Mara G. Freire, J. A. P. Coutinho, Phys. Chem. Chem. Phys., 2014, 16, 5723-5731.
195. K. A. Kurnia, M. G. Freire and J.A.P. Coutinho, J. Phys. Chem. B, 2014, 118, 297–308.
196. S.H. Li, C.Y. He, H.W. Liu, K. Li and F. Liu, J. Chromatogr. B, 2005, 826, 58-62.

197. Q.F. Liu, J. Yu, W.L. Li, X.S. Hu, H.S. Xia, H.Z. Liu and P. Yang, Sep. Sci Technol, 2006, 41, 2849-2858.
198. H. Passos, A.R. Ferreira, A.F.M. Claudio, J.A.P. Coutinho and M.G. Freire, Biochem. Eng. J., 2012, 67, 68-76.
199. Y.C. Pei, J.J. Wang, K. Wu, X.P. Xuan and X.J. Lu, Sep. Purif. Technol., 2009, 64, 288-295.
200. A. Soto, A. Arce and M.K. Khoshkbarchi, Sep. Purif. Technol., 2005, 44, 242-246.
201. H. Passos, A.C.A. Sousa, M. Ramiro Pastorinho, A.J.A. Nogueira, L.P.N. Rebelo, J.A.P. Coutinho and M.G. Freire, Anal. Method, 2012, 4, 2664-2667.
202. A. B. Wey and W. Thormann, J. Chromatogr., A, 2001, 916, 225–238.
203. M.M. Churley, T.P. Lyons, P.V. Robandt and M.R. Bruins, J. Anal. Toxicol., 2003, 27, 530–532.
204. M. Adachi, M. Harada, A. Shioi and Y Sato, J. Phys. Chem., 1991, 95, 7925-7931.
205 H. Itoh, M.P. Thien, T.A. Hatton and D. I. C. Wang, Biotechnol. Bioeng., 1900, 35, 853-860.
206. R. Hatti-Kaul, Mol. Biotechnol., 2001, 19, 269–277.
207. M.T. Zafarani-Moattar and S. Hamzehzadeh, Biotechnol. Prog., 2011, 27, 986-997.
208. A. Salabat, M.H. Abnosi, A. Motahari, J. Chem. Eng. Data,2008, 53, 2018-2021
209. M. Lu, F. Tjerneld, J. Chromatogr. A, 1997, 766, 99-108.
210. L.I.N. Tomé, V.R. Catambas, A.R.R. Teles, M.G. Freire, I.M. Marrucho and J.A.P. Coutinho, *Sep. Purif.Technol.*, 2010, *72*, 167-173.
211. C.M.S.S. Neves, P.J. Carvalho, M.G. Freire and J.A.P. Coutinho, J. Chem. Thermodyn., 2011, 43, 948–957.
212. F. Atefi, M. T. Garcia, R. D. Singer and P. J. Scammells, Green Chem., 2009, 11, 1595–1604.
213. A.F.M. Cláudio; A.M. Ferreira, C.S.R. Freire, A.J. D. Silvestre, M.G. Freire and J.A.P. Coutinho, Sep Purif. Technol., 2012, 97, 142–149.
214. A.F.M. Cláudio, C.F.C. Marques, I. Boal-Palheiros, M.G. Freire and J.A.P. Coutinho, Green Chem., 2014, 16, 259–268.
215. M.R. Almeida, H. Passos, M.M. Pereira, A.S. Lima, J.A.P. Coutinho and M.G. Freire, Sep. Purif. Technol.,2014, 128, 1–10.

2. Extractions using ABS and their Characterization

2.1. A Critical Assessment on the Formation of Ionic-Liquid-Based Aqueous Biphasic Systems in Acidic Media

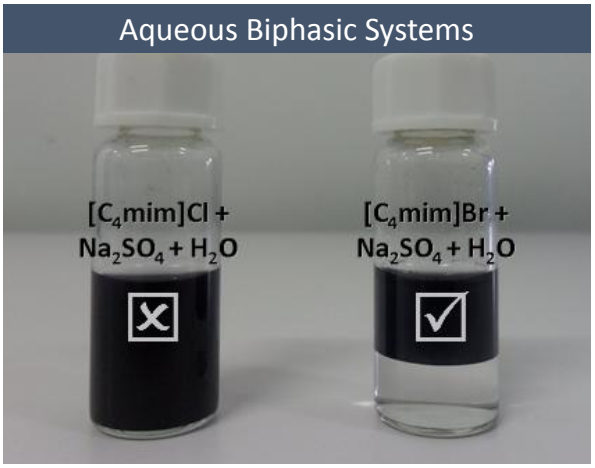

This chapter is based on the published manuscript: Cláudio, A. F. M.; Ferreira, A. M.; Shahriari, S., Freire, M. G. and Coutinho, J. A. P., A Critical Assessment on the Formation of Ionic-Liquid-Based Aqueous Two-Phase Systems in Acidic Media, J. Phys. Chem. B , 2011, 115, 11145-11153.

Abstract

In this work, the ability of Na_2SO_4 and ionic liquids (ILs) to induce the formation of acidic ABS is investigated. Ternary phase diagrams, tie-lines, and tie-line lengths for several systems were determined and reported at 298 K and atmospheric pressure. It is here shown that among the ILs studied only those containing long alkyl side chains at the ions and/or anions with low hydrogen bond basicity are capable of undergoing liquid-liquid demixing in the presence of Na_2SO_4 aqueous solutions. The results obtained indicate that besides the salting-out ability of the inorganic salt, the pH of the aqueous solution plays a crucial role towards the formation of IL-based ABS. In acidic media the range of ILs that are able to undergo ABS formation is substantially reduced when compared to alkaline aqueous salt solutions. The use of inorganic salts and ILs to promote acidic ABS is envisaged as particularly valuable in the extraction of compounds that exhibit low acid dissociation constants.

Introduction

Gutowski et al.[1] were the first to show that imidazolium-based ionic liquids (ILs) can form ABS in the presence of aqueous solutions of K_3PO_4, representing thus a step forward into the replacement of the conventional ABS based on polymer/polymer and polymer/salt mixtures. The authors[1] additionally indicated that 1-butyl-3-methylimidazolium chloride, $[C_4mim]Cl$, can form ABS with distinct "kosmotropic" salts, namely, KOH, K_2CO_3, Na_2HPO_4, and $Na_2S_2O_3$, while 1,3-dialkylimidazolium triflate- and tetrafluoroborate-based ILs form ABS with $CaCl_2$ and NaCl. Hence, adequate inorganic salts can salt-out hydrophilic ILs from aqueous solutions resulting in the formation of ABS. This observation has lead, in the past few years, to the exploration of IL-based ABS as novel extractive systems since a tailoring of the phases polarities could be achieved.[2-12] Most works have, however, been dealing with alkaline aqueous solutions, whereas the formation of IL-based ABS through the use

of neutral or acidic inorganic salts solutions is either contested or poorly understood. Nonetheless, the use of acidic aqueous solutions could be highly relevant in the extraction of biomolecules with low acid dissociation constants.

Phase diagrams containing several imidazolium-based ILs and distinct alkaline aqueous solutions of salts, namely, KOH, K_2HPO_4, K_2CO_3, and K_3PO_4 were described in literature.[6,9,13-19] Bridges et al.[19] reported ternary phase diagrams for imidazolium-, pyridinium-, ammonium-, and phosphonium-based chloride ILs, water, and K_3PO_4, K_2HPO_4, K_2CO_3, KOH, and $(NH_4)_2SO_4$. In this study[19], the only system capable of promoting ABS with the slightly acidic aqueous solution of $(NH_4)_2SO_4$ was the ammonium-based IL. Sadeghi et al.[20] studied the salting-out effect in aqueous solutions of 1-butyl-3-methylimidazolium bromide with trisodium citrate. Wang et al.[21] published experimental data on ABS formed by 1-butyl-3-methylimidazolium terafluoroborate ($[C_4mim][BF_4]$) and Na_2CO_3, $(NH_4)_2SO_4$, NaH_2PO_4, $MgSO_4$, Na_2SO_3, and NaOH. The authors[21] also postulated the inability of Na_3PO_4, Na_2HPO_4, K_2HPO_4, NH_4Cl, $NaCH_3CO_2$, $NaNO_3$, NaCl, and KCl to induce the phase separation of the tetrafluoroborate-based IL. Subsequently, Li et al.[22] showed that it was possible to promote ABS with aqueous solutions of $[C_4mim][BF_4]$ and Na_2CO_3, Na_3PO_4, Na_2SO_4, NaH_2PO_4, and NaCl. Curiously, contradictory results were found between the two research groups[21-22] for the formation of ABS composed of $[C_4mim][BF_4]$ and the inorganic salts Na_3PO_4 and NaCl.

The effect of inorganic salts on IL-based ABS formation has been widely studied,[1,3,4,19] and it was demonstrated that they typically follow the Hofmeister series (classification of ions based on their salting-out/-in aptitude).[23] Nevertheless, most of the inorganic salts studied present an alkaline or almost neutral character in aqueous solution.[1,5,6,13-21] Attempting at manipulating the pH values of IL-based ABS, He et al.[3] showed that systems containing 1-butyl-3-methylimidazolium chloride ($[C_4mim]Cl$) can undergo phase separation by the addition of appropriate amounts of diverse alkaline aqueous salt solutions, such as K_2HPO_4, K_3PO_4, K_2CO_3, KOH, Na_2HPO_4 and NaOH. However, when acidic to neutral salt solutions, namely KH_2PO_4, K_2SO_4, $(NH_4)_2SO_4$, KCl or NaCl, were added, the formation of IL-based ABS was not observed.[3] In the same line of investigation, Li et al.[4] reported ternary phase diagrams between water, $[C_4mim]Cl$, and distinct inorganic salts.

The authors[4] have exposed that ABS with [C_4mim]Cl can be formed by the adequate addition of alkaline aqueous solutions of the following salts: K_3PO_4, KOH, K_2HPO_4, NaOH, K_2CO_3, and Na_2HPO_4. Nevertheless, when using acidic or neutral salts, such as KH_2PO_4, $(NH_4)_2SO_4$, NaCl or KCl, no phase separation of the IL-rich phase was observed.[4] These reports[3,4] confirm that besides the salting-in/-out aptitude of the inorganic salts (Hofmeister series rank), the creation of IL-based ABS is strongly dependent on the pH of the aqueous solutions. For instance, if SO_4^{2-} is a stronger salting-out anion than HPO_4^{2-} or OH^-, ABS making use of sulfate-based salts should be more easily formed. In fact, this was not verified[3,4], meaning that the IL-based ABS formation capability largely depends on the aqueous medium pH induced by the inorganic salt.

Although previous works[3,4] have demonstrated the inability of acidic and neutral aqueous solutions to form IL-based ABS they have only focused on the [C_4mim]Cl. The ability of ILs to be tailored for specific applications suggests that adequate compounds, capable of undergoing liquid-liquid demixing in aqueous solutions, can be found - if the molecular interactions at the basis of the demixing phenomenon are correctly understood. The results gathered in previous works by our group indicate that for the formation of ABS with weaker salting-out agents, such as carbohydrates[24] or aminoacids,[25] more hydrophobic, yet water soluble ILs, must be employed. Such ILs are here defined as those fluids composed of long alkyl side chain lengths and/or anions with low hydrogen bond basicity values,[6,9] namely $[N(CN)_2]^-$, $[CF_3SO_3]^-$, and $[BF_4]^-$. Although it was previously[19] shown that [C_4mim][BF_4] is capable of forming ABS in the presence of sulfate-based salts this ionic liquid is not water stable and particular care should be taken when using these solutions for extraction purposes.[26] [BF_4]-based ILs suffer hydrolysis in contact with water, releasing fluoridric acid even at room temperature.[26]

In this work, the ability of Na_2SO_4 (with a pH value *circa* 7 in aqueous solution) for the formation of IL-based ABS is presented and discussed. For such a purpose, novel ternary phase diagrams composed of different water-stable ILs, water, and Na_2SO_4, at 298 K and atmospheric pressure, were determined. A large array of ILs was explored and it was verified that a proper selection of their structural features can lead to the liquid-liquid demixing, and to different pH values at their co-existing phases. Most of the investigated

ILs were shown to produce acidic aqueous systems. Finally, a close relation between the ILs aptitude to create ABS and their hydrogen bond basicity values is presented. This close pattern is shown to provide an *a priori* qualitative method to identify ILs that are capable of forming ABS with Na_2SO_4 (if hydrogen bond basicity values are previously known).

Experimental Section

Materials

The ILs used in this work to study the formation of acidic ABS were the following: 1-ethyl-3-methylimidazolium methylsulfate, [C_2mim][CH_3SO_4]; 1-ethyl-3-methylimidazolium trifluoromethanesulfonate, [C_2mim][CF_3SO_3]; 1-butyl-3-methylimidazolium chloride, [C_4mim]Cl; 1-hexyl-3-methylimidazolium chloride, [C_6mim]Cl; 1-heptyl-3-methylimidazolium chloride, [C_7mim]Cl; 1-butyl-3-methylimidazolium bromide, [C_4mim]Br; 1-butyl-3-methylimidazolium acetate, [C_4mim][CH_3CO_2]; 1-butyl-3-methylimidazolium methylsulfate, [C_4mim][CH_3SO_4]; 1-butyl-3-methylimidazolium ethylsulfate, [C_4mim][$C_2H_5SO_4$]; 1-butyl-3-methyl-imidazolium trifluoromethanesulfonate, [C_4mim][CF_3SO_3]; 1-butyl-3-methylimidazolium dicyanamide, [C_4mim][$N(CN)_2$]; 1-butyl-3-methylimidazolium hydrogenosulfate, [C_4mim][HSO_4]; 1-butyl-3-methylimidazolium tosylate, [C_4mim][TOS]; 1-butyl-3-methylimidazolium dimethylphosphate, [C_4mim][DMP]; 1-butyl-3-methylimidazolium trifluoroacetate, [C_4mim][CF_3CO_2]; 1-butyl-3-methylimidazolium octylsulfate, [C_4mim][OctylSO_4]; 1-butyl-3-methylimidazolium thiocyanate, [C_4mim][SCN]; 1-benzyl-3-methylimidazolium chloride, [C_7H_7mim]Cl; 1-benzyl-3-methylimidazolium ethylsulfate, [C_7H_7mim][$C_2H_5SO_4$]; 1-allyl-3-methylimidazolium ethylsulfate, [amim][$C_2H_5SO_4$]; 1-butyl-3-methylpyridinium chloride, [C_4mpy]Cl; 1-butyl-1-methylpiperidinium chloride, [C_4mpip]Cl; 1-butyl-1-methylpyrrolidinium chloride, [C_4mpyr]Cl, and 1-octylpyridinium dicyanamide, [C_8py][$N(CN)_2$]. All ionic liquids were supplied by Iolitec. To reduce the volatile impurities to negligible values, ILs individual samples were purified under constant agitation, at vacuum and moderate temperature (323 K), for a minimum of 48 hours. After this step, the purity of each IL was further checked by ^{1}H, ^{13}C and ^{19}F (whenever applicable) NMR

spectra and found to be > 99 wt % for all samples. The structures of ILs that were successful in the determination of the phase diagrams are shown in Figure 2.1.1.

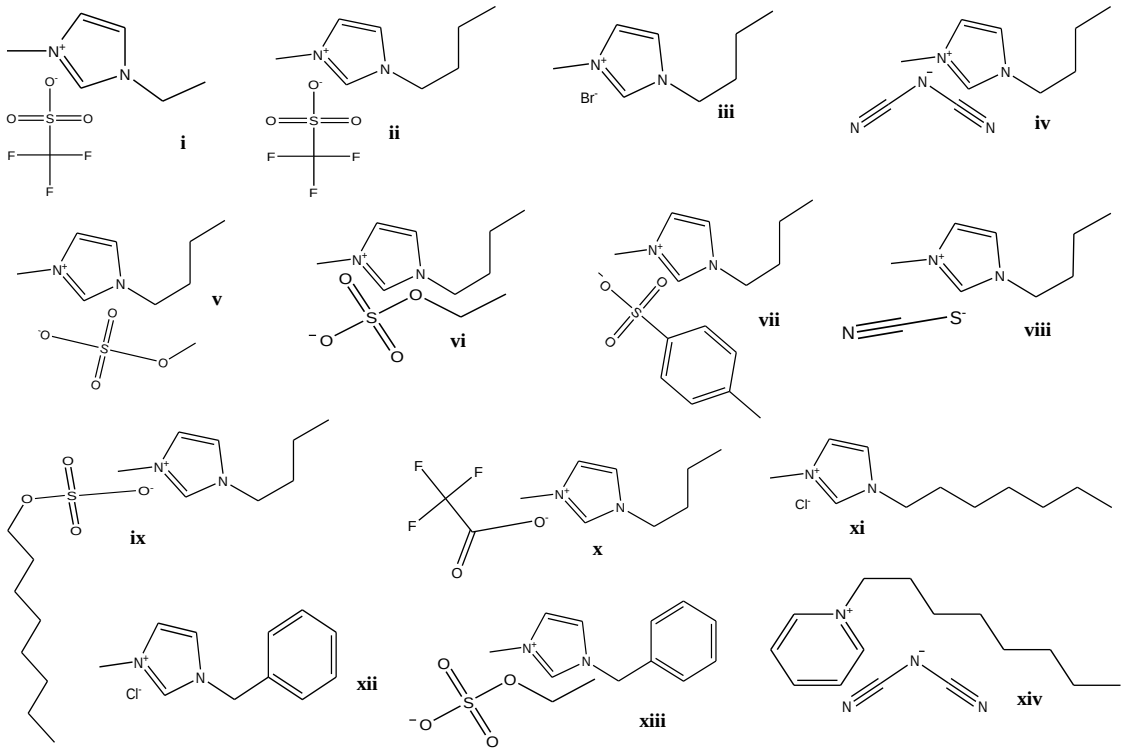

Figure 2.1.1: Ionic structures of the studied ionic liquids capable of forming ABS with Na_2SO_4 aqueous solutions: (i) $[C_2mim][CF_3SO_3]$; (ii) $[C_4mim][CF_3SO_3]$; (iii) $[C_4mim]Br$; (iv) $[C_4mim][N(CN)_2]$; (v) $[C_4mim][CH_3SO_4]$; (vi) $[C_4mim][C_2H_5SO_4]$; (vii) $[C_4mim][TOS]$; (viii) $[C_4mim][SCN]$; (ix) $[C_4mim][OctylSO_4]$; (x) $[C_4mim][CF_3CO_2]$; (xi) $[C_7mim]Cl$; (xii) $[C_7H_7mim]Cl$; (xiii) $[C_7H_7mim][C_2H_5SO_4]$; (xiv) $[C_8py][N(CN)_2]$.

The inorganic salt Na_2SO_4 was from LabSolve (purity > 99.8 wt %). The water employed was double distilled, passed across a reverse osmosis system and further treated with a Milli-Q plus 185 water purification equipment. The buffers used in the calibration of the pH meter equipment were the citric acid / sodium hydroxide / sodium chloride solution with a pH value of 4.00 (± 0.02), and the potassium dihydrogen phosphate / disodium hydrogen phosphate solution with a pH value of 7.00 (± 0.02), acquired from Fluka.

Phase Diagrams and Tie-Lines

Aqueous solutions of Na_2SO_4 at ≈ 25wt %, and aqueous solutions of the different hydrophilic ILs at ≈ 60 wt %, were prepared and used for the determination of the binodal curves. The phase diagrams were determined at 298 K (± 1 K) and at atmospheric

pressure through the cloud point titration method (previously validated by our group[5,6,9]). Drop-wise addition of the aqueous inorganic salt solution to each IL aqueous solution was carried out until the detection of a cloudy (biphasic) solution, followed by the drop-wise addition of ultra-pure water until the formation of a clear and limpid solution (monophasic region), as shown in Figure 2.1.2. Drop-wise additions were carried out under constant stirring. The ternary systems compositions were determined by weight quantification of all components within ± 10^{-4} g (using an analytical balance Mettler Toledo Excelence - XS205 Dual Range).

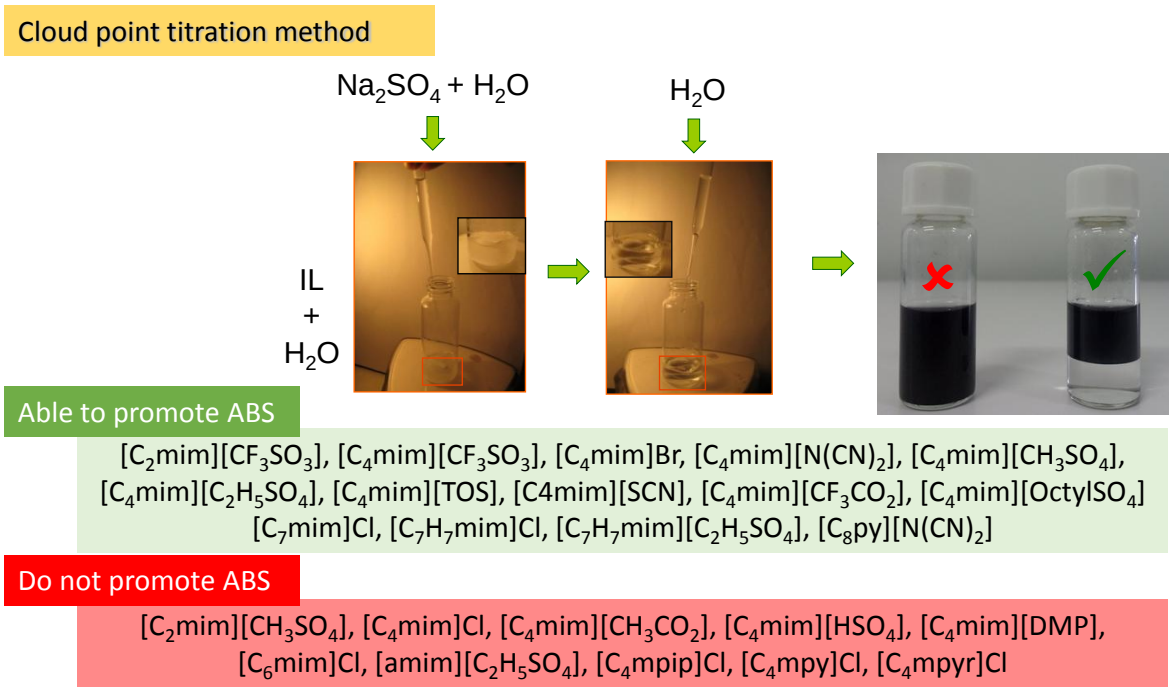

Figure 2.1.2: Experimental determination of the binodal curves for the IL-Na_2SO_4 ABS and identification of ILs able (or not) to form liquid-liquid systems.

The tie-lines (TLs) were determined by a gravimetric method originally proposed by Merchuk et al.[27] For the determination of TLs, a ternary mixture composed of Na_2SO_4 + water + IL at the biphasic region was gravimetrically prepared within ± 10^{-4} g, vigorously agitated, and left to equilibrate for at least 12 h, and at 298 K, aiming at a complete separation of the co-existing phases. In this step, small ampoules (10 cm^3) specifically designed for the purpose, were used. Both phases were carefully separated and individually weighed within ± 10^{-4} g. Each TL was determined by a mass balance approach

through the relationship between the top mass phase composition and the overall system composition. The experimental binodal curves were fitted accordingly to eq 2.1.1:[27]

$$Y = A\exp[(BX^{0.5}) - (CX^{3})] \qquad \text{eq. 2.1.1}$$

where *Y* and *X* are the ionic liquid and the inorganic salt weight fraction percentages, respectively, and *A*, *B* and *C* are constants obtained by the regression of the experimental binodal data.

For the TLs determination, the following system of four equations (eqs 2.1.2 to 2.1.5) and four unknown values (Y_T, Y_B, X_T and X_B) was solved:[27]

$$Y_T = A\exp[(BX_T^{0.5}) - (CX_T^{3})] \qquad \text{eq. 2.1.2}$$

$$Y_B = A\exp[(BX_B^{0.5}) - (CX_B^{3})] \qquad \text{eq. 2.1.3}$$

$$Y_T = \frac{Y_M}{\alpha} - \frac{1-\alpha}{\alpha} \times Y_B \qquad \text{eq. 2.1.4}$$

$$X_T = \frac{X_M}{\alpha} - \frac{1-\alpha}{\alpha} \times X_B \qquad \text{eq. 2.1.5}$$

where *T*, *B*, and *M* designate the top phase, the bottom phase and the mixture, respectively; *X* and *Y* represent, respectively, the weight fraction of Na_2SO_4 and ionic liquid; and *α* is the ratio between the mass of the top phase and the total mass of the mixture. The system solution results in the composition (wt %) of the ionic liquid and inorganic salt in the top and bottom phases, and thus, TLs can be directly represented.

For the calculation of the tie-lines length (TLL) it was employed the following eq,

$$\mathrm{TLL} = \sqrt{(X_T - X_B)^2 + (Y_T - Y_B)^2} \qquad \text{eq. 2.1.6}$$

where *T* and *B* symbolize, respectively, the top and bottom phases, and *X* and *Y* are the mass fraction percentages of inorganic salt and IL, as described before.

pH determination

The pH values (± 0.02) of the IL- and inorganic-salt-rich aqueous phases were measured at 298 (± 1) K using an HI 9321 Microprocessor pH meter (HANNA instruments). The

calibration of the pH meter was carried out with two buffers (pH values of 4.00 and 7.00). The compositions adopted at the biphasic region were composed of 15 wt % of Na_2SO_4, 60 wt % of water and 25 wt % of each ionic liquid. All mixtures were gravimetrically prepared within ± 10^{-4} g. The mixtures were prepared, vigorously stirred, and further kept still in small ampoules for phase separation, and for at least 12 h at (298 ± 1) K. After the careful separation of the phases, the pH of each aqueous phase was further measured.

Results and Discussion

Phase Diagrams

A broad range of ILs was studied to identify the ionic liquid structural features responsible for the formation of ABS in the presence of salt solutions of Na_2SO_4. The ionic liquids investigated were [C_2mim][CH_3SO_4], [C_2mim][CF_3SO_3], [C_4mim]Cl, [C_4mim]Br, [C_4mim][CH_3CO_2], [C_4mim][CF_3SO_3], [C_4mim][$N(CN)_2$], [C_4mim][HSO_4], [C_4mim][CH_3SO_4], [C_4mim][$C_2H_5SO_4$], [C_4mim][TOS], [C_4mim][DMP], [C_4mim][SCN], [C_4mim][CF_3CO_2], [C_4mim][OctylSO_4], [C_6mim]Cl, [C_7mim]Cl, [C_7H_7mim]Cl, [C_7H_7mim][$C_2H_5SO_4$], [amim][$C_2H_5SO_4$], [C_4mpip]Cl, [C_4mpy]Cl, [C_4mpyr]Cl, and [C_8py][$N(CN)_2$]. The compositions used for the evaluation of the possibility of forming liquid-liquid biphasic systems are reported in *Supporting Information* (Table S1). The ionic liquids that were able to promote ABS with Na_2SO_4 were the following: [C_2mim][CF_3SO_3], [C_4mim][CF_3SO_3], [C_4mim]Br, [C_4mim][$N(CN)_2$], [C_4mim][CH_3SO_4], [C_4mim][$C_2H_5SO_4$], [C_4mim][TOS], [C4mim][SCN], [C_4mim][CF_3CO_2], [C_4mim][OctylSO_4], [C_7mim]Cl, [C_7H_7mim]Cl, [C_7H_7mim][$C_2H_5SO_4$], and [C_8py][$N(CN)_2$], as shown in Figure 2.1.2. Therefore, despite the controversy found in literature postulating that acidic and neutral inorganic salts are not able to promote IL-based ABS, it is here shown that they can be created if an adequate choice of the ionic liquid is carried out.

In agreement with the results previously reported[4] we also found to be not possible to create the [C_4mim]Cl-Na_2SO_4 ABS, although an ABS formation was observed with [C_4mim]Br. These data are in good agreement with previous findings using the inorganic salt K_3PO_4[6,9] where [C_4mim]Br was shown to be more able to undergo the formation of ABS than the chloride counterpart.

The experimental phase diagrams obtained, at 298 K and at atmospheric pressure, for the ternary systems composed of Na_2SO_4 + water + ILs are presented in Figures 2.1.3 to 2.1.5. The phase diagrams are distributed by different figures to facilitate the individual analysis of the influence of the anion/cation structural effects. All phase diagrams are represented in molality units for a more comprehensive perception of the impact of diverse ionic liquids on the ABS formation (avoiding thus differences that could be a merely result of different molecular weights).The experimental weight fraction data for each phase diagram are reported in *Supporting Information* (Table S2 to S9).

Table 2.1.1 presents the parameters obtained by the regression of the experimental binodal curves (in weight fraction) using eq 2.1.1.

Table 2.1.1. Parameters (*A*, *B* and *C*) obtained by the regression of the experimental binodal data through the application of eq 2.1.1 (and respective standard deviations, σ) for the IL + Na_2SO_4 + H_2O systems at 298 K.

IL + Na_2SO_4 + Water system	***A* ± σ**	***B* ± σ**	***10^5C* ± σ**	***R^2***
[C_2mim][CF_3SO_3]	106.1 ± 2.1	-0.439 ± 0.010	16.2 ± 2.0	0.9990
[C_4mim][CF_3SO_3]	190.0 ± 9.4	-0.965 ± 0.002	2.0 ± 3.9	0.9923
[C_4mim]Br	97.5 ± 2.6	-0.393 ± 0.016	1.0 ± 5.8	0.9989
[C_4mim][CH_3SO_4]	105.4 ± 2.4	-0.396 ± 0.009	4.4 ± 0.4	0.9963
[C_4mim][$C_2H_5SO_4$]	95.4 ± 0.7	-0.393 ± 0.004	5.7 ± 0.2	0.9980
[C_4mim][$N(CN)_2$]	88.8 ± 1.0	-0.446 ± 0.006	20.2 ± 0.7	0.9997
[C_4mim][TOS]	102.1 ± 0.7	0.421 ± 0.003	18.2 ± 0.2	0.9996
[C_4mim][SCN]	85.8 ± 0.5	-0.433 ±0.003	49.0 ± 0.9	0.9995
[C_4mim][CF_3CO_2]	103.3 ± 1.6	-0.396 ± 0.008	5.0 ± 1.4	0.9995
[C_4mim][OctylSO$_4$]	158.0 ± 2.4	-0.575 ± 0.007	42.4 ± 1.1	0.9997
[C_7mim]Cl	91.6 ± 2.0	-0.287 ± 0.011	9.9 ± 1.5	1.0000
[C_7H_7mim]Cl	104.7 ± 7.4	-0.372 ± 0.036	4.9 ± 6.6	0.9982
[C_7H_7mim][$C_2H_5SO_4$]	100.6 ± 1.6	-0.383 ± 0.007	12.9 ± 0.5	0.9997
[C_8py][$N(CN)_2$]	195.2 ± 2.4	-1.079 ± 0.008	9.9 ± 2.3	0.9984

In all phase diagrams, the top-rich phase corresponds to the IL-rich phase while the bottom phase represents the Na_2SO_4-rich phase. An unique exception was observed with

the $[C_4mim][CF_3SO_3]$ system. This inversion of phases is directly related with the high density of the fluorinated ionic liquid.[28] The tie-lines and tie-line lengths for each system were determined through the application of eqs 2.1.2 to 2.1.6. Weight fraction compositions for the co-existing phases of each system (TLs), along with the respective tie-line lengths, are reported in Table 2.1.2.

Table 2.1.2: Mass fraction compositions (wt %) for the co-existing phases of the IL (Y) + Na_2SO_4 (X) + H_2O systems at 298 K, and respective values of α and TLL.

IL + Na_2SO_4 + water system	Weight fraction composition / wt %						α	TLL
	Y_T	X_T	Y_M	X_M	Y_B	X_B		
$[C_2mim][CF_3SO_3]$	63.37	1.37	17.95	14.96	5.55	18.67	0.79	60.35
	71.67	0.80	24.88	15.28	2.22	22.30	0.33	72.70
	73.70	0.69	24.89	15.94	1.71	23.18	0.32	75.43
$[C_4mim][CF_3SO_3]$	3.89	15.60	20.10	11.96	68.31	1.12	0.75	66.03
	3.02	17.47	15.13	14.99	85.13	0.69	0.85	83.81
	2.15	20.00	24.95	14.97	90.03	0.60	0.74	90.00
$[C_4mim]Br$	34.62	6.90	23.05	14.97	15.07	20.53	0.59	23.83
	39.71	5.21	24.96	15.22	12.73	23.52	0.55	32.60
$[C_4mim][CH_3SO_4]$	45.93	4.36	24.69	14.52	11.88	20.64	0.62	37.74
	55.70	2.59	28.64	14.27	10.01	22.31	0.59	49.77
$[C_4mim][C_2H_5SO_4]$	30.58	7.98	14.01	18.44	8.05	22.21	0.27	26.65
$[C_4mim][OctylSO_4]$	50.40	3.79	9.73	15.45	1.23	17.88	0.17	51.15
	59.73	2.81	16.02	14.88	0.66	19.12	0.26	61.29
	73.70	1.75	24.98	14.95	0.14	21.68	0.34	76.20
$[C_4mim][N(CN)_2]$	53.19	1.32	15.08	14.93	2.97	19.26	0.24	53.33
	57.54	0.95	20.18	14.91	1.29	21.98	0.34	60.06
	60.82	0.56	25.00	15.00	0.40	24.92	0.41	65.15
$[C_4mim][TOS]$	44.64	3.78	15.00	15.07	4.69	19.00	0.26	42.75
	55.41	2.10	20.24	15.59	1.63	22.73	0.35	57.61
	57.41	1.87	24.80	14.93	0.87	24.52	0.42	60.91
$[C_4mim][SCN]$	47.27	1.87	15.14	10.06	9.14	11.59	0.16	39.35
	52.65	1.27	19.97	10.05	3.85	14.38	0.33	50.53
	63.19	0.50	24.93	14.94	0.01	24.35	0.39	67.53
$[C_4mim][CF_3CO_2]$	45.00	4.38	24.95	14.99	7.03	24.48	0.53	42.97
	51.80	3.04	27.17	14.96	6.67	24.88	0.55	50.14
$[C_7mim]Cl$	63.27	1.66	25.05	15.00	12.88	19.25	0.76	53.37
$[C_7H_7mim]Cl$	32.54	9.22	28.79	11.40	11.34	21.56	0.82	24.54
	46.78	4.63	25.08	15.13	10.72	22.08	0.60	40.06
	47.37	4.49	25.92	14.92	10.09	22.60	0.58	41.44
$[C_7H_7mim][C_2H_5SO_4]$	47.37	3.79	20.00	15.00	5.23	21.04	0.35	45.54

	55.92	2.33	25.01	15.00	2.43	24.27	0.42	57.81
	61.51	1.15	20.08	10.15	2.66	13.93	0.30	60.22
$[C_8py][N(CN)_2]$	68.44	0.94	20.58	12.07	1.56	16.50	0.28	68.66
	71.35	0.87	24.59	14.52	0.48	21.56	0.34	73.83

The pH in the top and bottom phases of the ABS investigated was determined to evaluate the formation of acidic IL-based ABS (envisaging improved systems for the extraction of biomolecules with low acid dissociation constants). The pH values of the co-existing phases, displayed in Table 2.1.3, were measured in biphasic systems formed by 25 wt % of each IL + 15 wt % of Na_2SO_4 + 60 wt % of water.

Table 2.1.3: pH values of the co-existing phases in IL-Na_2SO_4-based ABS at the biphasic composition of 25 wt % of IL + 15 wt % of Na_2SO_4 + 60 wt % of water (at 298 K), and the Na_2SO_4 speciation[31] in aqueous solution.

IL-rich phase/Na_2SO_4-rich phase		
IL+ Na_2SO_4 + water system	pH	$[SO_4^{2-}]/[HSO_4^-]$
$[C_2mim][CF_3SO_3]$	2.71 / 3.32	$5.13 \times 10^0 / 2.09 \times 10^1$
$[C_4mim][CF_3SO_3]$	3.12 / 3.04	$1.32 \times 10^1 / 1.10 \times 10^1$
$[C_4mim]Br$	5.43 / 5.22	$2.69 \times 10^3 / 1.66 \times 10^3$
$[C_4mim][CH_3SO_4]$	1.88 / 1.57	$7.59 \times 10^{-1} / 3.72 \times 10^{-1}$
$[C_4mim][C_2H_5SO_4]$	2.29 / 1.29	$1.95 \times 10^0 / 1.95 \times 10^{-1}$
$[C_4mim][OctylSO_4]$	3.64 / 3.52	$4.37 \times 10^1 / 3.31 \times 10^1$
$[C_4mim][N(CN)_2]$	8.54 / 8.07	$3.47 \times 10^6 / 1.17 \times 10^6$
$[C_4mim][TOS]$	5.33 / 5.16	$2.14 \times 10^3 / 1.45 \times 10^3$
$[C_4mim][SCN]$	4.49 /4.29	$3.09 \times 10^2 / 1.95 \times 10^2$
$[C_4mim][CF_3CO_2]$	4.18 / 4.16	$1.51 \times 10^2 / 1.45 \times 10^2$
$[C_7mim]Cl$	4.15 / 4.16	$1.41 \times 10^2 / 1.45 \times 10^2$
$[C_7H_7mim]Cl$	4.44 / 4.64	$2.75 \times 10^2 / 4.37 \times 10^2$
$[C_7H_7mim][C_2H_5SO_4]$	2.08 / 2.05	$1.20 \times 10^0 / 1.12 \times 10^0$
$[C_8py][N(CN)_2]$	6.94 / 7.07	$8.71 \times 10^5 / 1.17 \times 10^5$

The respective compositions of each component at the IL- and Na_2SO_4-rich phases are reported in Table 2.1.2. Since the concentration of ionic liquid in each phase is not the

same, the pH values at the co-existing phases are slightly different. Nevertheless, close pH values for a common system at both aqueous phases are observed.

A general trend on the pH values at the IL-rich phase was observed: an increase in the alkyl side chain length at the cation and/or anion leads to an increase in the pH values. At the salt-rich phase no general pattern was observed. The main differences in the pH values were observed with distinct [C_4mim]-based ionic liquids combined with several anions. As result, when using a neutral salt, such as Na_2SO_4, the pH values of IL-based ABS are strongly dependent on the ionic liquid employed. Most IL-based ABS here studied are acidic with the exception of the [$N(CN)_2$]-based systems that, due to anion basicity, produces alkaline aqueous phases.

In order to investigate the inorganic anion speciation into $H_2SO_4/HSO_4^-/SO_4^{2-}$ at the pH values induced by the different ionic liquids, the ratio of the concentrations of the pairs H_2SO_4/HSO_4^- and HSO_4^-/SO_4^{2-} was determined taking into account the acid dissociation constants of the corresponding polyprotic acid.[29] The ratio between the concentrations of the species SO_4^{2-} and HSO_4^- is provided in Table 2.1.3. The ratio of the ionic concentrations corresponding to the first dissociation of the protons was considered to be marginal since the pH values are well above the pK_{a1} of H_2SO_4 (these results are however provided in *Supporting Information*). From the results obtained it can be seen that there is not a close relationship between the concentration of SO_4^{2-} and the ability of the ILs to be salted-out. For instance, for the [C_4mim]-based ionic liquids, the highest concentration of the sulfate anion, at both aqueous phases, is observed with the ionic liquid [C_4mim][$N(CN)_2$]. Nonetheless, among the [C_4mim]-based series, [C_4mim][$N(CN)_2$] is not the ionic liquid with the higher ability to be separated from the aqueous mixture. ILs with anions such as $[CF_3SO_3]^-$, $[SCN]^-$ and $[TOS]^-$ are easily salted-out from aqueous media albeit presenting lower pH values. Hence, for a common salt, the ability of the ILs to undergo liquid-liquid demixing does not strictly depend on the inorganic salt speciation, but instead on the ionic liquid structural features or hydrogen-bond ability as it will be discussed below. On the other hand, the pH of the aqueous media seems to be an important factor in the creation of ABS in the presence of a common salt. Contrarily to the large array of ionic liquids that were able to produce ABS in the presence of an alkaline aqueous solution of

K_3PO_4[6,9] in the presence of acidic or neutral aqueous solutions the number of ILs that are capable of forming ABS is largely reduced. Acidic or neutral salt solutions limit the range of ILs that are able to create ABS, as shown in Figure 2.1.2.

In complex mixtures, as those containing high charge density salts with an enhanced capacity for creating ion-water hydration complexes (such as Na_2SO_4), the capability to induce ABS increases with the decreasing on the ionic liquid affinity for water - the ionic liquid is salted-out by the inorganic ions. These hydrophobic ILs are those composed of long alkyl side chains[6,9] or constituted by anions with lower hydrogen-bond basicity values (anions with a low hydrogen bond acceptor strength).[6,9] The affinity of hydrogen-bond donors or acceptors is influenced by steric factors (accessibility of the donor or acceptor groups), as well as by electronic factors, such as electronegativity and hybridization.[30] The hydrogen-bonding ability of ionic liquids can be empirically estimated using a variety of solvatochromic probes as previously demonstrated in literature.[31] The solvatochromic parameters are derived from spectroscopic techniques specifically designed to measure only a single interaction (hydrogen-bonding). One of most interesting and widely used set of solvatochromic parameters are the Kamlet-Taft parameters. These parameters comprise the solvent dipolarity/polarizability (π*), the hydrogen-bond acidity (α), and the hydrogen-bond basicity (β).[31] The β-scale is a measure of the ability of the solvent to accept a proton (or donate an electron pair) in a solute-solvent hydrogen-bond. In ABS, water is the most cohesive solvent, dipolar, and a strong hydrogen-bond donor and acceptor. ILs display a complex combination of specific interactions including the ability to hydrogen-bond. Thus, in this work, the Kamlet-Taft parameters (particularly, the hydrogen-bonding basicity) will be used in the following discussion of the phase behavior since hydrogen-bond interactions of the pairs IL-water and inorganic-salt-water are competing for the creation of ABS.

The larger the biphasic region, the higher is the ability of each ionic liquid to promote ABS formation. From the gathered data, the overall tendency of the ILs in creating ABS, for instance in the presence of 0.5 mol·kg^{-1} of Na_2SO_4, follows the order: $[C_8py][N(CN)_2]$ > $[C_4mim][CF_3SO_3]$ >> $[C_4mim][OctylSO_4]$ > $[C_4mim][TOS]$ ≈ $[C_4mim][SCN]$ > $[C_4mim][N(CN)_2]$ > $[C_2mim][CF_3SO_3]$ ≈ $[C_7H_7mim][C_2H_5SO_4]$ > $[C_4mim][C_2H_5SO_4]$ > $[C_4mim][CF_3CO_2]$ ≈

$[C_4mim][CH_3SO_4]$ > $[C_4mim]Br$ > $[C_7H_7mim]Cl$> $[C_7mim]Cl$. The differences observed in the phase behavior for the different ILs formed by distinct cation/anion combinations are a clear reflection of their commonly attributed epithet of "designer solvents". The appropriate selection of the cation and/or anion composing an ionic liquid could thus provide ABS with tailored phase behavior and in acidic media.

The systems displayed in Figure 2.1.3 with a common cation, $[C_4mim]^+$, allow the investigation of the ability of the ionic liquids anions to promote ABS. The results (at 0.5 $mol \cdot kg^{-1}$ of Na_2SO_4) indicate that the anions influence follows the rank: $[CF_3SO_3]^-$ > $[OctylSO_4]^-$ > $[TOS]^-$ ≈ $[SCN]^-$ > $[N(CN)_2]^-$ > $[C_2H_5SO_4]^-$ > $[CF_3CO_2]^-$ ≈ $[CH_3SO_4]^-$ > Br^- (>> Cl^- that do not forms ABS with Na_2SO_4 aqueous solutions with this cation).

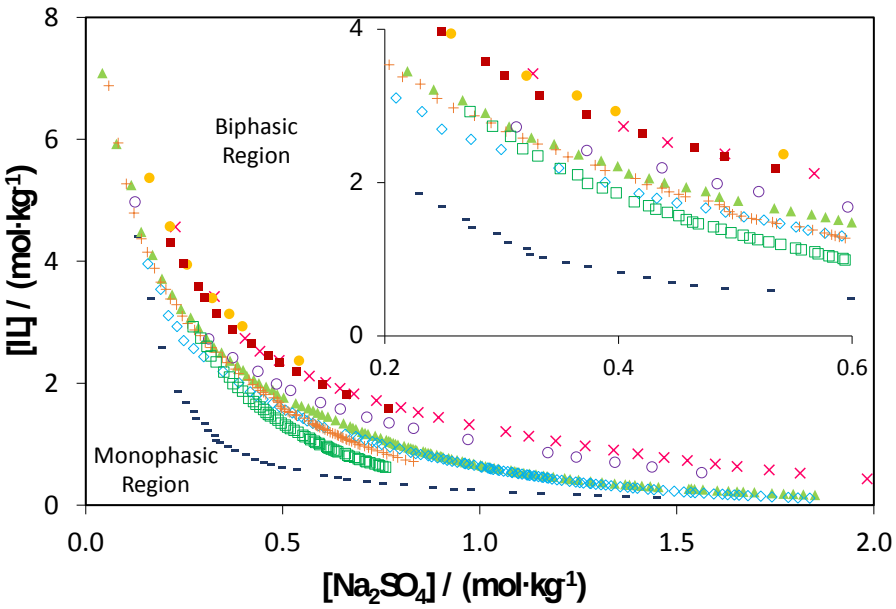

Figure 2.1.3: Ternary phase diagrams for $[C_4mim]$-based ILs at 298 K and atmospheric pressure: —, $[C_4mim][CF_3SO_3]$; ◇, $[C_4mim][TOS]$; +, $[C_4mim][SCN]$; ○, $[C_4mim][C_2H_5SO_4]$; ×, $[C_4mim][CH_3SO_4]$; ▲, $[C_4mim][N(CN)_2]$; □, $[C_4mim][OctylSO_4]$; ■, $[C_4mim][CF_3CO_2]$; ●, $[C_4mim]Br$.

The trend displayed by the ionic liquid anions to induce ABS agrees well with our previous results for ABS formed with K_3PO_4 aqueous solutions.[9] This close agreement suggests that this trend is not dependent on the pH of the medium or on the ions speciation (as discussed above) but only on the ionic liquid anion characteristics.[9] The anions rank obtained reflects thus the competition between the inorganic salt and the ionic liquid ions for the formation of water-ion hydration complexes.[32] Anions with highly dispersed

charges tend to preferentially interact with hydrophobic moieties and do not form hydration complexes.[32] Thus, the anions' hydrogen bonding accepting strength seems to be a main controlling factor in ABS formation for a common inorganic salt. As previously observed, anions with low hydrogen bond basicity values are more prone to undergo liquid-liquid demixing in aqueous media.[9] While $[C_4mim][CH_3CO_2]$ was not able to create Na_2SO_4-based ABS, on the other hand, $[C_4mim][CF_3CO_2]$ was be capable of forming ABS (the fluorination of the anion leads to lower β values).[9]

An increase in the alkyl side chain in both the ionic liquid cation or anion enhances the ability of the ionic liquid for ABS formation, as observed by comparing the two following sets depicted in Figure 2.1.4: $[C_2mim][CF_3SO_3]$/$[C_4mim][CF_3SO_3]$ and $[C_4mim][CH_3SO_4]$/$[C_4mim][C_2H_5SO_4]$/$[C_4mim][OctylSO_4]$.

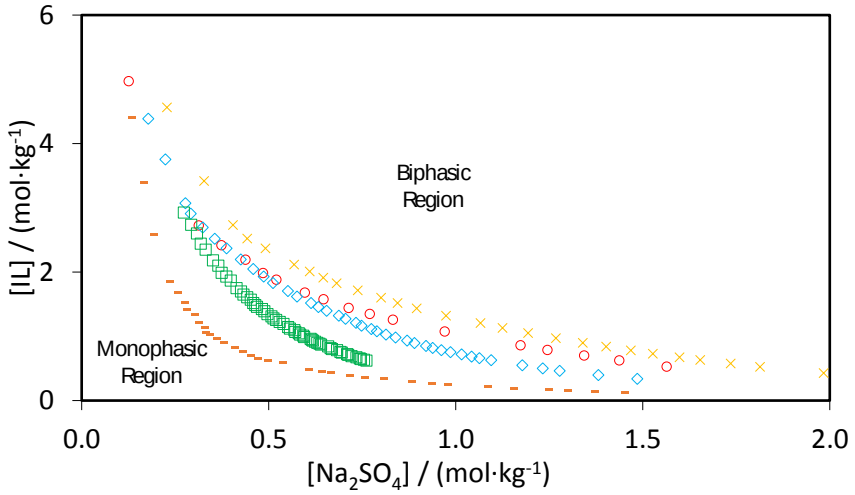

Figure 2.1.4: Ternary phase diagrams for selected ionic liquids at 298 K and atmospheric pressure (evaluation of the cation/anion alkyl chain length influence): —, $[C_4mim][CF_3SO_3]$; ◇, $[C_2mim][CF_3SO_3]$; ○, $[C_4mim][C_2H_5SO_4]$; ×, $[C_4mim][CH_3SO_4]$, □, $[C_4mim]$ $[OctylSO_4]$.

The previous trend is a direct outcome of solvophobic and entropic effects: increasing the alkyl side chain length of the ionic liquid cation and/or anion enhances the fluid overall hydrophobicity while increasing the entropy of solution of the ionic liquid in water, and therefore facilitates the phase separation.[33] Moreover, while $[C_4mim]Cl$ was not able to induce the phase separation, on the other hand, the chloride combination with different cations, such as $[C_7mim]^+$, leads to the formation of ABS with Na_2SO_4 aqueous solutions, as shown in Figure 2.1.5. The ability for ABS formation of $[C_7mim]Cl$ is also a direct consequence of the longer alkyl side chain cation.

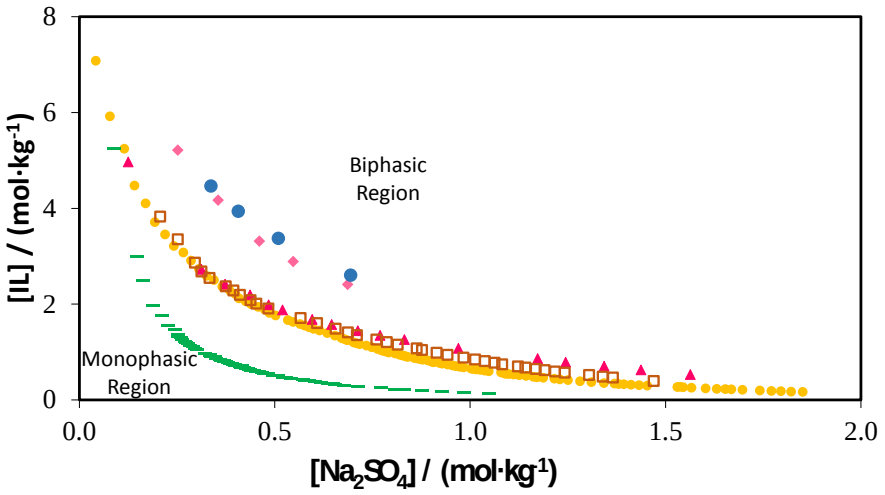

Figure 2.1.5: Ternary phase diagrams for selected ionic liquids at 298 K and atmospheric pressure (evaluation of the cation core and functionalized groups influence): —, $[C_8py][N(CN)_2]$; ▲, $[C_4mim][C_2H_5SO_4]$; ●, $[C_4mim][N(CN)_2]$; □, $[C_7H_7mim][C_2H_5SO_4]$; ♦ ,$[C_7H_7mim]Cl$; ●, $[C_7mim]Cl$.

Figure 2.1.5 illustrates additional information on the ionic liquid cation influence for liquid-liquid demixing using Na_2SO_4 aqueous solutions. Comparing $[C_4mim][C_2H_5SO_4]$ and $[C_7H_7mim][C_2H_5SO_4]$ it is observed that the later ionic liquid presents a slightly higher ability to induce the formation of ABS. Although the benzyl group present in $[C_7H_7mim][C_2H_5SO_4]$ enhances the ionic liquid affinity for water and ability to hydrogen-bond, this larger substituent also contributes for a decrease in the solubility of the ionic liquid in water when compared with $[C_4mim][C_2H_5SO_4]$. This pattern is also in close agreement with the results observed between $[C_7H_7mim]Cl$ and $[C_4mim]Cl$.

Figure 2.1.5 shows that the ionic liquid containing the cation $[C_8py]^+$ has the greatest capacity to promote ABS among all the ionic liquids studied. This enhanced capacity in creating ABS is a direct result of the anion low hydrogen bond basicity ($[N(CN)_2]^-$) coupled to a pyridinium cation that also contributes to a reduction of the overall hydrogen bond basicity of the ionic liquid. Although we were not able to found literature β values for this specific ionic liquid, a general trend between imidazolium- and pyridinium-based cations was found and support this statement. The hydrogen bond basicity values of pyridinium-based ionic liquids are consistently lower than their imidazolium-based counterparts (β values: $[C_4py][BF_4]$[34] = 0.213 and $[C_4mim][BF_4]$[35] = 0.376; $[C_8py][BF_4]$[34] = 0.340 and $[C_8mim][BF_4]$[36] = 0.630; $[C_4py][NTf_2]$[34] = 0.123 and $[C_4mim][NTf_2]$[36] = 0.420; $[C_8py][NTf_2]$[34] =

0.115 and $[C_8mim][NTf_2]$[36] = 0.470). Therefore, the lower the hydrogen bond basicity of an ionic liquid the greater is its ability for promoting ABS.

Most of the discussion on the ionic liquids aptitude for creating ABS was based on their hydrogen-bond basicity, since it was verified that with the salt Na_2SO_4, the ILs with lower β values are more ables to form ABS.[35-39] The β values for the distinct ionic liquids investigated in this work are reported in Table 2.1.4.

Table2.1.4: Hydrogen bond basicity values (β) for individual $[C_4mim]$-based ILs . The shaded rows correspond to ionic liquids that are able to create Na_2SO_4-based ABS.

Ionic liquid	β
$[C_4mim][PF_6]$	0.21[35]
$[C_4mim][NTf_2]$	0.24[35]
$[C_4mim][BF_4]$	0.38[35]
$[C_4mim][CF_3SO_3]$	0.46[37]
$[C_4mim][N(CN)_2]$	0.60[37]
$[C_4mim][CH_3SO_4]$	0.67[37]
$[C_4mim][SCN]$	0.71[38,39]
$[C_4mim][CF_3CO_2]$	0.74[38,39]
$[C_4mim][OctylSO_4]$	0.77[38,39]
$[C_4mim]Br$	0.87[38,39]
$[C_4mim]Cl$	0.95[36]
$[C_4mim][DMP]$	1.12[37]
$[C_4mim][CH_3CO_2]$	1.20[37]

Table 2.1.4 and Figure 2.1.6 reveal that it exists a close relationship between the ability of each ionic liquid to form ABS and their hydrogen bond basicity values – the lower the β value is, the more efficient the ionic liquid is in creating ABS.

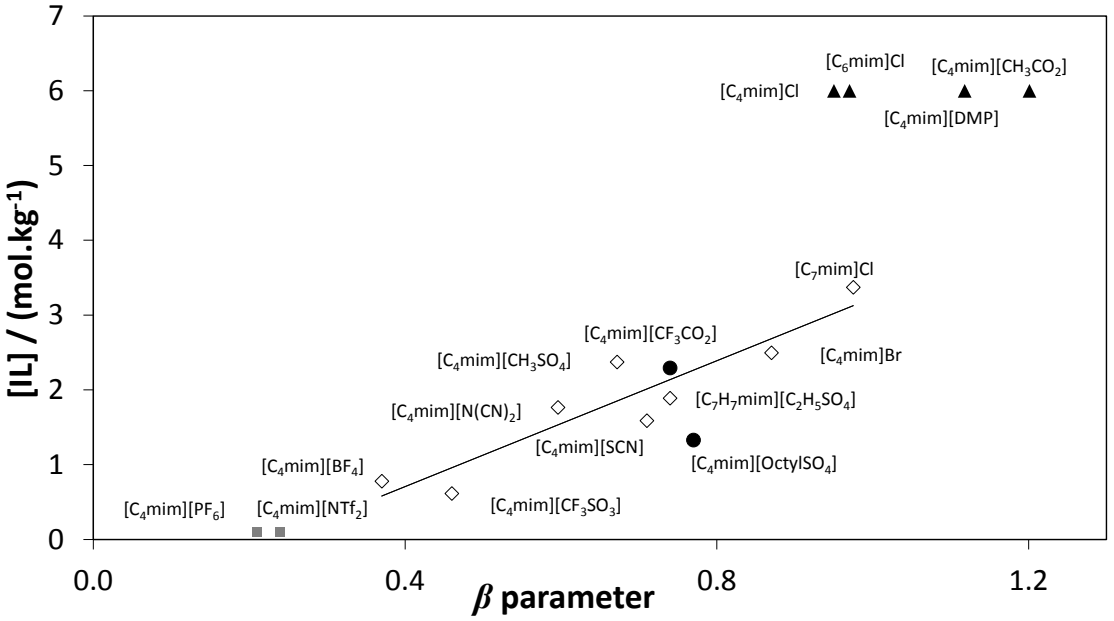

Figure 2.1.6: Ionic liquid molality, taken from each binodal curve and at which the Na_2SO_4 molality is equal to 0.5 mol·kg^{-1}, as a function of the hydrogen bond basicity values (β):[35-39] open diamonds represent the training set of ILs that formed ABS; full circles represent the test set of ionic liquids; full squares represent the hydrophobic ILs that are not completely miscible with water; and the full triangles represent the ILs that although miscible with water were not able to form ABS.

It should be remarked that albeit a qualitative trend is observed, the comparison of the solvatochromic parameters obtained by different authors and different techniques is not straightforward and general deviations exist.[35-39] To generalize this comparison the ionic liquids that were not able to form ABS were also included, as well as those at the opposite extreme – the $[PF_6]$- and $[NTf_2]$-based ionic liquids that present low hydrogen bond basicities, and as such, are not completely miscible with water,[33,40] and are thus unable to create ABS.

The results compiled in Table 2.1.4 and Figure 2.1.6 indicate that any ionic liquid with β values ranging between those displayed by the $[C_4mim][BF_4]$ and the $[C_4mim]Br$ should be able to form ABS with Na_2SO_4, while those below this range will be not water soluble, and those above will not be able to undergo liquid-liquid demixing in Na_2SO_4 aqueous solutions. Indeed, a training set of ILs ($[C_4mim][OctylSO_4]$ and $[C_4mim][CF_3CO_2]$ with β values ranging between 0.38- 0.87) was investigated and supported our main conclusions.

Conclusions

IL-based ABS are new approaches for recycling or concentrating hydrophilic ionic liquids from aqueous solutions or to perform selective separations of added-value products. In particular, when dealing with the extraction of compounds with low acid dissociation constants from aqueous media, the use of acidic IL-based ABS could be advantageous.

Contrarily to most literature reports that have suggested that IL-based ABS could not be formed with acidic or neutral salt aqueous solutions, it was here demonstrated that an adequate selection of the ionic liquids structural features can lead to ABS formation in acidic media. Phase diagrams, tie-lines and tie-line lengths were determined and reported at 298 K and atmospheric pressure. The results obtained indicate that both the ionic liquid cation and anion structural features have a large impact on the phase diagrams behavior. In general, an increase in the cation/anion alkyl chain length leads to an increase in the phases' separation ability, whereas a decrease in the hydrogen bond basicity of the ionic liquid promotes the formation of ABS. Particularly, the ability of ILs to create ABS was found to be largely dependent on their hydrogen bond basicity values – a measure of their capability to hydrogen-bond with water. This close relationship allowed to state that ionic liquids with β values ranging between $[C_4mim][BF_4]$ and $[C_4mim]Br$ are able to form ABS with Na_2SO_4, while those ionic liquids with β values outside this limited range will not form Na_2SO_4-based ABS. Besides the effect of the ionic liquid structural features towards the formation of IL-based ABS, the pH media of the inorganic salts show to be a determinant factor regarding the number of effective ionic liquids that are capable of undergo liquid-liquid demixing.

References

1. K.E. Gutowski, G.A. Broker, H.D. Willauer, G.J. Huddleston, R.P Swatloski, J.D. Holbrey and R.D. Rogers, J. Am. Chem. Soc., 2003, 125, 6632-6633.
2. A.F.M. Cláudio, M.G. Freire, C.S.R. Freire, A.J.D. Silvestre and J.A.P. Coutinho, Sep. Purif. Technol. 2010, 75, 39-47.
3. C. He, S. Li, H. Liu, K. Li and F. Liu, J. Chromatogr. A, 2005, 1082, 143-149.
4. Li, S.; He, C.; Liu, H.; Li, K.; Liu, F. J. Chromatogr. B, 2005, 826, 58-62.
5. C.L.S. Louros, A.F.M. Cláudio, C.M.S.S. Neves, M.G. Freire, I.M. Marrucho, J. Pauly and J.A.P. Coutinho, Int. J. Mol. Sci. 2010, 11, 1777-1791.
6. C.M.S.S. Neves, S.P.M. Ventura, M.G. Freire, I.M. Marrucho and J.A.P. Coutinho,J. Phys. Chem. B, 2009, 113, 5194-5199.
7. Y.C. Pei, J.J. Wang, K. Wu, X.P. Xuan and X. Lu, J. Sep. Purif. Technol., 2009, 64, 288-295.
8. A. Soto, A. Arce and M.K. Khoshkbarchi, Sep. Purif. Technol., 2005, 44, 242-246.
9. S.P.M Ventura, C.M.S.S. Neves, M.G. Freire, I.M. Marrucho, J. Oliveira and J.A.P. Coutinho, J. Phys. Chem. B,2009, 113, 9304-9310.
10. M.G. Freire, C.M.S.S. Neves, I.M. Marrucho, J.N.C. Lopes, L.P.N. Rebelo and J.A.P. Coutinho, Green Chem., 2010, 12, 1715-1718.
11. J.F.B. Pereira, A.S. Lima, M.G. Freire and J.A.P. Coutinho, Green Chem., 2010, 12, 1661-1669.
12. L.I.N. Tomé, V.R. Catambas, A.R.R. Teles, M.G. Freire, I.M. Marrucho and J.A.P Coutinho,. Sep. Purif.Technol. 2010, 72, 167-173.
13. Y.F. Deng, J. Chen and D.L. Zhang, J. Chem. Eng. Data 2007, 52, 1332-1335.
14. Z. Du, Y.L. Yu and J.H. Wang,Chem. Eur. J. 2007, 13, 2130-2137.
15. Z.Y. Li, Y.C. Pei, L. Liu and J.J. Wang, J. Chem. Thermodyn. 2010, 42, 932-937.
16. Y.C. Pei, Z.Y. Li, L. Liu, J.J. Wang and H.Y. Wang, Sci. China Chem., 2010, 57, 1554-1560.
17. Y. Pei, J. Wang, L. Liu, K. Wu and Y. J. Zhao,Chem. Eng. Data, 2007, 52, 2026-2031.
18. M. T. Zafarani-Moattar and S. Hamzehzadeh, J. Chem. Eng. Data, 2007, 52, 1686-1692.
19. N.J. Bridges, K.E. Gutowski and R.D. Rogers, Green Chem., 2007, 9, 177-183.
20. R. Sadeghi, R. Golabiazar and H. Shekaari, J. Chem. Thermodyn., 2010, 42, 441-453.
21. Y. Wang, X.H. Xu, Y.S. Yan, J. Han and Z. L. Zhang, Thermochim. Acta, 2010, 501, 112-118.
22. C.X. Li, J. Han, Y. Wang, Y.S. Yan, J.M. Pan, X.H. Xu and Z.L. Zhang, J. Chem. Eng. Data 2010, 55, 1087-1092.
23. F. Hofmeister, Arch. Exp. Pathol. Pharmakol. 1888, XXV, 1.
24. M.G. Freire, C.L.S. Louros, L.P.N. Rebelo and J.A.P. Coutinho, Green Chem., 2011, 13, 1536-1545.
25. M. Domínguez-Pérez, L.I.N. Tomé, M.G. Freire, I.M. Marrucho, O. Cabeza and J.A.P. Coutinho, Sep. Purif.Technol., 2010, 72, 85-91.
26. M.G. Freire, C.M.S.S. Neves, I.M. Marrucho, J.A.P. Coutinho and A.M Fernandes, J. Phys. Chem. A, 2010, 114, 3744-3749.
27. J.C. Merchuk, B.A. Andrews and J.A. Asenjo, J. Chromatogr. B, 1998, 711, 285-293.
28. R.L. Gardas, M.G. Freire, P.J. Carvalho, I.M. Marrucho, I.M.A. Fonseca, A.G.M. Ferreira and J.A.P. Coutinho, J. Chem. Eng. Data, 2007, 52, 1881-1888.
29. W.L. Marshall and E.V. Jones, J.Phys. Chem., 1966, 70, 4028-4040.
30. J.W. Steed and J.L. Atwood, Supramolecular Chemistry, Hardcover, 2$^{ed.}$ 2009.
31. C. Reichardt, Green Chem., 2005, 7, 339-351.
32. M.G. Freire, C.M.S.S. Neves, A.M.S. Silva, L.M.N.B.F. Santos, I.M. Marrucho, L.P.N. Rebelo, J.K. Shah, E.J. Maginn and J.A.P. Coutinho, J. Phys. Chem. B, 2010, 114, 2004-2014.
33. M.G. Freire, P.J. Carvalho, R.L. Gardas, I.M Marrucho, L.M.N.B.F. Santos and J.A.P. Coutinho, J. Phys. Chem. B, 2008, 112, 1604-1610.

34. N.D. Khupse and A. Kumar, J. Phys. Chem. B, 2010, 114, 376-381.
35. L. Crowhurst, P.R. Mawdsley,J.M. Perez-Arlandis,P.A. Salter and T. Welton, Phys. Chem. Chem. Phys., 2003, 5, 2790-2794.
36. R. Lungwitz, V. Strehmel and S. Spange, New J. Chem., 2010, 34, 1135-1140.
37. A. Brandt, J.P. Hallett, D.J. Leak, R.J. Murphy and T. Welton, Green Chem., 2010, 12, 672-679.
38. R. Lungwitz and S. Spange, New J. Chem., 2008, 32, 392-394.
39. R. Lungwitz, M. Friedrich, W. Linert and S. Spange, New J. Chem., 2008, 32, 1493-1499.
40. M.G. Freire, C.M.S.S. Neves, P.J. Carvalho, R.L. Gardas, A.M. Fernandes, I.M. Marrucho, L.M.N.B.F. Santos and J.A.P. Coutinho, J. Phys. Chem. B, 2007, 111, 13082-13089.

2.2. Evaluation of the Impact of Phosphate Salts on the Formation of Ionic-Liquid-Based Aqueous Biphasic Systems

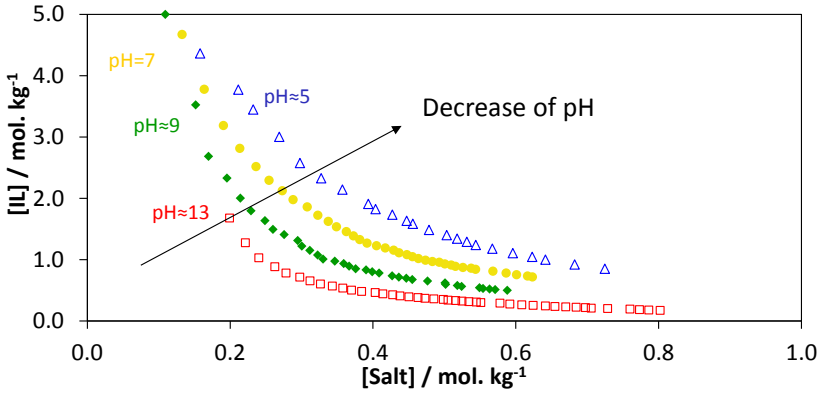

This chapter is based on the published manuscript: Mourão, T.; Cláudio, A. F. M.; Boal-Palheiros, I.; Freire, M. G.; Coutinho, J. A. P., "Evaluation of the Impact of Phosphate Salts on the Formation of Ionic-Liquid-Based Aqueous Biphasic Systems", J. Chem. Thermodyn., 2012, 54, 398-405.

Abstract

The present study aims at evaluating the capability of phosphate-based salts, whose anions can coexist in water depending on the media pH, to promote ABS formation with 1-butyl-3-methylimidazolium-based ionic liquids, as well as to infer on the influence of the ionic liquid anion in the overall process of liquid-liquid demixing. In this context, novel phase diagrams of ABS composed of several imidazolium-based ionic liquids and three phosphate salts and a mixture of salts (K_3PO_4, K_2HPO_4, K_2HPO_4 + KH_2PO_4, and KH_2PO_4) were determined by the cloud point titration method at 298 K and atmospheric pressure. The corresponding tie-line compositions, tie-line lengths, and pH values of the coexisting phases were also determined. The ILs ability to promote ABS is related with the hydrogen-bond basicity of the composing anion - the lower it is the higher the ability of the ionic fluid to undergo liquid-liquid demixing. Moreover, similar patterns on the ionic liquids sequence were observed with the different phosphate salts. The phosphate anion charge plays a determinant role in the formation of ABS. The two-phase formation aptitude (with a similar ionic liquid) decreases in the rank: K_3PO_4 > K_2HPO_4 > K_2HPO_4 + KH_2PO_4 > KH_2PO_4. Yet, besides the charge of the phosphate anion, the pH and ionic strength of the aqueous media also influence the phase separation ability.

Introduction

In spite of the efforts carried by a number of authors,[1-17] the formation of ionic-liquid-based ABS seems to be influenced by many variables besides the IL and salt identities and, as a result, a complete understanding of the mechanism and the underlying interactions has not yet been achieved. The picture more commonly accepted is that when a salt is dissolved in an aqueous solution, its ions are surrounded by a layer of water molecules, a process known as ionic hydration. In the present case, when an inorganic salt is added to an aqueous solution of an ionic liquid, the two solutes compete for the

solvent molecules. The competition is won by the inorganic ions (with a stronger interaction with the solvent), and those of the ionic liquid lose. There is a "migration" of solvent molecules away from the ions of the ionic liquid towards those of the inorganic salt, which, in turn, decreases the hydration and therefore the solubility of the ionic liquid in water. As a consequence, a phase rich in ionic liquid separates from the rest of the solution.[18,19] Moreover, a more prominent effect of the salt anion is to be expected: having a more diffuse valence electronic configuration than cations, they are more polarizable and have a higher aptitude to be hydrated.[7,18,20]

Most authors[14,16] stated that the Hofmeister series[21] is always obeyed and explained their ranks based on the Gibbs free energy of hydration of the ions[22], but there is considerable amount of evidence that the salting-out of ILs by inorganic salts from aqueous media is driven by an entropic process resulting from the preferential formation of water-ion complexes.[10,20,23] Hydration and hydrogen-bond formation are thus processes particularly relevant for the anions involved, whether they come from the salt or from the IL. Those processes are naturally pH dependent and this variable must also be accounted for. However, changing the pH of the salt´s solution almost invariably leads to changes in both the charge of the ions and on the extent of the hydrogen-bonding. Therefore, an evaluation of each factor independently is not a straightforward matter.

Henceforth, a systematic approach stems as a most valuable tool to study these effects. Since salting-in/-out effects are more pronounced when different anions are compared,[24,25] we propose here to study the IL anion influence in promoting ABS formation under different pH values obtained by the use of diverse phosphate-based salts. The cation 1-butyl-3-methylimidazolium was chosen due to its role as a model IL cation for which extensive data are available either from experimental studies[7,14,26-30] or from computer simulations.[31-33] In addition, the phosphate-based inorganic salts were selected because they are important ions in biological systems.[34] K_3PO_4 is indeed the most studied salt as a salting-out species[1,5,12,18,30,35-42] followed by KH_2PO_4 and KH_2PO_4/K_2HPO_4 mixtures which are also frequently used at the biotechnological field.[16,30,40,42,43] The present study aims at evaluating the ability of three phosphate salts, K_3PO_4, KH_2PO_4, and K_2HPO_4, and one of their mixtures (K_2HPO_4/KH_2PO_4), and whose anions can coexist in

water depending on the media pH, to promote the formation of ionic-liquid-based ABS, and also infer on the influence of the IL anion in the overall process. The results here obtained, along with data from previous works using K_3PO_4[18] and a buffered mixture KH_2PO_4/K_2HPO_4[43] enabled us to gather a broader picture on the evaluation of the influence of both the salt's anion charge and ionic liquid anion towards the formation of ABS.

Experimental Procedure

Materials

The ionic liquids used in this work were 1-butyl-3-methylimidazolium trifluoromethanesulfonate (triflate), $[C_4mim][CF_3SO_3]$; 1-butyl-3-methylimidazolium methanesulfonate, $[C_4mim][CH_3SO_3]$; 1-butyl-3-methylimidazolium acetate, $[C_4mim][CH_3CO_2]$; 1-butyl-3-methylimidazolium trifluoroacetate, $[C_4mim][CF_3CO_2]$; 1-butyl-3-methylimidazolium ethylsulfate, $[C_4mim][C_2H_5SO_4]$; 1-ethyl-3-methylimidazolium methylsulfate, $[C_4mim][CH_3SO_4]$; 1-butyl-3-methylimidazolium 4-methylbenzenesulfonate (tosylate), $[C_4mim][TOS]$; 1-butyl-3-methylimidazolium chloride, $[C_4mim]Cl$; 1-butyl-3-methylimidazolium bromide, $[C_4mim]Br$; 1-butyl-3-methylimidazolium dicyanamide, $[C_4mim][N(CN)_2]$; and 1-butyl-3-methylimidazolium dimethylphosphate, $[C_4mim][DMP]$. Their ionic structures are presented in Figure 2.2.1.

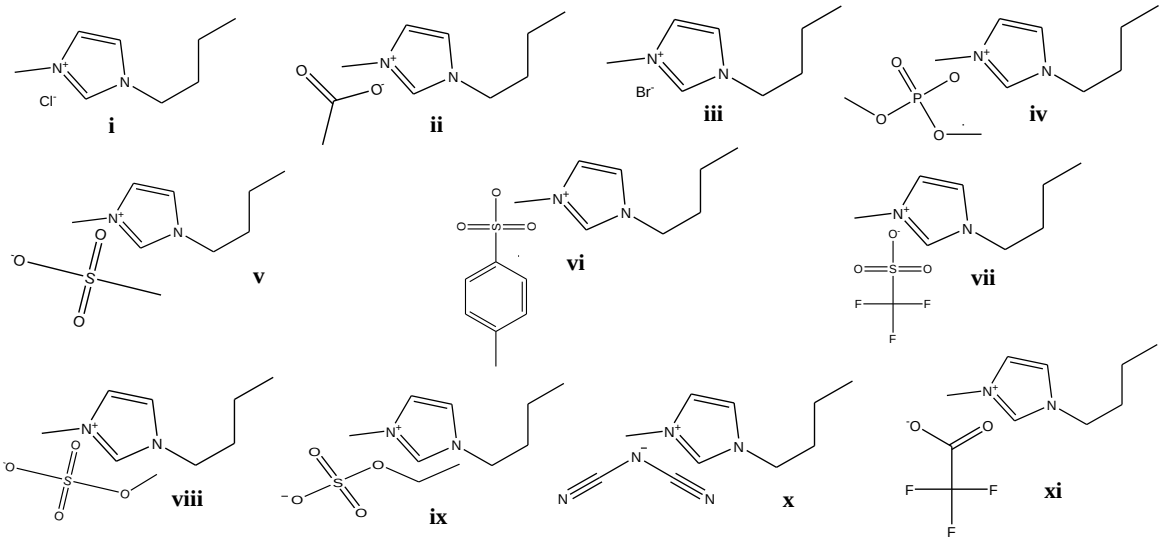

Figure 2.2.1: Chemical structures of the studied ILs: (i) [C_4mim]Cl; (ii) [C_4mim][CH_3CO_2]; (iii) [C_4mim]Br; (iv) [C_4mim][DMP]; (v) [C_4mim][CH_3SO_3]; (vi) [C_4mim][TOS]; (vii) [C_4mim][CF_3SO_3]; (viii) [C_4mim][CH_3SO_4]; (ix) [C_4mim][$C_2H_5SO_4$]; (x) [C_4mim][$N(CN)_2$]; (xi) [C_4mim][CF_3CO_2].

All ILs were supplied by Iolitec (Ionic Liquid Technologies, Germany). To reduce the volatile impurities content to negligible values, ILs individual samples were kept at constant agitation under vacuum and at a moderate temperature (323 K), for a minimum of 48 hours. After this purification step, the purity of each IL was further checked by ^{1}H, ^{13}C and ^{19}F NMR (when applicable) spectra and found to be > 98 wt % for all samples (water content < 1000 ppm as determined by Karl-Fischer titration and halogen content < 100 ppm). K_3PO_4 was from Sigma (purity > 98 wt %), K_2HPO_4 was from Riedel-de Haën (purity > 99 wt %), and KH_2PO_4 was from Panreac (purity > 99 wt %). The buffers used in the calibration of the pH meter equipment were the citric acid / sodium hydroxide / sodium chloride solution with a pH value of 4.00 (± 0.02), and the potassium dihydrogenphosphate / disodium hydrogenphosphate solution with a pH value of 7.00 (± 0.02), acquired from Fluka. Double distilled water, passed through a reverse osmosis system, and further treated with a Milli-Q plus 185 water purification equipment, was used in all experiments.

Phase Diagrams, Tie-Lines and pH measurements

The solubility curves of the systems composed of IL, water, and each of the phosphate salts were determined using the cloud point titration method at 298 K (± 1 K). The experimental procedure adopted in this work follows the method already validated by us

and described in **Chapter 2.1**. Aqueous solutions of each salt with variable mass fractions (50 wt % for K_3PO_4 and K_2HPO_4, 18 wt % for KH_2PO_4, and 40 wt % for the phosphate buffer composed of a mixture of the salts K_2HPO_4 and KH_2PO_4 with pH = 7.0 and Henderson-Hasselbalch equation equivalents = 1.09), and aqueous solutions of each IL in a range between 35-70 wt %, were prepared and used for the determination of the corresponding solubility curves. Repetitive drop-wise addition of the aqueous salt solution to each ionic liquid aqueous solution was carried out until the detection of a cloudy solution (the biphasic region), followed by the drop-wise addition of water until the formation of a clear and limpid solution (the monophasic region). To complete the phase diagrams the opposite addition of the ionic liquid aqueous solution to the salt solutions was also carried out. Drop-wise additions were carried out under constant stirring. The ternary systems compositions were determined by weight quantification of all components within ± 10^{-5} g.

The experimental binodal curves were fitted by least-squares regression according to equation 2.1.1 presented in **Chapter 2.1**.

For the determination of each tie-line (TL), a ternary mixture composed of phosphate salt + water + ionic liquid at the biphasic region was gravimetrically prepared as indicated in **Chapter 2.1**, and determined through the relationship between the weight of the top phase and the overall weight by the lever-arm rule using eqs. 2.1.2 to 2.1.6. Moreover, the tie-line length (TLL) was determined using equation 2.1.7.

Additionally, the pH values of the IL- and inorganic-salt-rich aqueous phases were measured at 298 K and as previously described (**Chapter 2.1**). The compositions at which the pH was measured correspond to the same compositions adopted for the TLs determination.

Results and Discussion

Since all systems studied on this work share the same IL cation, and the temperature (298 K) and pressure (1 bar) are also common, the comparison of the data allows the evaluation of the effect of the anion of the IL as well as the effect of the salt on the ABS formation.

Albeit ionic species are present in ionic liquid + inorganic salt ABS, and thus ion exchange might be expected, Bridges *et al*.[14] have shown that the ions migration in the coexisting phases of the ABS composed of $[C_4mim]Cl + K_3PO_4$ is not significant to yield inaccurate results on the concentration of each salt at both aqueous phases – taking into account the uncertainty already associated to the experimental procedure. This has been confirmed later on by Zafarani-Moattar and Hamzehzadeh[42] and by Neves *et al.*[44]; therefore, it may be assumed that the same is valid for the phosphate systems here studied.

Making use of the experimental data obtained in this work and those already published,[18,43] the main results can be grouped in four sets of phosphate-based ABS from highest to the least charge bearer salt: 1) potassium phosphate, K_3PO_4; 2) potassium hydrogenphosphate, K_2HPO_4; 3) phosphate buffer composed of potassium hydrogenphosphate + dihydrogenphosphate, $K_2HPO_4 + KH_2PO_4$; 4) potassium dihydrogenphosphate, KH_2PO_4. The weight fraction data for all the solubility curves measured in this work are presented in *Supporting Information* (Table S10 to S20).

Effect of Ionic Liquid on ABS Formation

Systems Composed of Potassium Phosphate, K_3PO_4

The binodal curves for $[C_4mim][CF_3SO_3]$, $[C_4mim]Br$, $[C_4mim][CH_3SO_3]$, $[C_4mim][N(CN)_2]$, $[C_4mim][CF_3SO_3]$, $[C_4mim]Cl$, $[C_4mim][CH_3CO_2]$, and $[C_4mim][CF_3CO_2]$ were reported in a previous paper[18] while new data for $[C_4mim][TOS]$, $[C_4mim][CH_3SO_4]$, $[C_4mim][C_2H_5SO_4]$ and $[C_4mim][DMP]$ are shown in Figure 2.2.2.

It should be stressed that all the phase diagrams are displayed in molality units to allow a more direct comparison among the different ionic liquids and salts effects.

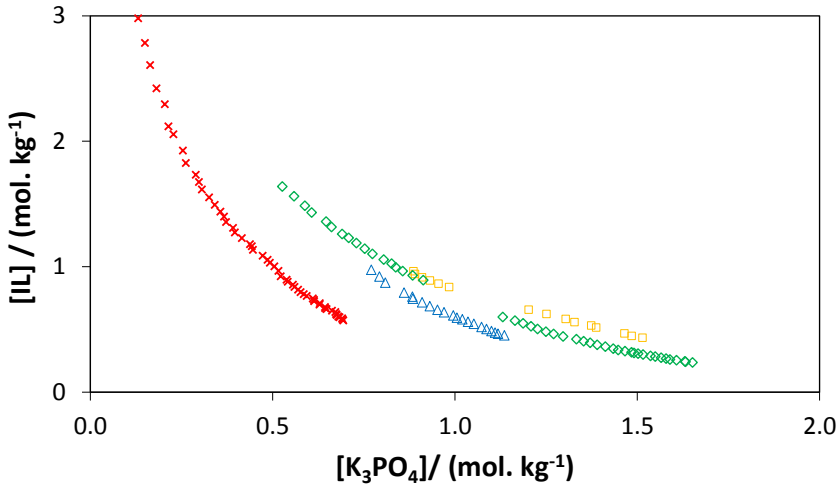

Figure 2.2.2: Ternary phase diagrams for [C_4mim]-based ILs + K_3PO_4 at 298 K and atmospheric pressure: ×, [C_4mim][TOS]; Δ, [C_4mim][$C_2H_5SO_4$]; □, [C_4mim][DMP]; ◇, [C_4mim][CH_3SO_4].

The parameters obtained for the regression of the solubility curves of the IL+ K_3PO_4 + H_2O systems using equation 2.1.1 are presented in Table 2.2.1.

Table 2.2.1: Parameters *A*, *B* and *C* of eq. 2.1.1 (and respective standard deviations, σ, and correlation coefficients, R^2) for the [C_4mim]-based ILs + phosphate salt + H_2O systems at 298 K.

IL + K_3PO_4 + Water	***A* ± σ**	***B* ± σ**	**10^5(*C* ± σ)**	**R^2**
[C_4mim][CH_3SO_4]	82.78 ± 1.90	-0.308 ± 0.007	6.67 ± 0.09	0.9998
[C_4mim][$C_2H_5SO_4$]	213.63 ± 57.22	-0.587 ± 0.079	5.48 ± 1.17	0.9984
[C_4mim][TOS]	89.88 ± 1.01	-0.378 ± 0.005	19.4 ± 0.53	0.9993
[C_4mim][DMP]	51.24 ± 12.04	-0.192 ± 0.065	4.57± 0.63	0.9996
IL + K_2HPO_4 + Water	***A* ± σ**	***B* ± σ**	**10^5(*C* ± σ)**	**R^2**
[C_4mim]Cl	92.70 ± 3.29	-0.370 ± 0.012	1.80 ± 2.01	0.9919
[C_4mim]Br	73.80 ± 1.27	-0.267 ± 0.004	4.77 ± 0.36	0.9970
[C_4mim][CH_3SO_4]	81.48 ± 3.17	-0.284 ± 0.010	3.67 ± 0.07	0.9989
[C_4mim][$C_2H_5SO_4$]	87.20 ± 4.11	-0.322 ± 0.017	3.85 ± 0.74	0.9985
[C_4mim][$N(CN)_2$]	84.27 ± 0.73	-0.378 ± 0.004	17.34 ± 0.51	0.9986
[C_4mim][TOS]	89.88 ± 0.62	-0.347 ±0.003	13.28 ± 0.02	0.9996
[C_4mim][DMP]	75.21 ± 1.00	-0.272 ± 0.004	2.28 ± 0.03	0.9996
[C_4mim][CH_3CO_2]	87.39 ± 2.54	-0.342 ± 0.009	1.64 ± 0.12	0.9992
[C_4mim][CH_3SO_3]	83.16 ±0.40	-0.291 ± 0.002	2.16± 0.03	0.9996
[C_4mim][CF_3SO_3]	225.87 ± 8.38	-0.965 ± 0.021	1.00 ± 5.85	0.9962

$[C_4mim][CF_3CO_2]$	86.34 ± 0.62	-0.308 ± 0.003	6.17 ± 0.06	0.9997
IL + K_2HPO_4/KH_2PO_4+ Water	***A ± σ***	***B ± σ***	**10^5(*C ± σ*)**	***R*^{2}**
$[C_4mim]Br$	80.80 ± 0.77	-0.301 ± 0.004	2.31 ± 1.58	0.9994
$[C_4mim][CH_3SO_4]$	72.42 ± 2.38	-0.246 ± 0.008	3.22 ± 0.07	0.9996
[C4mim][DMP]	74.36 ± 2.96	-0.258 ± 0.011	2.07 ± 0.14	0.9996
$[C_4mim][CF_3CO_2]$	114.81 ± 2.80	-0.415 ± 0.010	2.88 ± 0.03	0.9977
IL + KH_2PO_4 + Water	***A ± σ***	***B ± σ***	**10^5(*C ± σ*)**	***R*^{2}**
$[C_4mim][CF_3SO_3]$	126.95 ± 5.51	-0.542 ± 0.025	39.93 ± 6.70	0.9977

The ternary system compositions used at the biphasic region and the TL compositions, the respective tie-line lengths, and pH values are reported in Table 2.2.2.

Table 2.2.2: Compositions (mass fraction) for the $[C_4mim]$-based ILs + phosphate salt + H_2O systems at 298 K, and respective values of TLL, and pH of the coexisting phases.

IL	**100·(Mass fraction composition ± 2^{-4})** [a]						**TLL ±0.02**[a]	**pH_B ±0.02**[a]	**pH_T ±0.02**[a]
	$[IL]_T$	**$[Salt]_T$**	**$[IL]_M$**	**$[Salt]_M$**	**$[IL]_B$**	**$[Salt]_B$**			
IL + K_3PO_4 + Water									
$[C_4mim][CH_3SO_4]$	42.95	4.47	24.88	14.87	6.43	24.85	41.82	12.91	13.30
	52.07	2.27	29.54	14.51	3.22	28.82	55.60	12.94	13.07
$[C_4mim][C_2H_5SO_4]$	41.22	7.62	24.90	14.68	7.25	22.31	37.01	12.68	12.91
	53.46	5.49	29.99	14.68	5.37	24.32	51.64	12.67	12.90
$[C_4mim][TOS]$	52.82	1.96	29.79	10.27	3.93	19.58	52.00	12.56	12.99
	62.84	0.90	37.16	10.72	0.75	24.64	66.48	13.05	12.91
$[C_4mim][DMP]$	39.48	1.85	19.87	19.73	1.87	36.15	50.90	13.40	13.56
	46.53	0.25	24.65	19.87	0.58	41.45	61.72	13.54	13.77
IL + K_2HPO_4 + Water									
$[C_4mim]Cl$	37.86	5.81	33.37	9.81	4.58	35.45	44.57	9.46	9.46
	44.18	3.99	37.67	9.84	2.35	41.52	56.20	9.80	9.58
$[C_4mim]Br$	48.12	2.56	37.78	10.14	1.35	36.83	57.98	9.40	9.36
	57.78	0.84	44.76	10.60	0.22	44.02	71.96	9.60	9.57
$[C_4mim][CH_3SO_4]$	54.11	2.07	24.84	20.18	4.36	32.84	58.50	8.72	8.75

	60.39	1.11	29.93	20.07	2.11	37.39	68.65	8.81	9.08
$[C_4mim][C_2H_5SO_4]$	34.02	8.17	23.74	15.48	7.88	26.76	32.09	8.38	8.35
	49.48	3.08	25.29	19.90	2.08	36.03	57.73	8.52	8.72
$[C_4mim][N(CN)_2]$	49.50	1.97	30.00	10.14	2.50	21.65	50.95	8.46	9.25
	58.26	0.94	37.86	9.97	0.48	26.50	63.18	9.17	9.34
	43.04	4.38	29.88	10.11	5.88	20.57	40.53	9.10	9.32
$[C_4mim][TOS]$	53.76	2.19	25.35	14.90	1.75	25.46	56.98	9.18	9.59
	55.39	1.94	38.94	9.83	0.74	28.13	60.60	9.27	9.95
$[C_4mim][DMP]$	44.02	3.86	37.88	9.94	1.25	46.21	60.19	9.62	9.61
	57.26	1.01	29.52	24.87	0.68	49.75	74.64	10.02	10.20
$[C_4mim][CH_3CO_2]$	30.83	9.05	24.92	15.10	5.95	34.50	35.59	8.25	8.07
	38.61	5.65	29.88	15.08	1.90	45.27	54.01	8.07	8.08
$[C_4mim][CH_3SO_3]$	42.24	5.38	37.35	10.25	1.40	46.08	57.67	9.20	9.69
	44.79	4.50	30.64	19.74	0.47	52.25	65.15	9.44	9.89
$[C_4mim][CF_3SO_3]$	72.24	1.40	19.97	10.04	7.78	12.06	65.34	8.60	8.74
	69.50	1.49	37.91	9.95	3.03	19.30	68.81	9.09	9.26
IL + KH_2PO_4/K_2HPO_4 + Water									
$[C_4mim]Br$	46.00	3.49	37.89	10.03	3.77	37.56	54.26	7.45	7.47
	54.72	1.67	44.83	9.99	0.96	46.85	70.22	7.50	7.48
$[C_4mim][CH_3SO_4]$	43.95	4.08	24.98	19.98	2.32	38.95	54.31	7.09	7.27
	52.71	1.66	29.95	19.95	1.08	43.14	66.23	7.43	7.42
[C4mim][DMP]	44.58	3.91	38.00	9.98	2.82	42.50	56.87	7.50	7.53
	53.01	1.72	29.94	24.52	0.46	53.68	73.91	7.59	7.62
IL + KH_2PO_4 + Water system									
$[C_4mim][CF_3SO_3]$	45.29	3.50	30.05	9.92	0.10	22.54	49.03	5.08	4.75
	53.91	2.47	37.67	9.92	0.00	27.21	59.32	5.96	4.83

[a] Expanded uncertainty at the 0.95 confidence level evaluated from the standard deviation and applying a coverage factor k = 2.

In Figure 2.2.2, the closer the curve is to the axes the larger the biphasic area and the stronger the demixing ability of the ionic liquid anion. On the systems here studied we found that ability to increase in the order: $[C_4mim][TOS]$ >$[C_4mim][C_2H_5SO_4]$ > $[C_4mim][DMP] \approx [C_4mim][CH_3SO_4]$.

The PO_4^{3-} equilibrium concentration values were determined from the corresponding values of the total phosphate concentration and the basicity constant, Kb_3, (the two successive hydrolysis reactions can be neglected, as well as water hydrolysis) and were always greater than 90 % of the total amount. The triple charge and the ability of PO_4^{3-} to act as a hydrogen acceptor towards water do certainly have an important contribution in extensive formation of complexes with water; the competition for water molecules will lead to the dehydration of IL ions which release water molecules, and to an increase of the surface tension of the IL cavity. Therefore, PO_4^{3-} is a strong salting-out species and leads to the liquid-liquid demixing of a wide range of aqueous solutions of ionic liquids as shown in Table 2.2.4.

Anions interact with water molecules by an approximately linear hydrogen bond, suggesting that the dominant interactions are short range forces of a chemical nature.[45] Thus, the ability for a given anion to be preferentially hydrated depends on its ability to hydrogen bond. In fact, the ionic liquid anion forming ability for ABS follows a close trend to the one presented by their H-bond basicity values.[46,47]

The H-bond basicity is a descriptor of solvation interactions at a molecular level that relies on empirical scales based on solvent interactions with a reference solute.[49,50] Those scales are usually based on solvatochromic probes, such as the Reichardt $E_T(30)$[51] and the Kamlet-Taft.[52] If we consider the literature[48,50,53] values using the ionic solvatochromic probe $[Fe(phen)_2(CN)_2]ClO_4$, we notice some discrepancy among them, so we considered values from the least number of authors (Table 2.2.3).

Table 2.2.3: Hydrogen bond basicity (β) of $[C_4mim]$-based ILs with the solvatochromic probe $[Fe(phen)_2(CN)_2]ClO_4$.

Ionic liquid	β
$[C_4mim][CF_3SO_3]$	0.49[48]
$[C_4mim][N(CN)_2]$	0.60[48]
$[C_4mim][CH_3SO_4]$	0.66[48]
$[C_4mim][CH_3SO_3]$	0.85[50]
$[C_4mim]Br$	0.87[50]
$[C_4mim]Cl$	0.95[50]

$[C_4mim][DMP]$	1.12[48]
$[C_4mim][CH_3CO_2]$	1.20[48]

As it can be noticed the rank obtained from the binodal curves follows closely the H-bond basicity values of the ionic liquids, as depicted in Figure 2.3.3, and as previously discussed in **Chapter 2.1.**

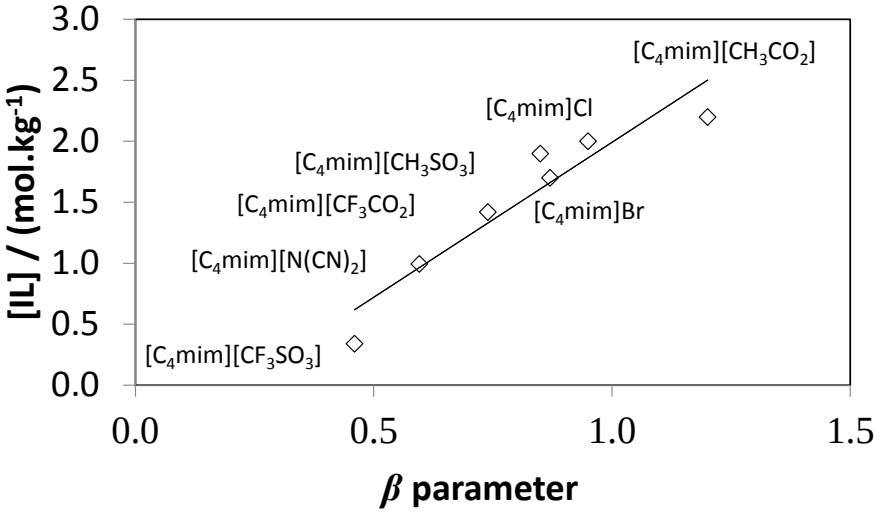

Figure 2.2.3: Ionic liquid molality, taken from each binodal curve and at which the K_3PO_4 molality is equal to 0.5 mol·kg^{-1}, as a function of the hydrogen bond basicity values (β).[48,50]

Systems Composed of Potassium Hydrogenphosphate, K_2HPO_4

A large range of ILs were studied using K_2HPO_4, and the experimental phase diagrams at 298 K and atmospheric pressure for the systems constituted by IL+ K_2HPO_4 + H_2O are presented in Figure 2.2.4. The parameters obtained for the regression of the corresponding solubility curves using equation 2.1.1 are presented in Table 2.2.1. The TL compositions, tie-line lengths, and pH values of the coexisting phases are reported in Table 2.2.2.

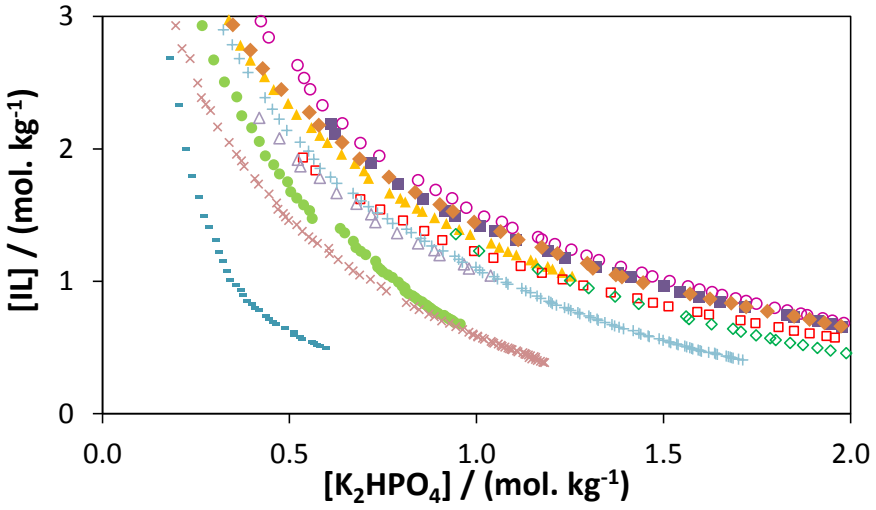

Figure 2.2.4: Ternary phase diagrams for [C_4mim]-based ILs + K_2HPO4 at 298 K and atmospheric pressure: -, [C_4mim][CF_3SO_3]; ●, [C_4mim][$N(CN)_2$]; ×, [C_4mim][TOS]; △, [C_4mim][$C_2H_5SO_4$]; +, [C_4mim][CF_3CO_2]; □, [C_4mim][DMP]; ◇, [C_4mim][CH_3SO_4]; ▲, [C_4mim]Br; ◆, [C_4mim][CH_3SO_3]; ■, [C_4mim][CH_3CO_2]; ○, [C_4mim]Cl

An example of the tie-lines obtained in this work can be appreciated in Figure 2.2.5 for the system composed of [C_4mim][$N(CN)_2$] + K_2HPO_4 + water.

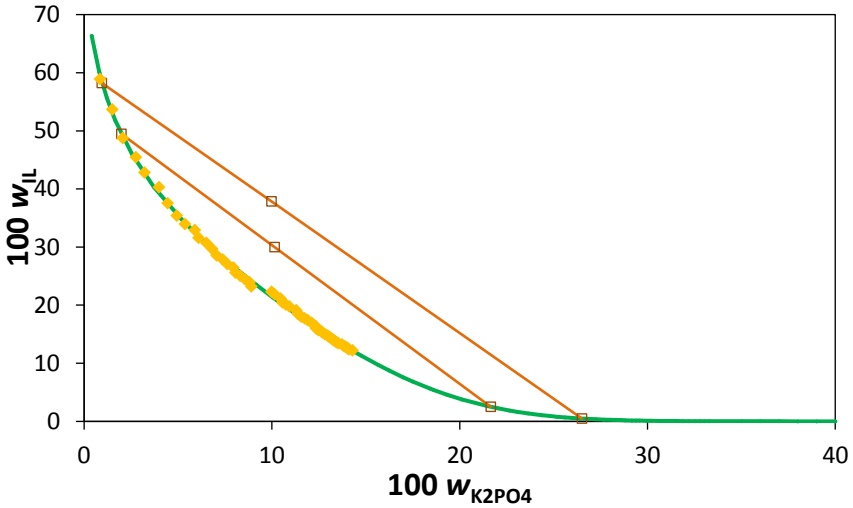

Figure 2.2.5: Ternary phase diagram for [C_4mim][$N(CN)_2$] + K_2HPO_4 + water at 298 K and atmospheric pressure: ◆, experimental binodal curve data; □, TL data, —, fitting by equation 2.1.1.

When considering the basicity equilibrium for the HPO_4^{2-} aqueous solutions (the species acidic character being negligible) small differences (< 1 %) between nominal and equilibrium values are to be expected and can be ignored.

If we choose the salt concentration of 1.0 mol·kg^{-1} to compare the relative ability of the IL for ABS formation we observe that it decreases according to the following order: [C_4mim][CF_3SO_3] > [C_4mim][TOS] ≈ [C_4mim][$N(CN)_2$] > [C_4mim][$C_2H_5SO_4$] > [C_4mim][CF_3CO_2] > [C_4mim]Br ≈ [C_4mim][CH_3SO_4] ≈ [C_4mim][DMP] > [C_4mim][CH_3CO_2] > [C_4mim][CH_3SO_3] > [C_4mim]Cl. The systems formed by the addition of K_2HPO_4 closely follow the trend observed for the K_3PO_4 series presented above; yet, with higher values for their saturation solubilities. This is not an unexpected result considering the comparatively lower charge density of HPO_4^{2-} and its inherent lower hydration capability.

Besides the general trend and that the ionic liquid extremes are almost the same, when comparing the sequences obtained with both salts, K_3PO_4 and K_2HPO_4, there are however slight differences in the ionic liquids rank. For instance, the acetate-based ionic liquid is more easily salted-out than [C_4mim]Cl when using K_2HPO_4. It should be noted that the interaction of IL with water is mainly dependent on the nature and concentration of the IL anion but also from the relative proportions of all players.[54-56] The processes seem to be surface phenomena and dominated by short range interactions with a marginal effect in the bulk water; the IL assumes therefore the prominent role.[54] Minor changes in pH may induce disturbances at the IL surface and in fact the difference in pH of both series is of several units, as can be seen in Table 2.2.2. Impurities may also affect the IL surface, making reproducibility difficult to achieve.[54] Nevertheless, the presence of impurities affecting these experiments can be overruled by the close agreement between them and previous results from our group[18] as well as from others[30,57]. In *Supporting Information (*Figure S1) the comparison of our results with literature ones for the systems [C_4mim]Cl, [C_4mim]Br and [C_4mim][CH_3CO_2] is presented.

Using K_2HPO_4 as salt, it is also possible to see the correlation between the ionic liquid anion ABS forming ability and the respective H-bond basicity values - Figure 2.2.6.

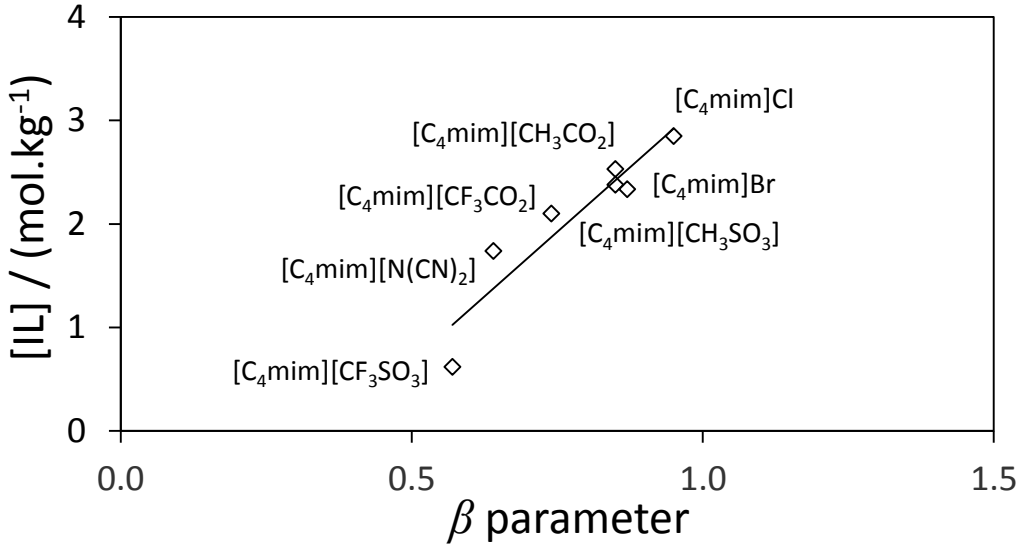

Figure 2.2.6: Ionic liquid molality, taken from each binodal curve and at which the K_2HPO_4 molality is equal to 0.5 mol·kg^{-1}, as a function of the hydrogen bond basicity values (β).[50]

Systems Composed of Potassium Hydrogenphosphate + Dihydrogenphosphate, K_2HPO_4 + KH_2PO_4

The combination of K_2HPO_4 + KH_2PO_4 (1.00 *m* + 1.09 *m*) to obtain a phosphate buffer solution at a neutral pH (7.0) and to be used in ABS formation was addressed in a previous study.[43] Nevertheless, to complete the study, new data for [C_4mim]Br, [C_4mim][CH_3SO_4], [C_4mim][DMP] and [C_4mim][CF_3CO_2] were obtained in this work. The regression parameters estimated by least-squares regression of the cloud-point data using equation 2.1.1 are presented in Table 2.2.1. In Table 2.2.2 are reported the ternary system compositions, and the respective tie-line lengths and pH values at the coexisting phases.

The experimental phase diagrams at 298 K and atmospheric pressure for the systems making use of the phosphate buffer are shown in Figure 2.2.7.

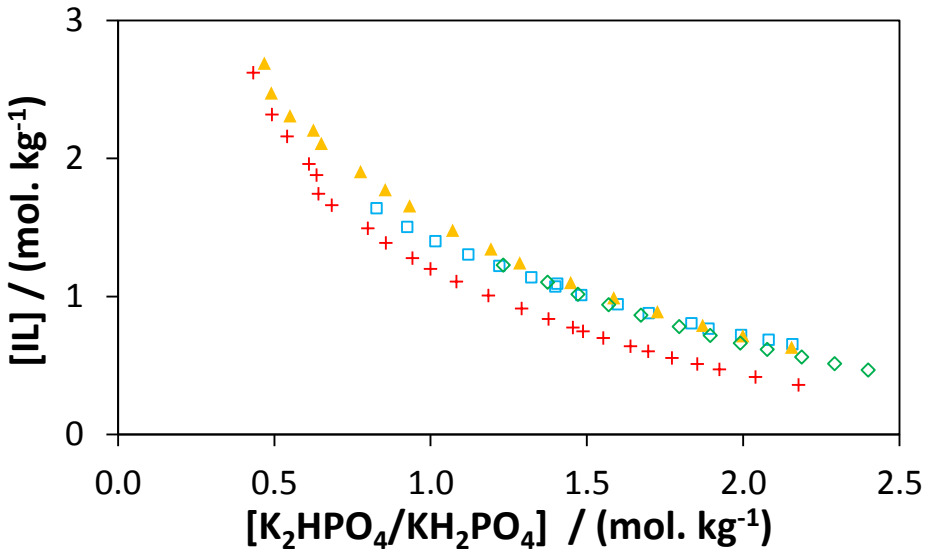

Figure 2.2.7: Ternary phase diagrams for [C_4mim]-based ILs + K_2HPO_4/KH_2PO_4 at 298 K and atmospheric pressure: +, [C_4mim][CF_3CO_2]; □, [C_4mim][DMP]; ◊, [C_4mim][CH_3SO_4]; ▲, [C_4mim]Br.

From the solubility curves we can order the ILs according to their ability to form biphasic systems: [C_4mim][CF_3CO_2] > [C_4mim][DMP] > [C_4mim][CH_3SO_4] >[C_4mim]Br. When considering also the ILs studied previously[43] with this mixture of salts a broader ranking is obtained. All these systems present consistently higher saturation solubility values when compared with the corresponding ones using K_2HPO_4 salt solution alone, thus revealing the importance of pH in the interactions among all ions present in solution and/or the importance of substituting a stronger salting-out anion (HPO_4^{2-}) by a weaker one ($H_2PO_4^-$). The ranking obtained for the ILs ability to promote ABS with this mixture of salts is much similar to the ones presented before using the other phosphate salt solutions. Since the cation is the same for all the ILs, that means that the IL anion demixing ability follows a trend close to the previous ones, indicating coincidental mechanisms of ABS formation for both phosphate salts. Additionally, the ability to form ABS also correlates with the H-bond basicity values of the investigated ILs and as shown in Figure 2.2.8.

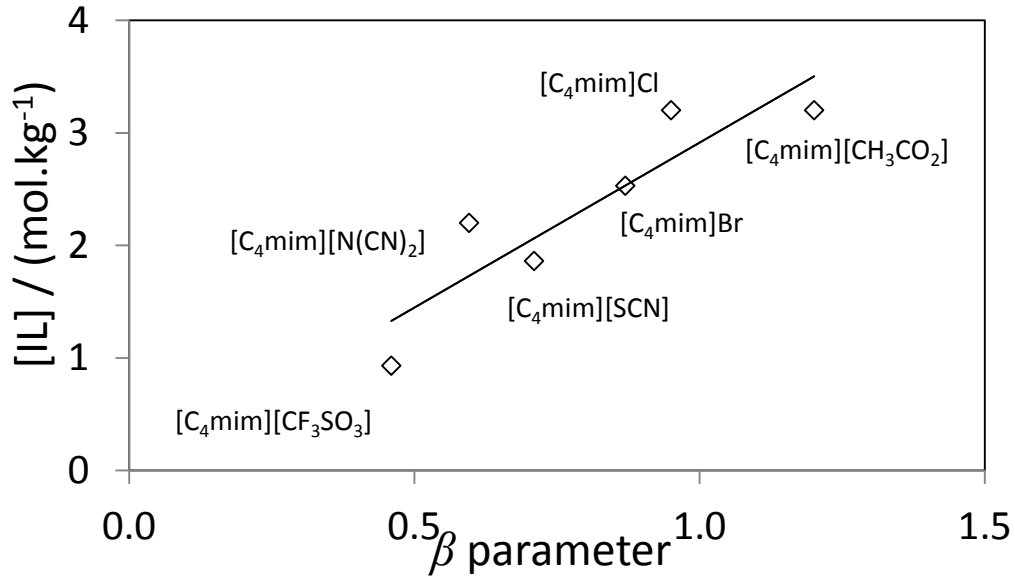

Figure 2.2.8: Ionic liquid molality, taken from each binodal curve and at which the K_2HPO_4/ KH_2PO_4 molality is equal to 0.5 mol·kg^{-1}, as a function of the hydrogen bond basicity values (β).[48]

Systems Composed of Potassium Dihydrogenphosphate, KH_2PO_4

To complete the study of the phosphate salt series, the ABS formation using the most protonated phosphate species, KH_2PO_4, was further investigated. Although acidic in aqueous solutions, the equilibrium and the nominal concentrations of $H_2PO_4^-$ are not significantly different. All the ILs investigated were combined with this salt, yet only the $[C_4mim][CF_3SO_3]$ was able to form a biphasic system. For the remaining systems solid-liquid phases were observed instead of liquid-liquid phases. Nevertheless, it should be remarked that although literature presents this phosphate anion as not amenable to inducing liquid-liquid demixing,[15] it was here observed the formation of ABS with $[C_4mim][CF_3SO_3]$ – an ionic liquid with low affinity for water. The binodal curve obtained with $[C_4mim][CF_3SO_3]$ and KH_2PO_4 solutions, along with the curves obtained for the same IL and all the other different phosphate solutions, are presented in Figure 2.2.9. The regression parameters obtained for the equation 2.1.1 estimated by least-squares regression of the cloud-point data are presented in Table 2.2.1 and the ternary system compositions, tie-line lengths, and pH values are reported in Table 2.2.2.

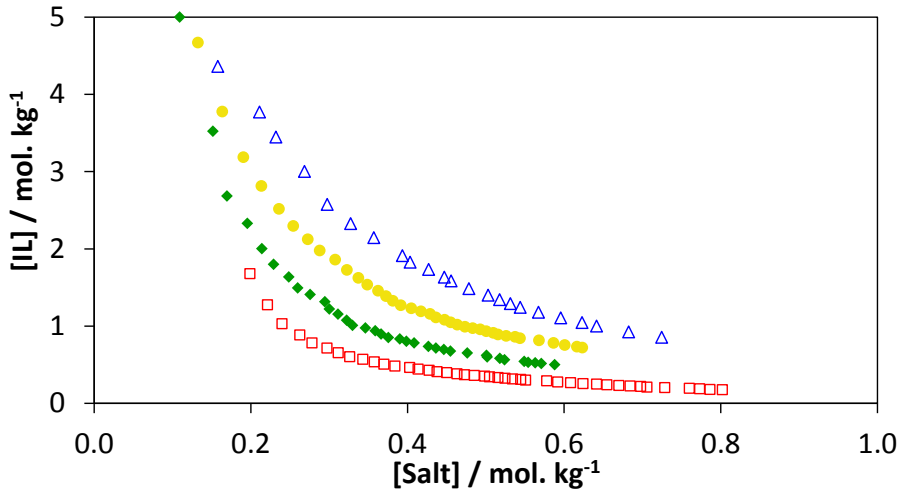

Figure 2.2.9: Ternary phase diagrams for $[C_4mim][CF_3SO_3]$ and different potassium-phosphate-based salts ABS at 298 K and atmospheric pressure: □, K_3PO_4 [20]; ◆, K_2HPO_4; ●, K_2HPO_4/KH_2PO_4[45] (pH= 7.0); Δ, KH_2PO_4.

Considering all the salt series studied, whose results are summarized in Table 2.2.4, we notice that $[C_4mim][CF_3SO_3]$ consistently proved to be the IL most prone to form biphasic systems. This strong ability was already acknowledged as this IL had been able to undergo liquid-liquid demixing with other weak salting-out species, such as NaCl,[17] polymers,[58] carbohydrates[59] and amino acids[38]. The ILs ability to promote ABS systems follows approximately the same order independently of the salt, which seems to emphasize the prominent role of the ILs anion identity and its hydrogen-bonding donor ability in the two phase formation.

Table 2.2.4: Ability of the various $[C_4mim]$-based ILs for phase separation (for 1 mo·kg^{-1} of phosphate salt).

Salts	Ability of $[C_4mim]$-based ILs for ABS formation
K_3PO_4	$[C_4mim][CF_3SO_3]$[18] > $[C_4mim][N(CN)_2]$[18] > $[C_4mim][TOS]$ > $[C_4mim][CF_3CO_2]$[18] > $[C_4mim][C_2H_5SO_4]$ > $[C_4mim]Br$[18] ≈ $[C_4mim][CH_3SO_4]$ > $[C_4mim][DMP]$ > $[C_4mim][CH_3SO_3]$[18] > $[C_4mim]Cl$[18]> $[C_4mim][CH_3CO_2]$[18]
K_2HPO_4	$[C_4mim][CF_3SO_3]$ > $[C_4mim][TOS]$ ≈ $[C_4mim][N(CN)_2]$ > $[C_4mim][C_2H_5SO_4]$ > $[C_4mim][CF_3CO_2]$ ≈ $[C_4mim][CH_3SO_4]$ ≈ $[C_4mim][DMP]$ > $[C_4mim]Br$ > $[C_4mim][CH_3CO_2]$ ≈ $[C_4mim][CH_3SO_3]$ > $[C_4mim]Cl$

K_2HPO_4/ KH_2PO_4	$[C_4mim][CF_3SO_3]$[43] > $[C_4mim][TOS]$[43] $[C_4mim][N(CN)_2]$[43] > $[C_4mim][CF_3CO_2]$ > $[C_4mim][C_2H_5SO_4]$[43] ≈ $[C_4mim][DMP]$ ≈ $[C_4mim][CH_3SO_4]$ > $[C_4mim][CH_3CO_2]$[43] ≈ $[C_4mim]Br$ > $[C_4mim]Cl$[43]> $[C_4mim][CH_3SO_3]$[43]
KH_2PO_4	$[C_4mim][CF_3SO_3]$

Effect of the Phosphate Salt on ABS Formation

A comparison of the different sets of results is now carried out aiming at determine the influence of the salt in the ABS forming ability. Figure 2.2.9 shows the effect of the replacement of the highly basic and charged PO_4^{3-} anion by less alkaline and less charged anions, $H_2PO_4^-$ and the phosphate buffer mixture, HPO_4^{2-} + $H_2PO_4^-$, ending up with the slightly acidic anion, $H_2PO_4^-$. This pattern reflects curves successively more apart from both axes revealing a decreased ability for biphasic systems promotion that follows the order: PO_4^{3-} > HPO_4^{2-} > (HPO_4^{2-} + $H_2PO_4^-$) > $H_2PO_4^-$.

The results shown in Figure 2.2.9 corroborate the qualitative trend on the salt anions ability to induce the salting-out of the ionic liquid that closely follows the Hofmeister series.[21] The anion which induces the strongest salting-out effect is PO_4^{3-} as previously observed by our group[10] and others[14]. Moreover, the salt´s ion charge plays a significant role being responsible for the formation of hydration complexes.[17] Although the hydration sphere of PO_4^{3-} ion seems to have less water molecules than those of HPO_4^{2-} and $H_2PO_4^-$,[60,61] which, in a superficial analysis, could suggest a comparatively weaker interaction of the PO_4^{3-} with water and a lower capability to create ABS, it should be stressed that the data refer to the number of water molecules in the first hydration shell (not the whole hydration sphere), and not to the strength of their interaction. Due to its higher charge, PO_4^{3-} will more strongly and readily hydrogen bond with water than the less charged phosphate species. Those studies[60,61] also suggest that the hydration sphere for both hydrogen and dihydrogen phosphate anions are similar, as far as the number of water molecules and their geometry are concerned; however, as shown here, a drastic reduction in the ABS formation ability is observed when changing from hydrogen to dihydrogen phosphate salt. A possible explanation for those results is to consider that the

higher the charge of the anion the more intense is the electric field, and the more aligned are the dipoles of the water molecules around the anion, with the exact number of hydrogen bonds being less important than the cohesion brought by the alignment of the dipoles of the surrounding water molecules. This would rank the interaction anion/water as obtained by us: $PO_4^{-3} > HPO_4^{-2} > H_2PO_4^-$. Other factors being equal, water molecules are held more strongly by molecules with a net charge than by molecules with no net charge.[62]

Apart from the charge of the salt´s anion, the replacement of PO_4^{3-} anions with increasingly protonated phosphate species carries other significant changes along, namely a decrease of the medium ionic strength and a decrease in solution´s pH. According to Tomé *et al.*[19] salting-in/-out effects are considerably dependent on the ionic strength and, in fact, when displacing K_3PO_4 with KH_2PO_4, the ionic strength varies six-fold from 6 *m* to 1 *m.* This in turn will cause significant changes in the surface tension that, together with the formation of hydration complexes, are particularly relevant to the solution behavior of high charge density ions such as PO_4^{3-} and HPO_4^{2-}.[12] Another dramatic change occurs concurrently when K_2HPO_4 replaces K_3PO_4: the OH^- concentration decreases nearly four orders of magnitude, and the corresponding decrease is close to five orders when the salt KH_2PO_4 replaces K_2HPO_4, as can be appreciated in Table 2.2.2. In fact, the pH difference between the two phases in equilibrium for the systems herein studied is usually smaller than 0.5 pH units. Identical differences were reported in **Chapter 2.1**,[63] where it was studied ionic-liquid-based ABS formation by the addition of Na_2SO_4 evidencing a considerable extension of the hydrogen ion equilibrium between both aqueous phases. Although the migration of ions in the coexisting phases of ABS might accomplish an irrelevant mass transfer to affect major ions,[14] for the most mobile ions in solution, hydronium and hydroxide, it is sufficient to allow convergent pH values for both phases. Since the pH of the IL solution follows closely the pH values of the solution of the salt, the hydroxide ion concentration in the IL solution decreases abruptly when changing the salt from K_3PO_4 to K_2HPO_4, and then to the buffer and to KH_2PO_4. The C2 carbon atom of the imidazolium cation shows a higher affinity for OH^- ions than for the identically charged monovalent anions.[64] The decrease of hydroxide ions in solution will

reduce the competition with the IL anions, making more difficult to bring the IL ions apart, and thus the ability of ABS formation is highest for PO_4^{3-} and severely reduced for the acidic $H_2PO_4^-$. The media pH may have a steady although small influence on ABS formation; the lower it is, the higher the saturation solubility values, but the effect turns from quantitative to qualitative when the pH goes from alkaline or neutral to moderately acidic (see Table 2.2.2).

The precise mechanism of salting-out is not fully understood, and different interactions have been proposed to explain the mechanisms involved[22,65] and where hydration phenomena stem as having a key role; specific hydration values for each ion in different pairs are acknowledged, but no real predictability exists yet.[66] Several studies however relate the IL salting-out with the Gibbs free energy and the entropy of hydration of the ions of the inorganic salt.[67] It was shown that solubility data of hydrophobic IL in aqueous salt solution correlates well with the molar entropy of hydration of the salt ions.[7,20,23] Shahariari *et al*.[17] in a recent study using $[C_4mim][CF_3SO_3]$ and an extensive range of salts concluded that the entropy of hydration of the inorganic salts, and not the free Gibbs energy, has a dominant role in the formation of ion-water complexes and in promoting ionic-liquid-based ABS. However caution should be used when generalizing these results, since when different salts are used discrepancies may occur.[65,66,68] Additionally it has to be considered that the aqueous solutions in ABS may be so concentrated that there is no "bulk" water present and all water molecules are interacting with one or more ions.[69]

Conclusions

Novel phase diagrams of ABS for several imidazolium-based ILs and three phosphate salts and a mixture of salts (K_3PO_4, K_2HPO_4, K_2HPO_4 + KH_2PO_4, and KH_2PO_4) were determined by the cloud point titration method at 298 K. From the gathered results, the ability of different IL anions, as well as the salt employed, to promote the formation of ABS was presented and discussed.

As far as the ability of creating ABS is concerned it was observed that the sequences of ILs follow similar patterns for the different phosphate salts series. In general, the lower the hydrogen bond basicity of the IL (*i.e.*, less affinity of the IL anion to interact with the protons of water), the higher the ability of the ionic fluid to undergo liquid−liquid demixing in the presence of the phosphate salt.

When considering the different forms of the phosphate anions as salting-out agents it was found that the charge of the phosphate anion plays the most determinant role (the higher it is the better the salting-out agent) and the liquid-liquid demixing of a similar ionic liquid decreases in the rank: K_3PO_4 > K_2HPO_4 > K_2HPO_4 + KH_2PO_4 > KH_2PO_4. However, this effect is attributable not only to the salt´s anion charge but also to pH and ionic strength changes. In fact there was a considerable reduction in the number of ABS formed when the acidic phosphate salt, KH_2PO_4, was used. Only [C_4mim][CF_3SO_3] was able to form ABS with this acidic salt.

Although the interactions among all players in a given ABS (water / IL / salt) are not yet completely understood we put forward a thorough set of results for the IL/phosphate salts based systems. The establishment of this correlation pattern, even if fraught with some empiricism, is of paramount importance as it provides a grounded basis for a proper choice of a system according to its purpose or application, as well as a guidance when pursuing further studies aiming at unveiling the intricate interactions in these systems.

References

1. C.L.S. Louros, A.F.M. Cláudio, C.M.S.S. Neves, M.G. Freire, I.M. Marrucho, J. Pauly and J. A. P. Coutinho, Int. J. Mol. Sci., 2010,11, 1777-1791.
2. A.F.M. Cláudio, M.G. Freire, C.S.R. Freire, A.J.D. Silvestre and J.A.P. Coutinho, Sep. Purif. Technol.,2010, 75, 39-47.
3. J.F.B. Pereira, A.S. Lima, M.G. Freire and J.A.P. Coutinho, Green Chem.,2010, 12, 1661-1669.
4. M.G. Freire; A.F.M. Cláudio; J.M.M Araújo; J.A.P. Coutinho; I.M.Marrucho; J.N. Canongia Lopes and L.P.N. Rebelo, Chem. Soc. Rev.,2012, 41, 4966-4995.
5. K.E. Gutowski, G.A. Broker, H.D. Willauer, J.G. Huddleston, R.P. Swatloski, J.D. Holbrey and R.D. Rogers, J. Am. Chem. Soc., 2003, 125,6632-6633.
6. A.M. Fernandes, M.A.A. Rocha, M.G. Freire, I.M. Marrucho, J.A.P. Coutinho and L.M.N.B.F. Santos, J. Phys. Chem. B, 2011,115,4033-4041.
7. M.G. Freire, P.J. Carvalho, A.M.S. Silva, L.M.N.B.F. Santos, L.P.N. Rebelo, I.M. Marrucho and J.A.P. Coutinho, J. Phys. Chem. B,2009, 113, 202-211.
8. E. Bogel-Łukasik, C. Lourenço, M.E. Zakrzewska and R. Bogel-Łukasik, J. Phys. Chem. B, 2010, 114, 15605-15609.
9. M.G. Freire, P.J. Carvalho, R.L. Gardas, I. M. Marrucho, L.M.N.B.F. Santos and J.A.P. Coutinho, J. Phys. Chem. B,2008, 112, 1604-1610.
10. M.G. Freire, P.J. Carvalho, A.M.S. Silva, L.M.N.B.F. Santos, L.P.N. Rebelo, I.M. Marrucho and J.A.P. Coutinho, J. Phys. Chem. B, 2009, 113, 202-211.
11. N.J. Bridges and R.D. Rogers, Sep. Purif. Technol.,2008, 43,1083-1090.
12. F.J. Deive, A. Rodriguez, I.M. Marrucho and L.P.N. Rebelo, J. Chem. Thermodyn.,2011, 43, 1565-1572.
13. B. Wu, Y.M. Zhang and H.P. Wang, J. Chem. Eng. Data, 2008, 53, 983-985.
14. N.J. Bridges, K.E. Gutowski and R.D. Rogers, Green Chem. 2007, 9, 177-183.
15. H. Wang, Q. Feng, J. Wang and H. Zhang, J. Phys. Chem. B, 2010, 114, 1380-1387.
16. Y. Li, L.S. Wang and S.F. Cai, J. Chem. Eng. Data, 2010, 55, 5289-5293.
17. S. Shariari, C.M.S.S. Neves, M.G. Freire and J.A.P Coutinho, J. Phys. Chem. B, 2012, 116, 7252–7258
18. S.P.M. Ventura, C.M.S.S. Neves, M.G. Freire, I.M. Marrucho, J. Oliveira and J.A.P. Coutinho, J. Phys. Chem. B, 2009, 113, 9304-9310.
19. L.I.N. Tomé, F.R. Varanda, M.G. Freire, I.M. Marrucho and J.A.P. Coutinho, J. Phys. Chem. B, 2009, 113, 2815-2825.
20. L.I.N. Tomé, M. Domínguez-Pérez, A.F.M. Cláudio, M.G. Freire, I.M. Marrucho, O. Cabeza and J.A.P. Coutinho, J. Phys. Chem. B, 2009, 113, 13971-13979.
21. J.H.W. Kunz and B.W. Ninham, Curr. Opin. Colloid Interface Sci., 2004, 9, 19-37.
22. Y. Marcus, Chem. Rev., 2009, 109, 1346-1370.
23. M.G. Freire, C.M.S.S. Neves, K. Shimizu, C.E.S. Bernardes, I.M. Marrucho, J.A.P. Coutinho, J.N. Canongia Lopes and L.P.N. Rebelo, J. Phys. Chem. B, 2010, 114, 15925-15934.
24. M.G. Freire, C.M.S.S. Neves, A.M.S. Silva, L.M.N.B.F. Santos, I.M. Marrucho, L.P.N. Rebelo, J.K. Shah, E.J. Maginn and J.A.P. Coutinho, J. Phys. Chem. B, 2010, 114, 2004-2014.
25. S. Katsuta, K. Nakamura, Y. Kudo and Y. Takeda, J. Phys. Chem. B,2012, 116, 852-859.
26. J.N. Canongia Lopes, M.F. Costa Gomes, P. Husson, A.H. Pádua, L.P.N. Rebelo, S. Sarraute and M. Tariq, J. Phys. Chem. B, 2011, 115, 6088-6099.
27. P.J. Carvalho, T. Regueira, L.M.N.B.F. Santos, J. Fernandez and J.A.P. Coutinho, J. Chem. Eng. Data, 2009, 55, 645-652.
28. U. Domańska and M. Królikowski, J. Chem. Eng. Data, 2010, 55, 4817-4822.

29. T.M. Letcher, A. Marciniak, M. Marciniak and U. Domańska, J. Chem. Eng. Data, 2005, 50, 1294-1298.
30. Y. Pei, J. Wang, L. Liu, K. Wu and Y. Zhao, J. Chem. Eng. Data, 2007, 52, 2026-2031.
31. M. Kohagen, M. Brehm, Y. Lingscheid, R. Giernoth, J. Sangoro, F. Kremer, S. Naumov, C. Iacob, J. Kärger, R. Valiullin and B. Kirchner, J. Phys. Chem. B, 2011, 115, 15280-15288.
32. K. Dong, Y. Song, X. Liu, W. Cheng, X. Yao and S. Zhang, J. Phys. Chem. B, 2011, 116, 1007-1017.
33. L.I.N. Tomé, M. Jorge, J.R.B. Gomes and J.A.P. Coutinho, J. Phys. Chem. B, 2012, 116, 1831-1842.
34. K. D. Collins, Biophys. Chem., 2006, 119, 271-281.
35. M. T. Zafarani-Moattar and S. Sarmad, J. Chem. Thermodynamics., 2010, 42, 1213-1221.
36. V. Najdanovic-Visak, J.N. CanongiaLopes, Z.P. Visak , J. Trindade and L.P.N. Rebelo, Int. J. Mol. Sci., 2007, 8, 736-748.
37. C.M.S.S. Neves, S.P.M. Ventura, M.G. Freire, I.M. Marrucho and J.A.P. Coutinho, J. Phys. Chem. B, 2009, 113, 5194-5199.
38 M. Domínguez-Pérez, L.I.N. Tomé, M.G. Freire, I.M. Marrucho, O. Cabeza and J.A.P. Coutinho, Sep. Purif. Technol.,2010, 72, 85-91.
39. Y. Deng, T. Long, D. Zhang, J. Chen and S. Gan, J. Chem. Eng. Data, 2009, 54, 2470-2473.
40. C. Wang, H. Luo, H. Li, X. Zhu, B. Yu and S. Dai, Chem. Eur. J., 2012, 18, 2153-2160.
41. X. Xie, J. Han, Y. Wang, Y. Yan, G. Yin and W. Guan, J. Chem. Eng. Data, 2005, 50, 4741-4745.
42. M.T. Zafarani-Moattar and S. Hamzehzadeh, J. Chem. Eng. Data, 2010, 55, 1598-1610.
43. S.P.M. Ventura, S.G. Sousa, L.S. Serafim, Á.S. Lima, M.G. Freire and J.A.P. Coutinho, J. Chem. Eng. Data, 2012, 57, 507-512.
44. C.M.S.S Neves, M.G. Freire and J.A.P. Coutinho, RSC Advances, 2012, 2, 10882-10890
45. K.D. Collins, G.W. Neilson and J.E. Enderby, Biophys. Chem., 2007, 128, 95-104.
46. C. Reichardt, Org. Process Res. Dev.,2006, 11, 105-113.
47. J.P. Hallett and T. Welton, Chem. Rev., 2011, 111, 3508-3576.
48. M.A. Ab Rani, A. Brant, L. Crowhurst, A. Dolan, M. Lui, N.H. Hassan, J.P. Hallett, P.A. Hunt, H. Niedermeyer, J.M. Perez-Arlandis, M. Schrems, T. Welton and R. Wilding, Phys. Chem. Chem. Phys., 2011, 13, 16831-16840.
49. S.N. Baker, G.A. Baker and F.V. Bright, Green Chem., 2002, 4, 165-169.
50. R. Lungwitz and S. Spange, New J. Chem., 2008, 32, 392-394.
51. C. Reichardt, Chem. Rev., 1994, 94, 2319-2358.
52. M.J. Kamlet and R.W. Taft, J. Am. Chem. Soc., 1976, 98, 377-383.
53. R. Lungwitz, M. Friedrich, W. Linert and S. Spange, New J. Chem., 2008, 34, 1493-1499.
54. L. Zhang, Z. Xu, Y. Wang and H. Li, J. Phys. Chem. B, 2008, 112, 6411-6419.
55. H. Wang, J. Wang, S. Zhang and X. Xuan, J. Phys. Chem. B, 2008, 112, 16682-16689.
56. B. Sun, Q. Jin, L. Tan, P. Wu and F. Yan, J. Phys. Chem. B, 2008, 112, 14251-14259.
57. Z. Li, Y. Pei, L. Liu and J. Wan, J. Chem. Thermodyn., 2010, 42, 932-937.
58. M.G. Freire, J.F.B. Pereira, M. Francisco, H. Rodriguez, L.P.N. Rebelo, R.D. Rogers and J. A.P. Coutinho, Chem. Eur. J., 2012, 18, 1831-1839.
59. M.G. Freire, C.L.S. Louros, L.P.N. Rebelo and J.A.P. Coutinho, Green Chem., 2011, 13, 1536-1545.
60. P.E. Mason, J.M. Cruickshank, G.W. Neilson and P. Buchanan, Phys. Chem. Chem. Phys., 2003, 5, 4686-4690.
61. C. Ebner, U. Onthong and M. Probst, J. Mol. Liq., 2005, 118, 15-25.
62. A.N. Troganis, C. Tsanaktsidis and I.P. Gerothanassis, J. Magn. Reson., 2003, 164, 294-303.
63. A.F.M. Cláudio, A.M. Ferreira, S. Shahriari, M.G. Freire and J.A.P. Coutinho, J. Phys. Chem. B, 2011, 115, 11145-11153.
64. Y. Gao, L. Zhang, Y. Wang and H. Li, J. Phys. Chem. B, 2010, 114, 2828-2833.

65. D.F. Parsons, M. Boström, T.J. Maceina, A. Salis and B.W. Ninham, Langmuir, 2009, 26, 3323-3328.
66. A. Salis, M.C. Pinna, D. Bilaničová, M. Monduzzi, P.L. Nostro and B.W. Ninham, J. Phys. Chem. B, 2006, 110, 2949-2956.
67. Y. Marcus, Chem. Rev., 2007, 107, 3880-3897.
68. B.W. Ninham, T.T. Duignan and D.F. Parsons, Curr. Opin. Colloid Interface Sci., 2011, 16, 612-617.
69. Y. Marcus, J. Solution Chem., 2009, 38, 513-516.

2.3. Extended Scale for the Hydrogen-Bond Basicity of Ionic Liquids

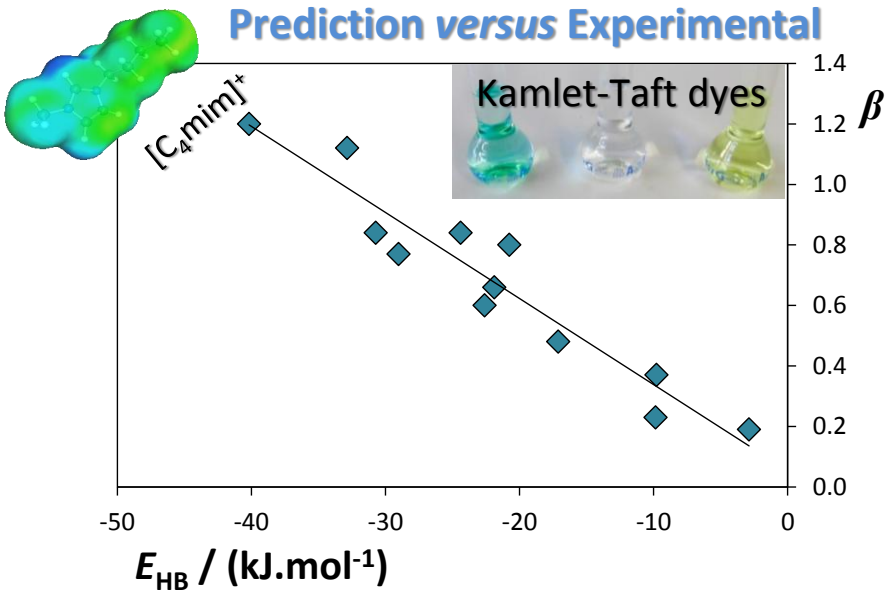

This chapter is based on the published paper: Cláudio, A. F. M.; Swift, L.; Hallett, J. P., Welton, T., Coutinho J. A. P. and Freire, M. G.,Extended Scale for the Hydrogen-Bond Basicity of Ionic Liquids, Phys. Chem. Chem. Phys, 2014, 16, 6593-6601.

Abstract

In the past decade, ionic liquids (ILs) have been the focus of intensive research regarding their use as potential and alternative solvents in many chemical applications. Targeting their effectiveness, recent investigations have attempted to establish polarity scales capable of ranking ILs according to their chemical behaviours. However, some major drawbacks have been found since polarity scales only report relative ranks because they depend on the set of probe dyes used, and they are sensitive to measurement conditions, such as purity levels of the ILs and procedures employed. Due to all these difficulties it is of crucial importance to find alternative and/or predictive methods and to evaluate them as *a priori* approaches able to provide the chemical properties of ILs. Furthermore, the large number of ILs available makes their experimental characterization, usually achieved by a trial and error methodology, burdensome. In this context, we firstly evaluated COSMO-RS, Conductor-Like Screening Model for Real Solvents, as an alternative tool to estimate the hydrogen-bond basicity of ILs. After demonstrating a straight-line correlation between the experimental hydrogen-bond basicity values and the COSMO-RS hydrogen-bonding energies in equimolar cation-anion pairs, an extended scale for the hydrogen-bond accepting ability of IL anions is proposed here. This new ranking of the ILs chemical properties opens the possibility to pre-screen appropriate ILs (even those not yet synthesized) for a given task or application.

Introduction

For all applications, an efficient and realistic use of ILs as solvents requires the previous knowledge of their physical and chemical properties. The main challenge consists therefore in the development of a “tailored solvent” for a target application. For that purpose, it is crucial to understand the solvation interactions at a molecular level in order to further evaluate the performance of a given solvent. Among the most important

features of an IL to be used as a solvent are the specific interactions occurring between the solvent and the dissolved substrate (solute-solvent interactions) which are usually related to the solvent polarity. It has previously been demonstrated that the IL polarity influences its solvation ability, reaction rates, reaction mechanisms, product yields and enzyme activity, among others.[1-6] Moreover, in **Chapters 2.1 and 2.2**, it was concluded that the ability of ILs to form ABS is closely correlated with their hydrogen-bond basicity, β.

The Kamlet-Taft parameters are well established for traditional solvents and it is one of the most accepted (used) polarity scales.[7,8] Nevertheless, for more recent solvents such as ILs, these parameters are still not definitive and are undergoing continuous experimental measurements by several research groups.[9-15] One of the major reasons behind this continuous research is the sensitivity of the Kamlet-Taft values to impurities.[9,10,16-18] In ILs, many of these impurities come from their own synthesis.[19] In this context, to simplify the experimental tasks, ILs should ideally be liquid at room temperature and non-coloured. Despite some divergences found between different authors and probe dyes, it is generally accepted that: (*i*) the dipolarity/polarizability (π^*) values are similar amongst several ILs and are higher than those of most molecular solvents (Coulombic interactions as well as dipole and polarizability effects occur in ILs); (*ii*) the hydrogen-bond basicity values cover a large range, from similar to acetonitrile to lower values, and are mainly controlled by the IL anion; and (*iii*) the hydrogen-bond acidity values of ILs are comparable to or lower than that of aniline and are mainly determined by the IL cation (although the anion also plays a secondary role since stronger cation-anion interactions further reduce the ability of the cation to interact with the dye).[9-15]

Aiming at overcoming the difficulties encountered with common solvatochromic probes and the establishment of polarity scales in ILs, several attempts have been carried out in order to find suitable alternatives. Due to all the difficulties found hitherto to establish a polarity scale for ILs, it is of vital importance to find alternative and/or predictive methods. These alternatives were already discussed in **Chapter 1.2: Characterization of solvents: Solvatocromic Parameters.** Moreover, the large number of ILs available from

their structural flexibility also represents a major drawback in that it is unfeasible to experimentally determine the solvatochromic parameters for all the cation/anion combinations which may form an IL. Therefore, we provide here novel results on the use of COSMO-RS, Conductor-Like Screening Model for Real Solvents,[20-23] as a valuable tool to estimate the hydrogen-bond basicity, β, of ILs. COSMO-RS is based on unimolecular quantum calculations and was mainly used for the prediction of the liquid-liquid equilibrium of binary mixtures (composed of ILs and water, alcohols or hydrocarbons) or of ternary mixtures (constituted by ILs and aromatic and aliphatic hydrocarbons or by ILs, water and ethanol).[24-28] COSMO-RS was also found to be valuable in the prediction of the excess properties of binary mixtures composed of molecular solvents and ILs, as well as between ILs and gases or other volatile compounds.[29-31] The results obtained allowed to establish the main criteria aiming at selecting the IL structures that promote favourable solute-solvent intermolecular interactions.[29-31] The use of COSMO-RS to predict the hydrogen-bond basicity of ILs, as a main solvatochromic parameter which defines the ability of a given IL to accept protons, is proposed here by means of the hydrogen-bonding energies of the corresponding IL cation-anion pairs.

Experimental Procedure

Materials

The ILs experimentally investigated were [C_4mim][CF_3SO_3] (99 wt % purity from Iolitec), [C_4mim][$C_8H_{17}SO_4$] (97 wt % purity form Merck), [C_4mim][$(CH_3O)_2PO_2$] (98 wt % purity from Iolitec) and [C_4mim][CF_3CO_2] (97 wt % purity from Iolitec). The purity of each IL was also checked by ^{1}H, ^{13}C, and ^{19}F (whenever applicable) NMR spectra and found to be in accordance with the purity levels given by the suppliers. The dyes used were *N*,*N*-diethyl-4-nitroaniline, 99% purity from Fluorochem, Reichardt dye, 90% purity from Sigma-Aldrich, and 4-nitroaniline, 99% purity from Aldrich. The deuterium oxide used was acquired at Aldrich with > 99.96 % D atoms. The 3-(trimethylsilyl)propionic-2,2,3,3-d4 acid sodium salt (TSP) was from Aldrich with >98 % D atoms.

Solvatochromic Assays

All the IL samples were dried under vacuum, at 323 K for 48 h, before use. The dried IL (0.5 mL) was taken and placed into an appropriate round-bottom flask and each dye was further added (Reichardt dye, *N*, *N*-diethyl-4-nitroaniline or 4-nitroaniline) in a dichloromethane solution. Dichloromethane was then removed under vacuum at 323 K (for 3 h). After cooling, the UV-Vis spectra of all samples were recorded at 298 K (thermostated sample holder) using a PC-controlled Perkin-Elmer Lambda 2 spectrophotometer. Further details on the experimental procedure can be found elsewhere.[9,10] Additional information regarding the procedure to determine the Kamlet-Taft parameters of ILs is described in **Chapter 1.2: Characterization of solvents: Solvatocromic Parameters.**

Nuclear Magnetic Resonance (NMR)

The ^{1}H NMR spectra were obtained with pure IL samples (and after drying under vacuum) placed in NMR spectroscopy tubes containing sealed reference capillaries with D_2O and TSP as the internal reference, and at 298 K. The ^{1}H NMR measurements were performed on a Bruker Avance 300 spectrometer operating at 300.13 MHz.

COSMO-RS

COSMO-RS[20-23] is a thermodynamic model that combines quantum chemistry, based on the dielectric continuum model known as COSMO (COnductor-like Screening MOdel for Real Solvents), with statistical thermodynamics calculations. COSMO calculations are performed in an ideal conductor, meaning that molecules are assumed as surrounded by a virtual conductor environment, and the interactions are completely made on the conductor interface, taking into account the electrostatic screening and the back-polarization of the solute molecule. Therefore, COSMO gives a discrete surface around the solute molecule which is characterized by its geometry and screening charge density (σ) that iteratively corresponds to a minimum energetic state at the conductor, stored in the so-called COSMO files. As a second step, COSMO-RS treats the surface around the solute molecule as segments, and it also similarly treats the screening charge density of the respective segment, σ'.

In the molecular interaction approach, the most significant molecular interaction energy modes are the electrostatic misfit energy, and the hydrogen-bonding energy, E_{HB}, defined according to the following equation,

$$E_{HB} = a_{eff} c_{HB} \min(0;\min(0;\sigma_{donor} + \sigma_{HB}) \times \max(0;\sigma_{acceptor} - \sigma_{HB})) \qquad \text{eq. 2.3.1}$$

which is described as a function of the polarization charges of the two interacting segments, ($\sigma_{acceptor}$,σ_{donor}) and where a_{eff} is the effective contact area between two surface segments, c_{HB} is the hydrogen-bond strength and σ_{HB} is the threshold for hydrogen-bonding. Generally, a hydrogen-bonding interaction, in COSMO-RS, can be expected if two sufficiently polar pieces of surface of opposite polarity are in contact. The van der Waals energy is also accounted; yet, it only depends on element specific van der Waals interaction parameters. The link between the microscopic surface interaction energies and the macroscopic thermodynamic properties of a liquid is provided by statistical thermodynamics. It should be remarked that since all molecular interactions in COSMO-RS consist of local pair wise interactions of surface segments, the statistical averaging can be done in the ensemble of interacting surface pieces.

To describe the composition of the surface segment ensemble regarding the interactions which depend on σ only, only the probability distribution of σ has to be known for all compounds X_i. Such probability distributions, $pX(\sigma)$, are known as "σ-profiles". The σ-profile of a whole system/mixture is the sum of the individual σ-profiles of the components weighted with their mole fractions in the target mixture.

A number of conformations are available for the IL ions studied. In all the studied examples the lowest energy conformer was employed in the COSMO-RS calculations. Moreover, independent files for the IL cation and anions were used. An equimolar cation-anion mixture was used to specifically determine the E_{HB} values of a pure IL. The quantum chemical COSMO calculation was performed in the Turbomole program package[27] with the BP density functional theory, giving the surface charge density and the Ahlrichs-TZVP (triple-ζ valence polarized large basis set).[27] The COSMOtherm program with the parameter file BP_TZVP_C2.1_1301 was used in all the calculations.[32-34]

Results and Discussion

Experimental Kamlet-Taft Solvatochromic Parameters

There are two major literature sources reporting the Kamlet-Taft parameters with the goal of appraising the effect of the IL anion through their hydrogen-bond basicity.[9,10,35-37] To expand this database, additional Kamlet-Taft solvatochromic parameters were here determined for 4 ILs based on the 1-butyl-3-methylimidazolium-($[C_4mim]^+$) cation. There are several sets of dyes that can be used to determine the Kamlet-Taft parameters. In this work, the Reichardt's dye, 4-nitroaniline and *N*,*N*-diethyl-4-nitroaniline were used. All spectra were recorded at 298 K, and thus, only ILs that are liquid at room temperature were considered. The values of the Kamlet-Taft solvatochromic parameters determined in this work are reported in Table 2.3.1.

Table 2.3.1: Kamlet–Taft parameters using the following set of dyes: Reichardt's Dye, N,N-diethyl-4-nitroaniline and 4-nitroaniline.

IL	α	β	π^*
$[C_4mim][CF_3SO_3]$	0.62	0.48	0.98
$[C_4mim][C_8H_{17}SO_4]$	0.65	0.80	0.93
$[C_4mim][(CH_3O)_2PO_2]$	0.48	1.12	0.96
$[C_4mim][CF_3CO_2]$	0.57	0.84	0.94

The solvatochromic data for $[C_4mim][CF_3SO_3]$ and $[C_4mim][(CH_3O)_2PO_2]$ are in close agreement with previous published data[9,10,38] whereas novel results are presented for the $[C_4mim][C_8H_{17}SO_4]$ and $[C_4mim][CF_3CO_2]$.

The π^* values are high for all the ILs investigated in comparison to non-aqueous molecular solvents[39-42] and slightly depend on the IL anion. π^* is a true measure of the ion-dye non-specific interactions (polarizability, and dipole-dipole and dipole-induced dipole interactions) and tends to decrease with the increase on the charge delocalization of the IL anion.[9,10] In fact, the octylsulphate-based IL is the one which presents the lowest π^* value – a consequence of the long aliphatic moiety present in the anion.

As previously demonstrated in the literature, the hydrogen-bond acidity of ILs is mainly determined by the IL cation;[9,10] yet, there is also a clear dependence on the IL anion, as shown here and in agreement with literature data.[9,10] The data presented in Table 2.3.1 reveal that the ability of the IL to act as a hydrogen-bond donor (mainly arising from the IL cation) is moderated by the hydrogen-bond acceptor ability of the anion composing the respective IL. For instance, the dimethylphosphate-based IL, having an anion with the highest ability to accept a hydrogen bond, is the one with the lowest α value. The high ability of this anion to hydrogen-bond with the IL cation limits its availability to interact as a hydrogen-bond donor to the dye.

The β value reflects the hydrogen-bond basicity of each IL acting as a solvent. As shown in Table 2.3.1, the β values are strongly dependent on the IL anion. Between the studied ILs, the dimethylphosphate-based fluid presents the highest ability to hydrogen-bond with the protons of the hydrogen-bond donor group (-NH_2) of the 4-nitroaniline dye.

Estimation of the Hydrogen-bond Basicity of ILs

Taking into account all the difficulties in experimentally determining the Kamlet-Taft solvatochromic parameters we tested the COSMO-RS as a viable and expeditious tool to estimate the hydrogen-bond basicity of ILs. Imidazolium-, pyridinium- and pyrrolidinium-based ILs were included and combined with a wide variety of anions as it can see in Table 2.3.2. In addition, IL cations with different alkyl side chain lengths, as well as with functionalized groups, were also comprised.

The hydrogen-bond basicity was chosen in this work since it is one of the most important parameters reflecting the hydrogen-bond acceptor ability of the IL anion. Most of the relevant properties of ILs regarding this solute-solvent interaction are significantly determined by the nature of the anion rather than the cation.[43-46] In fact, the β parameter is widely used to explain (and indeed correlates with) diverse properties, such as solvation ability and phase equilibrium behaviour of ILs.[47-50] Within this perspective, the hydrogen-bond basicity was here correlated with the hydrogen-bonding interaction energy in the equimolar cation-anion mixture (E_{HB} / (kJ·mol^{-1})) obtained from COSMO-RS to infer a possible dependence. It should be remarked that other attempts were also carried out, namely the correlation of the hydrogen-bond basicity with the van der Waals energy

derived from COSMO-RS – data shown in *Supporting Information* (Table S21 and Figure S2). Although, and as expected, the enhanced correlations with the experimental β values were gathered with the COSMO-RS hydrogen-bonding energies and as shown hereinafter.

Table 2.3.2: Hydrogen-bond basicity (β) data, experimental ^{1}H NMR chemical shift of the C2-proton (δ / ppm) and hydrogen-bonding interaction energy in the equimolar cation-anion mixture of several ILs (E_{HB} / (kJ·mol^{-1})) taken from COSMO-RS calculations.

IL	β [9,10]	β [35-37]	δ^{*} / ppm	E_{HB} / (kJ·mol^{-1})
$[C_2mim][N(CF_3SO_2)_2]$	0.23	n.a.	n.a.	-10.38
$[C_4mim][N(CF_3SO_2)_2]$	0.23	0.42	8.39	-9.86
$[C_4C_1mim][N(CF_3SO_2)_2]$	0.24	n.a.	n.a.	-5.54
$[C_5mim][N(CF_3SO_2)_2]$	0.26	n.a.	n.a.	-9.65
$[C_6mim][N(CF_3SO_2)_2]$	0.26	0.44	n.a.	-9.50
$[C_8mim][N(CF_3SO_2)_2]$	0.29	0.47	n.a.	-9.22
$[C_{10}mim][N(CF_3SO_2)_2]$	n.a.	0.49	n.a.	-8.90
$[C_4mpy][N(CF_3SO_2)_2]$	0.25	n.a	n.a	-7.61
$[C_4mpyr][N(CF_3SO_2)_2]$	0.25	n.a	n.a	-4.53
$[C_5mpyr][N(CF_3SO_2)_2]$	0.26	n.a	n.a	-8.98
$[(C_2OC_2)mpyr][N(CF_3SO_2)_2]$	0.28	n.a	n.a	-5.01
$[C_4mim][PF_6]$	0.19	0.44	8.11	-2.88
$[C_6mim][PF_6]$	n.a.	0.50	n.a.	-2.71
$[C_8mim][PF_6]$	n.a.	0.53	n.a.	-2.57
$[C_{10}mim][PF_6]$	n.a.	0.55	n.a.	-2.44
$[C_4mim][BF_4]$	0.37	0.55	8.37	-9.79
$[C_4C_1mim][BF_4]$	0.36	n.a.	n.a.	-5.84
$[C_6mim][BF_4]$	n.a.	0.60	n.a.	-9.35
$[C_8mim][BF_4]$	n.a.	0.63	n.a.	-8.99
$[C_{10}mim][BF_4]$	n.a.	0.65	n.a.	-8.63
$[C_4mim][CF_3SO_3]$	0.48*	0.57	8.72	-17.11
$[C_6mim][CF_3SO_3]$	n.a.	0.61	n.a.	-16.63
$[C_8mim][CF_3SO_3]$	n.a.	0.64	n.a.	-16.26
$[C_{10}mim][CF_3SO_3]$	n.a.	0.65	n.a.	-15.82
$[C_4mim][ClO_4]$	n.a.	0.55	n.a.	-13.11

$[C_4mim][C(CN)_3]$	n.a.	0.54	8.81	-16.73
$[C_4mim][N(CN)_2]$	0.60	0.64	8.99	-22.60
$[C_6mim][N(CN)_2]$	n.a.	0.69	n.a.	-22.05
$[C_8mim][N(CN)_2]$	n.a.	0.71	n.a.	-21.69
$[C_{10}mim][N(CN)_2]$	n.a.	0.75	n.a.	-21.20
$[C_4mim][SCN]$	n.a.	0.71	9.04	-17.01
$[C_4mim][NO_3]$	n.a.	0.74	n.a.	-24.21
$[C_6mim][NO_3]$	n.a.	0.76	n.a.	-23.58
$[C_8mim][NO_3]$	n.a.	0.80	n.a.	-23.13
$[C_{10}mim][NO_3]$	n.a.	0.81	n.a.	-22.60
$[C_4mim][CF_3CO_2]$	0.84*	0.74	n.a.	-24.38
$[C_4mim]I$	n.a.	0.75	n.a.	-19.97
$[C_4mim][CH_3SO_4]$	0.66	0.75	n.a.	-21.88
$[C_4mim][C_8H_{17}SO_4]$	0.80*	0.77	n.a.	-20.76
$[C_4mim][CH_3SO_3]$	0.77	0.85	n.a.	-29.03
$[C_4mim]Br$	n.a.	0.87	n.a.	-25.60
$[C_4mim]Cl$	0.84	0.95	n.a.	-30.72
$[C_6mim]Cl$	n.a.	0.97	n.a.	-30.11
$[C_8mim]Cl$	n.a.	0.98	n.a.	-29.69
$[C_{10}mim]Cl$	n.a.	0.98	n.a.	-29.18
$[C_4mim][(CH_3O)_2PO_2]$	1.12*	1.12	10.12	-32.85
$[C_4mim][CH_3CO_2]$	0.85	1.20	10.59	-40.17

*experimental data from this work

As previously mentioned, the solvatochromic parameters values determined by different authors are slightly different. In general, each group of researchers provide one relative polarity scale. Therefore, the E_{HB} values for each IL were independently correlated with the Kamlet-Taft β parameters published by Welton and co-workers[9,10] and by Lungwitz et al.[35-37]. These literature sources[9,10,35-37] were chosen since they represent the most complete databases found for ILs. These experimental values allow the inspection on the IL anion effect and the comparison between the hydrogen-bond basicity and the E_{HB}. The β experimental data[9,10,35-37] and the respective COSMO-RS results are compiled in Table

2.3.2. The definition of the IL acronyms is provided in **List of Abbreviations**. The complete description of the IL anions is provided in Table 2.3.3.

In general, the hydrogen-bond basicity values reported by Lungwitz et al.[35-37] are higher than those published by Welton and co-workers[9,10]. These differences are a main result of the different solvatochromic dyes used by the two research groups.[9,10,35-37]

Anions such as acetate, dimethylphosphate and halogens present high hydrogen-bond basicities and thus an expected strong coordinating ability in aqueous solutions or in other media able to donate protons. At the other extreme of the ILs β ranking, the fluorinated IL anions are found, such as $[N(CF_3SO_2)_2]^-$, $[PF_6]^-$, $[BF_4]^-$ and $[CF_3SO_3]^-$. These IL anions are weak hydrogen-bond acceptors, and when combined with the imidazolium cation, result in non-coordinating ILs. Structural changes to the IL anion, such as the introduction of electron withdrawing atoms or groups, also have a considerable influence on the hydrogen-bond basicity values. For instance, considering the cyano-based ILs, $[SCN]^-$, $[N(CN)_2]^-$ and $[C(CN)_3]^-$, there is a decrease in the IL anion's ability to accept hydrogen bonds with the increase number of –CN groups attached to the central atom, despite the growing number of possible sites for interaction. The more –CN groups are present, the smaller is the overall charge of the end group, and thus the electron density that is required for hydrogen-bonding. The introduction of fluorinated groups, from $[CH_3CO_2]^-$ to $[CF_3CO_2]^-$ and from $[CH_3SO_3]^-$ to $[CF_3SO_3]^-$, also leads to a decrease in the IL's hydrogen-bond basicity. The low polarizability of the fluorinated groups and their electron withdrawing effect weakens the hydrogen-bonding ability with the hydrogen-bond donor protons of the solvatochromic probe. Finally, there is an increase in the hydrogen-bond basicity with the increase of the alkyl side chain length attached to the IL anion, resulting from the electron-donating effect of the fatty groups, as shown in data for methylsulphate- and octylsulphate-based ILs. In summary, a large range of β values are achievable by the structural modification of the IL anion. This pattern opens the door to the creation of ILs with defined hydrogen-bond basicity capable of reproducing the chemical behaviour of typical molecular solvents for specific applications.

Figure 2.3.1 depicts the correlation between the experimental β parameter of each IL[9,10,35-37] and the respective E_{HB} COSMO-RS values. At a first sight, it can be seen that

there is a close relationship between the experimental hydrogen-bond basicity of ILs and the hydrogen-bonding energy of the pure cation-anion pairs estimated by COSMO-RS. This correlation indicates that anions with an absolute lower hydrogen-bonding interaction with the corresponding cation are also those that are less able to accept hydrogen bonds when acting as the solvent environment. However, a closer look at Figure 2.3.1 also points out to the existence of two different correlations for the experimental data taken from the two research groups.[9,10,35-37]

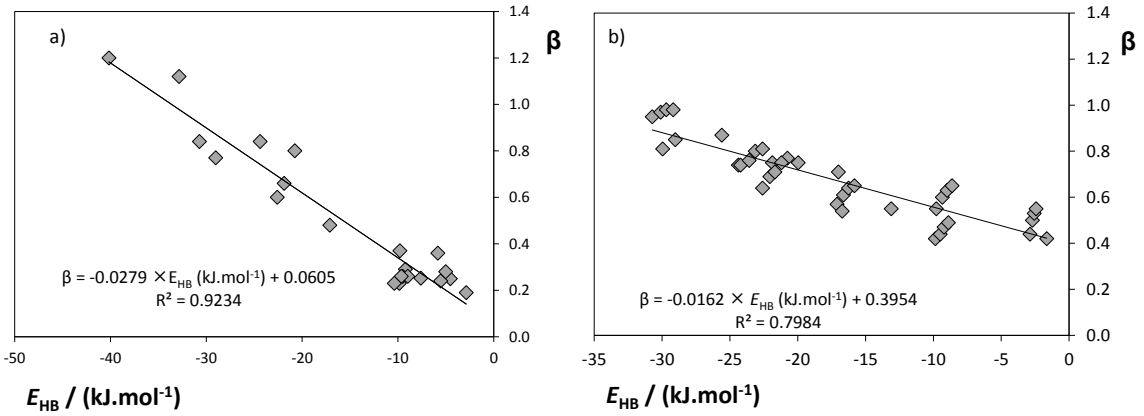

Figure 2.3.1: Correlation between the experimental values of hydrogen-bond basicity (β) and the E_{HB} predicted by COSMO-RS: (a) experimental data from Welton and co-workers[9,10]; **(b)** experimental data from Lungwitz et al.[35-37].

Higher correlation coefficients and a higher dependence on the E_{HB} values are observed with the experimental results from Welton and co-workers.[9,10] This discrepancy can be ascribed to the different sets of dyes used by both groups and to the respective hydrogen-bonding dependency of the IL anion with a given dye.[9,10,35-37] Nevertheless, both correlations depicted in Figure 2.3.1 reveal a good agreement between the experimental hydrogen-bond basicity and the estimated hydrogen-bonding energies of the IL ions pairs. Based on this linear dependence and on the respective correlations it seems plausible to predict the β values.

Figure 2.3.2 shows the relationship between the experimental and estimated β parameters. In both examples displayed in Figure 2.3.2 there is a close agreement between the predicted and experimental β values meaning that the equations provided in Figure 2.3.1 can be used to predict the hydrogen-bond basicity of a wide variety of ILs,

and independently of the IL cation core or alkyl side chain length, with reasonable accuracy.

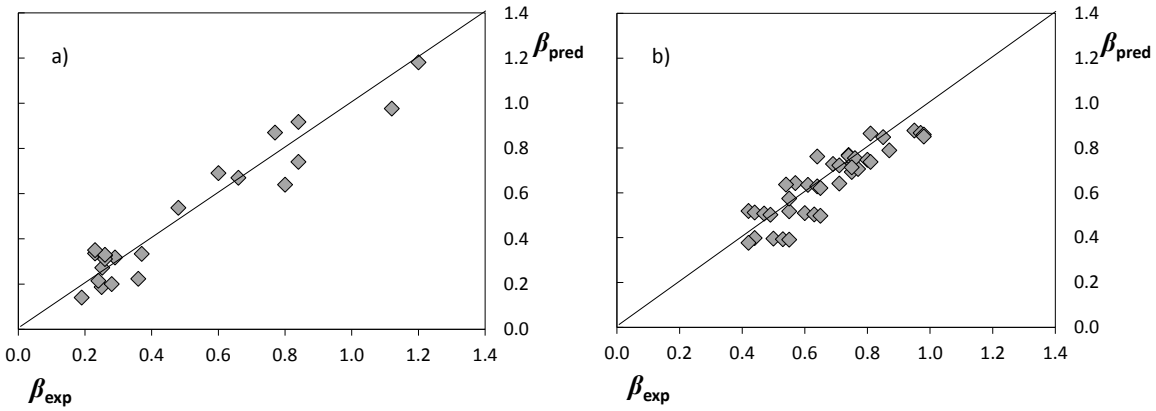

Figure 2.3.2: Correlation between the predicted and experimental values of hydrogen-bond basicity (β_{pred} and β_{exp}, respectively) based on the equations provided by the E_{HB} estimated by COSMO-RS: (a) experimental data from Welton and co-workers[9,10]; **(b)** experimental data from Lungwitz et al.[35-37].

Aiming at further evaluating the capability of COSMO-RS for the prediction of the IL anions to accept hydrogen bonds, additional ^{1}H NMR data were also determined in this work for pure ILs. The chemical shifts presented here were measured for pure ILs, using an internal capillary containing the solvent and reference, to avoid the influences of solvent-IL interactions and the concentration of the salt itself upon the chemical shifts. In this way, the chemical shifts of pure ILs represent the differences in their ability to hydrogen-bond with the IL cation and as a function of the respective anion.

The correlation between the ^{1}H NMR chemical shift of the proton in the C2-position of the imidazolium ring in [C_4mim]-based ILs against the E_{HB} estimated by COSMO-RS is depicted in Figure 2.3.3.

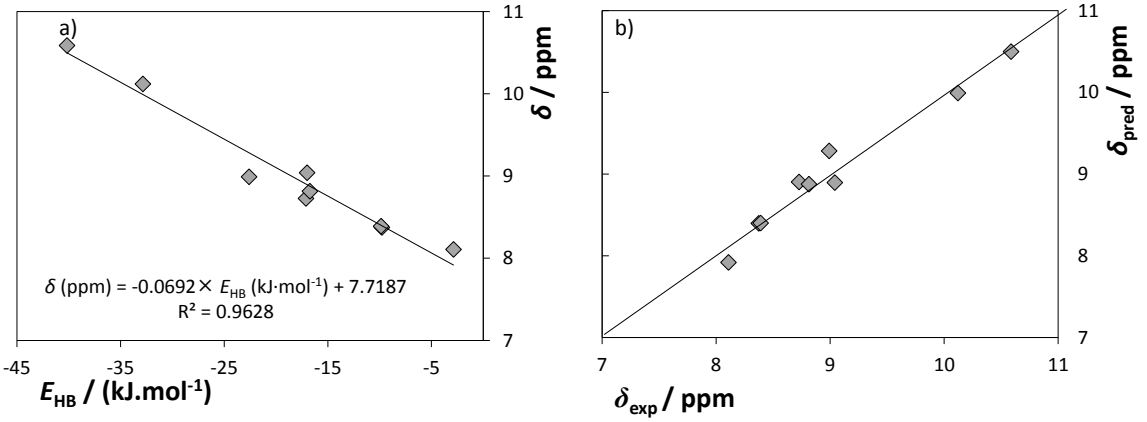

Figure 2.3.3: (a) Correlation between the experimental values of ^{1}H NMR chemical shift of the C2-proton of the imidazolium ring and the EHB estimated by COSMO-RS and (b) correlation between the predicted and experimental values of the ^{1}H NMR chemical shift of the proton in the C2-position of the imidazolium ring in [C_4mim]-based ILs (δ_{pred} and δ_{exp}, respectively).

The interaction of IL anions with $[C_4mim]^+$ is complex in nature with preferential hydrogen-bonding with the most acidic hydrogen at the imidazolium cation, in the C2 position. Bonhôte et al.[51] demonstrated that the ^{1}H NMR chemical shift of the most acidic proton in 1,3-dialkylimidazolium moves to lower field with the increase of the anion basicity (in acetone solvent), and later on, Lungwitz and Spange[35-37] revealed that the same chemical shift closely correlates with the hydrogen-bond basicity (β) of ILs with a common anion and can be used as a measure of its hydrogen-bonding strength. According to Figure 2.3.3, there is a close relationship between the interaction strength of the IL anion with the imidazolium ring (represented by the ^{1}H NMR chemical shift) and E_{HB} estimated by COSMO-RS for a series of [C_4mim]-based compounds. The linear function depicted in Figure 2.3.3 indicates that COSMO-RS is also able to predict the ^{1}H NMR chemical shift of the most acidic proton in the imidazolium ring as a result of the cation-anion hydrogen-bonding strength. Recently, a number of wavefunction-based methods, as well as density functional theory, were proposed to predict the proton NMR chemical shifts of a number of ILs incorporating the 1-ethyl-3-methylimidazolium cation combined with diverse anions.[52]

Extended scale of the Hydrogen-bond Basicity of ILs

A single "polarity" parameter is not sufficient to explain all the variations in experimental results in solvent-mediated processes. Simple solvents, like *n*-alkanes, are limited in the

number and type of interactions with the dissolved molecule. On the other hand, more complex solvents, with additional functional groups, are capable of having additional interactions, and ILs tend to fall within this category. Given their chemical structure and diversity of functional groups, ILs are able to establish dispersive, $\pi\cdots\pi$, $n\cdots\pi$, hydrogen-bonding and electrostatic interactions. The experimental polarity scales are a weighted average of solute-solvent interactions, and are thus more complex in nature for ILs. In this work we focused essentially on the hydrogen-bond basicity of ILs, which is strongly dominated by their anions. The β value is a numerical description of the hydrogen-bond basicity of ILs and describes the importance of the individual ability of each IL anion to accept hydrogen bonds. Table 2.3.3 lists the COSMO-RS hydrogen-bonding interaction energies for an extended number of IL anions, combined with the common and mostly studied $[C_4mim]^+$ cation, in a decreasing order of hydrogen-bond basicity.

Table 2.3.3: Hydrogen-bonding interaction energy in the equimolar cation-anion mixture (E_{HB} / ($kJ{\cdot}mol^{-1}$)) taken from COSMO-RS calculations for $[C_4mim]$-based ILs as a new and extended scale of hydrogen-bond basicity. The anions list is presented in a decreasing order of hydrogen-bond basicity of the IL anion.

$[C_4mim]$-based ILs		
Anion	Abbreviation	E_{HB} / ($kJ.mol^{-1}$)
Acetate	$[CH_3CO_2]^-$	-40.17
Decanoate	$[C_9H_{20}CO_2]^-$	-38.64
Bis(2,4,4-trimethylpentyl)phosphinate	$[C_{16}H_{34}O_2P]^-$	-38.45
Benzoate	$[(C_6H_5)CO_2]^-$	-34.35
Diethylphosphate	$[(C_2H_5O)_2PO_2]^-$	-33.41
Dimethylphosphate	$[(CH_3O)_2PO_2]^-$	-32.85
Dibutylphosphate	$[(C_4H_9O)_2PO_2]^-$	-32.46
Chloride	Cl^-	-30.72
Nitrite	$[NO_2]^-$	-29.96
Methanesulfonate	$[CH_3SO_3]^-$	-29.03
Bromide	Br^-	-25.60
Salicylate	$[C_7H_5O_3]^-$	-25.46
Toluene-4-sulfonate (tosylate)	$[C_7H_8SO_3]^-$	-25.05
Trifluoroacetate	$[CF_3CO_2]^-$	-24.38
Nitrate	$[NO_3]^-$	-24.21
Heptafluorobutanoate	$[C_3F_7CO_2]^-$	-22.64
Dicyanamide	$[N(CN)_2]^-$	-22.60
2-(2-methoxyethoxy)ethylsulphate	$[C_5OC_1SO_4]^-$	-22.12
Ethylsulfate	$[C_2H_5SO_4]^-$	-22.10

Methoxyethylsulphate	$[C_3H_7OSO_4]^-$	-21.92
Methylsulphate	$[CH_3SO_4]^-$	-21.88
Ethoxyethylsulphate	$[C_4H_9OSO_4]^-$	-21.78
Butylsulphate	$[C_4H_9SO_4]^-$	-21.56
Octylsulphate	$[C_8H_{17}SO_4]^-$	-20.76
Bis(malonato)borate	$[C_6H_4BO_8]^-$	-20.33
Iodide	I^-	-19.97
Tri(fluoromethane)sulfonate	$[CF_3SO_3]^-$	-17.11
Bis(pentafluoroethyl)phosphinate	$[PO_2(C_2F_5)_2]^-$	-17.09
Thiocyanate	$[SCN]^-$	-17.01
Tricyanomethane	$[N(CN)_3]^-$	-16.73
Bis(salicylato)borate	$[BC_{14}H_8O_6]^-$	-16.50
Bisbiphenyldiolatoborate	$[BC_{24}H_{16}O_4]^-$	-14.42
Perclorate	$[ClO_4]^-$	-13.11
Tetracyanoborate	$[B(CN)_4]^-$	-12.48
Bis(trifluoromethylsulfonyl)methane	$[CH(CF_3SO_2)_2]^-$	-11.16
Bis(oxalate)borate	$[B(C_2O_4)_2]^-$	-10.88
Bis(trifluoromethanesulfonyl)imide	$[N(CF_3SO_2)_2]^-$	-9.86
Tetrafluoroborate	$[BF_4]^-$	-9.79
Bis(pentafluoroethylsulfonyl)imide	$[N(C_2F_5SO_2)_2]^-$	-8.27
Tris(trifluoromethylsulfonyl)methide	$[C(SO_2CF_3)_3]^-$	-7.20
Boron tetrachloride	$[BCl_4]^-$	-4.13
Triiodide	$[I_3]^-$	-2.99
Hexafluorophosphate	$[PF_6]^-$	-2.88
Hexafluoroarsenate	$[AsF_6]^-$	-1.72
Hexafluorostibate	$[SbF_6]^-$	-1.65
Tetrachloroferrate	$[FeCl_4]^-$	-0.99
Tris(pentafluoroethyl)trifluorophosphate	$[(C_2F_5)_3PF_3]^-$	-0.74
Bis(nonafluorobutyl)trifluorophosphate	$[(C_4F_9)_2PF_3]^-$	-0.69

The information provided in Table 2.3.3 henceforward can be used to understand the effect of different IL anions towards chemical-mediated processes. This extended polarity scale of the ability of the IL anion to hydrogen-bond can provide *a priori* information to select an improved IL for a specific application before extensive and time-consuming experiments.

Aiming at predicting the solvatochromic parameters of ILs, previously, Hunt and co-workers[38] employed TD-DFT calculations to estimate the hydrogen-bond basicity and hydrogen-bond acidity of several ILs. Albeit the promising results, these approaches require a high computational cost and more expertise knowledge, and thus, are not suitable for routine screening. This major drawback is overcome with the COSMO-RS

methodology proposed here. COSMO-RS is an expedite method that can be used by researchers who deal with more applicative-related strategies and mainly require the ILs solvatochromic parameters for further correlations or predictions in phase behaviour, solvation performance, etc.

Conclusions

The great complexity of ILs to act either as hydrogen-bond donors or acceptors has resulted in great efforts in the literature aimed at characterizing these fluids according to a polarity scale. Furthermore, this complexity, achieved by innumerable chemical structural variations, is valuable for the creation of "tailor-made" compounds. However, an efficient and realistic employment of ILs in scientific research, or even in industrial applications, requires the accurate knowledge of their physical and chemical properties. One of the most important aspects of ILs when envisaging their use for replacing typical molecular solvents relies on the specific interactions occurring between the solvent and the dissolved solute. The reactivity of dissolved substrates, reaction rates and reaction mechanisms are dependent on the solvent-solute interactions. The quantification of these solvent characteristics is thus an important tool to understand the physicochemical phenomena and chemical behaviour of systems involving ILs. For that purpose, several solvent parameters and relative polarity scales for ILs have been proposed in the past few years. Nevertheless, these polarity scales are dependent on the set of solvatochromic dyes used, on the experimental procedure adopted and also on the purity of the ILs. Therefore, a proper comparison amongst different groups of research is not viable and we are always limited to a relative polarity scale for a restricted number of ILs.

Aiming at overcoming the difficulties encountered with the establishment of a polarity scale for ILs, we proposed here the use of the hydrogen-bonding interaction energies, occurring in the equimolar cation-anion mixtures (E_{HB} / (kJ·mol^{-1})), estimated from COSMO-RS calculations. Reasonable linear correlations between the experimental hydrogen-bond basicity values of a wide variety of ILs and the E_{HB} estimated from COSMO-RS were found, thus underlining the validity of the proposed methodology. Based on this dependence, we provided an extended polarity scale capable of characterizing the IL anions' abilities to hydrogen-bond when acting as solvent media. The E_{HB} values estimated from COSMO-RS can be adequately used for routine screening, before extensive and time-consuming experimental measurements by a trial and error approach, and allow for the correct choice of an improved IL for a specific application.

References

1. D.R. MacFarlane, J.M. Pringle, K.M. Jonansson, S.A. Forsyth and M. Forsyth, Chem. Commun., 2006, 1905-1917.
2. S.V. Dzyba and R.A. Bartsch, Tetrahedron Lett., 2002, 43, 4657-4659.
3. Y. Fukaya, A. Sugimoto and H. Ohno, Biomacromolecules, 2006, 7, 3295-3297.
4. R.M. Lau, M.J. Sorgedrager, G. Carrea, F.V. Rantwijk, F. Secundo and R.A. Sheldon, Green Chem., 2004, 6, 483-487.
5. L. Crowhurst, R. Falcone, N.L. Lancaste, V.L. Mestre and T. Welton, J. Org. Chem., 2006, 71, 8847-8853.
6. L. Crowhurst, M.L. Lancaster, J.M.P. Arlandis and T. Welton, J. Am. Chem. Soc., 2004, 126, 11549-11555.
7. Y. Marcus, Chem. Soc. Rev., 1993, 22, 409-416.
8. S. Spange, E. Vilsmeier, K. Fischer, A. Reuter, S. Prause, Y. Zimmermann, Ch. Schmidt, Macromol. Rapid Commun., 2000, 21, 643-659.
9. M.A. Ab Rani, A. Brant, L. Crowhurst, A. Dolan, M. Lui, N.H. Hassan, J.P. Hallett, P.A. Hunt, H. Niedermeyer, J.M. Perez-Arlandis, M. Schrems, T. Welton and R. Wilding, Phys. Chem. Chem,. Phys., 2011, 13, 16831-16840.
10. L. Crowhurst, P.R. Mawdsley, J.M. Perez-Arlandis, P.A. Salter and T. Welton, Phys. Chem. Chem,. Phys., 2003, 5, 2790-2794.
11. C. Chiappe and D. Pieraccini, J. Phys. Org. Chem., 2005, 18, 275-297.
12. C. Chiappe, C.S. Pomelli and S. Rajamani, J. Phys. Chem. B, 2011, 115, 9653-9661.
13. L. Crowhurst, P.R. Mawdsley, J.M. Perez-Arlandis, P.A. Salter and T. Welton, Phys. Chem. Chem. Phys., 2003, 5, 2790-2794;
14. T.V. Doherty, M. Mora-Pale, S.E. Foley, R.J. Linhardt and J.S. Dordick, Green Chem., 2010, 12, 1967-1975;
15. R. Lungwitz, V. Strehmel and S. Spange, New J. Chem., 2010, 34, 1135-1140.
16. S.N. Baker, G.A. Baker and F.V. Bright, Green Chem., 2002, 4, 165-169.
17. B.R. Mellein, S.N.V.K. Aki, R.L. Ladewski and J.F. Brennecke, J. Phys. Chem. B, 2007, 111, 131-138.
18. S. Trivedi, N.I. Malek, K. Behera and S. Pandey, J. Phys. Chem. B, 2010, 114, 8118-8125.
19. P. Wasserschied and T. Welton, Ionic Liquids in Synthesis, VCH Wiley, Weinheim, 2007.
20. A. Klamt, J. Phys. Chem., 1995, 99, 2224-2235.
21. A. Klamt, COSMO-RS from quantum chemistry to fluid phase thermodynamics and drug design, Elsevier, Amsterdam, Boston, 2005
22. A. Klamt and F. Eckert, Fluid Phase Equilibr., 2000, 172, 43-72.
23. A. Klamt and G. Schuurmann, J. Chem. Soc., 1993, 2, 799-805.
24. M.G. Freire, S.P.M. Ventura, L.M.N.B.F. Santos, I.M. Marrucho and J.A.P. Coutinho, Fluid Phase Equilibr., 2008, 268, 74-84.
25. M.G. Freire, L.M.N.B.F. Santos, I.M. Marrucho and J.A.P. Coutinho, Fluid Phase Equilibr., 2007, 255, 167-178.
26. A.R. Ferreira, M.G. Freire, J.C. Ribeiro, F.M. Lopes, J.G. Crespo and J.A.P. Coutinho, Ind. Eng. Chem. Res., 2011, 50, 5279-5294.
27. A.R. Ferreira, M.G. Freire, J.C. Ribeiro, F.M. Lopes, J.G. Crespo and J.A.P. Coutinho, Ind. Eng. Chem. Res., 2012, 51, 3483-3507.
28. C.M.S.S. Neves, J.F.O. Granjo, M.G. Freire, A. Robertson, N.M.C. Oliveira and J.A.P. Coutinho, Green Chem., 2011, 13, 1517-1526.
29. K.A. Kurnia and J.A.P. Coutinho, Ind. Eng. Chem. Res., 2013, 52, 13862-13874.

30. J. Palomar, M. Gonzalez-Miquel, A. Polo and F. Rodriguez, Ind. Eng. Chem. Res., 2011, 50, 3452-3463.
31. M. Gonzalez-Miquel, J. Palomar and F. Rodriguez, J. Phys. Chem. B, 2013, 117, 296-306.
32. A. Schäfer, A. Klamt, D. Sattel, J.C.W. Lohrenz and F. Eckert, Phys. Chem. Chem. Phys., 2000, 2, 2187-2193.
33. A. Schäfer, C. Huber and R. Ahlrichs, J. Chem. Phys., 1994, 100, 5829-5835.
34. A. Klamt and F. Eckert, COSMOtherm program (Version C3.0 Release 13.01), 2013, COSMOlogic GmbH & Co. KG: Leverkusen, Germany.
35. R. Lungwitz, M. Friedrich, W. Linert and S. Spange, New J. Chem., 2008, 32, 1493-1499.
36. R. Lungwitz and S. Spange, New J. Chem., 2008, 32, 392-394.
37. R. Lungwitz, V. Strehmel and S. Spange, New J. Chem., 2010, 34, 1135-1140.
38. H. Niedermeyer, C. Ashworth, A. Brandt, T. Welton and P.A. Hunt, Phys. Chem. Chem. Phys., 2013, 15, 11566-11578.
39. M.J. Kamlet and R.W. Taft, J. Am. Chem. Soc., 1976, 98, 377-383.
40. M.J. Kamlet and R.W. Taft, J. Am. Chem. Soc., 1976, 98, 2886-2894.
41. M.J. Kamlet, J.L. Abboud and R.W. Taft, J. Am. Chem. Soc., 1977, 99, 6027-6038.
42. M.J. Kamlet, J.L. Abboud, M.H. Abraham and R.W. Taft, J. Org. Chem., 1983, 48, 2877-2887.
43. M.G. Freire, L.M.N.B.F. Santos, A.M. Fernandes, J.A.P. Coutinho and I.M. Marrucho, Fluid Phase Equilib., 2007, 261, 449-454.
44. A.F.M. Cláudio, C.F.C. Marques, I. Boal-Palheiros, M.G. Freire and J.A.P. Coutinho, Green. Chem., 2014, 16, 259–268.
45. A.F.M. Cláudio, A.M. Ferreira, M.G. Freire and J.A.P. Coutinho, Green Chem., 2013, 15, 2002-2010.
46. A. George, K. Tran, T.J. Morgan, P.I. Benke, C. Berrueco, E. Lorente, B.C. Wu, J.D. Keasling, B.A. Simmons and B.M. Holmes, Green Chem., 2011, 13, 3375-3385.
47. T.P. Wells, J.P. Hallet, C.K. Williams, T. Welton, J. Org. Chem., 2008, 73, 5585-5588.
48. A.F.M. Cláudio, A.M. Ferreira, S. Shahriari, M.G. Freire and J.A.P. Coutinho, J. Phys. Chem. B, 2011, 115, 11145-11153.
49. Y. Fukayaa, K. Hayashia, M. Wadab and H. Ohno, Green Chem., 2008, 10, 44-46.
50. A. Brandt, M.J. Ray, T.Q. To, D.J. Leak, R.J. Murphy and T. Welton, Green Chem., 2011, 13, 2489-2499.
51. P. Bonhôte, A.P. Dias, N. Papagergiou, K. Kalyanasundaram and M. Grätzel, Inorg. Chem., 1996, 35, 1168-1178.
52. S. Chen, R. Vijayaraghavan, D.R. MacFarlane and E.I. Izgorodina, J. Phys. Chem. B, 2013, 117, 3186-3197.

2.4. Characterization of Aqueous Biphasic Systems Composed of Ionic Liquids and a Citrate-based Biodegradable Salt

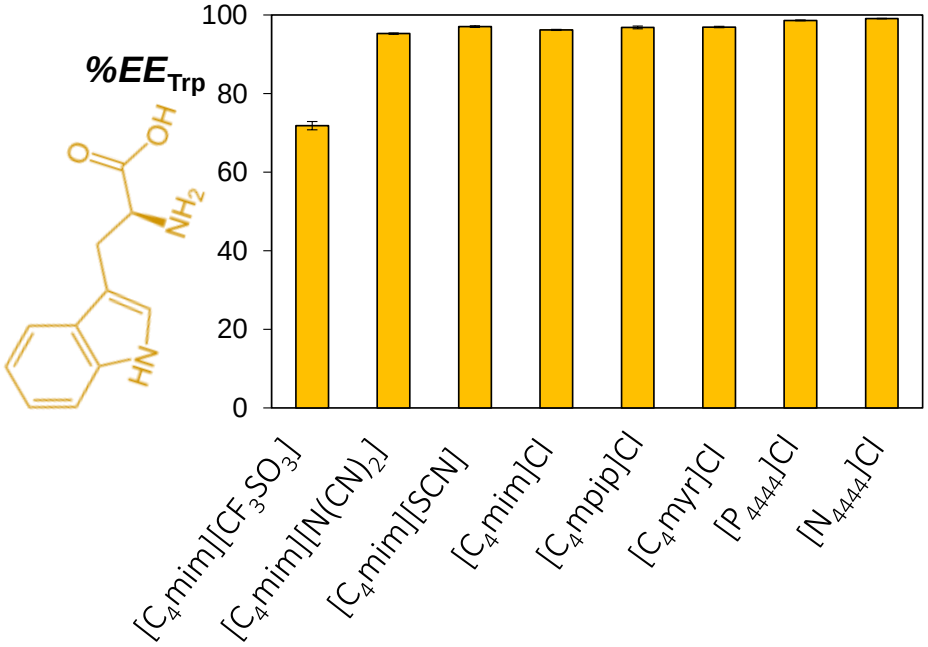

This chapter is based on the published paper: Passos, H.; Ferreira, A. R.; Cláudio, A. F. M.; Coutinho, J. A. P.; Freire, M. G., Characterization of Aqueous Biphasic Systems Composed of Ionic Liquids and a Citrate-Based Biodegradable Salt, Biochem. Eng. J., 2012, 67, 68-76.

Abstract

Albeit IL-based ABS have been largely explored as liquid-liquid extractive approaches for a large array of (bio)molecules, the application of biodegradable and nontoxic salts as phase constituents of these systems has been seldom investigated. In this work 15 ionic liquids were evaluated toward their ability to form ABS in the presence of a common biodegradable organic salt: potassium citrate. The ternary phase diagrams, tie-lines, and respective tie-line lengths, were determined at 298 K. The gathered data allowed the evaluation of the effects of the IL cation core, of the cation side alkyl chain length, and of the anion nature, to form two-phase systems. It is shown that the ILs aptitude to undergo liquid-liquid demixing is mainly controlled by their hydrophobicity. The large differences observed between the phase diagrams behaviour suggest the possibility of tailoring the aqueous phases' polarities for a specific extraction. Therefore, the partitioning of a hydrophobic amino acid produced by bacteria fermentation, L-tryptophan, was also addressed aiming at exploring the applicability of the proposed systems in the biotechnology field. Single-step extraction efficiencies of L-tryptophan for the IL-rich phase range between 72 % and 99 %.

Introduction

A large set of literature data has been focused on ionic-liquid-based ABS and where most of the salts used are based on phosphates, sulphates, and carbonate anions.[1-10] However, common inorganic salts lead to environmental concerns when discharged in high concentrations into the effluent streams. Recent works have introduced biodegradable and nontoxic organic salts, such as the citrate-, tartrate- or acetate-based,[11-21] or non-charged, biodegradable, nontoxic, and renewable feedstock organic compounds, such as carbohydrates[22] or amino acids,[8] in the formulation of IL-based ABS. Nevertheless, the works dealing with organic salts[11-21] addressed ILs based essentially on the imidazolium

cation with the bromide, chloride, and tetrafluoroborate counterions. Besides the water-stable chloride and bromide-based ILs, [BF_4]-based fluids tend to be the most largely explored,[11-21] and it should be stressed that [BF_4]-based ILs are not water stable and form hydrofluoridric acid in aqueous media.[23]

Since citrate-based salts are biodegradable and nontoxic, we studied here a large array of ionic-liquid-based ABS, making use of potassium citrate, as "greener" alternatives to the previously studied systems.[1-11] Moreover, aiming at achieving a proof of principle on the applicability of the studied systems, the partitioning of L-tryptophan was also addressed. Aromatic amino acids, such as L-tryptophan, L-phenylalanine, and L-tyrosine, can be produced by bacterial fermentation.[24] Two representative producer organisms are *Corynebacterium glutamicum* and *Escherichia coli*.[24] In particular, L-tryptophan is one of the amino acids difficult to obtain in a high level of production yield.[24] Hence, several attempts at strain improvement have been explored, namely the recombinant DNA technology.[25] It has been shown that to guarantee the cell viability and increase the rate of tryptophan production, 4 main parameters should be optimized, namely the efflux of tryptophan, the growth rate, the inhibition constant, and the tryptophan repressor level.[26] In this context, the application of ionic-liquid-based ABS could be a valuable alternative to guarantee a continuous tryptophan extraction step during fermentation.

Experimental Procedure

Materials

The determination of the liquid-liquid ternary phase diagrams was performed using aqueous solutions of potassium citrate tribasic monohydrate, $C_6H_5K_3O_7.H_2O$ (≥ 99 wt % pure from Sigma-Aldrich), and individual aqueous solutions of the following ILs: 1-butyl-3-methylimidazolium chloride, $[C_4mim]Cl$ (99 wt %); 1-hexyl-3-methylimidazolium chloride, $[C_6mim]Cl$ (> 98 wt %); 1-butyl-3-methylpyridinium chloride, $[C_4mpy]Cl$ (> 98 wt %); 1-butyl-1-methylpiperidinium chloride, $[C_4mpip]Cl$ (99 wt %); 1-butyl-1-methylpyrrolidinium chloride, $[C_4mpyr]Cl$ (99 wt %); tetrabutylammonium chloride, $[N_{4444}]Cl$ (≥ 97 wt %); tetrabutylphosphonium chloride, $[P_{4444}]Cl$ (98 wt %); 1-butyl-3-methylimidazolium bromide, $[C_4mim]Br$ (99 wt %); 1-butyl-3-methylimidazolium acetate, $[C_4mim][CH_3CO_2]$ (> 98 wt %); 1-butyl-3-methylimidazolium methanesulfonate, $[C_4mim][CH_3SO_3]$ (99 wt %); 1-butyl-3-methylimidazolium trifluoroacetate, $[C_4mim][CF_3CO_2]$ (> 97 wt %); 1-butyl-3-methylimidazolium trifluoromethanesulfonate, $[C_4mim][CF_3SO_3]$ (99 wt %); 1-butyl-3-methylimidazolium dicyanamide, $[C_4mim][N(CN)_2]$ (> 98 wt %); 1-butyl-3-methylimidazolium thiocyanate, $[C_4mim][SCN]$ (> 98 wt %); and 1-butyl-3-methylimidazolium dimethylphosphate, $[C_4mim][PO_4(CH_3)_2]$ (> 98 wt %). All imidazolium-, pyridinium-, and pyrrolidinium-based ionic liquids were purchased from Iolitec. The tetrabutylphosphonium chloride was kindly supplied by Cytec Industries Inc. The tetrabutylammonium chloride was from Aldrich. Chemical structures of studied ILs are depicted in Figure 2.4.1. To reduce the volatile impurities to negligible values, IL individual samples were purified under constant agitation, under vacuum, and at moderate temperature (323 K), for a minimum of 24 h. After this procedure, the purity of each ionic liquid was further checked by ^{1}H and ^{13}C NMR spectra and found to be in accordance with the stated purity level provided by the suppliers.

The water used was double distilled, passed through a reverse osmosis system, and further treated with a Milli-Q plus 185 apparatus. L-tryptophan (purity > 99.0 wt %) was from Sigma.

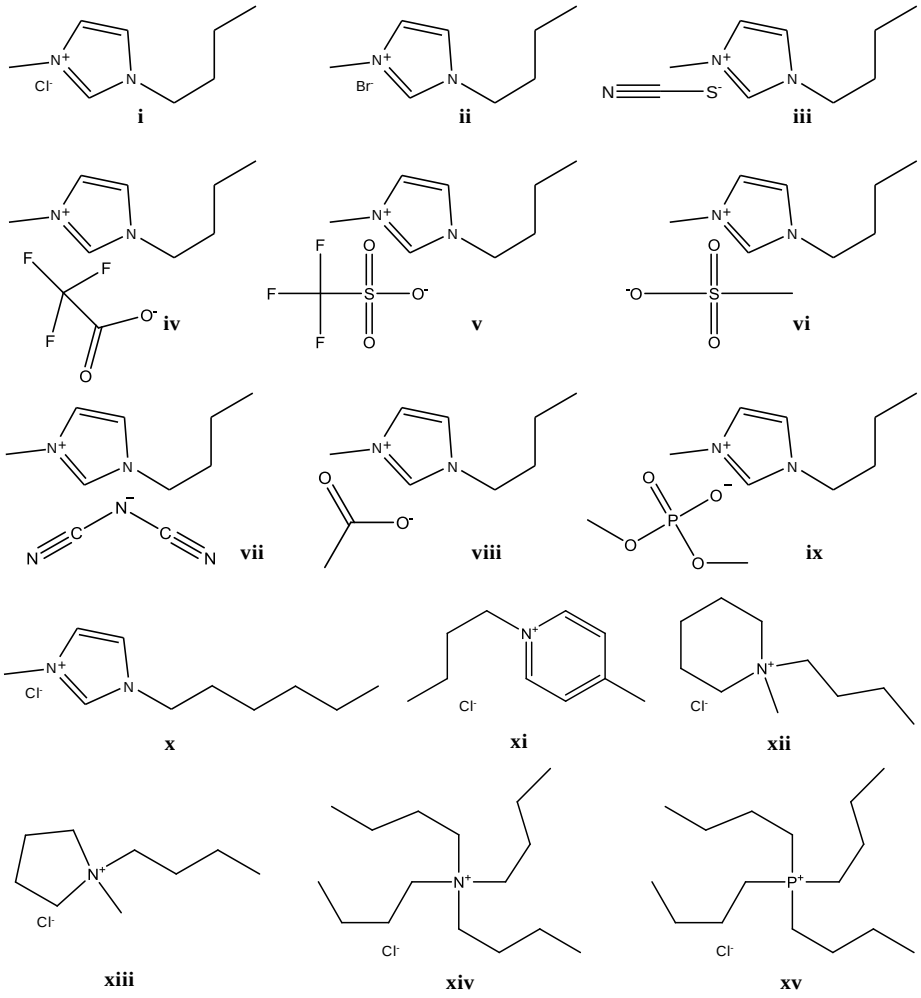

Figure 2.4.1: Chemical structures of the ionic liquids used to form ABS: (i) $[C_4mim]Cl$, (ii) $[C_4mim]Br$, (iii) $[C_4mim][SCN]$, (iv) $[C_4mim][CF_3CO_2]$, (v) $[C_4mim][CF_3SO_3]$, (vi) $[C_4mim][CH_3SO_3]$, (vii) $[C_4mim][N(CN)_2]$, (viii), $[C_4mim][CH_3CO_2]$, (ix) $[C_4mim][PO_4(CH_3)_2]$, (x) $[C_6mim]Cl$, (xi) $[C_4mpy]Cl$, (xii) $[C_4mpip]Cl$, (xiii) $[C_4mpyr]Cl$, (xiv) $[N_{4444}]Cl$, (xv) $[P_{4444}]Cl$.

Phase Diagrams, Tie-Lines and pH measurements

The solubility curves were determined through the cloud point titration method and at (298 ± 1) K and atmospheric pressure (and as previously described in **Chapters 2.1 and 2.2**). The experimental binodal curves were fitted by eq 2.1.1.

The tie-lines (TLs) were determined by a gravimetric method originally proposed by Merchuk et al.[27] for polymer-based ABS, and later on applied by Rogers and co-workers[1] to IL-based ABS. Further details on the determination of TLs and TLLs are described in **Chapter 2.1**.

The pH values of the IL- and organic-salt-rich aqueous phases were measured at 298 as described in **Chapter 2.1**. The compositions at which the pH was measured correspond to the same compositions adopted for the TLs determination.

Partitioning of L-tryptophan

The partitioning of L-tryptophan was evaluated in several systems composed of 20 wt % of $C_6H_5K_3O_7$, 40 wt % of each ionic liquid, and 40 wt % of an aqueous solution containing L-tryptophan at 0.77 g·dm^{-3} (3.8 × 10^{-4} mol·dm^{-3}). All mixtures were prepared by weight with an uncertainty of ± 10^{-4} g. The mixtures were prepared and vigorously stirred, and further allowed to equilibrate and phase separate for at least 12 h at (298 ± 1) K. Preliminary optimization studies showed that the partitioning of L-tryptophan was completely attained after 12 h of equilibrium.

After the separation of the phases, the amount of L-tryptophan was quantified through UV-spectroscopy, using a SHIMADZU UV-1700, Pharma-Spec Spectrometer, at a wavelength of 279 nm, and using a calibration curve previously established. Slight interferences of the salt and some ILs in the quantification of L-tryptophan were verified. Therefore, to minimize these interferences, ternary mixtures at the same weight fraction composition were prepared, using pure water instead of the L-tryptophan aqueous solution, and used as blank samples. At least three individual samples of each system were prepared for the quantification of L-tryptophan in both phases. The partition coefficient of L-tryptophan, K_{Trp}, was determined according to the following equation,

$$K_{Trp} = \frac{[Trp]_{IL}}{[Trp]_{Salt}} \qquad \text{eq. 2.4.1}$$

where $[Trp]_{IL}$ and $[Trp]_{Salt}$ are the concentrations of L-tryptophan in the ionic-liquid-rich and in the citrate-rich phase, respectively.

The extraction efficiencies of L-tryptophan were determined according to,

$$\%EE_{Trp} = \frac{[Trp]_{IL} \times w_{IL}}{[Trp]_{IL} \times w_{IL} + [Trp]_{Salt} \times w_{Salt}} \times 100 \qquad \text{eq. 2.4.2}$$

where w_{IL} and w_{Salt} are the weight of the ionic-liquid-rich phase and of the citrate-rich phase, respectively, and $[Trp]_{IL}$ and $[Trp]_{Salt}$ are the concentration of L-tryptophan in the ionic-liquid-rich phase and in the citrate-rich phase, respectively.

Results and Discussion

Novel ternary phase diagrams were determined for several ionic liquids + water + potassium citrate, at 298 K and at atmospheric pressure. The ionic structures of the ionic liquids that were able to create liquid-liquid systems with this salt are depicted in Figure 2.4.1. The respective ternary phase diagrams are illustrated in Figures 2.4.2 to 2.4.4. The experimental weight fraction data of each phase diagram are given in the *Supporting Information* (Tables S22 to S31).

The systems composed of potassium citrate, water, and $[C_4mim]Br$ or $[C_4mim]Cl$ have already been reported by Zafarani-Moattar and Hamzehzadeh.[16-17] It should be remarked that a good agreement was observed between our data and literature data.[16-17] The respective comparisons are provided in the *Supporting Information* (Figure S3).

In the studied ABS, the top phase corresponds to the IL-rich phase, while the bottom phase is mainly composed of the citrate-based salt. The only exception was observed with the $[C_4mim][CF_3SO_3]$-based system. This feature was already observed with other salts.[4,5]

In all phase diagrams, the biphasic region is localized above the solubility curve. The larger this region, the higher the ability of the IL to undergo liquid-liquid demixing, *i.e.*, the easier the IL is salted-out by the citrate-based salt.

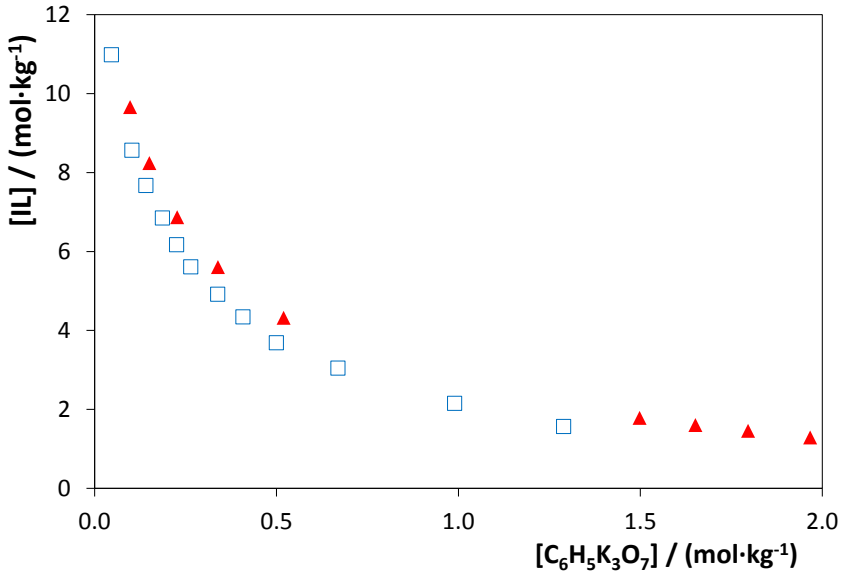

Figure 2.4.2: Evaluation of the cation alkyl side chain length in the ternary phase diagrams composed of ionic liquid + water + $C_6H_5K_3O_7$: ▲, [C_4mim]Cl; □, [C_6mim]Cl.

Figure 2.4.2 depicts the effect of the imidazolium side alkyl chain length in the formation of ABS. In general, an increase in the aliphatic chain facilitates the creation of ABS. Longer aliphatic chains at the cation contribute to an enhanced hydrophobicity displayed by the IL. Indeed, as the IL becomes more hydrophobic there is a reduction on the water-ionic-liquid affinity and, therefore, an improved phase separation occurs. Binary liquid-liquid equilibrium data further supports this idea: an increase in the cation side alkyl chain length decreases the solubility of the ionic liquid in water.[28] Moreover, this pattern is in close agreement with previous results on ILs-based ABS composed of distinct salts, and as already shown in this thesis.

It should be stressed that 3 additional ILs were tested according to their ability to form liquid-liquid aqueous phases, namely 1-ethyl-3-methylimidazolium chloride, 1-allyl-3-methylimidazolium chloride, and 1-hydroxyethyl-3-methylimidazolium chloride. However, we couldn't detect the coexisting liquid aqueous phases with these ionic liquids. Only solid-liquid equilibria were observed. The solid phases were further identified by ^{1}H and ^{13}C NMR spectra and correspond merely to the ionic liquid. Therefore, it is safe to admit that there is no ion exchange among the studied ILs and the citrate-based salt (at least not above the detection limit of the equipment). Since potassium citrate has a higher affinity for water compared to the ILs, there is the preferential exclusion of the IL from

the aqueous solution. The reason behind the formation of solid-liquid equilibrium instead of liquid-liquid equilibrium with these ILs is a consequence of their higher melting temperature (358 K for 1-ethyl-3-methylimidazolium chloride,[29] 325 K for 1-allyl-3-methylimidazolium chloride,[30] and 359 K for 1-hydroxyethyl-3-methylimidazolium chloride[31]) compared with the remaining ILs. Indeed, these ILs are more structurally similar to conventional salts and thus present higher melting temperatures.

The effect of the cation core is displayed in Figure 2.4.3. The ionic liquid cation ability to form ABS, for instance at 0.5 mol·kg^{-1} of potassium citrate, follows the order: $[P_{4444}]^+$ > $[N_{4444}]^+$ >> $[C_4mpy]^+$ ≈ $[C_4mpip]^+$ > $[C_4mpyrr]^+$ > $[C_4mim]^+$. This trend reflects the aptitude of the ionic liquid cation to be solvated by water (since the chloride anion is the counterion common to all ionic liquids), and which is regulated by steric and entropic contributions.[28,32]

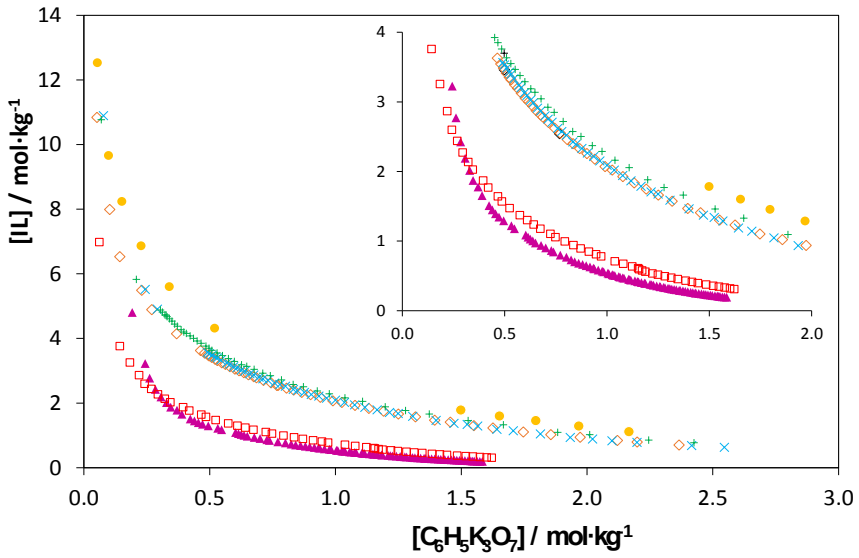

Figure 2.4.3: Evaluation of the cation core in the ternary phase diagrams composed of ionic liquid + water + $C_6H_5K_3O_7$: ●, $[C_4mim]Cl$; ◇, $[C_4mpip]Cl$; +, $[C_4mpyrr]Cl$; ×, $[C_4mpy]Cl$; ▲, $[P_{4444}]Cl$; □, $[N_{4444}]Cl$.

This trend follows the hydrophobic sequence of the IL cations. Quaternary phosphonium- and ammonium-based cations are those that present the higher ability to form ABS since they present four butyl chains which are responsible for their higher hydrophobicity. Their water miscibility essentially results from the strong solvation of the chloride anion. From the comparison among the cyclic nitrogen-based ILs, it is clear that the 6-sided ring

cations, such as pyridinium and piperidinium are more able to induce ABS when compared with the smaller 5-sided rings of imidazolium and pyrrolidinium. Hence, the inherent hydrophobicity of the cation, which is also ruled by their carbon number, is the main factor behind the ability of these compounds to form ABS. The trends obtained here are in agreement with the results previously reported for additional IL-based ABS composed of different salts[32] and also correlate with the solubility of these ILs in water.[33] From the results obtained it is evident that a large number of combinations of IL cations can be employed in the formation of IL-based ABS, and that these systems allow the tailoring of the phases' polarities aiming at performing specific extractions.

The effect of the anion nature on the ABS phase behaviour was studied with several ILs containing the common $[C_4mim]^+$ cation, while combined with the following anions: Cl^-, Br^-, $[CH_3SO_3]^-$, $[CH_3CO_2]^-$, $[CF_3SO_3]^-$, $[CF_3CO_2]^-$, $[SCN]^-$, $[N(CN)_2]^-$, and $[PO_4(CH_3)_2]^-$. The corresponding ternary phase diagrams are depicted in Figure 2.4.4.

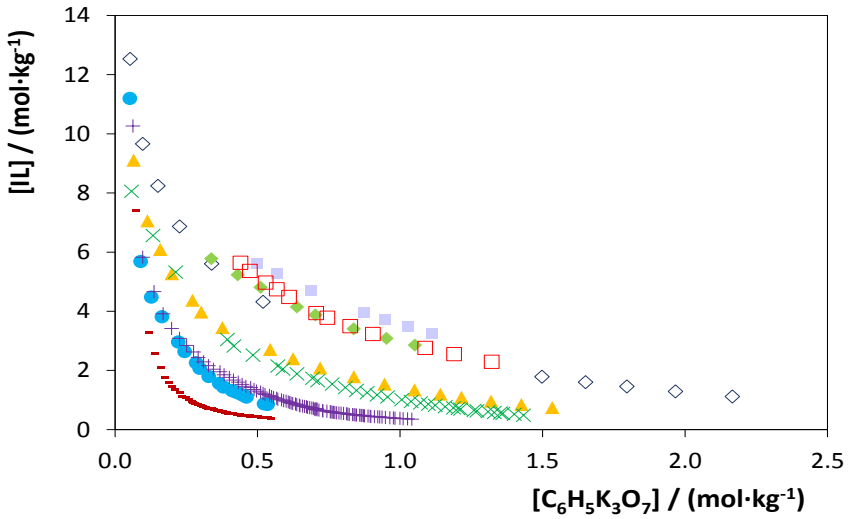

Figure 2.4.4: Evaluation of the anion nature in the ternary phase diagrams composed of ionic liquid + water + $C_6H_5K_3O_7$: ▬, $[C_4mim][CF_3SO_3]$; ●, $[C_4mim][SCN]$; +,$[C_4mim][N(CN)_2]$; ×, $[C_4mim][CF_3CO_2]$; ▲, $[C_4mim]Br$; ◇, $[C_4mim]Cl$; ◆, $[C_4mim][CH_3SO_3]$, □, $[C4mim][PO_4(CH_3)$, ■, $[C_4mim][CH_3CO_2]$.

Figure 2.4.4 reveals that a large number of ILs constituted by different anions can be combined with organic salts besides the chloride-, bromide-, and tetrafluoroborate-based fluids commonly investigated.[11-21] At 0.5 mol·kg^{-1} of potassium citrate, the IL anion ability

to form ABS is: $[CH_3CO_2]^-$ < $[PO_4(CH_3)_2]^-$ < $[CH_3SO_3]^-$ < Cl^- << Br^- < $[CF_3CO_2]^-$ << $[N(CN)_2]^-$ < $[SCN]^-$ < $[CF_3SO_3]^-$. This rank is in close agreement with previous works using inorganic salts such as K_3PO_4, K_2HPO_4 and Na_2SO_4, reported in **Chapters 2.1 and 2.2**. The good agreement on the anion trend observed among systems constituted by different salts suggests that the ionic liquid pattern for creating ABS is not affected by the salt nature or the pH of the aqueous salt solution employed.

The anions of ILs compete with the salt ions for the formation of hydration complexes. Usually this competition is won by the ions with a higher charge density, *i.e.*, ions that are capable of stronger interactions with water. For a common cation, ILs composed of anions with lower hydrogen bond basicity are more able to form ABS. Indeed, a close agreement exists between the tendency on the ILs ability to form ABS and the hydrogen bond basicity values determined by solvatochromic probes - Figure 2.4.5. Moreover, the fluorination of the anions, which further implies a lower ability of the anion for hydrogen-bonding, leads to an enhanced capability of the IL to undergo liquid-liquid demixing. For instance, $[C_4mim][CF_3CO_2]$ and $[C_4mim][CF_3SO_3]$ are more easily salted-out than $[C_4mim][CH_3CO_2]$ and $[C_4mim][CH_3SO_3]$, respectively. Therefore, fluorinated ILs require a less amount of salt to form two aqueous liquid phases.

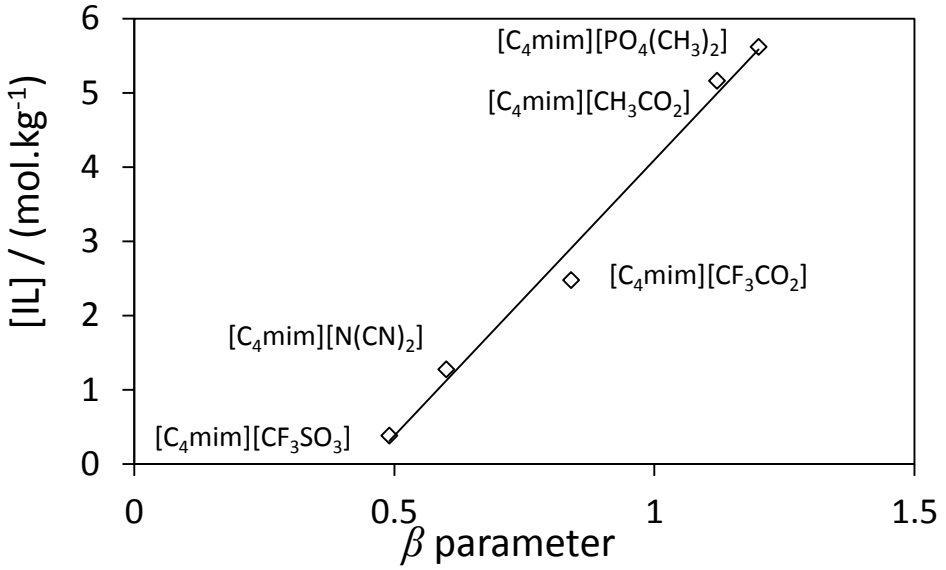

Figure 2.4.5: Ionic liquid molality, taken from each binodal curve and at which the $C_6H_5K_3O_7$ molality is equal to 0.5 mol·kg^{-1}, as a function of the hydrogen bond basicity values (β).[34,35]

For the studied systems, the experimental binodal data were further fitted by the empirical relationship described by eq 2.1.1. The regression parameters were estimated by the least-squares regression, and their values and corresponding standard deviations (σ) are provided in Table 2.4.1. In general, good correlation coefficients were obtained for all systems indicating that these fittings can be used to predict data in a given region of the phase diagram where no experimental results are available.

Table 2.4.1: *A*, *B* and *C* are constants obtained by the regression of the experimental binodal data through the application of eq 2.1.1 (and respective standard deviations, σ, and correlation coefficients, R^2) for the several systems at 298 K.

Ionic liquid	$A \pm \sigma$	$B \pm \sigma$	10^5 ($C \pm \sigma$)	R^2
$[C_4mim]Cl$	86.0 ± 0.5	-0.180 ± 0.003	0.84 ± 0.03	0.9998
$[C_4mim]Br$	92.4 ± 0.6	-0.228 ± 0.003	1.87 ± 0.06	0.9997
$[C_4mim][CF_3SO_3]$	208.8 ± 5.0	-0.829 ± 0.012	1.00 ± 1.44	0.9968
$[C_4mim][CF_3CO_2]$	93.7 ± 1.9	-0.222 ± 0.008	3.40 ± 0.15	0.9958
$[C_4mim][SCN]$	120.9 ± 4.3	-0.470 ± 0.019	13.34 ± 2.37	0.9951
$[C_4mim][N(CN)_2]$	121.8 ± 1.8	-0.444 ± 0.006	6.56 ± 0.24	0.9968
$[C_4mim][CH_3SO_3]$	85.0 ± 2.8	-0.123 ± 0.010	1.02 ± 0.15	0.9987
$[C_4mim][CH_3CO_2]$	82.6 ± 3.7	-0.117 ± 0.013	0.95 ± 0.13	0.9994
$[C_4mim][PO_4(CH_3)_2]$	112.2 ± 2.2	-0.179 ± 0.006	0.54 ± 0.05	0.9996
$[C_6mim]Cl$	85.9 ± 1.0	-0.173 ± 0.005	1.61 ± 0.14	0.9983
$[C_4mpip]Cl$	87.1 ± 0.3	-0.210 ± 0.001	0.85 ± 0.01	0.9997
$[C_4mpyr]Cl$	87.8 ± 0.5	-0.214 ± 0.002	0.74 ± 0.02	0.9993
$[C_4mpy]Cl$	94.3 ± 0.4	-0.232 ± 0.001	0.80 ± 0.01	0.9996
$[P_{4444}]Cl$	170.0 ± 5.7	-0.484 ± 0.011	1.64 ± 0.14	0.9944
$[N_{4444}]Cl$	99.3 ± 0.9	-0.318 ± 0.003	1.79 ± 0.06	0.9990

The experimental tie-lines, along with their respective length, are reported in Table 2.4.2. An example of the tie-lines obtained for this type of systems is depicted in the *Supporting Information* (Figure S4).

The pH values of both phases in each ABS, and for the compositions for which the TLs were determined, are given in Table 2.4.2. The pH values of these systems are in the alkaline region (pH = 8 - 10) and indicate their possible applicability for the extraction of a given (bio)molecule. Since an aqueous solution at 50 wt % of potassium citrate presents a pH value of *circa* 9.2, the differences observed in the pH values are due to the presence of the ILs in the aqueous media.

Table 2.4.2: Weight fraction percentage (wt %) for the coexisting phases of ionic liquid ([IL]) + potassium citrate ([Salt]) + H_2O, and respective values of TLL, and pH values of each phase.

Ionic liquid	weight fraction percentage / wt %								TLL
	$[IL]_{IL}$	$[Salt]_{IL}$	pH_{IL}	$[IL]_{M}$	$[Salt]_{M}$	$[IL]_{Salt}$	$[Salt]_{Salt}$	pH_{Salt}	
$[C_4mim]Cl$	52.68	7.33	9.00	39.74	20.35	5.83	54.47	8.98	66.46
	56.57	5.39	8.99	42.82	19.08	4.57	57.16	9.07	73.37
$[C_4mim]Br$	60.81	3.36	9.19	29.92	24.91	5.14	42.20	9.23	67.87
	73.40	1.02	9.52	40.01	25.03	1.07	53.04	9.04	89.08
$[C_4mim][CF_3SO_3]$	74.74	1.54	7.17	40.03	14.91	1.76	29.66	7.65	78.21
	82.48	1.26	7.20	39.82	20.41	0.73	37.96	7.67	89.61
$[C_4mim][SCN]$	56.77	2.57	7.79	14.93	15.05	9.61	16.64	7.84	49.21
	70.64	1.31	7.26	30.19	20.14	0.04	34.18	7.81	77.88
	74.25	1.08	7.06	39.94	20.02	0.00	42.07	7.78	84.81
$[C_4mim][N(CN)_2]$	47.57	4.43	8.76	21.82	15.14	9.67	20.19	8.83	41.05
	52.21	3.62	8.80	24.70	15.13	6.98	22.55	8.68	49.03
	58.81	2.68	8.87	29.95	14.97	3.98	26.04	8.66	59.60
	86.94	0.58	8.75	39.92	19.98	0.37	36.30	8.63	93.65
$[C_4mim][CH_3SO_3]$	61.89	6.49	9.36	36.88	29.91	2.95	61.68	8.93	80.74
$[C_6mim]Cl$	54.20	6.90	8.39	44.89	15.02	2.62	51.86	8.88	68.43
$[C_4mpip]Cl$	49.13	7.38	9.41	32.05	24.96	5.83	51.94	9.29	62.13
	54.23	5.04	9.52	40.00	20.06	3.98	58.11	9.32	73.08
	59.43	3.32	9.61	43.00	19.96	2.44	61.04	9.49	81.11
$[C_4mpyr]Cl$	54.34	4.99	9.31	39.93	19.92	4.54	56.62	10.09	71.73
	54.23	5.04	9.31	40.00	20.06	3.98	58.11	10.58	73.08
	55.52	4.56	9.30	41.98	18.59	4.07	57.86	10.04	74.08
$[C_4mpy]Cl$	45.12	9.90	8.31	30.03	25.05	8.70	46.47	8.23	51.61
	55.51	5.20	8.18	34.76	25.10	5.04	53.61	8.18	69.94
$[P_{4444}]Cl$	39.56	8.94	7.99	30.06	14.96	8.93	28.33	7.86	36.25
	50.66	6.23	8.32	34.80	15.21	7.14	30.88	8.22	50.01
	67.27	3.67	8.39	39.92	20.06	1.99	42.80	8.29	76.11
$[N_{4444}]Cl$	42.92	6.86	8.81	26.97	20.05	5.19	38.07	8.95	48.96
	52.43	4.02	9.12	31.81	20.18	3.08	42.70	9.03	62.70
	64.74	1.81	9.58	39.87	20.21	1.36	48.71	9.32	78.84

Figure 2.4.6 depicts the results obtained for the partition coefficients and percentage extraction efficiencies of L-tryptophan in several IL-based ABS. The composition of the coexisting phases corresponding to the common initial mixture are given in Table 2.4.2.

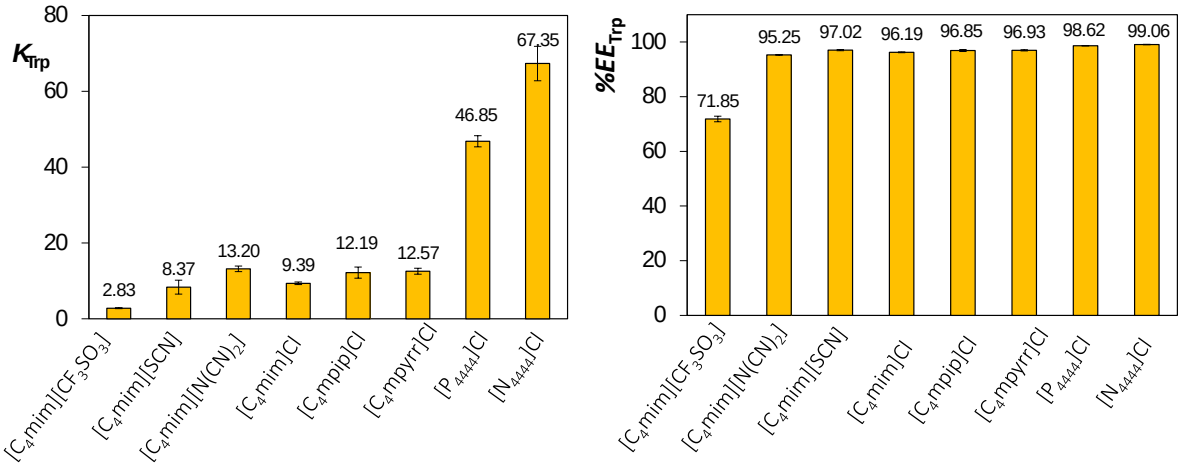

Figure 2.4.6: Partition coefficients (K_{Trp}) and extraction efficiencies (%EE_{Trp}) of L-tryptophan in ABS composed of ionic liquids and $C_6H_5K_3O_7$ at 298 K.

The partition coefficients of L-tryptophan range between 3 and 67, indicating thus a preferential partitioning of the amino acid for the IL-rich phase in all the investigated systems. The single-step extraction efficiencies range between 72 % and 99 %. Although small deviations are verified in this work, it should be stressed that an increase in the partition coefficient does not necessarily involves the increase in the extraction efficiency or *vice-versa*. The percentage extraction efficiencies are a result of the concentration of L-tryptophan in each phase combined with their total weight.

For the common mixture composition the partition coefficient of L-tryptophan increases in the order: $[C_4mim][CF_3SO_3]$ < $[C_4mim][SCN]$ < $[C_4mim]Cl$ < $[C_4mpip]Cl$ ≈ $[C_4mpyr]Cl$ < $[C_4mim][N(CN)_2]$ < $[P_{4444}]Cl$ < $[N_{4444}]Cl$.

It is well known that, depending on the pH of the solution, amino acids can be present in the form of different species due to the ionization/protonation of their characteristic functional groups: –COOH and $–NH_2$. Since for tryptophan, the protonation constants values are p*K*a1 = 2.38 and p*K*a2 = 9.39,[36] the amino acid is predominately on its cationic form (and therefore positively charged) in the systems with a pH below 2.38, it is mainly a zwitterion (with no net charge) if the pH is between 2.38 and 9.39, and it is negatively charged if the pH of the coexisting phases is higher than 9.39. The pH values of the IL-rich

phase in the mixtures used for the partitioning experiments are between p*K*a1 and p*K*a2. However, most of the pH values of the phases are alkaline and near the value of p*K*a2 meaning that in some examples there are already significant amounts of charged tryptophan that act as excellent counter ions for the cationic more hydrophobic phase containing the IL. In fact, two systems present pH values ranging between 7.06-7.20, and those are the ones where the lower partitioning coefficients were observed ($[C_4mim][CF_3SO_3]$ and $[C_4mim][SCN]$). For pH values above 8 the partition coefficients of L-tryptophan range between 13 and 67. Although $[N_{4444}]Cl$ presents the highest partition coefficient, which could be associated with high pH values, high partition coefficients in the $[C_4mpyr]Cl$-based system are not observed in spite of the similar high pH values at the coexisting phases. Moreover, no large differences in the partition coefficients of L-tryptophan are observed among the chloride and cyclic nitrogen-based ionic liquids, namely $[C_4mim]Cl$, $[C_4mpyr]Cl$ and $[C_4mpip]Cl$. Indeed, the systems containing these ILs present a similar TLL for the extraction point, reflecting thus the similarity in the composition of the coexisting phases among the 3 systems. Rogers and co-workers[1] already showed that the IL-rich phase becomes increasingly hydrophobic as the divergence between the two phases increases, *i.e.* with an increase in the TLL, making use of partitioning experiments of a series of short chain alcohols. On the other hand, larger differences are observed between these and $[P_{4444}]Cl$ and $[N_{4444}]Cl$. Systems formed by the two later ILs show a better performance for extracting the amino acid, with extraction efficiencies in the order of 99 %. These systems also show longer TLLs which further induce coexisting phases of progressive different polarities, albeit presenting different pH values. Finally, the effect of the IL anion seems to have a stronger effect on the partition coefficients of L-tryptophan. For the $[C_4mim]$-based ILs the partitioning of the amino acid for the IL-rich phase follows the order: $[C_4mim][CF_3SO_3] < [C_4mim][SCN] < [C_4mim]Cl < [C_4mim][N(CN)_2]$. In addition, this rank does not reflect the compositions of the coexisting phases as shown by the TLL values. Therefore, the results obtained seem to indicate that the partition coefficient of L-tryptophan depends on a delicate balance between the amount of charged species and the composition of the phases.

In our previous works, the partition coefficients of L-tryptophan in ABS composed of diverse ILs and K_3PO_4 have shown to be more dependent on the ionic liquid cation than on the ionic liquid anion.[4,5] This pattern is a direct consequence of the anionic nature of L-tryptophan in the systems formed by the highly alkaline K_3PO_4 (pH values > 12 in the coexisting phases). In the systems studied in this work, with lower pH values, the effect of the ionic liquid anion seems to be more relevant (especially if the extraction efficiencies are evaluated).

The partition coefficients obtained in this work are lower than those obtained before using K_3PO_4 and similar ILs.[4,5] However, it should be remarked that high extraction efficiencies are still observed here while using a biodegradable organic salt such as potassium citrate. Moreover, the extraction efficiencies obtained with the citrate salt are higher than those previously observed by our group with ABS formed by $[C_4mim][CF_3SO_3]$ and a large variety of carbohydrates, where the extraction efficiencies were close to 50 %.[22]

Zafarani-Moattar and Hamzehzadeh[21] provided the partitioning coefficients of several amino acids in ABS composed of 1-butyl-3-methylimidazolium bromide and potassium citrate at 298 K, and also investigated the effect of the pH of the aqueous media towards the partitioning behaviour. The authors[21] concluded that hydrophobic interactions were the main driving force for the amino acids partitioning, although salting-out effects and electrostatic interactions also play a role. The partitioning coefficients of L-tryptophan increase with the TLL and with the pH increase (from pH = 5.00 to 7.00).[21] However, based on the range of the partitioning coefficient values obtained by the authors[21] and those obtained here it seems that the tailoring of the partitioning of amino acids is more easily attained by the manipulation of the IL structure (if compared with the phases composition and pH values of the coexisting phases).

Finally, it should be stressed that the partition coefficients of L-tryptophan obtained in this work are significantly higher than those observed with polymer-based ABS: $K_{Trp} \approx 1$ in polymer-polysaccharide ABS[37,38] and $K_{Trp} \approx 1$-7 in polymer-salt ABS.[39]

Conclusions

Aiming at developing more benign systems, we propose here the use of a biodegradable salt as a main constituent of ionic-liquid-based ABS. Novel ternary phase diagrams, tie-lines, and tie-line lengths were determined making use of a large range of ILs and a common organic salt: potassium citrate. The large array of ILs investigated and the distinct phase behaviours observed indicate that the tailoring of the phases' polarities can be achieved. In general, the higher the hydrophobicity of the IL, the better is the IL performance in inducing the liquid-liquid demixing.

The applicability of the studied ABS was evaluated through the determination of the partition coefficients and extraction efficiencies of a hydrophobic aromatic amino acid (L-tryptophan). In all the investigated systems the amino acid preferentially partitions for the IL-rich phase. The partition coefficients obtained range between 3 and 67, and extraction efficiencies between 72 % and 99 % were achieved. The partition coefficients of L-tryptophan in IL-based ABS are substantially higher than those observed in conventional polymer-based ABS. Therefore, the application of the systems here investigated in biotechnological approaches, aiming at continuously extracting the amino acid and avoiding competing pathways, is straigthforward envisaged.

References

1. K.E. Gutowski, G.A. Broker, H.D. Willauer, J.G. Huddleston, R.P. Swatloski, J.D. Holbrey and R.D. Rogers, J. Am. Chem Soc., 2003, 125, 6632-6633.
2. N.J. Bridges, K.E. Gutowski, R.D. Rogers, Green Chem., 2007, 9, 177-183.
3. Y.C. Pei, J.J. Wang, L. Liu, K. Wu and Y. Zhao, J. Chem. Eng. Data, 2007, 52, 2026-2031.
4. C.M.S.S. Neves, S.P.M. Ventura, M.G. Freire, I.M. Marrucho and J.A.P. Coutinho, J. Phys. Chem. B, 2009, 113, (2009) 5194-5199.
5. S.P.M. Ventura, C.M.S.S. Neves, M.G. Freire, I.M. Marrucho, J. Oliveira, J.A.P. Coutinho, J. Phys. Chem. B, 113, 9304-9310.
6. A.F.M. Cláudio, A.M. Ferreira, S. Shahriari, M.G. Freire and J.A.P. Coutinho, J. Phys. Chem. B, 2011, 115, 11145-11153.
7. C.L.S. Louros, A.F.M. Cláudio, C.M.S.S. Neves, M.G. Freire, I.M. Marrucho, J. Pauly and J.A.P. Coutinho, Int. J. Mol. Sci., 2010, 11, 1777-1791.
8. M. Domínguez-Pérez, L.I.N. Tomé, M.G. Freire, I.M. Marrucho, O. Cabeza and J.A.P. Coutinho, Sep. Purif. Technol., 2010, 72, 85-91.
9. C.M.S.S Neves, M.G. Freire and J.A.P. Coutinho, RSC Advances, 2012, 2, 10882-10890.
10. T. Mourão, A.F.M. Cláudio, I. Boal-Palheiros, M.G. Freire and J.A.P. Coutinho, J. Chem. Thermodyn., 2012, 54, 398-405.
11. Z. Li, Y. Pei, L. Liu and J. Wang, J. Chem. Thermodyn., 2010, 42, 932-937.
12. J. Han, C. Yu, Y. Wang, X. Xie, Y. Yan, G. Yin and W. Guan, Fluid Phase Equilib., 2010, 295, 98-103.
13. M.T. Zafarani-Moattar and S. Hamzehzadeh, J. Chem. Eng. Data, 2009, 54, 833-841.
14. J.A. Han, R. Pan, X.Q. Xie, Y. Wang, Y.S. Yan, G.W. Yin and W.X. Guan, J. Chem. Eng. Data, 2010, 55, 3749-3754.
15. R. Sadeghi, R. Golabiazar and H. Shekaari, J. Chem. Thermodyn., 2010, 42, 441-453.
16. M.T. Zafarani-Moattar and S. Hamzehzadeh, J. Chem. Eng. Data, 2010, 55, 1598-1610.
17. M.T. Zafarani-Moattar and S. Hamzehzadeh, Fluid Phase Equilib., 2011, 304, 110-120.
18. J. Han, Y. Wang, Y. Li, C. Yu and Y. Yan, J. Chem. Eng. Data, 2011, 56, 3679-3687.
19. J. Han, Y. Wang, C.l. Yu, Y.S. Yan and X.Q. Xie, Anal. Bioanal. Chem., 2011, 399, 1295-1304.
20. Y. Lu, W. Lu, W. Wang, Q. Guo and Y. Yang, Talanta, 2011, 85, 1621-1626.
21. M.T. Zafarani-Moattar and S. Hamzehzadeh, Biotechnol. Prog., 2011, 27, 986-997.
22. M.G. Freire, C.L.S. Louros, L.P.N. Rebelo and J.A.P. Coutinho, Green Chem., 2011, 13,1536-1545.
23. M.G. Freire, C.M.S.S. Neves, I.M. Marrucho, J.A.P. Coutinho and A.M. Fernandes, J. Phys. Chem. A, 2010, 114, 3744-3749.
24. M. Ikeda, Appl. Microb. Biotechnol., 2005, 69, 615-626.
25. S. Aiba, H. Tsunekawa and T. Imanaka, New, Appl. Environm. Microbiol., 1982, 43, 289-297.
26. A. Marín-Sanguino and N.V. Torres, Biotechnol. Prog., 2000, 16, 133-145.
27. J.C. Merchuk, B.A. Andrews and J.A. Asenjo, J. Chromatogr. B, 1998,711, 285-293.
28. M.G. Freire, P.J. Carvalho, R.L. Gardas, I.M. Marrucho, L.M.N.B.F. Santos and J.A.P. Coutinho, J. Phys. Chem. B, 2008, 112, 1604-1610.
29. J.S. Wilkes, J.A. Levisky, R.A. Wilson and C.L. Hussey, Inorg. Chem., 1982, 21, 1263-1264.
30. W. Ning, Z. Xingxiang, L. Haihui and H. Benqiao, Carbohydr. Polym., 2009, 76, 482-484.
31. Online Database of Chemicals from Around the World at http://www.chemblink.com/.
32. S.P.M. Ventura, S.G. Sousa, L.S. Serafim, Á.S. Lima, M.G. Freire and J.A.P. Coutinho, J. Chem. Eng. Data, 2011, 56, 4253–4260.
33 M.G. Freire, C.M.S.S. Neves, S.P.M. Ventura, M.J. Pratas, I.M. Marrucho, J. Oliveira, J.A.P. Coutinho, A.M. Fernandes, Fluid Phase Equilib., 2010, 294, 234-240.

34. M.A. Ab Rani, A. Brant, L. Crowhurst, A. Dolan, M. Lui, N.H. Hassan, J.P. Hallett, P.A. Hunt, H. Niedermeyer, J.M. Perez-Arlandis, M. Schrems, T. Welton and R. Wilding, Phys. Chem. Chem,. Phys., 2011, 13, 16831-16840.
35. A.F.M.Cláudio, L. Swift, J.P. Hallett, T. Welton, J.A.P. Coutinho and M. G. Freire, J. Phys. Chem. Chem. Phys, 2014, 16, 6593 – 6601.
36. J. Wang, Y. Pei, Y. Zhao and Z. Hu, Green Chem., 2005, 7, 196-202.
37. M. Lu, F. Tjerneld, J. Chromatogr. A, 1997, 766, 99-108.
38. P.P. Madeira, J.A. Teixeira, E.A. Macedo, L.M. Mikheeva, B.Y. Zaslavsky, Fluid Phase Equilibr., 2008, 267, 150-157.
39. A. Salabat, M.H. Abnosi, A. Motahari, J. Chem. Eng. Data, 2008, 53, 2018-2021

2.5. Reversible pH-Triggered Aqueous Biphasic Systems

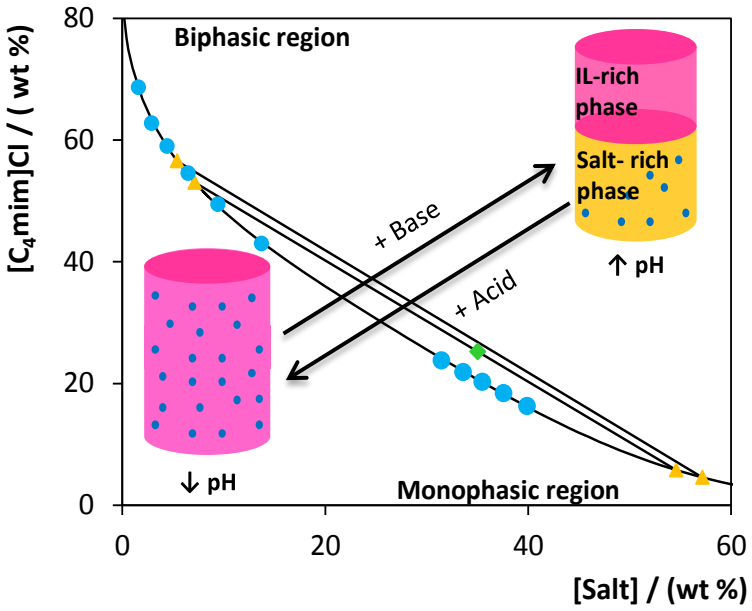

This chapter is based on the following manuscript: Ferreira, A. M., Cláudio, A. F. M. Rogers, R. D., Coutinho, J. A. P. and Freire, M.G., Reversible pH-Triggered Aqueous Biphasic Systems, under preparation (2014).

Abstract

In this work, reversible transitions between homogeneous solutions and biphasic systems triggered by a change in the pH of the aqueous media are demonstrated. In particular, reversible pH-dependent aqueous biphasic systems composed of several ILs and one organic salt that can suffer speciation are here disclosed. The potential application of the investigated reversible ABS is demonstrated with the selective separation of two dyes, chosen here as model molecules. Remarkably, the ABS constituted by $[C_4mim]Cl$ (the most hydrophilic IL investigated) is able to completely separate the two dyes for opposite phases with extraction efficiencies of 100% in a single-step procedure.

Introduction

Recently, a large interest has been devoted to the study of dynamic and reversible biphasic systems constituted by ionic liquids (ILs).[1-3] Specifically, it was demonstrated that phase transitions in mixtures involving ILs and other solvents can be induced by a temperature-driven phenomenon or by CO_2/N_2 flushing.[4-7] Some IL/solvent mixtures display an upper critical solution temperature (UCST)[8,9] whereas others present a lower critical solution temperature (LCST)[10-12]. These temperature-dependent phase transitions have shown to be advantageous in the selective separation of proteins[13] and metals[14]. However, common UCST and LCST behaviours in systems involving ILs typically occur at temperatures far from room temperature and a high energy input is required to trigger their phase switch. Furthermore, these systems are usually composed of an IL-rich phase (typically with hydrophobic characteristics) and a molecular-solvent-rich phase.[8-14] On the other hand, reversible liquid-liquid systems have been achieved with molecular solvents that react with CO_2 and thus form salts and/or ILs.[4-7] This reversibility pattern was accomplished by independent flush with gases and requires the use of specific

equipment. These reversible two-phase systems have been used in the separation of aliphatic and aromatic amines.[4-7]

Actually, the research in liquid-liquid extractions using ILs focuses on two main approaches: the direct use of non-water miscible hydrophobic ILs (where the reversible temperature- and CO_2/N_2-induced systems fall) and the use of aqueous biphasic systems (ABS) composed of ILs and organic/inorganic salts. IL-based ABS are benign and biocompatible options (present *circa* 70 wt % of water in the overall system) and also allow the complete extraction of a wide variety of compounds and high concentration factors.[15-18] In spite of all these advantages and enhanced performance, the pH-driven reversible behaviour of IL-based ABS has not been explored hitherto. Therefore, the major goal of this work is to show the reversibility of IL-based ABS triggered by a pH-dependent phenomenon and their potential application in selective separations here demonstrated with two textile dyes. Around 1–20% of the total world production of dyes is lost during the dying process and is released into the environment through effluents.[19,20] Textile dyes and their metabolites are commonly toxic and carcinogenic representing therefore a major environmental concern.[19,20]

Experimental Procedure

Materials

Potassium citrate tribasic monohydrate, $C_6H_5K_3O_7.H_2O$ (≥ 99 wt % pure) was from Sigma–Aldrich, citric acid monohydrate, $C_6H_8O_7.H_2O$ (100 wt % pure), was from Fisher Scientific and potassium hydroxide was from Pronolab. The ILs investigated were 1-butyl-3-methylimidazolium chloride, [C_4mim]Cl (99 wt % pure); 1-butyl-3-methylpyridinium chloride, [C_4mpy]Cl (> 98 wt % pure); 1-butyl-1-methylpiperidinium chloride, [C_4mpip]Cl (99 wt % pure); tetrabutylphosphonium chloride, [P_{4444}]Cl (98 w t% pure); 1-butyl-3-methylimidazolium bromide, [C_4mim]Br (99 wt % pure); 1-butyl-2,3-dimethylimidazolium chloride, [C_4C_1mim]Cl (98 wt % pure). All imidazolium-, pyridinium-, and pyrrolidinium-based ILs were purchased from Iolitec. The [P_{4444}]Cl was kindly supplied by Cytec Industries Inc. The chemical structures of the investigated ILs are depicted in Figure 2.5.1.

Before use each IL was dried for a minimum of 48h, at a moderate temperature (323 K), and under constant agitation and vacuum. For the extraction experiments, two dyes were employed, namely Sudan III from Merck and Pigment Blue 27 (PB27) from Daicolor.

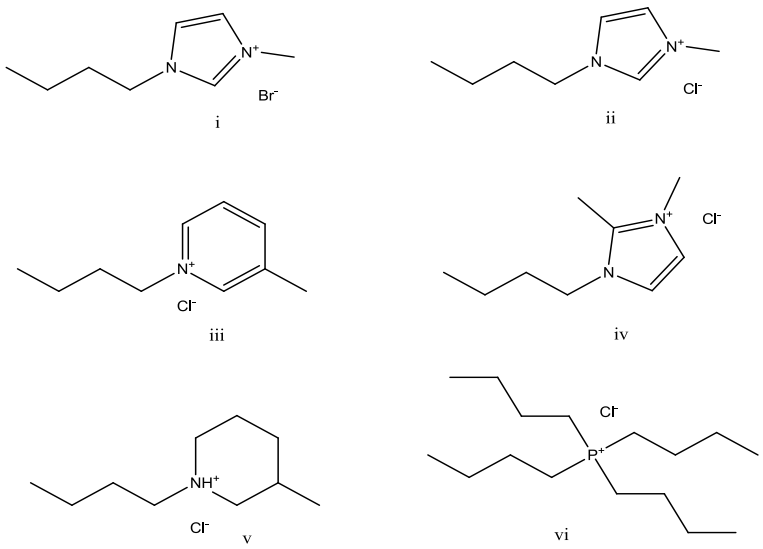

Figure 2.5.1: Chemical structures of the ionic liquids investigated: i) $[C_4mim]Br$, ii) $[C_4mim]Cl$, iii) $[C_4mpy]Cl$, iv) $[C_4C_1mim]Cl$, v) $[C_4mpip]Cl$, vi) $[P_{4444}]Cl$.

Phase Diagram, Tie-Lines and pH Measurements

The binodal curves were determined through the cloud point titration method (previously described in **Chapter 2.1**), at (298 ± 1) K and at atmospheric pressure, using aqueous solutions of salt/citric acid at around 50 wt % and aqueous solutions of the different hydrophilic ILs (with concentrations ranging from 60 wt % to 90 wt %). The ratio of potassium citrate and citric acid was changed in order to prepare buffer solutions and to determine the phase diagrams at given pH values. The tie-lines (TLs) were also determined as described in **Chapter 2.1**. The pH of each aqueous phase was measured at 298 K using an HI 9321 Microprocessor pH meter (HANNA instruments) – *cf.* **Chapter 2.1**.

Reversibility and Partitioning of Dyes

An initial ternary mixture at the biphasic region was prepared and allowed for phase separation for at least 3 h at 298 K. At this initial mixture composition, the pH values of the aqueous media of all IL-containing systems are *ca.* to 9. An aqueous solution of citric

acid at 50 wt % was added dropwise, under constant agitation, until the mixture became homogeneous (monophasic). Then, an aqueous solution of potassium hydroxide at 50 wt % was added, under agitation, to recover the initial pH value of 9. During these manipulations the pH of the aqueous solutions was experimentally controlled.

Thiss reversible procedure as carried out with 2 different textile dyes in solution. The quantification of sudan III and PB27 in each phase was performed by UV-Vis spetrocopy at the wavelengths of 348 nm and 615 nm. Further details are provided in **Chapter 2.4**. The extraction efficiencies are defined as the percentage ratio between the amount of each dye in one of phases to that in the total mixture, while considering the weight of the coexisting phases.

Results and discussion

Figure 2.5.2 sketches the principle of the reversible process that we aim to demonstrate in this work - a transition from the monophasic to the biphasic regimes could be attained by the alternate addition of an acid and a basis. For this purpose, we employed a citrate-based salt and halogen-based ILs as phase forming components of ABS. Citric acid ($C_6H_8O_7$) and potassium hydroxide (KOH) were additionally employed to change the medium pH without introducing new species into aqueous solution.

The pair potassium citrate/citric acid was selected due to their biodegradable and non-toxic characteristics. In fact, citric acid is currently recognized as safe (GRAS) and commonly used as a food additive.[21]

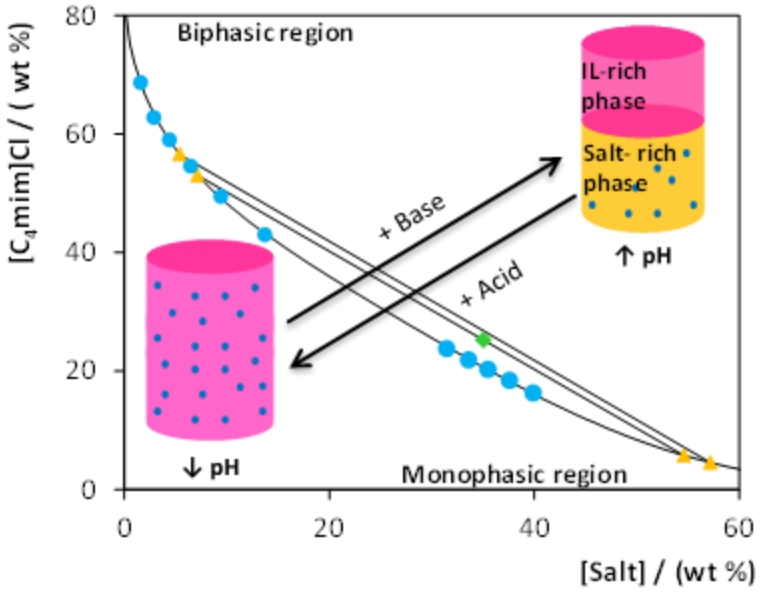

Figure 2.5.2: Ternary phase diagrams for $[C_4mim]Cl$ + water + $C_6H_5K_3O_7$ at 298 K and at pH ≈ 9 (●), tie-line data (▲), initial mixture composition (♦).

Aiming at studying the possibility of moving from monophasic to biphasic regimes in IL-based ABS, by a proper tailoring of the pH of the aqueous media, we initially determined the liquid-liquid ternary phase diagrams, at different pH values, of several hydrophilic ILs, namely $[C_4mim]Cl$, $[C_4C_1mim]Cl$, $[C_4mpip]Cl$, $[C_4mpy]Cl$, $[C_4mim]Br$ and $[P_{4444}]Cl$ combined with buffered solutions of the pair $C_6H_5K_3O_7/C_6H_8O_7$ in different molar ratios.

The ternary phase diagrams for the systems composed of water, organic salt/citric acid and several ILs at 298 K, and at different pH values, are illustrated in Figure 2.5.3. The experimental weight fraction data are presented in the *Supporting Information* (Tables S32 to S39).

The phase diagrams at pH≈ 9 were further characterized by the determination of diverse tie-lines and respective tie-line lengths to infer on the phases compositions - Table 2.5.1. In all investigated ABS, the top phase corresponds to the IL-rich phase while the bottom phase is mainly composed of salt and water.

Table 2.5.1: Weight fraction percentage (wt %) for the coexisting phases of IL + potassium citrate + H_2O (at a pH ≈ 9), and respective values of tie-line length (TLL) and pH values of each phase.

IL	Weight fraction composition / wt %								TLL
	$[IL]_{IL}$	$[salt]_{IL}$	pH_{IL}	$[IL]_{M}$	$[salt]_{M}$	$[IL]_{salt}$	$[salt]_{salt}$	pH_{salt}	
$[C_4mim]Cl$	53.04	7.13	9.32	25.25	35.03	5.77	54.58	9.30	66.98
$[C_4C_1mim]Cl$	47.88	10.76	8.93	25.02	34.90	9.78	51.00	8.67	55.42
$[C_4mpip]Cl$	55.91	4.46	9.26	25.13	34.75	4.40	55.15	9.34	72.27
$[C_4mpy]Cl$	55.74	5.13	8.44	24.62	35.47	4.39	55.19	8.16	71.71
$[C_4mim]Br$	76.93	0.65	8.93	35.08	32.04	0.42	58.03	8.92	95.64
$[P_{4444}]Cl$	72.93	3.06	9.34	24.97	35.03	0.58	51.29	9.14	86.95

In general, and for all ILs, there is a decrease on the ability for ABS formation with the pH reduction, *e.g.*, the higher the pH of the aqueous medium the larger is the biphasic region.

In Figure 2.5.3, the ABS are depicted at various pH values and the most acidic pH presented for each system denotes the lower limit for which ABS can no longer form. The overall results are summarized in Table 2.5.2.

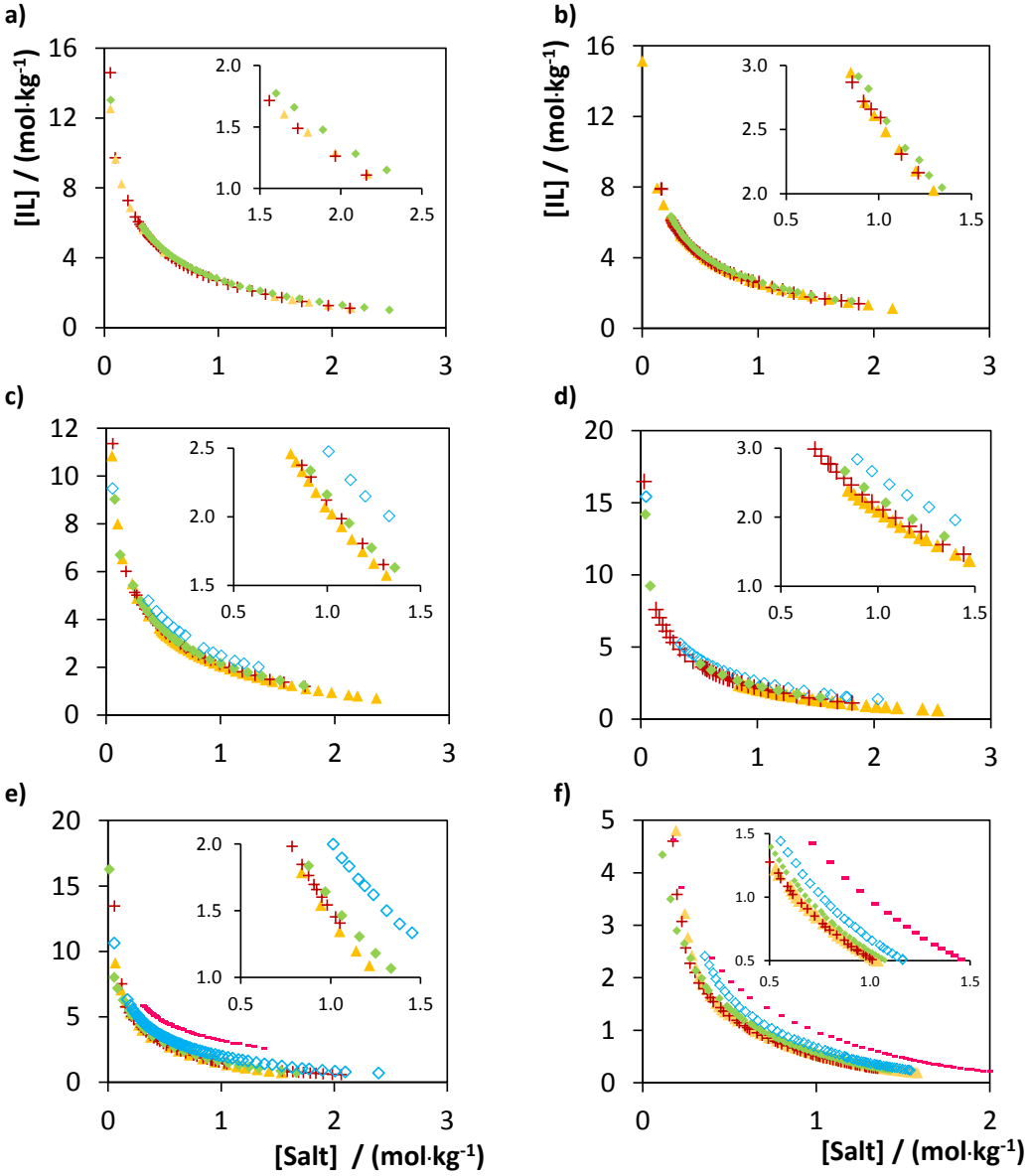

Figure 2.5.3: Evaluation of the pH effect in ternary phase diagrams composed of IL + water + $K_3C_6H_5O_7$/ $C_6H_8O_7$ at pH ≈ 9 (▲), pH ≈ 8 (+), pH ≈ 7 (♦), pH ≈ 6 (◊) and pH ≈ 5 (▬).The ILs are: **(a)** [C_4mim]Cl, **(b)** [C_4C_1mim]Cl, **(c)** [C_4mpip]Cl, **(d)** [C_4mpy]Cl, **(e)** [C_4mim]Br and **(f)** [P_{4444}]Cl. Some phase diagrams have been reported by other authors and are included here for comparison purposes.[22-24]

Table 2.5.2: Identification of the systems able (✓) or not able (×) to form two-phase systems as a function of the pH.

pH	9	8	7	6	5
$[C_4mim]Cl$	✓	✓	✓	×	×
$[C_4C_1mim]Cl$	✓	✓	✓	×	×
$[C_4mpip]Cl$	✓	✓	✓	✓	×
$[C_4mpy]Cl$	✓	✓	✓	✓	×
$[C_4mim]Br$	✓	✓	✓	✓	✓
$[P_{4444}]Cl$	✓	✓	✓	✓	✓

ILs with a higher hydrophobicity, achieved either with longer and more aliphatic moieties or with anions with lower hydrogen-bond basicity,[25,26] are capable of forming ABS at lower pH values. Examples of this pattern are perceived with $[P_{4444}]Cl$ and $[C_4mim]Br$ that form ABS even at a pH of 5. At a fixed pH, the IL ability to form ABS follows the order: $[P_{4444}]Cl$ > $[C_4mim]Br$ > $[C_4mpy]$ Cl ≈ $[C_4mpip]Cl$ > $[C_4C_1mim]Cl$ ≈ $[C_4mim]Cl$. This assortment mirrors the salting-out effect of the citrate-based salt over the IL.[15-18] Figure 2.5.4 illustrate all binodal curves with tested ILs at fixed pH values.

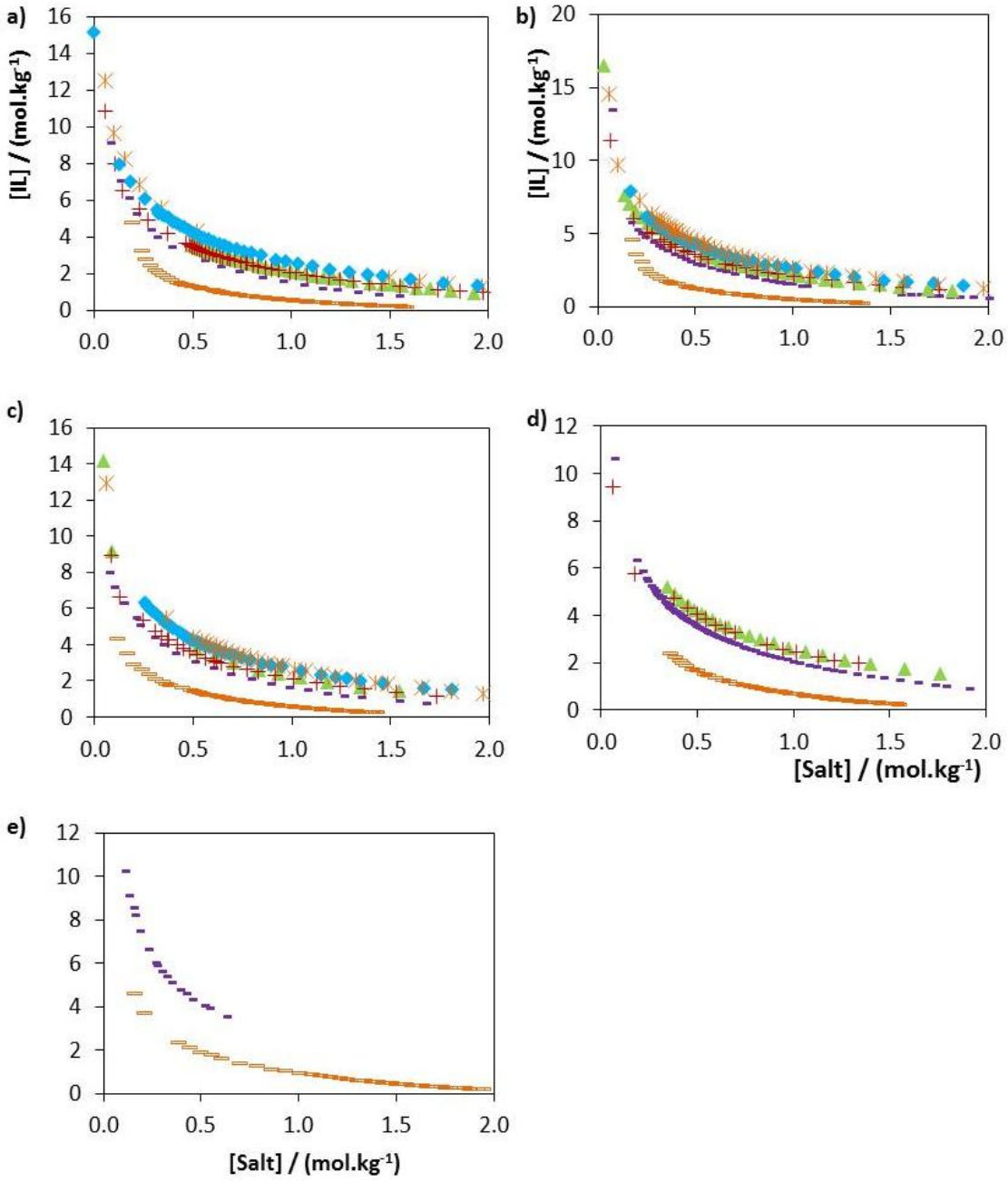

Figure 2.5.4: Phases diagrams for systems composed of **(a)** IL + water + $C_6H_5K_3O_7$ at pH ≈ 9; IL + water + $C_6H_5K_3O_7$/$C_6H_8O_7$ at **(b)** pH ≈ 8 (b); **(c)** pH ≈ 7; **(d)** pH ≈ 6; and **(e)** pH ≈ 5. The ILs used are (✳) [C_4mim]Cl, (◆) [C_4C_1mim]Cl, (+) [C_4mpip]Cl, (▲) [C_4mpy]Cl, (–) [C_4mim]Br and (▫) [P_{4444}]Cl.

The aptitude for ABS formation as a function of the pH is strongly related with the speciation performance of citric acid/potassium citrate. The speciation curves of citric acid are depicted in the *Supporting Information* (Figure S5). Citric acid present 4 pK_a values, namely 3.05, 4.67, 5.39 and 13.92.[27] At pH values lower than 3.05 the non-charged citric acid is mainly present and this neutral form is not able to form ABS with ILs.

At pH values above 4.67 and 5.39 there is the prevalence of the divalent and trivalent charged hydrogenocitrate and citrate anions, respectively. Therefore, it seems that only the most hydrophobic ILs investigated ([P_{4444}]Cl and [C_4mim]Br) are still capable of forming two-phase systems at a pH *ca.* 5 with a large amount of hydrogenocitrate ions in solution – a weaker salting-out species if compared with the trivalent citrate anion. On the other hand, ILs such as [C_4mim]Cl and [C_4C_1mim]Cl, which are amongst the most hydrophilic ILs investigated, do not form ABS at a pH of 6. The minimum pH value required for ABS formation with these ILs is 7.

After establishing the ternary phase diagrams and the pH values for which no liquid-liquid demixing is observed, the reversible IL-based ABS behaviour was appraised by the addition of citric acid and potassium hydroxide. For this purpose, an initial ternary mixture at the biphasic region at pH ≈ 9 was prepared. An aqueous solution of citric acid was added until the mixture became homogeneous (monophasic). Then, an aqueous solution of potassium hydroxide was added, to recover the initial pH value of 9. The differences in the phases' compositions are indeed negligible since a small amount of each aqueous solution (± 0.6 wt %) is enough to trigger the phase transition. The pH-driven reversibility was experimentally confirmed with the ILs [C_4mim]Cl, [C_4C_1mim]Cl, [C_4mpip]Cl, [C_4mpy]Cl, [C_4mim]Br and [P_{4444}]Cl.

In summary, it is possible to prepare reversible IL-based ABS playing around with the speciation behaviour of the organic salt. In addition, the cyclic reversibility was demonstrated with the [C_4mim]Cl-based ABS, at least 3 times, with no significant changes in the phases' composition. This phase reversibility takes place at room temperature and is achieved with low-cost compounds and already present in the mixture. Hence, these novel systems can be envisaged as potential alternatives to the more complex reversible systems that require additional energy inputs or the reaction of the phase-forming components with gases. Their reversibility is a major advantage on liquid-liquid extractions that can be used to perform selective separations as demonstrated hereinafter.

As a proof of principle, we tested the ability of the proposed systems for the separation of textile dyes. The mixture of the two dyes in the monophasic aqueous region (first step) is

shown in Figure 2.5.5. The introduction of KOH (aq.) moving the system into the biphasic region by increasing the pH leads to the selective separation of the two dyes for opposite phases. Figure 2.5.6 depicts the extraction efficiencies (*EE*%) of each dye (starting from the dyes binary mixture) in selected ABS.

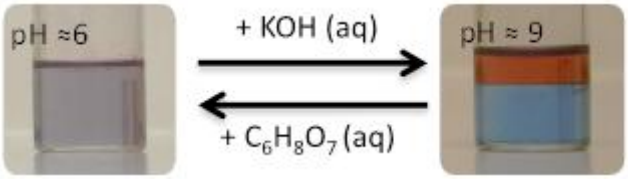

Figure 2.5.5: Selective separation of sudan III and PB27 from their initial mmonophasic mixture using the ABS composed of [C_4mim]Cl.

Sudan III preferentially migrates for the IL-rich phase whereas PB27 partitions for the citrate-rich layer. This trend reflects their octanol-water partition coefficients (K_{ow}): the log(K_{ow}) of sudan III is 7.47 and the log(K_{ow}) of PB27 is -0.26.[27] The extraction efficiencies and the selective separation of sudan III and PB27 for opposite phases is highly dependent on the IL cation. The selective partitioning of both compounds for opposite phases follows the order: [C_4mpip]Cl < [C_4mpy]Cl < [C_4C_1mim]Cl < [C_4mim]Cl.

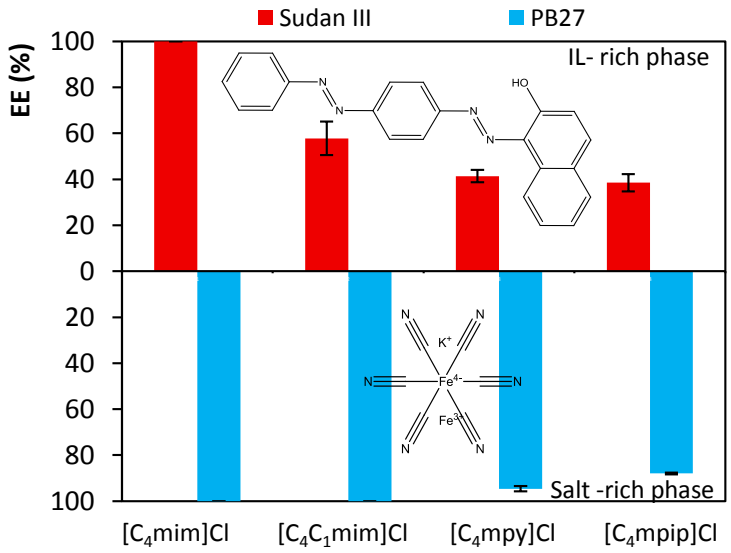

Figure 2.5.6: Percentage extraction efficiencies of sudan III and PB27, *EE*%, in the different ABS at 298 K. The chemical structures of both dyes are presented as inserts.

Remarkably, the ABS constituted by [C_4mim]Cl (the most hydrophilic IL investigated) is able to completely separate the two dyes for opposite phases with extraction efficiencies of 100% in a single-step procedure.

Conclusions

The results here reported show that low-cost and easily reversible ABS composed of ILs can be accomplished by a pH-driven phenomenon playing around with the speciation of the organic salt. Moreover, these systems have shown to be highly efficient in the selective separation of compounds with different hydrophobic natures albeit present in the same aqueous media. Hence, the application of the proposed reversible systems for use in the separation of diverse value-added compounds is envisaged.

References

1. Y. Kohno and H. Ohno, Chem. Commun., 2012, 48, 7119-7130.
2. P.G. Jessop, S.M. Mercera and D.J. Heldebrant, Energy Environ. Sci., 2012, 5, 7240-7253.
3. J. Luo, T.T. Xin and Y.L. Wang, New J. Chem., 2013, 37, 269-273.
4. S. Saita,Y. Kohno, N. Nakamura and H. Ohno,Chem. Commun., 2013, 49, 8988-8990.
5. D. Xiong, Z. Li, H. Wanga and J. Wang, Green Chem., 2013, 15, 1941-1948.
6. Y. Kohno, H. Arai and H. Ohno, Chem. Commun., 2011, 47, 4772-4774.
7. D.Z. Xiong, H.Y. Wang, Z.Y. Li and J.J. Wang, ChemSusChem, 2012, 5, 2255-2261.
8. M.G. Freire, C.M.S.S. Neves, K. Shimizu, C.E.S. Bernardes, I.M. Marrucho, J.A.P. Coutinho, J.N. Canongia Lopes and L.P.N. Rebelo, J. Phys. Chem. B, 2010, 114, 15925-15934.
9. P. Nockemann, B. Thijs, S. Pittois, J. Thoen, C. Glorieux, K. Van Hecke, L. Van Meervelt, B. Kirchner and K. Binnemans, J. Phys. Chem. B, 2006, 110, 20978-20992.
10. S. Saita, Y. Kohno and H. Ohno, Chem. Commun., 2013, 49, 93-95.
11. J. Lachwa, J. Szydlowski, A. Makowska, K.R. Seddon, J.M.S.S. Esperanca, H.J.R. Guedes and L.P.N. Rebelo, Green Chem., 2006, 8, 262-267.
12. K. Fukumoto and H. Ohno, Angew. Chemie, 2007, 46, 1852-1855.
13. Y. Kohno, S. Saita, K. Murata, N. Nakamura and H. Ohno, Polymer Chem.,2011, 2, 862-867.
14. Z.L. Xie and A. Taubert, Chem. Phys. Chem., 2011, 12, 364-368.
15. K.E. Gutowski, G.A. Broker, H.D. Willauer, J.G. Huddleston, R.P. Swatloski, J.D. Holbrey and R.D. Rogers, J. Am. Chem. Soc., 2003, 125, 6632-6633.
16. M.G. Freire, A.F.M. Cláudio, J.M.M. Araújo, J.A.P. Coutinho, I.M. Marrucho, J.N. Canongia Lopes and L.P.N. Rebelo, Chem. Soc. Rev., 2012, 41, 4966-4995.
17. M.G. Freire, C.L.S. Louros, L.P.N. Rebelo and J.A.P. Coutinho, Green Chem., 2011, 13, 1536-1545.
18. M.G.Freire, C.M.S.S. Neves, I.M. Marrucho, J.N. Canongia Lopes, L.P.N. Rebelo and J.A.P. Coutinho, Green Chem., 2010, 12, 1715-1718.
19. S. Sekar, M. Surianarayanan, V. Ranganathan, D.R. MacFarlane and A.B. Mandal, Environ. Sci. Technol., 2012, 46, 4902-4908.
20. U.G. Akpan and B.H. Hameed, J. Hazard.Mater., 2009, 170, 520-529.
21. J. Smith and L. Hong-Shum, Food Additives Data Book. Blackwell Science Ltd, 2003.
22. H. Passos, A.R. Ferreira, A.F.M. Claudio, J.A.P. Coutinho and M.G. Freire, Biochem. Eng. J., 2012, 67, 68-76.
23. M.T. Zafarani-Moattar and S. Hamzehzadeh, Fluid Phase Equilib., 2011, 304, 110-120.
24. H. Passos, M.P. Trindade, T.S.M. Vaz, L.P. Costa, M.G. Freire, J.A.P. Coutinho, Sep. Purif. Technol., 2013, 108, 174-180
25. A.F.M. Cláudio, A.M. Ferreira, S. Shahriari, M.G. Freire, J.A.P. Coutinho, J. Phys. Chem. B, 2011, 115, 11145-11153.
26. A.F.M. Cláudio, L. Swift, J. Hallett, T. Welton, J.A.P. Coutinho and M.G Freire, Phys. Chem. Chem. Phys., 2014, 16, 6593-6601.
27. Chemspider, The free chemical database at http://www.chemspider.com.

2.6. Optimization of the Gallic Acid Extraction using Ionic Liquid-Based Aqueous Biphasic Systems

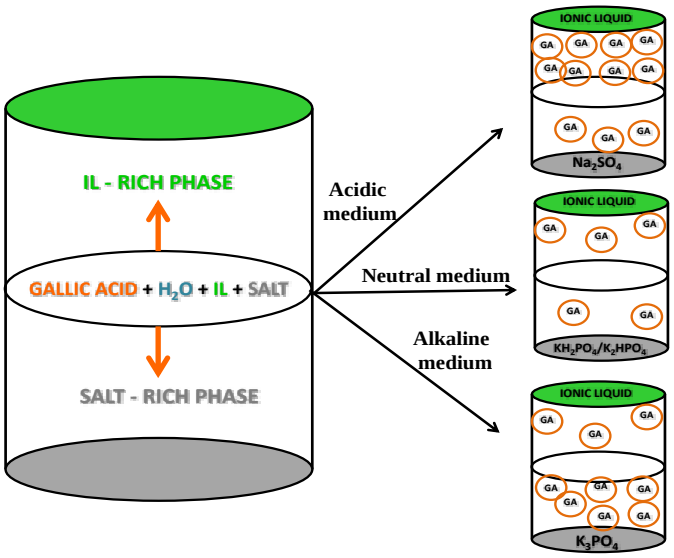

This chapter is based on the following published paper: Cláudio, A. F. M.; Ferreira, A. M.; Freire, C. S. R.; Silvestre, A. J. D.; Freire, M. G. and Coutinho, J. A. P., Optimization of the Gallic Acid Extraction using Ionic-Liquid-Based Aqueous Two-Phase Systems, Sep. Purif. Technol., 2012, 97, 142-149.

Abstract

Gallic acid is a phenolic, natural and interesting compound because of its antioxidant, anti-inflammatory, antifungal and antitumor properties. It is present in relatively high concentrations in a number of biomass sources and in industrial wastes from where it could be extracted. Aiming at developing benign and efficient extraction/purification processes for phenolic compounds (PhCs), ABS composed of ILs and inorganic salts were investigated. Several combinations of ILs and inorganic salts were studied to understand the influence of the IL structure and of the medium on the gallic acid partitioning. It is here shown that at low pH values the non-charged form of gallic acid preferentially migrates for the IL-rich phase whereas its conjugate base preferentially partitions for the salt-rich phase. The results indicate that IL-based ABS can be the basis of new extraction/purification processes of gallic acid from natural matrices, and improved extractions are obtained using acidic aqueous solutions.

Introduction

Phenolic compounds display relevant properties in the health and nutrition fields.[1,2] These features are mainly related to the antioxidative and radical scavenging properties of some phenolic structures[3], but also to their anticholesterolemic, hypertension depression and protection against cardiovascular diseases.[4] The use of natural phenolic compounds for nutraceutical and cosmetic applications is highly advantageous compared to synthetic substitutes that usually present adverse effects.[5] Besides, some phenolic compounds are also phytotoxic and toxic to bacteria, and can be used in biological wastewater treatments.[6-8]

Examples of simple phenolic structures are vanillic, gallic, protocatechuic, ellagic, and syringic acids, and quercetin, vanillin and resveratrol. These compounds are usually present in natural sources such as wood, barks, fruits and vegetables.[1,2,6,7] They may, in

many cases, be isolated from residues of industrial or agricultural activities, such as wastewaters from olive mills, cork powder and black condensates.[6-9] For instance, olive mills residues may contain 4-16 % of organic matter, and from which phenolic compounds represent 2-15 %.[6] To decrease the load of phenolic compounds on aqueous effluents, and at the same time to add economical value to them, there is a growing interest on their extraction from both industrial or agricultural wastes.

Hasmann et al.[10] have used ABS composed of two thermoseparating copolymers (ethylene oxide and propylene oxide) to remove phenolic compounds from a hydrolysate of rice straw. The extraction efficiencies of phenolic compounds (ferulic acid, siringic acid, furfural, vanillin and syringaldehyde) varied between 6 % and 80 % depending on the copolymer used.[10] Moreover, the authors[10] found that in a system containing 50 wt % of the copolymer with the higher molecular weight, no extraction of phenolic compounds was observed due to the high viscosity of the system. The application of IL-based systems to the extraction of phenolic compounds from natural sources has also been reported in literature.[1] Du et al.[1] applied a microwave-assisted technique to extract gallic acid, ellagic acid, quercentin, and trans-resveratrol from medicinal plants using aqueous solutions of hydrophilic ILs. The extraction yield of polyphenolic compounds was greatly improved by the addition of ILs when compared with pure water, and reached extraction yields equivalent to those obtained with methanol.[1] Furthermore, by using different ILs it was also observed that the ions that compose the ionic fluid, and especially the anions, control the extraction efficiencies.[1] In a previous work, we have studied the partitioning of vanillin with IL-based ABS composed of a large range of ILs and a common inorganic salt - K_3PO_4.[11] Additional parameters that could affect the partitioning of the molecule, namely the temperature and the available concentration of vanillin in the global system, were also evaluated.[11] In all systems and conditions tested, vanillin preferentially migrates for the IL-rich phase.[11]

In this work, ABS formed by various ILs and different inorganic salts were explored for the extraction of gallic acid (3,4,5-trihydroxybenzoic acid, $C_6H_2(OH)_3COOH$, pK_a = 4.41 at 298 K)[12] aiming at investigating the effect of the structural features of the IL and the medium

pH on the extraction efficiency. The molecular structure of gallic acid is depicted in Figure 2.6.1.

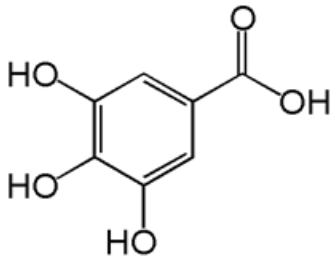

Figure 2.6.1: Chemical structure of gallic acid.

Experimental Procedure

Materials

The ILs used in this work to study the partitioning of gallic acid were 1-ethyl-3-methylimidazolium trifluoromethanesulfonate, $[C_2mim][CF_3SO_3]$; 1-butyl-3-methylimidazolium bromide, $[C_4mim]Br$; 1-butyl-3-methylimidazolium methylsulfate $[C_4mim][CH_3SO_4]$; 1-butyl-3-methylimidazolium ethylsulfate, $[C_4mim][C_2H_5SO_4]$; 1-butyl-3-methylimidazolium trifluoromethanesulfonate, $[C_4mim][CF_3SO_3]$; 1-butyl-3-methylimidazolium dicyanamide, $[C_4mim][N(CN)_2]$, 1-heptyl-3-methylimidazolium chloride, $[C_7mim]Cl$, 1-methyl-3-octylimidazolium chloride, $[C_8mim]Cl$, and 1-butyl-3-methylimidazolium octylsulfate, $[C_4mim][OctylSO_4]$. All ILs were supplied by Iolitec, with the exception of $[C_4mim][OctylSO_4]$ which was acquired from Merck. To reduce the volatile impurities content to negligible values, ILs individual samples were kept at constant agitation under vacuum and at a moderate temperature (323 K), for a minimum of 48 h. After this purification step, the purity of each IL was further checked by ^{1}H, ^{13}C and ^{19}F NMR (when applicable) spectra and found to be > 99 wt % for all samples. Na_2SO_4 was acquired at LabSolve (purity > 99.8 wt %), K_3PO_4 was from Sigma (purity > 98 wt %), K_2HPO_4 was from Riedel-de Haën (purity > 99 wt %), and KH_2PO_4 was from Panreac (purity > 99 wt %). NaOH was from EKA (purity 98 wt %). Gallic acid was acquired at Merck (> 99.5 wt % pure). The water used was double distilled, passed across a reverse osmosis system and further treated with a Milli-Q plus 185 water purification equipment. The

buffers used in the calibration of the pH meter equipment were the citric acid / sodium hydroxide / sodium chloride solution with a pH value of 4.00 (± 0.02), and the potassium dihydrogen phosphate / disodium hydrogen phosphate solution with a pH value of 7.00 (± 0.02), acquired from Fluka.

The ionic structures of the ILs used for the partitioning of gallic acid are shown in Figure 2.6.2.

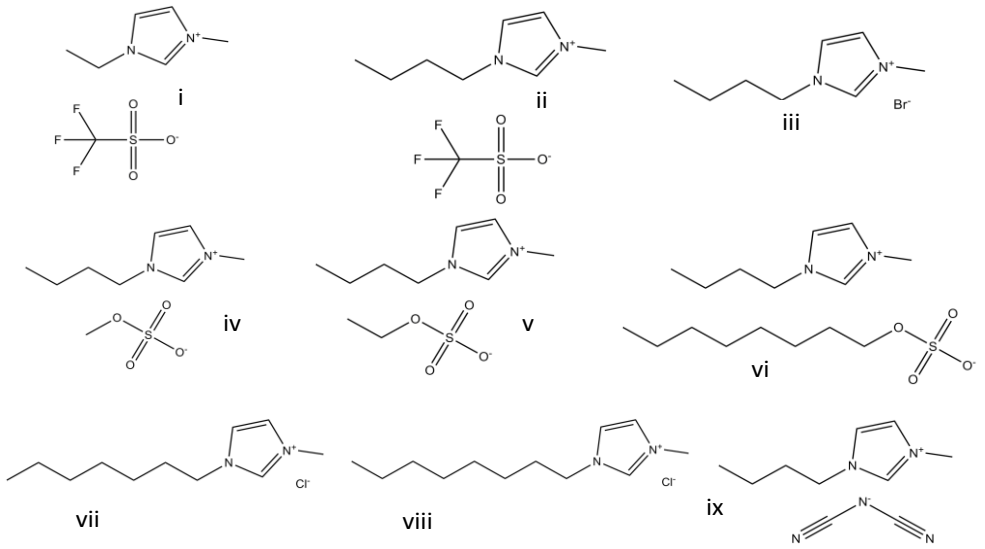

Figure 2.6.2: Chemical structures of the studied ILs: (i) $[C_2mim][CF_3SO_3]$; (ii) $[C_4mim][CF_3SO_3]$; (iii) $[C_4mim]Br$; (iv) $[C_4mim][CH_3SO_4]$; (v) $[C_4mim][C_2H_5SO_4]$; (vi) $[C_4mim][OctylSO_4]$; (vii) $[C_7mim]Cl$; (viii) $[C_8mim]Cl$; (ix) $[C_4mim][N(CN)_2]$.

Partitioning of Gallic Acid and pH Measurements

The compositions of the ternary mixtures used for the gallic acid partitioning were chosen based on the phase diagrams determined previously, and shown in **Chapters 2.1 and 2.2**. The composition used for the partitioning experiments consists on 15 wt % of inorganic salt (Na_2SO_4, K_3PO_4, or KH_2PO_4/K_2HPO_4 (phosphate buffer)), 60 wt % of an aqueous solution containing gallic acid (at 3.06×10^{-3} mol·dm^{-3}), and 25 wt % of each IL. Since it was not possible to perform extractions for all the biphasic systems with the phosphate buffer containing 25 wt % of IL, additional mixtures of 15 wt % of KH_2PO_4/K_2HPO_4, 55 wt % of a gallic acid aqueous solution and 30 wt % of different ILs were also prepared. To better understand the influence of the pH on the extraction of gallic acid further experimental tests were conducted. For the system composed of 15 wt % of Na_2SO_4, 60

wt % of an aqueous solution containing gallic acid (at 3.06×10^{-3} mol·dm^{-3}), and 25 wt % of [C_4mim][CF_3SO_3], small amounts of NaOH were progressively added to increase the pH of the aqueous media. The detailed compositions used for the determination of the partition coefficients are reported in the *Supporting Information* (Tables S40 to S42). The mixtures were prepared and gallic acid was quantified by UV-Vis spectroscopy at a wavelength of 262 nm, and using a calibration curve previously established. Further details are provided in **Chapter 2.4**. Moreover, the effects of the salt and medium pH towards the quantification of gallic acid by UV spectroscopy were taken into account. At the dilutions carried out, and salt compositions employed, no significant deviations due to these factors were observed in the values of the partition coefficients. Only slight interferences of the imidazolium-based ILs with the analytical method were observed. Therefore, to minimize these interferences, blank samples were always prepared. At least three individual samples were quantified to determine the gallic acid partition coefficients and the respective standard deviations – numerical values are presented in the Supporting Information. The partition coefficients of gallic acid, K_{GA}, were determined as the ratio of its concentration in the IL and in the inorganic salt (Na_2SO_4, K_3PO_4 or K_2HPO_4/KH_2PO_4) aqueous-rich phases, according to the following equation,

$$K_{GA} = \frac{[GA]_{IL}}{[GA]_{Salt}} \qquad \text{eq. 2.6.1}$$

where $[GA]_{IL}$ and $[GA]_{Salt}$ are the concentration of gallic acid in the IL- and in each of the inorganic salt-rich aqueous phases, respectively.

The extraction efficiencies of gallic acid were determined accordingly to eq. 2.6.2,

$$\%EE_{GA} = \frac{[GA]_{IL} \times W_{IL}}{[GA]_{IL} \times W_{IL} + [GA]_{Salt} \times W_{Salt}} \times 100 \qquad \text{eq. 2.6.2}$$

where w_{IL} and w_{Salt} are the weight of the IL-rich phase and of the inorganic–salt-rich phase, respectively.

At the conditions used in this work, in general, the top layer is the IL-rich phase while the bottom phase is the inorganic-salt-rich phase. Few exceptions were verified with the systems [C_2mim][CF_3SO_3] + K_3PO_4 + aqueous solution, [C_4mim][CF_3SO_3] + K_3PO_4 + aqueous solution, and [C_4mim][CF_3SO_3] + Na_2SO_4 + aqueous solution, where it was observed an

inversion on the phase densities. Each phase was qualitatively identified (IL-rich or inorganic-salt rich) by UV-spectroscopy, using a SHIMADZU UV-1700, Pharma-Spec Spectrometer, at wavelength of 211 nm (absorption peak for the imidazolium core). pH values of the IL- and organic-salt-rich aqueous phases were measured at 298 K as described in **Chapter 2.1**.

Results and Discussion

Effect of the Inorganic Salt in the Gallic Acid Partitioning

The effect of the inorganic salt in the partitioning of gallic acid in IL-based ABS was evaluated using Na_2SO_4, K_3PO_4, and a K_2HPO_4/KH_2PO_4 buffer solution. The three salt solutions employed were chosen based on the different pH values that they confer to the aqueous phases. In general, imidazolium-based ILs lead to acidic aqueous solutions. The pH of their solutions may be, or not, changed by the presence of the salt. The sodium sulfate, being a neutral salt, will maintain the acidity of the aqueous phase (except for the systems composed of dicyanamide, or other strong alkaline anions); the mixture of salts K_2HPO_4/KH_2PO_4 (phosphate buffer) leads to a pH close to a neutral value; the K_3PO_4 produces alkaline aqueous solutions. All the pH values of both top and bottom phases of the systems used for the partitioning studies of gallic acid are presented in Table 2.6.1. The detailed compositions are listed in the *Supporting Information* (Tables S43 to S45), and correspond to the mass fraction percentages used in the partitioning experiments. For all the systems, no significant deviations between the pH of the salt-rich phase and the IL-rich aqueous phase were observed. The differences observed in the pH values between the various Na_2SO_4-based ABS are more pronounced when compared with the remaining salts. Na_2SO_4 is a neutral salt and therefore the pH of the medium is more dependent on the IL employed.

The partition coefficients obtained for gallic acid are depicted in Figure 2.6.3. The salts studied lead to very different behaviors in the partitioning of the biomolecule, suggesting that the choice of the inorganic salt is a dominant parameter in the optimization of the extraction of gallic acid.

Table 2.6.1: pH values of the aqueous coexisting phases in IL-based ABS at 298 K.

		Na_2SO_4	K_2HPO_4/KH_2PO_4	K_3PO_4
IL+ inorganic salt + water system			**pH**	
$[C_2mim][CF_3SO_3]$	Salt-rich phase	3.32	7.28	13.09
	IL-rich phase	2.71	7.57	13.15
$[C_4mim][CF_3SO_3]$	Salt-rich phase	3.04	7.10	12.85

	IL-rich phase	3.12	7.37	13.10
$[C_4mim][CH_3SO_4]$	Salt-rich phase	1.57	7.33	13.12
	IL-rich phase	1.88	7.6	13.33
$[C_4mim][C_2H_5SO_4]$	Salt-rich phase	1.29	7.15	12.88
	IL-rich phase	2.29	7.40	13.28
$[C_4mim][OctylSO_4]$	Salt-rich phase	3.52	7.01	12.89
	IL-rich phase	3.64	7.23	13.01
$[C_4mim][N(CN)_2]$	Salt-rich phase	8.07	7.53	13.48
	IL-rich phase	8.54	7.82	13.98
$[C_4mim]Br$	Salt-rich phase	5.22	7.08	12.97
	IL-rich phase	5.43	7.31	13.27
$[C_7mim]Cl$	Salt-rich phase	6.63	7.22	12.85
	IL-rich phase	6.05	7.45	12.99
$[C_8mim]Cl$	Salt-rich phase	6.72	7.55	13.41
	IL-rich phase	6.69	7.69	13.29

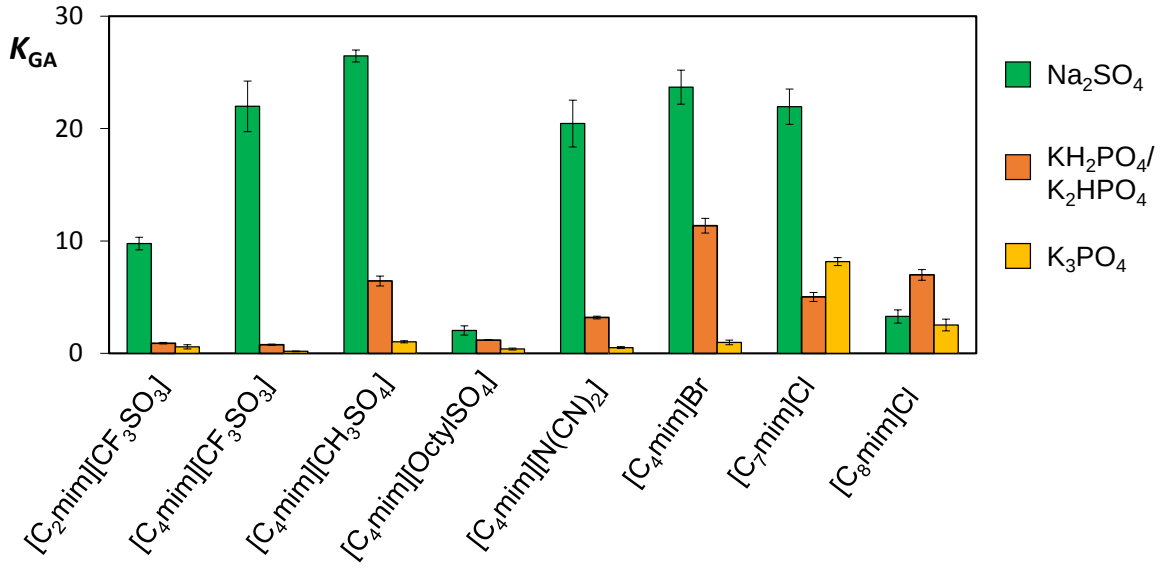

Figure 2.6.3: Partition coefficients of gallic acid in IL-based ABS formed by different inorganic salts at 298 K.

From Figure 2.6.3 it is possible to observe that, for most of the ILs investigated, the partition coefficients of gallic acid decrease in the following order of inorganic salts: Na_2SO_4 >> K_2HPO_4/KH_2PO_4 > K_3PO_4. However, this tendency is not obeyed for the systems with ILs with longer alkyl side chains at the cation, namely $[C_7mim]Cl$ and $[C_8mim]Cl$. The extraction of gallic acid with $[C_7mim]Cl$ is better with K_3PO_4, while with $[C_8mim]Cl$ the

phosphate buffer seems to yield enhanced extractions. This different pattern must be related with the ability of these ILs to form micelles, and thus with the influence of each salt in reducing or increasing the critical micelle concentration.[13]

Although K_3PO_4 is the strongest salting-out salt studied in this work, it seems that the pH of the aqueous media plays a major role in the partition behavior observed. For instance, the partition coefficients obtained with the systems containing $[C_4mim][CF_3SO_3]$ range between 0.18 and 21.98 when different salts are employed. Considering the pH values reported in Table 2.6.1, the partition coefficients obtained suggest that the neutral and less hydrophilic form of gallic acid, present in the acidic media of Na_2SO_4-based systems, is more easily extracted into the IL-rich phase than gallate. On the other hand, gallate, the charged conjugate base of gallic acid present in neutral or alkaline pH solutions formed by the phosphate-based salts, preferentially migrates for the salt-rich phase. In the systems considered here there are two aqueous phases of different nature: a predominant hydrophobic phase composed mainly of IL, and a more hydrophilic phase constituted majorly by the high charge density salts. These differences in the phases' polarities coupled to the charged or non-charged nature of gallic acid control the partition coefficients observed. Non-charged species tend to migrate to the most hydrophobic phase (IL-rich phase) while the charged species preferentially partition for the salt-rich-phase.

Effect of the IL Ions in the Gallic Acid Partitioning

The extraction of biomolecules using ABS (among other factors) is the result of their interactions with the compounds dissolved in the aqueous medium. Therefore, the chemical structures of the ionic liquid ions may have a significant impact on the gallic acid partitioning.

Figure 2.6.4 depicts the partition data obtained for gallic acid in ABS formed by alkaline aqueous solutions of K_3PO_4. The extraction efficiencies of gallic acid and the pH of the coexisting phases are also shown to allow comprehensive comparisons among different systems. The K_{GA} values in systems containing K_3PO_4 range between 0.18 and 8.16. The partitioning of the biomolecule towards the IL-rich phase is favorable for the $[C_4mim][CH_3SO_4]$, $[C_4mim]Br$, $[C_7mim]Cl$ and $[C_8mim]Cl$ containing systems (extraction

efficiencies higher than 50 %). Moreover, among the remaining systems, gallate preferentially migrates for the K_3PO_4-rich phase, and strongly depends on the IL structural features. In summary, the partition coefficients of gallic acid in K_3PO_4-based AS decrease in the following order: $[C_7mim]Cl$ >> $[C_8mim]Cl$ > $[C_4mim][CH_3SO_4]$ ≈ $[C_4mim]Br$ > $[C_2mim][CF_3SO_3]$ ≈ $[C_4mim][N(CN)_2]$ > $[C_4mim][OctylSO_4]$ > $[C_4mim][CF_3SO_3]$.

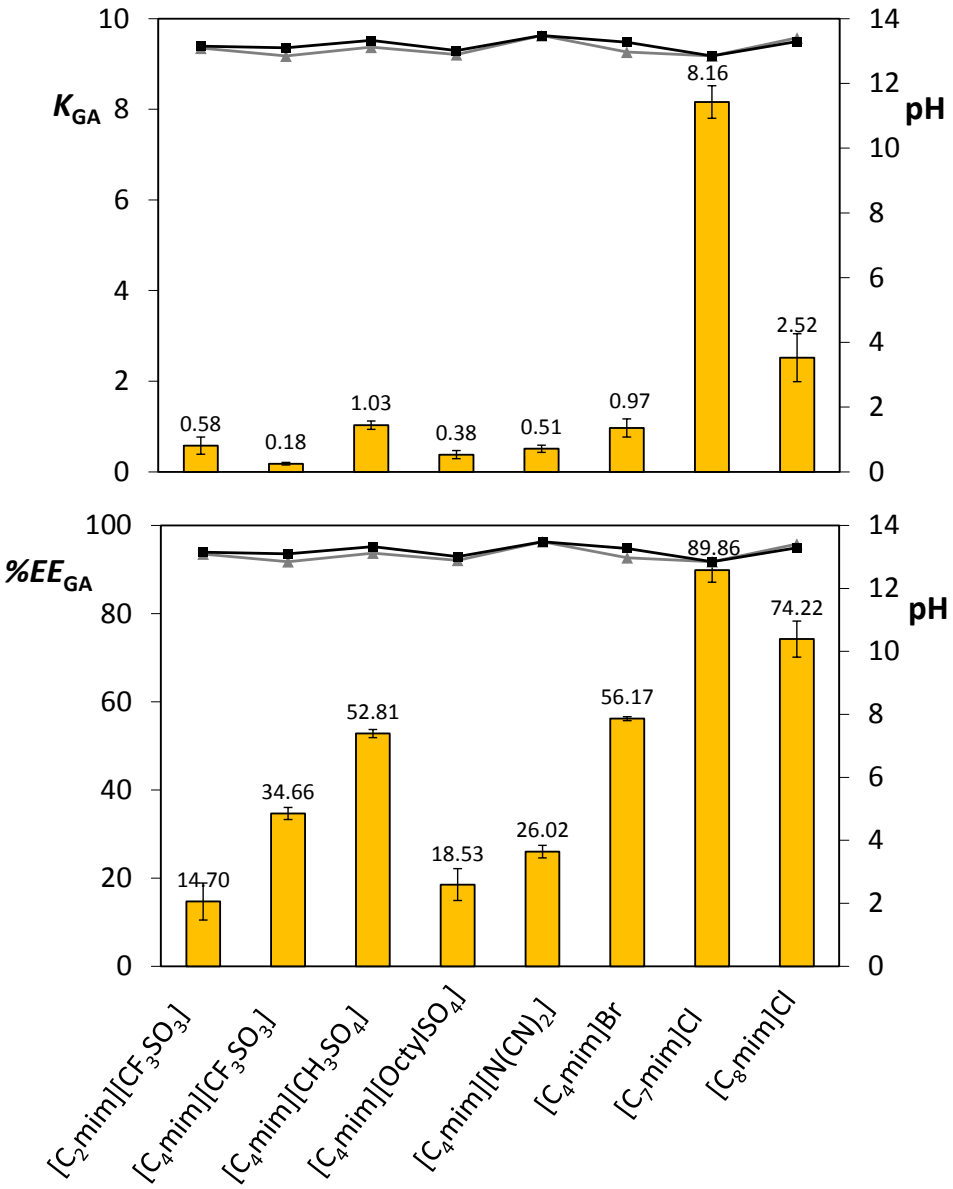

Figure 2.6.4: Partition coefficients (K_{GA}) and extraction efficiencies percentages ($\%EE_{GA}$) of gallic acid, and pH of both IL- (squares) and salt-rich phases (triangles), for different IL-K_3PO_4-based ABS at 298 K.

It should be stressed that an increase in the K_{GA} values does not necessarily involves the increase in the $\%EE_{GA}$ values. The $\%EE_{GA}$ values are a result of the concentration of gallic acid in each phase combined with their total weight.

The systems containing $[C_4mim]Br$ and $[C_4mim][CH_3SO_4]$ show extraction efficiencies *circa* 50 %. For the systems containing $[C_2mim][CF_3SO_3]$, $[C_4mim][N(CN)_2]$, $[C_4mim][OctylSO_4]$ and $[C_4mim][CF_3SO_3]$, the partition coefficient values are lower than 0.60, revealing that gallic acid migrates preferentially for the K_3PO_4–rich phase (extraction efficiencies below 35 %). The higher hydrophobicity of these ILs makes them less able to solvate the negative charged form of gallic acid. The hydrophobicity of these fluids can be confirmed by the ability of their anions to accept a proton (or donate an electron pair) in a solute-solvent hydrogen-bond.[14] The β values (hydrogen bond basicity values determined using solvatochromic probes) for the distinct $[C_4mim]$-based ionic liquids investigated are according to: $[C_4mim][CF_3SO_3]$ (β = 0.49)[15] > $[C_4mim][N(CN)_2]$ (β = 0.60)[15] > $[C_4mim][CH_3SO_4]$ (β = 0.75)[16] > $[C_4mim]Br$ (β = 0.87)[16], and thus support the idea of their higher hydrophobicity.

Albeit an increase in the cation side alkyl chain length also enhances the hydrophobicity of the IL,[17] the extraction efficiencies observed for $[C_7mim]Cl$ and $[C_8mim]Cl$, of 90 % and 74 %, respectively, suggest that the mechanism driving the partitioning of gallic acid in these systems is indeed more complex than expected, and must be certainly related with the ability of these long alkyl chain ILs to form micelles in aqueous media. With the gathered data we can postulate that the mechanism of extraction is not related with the solvation of the conjugate base of the gallic acid inside the micelle; instead, gallate reduces the repulsion between the imidazolium head groups and stabilizes the micelle, enhancing thus the formation of self-aggregated structures. This would also explain why the octylsulfate-based system, also able to form micelles in aqueous solutions, has a poorer performance in extracting gallate since both species are negatively charged.

In a previous work,[11] the extraction of vanillin was evaluated using systems composed of K_3PO_4 and several ILs. The partition coefficients of gallic acid and vanillin for a similar composition at the biphasic region, and at the same temperature in common IL-K_3PO_4-based ABS, are compared in the *Supporting Information* (Figure S6). For all the studied

systems, and at all the conditions analyzed, vanillin preferentially partitioned for the IL-rich phase.[11] Nonetheless, this pattern was not observed with gallic acid. Moreover, the partition coefficients obtained for vanillin[11] were substantially higher than those observed with gallic acid. This results from the fact that vanillin is less polar than gallic acid and is more easily extracted into the IL-rich phase.

Since the biphasic region for some IL-based ABS containing the phosphate buffer, K_2HPO_4/KH_2PO_4[17,18], is smaller than for the remaining salts, the concentration of the IL used in the phosphate-buffer-containing systems was of 30 wt %. Aiming at avoiding influences in the partition coefficient values that could be a merely result of the IL concentration, the systems containing the ILs $[C_4mim][CF_3SO_3]$, $[C_2mim][CF_3SO_3]$, and $[C_4mim][N(CN)_2]$ were also evaluated at 25 wt % with the phosphate buffer aqueous solution.

The partition coefficients and extraction efficiencies of gallic acid for the IL-rich phase and the pH of the coexisting phases of each system are sketched in Figure 2.6.5.

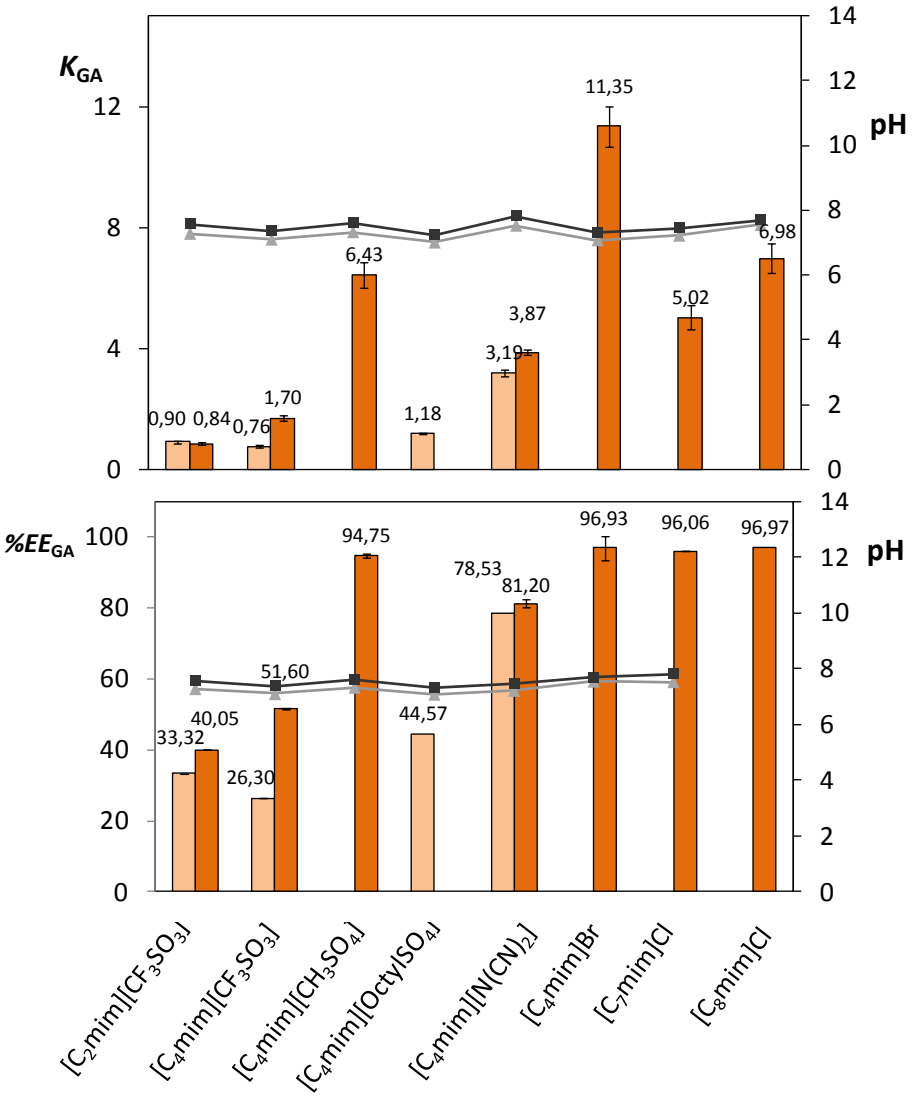

Figure 2.6.5: Partition coefficients (K_{GA}) and extraction efficiencies percentages ($\%EE_{GA}$) of gallic acid, and pH of both IL- (squares) and salt-rich phases (triangles), for different IL-K_2HPO_4/KH_2PO_4-based ABS at 298 K. The bars depicted in light orange correspond to systems containing 25 wt % of IL, while the bars in dark orange refer to systems with 30 wt % of IL.

The change in the partition coefficients when increasing the ionic liquid concentration from 25 wt % to 30 wt % is almost insignificant. The difference of 5 wt % in the IL concentration has thus a minor effect in the gallic acid partitioning that does not overlap with the larger differences observed among diverse ILs.

For the systems with 30 wt % of IL + 15 wt % of K_2HPO_4/KH_2PO_4 + 55 wt % of an aqueous solution of gallic acid (Figure 2.6.5), the K_{GA} values range between 0.84 and 11.35, and hence strongly depend on the IL employed. At the conditions investigated the partition

coefficients of gallic acid in K_2HPO_4/KH_2PO_4-based ABS decrease in the following order: [C_4mim]Br > [C_8mim]Cl > [C_7mim]Cl > [C_4mim][CH_3SO_4] > [C_4mim][$N(CN)_2$] > [C_4mim][OctylSO_4] ≈ [C_2mim][CF_3SO_3] ≈ [C_4mim][CF_3SO_3].

In the systems composed of 25 wt % of [C_2mim][CF_3SO_3] or [C_4mim][CF_3SO_3], and 30 wt % of [C_2mim][CF_3SO_3], the partition coefficients observed are lower than 1, meaning that the gallic acid preferentially partitions towards the salt-rich phase. For the remaining systems, gallic acid partitions for the IL-rich phase. Although the partition of the gallic acid towards the IL-rich phase is favored by the phosphate buffer when compared with the K_3PO_4 salt, the general behavior observed is identical to that previously discussed: there is a preferential partitioning of the biomolecule towards the salt-rich phase when the most hydrophobic ionic liquids are employed. Systems containing the most hydrophilic ILs are now favored with extraction efficiencies increasing from 50 % to 80-96 %. However, the partitioning in the systems with [C_7mim]Cl and [C_8mim]Cl, with extraction efficiencies > 96 %, seems still to be driven by a different extraction mechanism.

The partition coefficients, extraction efficiencies of gallic acid and pH values in aqueous biphasic systems composed of Na_2SO_4 and distinct ILs are reported in Figure 2.6.6. At pH values below 4.41 the dominant species is the non-charged form of gallic acid and the partitions are now all towards the IL-rich phase with K_{GA} values ranging from 2.04 to 29.58 (extraction efficiencies from 58 % to 99 %).

At the conditions evaluated, the partition coefficients of gallic acid in Na_2SO_4-based ABS decrease in the following order: [C_4mim][$C_2H_5SO_4$] > [C_4mim][CH_3SO_4] > [C_4mim]Br ≈ [C_4mim][CF_3SO_3] ≈ [C_7mim]Cl ≈ [C_4mim][$N(CN)_2$] >> [C_2mim][CF_3SO_3] >> [C_8mim]Cl > [C_4mim][OctylSO_4].

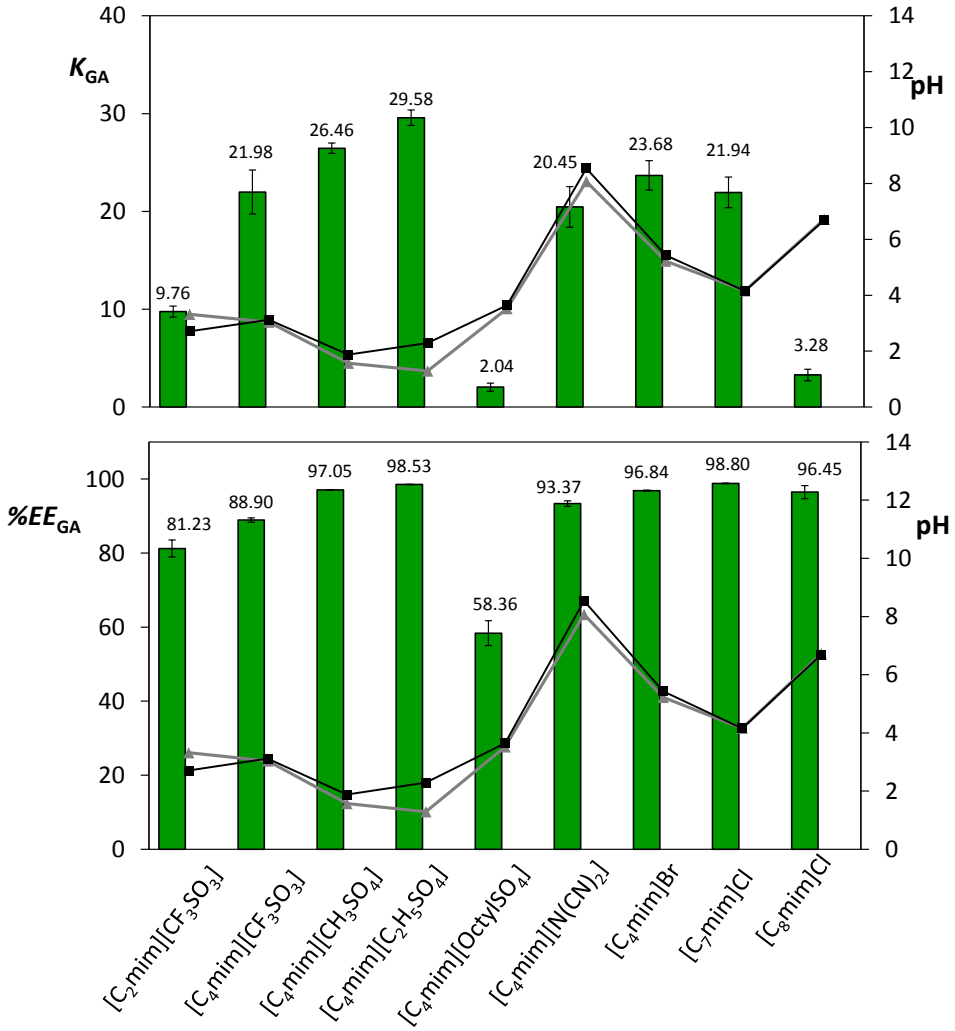

Figure 2.6.6: Partition coefficients (K_{GA}) and extraction efficiencies percentages (%EE_{GA}) of gallic acid, and pH of both IL- (squares) and salt-rich phases (triangles), for different IL-Na_2SO_4-based ABS at 298 K.

The sulfate-based ILs are, in this case, the improved ILs to extract gallic acid from aqueous media. The highly hydrophobic anions, such as $[CF_3SO_3]^-$ and $[OctylSO_4]^-$ present, on the other hand, the lowest extraction efficiencies. The good performance of the systems containing the $[C_7mim]Cl$, $[C_8mim]Cl$ and $[C_4mim][N(CN)_2]$ is related with their ability to extract gallate, present at the higher pH values observed for these systems, through the formation of micelles.[13,19]

Having established that acidic media favors the partition of gallic acid towards the IL-rich phase, this approach was also applied to the vanillin partitioning which was previously studied in alkaline medium.[11] It was observed that the partition coefficients of vanillin

(p*K*a = 8.2)[20] (for 25 wt % of IL + 15 wt % of inorganic salt, and at 298 K) ranged between 9.75 and 31.87 in K_3PO_4-IL-based ABS, and between 59.32 and 70.03 in Na_2SO_4-IL-based ABS for the ILs $[C_4mim][N(CN)_2]$ and $[C_4mim][CF_3SO_3]$, respectively. Further details on these values are provided in the *Supporting Information* (Table S46). Therefore, the use of Na_2SO_4 (although a weaker salting-out agent than K_3PO_4) enhances the partitioning of added-value phenolic compounds for the IL-rich phase, since in the Na_2SO_4-based systems the pH is lower than in the K_3PO_4-based systems. Moreover, and as shown before, the extraction of vanillin is always superior to that observed with gallic acid using common IL-based systems due to its lower polarity.

To better understand the influence of the pH on the extraction of gallic acid and aiming at getting a more comprehensive analysis on the mechanism driving its partitioning, further experimental studies were conducted. For the system composed of Na_2SO_4, $[C_4mim][CF_3SO_3]$, and an aqueous solution of gallic acid, small amounts of NaOH were progressively added to increase the pH of the coexisting phases. The results obtained are depicted in Figure 2.6.7.

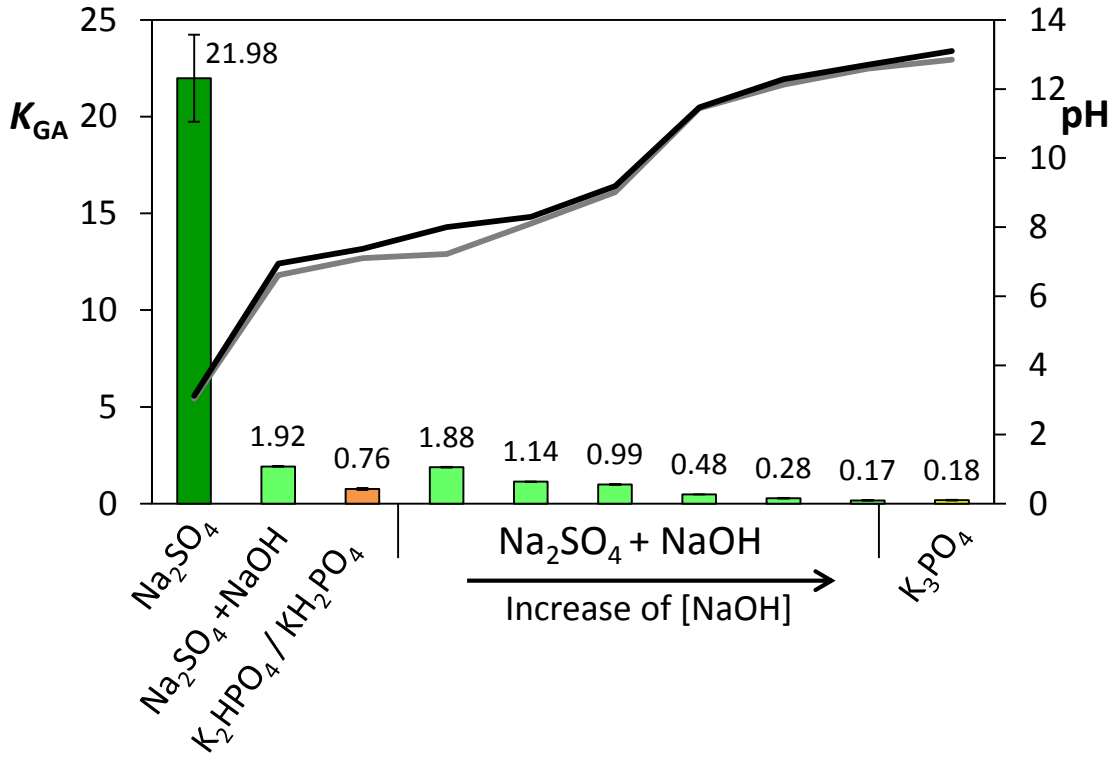

Figure 2.6.7: Partition coefficients of gallic acid (K_{GA}), and pH of both IL- (black) and salt-rich phases (gray), for $[C_4mim][CF_3SO_3]$-based systems composed of different inorganic salts at 298 K.

For pH values below the p*K*a of gallic acid (p*K*a = 4.4[12]), the uncharged molecule preferentially migrates for the IL-rich phase. On the opposite, when NaOH is added and the pH of the medium is superior to 4.4, gallate migrates for the salt-rich phase. Indeed, the higher the pH value the lower is the partition coefficient of gallic acid. A graphical representation of the extraction mechanism of gallic acid in the presence of different inorganic salts is summarized in the front cover of this chapter.

Conclusions

Diverse IL-based ABS were investigated regarding their extraction abilities for gallic acid – a phenolic compound of well-known interest. Several combinations of ILs and inorganic salts capable of creating ABS were explored. Comparing the extractions performed with ABS containing different inorganic salts (Na_2SO_4, K_2HPO_4/KH_2PO_4 and K_3PO_4) it was observed that Na_2SO_4-based systems provide an enhanced recovery of gallic acid at the IL-rich phase. From the results gathered at different pH values it was possible to recognize that there is a preferential partitioning of the non-charged molecule for the IL-rich phase, whereas the conjugate base tends to migrate for the salt-rich phase (more hydrophilic phase). Therefore, the choice of the inorganic salt, which in turns leads to different pH values, is a crucial factor in extraction approaches using IL-based ABS – especially with compounds that exhibit acid dissociation constants. This concept was also tested with success in the extraction of vanillin with systems composed of Na_2SO_4 instead of K_3PO_4.

References

1. F.Y. Du, X.H. Xiao, X.J. Luo and G.K. Li, Talanta, 2009, 78, 1177-1784.
2. M.D. Sanza, I.N. Dominguez, L.M.C. Carcel and L.N. Gracia, Anal. Chim. Acta, 2004,513, 229-237.
3. J.D. Habila, I.A. Bello, A.A. Dzikwi, H. Musa and N. Abubakar, Afr. J. Pharm. Pharacol., 2010, 4, 123-126.
4. Y. Zuo, H. Chen and Y. Deng, Talanta, 2002, 57, 307-316.
5. S.A.O. Santos, P. Pinto, A.J.D. Silvestre and C.P. Neto, Ind. Crops Prod., 2010, 31, 521-526.
6. A. Noubigh, A. Mgaidi, M. Abderrabba, E. Provost and W. Furst, J. Sci. Food Agric., 2007, 87, 783-788.
7. A. Noubigh, M., Cherif, E. Provost and M. Abderrabba, J. Chem. Eng. Data, 2008, 53, 1675.
8. E. Sergediene, K. Jonsson, H. Szymusiak, B. Tyrakowska, I.M. Rietjens, N. Cenas, Febs Lett., 1999, 462, 392-396.
9. A.F. Sousa, P. Pinto, A.J.D. Silvestre and C.P. Neto, J. Agric. Food Chem., 2006, 54, 6888-6893.
10. F.A. Hasmann, V.C. Santos, D.B. Gurpilhares, A. Pessoa-Junior and I.C. Roberto, J. Chem. Technol. Biotech., 2008, 83, 167-173.
11. A.F.M. Cláudio, M.G. Freire, C.S.R. Freire, A.J.D Silvestre and J.A.P. Coutinho, Sep. Purif. Technol., 2010, 75, 39-47.
12. P. Chuysinuan, N. Chimnoi, S. Techasakul and P. Supaphol, Macromol. Chem. Phys., 2009, 210 814-822.
13. M. Blesic, M.H. Marques, N.V. Plechkova, K.R. Seddon, L.P.N. Rebelo and A. Lopes, Green Chem., 2007, 9, 481-490.
14. C. Reichardt, Green Chem., 2005, 7, 339-351.
15. M.A. Ab Rani, A. Brant, L. Crowhurst, A. Dolan, M. Lui, N.H. Hassan, J.P. Hallett, H. Niedermeyer, J.M. Perez-Arlandis, M. Schrems, T. Welton and R. Wilding, Phys. Chem Chem Phys., 2011, 13, 16831-16840.
16. R. Lungwitz and S. Spange, New J. Chem., 2008, 32, 392-394.
17. S.P.M. Ventura, S.G. Sousa, L.S. Serafim, A.S. Lima, M.G. Freire and J.A.P. Coutinho, J. Chem. Eng Data, 2012, 57, 507-514.
18. S.P.M. Ventura, S.G. Sousa, L.S. Serafim, A.S. Lima, M.G. Freire and J.A.P. Coutinho, J. Chem. Eng. Data, 2011, 56, 4253-4260.
19. Y. Pei, Z.Y. Li, L. Liu, J.J. Wang and H.Y. Wang, Sci. China, 2010, 53, 1554-1560.
20. V.E. Tarabanko, Y.V. Chelbina, V.A. Sokolenko and N.V. Tarabanko, Solv. Ext. Ion Exch., 2007, 25, 99-107.

2.7. Development of Back-Extraction and Recyclability Routes for Ionic-Liquid-based Aqueous Biphasic Systems

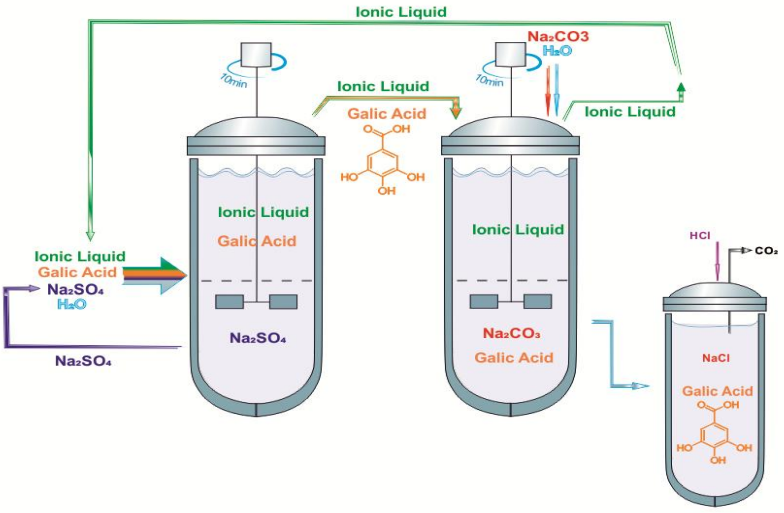

This chapter is based on the published paper: Cláudio, A. F. M.; Marques, C. F. C.; Boal-Palheiros, I,; Freire, M. G. and Coutinho, J. A. P., Development of Back-Extraction and Recyclability Routes for Ionic-Liquid-Based Aqueous Two-Phase Systems, Green Chem., 2014, 16, 259-268.

Abstract

Despite the exceptional achievements regarding the extraction of biomolecules using IL-based ABS, the ILs regeneration, recycling and reuse were lagged behind and still remain a challenging task towards the development of greener cost-effective processes. Aiming at overcoming these shortcomings, the phase diagrams of novel ABS composed of imidazolium-based ILs and Na_2CO_3 or Na_2SO_4 were determined and their extraction efficiencies for a model antioxidant – gallic acid - were evaluated. The most promising IL-based ABS were then used in sequential two-step cycles (product extraction/IL recovery) so as to evaluate the efficacy on the ILs recyclability and reusability. Extraction efficiency values ranging between 73% and 99% were obtained in four sequential partitioning experiments involving gallic acid while allowing the regeneration of 94-95% of the IL and further reutilization. Moreover, to support the vast applicability of the back-extraction routes and recyclability concept proposed here, the most prominent systems were further tested with two additional antioxidants, namely syringic and vanillic acids. In both examples, the extraction efficiencies were higher than 97%. The remarkable results obtained in this work support the establishment of IL-based ABS as a sound basis of greener cost-effective strategies with a substantial reduction in the environmental footprint and economical issues.

Introduction

To effectively apply IL-based ABS as extractive platforms, their phase diagrams must be established experimentally, and there is today a large amount of literature data reporting ternary phase diagrams of systems constituted by ILs, salts and water.[1-4] In addition to the phase diagrams, several works have been demonstrating the outstanding performance of IL-based ABS for extraction purposes.[5] Improved extraction efficiencies, in some examples

up to complete extraction, have been obtained for proteins, enzymes, alkaloids, antioxidants, antibiotics, endocrine disruptors, among others.[5]

ILs have been publicized as "green solvents" due to their negligible vapour pressures preventing thus further emissions to the atmosphere. Nevertheless, the design of entirely green ILs is still very limited and in most cases their toxicity, biocompatibility and biodegradability issues are only now being addressed.[6-11] In industrial applications, ILs are inevitably mixed with other products/solvents, and the development of efficient separation and recycling routes is a crucial attempt to decrease their environmental footprint.[12,13] Most ILs are also still expensive in comparison with more conventional molecular solvents reinforcing therefore the need for their recycling and reuse.[14,15] Envisaging this crucial objective, in the past few years, some researchers have been addressing the development of novel methodologies for the recovery and further reuse of ILs.[12,16-21] The main operations to recover ILs from aqueous solutions are based on the addition of salting-out species[21,22] and barrier (membrane) separations;[13] yet, the former were shown to be more adequate to an industrial implementation.[21] For instance, hydrophobic (water immiscible) ILs were successfully employed in the extraction of amino acids, phenols and amines[16-20] with the IL-rich phase being regenerated by back-extraction of the product, enabling thus the phase-forming compounds to be recycled. Hydrophilic (water-miscible) ILs used to extract α-tocopherol from a model mixture with methyl linoleate and caffeine from guaraná seeds were also recovered making use of organic solvents and reused several times.[16-20] The regeneration of ILs by liquid-liquid techniques may be economically viable; however, the use of volatile organic solvents in the overall process is a significant drawback. Hydrophilic ILs may be also recovered using $scCO_2$, but the process is expensive and consequently not easily amenable to the industrial scale.[21] The use of the unique solvent properties of ILs through the development of efficient separation/purification methods has been thoroughly investigated.[5] Even though, the ILs regeneration, recycling and reuse remains a demanding challenge that needs to be urgently faced.

In this work we propose a new strategy for the recycling and reuse of hydrophilic ILs commonly used as phase-forming components of ABS and usually employed as extractive

systems. For such purpose, a combination of two salt-type ABS was conducted for the extraction and back-extraction of gallic acid (p*K*a = 4.4; 9.4; 11.0)[23,24], and further confirmed with two other species, namely vanillic acid (p*K*a = 4.2; 10.2)[23,24] and syringic acid (p*K*a = 4.0; 9.6)[23,24]. These 3 compounds are representative molecules of phenolic acids and/or antioxidants (Figure 2.7.1). Phenolic compounds possess beneficial roles in the reduction of cancer appearance, neurodegenerative disorders, hypertension and cardiovascular diseases.[25] Besides, some phenolic compounds are also phytotoxic and bactericidal, and can be used in biological wastewater treatments.[26]

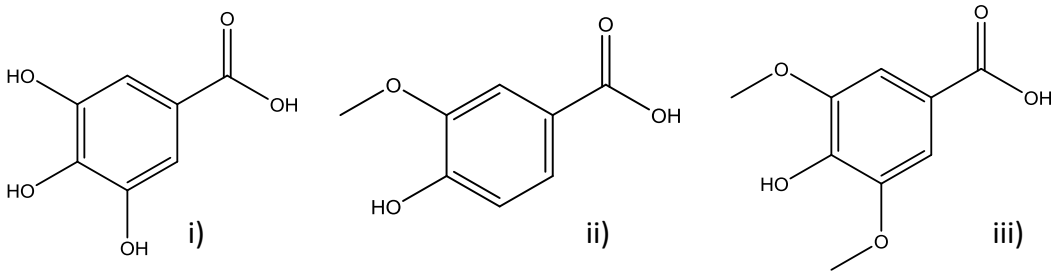

Figure 2.7.1: Chemical structures of gallic (i), vanillic (ii) and syringic (iii) acids.

In previous works[27-29] we thoroughly studied the partition behaviour of phenolic compounds using IL-based ABS and determined the optimal conditions for vanillin[28,29] and gallic acid[27] extraction. One example is reported in **Chapter 2.6**. In this context, improving the sustainability of the process was the step to follow. Hence, in this work, we aimed at recycling and reusing the ILs after the extraction stage to drastically minimize the environmental concerns and economical costs. After the efficient extraction of gallic acid for the IL-rich phase with Na_2SO_4-based ABS we therein investigated the combined use of IL-Na_2CO_3-based ABS to perform the antioxidant back-extraction for the salt-rich phase aiming at purifying the IL-rich phase. Na_2CO_3 was selected because it is highly soluble in water, environmentally safe, inexpensive and has a strong salting-out effect (forming ABS with a wide variety of ILs)[1-4]; under these circumstances, the ILs may be further chosen according to their ability to extract the molecule of interest. To additionally validate the back-extraction and recyclability/reusability of the IL, the enhanced ABS were further used in the extraction/back-extraction cycle of two additional molecules: vanillic and syringic acids.

Experimental Procedure

Materials

The ILs used in this work to form ABS with Na_2CO_3 were $[C_4C_1im][CF_3SO_3]$, $[C_4C_1im][SCN]$, $[C_4C_1im][CH_3SO_3]$, $[C_4C_1im][C_2H_5SO_4]$, $[C_4C_1im][CH_3SO_4]$, $[C_4C_1im][TOS]$, $[C_4C_1im]Br$, $[C_4C_1im][N(CN)_2]$, $[C_4C_1im][DMP]$, $[C_4C_1im]Cl$, and $[C_4C_1im][CH_3CO_2]$. All ILs were supplied by Iolitec and are depicted in Figure 2.7.2. To reduce the volatile impurities content to negligible values, ILs individual samples were kept at constant agitation under vacuum and at a moderate temperature (323 K), for a minimum of 48 h. After this purification step, the purity of each IL was further checked by ^{1}H, ^{13}C and ^{19}F NMR (when applicable) spectra and found to be > 98 wt % for all samples and according to the purity levels given by the supplier. Na_2SO_4 was acquired at LabSolve (purity > 99.8 wt %) and Na_2CO_3 was from Prolabo (purity > 99.9 wt %). Gallic, vanillic and syringic acids were acquired at Merck (> 99.5 wt % pure), Sigma-Aldrich (> 97 wt % pure) and Alfa Aesar (> 98 wt % pure), respectively. H_2SO_4, 95% pure, was from Sigma-Aldrich. The water used was double distilled, passed across a reverse osmosis system and further treated with a Milli-Q plus 185 water purification equipment. The buffers used in the calibration of the pH meter equipment were the citric acid/sodium hydroxide/sodium chloride solution with a pH value of 4.00 (± 0.02), and the potassium dihydrogen phosphate/disodium hydrogen phosphate solution with a pH value of 7.00 (± 0.02), acquired from Fluka.

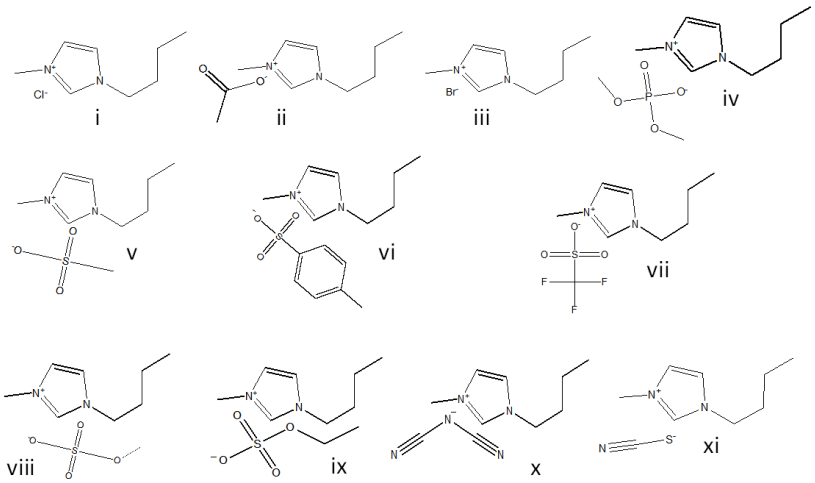

Figure 2.7.2: Chemical structures of the studied ILs: (i) $[C_4C_1im]Cl$; (ii) $[C_4C_1im][CH_3CO_2]$; (iii) $[C_4C_1im]Br$; (iv) $[C_4C_1im][DMP]$; (v) $[C_4C_1im][CH_3SO_3]$; (vi) $[C_4C_1im][TOS]$; (vii) $[C_4C_1im][CF_3SO_3]$; (viii) $[C_4C_1im][CH_3SO_4]$; (ix) $[C_4C_1im][C_2H_5SO_4]$; (x) $[C_4C_1im][N(CN)_2]$; (xi) $[C_4C_1im][SCN]$

Phase Diagrams

The solubility curves of the systems composed of IL, water, and sodium carbonate were determined using the cloud point titration method at (298 ± 1) K and atmospheric pressure. The experimental procedure adopted in this work follows the method already reported in **Chapters 2.1 and 2.2**. Aqueous solutions of Na_2CO_3 with a weight fraction of ≈ 20 wt %, and aqueous solutions of each IL with a weight fraction around 60 wt % were prepared and used for the determination of the corresponding solubility curves. To complete the phase diagrams the opposite addition of the IL aqueous solution, in this stage with a weight fraction of approximately 80 wt %, to the aqueous solution of the salt was also carried out. The experimental binodal curves were fitted by least-squares regression and corresponding tie-lines and tie-line lengths were determined using equations 2.1.1 to 2.1.6. Details on their determination are reported in **Chapter 2.1**.

Partitioning of Gallic, Syringic and Vanillic acids

For the determination of the gallic acid extraction efficiencies, both with Na_2SO_4 or Na_2CO_3, several ILs were investigated as phase-forming components of the ABS, namely $[C_4C_1im]Br$, $[C_4C_1im][CH_3SO_4]$, $[C_4C_1im][C_2H_5SO_4]$, $[C_4C_1im][CF_3SO_3]$ and $[C_4C_1im][N(CN)_2]$. The compositions of the biphasic mixtures used for the gallic acid partitioning were

chosen based on the phase diagrams determined in this chapter and **Chapter 2.1**. Several compositions were adopted while varying the IL and salt compositions. After the optimization investigations with gallic acid, the partitioning of vanillic and syringic acids was also investigated. In all of these compositions it was used an aqueous solution containing either gallic, syringic or vanillic acids at 3×10^{-3} mol·dm^{-3}. All extraction procedure was performed as described in **Chapters 2.4 and 2.6**. At least three individual samples were analysed to determine the extraction efficiencies and the respective standard deviations – the obtained numerical values are presented in the *Supporting Information* (Tables S47 and S48).

The extraction efficiencies (*%EE*) of each acid within the Na_2CO_3-based ABS (and thus into the salt-rich phase) was determined according to,

$$\%EE = \frac{[\text{antioxidant}]_{Na_2CO_3} \times w_{Na_2CO_3}}{[\text{antioxidant}]_{IL} \times w_{IL} + [\text{antioxidant}]_{Na_2CO_3} \times w_{Na_2CO_3}} \times 100 \qquad \text{eq. 2.7.1}$$

On the other hand, the extraction efficiencies (*%EE*) of gallic, syringic and vanillic acids into the IL-rich phase in the Na_2SO_4-based systems were determined according to,

$$\%EE = \frac{[\text{antioxidant}]_{IL} \times w_{IL}}{[\text{antioxidant}]_{IL} \times w_{IL} + [\text{antioxidant}]_{Na_2SO4} \times w_{Na_2SO_4}} \times 100 \qquad \text{eq. 2.7.2}$$

where w_{IL} is the weight of the IL-rich phase and w_{Na2SO4} and w_{Na2CO3} are the weight of the inorganic-salt-rich phases, respectively. $[\text{antioxidant}]_{IL}$ is the concentration of each phenolic acid in the IL-rich phase and $[\text{antioxidant}]_{Na2SO4}$ and $[\text{antioxidant}]_{Na2CO3}$ are the concentrations of the respective biomolecule in each of the inorganic salt enriched phases.

Back-Extraction Procedure and Recovery Efficiencies of IL

Aiming at developing a sustainable IL-recyclable strategy a two-step extraction process was performed twice. In the first step, systems composed of 20 wt % Na_2SO_4 + 25 wt % of IL + 55 wt % of an aqueous solution of gallic acid at 3.06×10^{-3} mol·dm^{-3} were used according to the optimized phase compositions determined in the individual extractions. In this step, the biomolecule was mainly extracted/separated into the IL-rich phase. Then,

in a second step, the IL-rich aqueous phase was separated and reused to form a new ABS with Na_2CO_3 in order to perform the back-extraction of gallic acid. This system was created with the top phase of the first system whereas Na_2CO_3 and water were further added to achieve the desired system composition: 10 wt % of Na_2CO_3, 20 wt % of IL and 70 wt % of water. In this step, gallic acid preferentially partitions for the Na_2CO_3-rich phase. After the back-extraction procedure, the recyclability and reusability of the IL aqueous solutions was then proved. The top phase of the Na_2CO_3-based system was separated and Na_2SO_4 and an aqueous solution of gallic acid were then added to attain the initial weight fraction percentages of each component and the overall process was repeated, *i.e.*, the regeneration/recycling step of the IL layer for a subsequent extraction. The two cycles of two steps were performed using $[C_4C_1im][CF_3SO_3]$ and $[C_4C_1im][N(CN)_2]$ – the ILs which provided the best extractive performances. Finally, and aiming at controlling the pH of each extractive system, H_2SO_4 at 4 M was added under the continuous measurement of the aqueous solution pH.

After all the optimization, the same procedure was applied to the extraction/back-extraction of vanillic and syringic acids (one cycle and 2 steps) and using $[C_4C_1im][CF_3SO_3]$. The vanillic and syringic acids aqueous solutions were at 3.20×10^{-3} mol·dm^{-3}.

The amount of IL lost in each cycle was determined based on their recovery efficiencies and calculated according to,

$$\%R_{IL} = \frac{[\mathrm{IL}]_{\mathrm{IL}} \times w_{\mathrm{IL}}}{[\mathrm{IL}]_{\mathrm{IL}} \times w_{\mathrm{IL}} + [\mathrm{IL}]_{\mathrm{salt}} \times w_{\mathrm{salt}}} \times 100 \qquad \text{eq. 2.7.3}$$

where ''IL'' and ''Salt'' symbolize, respectively, the IL- and salt- rich phases, [Salt] and [IL] are the weight fraction percentage of inorganic salt and ionic liquid and *w* is the weight of each phase.

pH Measurements

The pH of the IL- and inorganic-salt-rich aqueous phases was measured at (298 ± 1) K using a Mettler Toledo S47 SevenMultiTM dual meter pH/conductivity equipment with an uncertainty of ± 0.02.

Ultraviolet-Visible Spectroscopy / Inductively Coupled Plasma-optical Emission Spectrometry / Fourier Transform Infrared Spectroscopy

The TLs' compositions, for systems with $[C_4C_1im][CF_3SO_3]$ and $[C_4C_1im][N(CN)_2]$, were further confirmed by analytical techniques to check the possible ion exchange amongst the coexisting phases. The amount of the imidazolium cation in each aqueous phase was determined by Ultraviolet-Visible (UV-Vis) spectroscopy using a SHIMADZU UV-1700 Pharma-Spec Spectrophotometer at a wavelength of 211 nm (using calibration curves previously established). The sodium content at the coexisting phases was quantified by Inductively Coupled Plasma-Optical Emission Spectrometry (ICPOES) using a Jobin Yvon 70 plus, power 880 W, under a plasma gas flow of 16 $mL \cdot min^{-1}$ and pressure of 2.6 bar. The Fourier transform infrared (FTIR) spectra, with a resolution of 16 cm^{-1}, were obtained using a ABB MB 3000 spectrometer operating in the attenuated total reflection (ATR) mode (equipped with a Miracle Single Reflection ATR cell from Pike Technologies).

Results and Discussion

Planning of the Back-extraction and Recyclability Strategy

In **Chapter 2.6** we have shown the improved ability of IL-Na_2SO_4-based ABS for the extraction of gallic acid (extraction efficiencies up to 99%). In this step the gallic acid migrates for the IL-rich phase requiring a further process for the recovery of both the product and IL. Furthermore, we have found that the partition of phenolic acids is strongly pH dependent.[27] Charged species tend to partition for the salt-rich phase whereas neutral molecules preferentially partition for the IL-rich phase.[27] This pH-dependent behaviour was initially demonstrated by Visser et al.[30] using a simple indicator dye, thymol blue, although using ILs non-miscible with water (at room temperature). In this context, it is conceivable to use this reversible partitioning ability controlled by the pH of the medium to develop the back-extraction process. Amongst the possible salts capable of providing an alkaline medium, Na_2CO_3 was chosen because of its advantageous properties specified before. As a result, we designed a two-step ABS scheme (see

illustrative scheme in front cover of this chapter) to perform a greener IL-recyclable extraction procedure: (*i*) the biomolecule is extracted/separated into the IL-rich phase using Na_2SO_4-based ABS; *(ii*) the IL-rich aqueous phase is separated and reused to form a new ABS with Na_2CO_3 to carry out the back-extraction of the product of interest while regenerating the IL aqueous solution for subsequent reutilization.

In the first stage, and to manipulate the extraction of gallic acid for the IL-rich phase, Na_2SO_4 was used as the two-phase promoter alongside with several imidazolium-based ILs. This salt was chosen since it has a neutral character regarding the pH of its aqueous medium and is suitable to form ABS with distinct ILs. It should be remarked that an optimization was here carried out to improve the overall extraction efficiencies. In the second step, novel ABS composed of several imidazolium-based ILs and Na_2CO_3, which produces alkaline media, were determined with the goal of defining their immiscibility regions and to ascertain on the phases' composition.

ABS Formation Ability

The ability of eleven imidazolium-based ILs (Figure 2.7.2) to form ABS with Na_2CO_3 was first evaluated. The addition of inorganic salts to aqueous solutions of ILs leads to liquid-liquid demixing due to a preferential hydration of the high charge-density salt ions over the IL. In fact, the salting-out effect is the key element behind the formation of ABS comprising ILs and conventional salts.[31-33] Hence, salts composed of highly charged ions, such as PO_4^{3-}, CO_3^{2-} and SO_4^{2-}, display a high capability to form ABS with the low charge density ILs. Compared to the common salting-out inducing salts, ILs are generally weakly hydrated since they are made up of low-symmetry and charge-delocalized ions only capable of weak directional intermolecular interactions.[5] Consequently, the competition of the ions for water molecules will lead to the dehydration of the IL and to the liquid-liquid demixing.

With the exception of $[C_4C_1im][CH_3CO_2]$, all the ILs displayed in Figure 2.7.2 are able to form ABS at 298 K in presence of appropriate concentrations of Na_2CO_3. With the acetate-based IL, instead of the coexisting liquid phases, a solid-liquid equilibrium was observed in the whole composition range of the IL.

In the ABS composed of Na_2CO_3, the IL is almost completely segregated into the upper phase whereas the bottom layer corresponds to the inorganic-salt-rich phase, except with $[C_4C_1im][CF_3SO_3]$.The solubility curves for the systems composed of IL + Na_2CO_3 + water are depicted in Figure 2.7.3. The detailed weight fraction data and respective correlation, tie-lines and tie-line lengths are provided in the *Supporting Information* (Table S49) to S58. As mentioned before, sodium carbonate is a strong salting-out agent and leads to the liquid-liquid demixing of a wide variety of ILs in aqueous medium. This may be imparted to the carbonate's hydration ability. CO_3^{2-} is a base and acts as a hydrogen acceptor towards water, which certainly has an important contribution in the extensive formation of complexes with water.[34,35]

As may be appreciated in Figure 2.7.3, the solubility curves show a strong dependency on the IL; the closer the curve is to the origin, the less IL and/or salt is needed to induce the phase splitting and the wider is the biphasic region. From the depicted data, for 10 wt % of salt, a decreasing order for the ability of the $[C_4C_1im]$-based ILs to form ABS can be established as follows: $[C_4C_1im][CF_3SO_3]$ > $[C_4C_1im][SCN]$ > $[C_4C_1im][N(CN)_2]$ > $[C_4C_1im][TOS]$ > $[C_4C_1im][C_2H_5SO_4]$ > $[C_4C_1im]Cl$ ≈ $[C_4C_1im][CH_3SO_4]$ ≈ $[C_4C_1im]Br$ > $[C_4C_1im][CH_3SO_3]$ > $[C_4C_1im][DMP]$. Since all ILs share the same cation, this order is a direct result of the IL anion.

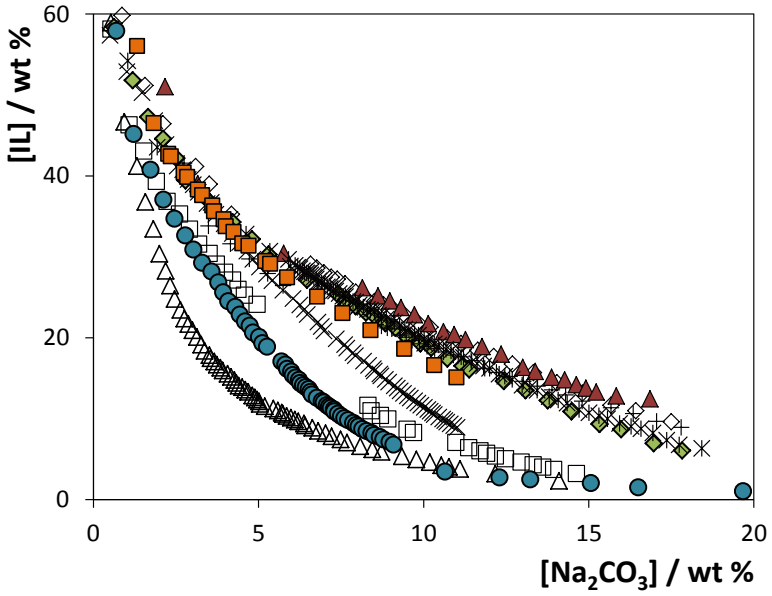

Figure 2.7.3: Binodal curves for the $[C_4C_1im]$-based ILs at 298K: (Δ) $[C_4C_1im][CF_3SO_3]$; (●) $[C_4C_1im][SCN]$; (□) $[C_4C_1im][N(CN)_2]$; (×) $[C_4C_1im][TOS]$; (■) $[C_4C_1im][C_2H_5SO_4]$; (+) $[C_4C_1im]Cl$; (♦) $[C_4C_1im][CH_3SO_4]$; (*) $[C_4C_1im]Br$; (◊) $[C_4C_1im][CH_3SO_3]$; (▲) $[C_4C_1im][DMP]$.

The IL anions interact with water molecules by an approximately linear hydrogen bond, suggesting that the dominant interactions are short range forces of a chemical nature.[36] As a result, the ability for a given anion to be preferentially hydrated depends on its ability to hydrogen bond with water which further rules the ABS formation aptitude. In fact, the IL anion forming ability for ABS closely follows the trend of their H-bond basicity values.[37,38] This trend is reported in Figure 2.7.4.

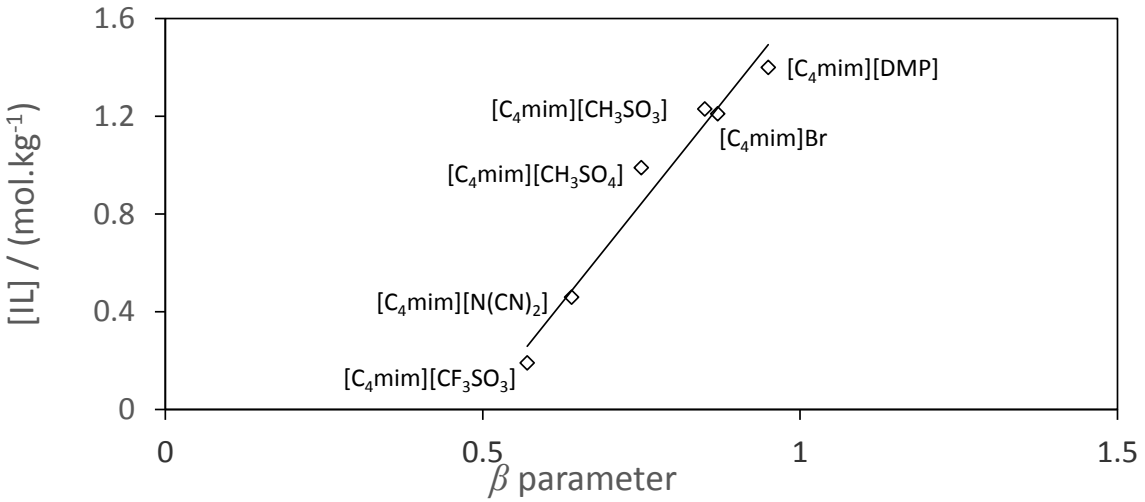

Figure 2.7.4: Ionic liquid molality, taken from each binodal curve and at which the Na_2CO_3 molality is equal to 1.0 mol·kg^{-1}, as a function of the hydrogen bond basicity values (β).[39]

A similar pattern is observed when comparing the solubility curves here obtained using Na_2CO_3 with the correspondent ones using Na_2SO_4 (**Chapter 2.1**) reinforcing the assumption of the major role that the IL anion plays in the ABS formation process. This allows the IL to be chosen according to the extraction purpose.

The correlation coefficients obtained for all systems are close to unity indicating that the fitting described by eq. 2.1.1 can be used to predict data in a given region of the phase diagram where no experimental results are available - reported in the *Supporting Information* (Table S59). The calculated TLs, that is, the compositions of the coexisting phases, along with their respective length, are also presented in the *Supporting Information* (Table S60). Moreover, in Figure S8 (*Supporting Information*) is depicted a binodal curve of the experimental data and respective fitting by equation 2.1.1 and several TLs.

Optimization of the Gallic Acid Extraction in Individual ABS

In the ABS constituted by Na_2CO_3, both aqueous phases present an alkaline pH imparted by the inorganic salt (the pH of the coexisting phases varies between 10 and 12 as presented in the *Supporting Information* (Table S48). In this range of pH values, gallic acid (pK_a = 4.41)[23,24] is predominantly in its deprotonated form, which is negative and has reduced affinity for the IL-rich phase bearing the less polar and more diffusedly charged ions. Although differences are observed amongst the different ILs, gallate ions tend to migrate to the salt-rich phase in most of the studied systems. The extraction efficiencies of gallic acid for the Na_2CO_3-rich phase, defined as the percentage ratio between the amount of gallic acid in the inorganic-salt-rich phase to that in the total mixture, are shown in Figure 2.7.5.

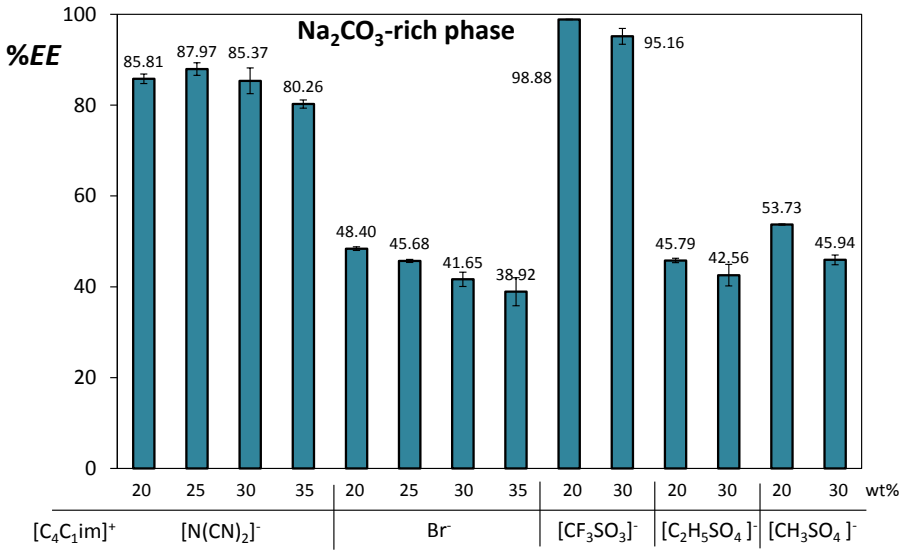

Figure 2.7.5: Extraction efficiencies (%*EE*) of gallic acid for the inorganic-salt-rich phase in ABS composed of 10 wt % of Na_2CO_3 and variable concentrations of $[C_4C_1im]$-based ILs at 298 K.

The extraction efficiencies of gallic acid range between 39% and 99% and are mostly dependent on the IL nature. The IL weight fraction was varied between 20% and 35%. On the other hand, the corresponding extraction efficiencies differed only slightly as a result of the IL content. This means that ABS with the lowest IL weight fraction (20%) still keep the optimal extracting performance - a result that has two major advantages: reduce of the downstream cost and decrease of the environmental impact that these systems may present.

Remarkable extraction efficiencies were observed with the most hydrophobic ILs investigated, namely 88% with $[C_4C_1im][N(CN)_2]$ and 99% with $[C_4C_1im][CF_3SO_3]$. When analysing the distribution behaviour of gallic acid it is reasonable to admit that its migration closely correlates with the aptitude of each IL for ABS formation (Figure 2.7.3). The hydrophobic character of the triflate anion accounts for the $[C_4C_1im][CF_3SO_3]$ strong liquid-liquid demixing ability as well as to its reduced affinity for gallate anions; dicyanamide ion displays a complex solvation shell with a subtle balance between the anion-water and water-water interactions[40] that may contribute to the lack of affinity towards gallate ions. The more moderate two phase promoters, $[C_4C_1im][CH_3SO_4]$ and $[C_4C_1im][C_2H_5SO_4]$, exhibit a considerable affinity for the phenolic molecule due to their more hydrophilic nature and higher water content at the IL-rich phase. The phases' compositions are provided in the *Supporting Information* (Table S48).

In **Chapter 2.7** we have shown that gallic acid preferentially migrates for the IL-rich phase in ABS composed of imidazolium-based ILs and Na_2SO_4.[27] In this work we expanded that study of the extraction efficiencies of gallic acid using several imidazolium-based ILs and different concentrations aiming at finding the best systems to be coupled with the back-extraction procedure. The extraction efficiencies of gallic acid for the IL-rich phase are depicted in Figure 2.7.6.

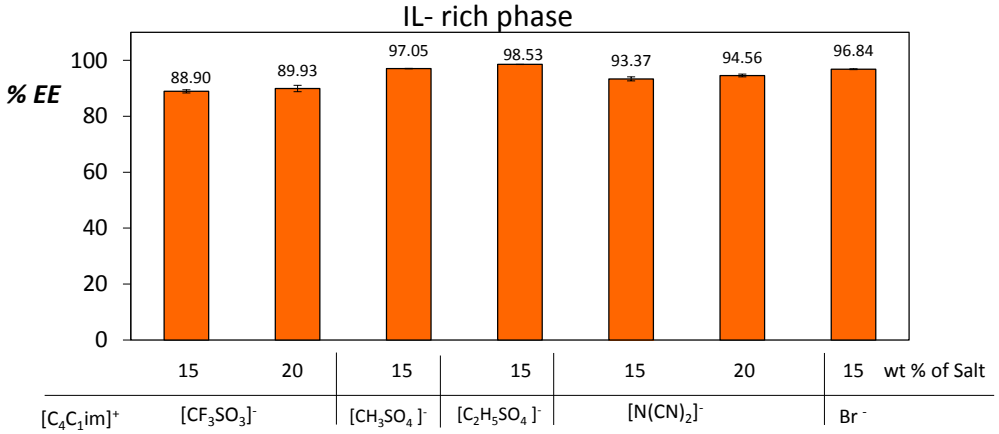

Figure 2.7.6: Extraction efficiencies (%*EE*) of gallic acid for the IL-rich phase in ABS composed of 25 wt % of $[C_4C_1im]$-based ILs and variable concentrations of Na_2SO_4 at 298 K.

The preferential migration of the gallic acid towards the IL-rich phase was observed for all the studied systems with extraction efficiencies ranging between 89% and 99%. Those differences can be attributed to the intrinsic nature of IL anions and also to the concurrent pH effect which they produce in the aqueous media and in the biomolecule itself. Being a neutral salt, Na_2SO_4 aqueous solutions have no buffering capacity, and hence, the inherent IL acidic/alkaline characteristics largely control the pH of the corresponding ABS.[27] Except for $[C_4C_1im][N(CN)_2]$, the pH values of both IL and Na_2SO_4 aqueous phases are slightly acidic as presented in the *Supporting Information* (Table S49). Amongst the studied ABS constituted by $[C_4C_1im]$-based ILs, outstanding results were obtained with $[C_4C_1im][CF_3SO_3]$ and $[C_4C_1im][N(CN)_2]$ – more hydrophobic ILs with a lower water content at the IL-rich phase as can be appreciated in their phases' compositions presented in the *Supporting Information* (Table S60). Taking into account the overall results obtained it is evident that the best ILs to be considered in the next steps of back-extraction and recyclability are those that allowed the higher extraction efficiencies for both the IL- and salt-rich phase, namely $[C_4C_1im][CF_3SO_3]$ and $[C_4C_1im][N(CN)_2]$.

Back-extraction of Gallic acid and ILs Recyclability and Reusability

As mentioned before, the main goal of this work was to develop a procedure that uses the promising IL-based ABS, not only for the extraction/purification of biomolecules as it has been extensively shown in literature,[5] but also for efficiently accomplish their back-extraction while allowing the IL recyclability and reusability. This combined procedure should allow an enhanced recovery of the added-value biomolecules and the IL cleaning and recycling, reducing therefore both economic and environmental loads.

Using the extraction efficiencies obtained in single-step procedures, either into the IL-rich phase using Na_2SO_4 or into the inorganic-salt-rich phase when Na_2CO_3 was employed, we proceeded to investigate the back-extraction of gallic acid and the recyclability of the ILs in a combined approach. For this purpose, the extraction of gallic acid was performed in two cycles, each one involving a first step with Na_2SO_4 + IL ABS, followed by a second step, using Na_2CO_3+ IL aqueous systems. This second step "cleans" the IL aqueous solution thus preparing it for reutilization in a new cycle using identical procedures. For this study the two most efficient ILs in both extractions, $[C_4C_1im][N(CN)_2]$ and $[C_4C_1im][CF_3SO_3]$, were chosen and the most favourable compositions were used. The results obtained for the gallic acid extraction in each of the four sequential single-step procedures, in the two cycles, are summarized in Table 2.7.1. Details of composition are reported in the *Supporting Information* (Table S61). As may be appreciated, although differences between the two ILs were observed for each of the different steps, the second cycle always produces poorer results at non-adjusted pH conditions. A closer observation reveals that there is an increase in the medium pH after the first back-extraction with sodium carbonate; this salt being a base of considerable strength, its concentrated solution imparts to both aqueous phases an alkaline pH ($9 < pH < 12$). This effect is even more remarkable for the least acidic IL, $[C_4C_1im][N(CN)_2]$. The pH effect is thus responsible for the reduced migration of gallic acid towards the IL-rich phase in the recycling step. At alkaline pH values the biomolecule is mostly in its anionic form preferring, therefore, the inorganic salt enriched phase as discussed before.

Table 2.7.1: Extraction efficiencies (%EE) of gallic acid and aqueous phases pH values in ABS at 298 K for two sequential cycles composed of 25 wt % of IL + 20 wt % of Na_2SO_4 and 20 wt % of IL + 10 wt % of Na_2CO_3.

Step		$[C_4C_1im][N(CN)_2]$		$[C_4C_1im][CF_3SO_3]$	
		non-adjusted pH	adjusted pH	non-adjusted pH	adjusted pH
		1st Cycle			
1 (to IL-rich phase)	% EE_{IL}	94.6 ± 0.5	93.1 ± 0.2	89.9 ± 1.1	93.3 ± 3.7
	pH IL/Salt	7.4/7.7	7.5/7.5	4.6/4.6	4.0/3.3
2 (to Na_2CO_3-rich phase)	% EE_{Salt}	70.6 ± 0.7	72.4 ± 1.2	98.7 ± 2.5	98.3 ± 1.7
	pH IL/Salt	11.2/11.3	11.7/11.7	11.1/11.5	11.1/11.1
		2nd Cycle			
3 (to IL-rich phase)	% EE_{IL}	50.1 ± 3.7	96.7 ± 3.3	35.6 ± 5.0	95.5 ± 2.6
	pH IL/Salt	8.7/9.9	6.4/6.3	8.6/8.5	2.9/2.9
4 (to Na_2CO_3-rich phase)	% EE_{Salt}	79.4 ± 4.2	78.7 ± 2.0	91.1 ± 2.1	99.2 ± 0.8
	pH IL/Salt	11.3/11.8	11.1/11.3	11.4/11.5	11.4/11.3

If the media pH are neutralized or adjusted to slight acidic values better results can be obtained. The whole extraction procedure was then repeated for both ILs. At this stage we conducted a pH adjustment between the cycles with the addition of H_2SO_4 4 M to the systems composed of $[C_4C_1im][CF_3SO_3]$ and $[C_4C_1im][N(CN)_2]$ (guarantying that SO_4^{2-} is the main anion in the ABS) and outstanding results were achieved as expected. This addition was carried out under a continuous control of the medium pH and until attaining the desired value. The small amount of acid solution required to change the pH has an insignificant impact on the overall system composition (lower than 0.2 wt %).

Figure 2.7.7 depicts the extraction efficiencies of gallic acid in the four sequential steps. For the ABS composed of $[C_4C_1im][CF_3SO_3]$, the extraction efficiencies values are always higher than 93%. This excellent performance is similar in the two cycles further confirming the IL aqueous phase regeneration and reusability. For the other IL studied, $[C_4C_1im][N(CN)_2]$, the extraction efficiencies values are higher than 93 % for the IL-rich phase and 72 % for the salt-rich layer. In summary, the initial extraction efficiencies are always reached after the ILs recyclability without a decrease in their extractive performance. In addition, due to the high ability of Na_2CO_3 as a two-phase promoter, a relatively small amount of salt is enough to induce the liquid-liquid demixing (10 wt % of Na_2CO_3 is sufficient to produce ABS with a wide range of ILs).

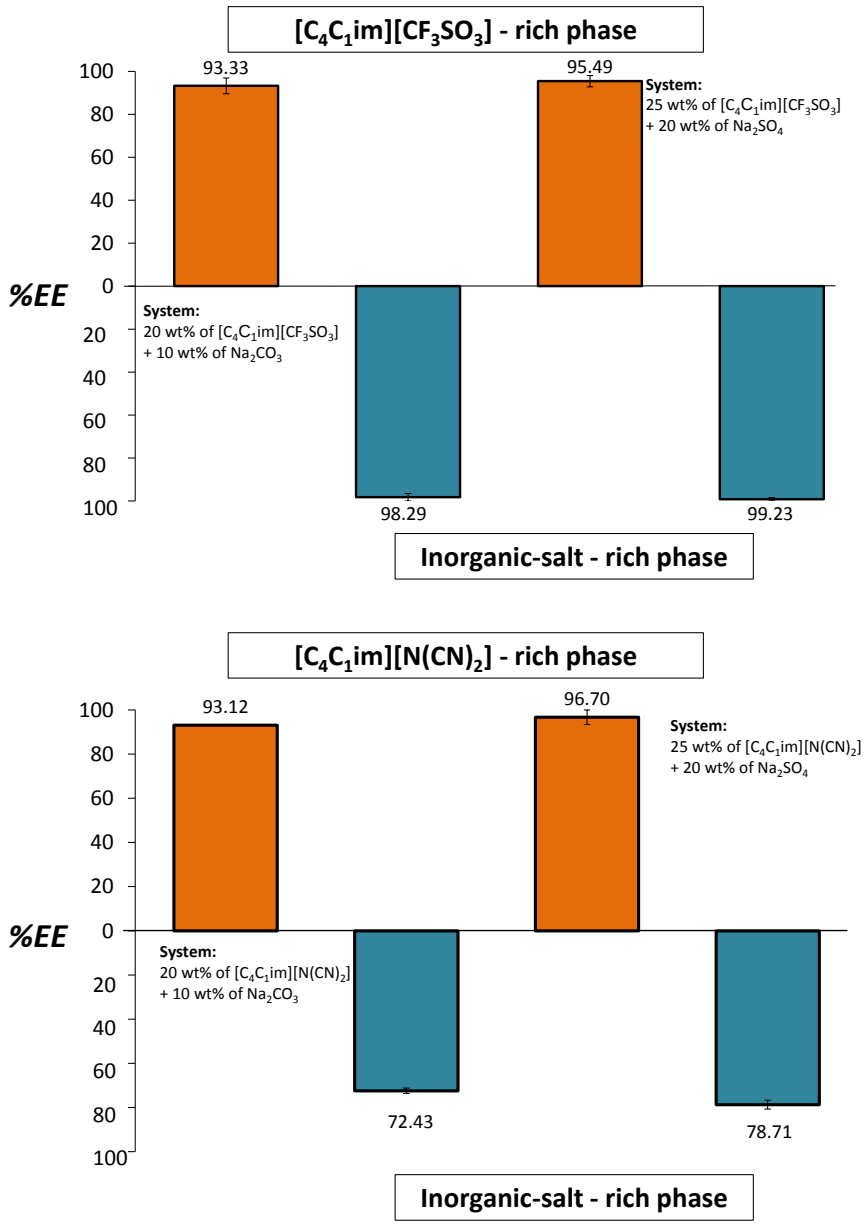

Figure 2.7.7: Extraction efficiencies (%*EE*) of gallic acid in sequential ABS composed of 25 wt % of IL + 20 wt % Na_2SO_4 (orange bars) and 20 wt % of IL + 10 wt % Na_2CO_3 (blue bars) at 298 K.

After the last stage, the biomolecule is mainly concentrated at the carbonate-rich aqueous solution (with a concentration of IL lower than 2 wt % - see Table S60 with the phases' compositions the *Supporting Information*). The biomolecule isolation may finally be achieved through the addition of HCl leaving NaCl in solution - a biocompatible salt - although it can be removed by ion exchange if high purity standard levels of the antioxidant are foreseen.

The scheme provided in the cover front of this chapter summarizes the optimized strategy for the extraction and back-extraction of gallic acid while allowing the reutilization of the IL aqueous phase. This optimized procedure highlights the "greener" nature of IL-based ABS if a proper selection of the inorganic salts and ILs is carried out based on the extraction efficiencies that they afford. In this context, the use of combined ABS for the extraction and recovery of other value-added compounds is straightforward envisaged.

The combination of ABS constituted by inorganic salts and ILs that is here reported yielded an almost complete recovery of gallic acid and a subsequent IL phase depletion, thus regenerating the IL aqueous solution for subsequent reutilizations with the same efficacy shown in the first cycle. The IL is only lost in the Na_2CO_3-rich solution during the back-extraction step. The IL present in the Na_2SO_4-rich phase is completely recovered and reused. Based on the TL compositions, and on the mixture compositions and total weight of each phase, there is a loss of 6 % of $[C_4C_1im][N(CN)_2]$ and 5 % of $[C_4C_1im][CF_3SO_3]$ at the end of each cycle of two steps. Further process improvements aiming the complete recovery of ILs are thus required. The addition of stronger salting-out salts to generate a second IL-rich phase or their adsorption onto activated carbon, as previously demonstrated by our group[41,42], are two of the possibilities to be evaluated.

Since the proposed process deals in aqueous solution with two charged species (IL + inorganic salt) one of the major concerns regarding the development of the back-extraction procedure relays on the possibility of ion exchange between the salts and the ionic liquid. Therefore, aiming at evaluating if any ion exchange takes place during the formation of the ABS and further phase separation, several analytical and spectroscopic techniques were applied to the characterization and quantification of the coexisting phases of the systems composed of $[C_4C_1im][CF_3SO_3]$ and $[C_4C_1im][N(CN)_2]$, combined with both salts, at the mixture compositions presented in Figure 2.7.7. The detection of the sulphate and carbonate anions was carried out with Fourier Transform Infrared spectroscopy. The sodium cation, at both aqueous phases, was quantified by Inductively Coupled Plasma Optical Emission Spectrometry. The imidazolium cation content was determined by UV-Vis spectroscopy. From the results obtained it is possible to establish

that there is no ion exchange in the studied systems, and that the amount of each ion at each phase is in good agreement with those estimated from the tie-lines. The experimental results are shown in the *Supporting Information* (Table S62 and S63). These results are in close agreement with previous studies involving ILs and other inorganic salts.[43,44] The inorganic anions of the salts commonly used to form ABS with ILs are of high charge density and with a great propensity to form hydration complexes.[45,46] Furthermore, these anions usually exhibit a stronger cation-anion interaction strength with less organic (more complex) and high charge density cations.[47] All of these factors contribute to a negligible ion exchange in this type of systems (composed of inorganic salts with high charge density ions *versus* low charge density IL ions).

Application of the Back-extraction Concept to Other Species

To further support the applicability of the back-extraction process, we further used the ABS composed of $[C_4C_1im][CF_3SO_3]$ + Na_2SO_4/Na_2CO_3 to study the extraction efficiencies and back-extraction possibility of two additional antioxidants: vanillic acid and syringic acid. Figure 2.7.8 depicts the results obtained. In both examples the extraction efficiencies are above 97 %. The detailed results and phases' compositions are provided in the *Supporting Information* (Table S64).

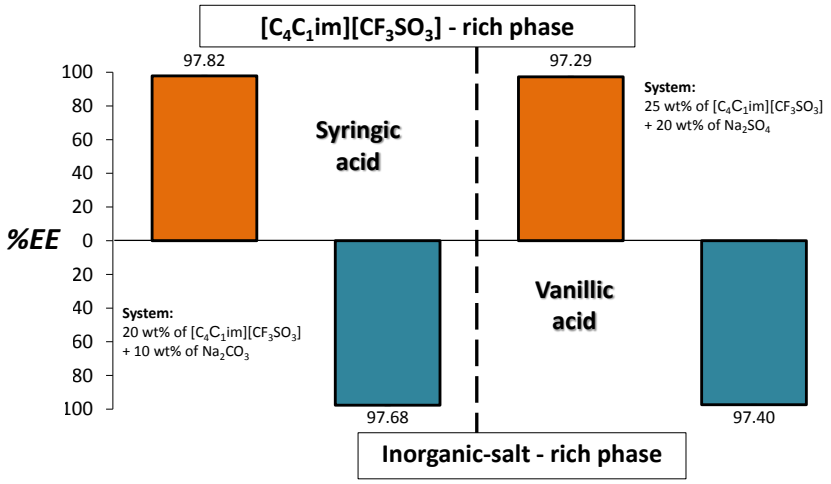

Figure 2.7.8: Extraction efficiencies (%*EE*) of syringic and vanillic acid in sequential ABS composed of 25 wt % of IL + 20 wt % Na_2SO_4) (orange bars) and 20 wt % of IL + 10 wt % Na_2CO_3 (blue bars) at 298 K.

In summary, the results reported here demonstrate that a judicious choice of the ABS forming components, media composition and pH ensures outstanding results in the

separation/extraction of added-value products and in the following back-extraction procedures. The industrial implementation of the proposed recovery procedure does not only minimize the environmental load of the industrial wastes but performs, at the same time, the retrieval of the valuable ILs.

Conclusions

Despite the large interest devoted to IL-based ABS as extractive systems of outstanding performance, the recovery of the extracted added-value products and the systems recyclability and reusability have been seldom studied. An efficient and environmentally safe extraction/purification combined process for IL-based ABS was here proposed. As a proof of principle, a model antioxidant was firstly employed – gallic acid. In a first step, Na_2SO_4 + IL ABS were used to extract gallic acid from an aqueous solution to the IL-rich phase; then, another ABS composed of IL and Na_2CO_3 was used to perform the back-extraction of the biomolecule and to "clean" the IL-rich phase for its subsequent reutilization. The use of Na_2SO_4 allowed near complete extractions into the IL enriched phase. The back-extraction that followed, using Na_2CO_3, also led to remarkable results, stripping the biomolecule almost entirely from the IL. In each cycle, the IL recovery efficiency was between 94-95%. The recycling of the IL and its further recyclability was established without losses in the extractive performance of the corresponding ABS. This two-step cycle was repeated twice proving the IL recyclability and reusability. Furthermore, the optimized systems were also applied to the extraction/back-extraction of syringic and vanillic acids. Extraction efficiencies above 97% were obtained supporting thus the vast applicability of the recommended strategy.

References

1. M.G. Freire, C.M.S.S. Neves, I.M. Marrucho, J.N. Canongia Lopes, L.P.N. Rebelo and J.A.P. Coutinho, Green Chem., 2010, 12, 1715-1718.
2. C.F.C. Marques, T.Mourão, C.M.S.S. Neves, A.S. Lima, I.Boal-Palheiros, J.A.P. Coutinho and M.G. Freire, Biotechnol. Prog., 2013, 29, 645-654.
3. H. Passos, A.C.A. Sousa, M. Ramiro Pastorinho, A.J.A. Nogueira, L.P.N. Rebelo, J.A.P. Coutinho and M.G. Freire, Anal. Methods, 2012, 4, 2664-2667.
4. S. Shahriari, L.C. Tomé, J.M.M. Araújo, L.P.N. Rebelo, J.A.P. Coutinho, I.M. Marrucho and M.G. Freire, RSC Adv., 2013, 3, 1835-1843.
5. M.G. Freire, A.F.M. Cláudio, J.M.M. Araújo, J.A.P. Coutinho, I.M. Marrucho, J.N. Canongia Lopes and L.P.N. Rebelo, Chem. Soc. Rev., 2012, 41, 4966-4995.
6. D. Coleman and N. Gathergood, Chem. Soc. Rev., 2010, 39, 600-637.
7. J. Ranke, S. Stolte, R. Störmann, J. Arning and B. Jastorff, Chem. Rev., 2007, 107, 2183-2206.
8. S. Stolte, S. Abdulkarim, J.R. Arning, A.K. Blomeyer-Nienstedt, U. Bottin-Weber, M. Matzke, J. Ranke, B. Jastorffa and J. Thoming, Green Chem., 2007, 10, 214-224.
9. S.P.M. Ventura, A.M.M. Gonçalves, F. Gonçalves and J.A.P. Coutinho, Aquat. Toxicol., 2010, 96, 290-297.
10. S.P.M. Ventura, C.S. Marques, A.A. Rosatella, C.A.M. Afonso, F. Gonçalves and J.A.P. Coutinho, Ecotox. Environ. Saf., 2012, 76, 162-168.
11. S.P.M. Ventura, A.M.M. Gonçalves, T. Sintra, J.L. Pereira, F. Gonçalves and J.A.P. Coutinho, Ecotoxicol., 2013, 22, 1-12.
12. J.F. Fernández, J. Neumann and J.Thöming, Curr. Org. Chem., 2011, 15, 1992-2014.
13. K. Haerens, S.V. Deuren, E. Matthijs and B.V. Bruggen, Green Chem., 2010, 12, 2182-2188.
14. N.V. Plechkova and K.R. Seddon, Chem. Soc. Rev., 2008, 37, 123-150.
15. Y. Zhang, B.R. Bakshi and E.S. Demessie, Environ. Sci. Technol., 2008, 42, 1724-1730.
16. A.F.M. Cláudio, A.M. Ferreira, M.G. Freire and J.A.P. Coutinho, Green Chem., 2013, 15, 2002-2010.
17. V.M. Egorov, S.M. Smirnova and I.V. Pletnev, Sep. Pur. Technol., 2008, 63, 710-715.
18. L. Huaxi, L. Zhuo, Y. Jingmei, L. Changping, C. Yansheng, L. Qingshan, Z. Xiuling and W.B. Urs, Green Chem., 2012, 14, 1721-1727.
19. X. Ni, H. Xing, Q. Yang, J. Wang, B. Su, Z. Bao, Y. Yang and Q. Ren, Ind. Eng. Chem. Res., 2012, 51, 6480-6488.
20. E.M. Siedlecka, M. Czerwicka, J. Neumann, P. Stepnowski, J.F. Fernández and J. Thöming, Ionic Liquids: Theory, Properties, New Approaches, Ed. A. Kokorin, 2011.
21. B. Wu, W. Liu, Y. Zhang and H. Wang, Chem. Eur. J., 2009, 15, 1804-1810.
22. C.M.S.S. Neves, M.G. Freire and J.A.P. Coutinho, RSC Adv., 2012, 2, 10882-10890.
23. P. Chuysinuan, N. Chimnoi, S. Techasakul and P. Supaphol, Macromol Chem. Physic., 2009, 210, 814-822.
24. ChemSpider – The free chemical database at www.chemspider.com.
25. J. Teixeira, T. Silva, S. Benfeito, A. Gaspar, E.M. Garrido, J. Garrido and F. Borges, Eur. J. Med. Chem., 2013, 62, 289-296.
26. A. Noubigh, A. Mgaidi, M. Abderrabba, E. Provost and W. Furst, J. Sci. Food Agric., 2007, 87, 783-788.
27. A.F.M. Cláudio, A.M. Ferreira, C.S.R. Freire, A.J.D. Silvestre, M.G. Freire and J.A.P. Coutinho, Sep. Purif. Technol., 2012, 97, 142-149.
28. A.F.M. Cláudio, M.G. Freire, C.S.R. Freire, A.J.D. Silvestre and J.A.P. Coutinho, Sep. Pur. Technol., 2010, 75, 39-47.

29. C.L.S. Louros, A.F.M. Cláudio, C.M.S.S. Neves, M.G. Freire, I.M. Marrucho, J. Pauly and J.A.P. Coutinho, Int. J. Mol. Sci., 2010, 11, 1777-1791.
30. A.E. Visser, R.P. Swatloski and R.D. Rogers, Green Chem., 2000, 2, 1-4.
31. M.G. Freire, P.J. Carvalho, A.M.S. Silva, L.M.N.B.F. Santos, L.P.N. Rebelo, I.M. Marrucho and J.A.P. Coutinho, J. Phys. Chem. B, 2009, 113, 202-211.
32. M.G. Freire, C.M.S.S. Neves, A.M.S. Silva, L.M.N.B.F. Santos, I.M. Marrucho, L.P.N. Rebelo, J.K. Shah, E.J. Maginn and J.A.P. Coutinho, J. Phys. Chem. B, 2010, 114, 2004-2014.
33. T. Mourão, A.F.M. Cláudio, I. Boal-Palheiros, M.G. Freire and J.A.P. Coutinho, J. Chem. Thermodyn., 2012, 54, 398-405.
34. S. Shahriari, C.M.S.S. Neves, M.G. Freire and J.A.P. Coutinho, J. Phys. Chem. B, 2012, 116, 7252–7258.
35. Y. Marcus, Chem. Rev., 2009, 109, 1346-1370.
36. K.D. Collins, G.W. Neilson and J.E. Enderby, Biophys. Chem. 2007, 128, 95-104.
37. J.P. Hallett and T. Welton, Chem. Rev., 2011, 111, 3508-3576.
38. C. Reichardt, Org. Process Res. Dev., 2006, 11, 105-113.
39. R. Lungwitz and S. Spange, New J. Chem., 2008, 32, 392-394.
40. B. Jagoda-Cwiklik, X.B. Wang, H.K. Woo, J. Yang, G.J. Wang, M. Zhou, P. Jungwirth and L.S. Wang, J. Phys. Chem. A, 2007, 111, 7719-7725.
41. C.M.S.S. Neves, M.G. Freire and J.A.P. Coutinho, RSC Adv., 2012, 2, 10882-10890.
42. J. Lemus, C.M.S.S. Neves, C.F.C. Marques, M.G. Freire, J.A.P. Coutinho and J. Palomar, Environ. Sci. Proc. Impacts, 2013, 15, 1752-1759.
43. K.E. Gutowski, G.A. Broker, H.D. Willauer, J.G. Huddleston, R.P. Swatloski, J.D. Holbrey and R. D. Rogers, J. Am. Chem. Soc., 2003, 125, 6632-6633.
44. C.M.S.S. Neves, M.G. Freire and J.A.P. Coutinho, RSC Adv., 2012, 2, 10882-10890.
45. M.G. Freire, P.J. Carvalho, A.M.S. Silva, L.M.N.B.F. Santos, L.P.N. Rebelo, I.M. Marrucho and J.A.P. Coutinho, J. Phys. Chem. B, 2009, 113, 202-211.
46. M.G. Freire, C.M.S.S. Neves, A.M.S. Silva, L.M.N.B.F. Santos, I.M. Marrucho, L.P.N. Rebelo, J.K. Shah, E.J. Maginn and J.A.P. Coutinho, J. Phys. Chem. B, 2010, 114, 2004-2014.
47. A.M. Fernandes, M.A.A. Rocha, M.G. Freire, I.M. Marrucho, J.A.P. Coutinho and L.M.N.B.F. Santos, J. Phys. Chem. B, 2011, 115, 4033-4041.

3. Solid-Liquid Extractions (from Biomass)

3.1. Enhanced Extraction of Caffeine from Guaraná Seeds using Aqueous Solutions of Ionic Liquids

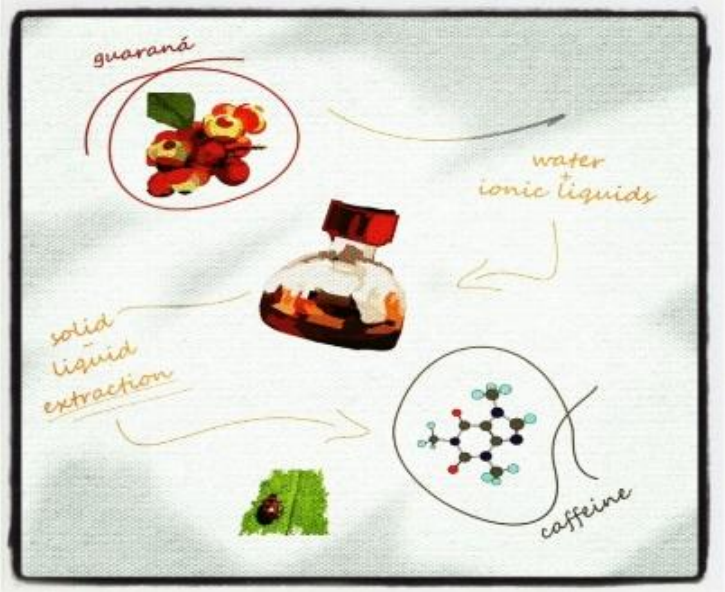

This chapter is based on the published paper: Cláudio, A. F. M.; Ferreira, A. M.; Freire, M. G. and Coutinho, J. A. P., Enhanced Extraction of Caffeine from Guaraná Seeds using Aqueous Solutions of Ionic Liquids, Green Chem., 2013, 15, 2002-2010.

Abstract

The extraction of caffeine from bioresources using more benign and cost-effective processes is of fundamental relevance towards the finding of alternative (bio)pesticides. Classically, the best attempts to extract caffeine from biomass have resulted in low efficiency and in a large consume of hazardous organic solvents and/or energy requests. In this work, we report an enhanced and selective extraction of caffeine from guaraná (*Paullinia cupana*, Sapindaceae) seeds using aqueous solutions of ILs. Several ILs composed of imidazolium or pyrrolidinium cations combined with the chloride, acetate and tosylate anions were investigated. Furthermore, the effect of the cation alkyl side chain length and the presence of functionalized groups were also addressed. Additional conditions such as the IL concentration, the contact time, the solid-liquid ratio and temperature were further optimized by a response surface methodology. Outstanding extraction yields (up to 9 wt % of caffeine *per* guaraná dry weight) were obtained at a moderate temperature and in a short-time. The recyclability and reusability of the ILs were also confirmed. For the first time it is shown that aqueous solutions of ILs are superior alternatives for the solid-liquid extraction of caffeine from biomass samples and, as a result, the development of an IL-based process is straightforward envisaged.

Introduction

Guaraná (*Paullinia cupana*, Sapindaceae) is a Brazilian native plant and its seeds are the only part suitable for human consumption.[1] Guaraná seeds are the richest vegetable source of caffeine with a concentration two to three times higher than those of coffee beans, tea leaves and cola nuts. The concentration of caffeine on a dry basis generally ranges from 3 to 7%.[2-4] Nevertheless, the place and method of cultivation and the drying procedure can lead to different amounts of caffeine. Guaraná also possesses other methylxanthines, tannins, saponins, starch and fats.[5] As a result of its rich composition, guaraná is typically used as a medicinal plant, either in natural products or by the pharmaceutical companies, as well as in the food industry.[6]

Caffeine (1,3,7-trimethylxanthine) belongs to the alkaloids family, more specifically to xanthines (2,6-dihydroxypurine). Theobromine (3,7-dimethylxanthine) and theophylline (1,3-dimethylxanthine), albeit in lower amounts, are the two other xanthines that can be found in guaraná.[5] Caffeine (Figure 3.1.1) is the bioactive ingredient mostly ingested by humans. It is also used in pharmaceutical products for therapeutic purposes because of its stimulant effects on the nervous, muscular and cardiovascular systems.[5] Nonetheless, besides these particular properties, caffeine also displays antibacterial and antifungal features.[7-10] It can act as a natural pesticide protecting plants - principal function in guaraná, coffee, tea and cocoa.

Taking into account the harmful and hazardous nature of pesticides commonly used in farming, caffeine can be foreseen as an alternative (bio)pesticide. Several works reported on the use of caffeine as a natural pesticide effective in killing/repelling slugs, snails, birds and insects.[7-10] Therefore, caffeine can be used as a repellent or a more benign pesticide while being an efficient economic alternative if extracted from residues, such as spent coffee or low added-value bioresources such as the guaraná seeds. In this context, the extraction and purification of xanthines (mainly caffeine) from natural plants, *e.g.* guaraná, through economic and benign processes, is of huge interest for their further applications as greener substitutes to common pesticides.

Currently, there is a great demand for natural ingredients and the discrimination among natural and synthetic caffeine has received an enormous attention. In the past few years,

the Food and Drug Administration (FDA) regulated that any added caffeine must be labelled on human consumption products owing to possible adulteration and health concerns.[11] Actually, caffeine extraction (essentially for decaffeination purposes and human intake) is carried out using supercritical carbon dioxide or related mixtures making use of co-solvents, such as alcohols and water, to improve the extraction yields.[12-16] Other conventional methods include the extraction of caffeine by water at high temperatures,[17] the use of organic solvents,[18-20] namely chloroform, methylene chloride and ethyl acetate, and the use of water-organic solvent mixtures (water-ethanol, water-methanol and water-acetone)[21]. These methods have some disadvantages since they require several hours of extraction, present low yields of caffeine and lead to human risks and safety issues.[12-21] In recent years, ILs emerged as alternative solvents for separation processes.[22-24] Taking into account the large content of caffeine in guaraná seeds and its non-effective, non-selective or poor extraction by conventional methods and/or solvents, and based on previous experience of our group in the extraction of alkaloids[25-28], we propose here, for the first time, the use of ionic liquids' aqueous solutions as alternative solvents for the selective extraction of caffeine from bioresources.

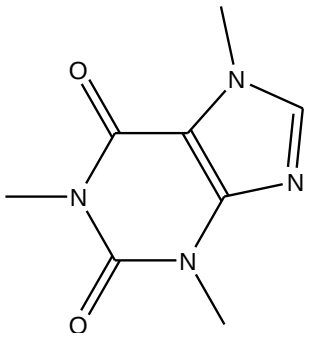

Figure 3.1.1: Chemical structure of caffeine.

Experimental Procedure

Materials

Guaraná seeds were purchased at a local market in Aracaju, Sergipe, Brazil. They were kept in sealed plastic bags at 4 ^{o}C until use. The seeds preparation for extraction purposes involved their initial grinding with a commercial coffee grinder. The samples of grinded guaraná were further divided and classified according to the particle size by means of stainless steel sieves. Two groups of different particles diameter (*d*) were isolated: d < 0.4 mm and 0.4 mm < *d* < 1.0 mm. The solvents used for the extraction of caffeine from guaraná seeds include water, aqueous solutions of sodium chloride and aqueous solutions of ionic liquids. Double distilled water, passed through a reverse osmosis system, and further treated with a Milli-Q plus 185 water purification equipment, was used in all experiments. NaCl, 99.9 wt % pure, was from Normapur.

The ionic liquids [C_4mim]Cl, [C_4mim][TOS], [C_4mpyrr]Cl, [C_2mim]Cl, [OHC_2mim]Cl and [C_2mim][CH_3CO_2] were purchased from Iolitec. Their chemical structures are depicted in Figure 3.1.2. All ionic liquid samples were dried, at least for 48 h, under vacuum and at a moderate temperature (≈ 323 K) before use. Their purities were further confirmed by ^{1}H and ^{13}C NMR spectra and showed to be ≥ 98-99 wt %. The water content of all ionic liquids, after the drying procedure, was < 1000 ppm as determined by Karl-Fischer titration.

The water immiscible solvents tested for the re-extraction of caffeine from an aqueous phase were chloroform, > 99 % pure from Carlos Erba, ethyl acetate, 99.5% pure from Fluka, hexane, 99.63% pure from Acros Organics, diethyl ether and toluene, 99.5% and 99.9% pure, respectively, from Prolabo, 1-butanol, 99.5% pure from Panreac, and xylene, 95% pure from Pronalys.

The high purity caffeine, used as a standard in the several quantitative and qualitative techniques, was obtained from Marsing & Co. Ltd. with a nominal purity ≥ 98.5 wt %. The other two methylxanthines, theophylline and theobromine, used in capillary electrophoresis and spectroscopic analysis were from Sigma and ≥ 99.0 wt % pure.

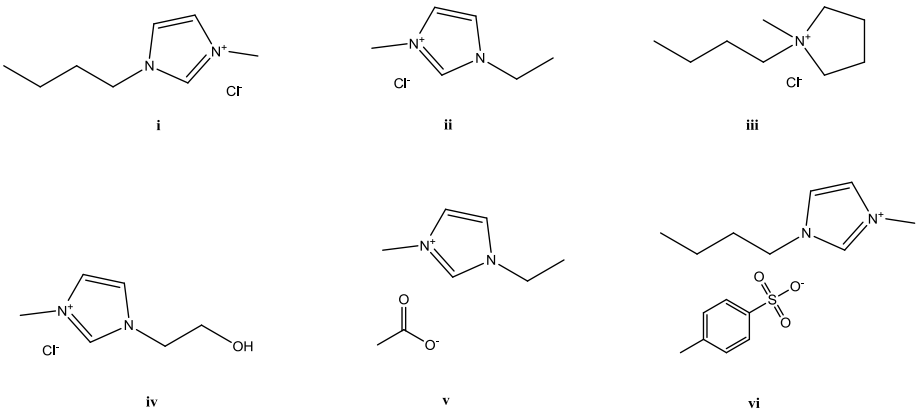

Figure 3.1.2: Chemical structures of the ionic liquids used in the extraction of caffeine from guaraná seeds: (i) $[C_4mim]Cl$; (ii) $[C_2mim]Cl$; (iii) $[C_4mpyrr]Cl$; (iv) $[OHC_2mim]Cl$; (v) $[C_2mim][CH_3CO_2]$; (vi) $[C_4mim][TOS]$.

Extraction of Caffeine

All the aqueous solutions were prepared gravimetrically within 10^{-4} g (using an analytical balance Mettler Toledo Excelence - XS205 Dual Range). Mixtures of specific amounts of guaraná grounded seeds and aqueous solutions were also prepared by weight and in specific sealed glass vials. Several concentrations of the solvent of extraction and different solid-liquid ratios were used according to the surface response methodology described below.

The extractions were carried out in a commercial Carousel Radleys Tech equipment able to both stirring and maintain the temperature within $\pm$ 0.5 ºC. In all experiments the stirring was kept constant at 250 rpm. After the extractions, the overall solution and extract were filtered under vacuum using a 0.45 µm cellulose membrane. After filtration, the extracted liquid solution was quantified through UV-spectroscopy, using a SHIMADZU UV-1700, Pharma-Spec Spectrometer, at a wavelength of 274 nm using a calibration curve previously established for caffeine. The effect of each ionic liquid on the quantification technique was evaluated and it was found to be of no major influence taking into account the dilutions carried out. To confirm that caffeine is the predominant methylxanthine being extracted we further employed NMR and capillary electrophoresis analysis in the aqueous extract of several samples to evaluate if any other alkaloids, at least in concentrations higher than the detection limit of the equipment, were concomitantly extracted from the guaraná seeds. The NMR spectra and capillary electrophoresis data

were acquired for pure caffeine, guaraná extract after the extraction with water, and guaraná extract after the extraction with [C_4mim]Cl at a concentration of 0.5 M. The ^{1}H NMR spectra were recorded using a Bruker Avance 300 at 300.13 MHz using deuterated dimethylsulfoxide as solvent. The capillary electrophoresis analysis was carried out using a P/ACE™ MDQ Beckman Coulter system using a 0.5 m (0.4 m to the detector) × 50 µm I.D. fused silica capillary. A 0.5 M acetic acid + 100 mM sodium dodecyl sulphate (SDS) solution was used. The separation was achieved at 20 kV (reverse polarity) by direct UV detection at 270 nm. Both techniques revealed that no other alkaloids are being extracted in measurable amounts from the guaraná seeds and support the adequacy of the UV spectroscopy as the major quantification technique.

The amount of caffeine present in the dry seeds was calculated according to the weight of pure caffeine present in the extract divided by the total weight of dry biomass used. At least three individual samples were prepared, and three samples of each aqueous phase were quantified, allowing us to determine the average extraction yield and corresponding standard deviation.

Surface Response Methodology

The factorial planning allows the simultaneous analysis of various factors and more than one answer.[29] In the 2^k factorial planning there are *k* factors that can contribute to a different response and the data are treated according to a second order polynomial equation:

$$y = \beta_o + \sum \beta_i \chi_i + \sum \beta_{ii} \chi_i^2 \sum_{i<j} \beta_{ij} \chi_i \chi_j \qquad \text{eq. 3.1.1}$$

where *y* is the response variable and β_0, β_i, β_{ii} and β_{ij} are the adjusted coefficients for the intercept, linear, quadratic and interaction terms, respectively, and χ_i and χ_i are independent variables. The 2^3 factorial planning is provided in the *Supporting Information* (Table S65). This mathematical model allows the drawing of surface response curves and through their analysis the optimal conditions can be determined.

In this work it was used a 2^3 factorial planning with the goal of optimizing the amount of extracted caffeine from guaraná seeds as well as to identify the most significant

parameters and their interactions. This planning has been defined by the central point (zero level), the factorial points (1 and -1, level one) and the axial points (level α). The axial points are encoded at a distance α from the central point:[24]

$$\alpha = \left(2^k\right)^{1/4} \qquad \text{eq. 3.1.2}$$

The obtained results were statistically analysed with a confidence level of 95%. The Student's t-test was used to check the statistical significance of the adjusted data.[30] The adequacy of the model was determined by evaluating the lack of fit, the regression coefficient (R^2) and the F-value obtained from the analysis of variance (ANOVA) that was generated.[30] Three-dimensional surface response plots were generated by varying two variables within the experimental range and holding the other factors constant at the central point.

In each factorial planning the central point was experimentally addressed at least in triplicate. Additional 12-20 experiments *per* factorial planning were conducted, for which several operational conditions were repeated to guarantee the accuracy of the data. The number of isolated experiments was limited by the operational conditions capability.

The Statsoft Statistica 8.0© software was used for all the statistical analysis, and Matlab R2010a, The MathWorks, was used for representing the response surfaces and contour plots.

SEM, FTIR and TGA

The SEM pictures, used to evaluate the morphology of the guaraná particles after extraction, were acquired using a Hitachi SU–70 microscope (after carbon evaporation) with a 15 kV acceleration voltage. The FTIR spectra, with a resolution of 4 cm^{-1}, were obtained using a Perkin Elmer BX spectrometer operating in the attenuated total reflection (ATR) mode (equipped with a single horizontal Golden Gate ATR cell). TGA assays were performed with a SETSYS Evolution 1750 analyser, from Setaram Instrumentation. Samples were heated at a constant rate of 10 ºC·min^{-1} from 20 to 540 ºC under a nitrogen flow of 200 cm^3·min^{-1}.

Results and Discussion

Initial Screening: Concentration and Structural Features of Ionic Liquids and Guaraná' Particles Diameter

Apart from the unique solvent properties of ionic liquids for biomass processing, namely cellulose, chitin and wood,[31-34] the ability of ILs to swell and dissolve raw biomass can lead to an improved access to the valuable ingredients embedded in biopolymer matrices. In particular, the use of aqueous solutions of ILs can avoid the cellulosic matrix dissolution[31-34] while allowing the extraction of target compounds, *e.g.* caffeine. On the other hand, there are already experimental evidences that water can act as a co-solvent (with supercritical CO_2) to improve the selective extraction of caffeine from crude biomass.[18]

With the goal of selectively extract high yields of caffeine from guaraná seeds, several aqueous solutions of ILs (Figure 3.1.2) were therefore investigated.

As a first screening test only aqueous solutions of $[C_4mim]Cl$ were used. For comparison purposes, we also accomplished the extraction of caffeine with water and aqueous solutions of NaCl. The same operational conditions were kept in all experiments, namely a guaraná-solvent ratio of 1:10, an extraction time of 30 min at 70 ^{o}C (343 K) and with guaraná particles diameter within 0.4 - 1.0 mm. The effects of the ILs and NaCl concentration through the extraction yield of caffeine are depicted in Figure 3.1.3. To confirm that caffeine is the predominant methylxanthine being extracted and to prove the selectivity of the aqueous solutions involving ionic liquids we used UV-Vis and nuclear magnetic resonance (NMR) spectroscopies and capillary electrophoresis to analyse the aqueous extract of several samples. It is safe to admit that other methylxanthines are not being extracted from the guaraná seeds, at least in concentrations higher than the detection limit of the equipment.

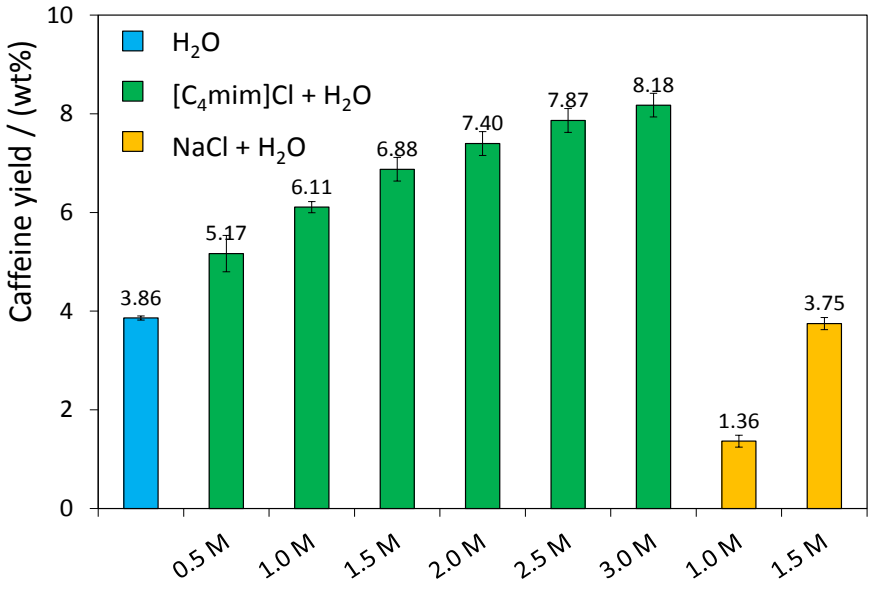

Figure 3.1.3: Yield of caffeine extracted from guaraná seeds (guaraná' particles diameter within 0.4 - 1.0 mm, T = 70 °C (343 K) , S/L ratio = 0.10 and t = 30 min).

The yield of caffeine strongly depends on the salt employed. As shown in Figure 3.1.3, the presence of IL has a huge influence in the extraction of caffeine from the bioresource with extraction yields up to 8 wt %. This value is significantly higher than those achieved with the extractions with water or the aqueous solutions of NaCl (used as model electrolyte solutions). In both salt solutions the extraction yield increases with the concentration of NaCl or [C_4mim]Cl. However, unlike what is observed with NaCl, the presence of IL always leads to increased extraction efficiencies when compared with pure water. The NaCl seems to be acting as a moderately salting-out agent reducing therefore the saturation solubility of caffeine in aqueous media.[35] In general, the combined results gathered with both NaCl and [C_4mim]Cl show that the ionic strength is a not relevant factor regarding the caffeine extraction. Aqueous solutions of [C_4mim]Cl, or other ionic liquids as shown below, prove to be suitable and enhanced extractive solvents for caffeine, and the best results are achieved with the higher concentrations of ionic liquid (2.5-3.0 M). The low viscosity of aqueous solutions of ILs, at least at the concentrations used, allows an easier penetration of the solvent into the sample matrix and a rapid mass transfer of the desired extracts into the liquid phase.

The enhanced extraction yields obtained with [C_4mim]Cl further motivated the study of other IL solutions as extractive solvents for caffeine. Based on the tailored ability of ILs,

their chemical structures were varied so that the cation core, the alkyl side chain length, the presence of functionalized groups and the anion nature effects could be evaluated. In addition, the influence of the guaraná' particles diameter was also investigated. The results obtained for the aqueous solutions of $[C_4mim]Cl$, $[C_4mim][TOS]$, $[C_4mpyrr]Cl$, $[C_2mim]Cl$, $[OHC_2mim]Cl$ and $[C_2mim][CH_3CO_2]$ at 0.5 M are depicted in Figure 3.1.4. For the systems composed of $[C_4mim]Cl$ and $[C_4mim][TOS]$ the effect of the particles diameter is also shown.

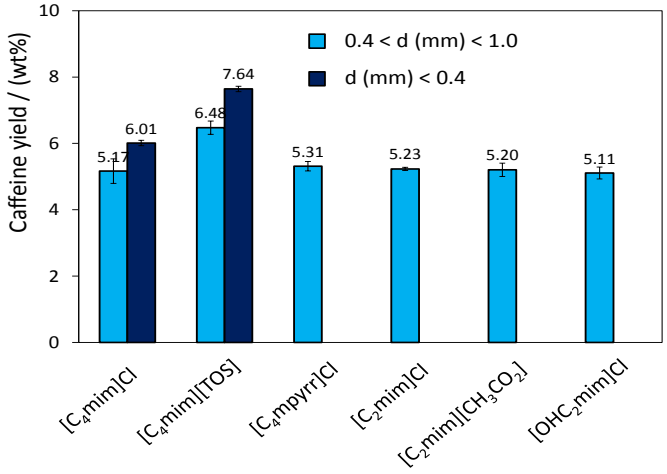

Figure 3.1.4: Yield of caffeine extracted from guaraná seeds with different ionic liquids ([IL] = 0.5 M, T = 70 °C (343 K), S/L ratio = 0.10 and t = 30 min).

For the larger guaraná' particles the obtained results reveal that the percentage of extracted caffeine is similar for the various ILs. One exception was observed with $[C_4mim][TOS]$ where an increase on the caffeine yield was observed due to its anion aromatic nature. Indeed, non-covalent π···π interactions between caffeine and various aromatic compounds in physiological media have been reported.[36-38] Nevertheless, the influence of an aromatic ring at the cation seems to be more limited since $[C_4mim]Cl$ and $[C_4mpyrr]Cl$ do not show significant differences in the extraction yields of caffeine within the associated uncertainty.

It was already demonstrated that the choice of the IL anion determines the dissolution process of crude biomass.[39] However, in this work, and besides the data obtained with $[C_4mim][TOS]$, there is no significant effect of the anion nature, when comparing the chloride- with the acetate-based IL, on the selective extraction of caffeine even though it

was already shown that [CH_3CO_2]-based ILs are better solvents for the dissolution of cellulose.[31-34] Furthermore, an increase in the cation alkyl side chain length (from [C_2mim]Cl to [C_4mim]Cl) or the inclusion of a hydroxyl group at the longest aliphatic chain ([OHC_2mim]Cl) do not lead to significant variations in the caffeine extraction yields meaning that dispersive-type interactions and hydrogen-bonding are not playing a crucial role. Therefore, the extraction mechanism must be mainly related with the enhanced solubility and the IL effect on the biomass structure as discussed below. On the other hand, as illustrated in Figure 3.1.4, the size of the guaraná particles is of more significance. Smaller particles of guaraná have a larger surface area, and thus, higher amounts of caffeine are extracted.

Optimization of the Operational Conditions: Response Surface Methodology

The univariate method for the optimization of the operational conditions does not consider the interaction among the factors and may not corresponds to the overall optimized conditions. With the goal of optimizing the operational conditions to obtain high extraction yields, *e.g.* identification of the most significant processing parameters, we used herein a response surface methodology (RSM). This type of strategy allows the exploitation of the relationship between the response (yield of caffeine) and the independent variables that can mould the extraction.

In this work, three 2^3 (3 factors and 2 levels) factorial plannings were executed. The first factorial planning was carried out with pure water and where the temperature, the solid-liquid ratio and time of extraction were optimized. The results obtained for water are presented in the *Supporting Information* (Tables S66 to S69) and Figure S9. In the second and third factorial plannings aqueous solutions of [C_4mim]Cl were employed. Although higher extraction yields were achieved with [C_4mim][TOS], [C_4mim]Cl was used in the optimization procedure because it is a cleaner (synthesis in one step), more stable and cheaper compound.

In the second factorial planning we varied the solid-liquid ratio, the extraction time and the extraction temperature. In this stage, the guaraná particles diameter was between 0.4 mm and 1.0 mm and the concentration of [C_4mim]Cl was maintained at 1.0 M. The

influence of the three variables towards the extraction yields of caffeine is illustrated in Figure 3.1.5.

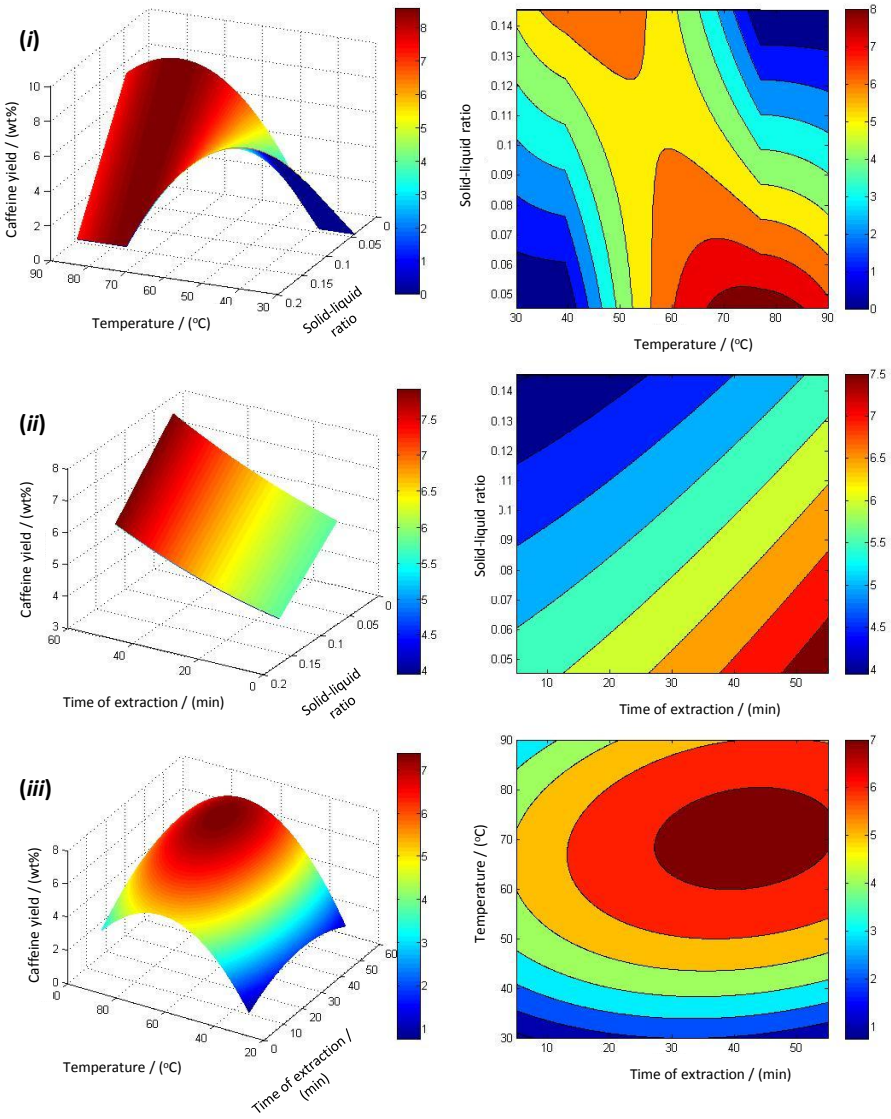

Figure 3.1.5: Response surface plots (left) and contour plots (right) on the yield of caffeine with the combined effects of (i) T and S/L ratio, (ii) t and S/L ratio and (iii) T and t using aqueous solutions of [C_4mim]Cl at 1.0 M and guaraná particles with a diameter within 0.4 - 1.0 mm.

The experimental points used in the second factorial planning, the model equation, the yield of caffeine obtained experimentally and the respective calculated values using the correlation coefficients obtained in the statistical treatment, as well as all the statistical analysis, are shown in the *Supporting Information* (Table S70 to S72). The average relative

deviation between the experimental and the predicted values is -0.16 % supporting the good description of the experimental results by the statistical model.

According to the statistical analysis shown in the *Supporting Information* (Table S71) and the data depicted in Figure 3.1.5, it is evident that temperature is the most significant parameter leading to a region of maximum yield of extraction. Higher extraction temperatures are profitable for the extraction of caffeine. Moreover, an increase in temperature contributes to a decrease in viscosity of the IL solutions and to enhance their swelling ability. The solid-liquid ratio also leads to different yields of caffeine. In general, the amount of extracted caffeine increases with the solvent volume. The time was the variable with the weakest influence in the extraction of the alkaloid. The optimized conditions occur at temperatures ranging from 65 ^{o}C and 85 ^{o}C (338-358 K) and for low solid-liquid ratios and moderate extraction times (between 30 and 50 min). In fact, extraction yields up to 8 wt % are observed with low concentrations of IL by the simple adjustment of the operational conditions.

Since in the statistical analysis of the previous 2^3 factorial planning it was found that time is not a significant variable for the caffeine extraction it was further carried out the third and last factorial planning with the time fixed at 30 min. The variables investigated in this methodology were the temperature, the solid-liquid ratio and the ionic liquid ([C_4mim]Cl) concentration. In this optimization process particles of smaller diameter (< 0.4 mm) were also used aiming at attaining the highest yields of extraction. All the statistical analysis is provided in the *Supporting Information* (Tables S73 to S76). The average relative deviation between the model results and the experimental data is -0.50 %. The response surface and contour plots are shown in Figure 3.1.6. Furthermore, based on the statistical analysis provided in *Supporting Information* (Table S75) and on the data depicted in Figure 3.1.6, it can be concluded that the most significant parameters are temperature, and the combined effects of temperature - solid-liquid ratio and ionic liquid concentration - solid-liquid ratio (*P*-value < 0.05).

Outstandingly, by the results obtained in this last factorial planning, extraction yields of caffeine up to 9 wt % were attained. This high value of caffeine was achieved within 30 min at 70 ^{o}C (343 K) (using an aqueous solution of [C_4mim]Cl at 2.34 M and a solid-liquid

ratio of 0.1. At this optimum point the predicted extraction yield of caffeine by the statistical approach is 9.49 wt % whereas the experimental value is 9.43 wt %.

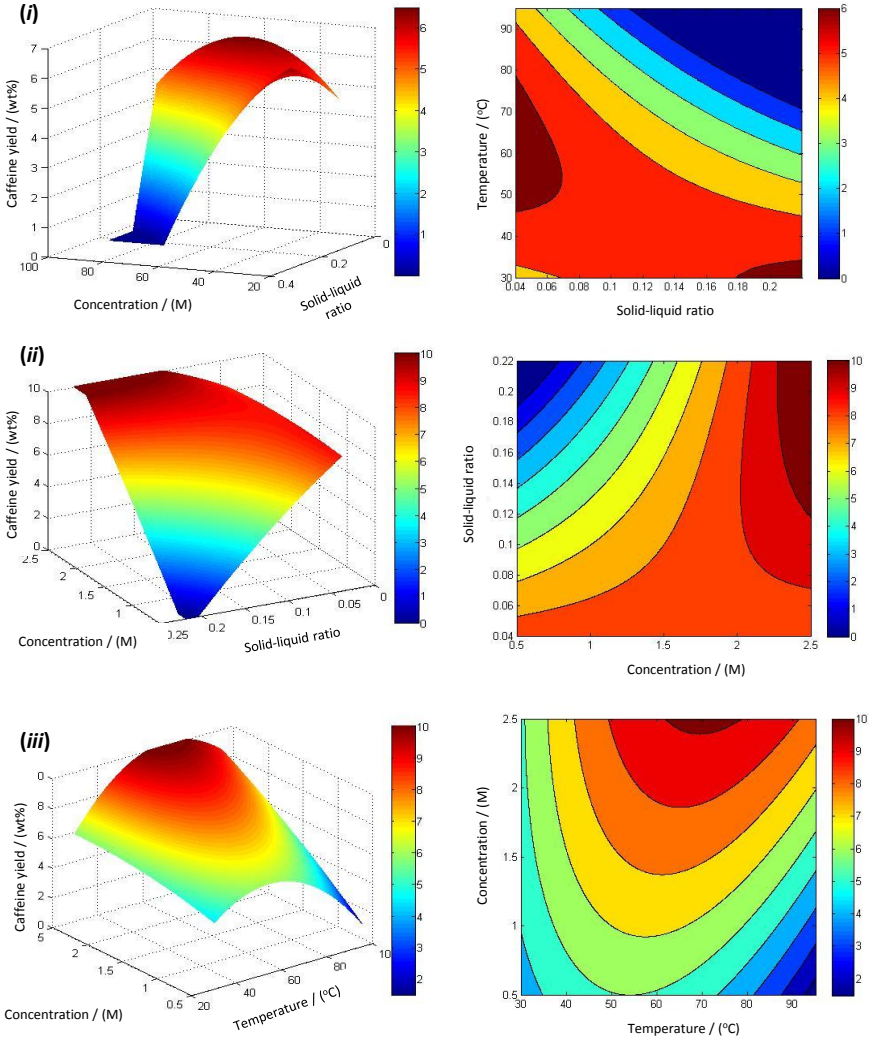

Figure 3.1.6: Response surface plots (left) and contour plots (right) on the yield of caffeine with the combined effects of (i) T and S/L ratio, (ii) [IL] and S/L ratio and (iii) T and [IL] using aqueous solutions of [C_4mim]Cl for 30 min of contact time and guaraná particles with a diameter inferior to 0.4 mm.

To support the high yields obtained, the extraction of caffeine from the same biomass sample using dicloromethane in soxhlet extraction during 270 min was also carried out for comparison purposes. The maximum yield of caffeine achieved was 4.30 wt %. Despite the use of a hazardous organic solvent and for an extended time, the extraction of caffeine by this conventional approach is significantly less efficient when compared with the enhanced results achieved with the IL aqueous solutions.

Recyclability and Reusability of the Solvent

Once the optimum conditions were identified, the isolation of caffeine from the aqueous media and the recyclability and reusability of the solvent were then investigated.

The first task consisted on the exploration of the reusability of the aqueous solutions without performing any pre-extraction of caffeine from the IL-based medium. Thus, the aqueous solution of $[C_4mim]Cl$ at 2.34 M was used for three successive extractions at the optimized operational conditions (solid-liquid ratio of 0.1 for 30 min and at 343 K (70 ^{o}C)). After each extraction the solid-liquid mixture was filtered and the aqueous solution was reused with a new sample of guaraná particles. Remarkably, in all samples, *circa* 9 wt % of caffeine was extracted with the overall solution reaching a caffeine concentration three times higher. The aqueous solution of IL can thus be reused at least three times without reaching saturation.

After settling the reusability of the IL aqueous solutions the next step was to confirm their recyclability. To this end, the first step consisted on the choice of a suitable solvent capable of re-extracting caffeine from the ionic liquid medium. At this stage, several organic solvents non-miscible with water were tested. The extraction was performed by placing the several organic solvents in contact with an aqueous solution containing caffeine at 22 $g \cdot L^{-1}$ (concentration similar to that found in the real experiments) and in a volume ratio of 1:3. This procedure was repeated for three times. The amount of caffeine in the aqueous solution after the re-extraction procedure is depicted in Figure 3.1.7. The results shown in Figure 3.1.7 represent an evaluation of the ability of several organic solvents to re-extract caffeine from aqueous solutions. The best extraction solvents are chloroform and dichloromethane. Indeed, chloroform shows to be capable of completely extract caffeine from the aqueous solution. These solvents are in fact the fluids of choice to extract caffeine from bioresources as presented earlier.[18-20] Nevertheless, we also found that butanol can be a good candidate to extract caffeine and can replace the more toxic and hazardous ethyl acetate currently used.[18-20]

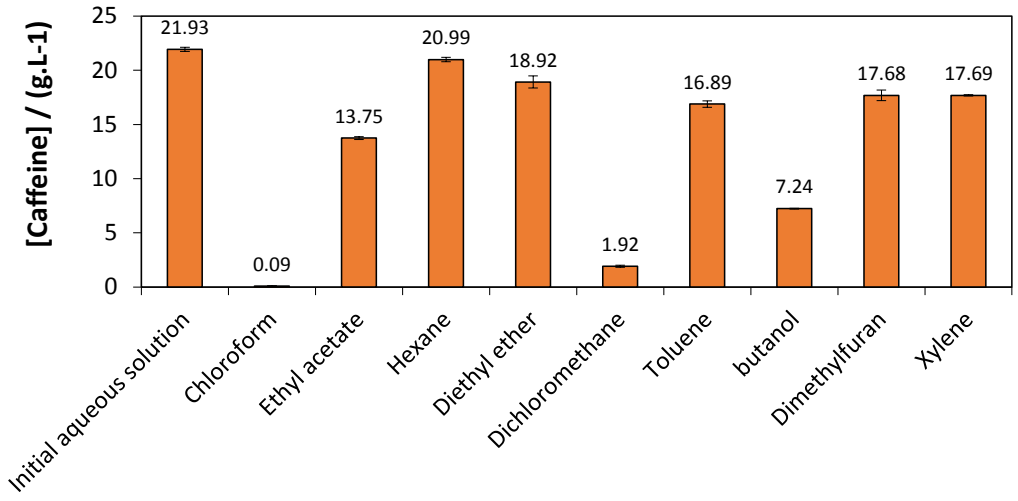

Figure 3.1.7: Concentration of caffeine in the aqueous solution after the liquid-liquid extraction by different organic solvents non-miscible with water.

After the selection of the best extractive solvents, chloroform and butanol were used to extract caffeine from the real samples containing caffeine extracted at the optimum operational conditions (aqueous solution of caffeine obtained from the guaraná seeds after 30 min at 70 ^{o}C (343 K) and using an aqueous solution of [C_4mim]Cl at 2.34 M and a solid-liquid ratio of 0.1). Even though chloroform is an organic, volatile and toxic solvent it should be emphasized that it was here used only with the intent of proving the recyclability of the IL aqueous solutions to extract caffeine from new guaraná seeds. More benign approaches, such as the use of supercritical CO_2 or butanol, are recommended at this stage.

Both the highly concentrated caffeine aqueous solution (after three extractions with new guaraná seeds) and a sample where a single extraction was performed were investigated. The aqueous solutions were placed in equilibrium with chloroform or butanol for three times, as previously described, and reused for a new extraction at the optimized conditions. This process was repeated for twice more and the aqueous solutions of [C_4mim]Cl always shown to be capable of extracting the maximum 9 wt % of caffeine.

Due to the low-volatility of alkaloids, their separation from the feedstock has to be accomplished essentially by solid-liquid extraction methodologies. Although some progress in the use of ILs as extractive media for added-value compounds from bioresources has been reported, these investigations are mostly restricted to the

identification and quantification of the bioactive structures.[40] A scalable isolation process for the target compounds from the IL solution as well as the recovery strategy of both the solute and solvent are still critical for the scale-up implementation. Figure 3.1.8 depicts the optimized strategy for the extraction of caffeine from guaraná seeds highlighting the recyclability and reusability of the ionic liquid aqueous solutions. Moreover, after the extraction of this biocompound, that has shown to be successful by IL aqueous solutions, and since the dry biomass consists mainly of carbohydrates, the processed guaraná can further proceed for biomass conversions approaches within an integrated biorefinery concept.

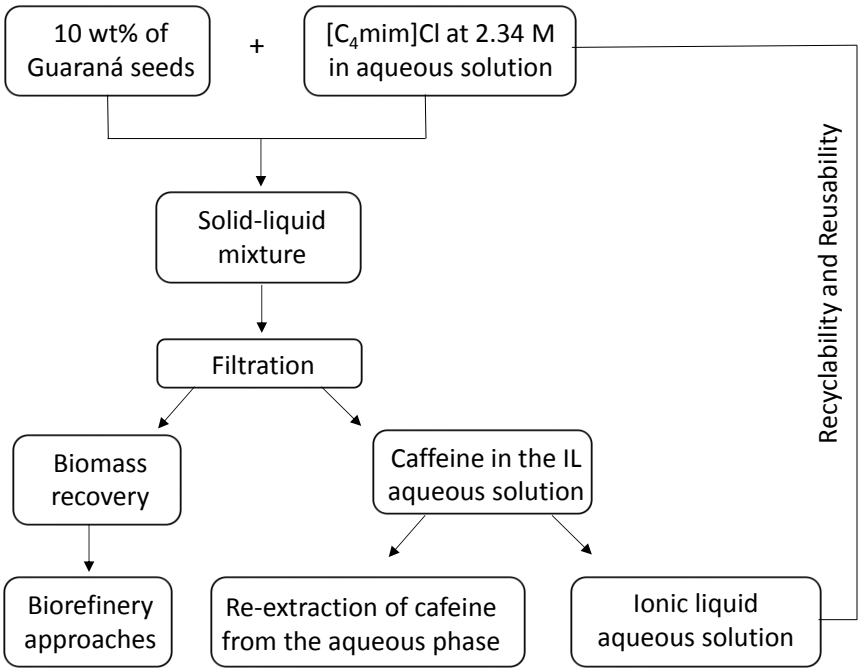

Figure 3.1.8: Flowchart for the extraction of caffeine from guaraná seeds.

Feedstock Analysis to Infer on the Mechanisms of Extraction

The gathered results show that temperature is the main factor affecting the extraction of caffeine, followed by the combined effects of temperature - solid-liquid ratio and IL concentration - solid-liquid ratio. With the goal of inferring on the reasons behind the enhanced extraction of caffeine by IL solutions we further applied scanning electron microscopy (SEM) to the guaraná samples after the extraction procedure. The SEM

images of guaraná after the treatment with water and an aqueous solution of $[C_4mim]Cl$, at the optimal conditions described before, are shown in Figure 3.1.9.

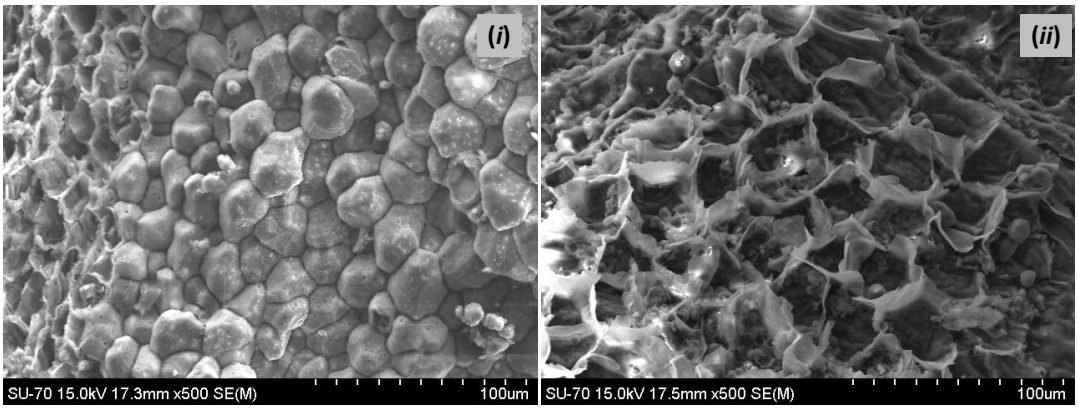

Figure 3.1.9: SEM images of the guaraná samples after extraction with (i) water and (ii) an aqueous solution of $[C_4mim]Cl$.

The sample structure that was in contact with pure water is less affected than the one treated with the IL aqueous solution. Albeit broken cells are seen in both samples, there is an increase in the ratio of broken cells to intact cells in the presence of the IL medium. This change in structure favours the extraction of caffeine to the aqueous phase. Hence, the extraction yield of the alkaloid is greatly improved in the presence of ILs since, besides enhancing the solubility of the alkaloid in aqueous medium, they further permit a better access to the valuable ingredients embedded in the biopolymer matrix.

As Fourier Transform Infrared spectroscopy (FTIR) can provides useful information for identifying the presence of certain functional groups or chemical bonds it was additionally applied to investigate the changes in the chemical structure of guaraná seeds. Figure 3.1.10 shows the results obtained for the original feedstock and after extraction with water and aqueous solutions of three different ILs. Moreover, the FTIR spectrum of a caffeine standard is also included for comparison purposes. The infrared spectrum of caffeine displays two characteristic bands corresponding to the carbonyl (C=O) vibration frequency at *circa* 1655 and 1700 cm^{-1}.[41] Interestingly, the high relative strength band at 1655 cm^{-1}, indicative of caffeine, is seen in the spectrum of the guaraná sample before extraction; yet, it is not visible in the spectra of the guaraná seeds after the extraction procedures and that can be associated to the dissolution of caffeine by the aqueous

media. In addition, the FTIR spectra show that the signal positions and intensity of the major absorption bands related with the polymeric matrix of guaraná do not significantly change after the extraction procedure. These results indicate that the chemical structures of the carbohydrates, and thus of the cellulose-polymeric matrix (intense characteristic bands in the fingerprint region from 900-1400 cm^{-1} of the mid-infrared spectral range), do not significantly change after the treatment with aqueous solutions. The bands in the region 900–1153 cm^{-1} are assigned to C–O and C–C stretching modes, while those in the 1400–1199 cm^{-1} region are due to O–C–H, C–C–H and C–O–H bending vibrational modes of the carbohydrates. These results disclose that the carbohydrate fraction is not significantly dissolved by the water-ionic-liquid mixtures.

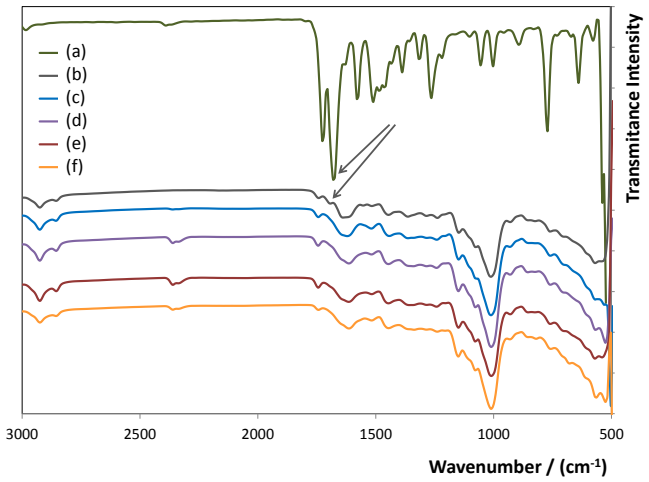

Figure 3.1.10: FTIR spectra of caffeine (a), guaraná sample before extraction (b), and guaraná samples after extraction with water (c), and aqueous solutions of [C_4mim]Cl (d), [C_2mim]Cl (e) and [C4mim][TOS] (f).

Thermogravimetric assays (TGA) were also used to assess on the structural integrity of the biomass sample and to support the non-dissolution of significant amounts of carbohydrates or polysaccharides from the guaraná seeds by the ILs aqueous solutions. The TGA results are depicted in Figure 3.1.11.

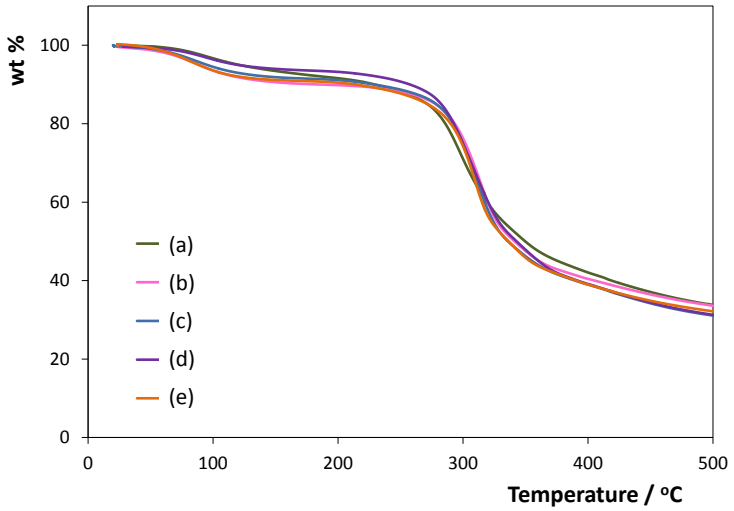

Figure 3.1.11: TGA of a guaraná sample before extraction (a), and of guaraná samples after extraction with water (b), and aqueous solutions of $[C_4mim]Cl$ (c), $[C_2mim]Cl$ (d) and $[C_4mim][TOS]$(e).

The thermal stabilities and the onset degradation temperatures of the guaraná samples after the extraction procedure are identical to the original sample. Likewise, no major differences are observed with the diverse samples exposed to different aqueous solutions. These results further confirm that the predominant polymeric matrix is not affected or significantly dissolved by the aqueous solutions of ionic liquids.

In summary, although ionic liquids were previously shown to be good candidates for the dissolution of biomass[31-34], the presence of water prevents the dissolution of the biopolymers while allowing the selective extraction of caffeine.

Conclusions

This work shows that aqueous solutions of ILs are enhanced solvents for the extraction of caffeine from bioresources, *e.g.* guaraná seeds. Compared with traditional extraction methods this new strategy proves to be selective towards caffeine and capable of providing extraction yields up to 9 wt %.

The recovery and reusability of the ILs were successfully demonstrated supporting the economic viability and weak environmental footprint of the proposed methodology. The time and temperature of extraction were greatly reduced compared to conventional methods. These advantages coupled to the high extraction yields make the proposed technique promising for large-scale applications. In this context, the use of aqueous solutions of ILs for the extraction of value-added ingredients from other biomass sources is straightforward envisaged.

References

1. D.V. de Freitas, C.R. Carvalho, F. Filho and S. Astolfi-Filho, J. Plant Res., 2007, 120, 399-404.
2. D.K. Bempong and P.J. Houghton, J. Pharm. Pharmacol., 1992, 44, 769-771
3. C.B. Mehr, R.N. Biswal, J.L. Collins and H.D. Cochran, J. Supercrit. Fluids, 1996, 9, 185-191.
4. C.S. Weckerle, M.A. Stutz and T.W. Baummann, Phitochemistry, 2003, 64, 735-742.
5. E. Cassel, R.M.F. Vargas, G.W. Brun, D.E. Almeida, L. Cogoi, G. Ferraro and R. Filip, J. Food Eng., 2010, 100, 656-661.
6. M.D.A. Saldana, C. Zetzl, R.S. Mohamed and G.Brunner, J. Supercrit. Fluids, 2002, 22, 119-127.
7. M.L. Avery, S.J. Werner, J.L. Cummings, J.S. Humphrey, M.P. Milleson, J.C. Carlson, T.M. Primus and M.J. Goodall, Crop Prot., 2005, 24, 651-657.
8. S.J. Werner, J.L. Cummings, S.K. Tupper, J.C. Hurley, R.S. Stahl and T.M. Primus, J. Wildl. Manage., 2007, 71, 1676-1681.
9. R.G. Hollingsworth, J.W. Armstrong and E. Campbell, Nature, 2002, 417, 915-916.
10. A.T. Laranja, A.J. Manzato and H. Bicudo, Rev. Saúde Pública, 2006, 40, 1112-1117.
11. L. Zhang, D.M. Kujawinski, E. Federherr, T.C. Schmidt and M.A. Jochmann, Anal. Chem., 2012, 84, 2805-2810.
12. C.B. Mehr, R.N. Biswal and J.D. Collins, J. Supercrit. Fluids, 1996, 9, 185-191.
13. H. Içen and M. Gürü, J. Supercrit. Fluids, 2009, 50, 225-228.
14. H. Içen and M. Gürü, J. Supercrit. Fluids, 2010, 55, 156-160.
15. M.D.A. Saldaña, C. Zetzl, R.S. Mohamed and G. Brunner, J. Agric. Food Chem., 2002, 50, 4820-4826.
16. W.J. Kim, J.D. Kim, J. Kim, S.G. Oh and Y.W. Lee, J. Food Eng., 2008, 89, 303-309.
17. H.L. Liang, Y.R. Liang, J.J. Dong, J.L. Lu, H.R. Xu and H.Wang, Food Chem., 2007, 101, 1468-1473.
18. G.J. Hulbert, R.N. Biswal, C.B. Mehr, T.H. Walker and J.L. Collins, Food Sci. Technol. Int., 1998, 4, 53-58.
19. T. Onami and H. Kanazawa, J. Chem. Educ., 1996, 73, 556-557.
20. H. Wang and K. Helliwell, Food Chem., 2000, 70, 337-344.
21. L. Majhenič, M. Škerget and Ž. Knez, Food Chem., 2007, 104, 1258-1268.
22. M.D. Joshi and J.L. Anderson, RSC Adv., 2012, 2, 5470-5484.
23. D. Han and K.H. Row, Molecules, 2010, 15, 2405-2426.
24. M.G. Freire, A.F.M. Cláudio, J.M.M. Araújo, J.A.P. Coutinho, I.M. Marrucho, J.N. Canongia Lopes and L.P.N. Rebelo, Chem. Soc. Rev., 2012, 41, 4966-4995.
25. M.G. Freire, C.M.S.S. Neves, I.M. Marrucho, J.N. Canongia Lopes, L.P.N. Rebelo and J.A.P. Coutinho, Green Chem., 2010, 12, 1715-1718.
26. M.G. Freire, A.R.R. Teles, J.N. Canongia Lopes, L.P.N. Rebelo, I.M. Marrucho and J.A.P. Coutinho, Sep. Sci. Technol., 2012, 47, 284-291.
27. M. Domínguez-Pérez, L.I.N. Tomé, M.G. Freire, I.M. Marrucho, O. Cabeza and J.A.P. Coutinho, Sep. Purif. Technol., 2010, 72, 85-91.
28. M.G. Freire, C.L.S. Louros, L.P.N. Rebelo and J.A.P. Coutinho, Green Chem., 2011, 13, 1536-1545.
29. M.I.I. Rodrigues and A. Francisco, Planejamento de Experimentos e Optimização de Processos, C.D.P. Editora, Campinas, Brazil, 2005.
30. J.N. Miller and J.C. Miller, Statistics and Chemometrics for Analytical Chemistry, 5th Ed., Pearson Prentice Hall, Harlow, England,2005.
31. H. Wang, G. Gurau and R. D. Rogers, Chem. Soc. Rev., 2012, 41, 1519-1537.
32. S.S. Tan and D.R. MacFarlane, Top Curr. Chem., 2010, 290, 311-339.
33. M.E. Zakrzewska, E. Bogel-Łukasik and R.Bogel-Łukasik, Energy Fuels, 2010, 24, 737-745.

34. M.G. Freire, A.R.R. Teles, R.A.S. Ferreira, L.D. Carlos, J.A. Lopes-da-Silva and J.A.P. Coutinho, Green Chem., 2011, 13, 3173-3180.
35. A. Al-Maaieh and D. R. Flanagan, J. Pharm. Sci., 2002, 91, 1000-1008.
36. J. Florian, J. Sÿponer and A. Warshel, J. Phys. Chem. B, 1999, 103, 884-892.
37. K. Ulanowska, J. Piosik, G. Gwizdek-Wisniewska and G. Wegrzyn, Bioorg. Chem., 2005, 33, 402-413.
38. G. Gattuso, G. Manfredi and S. Sammartano, Fluid Phase Equilibr., 2011, 308, 47-54.
39. A. Stark, Energy Environ. Sci., 2011, 4, 19-32.
40. B. Tang, W. Bi, M. Tian and K.H. Row, J. Chromatogr. B, 2012, 904, 1-21.
41. B.R. Singh, M.A. Wechter, Y. Hu and C. Lafontaine, Biochem. Educ., 1998, 26, 243-247.

3.2. Extraction of Caffeine from Spent Coffee using Aqueous Solutions of Ionic Liquids

This chapter is based on an ogoing work still with the following authors involved: Ana M. Ferreira, Hugo Gomes, João A. P. Coutinho and Mara G. Freire.

Abstract

Spent coffee grounds (SCG) are a major residue from the production of drinkable coffee. They have no commercial value and are discarded as a solid waste. However, SCG are rich in organic matter, as well as in other compounds, such as caffeine, tannins and polyphenols. In this study, the extraction of caffeine from SCG was performed using aqueous solutions of protic ILs (ethanolammonium-based cations combined with anions derived from carboxylic acids) and one aprotic IL, $[C_4mim][CH_3CO_2]$, for comparison purposes. The major goal of this work consists on the replacement of the imizadolium-based ILs commonly used for extraction approaches. The synthesized PILs are less expensive and more benign, biocompatible and biodegradable when compared to imidazolium-based counterparts. In general, all ILs solutions perform better than pure water. In addition, the extraction improves with the increase of hydroxyl groups at the cation of the IL, and where the results obtained confirm the higher performance of protic ILs to extract caffeine (up to 3.57 wt %) when compared with imidazolium-based fluids.

Introduction

Coffee is one of the world's most widely consumed beverages and is a major commodity in the world economy (just after petroleum).[1] In Portugal, where coffee consumption is so deeply rooted in the cultural habits, the total imports of coffee in 2006 was over 40 thousand tons.[2,3]

Spent coffee grounds (SCG), the solid residues obtained from the treatment of coffee powder with hot water to prepare coffee, are the main coffee industry residues with a worldwide annual generation of 6 million tons.[2,3] Most SCG remain unused, are discharged to the environment or burned.[4,5] Since SCG are actually considered a waste, these can be explored as a rich source of high-value components before their discharge. In spite of their large availability and high content in compounds of industrial interest, such as carbohydrates, proteins, caffeine and phenolic compounds,[6] SCG are not used as raw material for other processes. In a recent study[7], extracts from SCG exhibited anti-

tumor and anti-allergic activities, which were related to the presence of phenolic compounds in their composition, such as chlorogenic acid (most abundant PhC in SCG).

After the optimization carried out with guaraná seeds (*Chapter 3.1*), we explore here the extraction of caffeine from spent coffee with the goal of valorizing this residue, since the amount of caffeine on these wastes ranges from 3.59 to 8.09 mg/g of SCG.[8] Indeed, SCG is a residue with almost no commercial value with still a significate amount of caffeine. In order to valorize this residue, aqueous solutions of three PILs and one imidazolium-based IL were used as extractive solvents for caffeine.

The synthesis of PILs occurs *via* proton exchange in stoichiometric conditions through the reaction of a primary amine and a Brønsted acid. These reagents (acid and base) have a low cost and the synthesis of PILs is very simple, and thus the production of PILs for further applications is much simpler and economical when compared with their aprotic IL analogues.

Experimental Procedure

Materials

The spent coffee grounds were supplied by the *Cafeteria* of the Chemistry Department of University of Aveiro, in Portugal. The samples were dried until constant weight (≈ for 6 days at 373 K). SCG contained a humidity content of (59.52 ± 2.53) %. After this step, the SCG with particles diameter (d) < 0.4 mm were isolated. The solvents used for the solid-liquid extraction of caffeine from SCG were water and aqueous solutions of 4 ionic liquids. Moreover, extraction of caffeine using soxhlet extraction was also carried out using ethanol, dichloromethane and petroleum ether. Petroleum ether, dichloromethane, ethanol were purchased from sigma-Aldrich, BDH Prolabo and Carlo Erba, respectively, with 99.9 % of purity. Double distilled water, passed through a reverse osmosis system, and further treated with a Milli-Q plus 185 water purification equipment, was used in all experiments. The IL $[C_4mim][CH_3CO_2]$ was purchased from Iolitec, whereas the three PILs were synthetized by us. Their purities were confirmed by ^{1}H and ^{13}C NMR spectra. The chemical structures of the studied ILs are depicted in Figure 3.2.1. All ionic liquid samples

were dried for at least 48 h, under vacuum and at a room temperature (≈ 298 K), before use. The reagent used in Karl-Fischer titration was Hydranal-Coulomat AG from Riedel-de Haën.

The PILs used in this work were synthetized by us using amines and acetic acid to obtain ethanolammonium-based cations combined with the acetate anion. Ethanolamine (99%), diethanolamine (99%), triethanolamine (99%) and acetic acid (99.99%) were purchased from Sigma-Aldrich and used as received.

The high purity caffeine, used as a standard in the calibration curves, was obtained from Marsing & Co. Ltd. with a nominal purity ≥ 98.5 wt %.

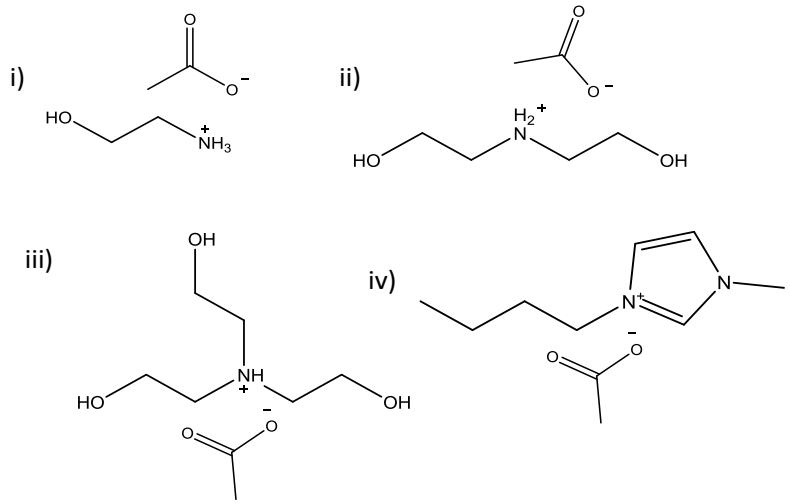

Figure 3.2.1: Chemical structures of the ionic liquids used in the extraction of caffeine from SCG: (i) [EA][CH_3CO_2]; (ii) [DEA][CH_3CO_2]; (iii) [TEA][CH_3CO_2]; (iv) [C_4mim][CH_3CO_2]

Synthesis of Protic ILs

Two hundreds mmol of amine was placed in a 100 mL glass vial and was cooled using an ice bath under vigorously stirring. Into this cold solution, two hundreds mmol of acetic acid were added drop-wise while maintaining the temperature at 0 °C since this reaction is exothermic. The mixture was then allowed to reach room temperature and kept under constant stirring for 12h. To reduce the volatile impurities to negligible values, all synthetized PILs were dried under constant agitation at vacuum and room temperature (298 K) for 48 h.

Characterization of PILs

The synthetized PILs were characterized using several techniques, namely, ^{1}H and ^{13}C NMR, density, viscosity, refractive index and melting temperature. The water content of each ionic liquid, after the drying step and immediately before the measurements of the thermophysical properties was determined by Karl Fischer titration using a Metrohm 831 Karl Fischer coulometer (< 1000 ppm).

The density and viscosity of the pure PILs were measured using an automated SVM 3000 Anton Paar rotational Stabinger viscometer-densimeter in the temperature range from (318.15 to 368.15) K, with a temperature uncertainty of ± 0.02 K. The dynamic viscosity has a relative uncertainty within 0.35 %, while the absolute uncertainty in density is ± 5 × 10^{-4} g·cm^{-3}.

Measurements of refractive index ($\boldsymbol{n_D}$) were performed at 589.3 nm using an automated Abbemat 500 Anton Paar refractometer, developed for measuring both liquid and solid samples. The Abbemat Anton Paar refractometer uses reflected light to measure the refractive index, where the sample on the top the measuring prism is irradiated from different angles by a LED. Refractive index measurements were carried out in the temperature range (288.15 to 353.15) K for pure PILs at atmospheric pressure. The maximum deviation in temperature is ± 0.01 K and the maximum uncertainly in the refractive index is ± 0.00002.

The melting temperatures of PILs were determined using a BX51 Olympus polarized optical microscope (Olympus Co., Tokyo, Japan) equipped with a LTS120 Linkam temperature-controlled stage (Linkam Scientific Instruments, Ltd., Tadworth, U.K.) that in this study operated between 248.15 and 353.15 K. The PILs samples (2mg, approximately) were placed under argon, in concave slides with coverslips sealed with thermal joint silicone, cooled to 248.15 K, and allowed to stay at this temperature for 30 min. After this step, the samples were subjected to a 0.1 K·min^{-1} heating run. The uncertainty of the temperature obtained from POM measurements was taken as not higher than 1.0 K.

Caffeine Extraction

In order to extract caffeine from SCG, mixtures of specific amounts of SCG and aqueous solutions were prepared by weight and in specific sealed glass vials as described in **Chapter 3.1**-*Extraction of caffeine.* All equipment and conditions were those the same as described in *Chapter 3.1*.

The amount of caffeine present in the SCG was calculated according to the weight of pure caffeine present in the extract divided by the total weight of dry biomass used.

Moreover, Soxhlet extractions with organic solvents were also conducted during 7 hours (420 min). For UV analysis it was necessary a calibration curve to quantify the amount of caffeine (λ=274 nm) obtained in different extractions with the solvent used.

Surface Response Methodology

The factorial planning allows the simultaneous analysis of various factors.[9] In this work a 2^3 factorial planning was also used and as presented in **Chapter 3.1** to identify the most significant parameters and their interactions. This planning has been defined by the central point (zero level), the factorial points (1 and -1, level one) and the axial points (level α), reported in the *Supporting Information* (Table S77).

Results and Discussion

Density, Viscosity, Melting Temperatures and Refraction Index Measurements

In this work, three PILs were synthesized aiming to replace the commonly used imidazolium-based ILs for the extraction of value-added compounds from biomass. They were characterized according to their NMR spectra, density, viscosity, refraction index and melting temperatures. The density, viscosity, and refractive index of the synthesized PILs are given in Figures 3.2.2 to 3.2.4. Detailed data are provided in the *Supporting Information* (Table S78).

For all ILs, the density decreases with an increase in temperature. In addition, the density of the [DEA]-based IL is similar to that displayed by the [TEA]-based compound at the same conditions. However, there is a significant decrease of density when the ammonium cation presents only one hydroxyl group, namely with the [EA]-based IL. In the literature[10,11] some properties for acetate-based ILs have already been reported. Comparing the experimental data obtained in this work (Figure 3.2.2) and those reported in the literature for a given temperature, for instance at 298.15 K, the density decreases in the following order: $[TEA][CH_3CO_2] \approx [DEA][CH_3CO_2] > [EA][CH_3CO_2] > [C_2mim][CH_3CO_2] > [C_4mim][CH_3CO_2] > [C_2im][CH_3CO_2] > [C_4mpyr][CH_3CO_2] > [N_{0112}][CH_3CO_2]$.

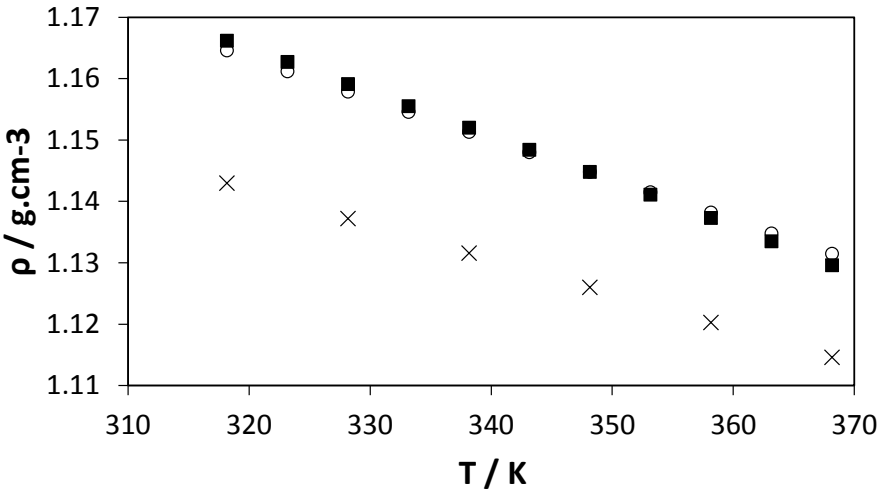

Figure 3.2.2: Density data for the studied ILs : ×, $[EA][CH_3CO_2]$; ○, $[DEA][CH_3CO_2]$; ■, $[TEA][CH_3CO_2]$.

From the obtained results, it seems that the ammonium-based ILs with hydroxyl groups are more dense than the non-hydroxylated ones. In addition, the increase in the number of hydroxyl groups attached to the ammonium cation increases the density of the IL.

The refractive index specifies the dielectric response to an electrical field induced by electromagnetic waves (light) and is thus an optical property of materials. The experimental refractive index data of the measured ILs are depicted in Figure 3.2.3. The refractive index was measured upward and downward on temperature, with no hysteresis effects observed, and within the temperature range from 283.15 to 353.15 K. For all ILs, the refractive index decreases with the temperature increase. The refractive

index values for the $[CH_3CO_2]$-based ILs, making use of already published data,[10] decrease in the following sequence: $[C_2mim][CH_3CO_2]$ > $[C_4mim][CH_3CO_2]$ > $[TEA][CH_3CO_2]$ > $[DEA][CH_3CO_2]$ >$[EA][CH_3CO_2]$ > $[C_4mpyr]$ $[CH_3CO_2]$ > $[N_{0112}]$ $[CH_3CO_2]$ > $[C_2im][CH_3CO_2]$. Densities and refractive indices for $[EA][CH_3CO_2]$ and $[DEA][CH_3CO_2]$ were also found in literature[11] and a close agreement with our data was found.

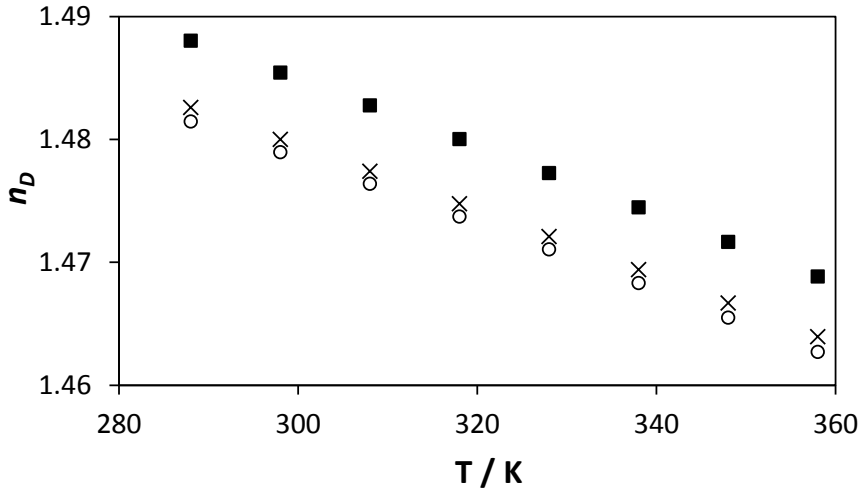

Figure 3.2.3: Refractive index data for the studied ILs : ○, $[DEA][CH_3CO_2]$ ×, $[EA][CH_3CO_2]$, ■, $[TEA][CH_3CO_2]$.

Viscosity is the internal resistance of a fluid to a shear stress, and in general, ILs present higher viscosities than conventional molecular solvents. Viscosity is an important property of ILs as it influences ionic conductivity and mass transport phenomena. The viscosity of the IL also influences the mass transfer during extractions.

The experimental viscosity data for the investigated ILs are depicted in Figure 3.2.4. At all the studied temperatures, the viscosity of $[EA][CH_3CO_2]$ is similar to that displayed by $[DEA][CH_3CO_2]$. However, contrarly to that observed with density, the addition of one more hydroxyl group (from $[DEA]^+$ to $[TEA]^+$) leads to a decrease in the viscosity. Comparing the experimental data obtained in this work and those reported in the literature[10] for a given temperature, for instance at 298.15 K, viscosity decreases in the following sequence: $[EA][CH_3CO_2]$ ≈ $[DEA][CH_3CO_2]$ > $[TEA][CH_3CO_2]$ > $[C_4mim][CH_3CO_2]$ > $[C_2mim][CH_3CO_2]$ > $[C_4mpyr][CH_3CO_2]$ > $[N_{0112}][CH_3CO_2]$ > $[C_2im][CH_3CO_2]$.

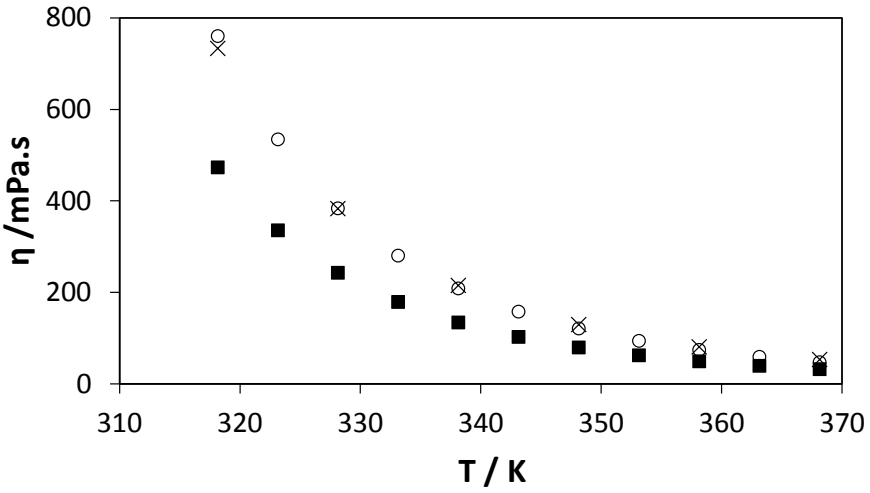

Figure 3.2.4: Viscosity data for the studied ILs : ×, [EA][CH_3CO_2]; ○, [DEA][CH_3CO_2]; ■, [TEA][CH_3CO_2].

Finally, the melting point of each PIL was determined using a Light-Polarized Optical Microscopy (POM), and as previously validated by us.[12] Since [DEA][CH_3CO_2] always remained liquid at the temperature range investigated it was only possible to determine the melting temperatures of the two other PILs. The melting point of [EA][CH_3CO_2] is 334 ± 1 K (61 ± 1 ^oC) and of [TEA][CH_3CO_2] it is 349 ± 1 K (76 ± 1 ^oC).

Optimization of the Operational Conditions using Water as the Main Solvent: Response Surface Methodology

With the goal of optimizing the operational conditions to obtain high extraction yields, we used herein a response surface methodology (RSM). This type of strategy allows the exploitation of the relationship between the response (yield of caffeine) and the independent variables that can influence the extraction. In this work, a 2^3 factorial planning was carried out with pure water and the temperature, the solid-liquid ratio and time of extraction were optimized. The central point used in the planning was 343 K (70°C), a solid-liquid ratio of 1:10 and a time of 30 min (since these conditions were the optimal ones found in the extraction of caffeine from guaraná (**Chapter 3.1**)). The results obtained for are presented in the *Supporting Information* (Table S79 to S80).

According to the statistical analysis and the data depicted in Figure 3.2.5, it is evident that the extraction efficiency improves with an increase in temperature, with a decrease in the

solid-liquid ratio and with longer times of extraction. From the optimization approach, and using water as the main solvent, it can be concluded that the optimum conditions required for an effective extraction of caffeine are: temperature at 358 K (85°C), 45 min of extraction and a $R_{S/L}$ of 1:10. Under these optimium operational conditions, the extraction yield of caffeine achieved the maximum value, namely 1.50 wt %.

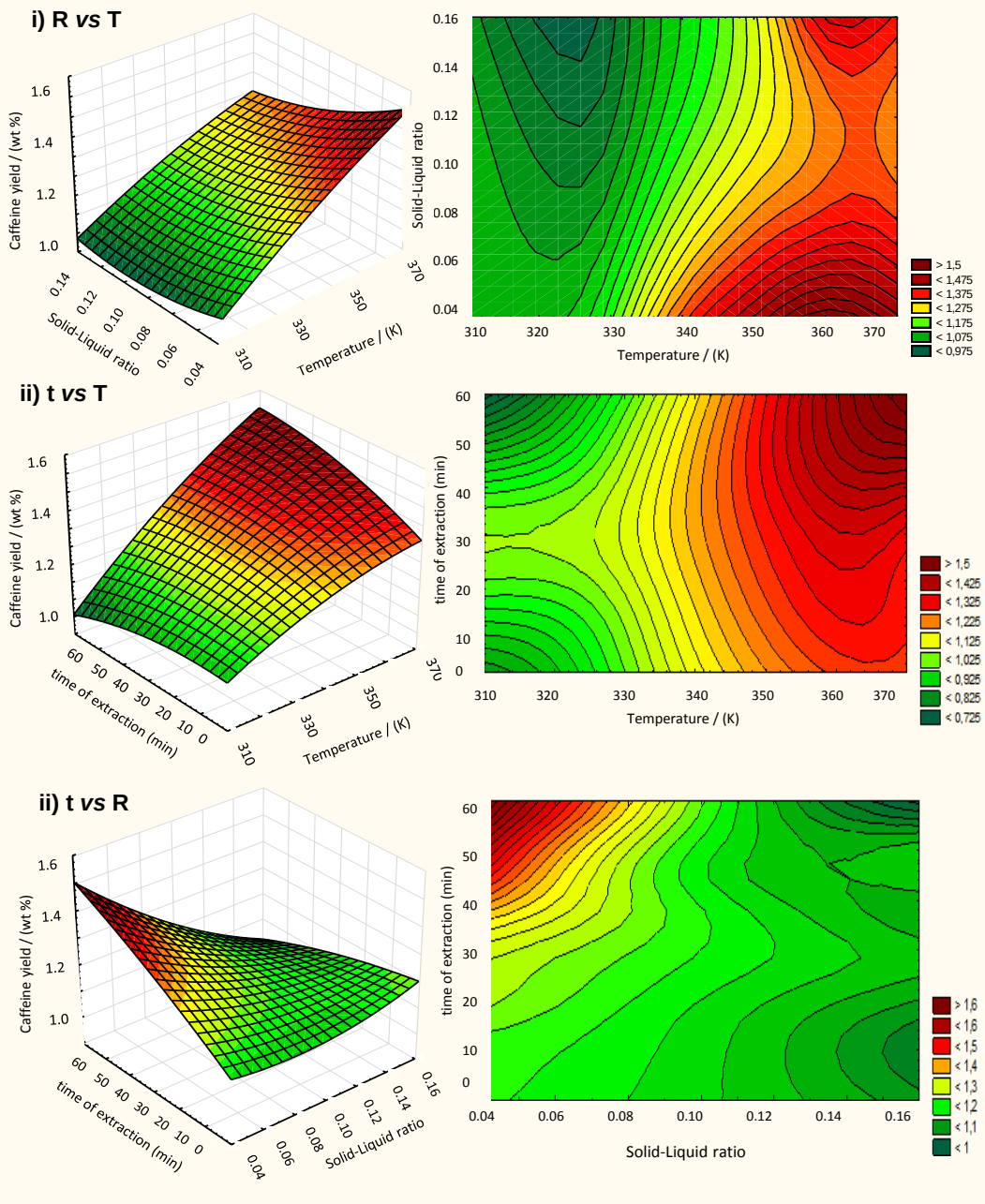

Figure 3.2.5 Response surface plots (left) and contour plots (right) on the yield of caffeine with the combined effects of (i) T and S/L ratio, (ii) t and S/L ratio and (iii) T and t using water and SCG particles with a diameter < 0.4 mm.

Effect of the Ionic Liquid Structure

We started by demonstrating the successful application of aqueous solutions of ILs in the extraction of caffeine from guaraná seeds (**Chapter 3.1***).* Our major goal is now to apply that knowledge to extract caffeine from wastes, namely SCG, while using cheaper and more biocompatible and biodegrable ILs.

The ILs synthesized and investigated in this work consist on alkylethanolammonium cations combined with anions derived from carboxylic acids (in particular the acetate anion). One imidazolium IL with the acetate anion was also studied for comparison purposes.

The results reported in Figure 3.2.5, show that high temperatures, a low solid-liquid ratio, and times higher than 40 min are the optimal conditions for the extraction. Therefore, these conditions were used to evaluate the extraction performance of caffeine from SCG using aqueous solutions of ILs (at a 2M concentration). Pure water was also used at the same operational conditions for comparison purposes. The fixed operational conditions were $R_{S/L}$= 1:10, 358 K (85^{o}C) and 45 min (with particles diameter < 0.4 mm).

Figure 3.2.6 reveals that all ILs solutions perform better than pure water. In addition, the extraction of caffeine increases according to the following rank: water < [EA][CH_3CO_2] < [DEA][CH_3CO_2] < [C_4mim][CH_3CO_2] < [TEA][CH_3CO_2]. For PILs, I general, the extraction yield increases with the increase on the number of hydroxyl groups at the cation of the PIL. Remarkably, an extraction yield of caffeine of 3.57 wt % was achieved with the aqueous solutions of [TEA][CH_3CO_2], confirming that protic ILs can be better extractive solvents that their more expensive and less-benign imidazolium-based counterparts.

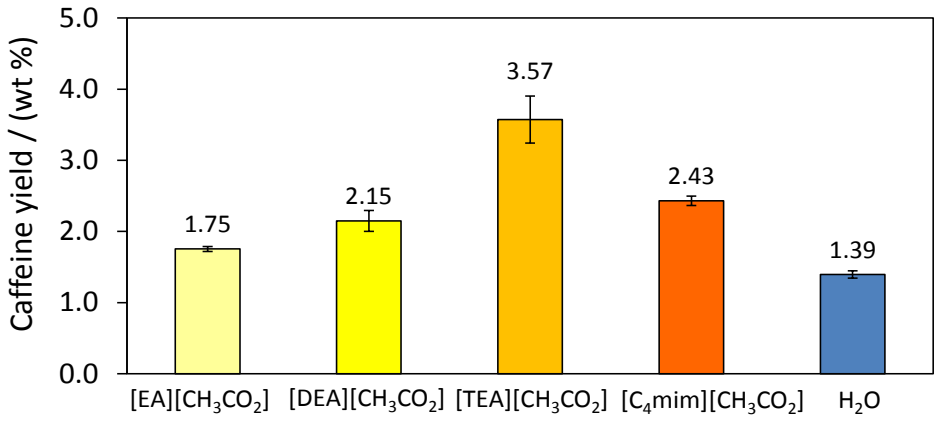

Figure 3.2.6: Yield of caffeine extracted from SCG with different ionic liquids ([IL] = 2 M, T = 85°C (358 K), S/L ratio = 1:10 =0.10 and t = 40 min).

The extraction of caffeine from SCG was also conducted by soxhlet extraction with three organic solvents (petroleum ether, dichloromethane and ethanol) during 420 min. However, substantially lower extraction yields were obtained, namely 0.24 wt %, 0.59 wt % and 1.59 wt % with petroleum ether, dichloromethane and ethanol, respectively. In addition, NMR analyses of these extracts only revealed the presence of caffeine for the extraction carried out with ethanol. Therefore, higher extraction yields can be obtained with aqueous solutions of ILs at more moderate conditions.

Conclusions

Three new PILs were synthetized, characterized, and further used in the extraction of caffeine (as aqueous solutions) from SCG. From the data obtained it was confirmed that cheaper and more benign PILs can be used for the extraction of added-values compounds of biomass instead of the well-studied imidazolium-based compounds. Extraction yields of caffeine up to 3.57 wt % were achieved with an aqueous solution of 2 M of [TEA][CH_3CO_2].

References

1. R.C. Borreli, A. Visconti, C. Mennella, M. Anese and V.J. Fogliano, Agric. Food Chem., 2002, 50, 6527-6533.
2. T. Tokimoto, N. Kawasaki, T. Nakamura, J. Akutagawa and S. Tanada, J. Colloid Interface Sci., 2005, 281, 56-61.
3. S.I. Mussatto, E.M.S. Machado, S. Martins and J.A. Teixeira, Food Bioprocess Tech., 2011, 4, 661–672.
4. L. Fan, A. Pandey, R. Mohan and C.R. Soccol, Acta Biotechnol., 2000, 20, 41–52.
5. F. Leifa, A. Pandey and C.R. Soccol, J. Basic Microbiol., 2000, 40, 187–197.
6. S.I. Mussatto, L.M. Carneiro, J.P.A. Silva, I.C. Roberto and J.A. Teixeira, Carbohyd. Polym., 2011, 83, 368–374.
7. K. Ramalakshmi, L.J.M. Rao, Y. Takano-Ishikawa and M. Goto, Food Chem., 2009, 115, 79-85.
8. J. Bravo, I. Juániz, C. Monente, B. Caemmerer, L. W. Kroh, M. P. De Peña and C. Cid, J. Agric. Food Chem. 2012, 60, 12565−12573
9. M.I.I. Rodrigues and A. Francisco, Planejamento de Experimentos e Optimização de Processos, C.D.P. Editora, Campinas, Brazil, 2005.
10. H.F.D. Almeida, H. Passos, J.A. Lopes-da-Silva, A.M. Fernandes, M.G. Freire and J.A.P. Coutinho, J. Chem. Eng. Data, 2012, 57, 3005−3013.
11. K.A. Kurnia, C.D. Wilfred and T. Murugesan, J. Chem, Thermodyn., 2009, 41, 517-521
12. G.J. Maximo, R.J.B.N. Santos, P. Brandão, J.M.S.S. Esperança, M.C. Costa, A.J.A. Meirelles, M.G. Freire and J.A.P. Coutinho, Cryst. Growth Des., 2014, 14, 4270–4277.

3.3. Ionic Liquids as Hydrotropes: A Study on the Enhanced Solubility of Gallic acid, Vanillin and Caffeine in Water

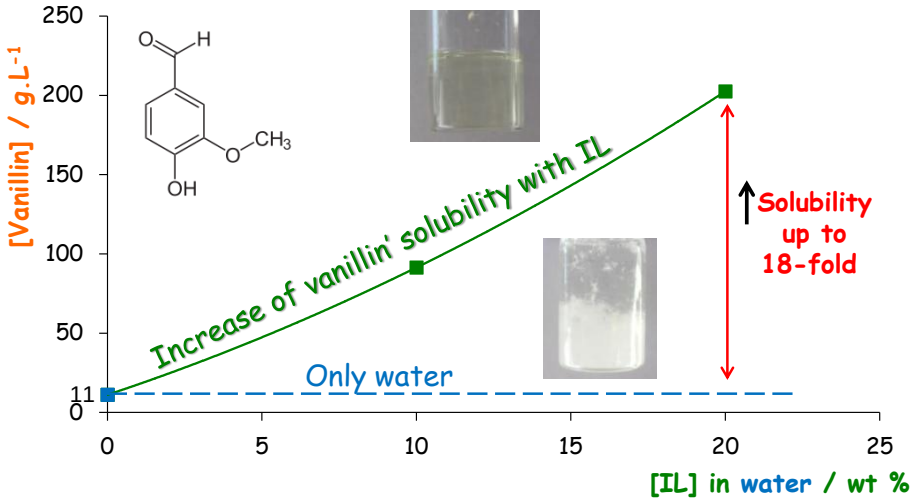

This chapter in based on a manuscript under preparation with the following authors: A.F.M. Cláudio, M.C. Neves, M.G. Freire and J.A.P. Coutinho, Ionic liquids as hydrotropes: A study on the enhanced solubility of antioxidants in water (2014).

Abstract

Hydrotropes are compounds that enhance the solubility of hydrophobic substances in water. They are widely used in formulation of drugs, cleaning and personal care products, as well as in extraction processes. In this work, it is shown that ILs are powerful hydrotropes and can increase the solubility of biomolecules in aqueous media (and which are considerable poorly soluble in pure water). Gallic acid and vanillin (both antioxidants) and caffeine (alkaloid) were used as model biomolecules in this study. The effects of the hydrotrope structure, concentration, and temperature on the solubility of the biomolecules were evaluated. The gathered results show that the solubility of the biomolecules studied go through a maximum in aqueous solutions of ILs with solubilities much higher than in any of the pure solvents. Increases in the solubility of more than 18-fold were observed for vanillin using 20 % wt of IL (0.7-1.4 $mol.L^{-1}$ depending of the IL). The enhanced solubility mechanism is shown to result from the formation of aggregates of ILs with the solute (by Dynamic Ligth Scattering studies). These evidences may have a large impact on explaining the role of ILs in the extraction of biocompounds as well as in designing process for their recovery from solution.

Introduction

The dissolution of compounds of low solubility in pure and mixed solvents plays an important role in the formulation of drugs, cleaning agents and personal care products, and is also relevant in industrial processes such as crystallization, extraction and other separation processes.[1] To achieve the required concentration levels of hydrophobic compounds in aqueous solutions it is common to use hydrotropes. These are a class of highly water soluble salts or molecules that are characterized by an amphiphilic molecular structure (constituted by one hydrophilic and one hydrophobic functional groups) with the ability to dramatically increase the solubility of sparingly soluble organic compounds

in water, often by several orders of magnitude.[2,3] The conventional hydrotropes used in industry are often compounds composed of a phenyl group (hydrophobic part) attached to an anionic group (hydrophilic part) accompanied by a counter ion such as ammonium, calcium, potassium or sodium.[4] It should be noted that although the hydrotropes are used to solubilize compounds in water they are not surfactants. The apolar part of the hydrotropes is smaller than traditional surfactants and they do not present a CMC or form aggregates in the absence of a solute.[5,6] The phenomenon of hydrotropy was first reported by Neuberg in 1916[3] in the solubilization of sparingly soluble compounds in water and its mechanism of action is still not fully understood.[7] Over the years, the phenomenon of hydrotropy has not been clearly explained; therefore, several theories to justify the increased solubility of a compound in water with hydrotropes were further proposed. Some authors, [8-10] suggest that hydrotropic solubilisation is based on changes in the nature and structure of the solvent, *i.e.*, there is a disruption of the water structure by the hydrotropes and, consequently, an increase of the solubility of the solute (molecule of interest) in water is observed. Another point of view is that the increase in solubility of the molecule is due to the formation of solute-hydrotropes complexes.[11-14] According to this theory, the increase of solubility is the result of a collective molecular phenomenon that occurs by the aggregation of the solute with the hydrotropes and the formation of molecular complexes at low hydrotrope concentrations.[11-14] Furthermore, recent studies[15-19] suggested that self-aggregation is responsible for the hydrotropic solubilisation mechanisms – a theory based on the self-assembly of hydrotrope molecules leading to an increase in the solute solubility.

Due to their nature, hydrotropes present, in general, a low toxicity and have a low bioaccumulation potential (octanol:water partition coefficient < 1.0).[20]

If the recovery of the solute is intended it can be easily achieved using water as antisolvent by reducing the concentration of the hydrotrope by dilution. Further, the contamination of the final product can be reduced to values below an acceptable level by washing with water.[21] In addition to the ability of increasing the solubility of compounds in water, hydrotropes may also play a role in the stabilization of solutions, change in viscosity, modifying the cloud-point and limiting the low temperature phase separation.

Although their solvation ability for a wide range of solutes is well known, and they have been proposed as potential replacements for the conventional organic solvents used in extraction techniques,[22-24] the use of ILs as hydrotropes has never, to the best of our knowledge, been previously investigated or reported.

Some works on the use of ILs for the extraction and purification of phenolic compounds have been previously reported.[23-27] Vanillin is one of the most appreciated fragrant substances used to create artificial flavors with many applications in the food, dietary, health care and pharmaceutical industries. The large interest in vanillin is also related to its relevant properties in the human health due to its antioxidant, anti-inflammatory, radical scavenger and antimicrobial characteristics. Due to the limited availability of vanillin from natural sources, the synthesis and extraction of this compound from alternative sources has been explored.[24,28,29] Likewise, gallic acid is a phenolic compound that possesses important properties in the health and nutrition fields related with its anti-inflammatory, antibacterial, antifungal, antioxidative, phytotoxic and radical scavenging activities.[23,30] These biomolecules are present in high concentrations in a variety of biomass sources, such as fruits, vegetables and wood, and also in many residues from industrial or agricultural activities.[20,31-33] Therefore, novel techniques that could make economically viable their extraction and purification from alternative sources would be very relevant.

The solubility of vanillin in water (12.78 $g.L^{-1}$) or non-polar solvents, such as hexane, is low, but it is significantly higher in mildly polar solvents, such as ethanol and methanol.[34] Thus, alcoholic solvents have been commonly employed to extract phenolic compounds from natural sources, because they give a relatively high yield of total extract, even though they are not highly selective for phenols. Particularly, mixtures of alcohols, such as 2-propanol and ethanol,[35,36] as well as with water have revealed to be more efficient in extracting phenolic constituents than the corresponding pure solvent systems.[37] Furtheremore, the solubility of vanillin in aqueous solution is recognized to increase in presence of hydrotropes such as nicotinamide, sodium salicylate, resorcinol and citric acid.[28]

Regarding gallic acid, its solubility at 303 K in common solvents follows the trend: ethyl acetate (12.9 $g.L^{-1}$ = 0.075 $mol.L^{-1}$) < water (16.1 $g.L^{-1}$ = 0.095$mol.L^{-1}$) < ethanol (189.4 $g.L^{-1}$ = 1.113 $mol.L^{-1}$) < methanol (288.3 $g.L^{-1}$ = 1.695 $mol.L^{-1}$).[38]. The gallic acid solubility in (water + ethanol)[39] mixtures was reported to be non-monotonical. No previous studies on the hydrotropic solubilization of gallic acid were reported.

Concerning the effect of inorganic salts on the solubility of phenolic compounds these have been investigated by Noubigh et al.[31,32,40] These authors reported data on the solubility of several phenolic compounds presente in olive mill wastewater, namely, gallic acid, protocatechuic acid, vanillic acid, vanillin, syringic acid and ferulic acid in water and aqueous solutions of three chloride salts (LiCl, NaCl, KCl).[32,39,40] They showed that the solubility of the phenolic compounds decreases with increasing the salt concentration, with a salting-out effect following the order: LiC l> NaC l> KCl. Furthermore, Noubighet al.[31] also shown that the solubility of gallic acid, vanillin, syringic acid and protoctechuic acid decrease with the concentration of Na_2SO_4. With the amphiphilic behavior of ILs in mind,[39] that seems to be the driving force behind their ability to dissolve a wide range of compounds, the potential of ILs to act as hydrotropes was here investigated based on their ability to enhance the solubility of two phenolic compounds in water, namely vanillin and gallic acid, whose structures are depicted in Figure 3.3.1.

In order to extend this study to other molecules, caffeine was chosen as model molecule of the alkaloids family. Caffeine is an important alkaloid present in various plant species, namely, coffee and guaraná seeds, cacao and tea. Moreover, this compound can be found in other products as food and beverages and is one of the most consumed and socially accepted natural stimulants. The chemical structure of caffeine is also reported in Figure 3.3.1. The use of a large amount of caffeine can cause cardiac stimulation and excitation of the central nervous, muscular and circulatory systems, since caffeine blocks adenosine receptors on presynaptic terminals of nerves due to their structural similarities. Caffeine is widely used in pharmaceutical formulations.[42] The solubility of caffeine in water at 303 K (as measured in this work) is 23.09 $g.L^{-1}$.

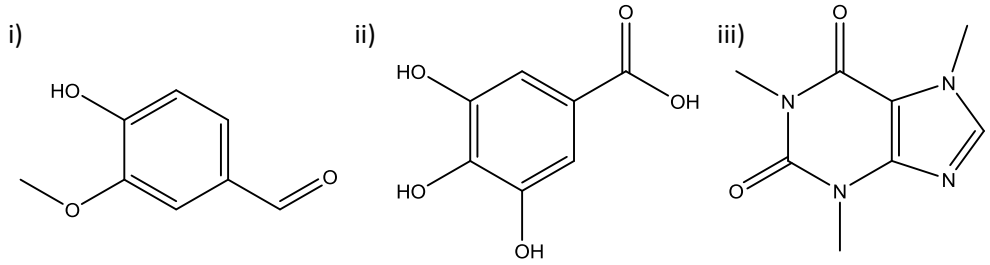

Figure 3.3.1: Chemicalstructures of vanillin (i), gallic acid (ii) and caffeine (iii).

The hydrotropicity was here evaluated by comparing the solubility of these compounds in water, aqueous solutions of ILs, aqueous solutions of well-known hydrotropes and salting-in inducing salts (such as sodium benzoate, sodium citrate and sodium thiocyanate). The importance and relevance of the gathered results for the extraction and purification of biomolecules from biomass (or other sources) by cost-effective and environmentally-safe processes are here discussed.

Experimental Procedure

Chemicals

A large variety of ionic liquids (ILs) was investigated, namely, 1-ethyl-3-methylimidazolium chloride, $[C_1C_2im]Cl$, 1- ethyl-3-methylimidazolium dicyanimide, $[C_2C_1im][N(CN)_2]$, 1-butyl-3-methylimidazolium trifluoromethanesulfonate (triflate), $[C_4C_1im][CF_3SO_3]$, 1-butyl-3-methylimidazolium thiocyanate, $[C_4C_1im][SCN]$, 1-butyl-3-methylimidazolium methylsulfate, $[C_4C_1im][CH_3SO_4]$, 1-butyl-3-methylimidazolium tosylate, $[C_4C_1im][TOS]$, 1-butyl-3-methylimidazolium bromide, $[C_4C_1im]Br$, 1-butyl-3-methylimidazolium dicyanamide, $[C_4C_1im][N(CN)_2]$, 1-butyl-3-methylimidazolium chloride, $[C_4C_1im]Cl$, 1-hexyl-3-methylimidazolium chloride, $[C_6C_1im]Cl$, 1-methyl-3-octylimidazolium chloride, $[C_8C_1im]Cl$, 1-decyl-3-decylimidazolium chloride, $[C_{10}C_1im]Cl$, 1-dodecyl-3-methylimidazolium chloride, $[C_{12}C_1im]Cl$, 1-tetradecyl-3-methylimidazolium chloride, $[C_{14}C_1im]Cl$, 1-butyl-3-methylpyridinium chloride, $[C_4C_1py]Cl$, 1-butyl-1-methylpiperidinium chloride, $[C_4C_1pip]Cl$, 1-butyl-1-methylpyrrolidinium chloride, $[C_4C_1pyrr]Cl$; tetrabutylammonium chloride, $[N_{4444}]Cl$, tetrabutylphosphonium chloride,

$[P_{4444}]Cl$, cholinium chloride, $[N_{1112}OH]Cl$, and tetrabutylammonium tosylate, $[N_{4444}][TOS]$. The imidazolium-, pyridinium-, and pyrrolidinium-based ILs were purchased from Iolitec. The tetrabutylphosphonium chloride was kindly offered by Cytec Industries Inc. The tetrabutylammonium chloride was obtained from Aldrich and Cholinium chloride from Sigma. All ionic liquids used have a purity level of at least 98 wt %. Before use, and in order to reduce the water and volatile compounds content to negligible values, IL samples were dried under constant agitation at vacuum and moderate temperature (333 K) for a minimum of 48 h. After this procedure, the purity of each IL was further checked by ^{1}H and ^{13}C NMR.

Sodium benzoate, ($NaC_7H_5O_2$) > 99.0 wt % pure, was supplied by Panreac. Sodium thiocyanate, (NaSCN) > 98.0 wt % pure, was supplied by Fluka. Sodium chloride, (NaCl) > 98.0 wt % pure, was provided by ChemLab and sodium citrate, ($NaC_6H_7O_7$) > 98.0 wt % pure, from JMGS. All of these compounds were, like the ionic liquids, dried before use.The structures of anions and cations of all used salts are represented in Figure 3.3.2.

Vanillin, > 99 wt % pure, was supplied by Acros and gallic acid,> 99.5 wt.% pure, was acquired from Merck. Caffeine was obtained from Marsing & Co. Ltd. with a nominal purity ≥ 98.5 wt %. All solutes were used as received.

The water employed was double distilled, passed across a reverse osmosis system, and further treated with a Milli-Q plus 185 water purification apparatus.

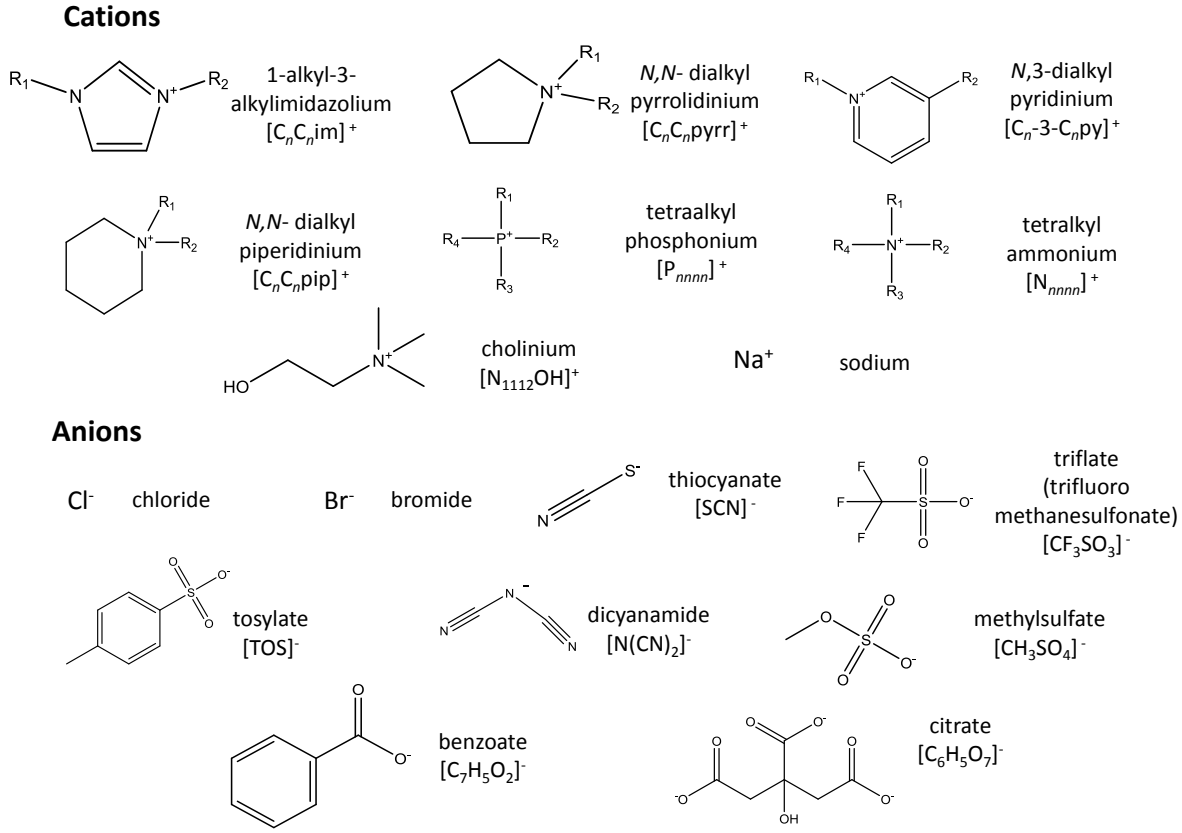

Figure 3.3.2: Chemical structures of the IL and salt anions and cations.

Solubility of Biomolecules

Each biomolecule (vanillin, gallic acid and caffeine) were added in excess amounts to each aqueous solution and equilibrated in an air oven under constant agitation using an Eppendorf Thermomixer Comfort equipment, at each selected temperature (± 0.5 K). Previously optimized equilibration conditions were established: stirring velocity of 750 rpm and equilibration time of at least 72 h. After the saturation was reached, all samples were centrifuged in a HettichMikro 120 centrifuge during 20 minutes at 4500 rpm to separate the macroscopic phases. After centrifugation, samples were put in an air bath equipped with a Pt 100 probe and PID controller at the temperature used in equilibrium assays during 2 h. Then, the samples of the liquid phase were carefully collected and the amount of vanillin, gallic acid and caffeine were quantified through UV-spectroscopy, using a SHIMADZU UV-1700, Pharma-Spec Spectrometer, at a wavelength of 280 nm, 262 nm and 274 nm, respectively, using calibration curves previously established. At least

three individual samples of each solution were quantified to determine the solubility of the biomolecule and the respective standard deviations.

Dynamic Light Scattering (DLS)

To evaluate the presence of aggregates and to determine their size in solutions composed of $[C_4C_1im][TOS]$, water and vanillin, dynamic light scattering (DLS) was employed, using a Nano-ZS, ZetaSizer from Malvern Instruments. A solution with 20 wt % of $[C_4C_1im][TOS]$ was prepared and where vanillin (at 109.5 $g.L^{-1}$) was solubilized at 298 K. In order to analyze the presence of aggregates, aliquots of solvent (aqueous solutions of $[C_4C_1im][TOS]$) were added, decreasing the concentration of vanillin in solution (93.9 $g.L^{-1}$, 82.1 $g.L^{-1}$, 73.0 $g.L^{-1}$, 65.7 $g.L^{-1}$, 59.7 $g.L^{-1}$, 54.8 $g.L^{-1}$ and 50.5 $g.L^{-1}$). The same procedure was performed adding water and simultaneously diluting both the hydrotrope and vanillin while keeping their ratio constant. Moreover, the same measurements were repeated at 323 K in order to evaluate the influence of temperature.

Before the measurements, all solutions were filtered using a 0.2mm PTFE membrane filter to remove all dust particles.

Results and Discussion

Aiming at investigating the potential of ILs to act as hydrotropes, the solubilities of vanillin, gallic acid and caffeine were measured in aqueous solutions with variable concentrations of these compounds, and compared with common hydrotropes and salting-in inducing salts. The solubility in pure water of vanillin, gallic acid and caffeine at 303 K, as measured in this work, are respectively (11.12 ± 0.025) $g.L^{-1}$ (0.073 $mol.L^{-1}$), (14.38 ± 0.41) g. L^{-1} (0.084 $mol.L^{-1}$), and (23.09 ± 1.36) $g.L^{-1}$ (0.119 $mol.L^{-1}$), and which are in good agreement with data previously reported in the literature.[38,40,43] All measured values, with the respective standard deviations, are reported in the *Supporting Information* (Table S81).

Effect of the IL Concentration in the Biomolecules Solubility

The solubility of gallic acid in aqueous solutions of $[C_4C_1im][N(CN)_2]$ and $[C_4C_1im]Cl$, of vanillin in aqueous solutions of $[C_2C_1im][N(CN)_2]$, $[C_4C_1im][TOS]$ and $[C_4C_1im]Cl$, and of caffeine in aqueous solutions of $[C_2C_1im][N(CN)_2]$ were studied in the entire concentration range from pure water to pure IL at 303 K (except for $[C_4C_1im][TOS]$ and $[C_4C_1im]Cl$ because they are solid at this temperature). The results obtained are shown in Figure 3.3.3.

S and S_0 are the solubility ($mol.L^{-1}$) of the biomolecules in presence of the hydrotrope and in pure water, respectively. Therefore, S/S_0 represents the solubility enhancement. The results show a synergetic effect of the two solvents upon the solubility of the biomolecules with aqueous solutions of the IL displaying a much higher solubility of both antioxidants than any of the two pure compounds, with solubility enhancements that may reach 40-fold. They clearly establish the capacity of the ILs to act as hydrotropes by enhancing the solubility of the biomolecules in water. The values of the solubility of the three compounds in each aqueous solution of IL are reported in the *Supporting Information* (Figure S10).

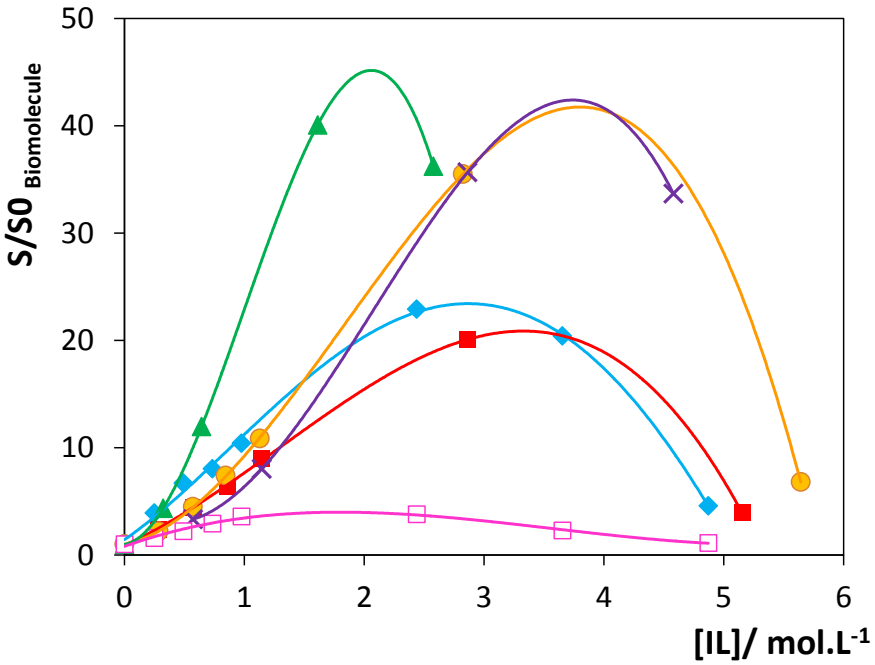

Figure 3.3.3: Influence of the ILs concentration in the solubility of gallic acid in aqueous solutions of ◆, $[C_4C_1im][N(CN)_2]$ and ■, $[C_4C_1im]Cl$; and vanillin in aqueous solutions of ●, $[C_2C_1im][N(CN)_2]$, ▲, $[C_4C_1im][TOS]$, ×, $[C_4C_1im]Cl$, caffeine in aqueous solutions of □, $[C_4C_1im][N(CN)_2]$ at 303 K. Lines have no scientific meaning and are only guides for the eye.

Effect of the Salt Anion and Cation in the Biomolecules Solubility

In the studies reported below the concentration region up to 20 wt % of the IL will be used to study the impact of the IL structural features upon their ability to enhance the solubility of the antioxidants here investigated.

The results for a range of IL and salts on the solubility of vanillin at 303 K are presented in Figure 3.3.4. The same figure expressed in wt % of IL is depicted in the *Supporting Information* (Figure S11). Similar results for gallic acid and caffeine are also presented in *Supporting Information* (Figures S12 and S13). These results emphasize the role of the ILs structure upon the solubility of the studied biomolecules and their superior performance when compared with the more conventional salts investigated.

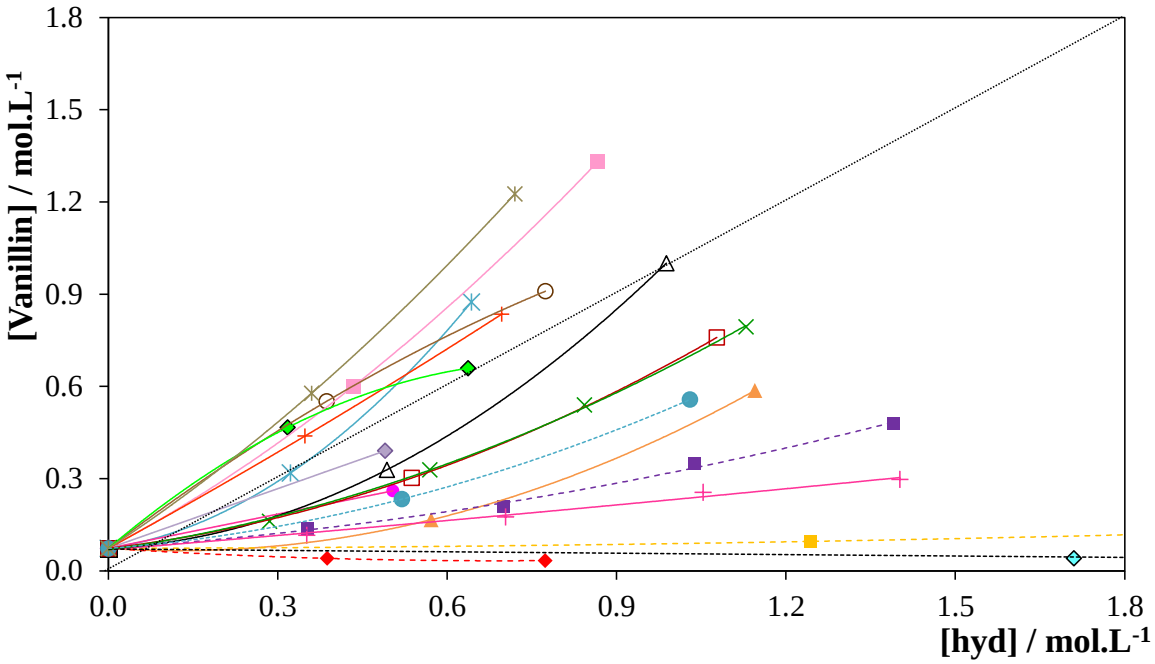

Figure 3.3.4: Influence of hydrotropes at different concentrations at 303 K in the vanillin's solubility in water (■) and in aqueous solutions of +, [C_2C_1im]Cl, ▲, [C_4C_1im]Cl, △, [C_6C_1im]Cl, ■, [C_8C_1im]Cl, ○, [$C_{10}C_1$im]Cl, +, [$C_{12}C_1$im]Cl, ◆, [$C_{14}C_1$im]Cl, ×, [C_2C_1im][$N(CN)_2$], ◆, [C_4C_1im][$N(CN)_2$], ✳, [C_4C_1im][TOS], ●, [C_4C_1im][SCN], □, [C_4C_1py]Cl, ■, [Na][$C_7H_5O_2$], ■, [Na][SCN], ◆, [Na][$C_6H_5O_7$], ◆,NaCl, ✳, [N_{4444}]Cl, ●,Na[TOS].

For a more detailed analysis of the IL major features (anion, cation and cation alkyl chain length) the results were further independently assessed based on equation 3.3.1,

$$S = S_0 + K_{Hyd} \times [Hyd] \qquad \text{eq. 3.3.1}$$

where S and S_0 are the solubility (mol.L^{-1}) of the biomolecule in presence of the hydrotrope and in pure water, repectively, [Hyd] is the concentration of hydrotrope in aqueous solution (mol.L^{-1}) and K_{Hyd} ($mol_{biomoecule}/mol_{Hydrotrope}$) is the hydrotropy constant used to compare the influence of hydrotropes on the solubility behavior. These constants were estimated for each system studied and are reported in Table 3.3.1.

Table 3.3.1: K_{Hyd} values for vanillin, gallic acid and caffeine for the various hydrotropes studied.

Hydrotrope	K_{Hyd} / ($mol_{biomolecule}.mol^{-1}_{hydrotrope}$)		
	Vanillin	Gallic acid	Caffeine
$[C_2C_1im]Cl$	0.163 ± 0.006		
$[C_4C_1im]Cl$	0.424 ± 0.014	0.556 ± 0.041	0.181 ± 0.002
$[C_6C_1im]Cl$	0.866 ± 0.031		
$[C_8C_1im]Cl$	1.422 ± 0.042		
$[C_{10}C_1im]Cl$	1.127 ± 0.064		
$[C_{12}C_1im]Cl$	1.099 ± 0.038		
$[C_{14}C_1im]Cl$	0.997 ± 0.023		
$[C_4C_1im]Br$		0.311 ± 0.012	0.080 ± 0.002
$[C_4C_1im][SCN]$	0.376 ± 0.017	0.460 ± 0.016	0.465 ± 0.006
$[C_4C_1im][TOS]$	1.164 ± 0.053	0.633± 0.048	0.463 ± 0.015
$[C_4C_1im][CH_3SO_4]$		0.438 ± 0.031	0.115 ± 0.014
$[C_4C_1im][CF_3SO_3]$		0.414 ± 0.024	0.319 ± 0.034
$[C_4C_1im][N(CN)_2]$	0.656 ± 0.021	0.844 ± 0.049	0.541 ± 0.029
$[C_2C_1im][N(CN)_2]$	0.584 ± 0.039		
$[C_4C_1py][N(CN)_2]$		1.533 ± 0.023	0.715 ± 0.031
$[C_4C_1py]Cl$		0.612 ± 0.036	0.034 ± 0.003
$[C_4C_1pip]Cl$		0.501 ± 0.015	-0.021 ± 0.008
$[C_4C_1pyrr]Cl$		0.444 ± 0.042	-0.017 ± 0.003
$[N_{1112}OH]Cl$		0.129 ± 0.011	-0.049 ± 0.001
$[N_{4444}]Cl$	1.583 ± 0.009	-0.107 ± 0.002	0.130 ± 0.004
$[P_{4444}]Cl$		-0.103 ± 0.001	0.103 ± 0.002
[Na][SCN]	0.030 ± 0.002	-0.005 ± 0.001	0.374 ± 0.026
$[Na][C_7H_5O_2]$	0.270 ± 0.003	0.083 ± 0.003	0.660 ± 0.056
$[Na][C_6H_5O_7]$	-0.059 ± 0.008	0.238 ± 0.004	-0.162 ± 0.003
NaCl	-0.016 ± 0.002	-0.013 ± 0.002	
[Na][TOS]	0.444 ± 0.034	0.218 ± 0.025	

The effect of the IL cation upon the solubility of vanillin, gallic acid and caffeine was assessed using a series of chloride-, dicyanamide- and tosylate-based ILs. The results are plotted in Figures S11 to S13 in the *Supporting Information* and the results for the hydrotropy constants, K_{Hyd}, reported in Table 3.3.1.

Table 3.3.1 show that the hydrotropes impact upon the solubility of vanillin follows the order: [Na][Citrate] < NaCl< [Na][SCN] < $[C_2C_1im]Cl$ < [Na][benzoate] < $[C_4C_1im][SCN]$ < $[C_4C_1im]Cl$ < [Na][TOS] < $[C_2C_1im][N(CN)_2]$ < $[C_4C_1im][N(CN)_2]$ < $[C_6C_1im]Cl$ < $[C_{14}C_1im]Cl$ < $[C_{12}C_1im]Cl$ < $[C_{10}C_1im]Cl$ < $[C_4C_1im][TOS]$ < $[C_8C_1im]Cl$ < $[N_{4444}]Cl$. Moreover, the results for

vanillin allow the evaluation of the effect of the cation alkyl chain from ethyl (C_2) to tetradecyl (C_{14}) with the hydrotropy constants, K_H, presenting a non-monotonical behavior, and as shown in Figure 3.3.5.

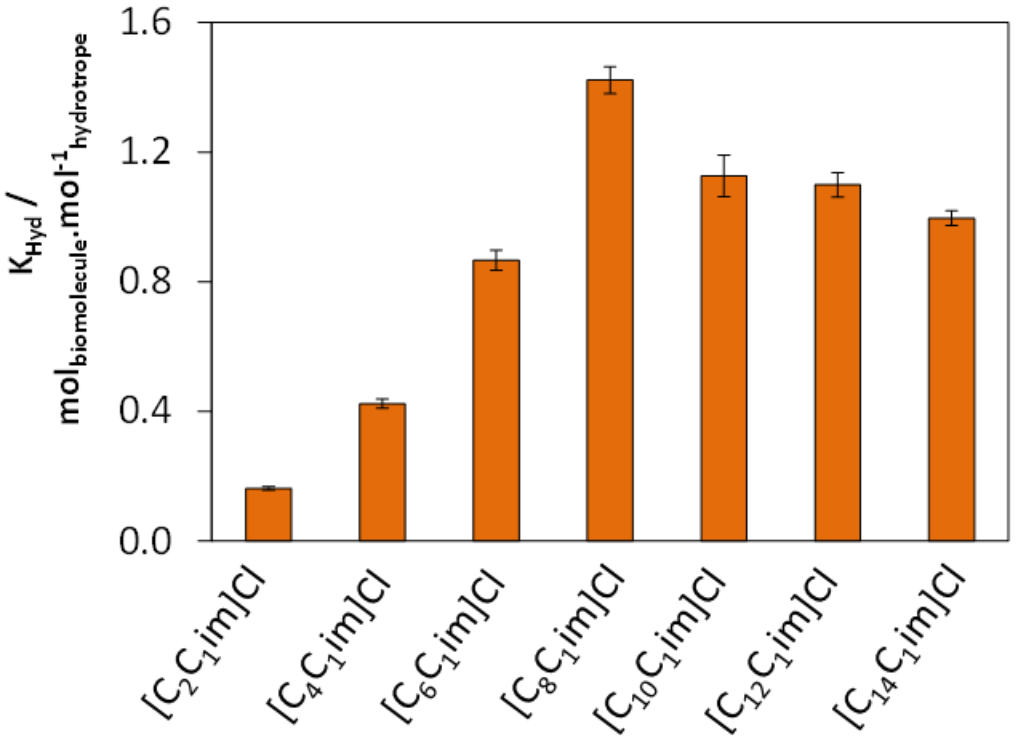

Figure 3.3.5: K_{Hyd} values for vanillin with [$C_nC_1$mim]Cl ILs, n = 2, 4, 6, 8, 10, 12, 14.

The impact of the IL on the solubility of vanillin increases from [C_2C_1im]Cl to [C_8C_1im]Cl, with an increase in the solubility of nearly 20-fold, and then decreases with the further increase of the cation alkyl chain length. Although the hydrotropic effect can be attributed to the formation of co-aggregates between the solute and the hydrotropes, as shown below, the decrease on the hydrotropic effect observed for the ILs that can form micelles, *i.e.*, those larger than [C_8C_1im]Cl, suggests that the formation of micelles is deleterious to this phenomenon. The increase in solubility with the cation alkyl chain length is also observed for [$N(CN)_2$]-based ILs – data shown in Figure S11 in the *Supporting Information*.

The results obtained for gallic acid allow the evaluation of the effect of a broad range of cation families upon the hydrotropic effect achieved by the ILs. According to the values of the hydrotropy constants, K_{Hyd}, reported in Table 3.3.1, the effects on the gallic acid solubility follow the order: [N_{4444}]Cl < [P_{4444}]Cl < [Na][SCN] < NaCl < [Na][benzoate] <

$[N_{1112}OH]Cl$ < [Na][TOS] < [Na][Citrate] < $[C_4C_1im]Br$ < $[C_4C_1im][CF_3SO_3]$ < $[C_4C_1im][CH_3SO_4]$ < $[C_4C_1pyrr]Cl$ < $[C_4C_1im][SCN]$ < $[C_4C_1pip]Cl$ < $[C_4C_1im]Cl$ < $[C_4C_1py]Cl$ < $[C_4C_1im][TOS]$ < $[C_4C_1im][N(CN)_2]$ < $[C_4C_1py][N(CN)_2]$.

Quaternary phosphonium and ammonium cations, $[N_{4444}]Cl$ and $[P_{4444}]Cl$, decrease the solubility of gallic acid in water ($K_{Hyd} < 0$), presenting a minor salting-out inducing behavior similar to that witnessed for sodium thiocyanate, and sodium citrate for vanillin. The absence of the hydrotropic capability of these cations may be related with their symmetry and low polarity since another quaternary ammonium, namely cholinium chloride, presents a minor hydrotropic activity (K_{Hyd} = 0.129 ± 0.011). The cations with ring structures, in particular those with an aromatic nature, present the strongest hydrotropic effect, and thus a higher impact upon the gallic acid solubility. The $[C_4C_1py][N(CN)_2]$ is shown to enhance the solubility of gallic acid in water up to 20-fold (from 14.38 ± 0.41 $g \cdot L^{-1}$ = 0.085 $mol \cdot L^{-1}$ to 263.46 ± 1.63 $g \cdot L^{-1}$ = 1.549 $mol \cdot L^{-1}$) at the highest concentration studied (20 wt % = 0.93 $mol \cdot L^{-1}$).

The effect of the counter ion on the hydrotropic effect is seldom explored but the results here reported show that it seems to be relevant as demonstrated by the K_{Hyd} presented in Table 3.3.1. Here the effect of the IL anion on the vanillin, gallic acid and caffeine solubilities was evaluated for a wide range of anions. For vanillin, the trend on solubility in the $[C_4C_1im]$-based ILs aqueous solutions follows the series: $[SCN]^- < Cl^- < [N(CN)_2]^- < [TOS]^-$ .Concerning the common salts, sodium citrate and sodium chloride decrease the solubility of vanillin ($K_{Hyd} < 0$). However, sodium thiocyanate induces a minor increase on the solubility of vanillin (K_{Hyd} = 0.030 ± 0.002) - an effect typical of a salting-in inducing salt. Moreover, sodium benzoate and sodium tosylate act as hydrotropes while increasing the solubility of vanillin 6.6 and 7.7 times over the water solubility at the higher concentration of salt (K_{Hyd} = 0.270 ± 0.003 and 0.444 ± 0.034).

While the $[SCN]^-$ and Cl^- anions do not seem to have a significant effect on the solubility, showing a minor salting-in inducing effect, the $[N(CN)_2]^-$ and $[TOS]^-$ reveal a strong hydrotropic effect. Tosylate, a common name for *p*-toluene sulfonate is a well-known hydrotrope,[4] but the action of $[N(CN)_2]^-$ as hydrotrope is here reported for the first time.

The results for $[TOS]^-$ suggest that the hydrotropy may be additive with the cation and anion - acting each ion as hydrotrope since the values of K_H are constant.

The hydrotropic solubility of gallic acid was assessed for an even larger number of anions. For gallic acid, the trend on the enhanced solubility by the $[C_4C_1im]$-based ILs follows the series: $Br^- < [CF_3SO_3]^- < [CH_3SO_4]^- < [SCN]^- < Cl^- < [TOS]^- < [N(CN)_2]^-$.

In what concerns the salts, the sodium thiocyanate has no effect on the solubility of gallic acid while the effect of the sodium benzoate is much smaller than for vanillin (K_{Hyd} of 0.083 ± 0.003 instead of 0.270 ± 0.003) showing that the hydrotropic effect is related not only with the nature of the hydrotrope but also with that of the solute. Further, the aromatic anions have a much lower effect upon the solubility of gallic acid than vanillin since the K_{Hyd} for $[C_4C_1im][TOS]$ is much lower for gallic acid (0.633 ± 0.048 *vs*. 1.16 ± 0.053). This suggests that the hydrotrope-solute interactions on the gallic acid aggregates are of a different nature than those with vanillin where the π- π interactions seem to be more relevant.

Other example, where the effect of IL is completely different in solubilizing both antioxidants is with $[N_{4444}]Cl$. This IL significantly favors the solubility of vanillin (K_{Hyd} = 1.583 ± 0.009); however, it decreases the solubility of gallic acid in water (K_{Hyd} = -0.107 ± 0.002), presenting a salting-out inducing behaviour.

Here, it is possible to show that the capability of each IL to improve the solubility of each antioxidant is different, depending on their characteristics, hydrophobicity and the way the molecule interacts with an aqueous solution of IL. The log(K_{OW}) for vanillin is 1.22 [46] while for gallic acid is 0.72,[46] revealing that vanillin is more hydrophobic than gallic acid. Therefore, the interactions with hydrotropes are consequently different. For these reasons the dissolution of gallic acid is favorable for ILs composed of anions with a more hydrophobic character and a higher hydrogen bonding accepting character, such as $[N(CN)_2]^-$ and $[SCN]^-$. Moreover, as with vanillin, the $[C_4C_1im][TOS]$ also improves the dissolution of gallic acid. All common salts, that appear in literature as a hydrotropes, increase less the solubility than the new hydrotropes (ILs).

The evaluation of the anion effect for the vanillin solubility behaviour was not possible since $[C_4C_1py][N(CN)_2]$ promoted a two-phase separation, and the same was observed for

aqueous solutions of 20 wt % of $[C_4C_1im][N(CN)_2]$. The top and bottom phases of the system created by vanillin, $[C_4C_1im][N(CN)_2]$ and water were analysed, and the bottom phase have twice the concentration of IL and 5 times more vanillin than the top phase. Aqueous solutions of $[N_{4444}][TOS]$ at concentrations of 10 wt % and 20 wt % were also tested for solubilisation of vanillin and gallic acid. In all cases the system separated into two liquid phases. The bottom phase has almost 21 times more IL and 18 times more vanillin than the top phase.

In addition to the comprehensive study of the effect of salts and ILs through the solubility of the two antioxidants, the effect of some ILs and common salts on the solubility of caffeine was also studied.

As can be seen by the K_{Hyd} values in Table 3.3.1 , the solubility of caffeine increases in the following sequence: sodium citrate (-0.1618) < $[N_{1112}OH]Cl$ (-0.0493) < $[C_4C_1pip]Cl$ (-0.0212) < $[C_4C_1pyrr]Cl$ (-0.0168) < $[C_4C_1py]Cl$ (0.0336) < $[C_4C_1im]Br$ (0.080) < $[P_{4444}]Cl$ (0.103) < $[C_4C_1im][CH_3SO_4]$ (0.115) < $[N_{4444}]Cl$ (0.130) < $[C_4C_1im]Cl$ (0.181) < $[C_4C_1im][CF_3SO_3]$ (0.319) < [Na][SCN] (0.374) < $[C_4C_1im][TOS]$ (0.463) < $[C_4C_1im][SCN]$ (0.465) < $[C_4C_1im][N(CN)_2]$ (0.541) < [Na][benzoate] (0.660) < $[C_4C_1py][N(CN)_2]$ (0.715).

Caffeine is a structurally different molecule compared with the two phenolic compounds previously studied with a K_{OW} value of 0.85[46]. As previously seen, the values of K_{Hyd} are here also different compared with the K_{Hyd} values for vanillin and gallic acid. For instance, adding $[C_4C_1im][TOS]$ to water, the K_{Hyd} for vanillin, gallic acid and caffeine is 1.164 ± 0.053, 0.633 ± 0.048, and 0.465 ± 0.015, respectively. With $[N_{4444}]Cl$ the results obtained for vanillin, gallic acid and caffeine are, respectively, 1.583 ±0.009, -0.107 ± 0.002 and 0.130 ± 0.004, while with [Na][Benzoate] they are 0.270 ± 0.003, 0.083 ± 0.003 and 0.660 ± 0.056.

According to the values of the hydrotropy constants reported in Table 3.3.1, the cations effect on the caffeine solubility follow sthe order: $[N_{1112}OH]Cl$ < $[C_4C_1pip]Cl$ < $[C_4C_1pyrr]Cl$ < $[C_4C_1py]Cl$ < $[P_{4444}]Cl$ < $[N_{4444}]Cl$ < $[C_4C_1im]Cl$ and $[C_4C_1im][N(CN)_2]$ < $[C_4C_1py][N(CN)_2]$. It should be noted that $[N_{1112}OH]Cl$, $[C_4C_1pip]Cl$ and $[C_4C_1pyrr]Cl$ decrease the solubility of this alkaloid in water. On the other hand, $[C_4C_1py]Cl$ induces a minor increase on the solubility of caffeine, whereas $[P_{4444}]Cl$, $[N_{4444}]Cl$ and $[C_4C_1im]Cl$ favour the solubility of

caffeine. The aromating ring in $[C_4C_1im][SCN]$ also favors the caffeine solubility compared with [Na][SCN].

The hydrotropic solubility of caffeine was evaluated for an even larger number of anions. For caffeine, the trend on the enhanced solubility by the $[C_4C_1im]$-based ILs follows the series: $Br^- < [CH_3SO_4]^- < Cl^- < [CF_3SO_3]^- < [TOS]^- < [SCN]^- < [N(CN)_2]^-$. Moreover, using $[C_4C_1py]$-based ILs it was verified that ILs with $[N(CN)_2]^-$ significantly increase the solubility of caffeine compared with the Cl^- anion. Finally, comparing [Na][SCN] and [Na][benzoate], it can be inferred that the presence of an aromatic ring at the anion favors the caffeine solubility – results that agree with the favorable extraction of caffeine from guaraná seeds shown in **Chapter 3.1**.

Effect of Temperature in the Biomolecules Solubility

The temperature impact is also here evaluated and discussed. To study the influence of temperature in the solubility of vanillin in presence of hydrotropes, two of the compounds studied, $[C_2C_1im][N(CN)_2]$ (IL) and sodium benzoate (salt), were used. Table 3.3.2 shows the effect of temperature upon the K_{Hyd} between 303 K and 323 K. The solubility results are presented in the *Supporting Information* (Figure S14).

A significant increase in the solubility of vanillin with temperature is observed, mainly when the hydrotrope is $[C_2C_1im][N(CN)_2]$. A similar trend was observed in literature for other hydrotropes.[38]

The aqueous solution of 20 wt % of $[C_2C_1im][N(CN)_2]$, at 323 K, formed an aqueous biphasic system and could not be used in this type of studies.

Table 3.3.2: K_{Hyd} values for vanillin using $[C_2C_1im][N(CN)_2]$ and [Na][Benzoate] at 303, 313 and 323 K.

	K_{Hyd} / ($mol_{biomolecule}.mol^{-1}_{hydrotrope}$)
Hydrotrope	Vanillin
303 K	
$[C_2C_1im][N(CN)_2]$	0.609
[Na][Benzoate]	0.277
313 K	
$[C_2C_1im][N(CN)_2]$	1.944
[Na][Benzoate]	0.442

323 K	
$[C_2C_1im][N(CN)_2]$	2.095
[Na][Benzoate]	0.866

DLS Analysis

In order to confirm the mechanism of hydrotropy by the formation of aggregates, dynamic light scattering (DLS) measurements were performed for systems composed of vanillin in a 20 wt % aqueous solution of $[C_4C_1im][TOS]$. Aliquots of water and solvent (20 wt % of aqueous solution of $[C_4C_1im][TOS]$) were added to an initial solution while decreasing concentration of vanillin. In Figure 3.3.6 it is observed the decrease of the aggregates size with the decrease of the vanillin content in solution. These data thus confirm that the mechanism of increasing the solubility is related with formation of IL-solute aggregates. Dhinakaranet al.[28] referred that the increased solubility of vanillin in hydrotrope solutions is justified as a collective molecular phenomenon, possibly occurring by the aggregation of a solute with the hydrotrope aggregates or by improved hydrogen-bonding. The solute molecules may also take part in the aggregation process of the hydrotrope, thus forming coaggregates with the hydrotrope molecules in aqueous solutions. The formation of a stable coaggregate depends on the molecular structure as well as on the functional group(s) attached to the carbon skeleton of the solute as it would govern the intercalation of the solute between the hydrotrope molecules. The solubilization of a solute is influenced by the hydrophobic part of a stable co-aggregate formed between the solute molecules and the hydrotrope and is also influenced by the chain length of an alkyl group of a hydrotrope. Therefore, the increase in solubility largely depends on the IL nature.

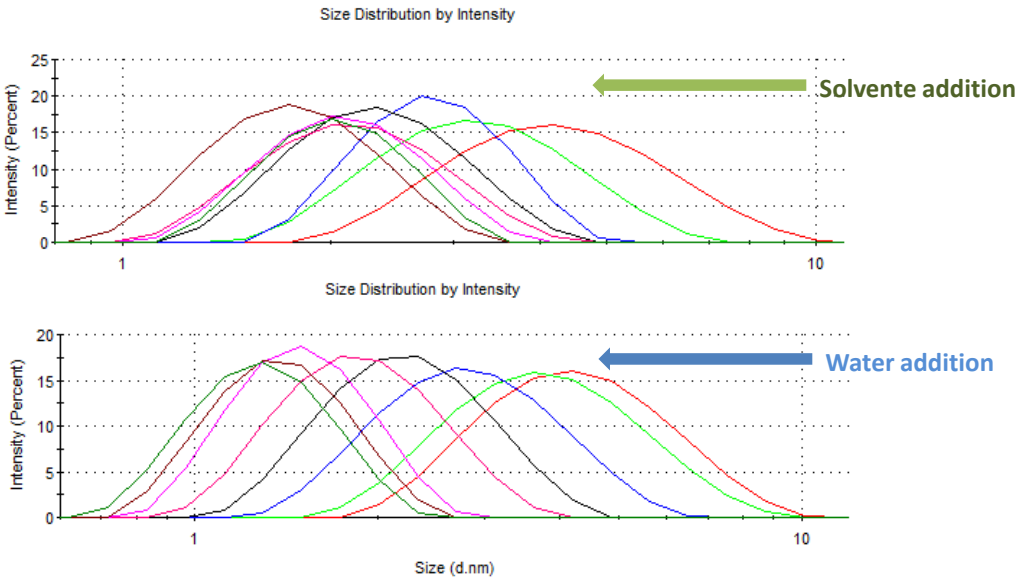

Figure 3.3.6: Particle size distribution adding aliquots of solvent or water while decreasing the concentration of vanillin.

Additionally, the impact of temperature was also evaluated. The solutions were measured at 298 K and 323 K. The increase of temperature also decreased the aggregates size as can be seen in Figure 3.3.7.

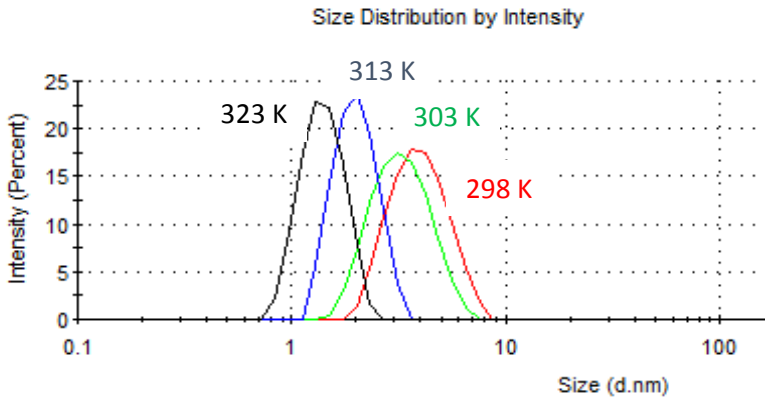

Figure 3.3.7: Particle size distribution at 298 K, 303 K, 313 K and 323 K.

ILs show potential environmental benefits as "green" replacements of conventional salts or volatile organic solvents; however, their toxicity must also be addressed. It should be emphasized that hydrophobic IL have a higher toxicity than hydrophilic ILs.[48] In this work, only hydrophilic ionic liquids were used. Several studies[48] were conducted to evaluate the toxicity of ILs, combining different anions and cations, as well as changing the alkyl group

chain length and number of alkyl groups substituted at the cation ring. These studies revealed that the ILs toxicity is primordially determined by the cation nature and it is directly correlated with the length of the side alkyl chain and number of alkyl groups. Commonly, the anion has a smaller influence than the cation, and generally short cation alkyl chains or hydrophilic ILs present low or no toxicity.[49] Usually, the ILs aqueous solubility decreases with the alkyl chain length increase, which for its turn is positive because the more toxic ILs (higher alkyl chain lengths) are poorly water soluble at room temperature, minimizing thus the environmental impact of ILs in aquatic streams.[49]

Precipitation of Vanillin

The solubility of vanillin and other compounds are an important characteristic to take into account in studies of extraction and purification of this biomolecule from a complex solution.

The recovery of vanillin from the hydrotrope solution can be attained by a simple dilution with distilled water and/or a decrease of temperature, since vanillin solubility is extremely sensitive to the hydrotrope concentration and temperature, as shown before.

Aiming to demonstrate the recovery of vanillin from hydrotrope solutions using water as antisolvent, some experimental tests were carried out. Indeed, it was tested the precipitation of vanillin by the simple addition of water and by lowering the temperature. For this purpose, an aqueous solution with 20 wt % of $[C_4C_1im]Cl$ was prepared and saturated with vanillin at 323 K. To recover the vanillin dissolved, the temperature of the solution was decreased from 323 K to 298 K and water was added, which leads to the precipitation of vanillin - Figure 3.3.8. The precipitated vanillin was further recovered by filtration, washed with cold water and dried. The appearance of the recovered vanillin is the same as the initial compound, as shown in Figure 3.3.8, and its purity was ascertained by ^1H NMR. Figure 3.3.8 shows no differences in the NMR spectra of the initial sample and after its recovery.

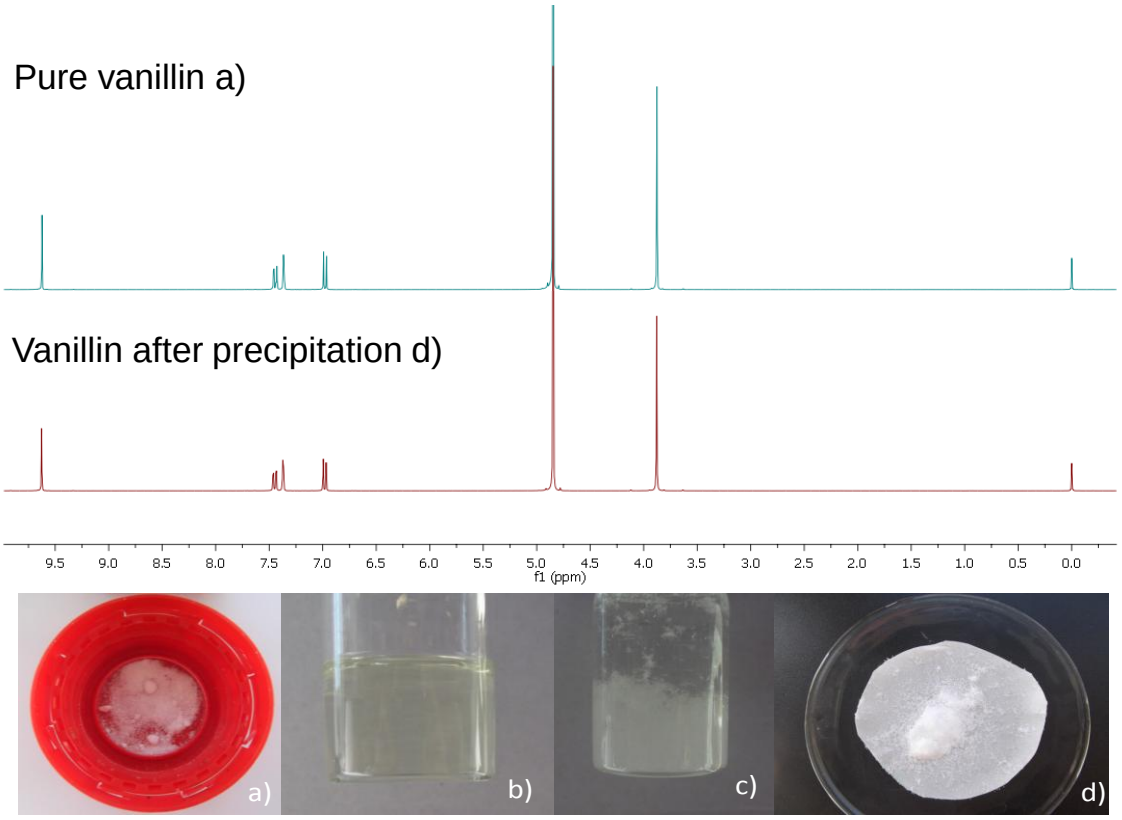

Figure 3.3.8: a) appearance of commercial vanillin and respective ^{1}H NMR spectrum; **b)** vanillin dissolved in a 20 wt % aqueous solution of $[C_4C_1im]Cl$ at 323 K; **c)** precipitation of vanillin with the addition of water and decrease of temperature; **d)** precipitated vanillin and respective ^{1}H NMR spectrum.

Conclusion

The solubility of vanillin, gallic acid and caffeine in water shows an outstanding increase in the presence of hydrotropes. It was found that aqueous solutions of ILs may enhance the solubility of these biomolecules more than 40-fold. The results show that the choice of the IL anion and cation is a crucial factor regarding the solubility increase. However, the temperature and concentration of hydrotrope are also important parameters. Finally, based on the hydrotropy concept, it is shown that biomolecules can be further recovered by a simple dilution with water or by a decrease in temperature.

References

1. C.V. Subbarao, I.P.K. Chakravarthy, A.V.S.L.S. Bharadwaj and K.M.M.K. Prasad, Chem. Eng. Technol., 2012, 35, 225-237.
2. Y.I. Korenman and T.V., Makarova, J. Phys. Chem, 1974, 48, 385-387.
3. Neuberg, C., Biochem. 1916, 76, 107-176.
4. T.K. Hodgdon and E.W. Kaler, Curr. Opin. Colloid Interface Sci., 2007, 12, 121–128
5. V. Srinivas, G.A. Rodley, K Ravikumar, W.T. Robinson, M.M Turnbull and D. Bala-subramanian, Langmuir, 1997, 13, 3235–3239.
6. D., Subramanian, C.T. Boughter, J.B. Klauda, B Hammouda and M.A. Anisimov, Faraday Discuss., 2013, 167, 217-238.
7. S. Shimizu, J.J. Bootha and S. Abbott, *Phys. Chem. Chem. Phys.,* 2013, 15, 20625-20632.
8. G.S.S Ferreira, D.M. Perigo, M.J. Politi and S. Schreier, Photochem. Photobiol.1996, 63, 755–761.
9. A. Matero, A. Mattsson and M.J. Svensson, Surfactants Deterg, 1998, 1, 485–489.
10. P. Bauduin, A. Renoncourt, A. Kopf, D. Touraud and W. Kunz, Langmuir 2005, 21, 6769–6775.
11. R. Sanghvi, D. Evans and S.H. Yalkowsky, Int. J. Pharm., 2007, 336, 35–41.
12. H. Suzuki and H. Sunada,Chem. Pharm. Bull, 1998, 46, 125–130.
13. A.A. Rasool, A.A. Hussain and L.W. Dittert, J. Pharm. Sci.,1991,80, 387–393.
14. M.A. Hussain, R.C. DiLuccio and M.B. Maurin, J. Pharm. Sci.,1993, 82, 77–79.
15. J. Lee, S. C. Lee, G. Acharya, C.J. Chang and K. Park,Pharm. Res., 2003, 20, 1022–1030.
16. D. Balasubramanian, V. Srinivas, V.G. Gaikar and M.M. Sharma, J. Phys. Chem.,1989, 93, 3865–3870.
17. R.E. Coffman and D.O. Kildsig, Pharm. Res.,1996,13, 1460–1463.
18. M.G. Neumann, C.C. Schmitt, K.R Prieto and B.E. Goi, J. Colloid Interface Sci.,2007,315, 810–813.
19. W.N. Charman, C.S.C. Lai, D.J Craik, B.C. Finnin and B.L. Reed, Aust. J. Chem.,1993, 46,377–385.
20. K. Stanton, C. Tibazarwa, H. Certa, W. Greggs, D. Hillebold, L. Jovanovich, D. Woltering and R. Sedlak, Integrated Environ Assess Manag, 2010, 6, 155–163.
21. V.B. Wagle, P.S. Kothari and W.G. Gaikar, J. Mol. Liq., 2007, 133, 68-76.
22. F. van Rantwijk and R.A. Sheldon, Chem. Rev. 2007, 107, 2757-2785.
23. A.F.M. Cláudio, A.M. Ferreira, C.S.R. Freire, A.J.D. Silvestre, M.G. Freire and J.A.P. Coutinho, Sep. Purif. Technol, 2012, 97, 142-149.
24. A.F.M. Cláudio, M.G Freire, C.S.R. Freire, A.J.D. Silvestre and J.A.P. Coutinho, Sep. Purif. Technol., 2010, 75, 39-47.
25. R.Bogel-Lukasik, L.M. Nobre Goncalves and E.Bogel-Lukasik, Green Chem., 2010, 12, 1947-1953.
26. M.R Almeida, H. Passos, M., Pereira, A.S. Lima, J.A.P Coutinho, M.G. Freire, Sep. Purif. Technol., 2014, 128, 1-10.
27. A.F.M. Cláudio, C.F.C. Marques, I Boal-Palheiros, M.G. Freire and J.A.P. Coutinho, Green Chem., 2014, 16, 259–268.
28. M. Dhinakaran, A.B. Morais and N.N. Gandhi, Asian J. Chem.,2013, 25, 231-236.
29., D Jadhav., B.N. Rekha,, P.R. Gogate and V.K. Rathod, J. Food Eng., 2009, 93, 421-426.
30. J. Teixeira, T. Silva, S. Benfeito, A. Gaspar, E. M. Garrido, J. Garrido and F. Borges, Eur. J. Med. Chem., 2013, 62, 289-96.
31. A. Noubigh, M. Cherif, E. Provost and M. Abderrabba, J. Chem. Eng. Data, 2008, 53, 1675-1678.

32. A.,Noubigh, A. Mgaidi, M. Abderrabba, E. Provost and W. Furst, J. Sci. Food Agric., 2007, 87, 783-788.
33. A.F. Sousa, P.C.R.O. Pinto, A.J.D. Silvestre and C.P Neto, J. Agric. Food Chem., 2006, 54, 6888-6893.
34., J. Dnyaneshwar, B.N. Rekha, R.G. Parag and K.R. Virendra, J. Food Eng., 2009, 93, 421- 426.
35. K. Hussain, G. Thorsen and D. Malthe-Sorenssen, Chem. Eng. Sci., 2001, 56, 2295-2304.
36. O. Pino-Garcia, Royal Institute of Technology, Stockholm, 2004.
37. S. Fernando, S. Adhikari, C. Chandrapal and N. Murali, EnergyFuels 2006, 20, 1727-1737.
48. A. Daneshfar, H.S. Ghaziaskar and N.J. Homayoun, Chem. Eng. Data 2008, 53, 776–778.
39. A. Noubigh, C. Jeribi, A. Mgaidi, M. Abderrabba, J. Chem. Thermodyn.,2012, 55, 75–78.
40. A. Noubigh, M. Abderrabba and E.J. Provost, Chem. Thermodyn., 2007, 39, 297-303.
41. M.L.S. Batista, C.M.S.S. Neves, P.J. Carvalho, R. Gani and J.A.P. Coutinho, J. Phys. Chem. B, 2011, 115, 12879-12888.
42. F. Belliardo, A. Martelli and M.G. Valle, Z LebensmUntersForsch., 1985, 180, 398-401
43. L.L. Lu and X.Y. Lu, J. Chem. Eng. Data, 2007, 52, 37–39.
44. M.G. Freire, P.J. Carvalho, A.M.S. Silva, L.M.N.B.F. Santos, L.P.N. Rebelo, I.M. Marrucho, J.A.P. Coutinho, J. Phys. Chem.B, 2009, 113, 202-211.
45. M.G. Freire, C.M.S.S. Neves, A.M.S. Silva, L.M.N.B.F. Santos, I.M. Marrucho, Rebelo, L.P.N., J. K. Shah, E. J. Maginn and J.A.P. Coutinho, J.Phys. Chem. B, 2010, 114, 2004-2014.
46. ChemSpider, *www.chemspider.com*: The free chemical database.
47. F.Y. Du, X.H. Xiao, X.J. Luo and G.K. Li, Talanta, 2009, 78, 1177-1184.
48. M. Petkovic, K.R. Seddon, L.P.N. Rebelo and C.P. Pereira, Chem. Soc. Rev., 2011, 40, 1383-1403
49. M.G. Freire, P.J. Carvalho, R.L. Gardas, I.M. Marrucho, L.M.N.B.F. Santos and J.A.P. Coutinho, J. Phys. Chem. B, 2008, 112, 1604-1610.
50. J.G. Huddleston, A.E. Visser, W.M. Reichert, H.D. Willauer, G.A. Broker and R.D. Rogers, Green Chem., 2001. 3, 156-164.

4. Final Remarks and Future Work

The present work reports a comprehensive study on the use of ILs as alternative solvents for the extraction of high-value biomolecules.

IL-based ABS are new approaches to perform selective separations of added-value products and may be further used for recycling or concentrating hydrophilic ionic liquids from aqueous solutions. In this thesis, the extrinsic and intrinsic properties of IL-based ABS aiming at optimizing the extraction efficiencies and the recycling of ILs were studied. The results obtained indicate that, overall, both the IL cation and anion structural features have a large impact on the phase diagrams behavior. In general, an increase in the cation/anion alkyl chain length leads to an increase in the phases' separation ability, whereas a decrease in the hydrogen bond basicity of the IL promotes the formation of ABS. Besides the effect of the IL structural features on the formation of IL-based ABS, the pH media of the inorganic salts is shown to be a determinant factor regarding the number of effective ILs that are capable of undergo liquid-liquid demixing.

The great complexity of ILs to act either as hydrogen-bond donors or acceptors has resulted in great efforts in the literature aimed at characterizing these fluids according to a polarity scale. Furthermore, this complexity, achieved by innumerable chemical structural variations, is valuable for the creation of "tailor-made" compounds. The reactivity of dissolved substrates, reaction rates and reaction mechanisms are dependent on the solvent-solute interactions. The quantification of these solvent characteristics is thus an important tool to understand the physicochemical phenomena and chemical behaviour of systems involving ILs. For that purpose, several solvent parameters and relative polarity scales for ILs have been proposed. However, the measurement of these parameters is a burdensome task. Therefore, it is of crucial importance to find alternative and/or predictive methods. In this thesis, reasonable linear correlations between the experimental hydrogen-bond basicity values of a wide variety of ILs and the E_{HB} (hydrogen-bonding interaction energies ($kJ \cdot mol^{-1}$)) estimated from COSMO-RS were found. Based on this dependence, we provided an extended polarity scale capable of characterizing the IL anions' abilities to hydrogen-bond when acting as solvent media. The E_{HB} values estimated from COSMO-RS can be adequately used for routine screening,

before extensive and time-consuming experimental measurements by a trial and error approach, and allow for the correct choice of an improved IL for a specific application.

The applicability of the studied ABS was also evaluated through the determination of the partition coefficients and extraction efficiencies of alkaloids, aminoacids, phenolic compounds and dyes. It was verified that the choice of the salt, pH and IL structure, are crucial factors in extraction approaches using IL-based ABS. Tuning the conditions of the system it is possible to reach complete extractions in a single-step.

Despite the large interest devoted to IL-ABS as extractive systems of outstanding performance, the recovery of the extracted added-value products and the systems recyclability and reusability have been seldom studied. An efficient and environmentally safe extraction/purification combined process for IL-ABS was proposed in this thesis. In each cycle, the IL recovery efficiency was between 94-95%. The recycling of the IL and its further recyclability was established without losses in the extractive performance of the corresponding ABS.

Solid-liquid extractions from biomass using aqueous solutions of ILs were also investigted in this thesis. The extraction of caffeine from bioresources, *e.g.* guaraná seeds and spent coffee, was carried out with aqueous solutions of a large variety of ILs. Compared with traditional extraction methods this new strategy proved to be selective towards caffeine and capable of providing high extraction yields. The recovery and reusability of the ILs were successfully demonstrated supporting the economic viability and low environmental footprint of the proposed methodology. The time and temperature of extraction were greatly reduced compared to conventional methods. These advantages coupled to the high extraction yields make the proposed technique promising for large-scale applications. In this context, the use of aqueous solutions of ILs for the extraction of value-added compounds from other biomass sources is straightforward envisaged.

Finally, it was found that aqueous solutions of ILs may considerably enhance the solubility of vanillin, gallic acid and caffeine, playing the role of hydrotropes. In some cases, it was observed an increase in solubility of more than 40-fold. This phenomenon is of utmost important, since molecules can be further recovered from the hydrotrope solution by a

simple dilution with water or by a decrease in temperature because its solubility is highly sensitive to the hydrotrope concentration and temperature of equilibrium.

As future work it would be interesting to extend this type of extractions followed by purification to other high-value products, for instance triterpenic compounds, from Portuguese agroflorestry biomass, namely, residues of the cork, pulp and olive industries. To this end, aqueous or ethanol solutions of ionic liquids (ILs) should be investigated. The screening of the ILs to be employed can be carried out using the polarity scale developed in this work, along with experimental measurements of solubility of triterpenic compounds in ILs. Microwave- and ultrasound–assisted extractions also deserve to be addressed aiming at decreasing the IL concentration and time of extraction.

Supporting Information

Referring to Chapter 2.1: A Critical Assessment on the Formation of Ionic-Liquid-Based Aqueous Biphasic Systems in Acidic Media

Table S1: Initial weight fraction compositions used in the determination of the phase diagrams and indication of the possibility of forming liquid-liquid equilibrium systems.

IL + Na_2SO_4 + Water system	Weight fraction composition / (wt %)		LLE
	IL	Na_2SO_4	
$[C_2mim][CH_3SO_4]$	59.94	24.89	×
$[C_2mim][CF_3SO_3]$	59.17	24.89	✓
$[C_4mim]Cl$	79.61	24.89	×
	78.38	24.89	×
	69.70	24.89	×
	79.43	24.17	×
	70.05	24.17	×
	63.73	24.08	×
	54.80	24.08	×
	49.69	24.08	×
$[C_4mim]Br$	59.40	24.89	✓
$[C_4mim][CH_3CO_2]$	62.06	24.89	×
$[C_4mim][CF_3SO_3]$	59.41	24.98	✓
$[C_4mim][N(CN)_2]$	60.45	24.98	✓
$[C_4mim][HSO_4]$	60.05	24.98	×
$[C_4mim][CH_3SO_4]$	59.46	24.98	✓
$[C_4mim][C_2H_5SO_4]$	60.83	24.98	✓
$[C_4mim][TOS]$	59.43	24.98	✓
$[C_4mim][SCN]$	59.29	24.48	✓
$[C_4mim][CF_3CO_2]$	59.84	23.85	✓
$[C_4mim][OctylSO_4]$	59.27	24.15	✓
$[C_6mim]Cl$	61.52	24.89	×
$[C_7mim]Cl$	59.27	24.98	✓
$[amim][C_2H_5SO_4]$	63.51	24.89	×
$[C_7H_7mim]Cl$	78.64	24.98	×
	60.68	24.50	✓
$[C_7H_7mim][C_2H_5SO_4]$	60.36	24.50	✓

$[C_4mim][DMP]$	58.74	24.98	×
$[C_4mpyr]Cl$	59.85	24.98	×
	46.60	24.98	×
$[C_4mpip]Cl$	59.19	24.98	×
$[C_4mpy]Cl$	59.58	24.89	×
$[C_8py][N(CN)_2]$	60.42	24.98	✓

×: a liquid-liquid two-phase system was not observed

✓: a liquid-liquid two-phase system was observed

Table S2: Weight fraction binodal data for the ternary systems with the ILs (1) $[C_4mim]Br$ and $[C_7mim]Cl$, Na_2SO_4 (2) and water (3) at 298 K.

$[C_4mim]Br$ *Mw* = 219.12		$[C_7mim]Cl$ *Mw* = 216.75	
100 w_1	100 w_2	100 w_1	100 w_2
54.0393	2.2450	49.1640	4.5704
50.0374	2.9426	46.0364	5.4667
46.3758	3.5181	42.2129	6.7470
42.6690	4.3629	36.0936	8.9788
40.7340	4.9203		
39.1392	5.3432		
34.1860	7.1392		

Table S3: Weight fraction binodal data for the ternary systems with the ILs (1) $[C_4mim][CF_3SO_3]$ and $[C_7H_7mim]Cl$, Na_2SO_4 (2) and water (3) at 298 K.

$[C_4mim][CF_3SO_3]$ *Mw* = 288.29				$[C_7H_7mim]Cl$ *Mw* = 208.69	
100 w_1	100 w_2	100 w_1	100 w_2	100 w_1	100 w_2
55.9574	1.7420	15.1997	6.4856	52.1187	3.4585
49.4163	2.1839	14.4891	6.9713	46.5538	4.8036
42.6622	2.5451	12.2491	7.8038	40.8953	6.1407
34.8741	3.1113	11.5476	8.2326	37.6422	7.2163
32.6968	3.3737	11.0102	8.5085	33.4692	8.8851
30.5625	3.6435	10.0308	9.1107		
29.0106	3.7196	9.3828	9.5904		
27.7697	3.9934	8.8289	10.1775		
26.0803	4.1160	7.7806	11.0171		
24.7855	4.3262	7.1237	11.6274		
23.4750	4.3606	6.7579	12.1002		
22.8571	4.5089	5.8257	13.2419		
21.6940	4.7606	5.2346	13.9924		
20.6162	5.0007	4.6460	14.9558		
19.2576	5.3606	4.2967	15.4922		
17.9431	5.6416	3.8793	16.2220		
16.7055	5.9138	3.5031	16.9919		
16.0429	6.1503				

Table S4: Weight fraction binodal data for the ternary system with the IL (1) [C_4mim][TOS], Na_2SO_4 (2) and water (3) at 298 K.

[C_4mim][TOS] *Mw* = 310.42					
100 w_1	100 w_2	100 w_1	100 w_2	100 w_1	100 w_2
55.1134	2.1965	19.3974	11.2545	11.2386	14.6425
52.3394	2.6370	19.0500	11.4263	10.8706	14.8501
49.0955	2.8920	18.5964	11.5308	10.5177	15.0144
47.6123	3.1879	18.2917	11.6676	10.3712	15.1164
45.5860	3.4124	17.9707	11.8142	10.1745	15.2113
44.3467	3.7432	17.6109	12.0100	10.0096	15.3772
43.0472	4.0834	17.4088	12.0376	9.8803	15.4039
40.4762	4.7220	17.1820	12.1230	9.6622	15.5324
38.3937	5.2297	16.8909	12.2817	9.4526	15.6658
36.5879	5.6003	16.4149	12.4691	9.2542	15.7874
35.8001	5.7930	16.2235	12.4916	9.0369	15.9254
35.0292	6.0081	15.9246	12.6629	8.6186	16.1558
34.1439	6.3172	15.7350	12.7080	8.3261	16.3428
33.3922	6.5271	15.5763	12.7441	8.0952	16.4750
32.5639	6.7218	15.4164	12.8053	7.9051	16.5861
31.9451	6.9343	15.1744	12.9359	7.5276	16.8535
31.2862	7.1026	15.0058	12.9715	7.2816	17.0011
30.6430	7.2707	14.7916	13.0911	6.9570	17.2276
30.0079	7.3962	14.5786	13.2072	6.6214	17.5031
29.4015	7.5716	14.3603	13.3118	6.2816	17.7352
28.8451	7.7471	14.2303	13.3293	6.0770	17.9045
28.3121	7.9154	13.9992	13.4720	5.9626	18.0061
26.5392	8.5570	13.8788	13.4957	5.7514	18.2244
25.8754	8.8774	13.6864	13.5946	5.4535	18.4622
25.5197	8.9404	13.3823	13.7201	5.2532	18.6667
24.9577	9.1554	13.2580	13.7511	5.1007	18.7947
24.4377	9.3715	13.1571	13.7965	4.9191	18.9523
24.0474	9.4984	12.9707	13.9066	4.8301	19.0611
23.5909	9.6437	12.8544	13.9330	4.6437	19.2740
22.8076	9.8880	12.6924	14.0296	4.3385	19.5714
22.2451	10.1692	12.5264	14.1223	4.0870	19.8312
21.2068	10.4920	12.4110	14.1580	3.8341	20.2070
20.8417	10.6302	12.2465	14.2600	3.6212	20.4269
20.4646	10.7767	12.1334	14.2944	3.4326	20.6973
20.0577	10.9956	11.7681	14.3944	3.2827	20.8456
19.7507	11.0861	11.4662	14.5194		

Table S5: Weight fraction binodal data for the ternary system with the IL (1) $[C_4mim][N(CN)_2]$, Na_2SO_4 (2) and water (3) at 298 K.

$[C_4mim][N(CN)_2]$ Mw = 205.26					
100 w_1	100 w_2	100 w_1	100 w_2	100 w_1	100 w_2
59.2507	0.5991	19.3120	9.2399	10.5544	13.2900
54.8690	1.1009	18.9342	9.4514	10.2598	13.3806
51.8550	1.6138	18.4497	9.6099	10.1166	13.4258
47.9001	1.9655	17.9810	9.7746	10.0147	13.5064
45.7296	2.3546	17.7649	9.8481	9.8187	13.6411
43.2478	2.6726	17.5410	9.9005	9.6239	13.7901
41.4875	3.0222	17.3206	9.9768	9.3697	13.9669
39.7641	3.3222	17.1234	10.0482	9.0471	14.1683
38.7154	3.6490	16.9255	10.1182	8.8929	14.2606
37.4124	3.9044	16.6287	10.2968	8.7105	14.4260
35.9524	4.1705	16.2728	10.4175	8.3211	14.7223
34.7078	4.4181	16.0995	10.4923	8.0822	14.8679
33.9512	4.6701	15.9253	10.5539	7.8427	15.0854
32.7114	4.9416	15.7515	10.6159	7.4506	15.4000
31.9583	5.1872	15.5882	10.6604	7.1248	15.6940
31.2631	5.3689	15.3151	10.8452	6.7903	16.0136
30.3312	5.4886	15.1581	10.9127	6.5486	16.2837
29.6970	5.7078	14.9995	10.9872	6.4309	16.3862
29.1123	5.8740	14.8507	11.0481	6.3199	16.5247
28.5183	6.1085	14.6931	11.0881	6.1377	16.7014
27.9697	6.3166	14.4710	11.2360	5.9503	16.9071
27.1516	6.4626	14.1961	11.3348	5.7490	17.1101
26.5973	6.6612	14.0631	11.3673	5.3191	17.9163
25.5167	7.0438	13.9227	11.4104	5.2314	17.8581
25.0388	7.2168	13.7166	11.5710	5.1330	17.9955
24.5804	7.4327	13.4617	11.6521	5.0040	18.2019
24.1565	7.5785	13.1654	11.8092	4.7432	18.5431
23.7470	7.7101	12.8565	11.9486	4.5561	18.8122
23.3335	7.8485	12.6568	12.0365	4.4179	19.0152
22.9589	8.0339	12.4205	12.1512	4.3237	19.1583
22.2747	8.2669	12.2737	12.2618	4.1728	19.4197
21.6125	8.5008	11.9127	12.4634	3.9017	19.8292
20.9677	8.7064	11.7399	12.5114	3.7390	20.1007
20.6801	8.7899	11.6039	12.5993	3.6139	20.3203
20.3732	8.8735	11.3870	12.7199	3.4851	20.5542
19.8287	9.0598	11.1653	12.8373	3.3498	20.8181
19.5651	9.1478	10.9648	12.9529		

Table S6: Weight fraction binodal data for the ternary systems with the ILs (1) $[C_8py][N(CN)_2]$ and $[C_2mim][CF_3SO_3]$, Na_2SO_4 (2) and water (3) at 298 K.

$[C_8py][N(CN)_2]$ *Mw* = 258.36				$[C_2mim][CF_3SO_3]$ *Mw* = 260.24	
100 w_1	100 w_2	100 w_1	100 w_2	100 w_1	100 w_2
57.5580	1.2385	15.1578	5.5323	53.3158	2.4638
43.6287	2.0683	15.0073	5.5637	49.4139	3.0753
39.1437	2.2653	14.8937	5.6462	44.4428	3.7831
33.8130	2.6257	14.7083	5.7134	43.1016	3.9712
31.2184	2.9191	14.5026	5.7610	41.2364	4.3877
28.7135	3.1255	14.3661	5.7754	39.5981	4.8028
27.4374	3.3485	14.2455	5.8154	38.1521	5.2062
26.1565	3.4498	14.1186	5.8513	36.4040	5.6931
25.4447	3.4785	13.9139	5.8647	34.7971	6.1124
25.1179	3.5793	13.8500	5.9203	33.4398	6.4554
24.4985	3.6185	13.6765	5.9861	32.2907	6.7684
24.0542	3.6921	13.3575	6.0368	30.7529	7.2544
23.7701	3.7390	13.2439	6.0828	29.6633	7.5532
23.2812	3.8205	13.1093	6.1252	28.3340	8.0048
22.8095	3.8829	12.8933	6.2292	27.4934	8.2396
22.2150	3.9714	12.6171	6.3006	26.6661	8.5056
21.7859	4.0411	12.4076	6.4226	25.5859	8.8881
21.4472	4.1088	11.8153	6.5740	24.8934	9.1017
20.0571	4.3784	11.5904	6.7487	23.9731	9.4298
19.7457	4.5182	11.0104	6.8955	23.3184	9.5977
19.3349	4.5297	10.7827	6.9758	22.5173	9.9069
19.0429	4.5861	10.4877	7.1538	21.9252	10.0743
18.8071	4.7018	9.9474	7.5127	21.1417	10.3506
18.3628	4.7188	9.4912	7.5706	20.3808	10.6432
18.0543	4.8616	9.2734	7.7176	19.5504	10.9968
17.6229	4.8907	8.9230	7.8876	18.9203	11.2141
17.4320	4.9866	8.5210	8.0841	18.1378	11.5603
17.1705	5.0127	8.2254	8.2800	17.6013	11.7560
17.0422	5.0789	7.9646	8.4414	17.0099	12.0153
16.8599	5.1180	7.7605	8.4937	16.4263	12.2785
16.7032	5.1333	7.2879	8.7874	15.7777	12.6050
16.5480	5.1933	6.8013	9.1839	15.1860	12.8932
16.4349	5.2182	6.0454	9.8807	14.6977	13.1162
16.3280	5.2782	5.5230	10.3016	14.0930	13.4521
16.1708	5.2916	5.2292	10.5481	12.5720	14.3292
16.0378	5.3457	4.7336	11.0829	11.5895	14.8978
15.8360	5.3427	4.2814	11.6575	10.8252	15.3583
15.7188	5.3703	3.8289	12.2741	9.4095	16.4006
15.4709	5.5858	3.4029	12.9468	8.1689	17.4210

Table S7: Weight fraction binodal data for the ternary systems with the ILs (1) $[C_7H_7mim][C_2H_5SO_4]$, $[C_4mim][CH_3SO_4]$ and $[C_4mim][C_2H_5SO_4]$, Na_2SO_4 (2) and water (3) at 298 K.

$[C_7H_7mim][C_2H_5SO_4]$ *Mw* = 298.36		$[C_4mim][CH_3SO_4]$ *Mw* = 250.32		$[C_4mim][C_2H_5SO_4]$ *Mw* = 265.35	
100 w_1	100 w_2	100 w_1	100 w_2	100 w_1	100 w_2
53.3251	2.8555	53.3183	3.1271	56.8853	1.7503
50.0374	3.4612	46.1214	4.4358	41.9873	4.2498
46.1067	4.0318	40.6256	5.4312	39.0972	5.0302
44.4395	4.2513	38.7093	5.9070	36.8093	5.8472
43.1716	4.5200	37.2599	6.5209	34.5103	6.4383
41.4795	5.0534	34.6465	7.4609	33.3151	6.8799
40.5604	5.3062	33.4808	7.9653	30.8742	7.8076
39.5924	5.5147	32.3996	8.4007	29.5095	8.4032
38.3225	5.8618	31.3748	8.8180	27.6936	9.1974
37.5132	6.0479	30.0638	9.4826	26.3776	9.8560
36.2727	6.4353	28.6195	10.2025	25.0556	10.5662
33.7954	7.4438	27.5691	10.7060	22.2210	12.1135
32.3485	7.9584	26.4669	11.2814	18.6276	14.2831
30.7323	8.5199	24.8772	12.1464	17.3126	15.0240
29.6636	8.8972	23.2223	13.1486	15.7241	16.0192
28.7666	9.1631	22.0758	13.7757	14.2479	16.9511
27.3528	9.7434	20.8716	14.4885	12.3795	18.1727
26.4785	10.0547	19.5884	15.2581		
25.6092	10.3728	18.4211	15.9849		
24.3068	10.9243	17.4049	16.6016		
23.7376	11.0762	16.3759	17.2508		
22.7202	11.4954	15.4763	17.8197		
21.9493	11.8047	14.4705	18.4983		
20.8771	12.2551	13.6965	19.0167		
20.1465	12.5739	12.6420	19.7702		
19.4855	12.8456	11.6527	20.4815		
18.8382	13.1165	9.7585	21.9799		
18.1796	13.3200				
17.2887	13.7520				
16.8193	13.9515				
16.2200	14.2279				
15.6623	14.4678				
15.0916	14.7390				
14.5730	14.9957				
13.4582	15.6343				
12.7531	15.9859				
12.2490	16.2463				
10.5122	17.2697				

Table S8: Weight fraction binodal data for the ternary system with the IL (1) [C_4mim][SCN], Na_2SO_4 (2) and water (3) at 298 K.

[C_4mim][SCN] *Mw* = 197.30					
100 w_1	100 w_2	100 w_1	100 w_2	100 w_1	100 w_2
57.5738	0.8303	27.0777	5.9257	18.7073	8.2460
53.9628	1.1600	26.7329	6.0279	18.5045	8.3199
50.9712	1.4404	26.3934	6.1002	18.3465	8.3502
48.5957	1.7133	25.7872	6.3460	18.1373	8.4248
46.2918	1.9667	25.2506	6.4612	17.9912	8.4612
44.9986	2.1794	24.9732	6.5155	17.8621	8.4865
43.3866	2.4218	24.2380	6.5705	17.6217	8.5751
41.9224	2.6317	23.8769	6.6026	17.4784	8.6025
41.1097	2.8108	23.5712	6.6940	17.2918	8.6740
40.0127	2.9660	23.2450	6.8028	17.0928	8.7502
39.3305	3.1692	23.0628	6.8562	16.8122	8.8477
37.9443	3.3599	22.6677	7.0242	16.4956	8.9395
37.0014	3.5453	22.4352	7.0664	16.2992	8.9908
36.1788	3.7815	21.9488	7.3073	16.0377	9.1371
35.4258	3.9700	21.4429	7.4431	15.6756	9.2550
34.4680	4.1346	20.9500	7.5668	15.3430	9.3395
33.7604	4.3214	20.6933	7.6422	14.9245	9.5164
33.0829	4.4905	20.4880	7.6787	14.5155	9.6889
32.4038	4.6906	20.3089	7.7213	14.1601	9.7929
31.5563	4.8243	20.1169	7.7828	13.7544	9.9780
30.5506	5.1218	19.8958	7.8798	13.3260	10.1127
29.8752	5.2292	19.6628	7.9419	12.7376	10.3386
28.8476	5.5606	19.4473	8.0189	12.3677	10.5710
28.0485	5.6835	19.0982	8.0954		
27.5575	5.8476	18.8970	8.1739		

Table S9: Weight fraction binodal data for the ternary systems with the IL (1) $[C_4mim][OctylSO_4]$ and $[C_4mim][CF_3CO_2]$, Na_2SO_4 (2) and water (3) at 298 K.

$[C_4mim][OctylSO_4]$ M*w* = 348.50		$[C_4mim][CF_3CO_2]$ *Mw* = 252.23			
100 w_1	100 w_2	100 w_1	100 w_2	100 w_1	100 w_2
50.4923	3.7322	27.6961	7.4667	52.0163	2.9569
48.8330	3.9844	27.2000	7.4998	50.0083	3.4104
47.5778	4.1861	26.7533	7.6143	47.4128	3.9047
46.0034	4.3229	26.4212	7.6527	46.1852	4.1153
45.0137	4.4907	26.0906	7.7589	44.2050	4.5090
43.2074	4.7404	25.6888	7.7814	42.1174	5.0320
42.2903	4.9300	25.1558	7.9939	40.0146	5.6424
40.9665	5.0396	24.8323	8.0256	38.2476	6.1923
40.2341	5.1995	24.5738	8.0619	37.1187	6.5210
39.4277	5.3508	24.2490	8.1319	35.4945	7.0556
37.8899	5.5494	23.9253	8.2085	33.3666	7.8645
37.1916	5.7023	23.6289	8.2789	31.4022	8.5822
36.5527	5.7813	23.3233	8.3292	28.4571	9.8569
35.9582	5.9066	22.7524	8.5529		
35.3766	6.0282	22.1483	8.6323		
34.6075	6.1082	21.8718	8.6771		
34.1392	6.1778	21.5108	8.8381		
33.7578	6.2388	20.9420	8.9397		
33.1989	6.3988	20.6728	8.9856		
32.6786	6.4804	20.1839	9.1524		
31.9347	6.5848	19.9185	9.1854		
31.4104	6.7138	19.4921	9.2927		
30.8496	6.7845	19.0831	9.4403		
30.4399	6.8696	18.6507	9.5428		
29.9646	6.9850	18.4249	9.5825		
29.4289	7.1115	18.1628	9.6761		
28.5336	7.2650	17.8320	9.7534		
28.1409	7.3259				

Referring to **Chapter 2.2: Evaluation of the impact of phosphate salts on the formation of ionic-liquid-based aqueous biphasic systems –**

Table S10: Weight fraction data for the ternary systems composed of IL (1), K_3PO_4 (2) and water (3) at 298 K.

[C_4mim][TOS] Mw = 310.36					
100 w_1	100 w_2	100 w_1	100 w_2	100 w_1	100 w_2
48.05	2.71	26.51	8.60	17.39	12.02
46.35	3.08	26.04	8.65	17.18	12.03
44.72	3.37	25.23	9.11	17.03	12.09
42.90	3.71	24.64	9.36	16.75	12.34
41.59	4.16	24.24	9.46	16.52	12.49
39.66	4.35	23.72	9.68	16.19	12.51
38.94	4.62	23.06	9.87	16.02	12.55
37.41	5.11	22.26	9.98	15.73	12.62
36.18	5.27	21.75	10.26	15.63	12.67
34.96	5.79	21.44	10.31	15.41	12.79
34.20	5.95	20.99	10.55	15.23	12.81
33.40	6.09	20.64	10.63	17.03	12.09
32.50	6.47	20.23	10.79		
31.66	6.75	19.83	10.90		
30.86	7.04	19.48	11.05		
30.26	7.22	19.19	11.19		
29.61	7.32	18.81	11.47		
28.89	7.68	18.57	11.51		
28.32	7.76	18.35	11.53		
27.60	8.11	18.02	11.79		
26.80	8.50	17.80	11.78		

Table S11: Weight fraction data for the ternary systems composed of IL (1), K_3PO_4 (2) and water (3) at 298 K.

$[C_4mim][CH_3SO_4]$ *Mw* = 250.32		$[C_4mim][C_2H_5SO_4]$ *Mw* = 265.35		$[C_4mim][DMP]$ *Mw* = 264.14	
100 w_{1*}	100 w_{2*}	100 w_{1*}	100 w_{2*}	100 w_{1*}	100 w_{2*}
29.09	10.05	20.48	14.06	20.27	15.83
28.09	10.60	19.59	14.40	19.91	15.90
27.11	11.10	18.74	14.65	19.45	16.19
26.36	11.42	17.33	15.45	19.02	16.52
25.39	12.07	16.75	15.79	18.58	16.86
24.77	12.31	16.45	15.81	18.11	17.28
23.98	12.79	15.90	16.19	14.76	20.34
23.52	13.07	15.32	16.50	14.11	20.98
22.91	13.41	14.79	16.81	13.32	21.68
22.25	13.77	14.38	17.08	12.81	22.00
21.60	14.11	13.89	17.45	12.27	22.58
20.92	14.59	13.55	17.59	11.95	22.76
20.39	14.92	13.30	17.80	10.98	23.72
19.93	15.09	12.90	18.02	10.57	23.97
19.43	15.39	12.57	18.25	10.27	24.33
18.88	15.80	12.06	18.55		
18.26	16.23	11.74	18.74		
		11.40	18.93		
		11.15	19.07		
		10.93	19.18		
		10.70	19.42		

Table S12: Weight fraction data for the ternary systems composed of IL (1), K_2HPO_4 (2) and water (3) at 298 K.

$[C_4mim][CF_3SO_3]$ *Mw* = 288.29		$[C_4mim][N(CN)_2]$ *Mw* = 205.26			
100 w_1	100 w_2	100 w_1	100 w_2	100 w_1	100 w_2
59.04	1.87	58.93	0.84	16.52	12.24
50.38	2.57	53.68	1.48	16.31	12.35
43.62	2.87	48.77	2.05	15.97	12.35
40.18	3.29	45.48	2.75	15.70	12.47
36.61	3.60	42.82	3.20	15.47	12.62
34.13	3.84	40.31	3.98	15.25	12.71
32.03	4.15	37.57	4.44	14.99	12.81
30.11	4.33	35.43	4.92	14.79	12.95
28.89	4.58	33.97	5.37	14.59	13.01
27.45	4.88	32.93	5.89	14.40	13.12
26.04	4.97	31.60	6.09	14.24	13.17
24.93	5.15	30.71	6.49	14.10	13.24
23.66	5.32	29.68	6.81	13.92	13.30
22.52	5.44	28.57	7.05	13.75	13.38
21.95	5.69	27.85	7.38	13.59	13.46
21.28	5.88	27.10	7.61	13.43	13.53
20.51	6.00	26.46	7.93	13.23	13.73
19.71	6.14	25.60	8.06	12.96	13.83
19.35	6.36	25.05	8.30	12.81	13.91
18.77	6.49	24.46	8.57	12.66	14.00
18.37	6.64	23.95	8.79	12.51	14.05
17.51	6.92	23.23	8.89	12.39	14.10
17.09	7.06	22.32	9.97	12.21	14.28
16.70	7.22	21.90	10.13		
16.31	7.34	21.10	10.46		
15.78	7.66	20.48	10.55		
15.17	8.02	20.14	10.73		
14.71	8.04	19.78	10.92		
14.33	8.28	19.12	11.28		
13.98	8.36	18.55	11.36		
13.52	8.73	18.28	11.47		
13.26	8.80	18.01	11.55		
13.08	8.93	17.71	11.74		
12.88	9.04	17.45	11.89		
12.59	9.29	16.96	12.11		

Table S13: Weight fraction data for the ternary systems composed of IL (1), K_2HPO_4 (2) and water (3) at 298 K,

[C_4mim][TOS] Mw = 310.36					
100 w_1	100 w_2	100 w_1	100 w_2	100 w_1	100 w_2
50.99	2.79	20.69	12.39	11.67	16.79
48.59	3.02	20.09	12.68	11.62	16.57
47.64	3.29	19.61	12.85	11.41	16.66
46.11	3.57	18.93	13.19	11.27	16.78
45.43	3.92	18.51	13.38	11.11	16.84
43.68	4.25	17.88	13.64	10.94	16.94
42.57	4.40	17.49	13.91	10.83	17.01
42.05	4.59	16.94	14.13	10.76	17.03
41.55	4.79	16.46	14.36	10.71	17.07
40.20	5.09	16.05	14.58		
38.87	5.57	15.76	14.70		
37.83	5.87	15.57	14.73		
37.22	6.08	15.41	14.86		
36.70	6.19	15.25	14.87		
35.53	6.62	15.05	15.04		
35.00	6.77	14.84	15.10		
33.99	7.20	14.49	15.33		
33.06	7.50	14.31	15.37		
32.40	7.55	14.20	15.41		
31.94	7.77	14.04	15.56		
31.58	7.85	13.83	15.65		
31.18	7.97	13.64	15.69		
30.69	8.30	13.51	15.78		
29.97	8.51	13.39	15.88		
29.30	8.76	13.21	15.93		
28.96	8.90	13.14	15.98		
28.55	9.10	13.06	16.02		
27.95	9.53	12.84	16.16		
27.30	9.56	12.67	16.21		
26.54	9.89	12.54	16.37		
25.66	10.29	12.38	16.44		
25.10	10.45	12.27	16.44		
24.53	10.69	12.20	16.48		
23.96	11.09	12.11	16.55		
22.99	11.48	11.96	16.62		
22.32	11.67	11.81	16.73		

Table S14: Weight fraction data for the ternary systems composed of IL (1), K_2HPO_4 (2) and water (3) at 298 K.

$[C_4mim][CH_3SO_4]$ *Mw* = 250.32				$[C_4mim][C_2H_5SO_4]$ *Mw* = 265.35	
100 w_1	100 w_2	100 w_1	100 w_2	100 w_1	100 w_2
25.34	14.12	8.73	27.28	37.14	6.80
23.54	14.92	8.41	27.57	35.49	7.61
21.44	16.85	8.17	27.84	33.64	8.34
20.13	17.88	8.02	27.98	33.07	8.44
19.20	18.46	7.76	28.26	32.03	9.19
18.15	19.27	7.58	28.52	30.59	9.83
17.19	19.98	7.42	28.67	29.53	10.57
15.52	21.37	7.25	28.85	28.49	11.12
15.18	21.45	7.06	29.08	27.67	11.27
14.47	22.09	6.88	29.30	26.51	12.06
13.82	22.70	6.67	29.59	25.38	12.81
13.44	22.92	6.49	29.79	24.63	13.38
12.90	23.33	6.30	30.06	24.06	13.57
12.51	23.72	6.12	30.32	22.99	14.40
12.24	23.87	5.96	30.54	22.49	14.57
11.81	24.25	5.67	30.96	21.62	15.31
11.49	24.60	5.41	31.28		
11.07	24.97	5.22	31.61		
10.67	25.32	4.89	32.24		
10.26	25.73	4.65	32.55		
9.92	26.14	4.42	32.92		
9.70	26.27	4.12	33.47		
9.34	26.67	3.85	34.01		
9.13	26.91	3.60	34.49		
9.02	26.95	3.36	34.99		

Table S15: Weight fraction data for the ternary systems composed of IL (1), K_2HPO_4 (2) and water (3) at 298 K.

[C_4mim]Cl *Mw* = 174.67				[C_4mim]Br *Mw* = 219.12	
100 w_1	100 w_2	100 w_1	100 w_2	100 w_1	100 w_2
46.99	4.64	11.52	24.71	59.54	0.45
39.45	5.10	11.20	25.11	56.23	1.15
36.98	5.53	10.95	25.37	53.34	1.74
35.36	6.14	10.70	25.66	47.09	3.11
34.12	6.87	10.43	25.97	45.20	3.30
33.18	7.19	10.20	26.23	44.53	3.61
31.50	8.32	9.95	26.53	42.09	4.87
30.70	8.58	9.72	26.83	39.47	5.56
29.98	8.81	9.48	27.15	37.88	6.04
28.93	9.29	9.28	27.35	36.91	6.44
27.69	10.05	9.11	27.63	35.80	7.01
26.33	10.72	8.93	27.82	34.91	7.39
25.39	11.42	8.72	28.10	33.94	7.96
23.56	12.81	7.91	28.19	33.13	8.29
22.80	13.43	7.79	28.29	32.15	8.87
22.12	14.00	8.54	28.30	31.53	9.19
21.38	14.49	7.62	28.55	30.99	9.48
20.64	15.09	8.30	28.64	30.04	10.02
20.19	15.68	7.49	28.71	29.29	10.52
19.69	16.03	8.13	28.84	28.67	10.86
18.90	16.86	7.38	28.88	28.04	11.02
18.69	16.98	7.23	29.12	26.76	11.79
18.29	17.40	7.04	29.42	26.28	12.18
17.79	17.92			25.95	12.36
17.26	18.39			25.39	12.77
16.86	18.78			25.09	12.96
16.23	19.45			24.51	13.39
15.70	20.08			23.96	13.80
15.35	20.39			23.37	14.24
14.88	20.89			22.87	14.62
14.39	21.42			22.01	15.32
14.09	21.75			21.59	15.59
13.84	22.11			21.18	15.88
13.54	22.39			20.82	16.16
13.21	22.77			20.29	16.63
12.94	23.06			19.99	16.79
12.68	23.34			19.61	17.18
12.27	23.84			19.32	17.32
11.98	24.17			18.94	17.63
11.66	24.54			18.56	17.94

Table S16: Weight fraction data for the ternary systems composed of IL (1), K_2HPO_4 (2) and water (3) at 298 K.

[C_4mim][DMP] *Mw* = 264.14				[C_4mim][CH_3CO_2] *Mw* = 198.26	
100 w_1	100 w_2	100 w_1	100 w_2	100 w_1	100 w_2
33.81	8.54	12.36	26.39	30.24	9.63
32.68	9.03	12.02	26.73	29.54	9.76
29.95	10.72	11.62	27.19	27.26	11.10
28.95	11.46	11.31	27.51	26.31	11.65
27.81	12.28	11.09	27.72	25.56	12.11
26.70	13.04	10.98	27.81	24.32	13.00
25.73	13.66	10.69	28.16	23.30	13.76
24.48	14.75	10.48	28.44	22.88	14.11
23.71	15.41	10.27	28.61	21.92	14.95
22.74	16.31	10.02	28.89	21.45	15.44
21.93	16.99	9.69	29.31	20.63	16.16
21.14	17.65	9.55	29.43	19.58	17.16
20.37	18.30	9.32	29.75	18.97	17.73
19.47	19.14	9.13	29.95	18.73	17.97
18.69	19.94	8.91	30.23	18.06	18.68
18.13	20.41	7.77	32.64	17.41	19.36
17.63	20.86	7.17	32.68	17.02	19.76
16.87	21.69	6.99	32.61	16.09	20.72
16.50	22.03	6.86	32.76	15.44	21.19
15.71	22.91	6.67	33.05	14.94	21.73
15.28	23.32	6.51	33.27	14.38	22.33
14.73	23.94			13.76	23.03
14.19	24.36			12.90	24.18
13.78	24.78			12.67	24.36
13.40	25.21			12.18	25.00
13.19	25.43			11.85	25.34
12.74	25.99			11.54	25.62

Table S17. Weight fraction data for the ternary systems composed of IL (1), K_2HPO_4 (2) and water (3) at 298 K.

[C_4mim][CH_3SO_3] *Mw* = 234.31					
100 w_1	100 w_2	100 w_1	100 w_2	100 w_1	100 w_2
56.91	1.64	20.47	18.59	9.96	29.37
52.94	2.54	19.73	19.29	9.74	29.57
47.50	3.71	19.50	19.48	9.44	29.93
43.86	5.18	18.84	20.11	9.22	30.17
40.77	5.73	17.50	21.48	8.91	30.60
39.14	6.44	16.91	22.05	8.67	30.92
37.92	6.94	16.37	22.65	8.46	31.14
36.47	7.68	15.91	23.06	8.23	31.51
34.79	8.78	15.37	23.64	7.88	31.89
33.81	9.15	14.73	24.36	7.65	32.19
32.44	10.03	14.30	24.77	7.35	32.53
31.09	10.69	13.86	25.16	7.19	32.79
29.52	11.77	13.42	25.59	7.00	33.03
28.17	12.71	13.08	25.96	6.83	33.28
27.03	13.58	12.66	26.40		
26.36	14.02	12.31	26.75		
25.32	14.75	11.87	27.23		
24.39	15.64	11.50	27.66		
23.56	16.22	11.08	28.18		
22.77	16.98	10.71	28.60		
22.08	17.48	10.44	28.79		
21.03	18.42	10.15	29.16		

Table S18: Weight fraction data for the ternary systems composed of IL (1), K_2HPO_4/KH_2PO_4 (2) and water (3) at 298 K.

[C_4mim][CF_3CO_2] *Mw* = 252.23					
100 w_1	100 w_2	100 w_1	100 w_2	100 w_1	100 w_2
57.40	2.69	24.38	12.88	14.99	19.59
49.07	4.63	23.22	13.55	13.90	20.46
39.80	6.36	21.84	14.51	13.20	21.02
36.90	7.17	20.24	15.67	12.29	21.75
35.26	7.83	18.70	16.84	11.39	22.52
29.51	9.69	17.44	17.77	10.62	23.18
27.37	11.14	16.35	18.58	9.53	24.24
25.94	11.84	15.87	18.93	8.29	25.46

Table S19: Weight fraction data for the ternary systems composed of IL (1), K_2HPO_4/KH_2PO_4 (2) and water (3) at 298 K.

[C_4mim]Br		[C_4mim][DMP]		[C_4mim][CH_3SO_4]	
Mw = 219.12		Mw = 264.14		Mw = 250.32	
100 w_1	100 w_2	100 w_1	100 w_2	100 w_1	100 w_2
59.55	1.03	30.21	11.43	23.51	16.12
53.05	2.13	28.43	12.61	21.64	17.64
48.08	2.80	22.39	17.98	20.26	18.66
44.12	4.03	27.00	13.67	19.06	19.66
42.26	4.73	25.61	14.88	17.77	20.68
39.79	5.13	24.39	15.98	16.36	21.87
37.09	6.80	23.13	17.10	15.24	22.80
35.15	7.11	22.04	17.91	14.21	23.69
33.60	7.90	21.03	18.77	13.35	24.45
32.58	8.87	19.92	19.95	12.34	25.42
31.60	9.20	18.84	20.93	11.39	26.33
29.43	10.79	17.54	22.24	10.48	27.22
27.99	11.76	16.83	22.76		
26.64	12.69	15.98	23.71		
24.50	14.30	15.32	24.50		
22.74	15.68	14.71	25.17		
21.41	16.70				
19.42	18.42				
17.83	19.82				
16.30	21.20				
14.79	22.58				
13.57	23.76				
12.16	25.14				
10.65	26.78				

Table S20: Weight fraction data for the ternary systems composed of IL (1), KH_2PO_4 (2) and water (3) at 298 K.

[C_4mim][CF_3SO_3] *Mw* = 288.29					
100 *w*1	100 *w*2	100 *w*1	100 *w*2	100 *w*1	100 *w*2
55.71	2.10	34.48	5.21	26.34	6.89
52.08	2.79	33.30	5.49	25.34	7.17
49.85	3.06	31.99	5.74	24.17	7.50
46.40	3.53	31.35	5.84	23.15	7.81
42.61	3.89	29.96	6.11	22.35	8.03
40.14	4.26	28.76	6.41	21.00	8.50
38.19	4.64	27.90	6.58	19.74	8.98
35.51	5.08	27.10	6.74		

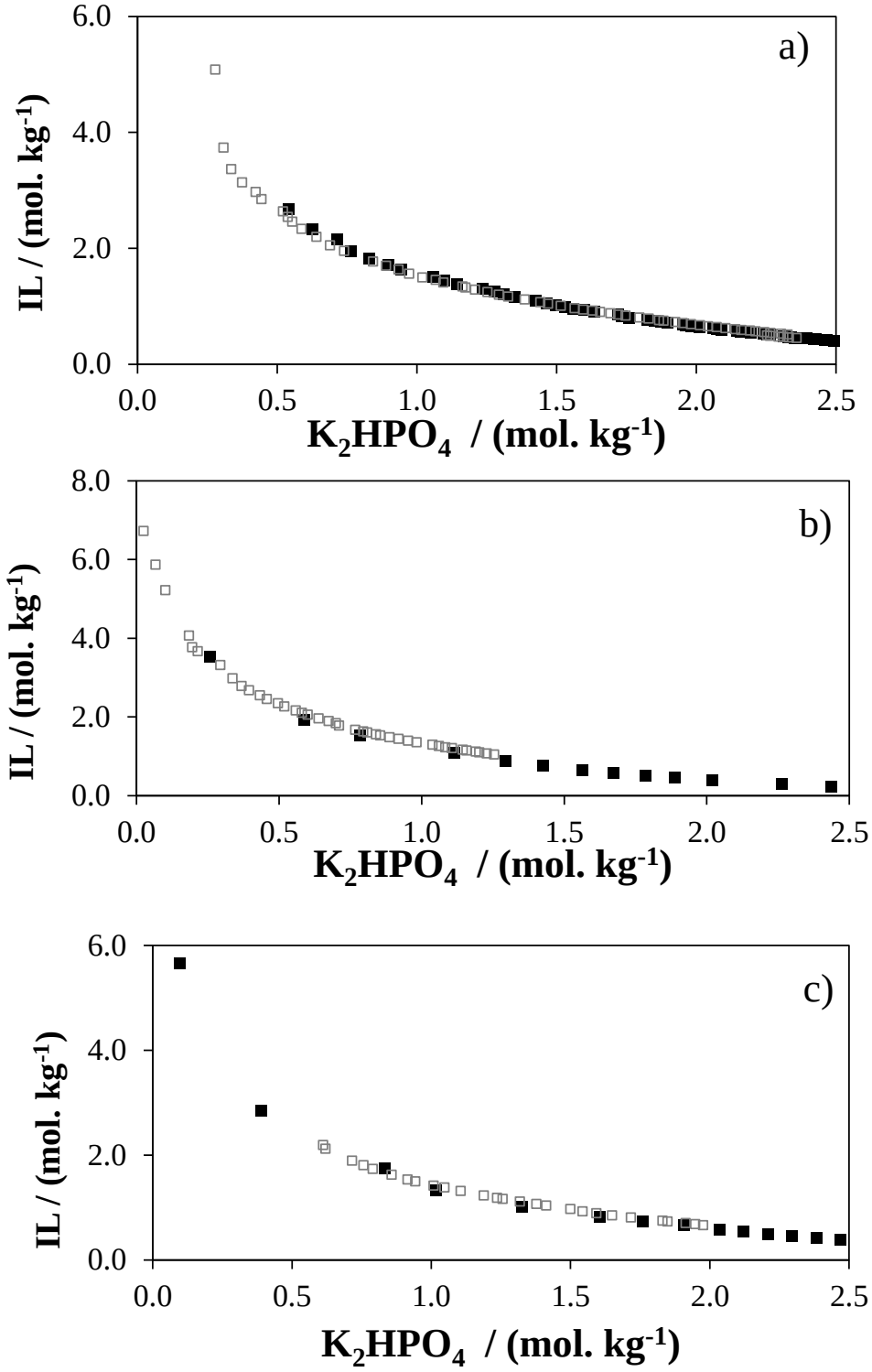

Figure S1: Phase diagram for the ternary system composed of IL + K_2HPO_4+ H_2O at 298 K: a) [C_4mim]Cl; b) [C_4mim]Br; c) [C_4mim][CH_3CO_2]. The empty symbols correspond to data gathered in this work while the full symbols correspond to literature data[18,30,57].

Referring to Chapter 2.3: Extended Scale for the Hydrogen-Bond Basicity of Ionic Liquids

Table S21: Hydrogen-bond basicity (β) data and van der Waals interaction energy in the equimolar cation-anion mixture (E_{vdW} / (kJ·mol^{-1})) taken from COSMO-RS calculations for [C_4mim]-based ILs.

IL	$\mathcal{B}^{10}$	$\mathcal{B}^{18}$	E_{vdW} / (kJ·mol^{-1})
[C_2mim][$N(CF_3SO_2)_2$]	0.23	n.a.	-57.77
[C_4mim][$N(CF_3SO_2)_2$]	0.23	0.42	-65.32
[C_4C_1mim][$N(CF_3SO_2)_2$]	0.24	n.a.	-67.91
[C_5mim][$N(CF_3SO_2)_2$]	0.26	n.a.	-69.16
[C_6mim][$N(CF_3SO_2)_2$]	0.26	0.44	-73.00
[C_8mim][$N(CF_3SO_2)_2$]	0.29	0.47	-80.81
[C_{10}mim][$N(CF_3SO_2)_2$]	n.a.	0.49	-88.72
[C_4mpy][$N(CF_3SO_2)_2$]	0.25	n.a	-67.68
[C_4mpyr][$N(CF_3SO_2)_2$]	0.25	n.a	-67.17
[C_5mpyr][$N(CF_3SO_2)_2$]	0.26	n.a	-70.26
[(C_2OC_2)mpyr][$N(CF_3SO_2)_2$]	0.28	n.a	-66.47
[C_4mim][PF_6]	0.19	0.44	-49.96
[C_6mim][PF_6]	n.a.	0.50	-57.97
[C_8mim][PF_6]	n.a.	0.53	-66.06
[C_{10}mim][PF_6]	n.a.	0.55	-74.20
[C_4mim][BF_4]	0.37	0.55	-48.81
[C_4C_1mim][BF_4]	0.36	n.a.	-51.51
[C_6mim][BF_4]	n.a.	0.60	-56.87
[C_8mim][BF_4]	n.a.	0.63	-64.99
[C_{10}mim][BF_4]	n.a.	0.65	-73.16
[C_4mim][CF_3SO_3]	0.48*	0.57	-55.71
[C_6mim][CF_3SO_3]	n.a.	0.61	-63.67
[C_8mim][CF_3SO_3]	n.a.	0.64	-71.71
[C_{10}mim][CF_3SO_3]	n.a.	0.65	-79.82
[C_4mim][ClO_4]	n.a.	0.55	-52.75
[C_4mim][$C(CN)_3$]	n.a.	0.54	-63.78
[C_4mim][$N(CN)_2$]	0.60	0.64	-56.70
[C_6mim][$N(CN)_2$]	n.a.	0.69	-64.55
[C_8mim][$N(CN)_2$]	n.a.	0.71	-72.50
[C_{10}mim][$N(CN)_2$]	n.a.	0.75	-80.49
[C_4mim][SCN]	n.a.	0.71	-59.37
[C_4mim][NO_3]	n.a.	0.74	-50.83
[C_6mim][NO_3]	n.a.	0.76	-58.83
[C_8mim][NO_3]	n.a.	0.80	-66.91
[C_{10}mim][NO_3]	n.a.	0.81	-75.06
[C_4mim][CF_3CO_2]	0.84*	0.74	-52.72
[C_4mim]I	n.a.	0.75	-61.86
[C_4mim][CH_3SO_4]	0.66	0.75	-59.38
[C_4mim][$C_8H_{17}SO_4$]	0.80*	0.77	-88.15
[C_4mim][CH_3SO_3]	0.77	0.85	-57.95
[C_4mim]Br	n.a.	0.87	-56.46
[C_4mim]Cl	0.84	0.95	-53.53
[C_6mim]Cl	n.a.	0.97	-61.62
[C_8mim]Cl	n.a.	0.98	-69.78
[C_{10}mim]Cl	n.a.	0.98	-77.99
[C_4mim][$(CH_3O)_2PO_2$]	1.12*	1.12	-65.04
[C_4mim][CH_3CO_2]	0.85	1.20	-55.57

*experimental data from this work

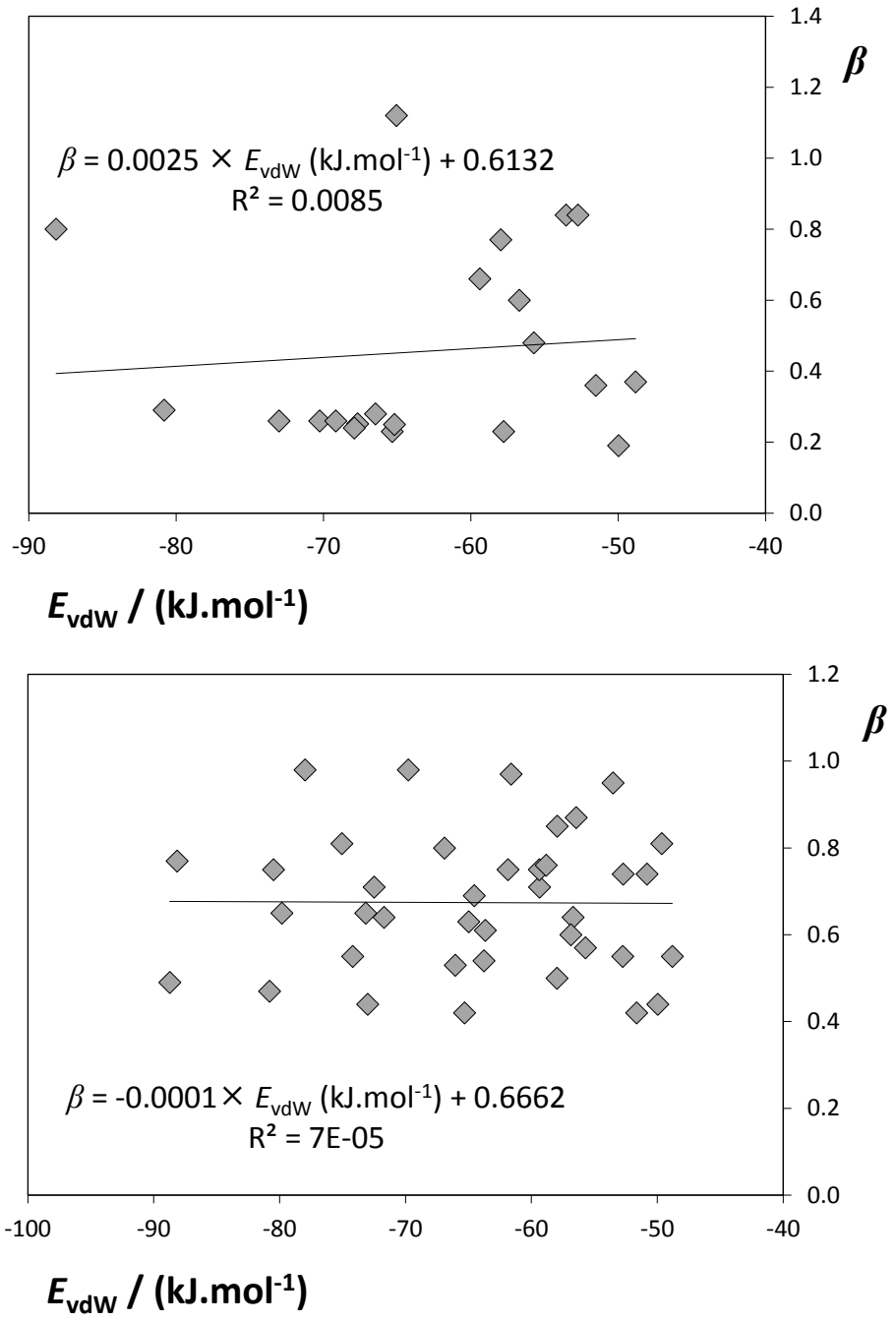

Figure S2: Correlation between the experimental values of hydrogen-bond basicity (β) and the E_{vdW} predicted by COSMO-RS: (a) experimental data from Welton and co-workers[10]; (b) experimental data from Lungwitz et al.[18].

Referring to Chapter 2.4: Characterization of Aqueous Biphasic Systems Composed of Ionic Liquids and a Citrate-Based Biodegradable Salt

Table S22. Weight fraction data for the system composed of IL (1) + $C_6H_5K_3O_7$ (2) + H_2O (3) at 298 K.

[C_4mim]Cl		[C_4mim]Br		[C_4mim][SCN]	
100 w_1	100 w_2	100 w_1	100 w_2	100 w_1	100 w_2
68.64	1.60	66.63	1.98	68.82	1.59
62.79	2.90	60.73	3.39	52.82	2.69
59.00	4.41	57.16	4.65	46.89	3.76
54.54	6.50	53.60	5.75	42.90	4.81
49.47	9.42	48.95	7.70	36.83	6.38
43.00	13.74	46.55	8.49	34.20	6.98
23.78	31.46	43.04	10.37	30.77	8.04
21.87	33.60	37.25	14.30	28.98	8.36
20.28	35.50	34.42	16.07	26.13	9.17
18.40	37.60	31.34	18.07	23.50	10.08
16.30	39.90	28.11	20.44	22.09	10.45
		25.24	22.47	20.63	11.18
		22.76	24.36	20.10	11.47
		20.81	25.92	19.47	11.76
		19.28	27.14	18.61	12.08
		17.38	28.80	18.21	12.32
		15.67	30.41	17.80	12.40
		14.06	31.98	14.64	13.83
				14.31	14.10

Table S23. Weight fraction data for the system composed of IL (1) + $C_6H_5K_3O_7$ (2) + H_2O (3) at 298 K.

$[C_4mim][CF_3CO_2]$		$[C_4mim][CF_3SO_3]$			
100 w_1	100 w_2	100 w_1	100 w_2	100 w_1	100 w_2
67.01	1.75	68.13	1.84	12.21	11.71
62.33	3.93	48.63	3.19	11.91	12.36
57.31	6.13	42.43	3.79	11.68	12.41
43.44	10.78	37.82	4.37	11.33	12.89
41.60	11.33	33.84	4.73	11.19	13.01
38.84	12.92	31.67	5.12	10.92	13.26
35.14	14.90	29.58	5.41	10.66	13.46
34.05	15.29	27.89	5.73	10.51	13.53
32.22	16.36	26.42	6.20	10.38	13.64
30.43	17.52	24.37	6.36	10.14	13.84
29.44	17.90	23.62	6.75	9.99	14.11
27.98	18.93	22.61	7.01		
26.33	19.86	21.66	7.27		
25.03	20.61	20.72	7.39		
23.93	21.33	20.17	7.61		
22.78	21.98	19.77	7.85		
21.71	22.67	19.12	8.15		
20.27	23.56	18.48	8.36		
19.32	24.15	17.83	8.56		
18.55	24.73	17.28	8.80		
17.80	25.20	16.91	9.09		
17.14	25.62	16.36	9.26		
16.33	26.20	16.03	9.58		
15.65	26.69	15.54	9.77		
15.19	26.95	15.12	9.93		
14.79	27.10	14.87	10.10		
14.02	27.86	14.51	10.28		
13.72	28.01	14.20	10.41		
13.19	28.63	13.88	10.55		
12.73	28.97	13.46	10.99		
12.35	29.30	13.11	11.31		
12.08	29.42	12.86	11.41		
11.57	30.04	12.61	11.53		
10.93	30.52	12.45	11.66		

Table S24: Weight fraction data for the system composed of IL (1) + $C_6H_5K_3O_7$ (2) + H_2O (3) at 298 K.

$[C_4mim][N(CN)_2]$					
100 w_1	100 w_2	100 w_1	100 w_2	100 w_1	100 w_2
67.80	1.91	16.73	15.36	10.44	19.24
54.43	2.90	16.43	15.54	10.33	19.41
48.91	4.03	16.07	15.71	10.23	19.56
44.53	4.92	15.87	15.81	10.04	19.73
41.22	5.74	15.56	15.92	9.84	19.93
38.74	6.50	15.25	16.04	9.65	20.02
36.85	7.16	15.01	16.25	9.55	20.12
34.97	7.80	14.69	16.36	9.42	20.35
33.34	8.22	14.47	16.55	9.32	20.44
31.96	8.69	14.18	16.60	9.24	20.52
30.69	9.14	13.98	16.79	9.14	20.62
29.49	9.58	13.80	16.93	9.02	20.83
28.61	10.14	13.63	17.08	8.94	20.93
27.52	10.51	13.36	17.16	8.86	20.99
26.56	10.95	13.17	17.31	8.77	21.08
25.57	11.31	13.01	17.47	8.69	21.15
24.76	11.71	12.86	17.59	8.58	21.39
23.88	12.04	12.69	17.77	8.43	21.53
23.06	12.33	12.48	17.85	8.34	21.58
22.53	12.74	12.38	17.69	8.23	21.81
21.77	13.01	12.16	17.70	8.12	22.04
21.07	13.21	12.02	17.85	7.99	22.16
20.64	13.54	11.89	17.98	7.90	22.31
20.07	13.73	11.65	18.26	7.74	22.52
19.61	13.90	11.49	18.26	7.57	22.81
19.18	14.25	11.27	18.56	7.42	23.04
18.66	14.41	11.03	18.80	7.31	23.14
18.16	14.57	10.87	18.85	7.14	23.46
17.83	14.82	10.76	18.94	7.01	23.65
17.35	14.89	10.66	19.03	6.87	23.93
17.07	15.19	10.56	19.12	6.71	24.20

Table S25: Weight fraction data for the system composed of IL (1) + $C_6H_5K_3O_7$ (2) + H_2O (3) at 298 K.

$[C_4mim][PO_4(CH_3)_2]$		$[C_4mim][CH_3SO_3]$	
100 w_1	100 w_2	100 w_1	100 w_2
59.81	11.89	57.50	9.38
58.62	12.67	55.05	11.66
56.74	13.95	52.98	13.54
55.60	14.82	49.26	16.37
54.20	15.78	47.60	17.73
50.97	17.79	44.39	20.42
49.95	18.60	41.94	22.60
47.97	20.19	40.07	24.39
46.03	21.71		
42.16	25.01		
40.22	26.72		
37.68	28.84		

Table S26: Weight fraction data for the system composed of IL (1) + $C_6H_5K_3O_7$ (2) + H_2O (3) at 298 K.

$[C_4mim][CH_3CO_2]$		$[C_6mim]Cl$	
100 w_1	100 w_2	100 w_1	100 w_2
52.65	13.21	69.00	1.41
51.12	14.82	63.45	3.05
48.30	17.43	60.87	4.15
43.98	21.11	58.12	5.41
42.40	22.50	55.58	6.47
40.80	23.96	53.21	7.50
39.25	25.43	49.91	9.40
		46.83	11.11
		42.78	13.69
		38.18	17.02
		30.37	23.27
		24.10	28.32

Table S27: Weight fraction data for the system composed of IL (1) + $C_6H_5K_3O_7$ (2) + H_2O (3) at 298 K.

[C_4mpyr]Cl					
100 w_1	100 w_2	100 w_1	100 w_2	100 w_1	100 w_2
65.68	2.06	41.08	12.12	30.79	21.10
50.88	6.01	40.64	12.50	29.66	22.13
46.44	8.53	40.06	12.93	28.91	23.01
46.11	8.74	39.66	13.21	27.76	24.13
45.64	8.98	39.24	13.48	26.75	25.34
45.62	9.12	38.69	13.96	25.06	26.85
45.36	9.20	38.13	14.45	23.92	28.14
45.01	9.43	37.52	14.96	22.80	29.61
44.63	9.68	36.90	15.49	20.62	31.88
44.13	9.95	36.16	16.11	19.11	33.82
43.76	10.21	35.81	16.55	16.29	36.60
43.13	10.58	35.11	17.18	15.36	38.13
42.75	10.85	34.20	17.89	13.20	40.75
42.48	11.10	33.62	18.51	12.07	42.63
42.03	11.46	32.58	19.39		
41.57	11.78	31.40	20.32		

Table S28: Weight fraction data for the system composed of IL (1) + $C_6H_5K_3O_7$ (2) + H_2O (3) at 298 K.

[C_4mpy]Cl					
100 w_1	100 w_2	100 w_1	100 w_2	100 w_1	100 w_2
66.91	2.32	34.20	17.58	24.07	27.13
50.60	6.94	33.82	17.90	23.73	27.68
47.68	8.21	33.46	18.29	22.78	28.60
39.83	13.07	32.71	18.86	21.39	30.03
39.60	13.25	32.33	19.26	20.32	31.07
39.30	13.51	31.89	19.71	19.92	31.83
38.88	13.79	31.04	20.33	19.31	32.42
38.68	13.99	30.74	20.63	18.08	33.47
38.22	14.29	30.21	21.17	17.52	34.34
37.57	14.83	29.62	21.69	16.29	35.74
37.29	15.09	29.16	22.26	14.79	37.20
36.74	15.43	28.56	22.81	14.13	38.26
36.49	15.72	27.95	23.45	13.43	39.14
35.96	16.09	27.28	24.08	12.70	40.25
35.67	16.39	26.51	24.80	11.29	42.54
35.08	16.81	25.73	25.50	10.51	43.82
34.76	17.15	24.93	26.31		

Table S29:. Weight fraction data for the system composed of IL (1) + $C_6H_5K_3O_7$ (2) + H_2O (3) at 298 K.

[C_4mpip]Cl					
100 w_1	100 w_2	100 w_1	100 w_2	100 w_1	100 w_2
67.51	1.56	36.91	15.54	27.92	23.90
60.51	3.05	36.53	15.90	26.98	24.82
55.60	4.19	36.05	16.30	26.03	25.76
51.29	6.58	35.54	16.69	25.09	26.74
48.39	7.63	35.05	17.14	24.15	27.69
44.29	10.14	34.78	17.37	23.18	28.77
41.03	12.44	34.13	17.95	21.96	29.94
40.47	12.83	33.46	18.56	21.25	30.86
40.07	13.14	32.83	19.14	19.97	32.20
39.89	13.24	32.78	19.04	19.10	33.25
39.55	13.46	32.04	19.80	17.45	34.86
39.14	13.78	31.51	20.35	16.38	36.26
38.89	13.97	30.87	20.97	15.26	37.67
38.38	14.38	30.21	21.64	13.89	39.39
37.99	14.70	29.46	22.36	13.24	40.26
37.48	15.10	28.43	23.27	11.83	42.03

Table S30: Weight fraction data for the system composed of IL (1) + $C_6H_5K_3O_7$ (2) + H_2O (3) at 298 K.

[C_4mpip]Cl					
100 w_1	100 w_2	100 w_1	100 w_2	100 w_1	100 w_2
67.51	1.56	36.91	15.54	27.92	23.90
60.51	3.05	36.53	15.90	26.98	24.82
55.60	4.19	36.05	16.30	26.03	25.76
51.29	6.58	35.54	16.69	25.09	26.74
48.39	7.63	35.05	17.14	24.15	27.69
44.29	10.14	34.78	17.37	23.18	28.77
41.03	12.44	34.13	17.95	21.96	29.94
40.47	12.83	33.46	18.56	21.25	30.86
40.07	13.14	32.83	19.14	19.97	32.20
39.89	13.24	32.78	19.04	19.10	33.25
39.55	13.46	32.04	19.80	17.45	34.86
39.14	13.78	31.51	20.35	16.38	36.26
38.89	13.97	30.87	20.97	15.26	37.67
38.38	14.38	30.21	21.64	13.89	39.39
37.99	14.70	29.46	22.36	13.24	40.26
37.48	15.10	28.43	23.27	11.83	42.03

Table S31: Weight fraction data for the system composed of IL (1) + $C_6H_5K_3O_7$ (2) + H_2O (3) at 298 K.

[N_{4444}]Cl					
100 w_1	100 w_2	100 w_1	100 w_2	100 w_1	100 w_2
65.99	1.83	25.61	16.43	13.48	26.67
51.10	4.18	24.67	17.11	12.98	27.23
47.50	5.31	23.48	18.14	12.60	27.66
44.35	6.29	22.70	18.64	12.11	28.20
41.94	6.89	21.70	19.55	11.66	28.69
40.41	7.57	20.79	20.38	11.21	29.19
38.72	8.27	19.91	21.05	10.72	29.78
37.26	8.96	19.09	21.82	10.32	30.24
36.04	9.52	18.40	22.48	9.95	30.66
34.21	10.78	17.83	22.92	9.47	31.26
32.97	11.37	16.51	24.13	9.10	31.75
31.37	12.51	15.78	24.84	8.77	32.14
30.39	12.95	15.06	25.60	8.46	32.54
29.07	13.83	14.51	26.08	8.17	32.91
27.63	14.95	14.25	26.16	7.94	33.19
26.59	15.75	13.86	26.41		

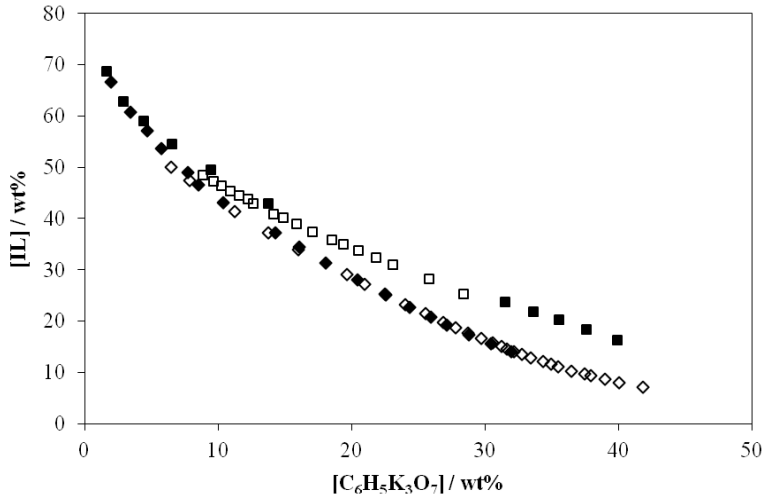

Figure S3: Phase diagram for the ternary system composed of $C_6H_5K_3O_7$ + H_2O + [C_4mim]Cl (■) and $C_6H_5K_3O_7$ + H_2O + [C_4mim]Br (◆) at 298 K. The full symbols represent the data obtained in this work while the empty symbols correspond to literature data.[16,17]

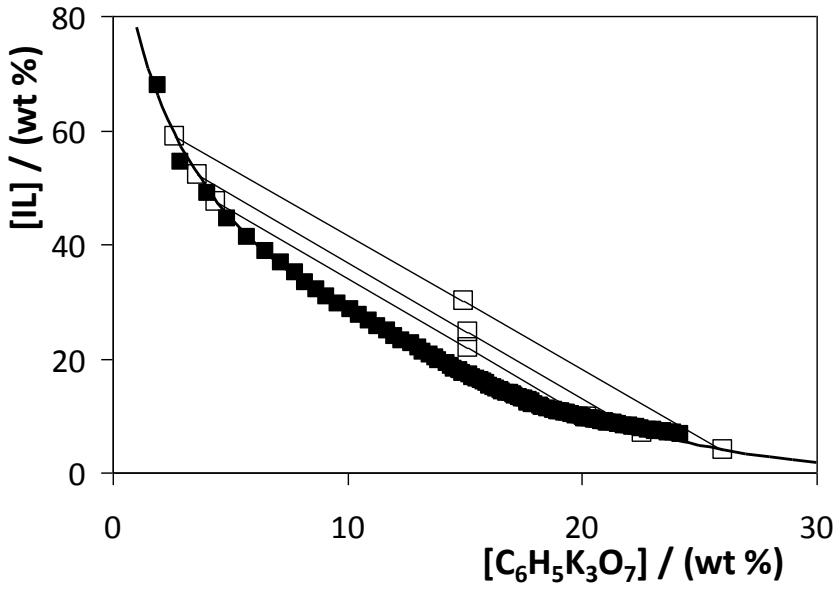

Figure S4: Phase diagram for the ternary system composed of [C_4mim][$N(CN)_2$] + $C_6H_5K_3O_7$ + H_2O, at 298 K and atmospheric pressure: binodal curve data (■), TL data (□), adjusted binodal data through eq (1) (—).

Referring to Chapter 2.5: Reversible pH-Triggered Aqueous Biphasic Systems

Table S32: Experimental weight fraction data for the systems composed of IL (1) + salt (2) + H_2O (3) at 298 K and at atmospheric pressure.

[C_4C_1mim]Cl							
pH ≈ 9				pH ≈ 8			
100 w1	100 w2	100 w1	100 w2	100 w1	100 w2	100 w1	100 w2
17.56	39.84	41.84	15.11	22.42	35.33	43.55	13.92
20.06	37.41	42.64	14.51	23.34	33.49	44.05	13.57
21.63	35.27	43.12	14.03	26.12	30.66	44.73	13.02
23.69	33.04	43.99	13.43	27.86	28.84	45.13	12.74
25.66	31.02	44.76	12.88	28.80	27.75	45.77	12.29
26.59	29.85	45.80	12.28	29.92	26.91	46.45	11.79
27.67	28.42	46.45	11.82	30.76	25.65	47.16	11.37
29.13	26.88	47.07	11.38	32.62	23.94	48.25	10.65
30.66	25.40	47.54	11.01	34.71	22.20	48.80	10.28
31.91	24.13	48.16	10.62	35.47	21.18	49.20	9.99
33.00	23.00	48.60	10.30	36.19	20.33	49.88	9.57
33.84	22.06	49.07	9.98	37.40	19.20	50.79	9.05
35.71	20.65	49.50	9.67	38.46	18.30	51.91	8.41
36.77	19.69	50.06	9.36	39.33	17.54	52.57	7.99
37.47	18.91	50.57	9.04	39.86	16.99	53.25	7.69
38.29	18.20	42.41	14.54	40.39	16.50	53.76	7.40
39.11	17.47	49.83	9.17	41.23	15.89	54.48	7.01
39.63	16.94	53.17	7.35	41.76	15.43	59.84	4.80
40.34	16.30	56.90	5.30	42.57	14.74	80.75	1.54
40.96	15.76	59.99	3.78	43.05	14.40		

Table S33: Experimental weight fraction data for the systems composed of IL (1) + salt (2) + H_2O (3) at 298 K and at atmospheric pressure.

[C_4C_1mim]Cl pH ≈ 7					
100 w_1	100 w_2	100 w_1	100 w_2	100 w_1	100 w_2
22.42	35.33	39.33	17.54	47.16	11.37
23.34	33.49	39.86	16.99	48.25	10.65
26.12	30.66	40.39	16.50	48.80	10.28
27.86	28.84	41.23	15.89	49.20	9.99
28.80	27.75	41.76	15.43	49.88	9.57
29.92	26.91	42.57	14.74	50.79	9.05
30.76	25.65	43.05	14.40	51.91	8.41
32.62	23.94	43.55	13.92	52.57	7.99
34.71	22.20	44.05	13.57	53.25	7.69
35.47	21.18	44.73	13.02	53.76	7.40
36.19	20.33	45.13	12.74	54.48	7.01
37.40	19.20	45.77	12.29		
38.46	18.30	46.45	11.79		

Table S34: Experimental weight fraction data for the systems composed of IL (1) + salt (2) + H_2O (3) at 298 K and at atmospheric pressure.

[C_4mpip]Cl					
pH ≈ 8		pH ≈ 7		pH ≈ 6	
100 w_1	100 w_2	100 w_1	100 w_2	100 w_1	100 w_2
18.59	34.74	19.13	34.29	27.76	27.84
20.83	32.23	21.77	31.48	29.17	25.87
22.17	30.49	23.79	29.15	30.31	24.57
24.04	28.49	25.36	27.22	32.18	22.60
25.69	26.70	27.23	25.23	33.34	21.31
27.56	24.79	29.30	23.19	34.86	19.81
28.91	23.36	30.93	21.58	38.96	16.72
30.49	21.85	32.75	19.85	40.03	15.67
31.29	20.92	33.91	18.76	41.21	14.60
32.48	19.84	35.35	17.45	42.63	13.43
33.61	18.79	36.95	16.13	43.92	12.44
34.90	17.65	37.97	15.26	45.42	11.32
36.15	16.58	39.03	14.38	47.86	9.68
38.56	14.58	40.36	13.39	52.74	4.62
39.46	13.85	41.55	12.49	64.49	1.62
40.53	13.05	42.40	11.84		
41.78	12.15	43.59	11.01		
44.09	10.61	45.21	9.99		
44.76	10.09	46.54	9.15		
45.92	9.36	47.80	8.36		
46.89	8.74	50.96	6.66		
48.99	7.61	56.21	3.60		
49.57	7.10	63.38	2.27		
53.51	5.09				
68.53	1.79				

Table S35: Experimental weight fraction data for the systems composed of IL (1) + salt (2) + H_2O (3) at 298 K and at atmospheric pressure.

[C_4mpy]Cl						[C_4mim]Cl	
pH ≈ 8		pH ≈ 7		pH ≈ 6		pH ≈ 8	
100 w_1	100 w_2	100 w_1	100 w_2	100 w_1	100 w_2	100 w1	100 w2
16.93	35.64	21.58	31.74	22.21	33.77	16.20	39.76
18.27	34.03	24.25	28.86	24.48	31.28	18.04	37.57
20.24	32.05	26.76	26.25	26.65	28.83	20.63	34.66
21.39	30.62	29.08	23.90	28.47	26.79	23.03	32.30
22.92	29.02	31.08	21.92	30.08	24.99	24.96	30.22
24.94	27.24	33.09	20.05	31.47	23.45	26.68	28.40
25.72	26.23	36.14	17.47	33.11	21.93	28.79	26.36
26.94	25.05	38.67	15.42	34.49	20.57	30.06	24.92
28.09	23.93	41.35	13.37	35.88	19.21	31.97	23.23
29.18	22.91	32.00	20.18	36.99	18.14	33.43	21.87
30.17	21.98	37.49	15.64	38.18	17.11	34.30	20.97
31.41	20.93	40.87	13.16	39.46	15.99	35.39	19.98
32.24	20.18	45.80	9.86	40.42	15.16	36.53	19.02
33.00	19.44	48.13	8.51	41.50	14.29	37.26	18.33
34.01	18.58	50.98	6.95	42.48	13.53	38.21	17.55
34.89	17.82	53.40	5.81	43.14	13.05	39.02	16.81
35.66	17.16	63.12	2.47	44.21	12.28	39.81	16.14
36.49	16.51	72.48	1.26	45.40	11.45	41.02	15.31
37.22	15.93			46.47	10.69	41.90	14.63
38.05	15.28			47.82	9.84	42.73	14.03
38.98	14.84			49.21	9.00	43.70	13.35
39.46	14.49			74.14	1.29	44.72	12.69
40.07	13.99					45.39	12.17
42.62	12.07					46.20	11.62
45.24	10.41					46.85	11.17
47.27	9.28					47.33	10.84
49.66	7.86					48.00	10.42
51.24	7.14					48.62	10.02
53.05	6.30					49.11	9.71
54.79	5.50					49.75	9.33
56.63	4.68					50.30	9.00
58.50	3.90					50.79	8.70
75.36	0.93					51.38	8.36
						52.51	7.65
						55.96	5.94
						62.91	2.79
						71.81	1.55

Table S36: Experimental weight fraction data for the systems composed of IL (1) + salt (2) + H_2O (3) at 298 K and at atmospheric pressure.

$[P_{4444}]Cl$					
pH ≈ 8					
100 w_1	100 w_2	100 w_1	100 w_2	100 w_1	100 w_2
57.55	5.11	21.90	16.80	11.39	25.12
51.38	5.72	21.08	17.42	11.12	25.45
47.51	6.49	20.04	18.17	10.82	25.66
43.09	7.07	18.91	18.97	10.56	25.92
40.14	7.72	18.40	19.23	10.26	26.26
38.22	8.50	17.87	19.69	10.03	26.47
35.90	9.04	17.14	20.36	9.80	26.71
34.51	9.73	16.28	21.08	9.60	26.88
33.28	10.27	15.24	21.75	9.18	27.29
32.31	10.69	14.71	22.25	9.01	27.45
31.26	11.09	14.49	22.36	8.81	27.69
29.67	12.12	13.98	22.87	8.43	28.15
28.64	12.49	13.65	23.08	8.31	28.22
27.33	13.30	13.27	23.43	8.21	28.29
25.95	14.28	13.01	23.66	7.99	28.54
25.20	14.54	12.74	23.84	7.80	28.77
24.20	15.31	12.36	24.16	7.65	28.92
23.64	15.60	12.05	24.51	7.50	29.11
23.12	15.86	11.71	24.82	7.35	29.28

Table S37: Experimental weight fraction data for the systems composed of IL (1) + salt (2) + H_2O (3) at 298 K and at atmospheric pressure.

[P_{4444}]Cl					
pH ≈ 6					
100 w_1	100 w_2	100 w_1	100 w_2	100 w_1	100 w_2
41.56	9.43	17.69	21.69	10.06	27.33
39.80	10.01	16.85	22.19	9.80	27.56
38.18	10.56	16.21	22.68	9.51	27.88
36.87	10.87	15.46	23.35	9.37	28.03
35.40	11.39	15.03	23.61	9.18	28.16
33.85	12.09	14.57	23.96	9.03	28.32
32.62	12.60	14.09	24.35	8.92	28.40
31.03	13.40	13.59	24.74	8.69	28.68
29.82	13.88	13.08	25.21	8.48	28.87
28.51	14.65	12.94	25.21	8.31	29.02
27.20	15.50	12.70	25.36	8.17	29.20
25.81	16.14	12.47	25.44	7.98	29.40
24.61	16.90	12.21	25.50	7.78	29.60
23.45	17.71	11.80	25.89	7.60	29.79
22.35	18.36	11.56	26.06	7.36	30.03
21.48	18.90	11.27	26.32	7.18	30.24
20.51	19.54	11.02	26.49	6.94	30.47
19.63	20.21	10.72	26.76	6.78	30.68
19.10	20.60	10.50	26.97	6.66	30.79
18.37	21.20	10.29	27.15	6.52	30.92

Table S38. Experimental weight fraction data for the systems composed of IL (1) + salt (2) + H_2O (3) at 298 K and at atmospheric pressure.

$[P_{4444}]Cl$					
pH ≈ 5					
100 w_1	100 w_2	100 w_1	100 w_2	100 w_1	100 w_2
57.71	4.17	18.37	24.10	9.96	30.82
52.34	5.35	17.47	24.83	9.61	31.16
41.17	9.45	16.59	25.43	9.26	31.47
38.49	10.76	15.62	26.24	8.96	31.74
36.24	11.95	14.88	26.77	8.61	32.10
34.37	13.09	14.17	27.33	8.34	32.37
32.27	14.15	13.66	27.72	8.07	32.65
29.59	15.99	13.08	28.15	7.59	33.15
27.32	17.62	12.46	28.71	7.17	33.58
25.36	18.99	12.01	29.04	6.88	33.87
23.57	20.28	11.59	29.36	6.51	34.30
21.83	21.57	11.15	29.73	6.14	34.70
20.58	22.59	10.70	30.13	5.77	35.16
19.44	23.34	10.31	30.49		

Table S39: Experimental weight fraction data for the systems composed of IL (1) + salt (2) + H_2O (3) at 298 K and at atmospheric pressure.

[C_4mim]Br							
pH ≈ 8				pH ≈ 6			
100 w_1	100 w_2	100 w_1	100 w_2	100 w_1	100 w_2	100 w_1	100 w_2
74.67	1.71	14.74	31.13	13.13	40.93	42.51	13.03
62.23	3.59			14.64	37.81	42.86	12.76
55.80	4.57			15.44	36.76	43.23	12.52
53.74	5.49			16.63	35.43	43.55	12.28
52.44	6.03			18.02	34.01	43.90	12.07
51.12	6.60			18.67	33.22	44.20	11.86
49.27	7.62			19.95	32.05	44.63	11.58
47.97	8.31			21.44	30.79	45.05	11.33
46.83	8.76			22.62	29.62	45.34	11.12
45.63	9.37			23.47	28.62	45.80	10.87
43.97	10.30			24.73	27.53	46.13	10.66
42.58	11.06			26.18	26.40	46.40	10.48
41.50	11.75			26.98	25.64	46.69	10.29
40.50	12.33			27.54	25.06	46.93	10.13
39.26	13.05			28.63	24.22	47.25	9.93
38.30	13.66			29.33	23.52	47.40	9.75
36.84	14.69			30.43	22.72	47.72	9.56
35.35	15.70			30.99	22.13	48.06	9.38
34.29	16.45			31.68	21.57	48.36	9.21
33.02	17.36			32.44	20.87	48.67	9.05
31.11	18.85			32.85	20.41	48.97	8.88
30.25	19.38			33.33	19.97	49.29	8.70
28.80	20.48			34.07	19.48	49.63	8.53
27.86	21.16			34.48	19.06	50.06	8.29
27.10	21.73			35.32	18.47	50.80	7.88
26.65	22.00			35.65	18.09	51.14	7.73
25.95	22.53			36.35	17.60	51.36	7.61
25.25	23.07			36.77	17.23	51.65	7.47
24.14	23.91			37.56	16.75	52.00	7.32
23.55	24.34			37.87	16.41	52.21	7.21
20.87	25.22			38.49	16.01	52.52	7.08
20.23	25.78			38.76	15.70	52.91	6.89
19.56	26.39			39.22	15.39	53.55	6.59
18.92	26.99			39.55	15.11	54.45	6.20
18.38	27.49			40.08	14.74	54.93	6.00
17.68	28.17			40.56	14.41	54.95	5.90
17.09	28.72			40.98	14.10	56.27	5.48
16.38	29.43			41.39	13.81	58.01	4.74
15.54	30.30			41.83	13.51	69.94	1.61

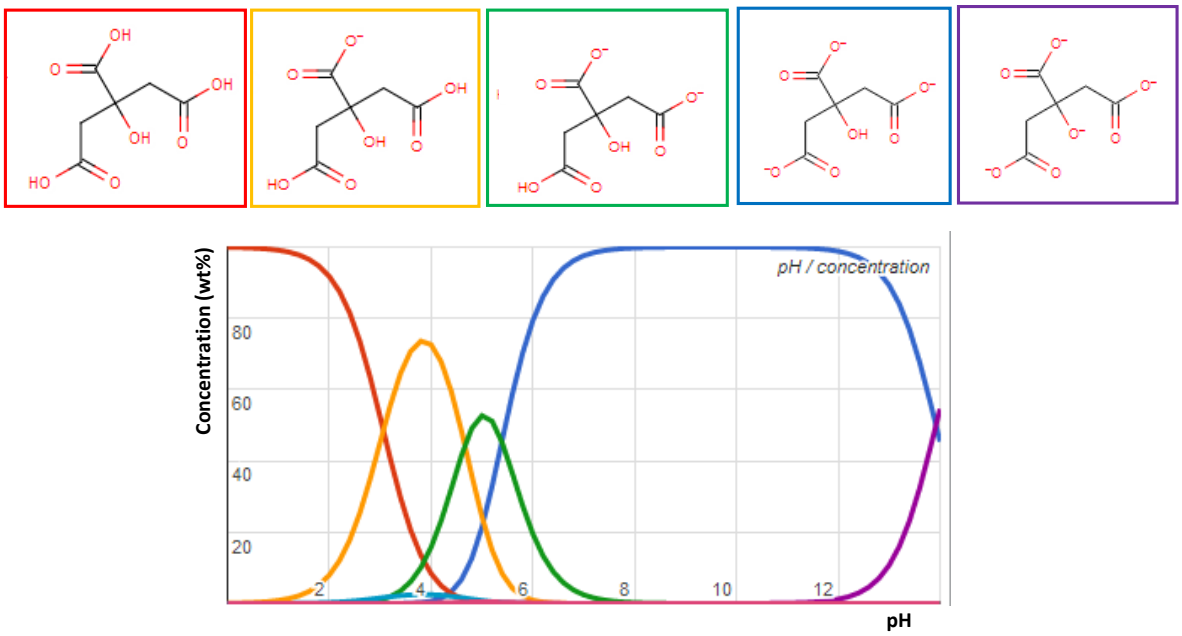

Figure S5. Speciation curve of acid citric as a function of pH.[27]

Referring to Chapter 2.6: Optimization of the Gallic Acid Extraction using Ionic Liquid-Based Aqueous Biphasic Systems

Table S40: Experimental weight fraction composition and partition coefficients of gallic acid in ILs + Na_2SO_4 ABS at 298.15 K.

IL + Na_2SO_4 + water system	Weight fraction composition / wt %		$K_{GA} \pm \sigma^a$	$EE\%_{GA} \pm \sigma^a$
	IL	Na_2SO_4		
$[C_2mim][CF_3SO_3]$	24.88	15.28	9.76 ± 0.56	81.23 ± 2.31
$[C_4mim][CF_3SO_3]$	24.95	14.97	21.98 ± 2.25	88.90 ± 0.60
$[C_4mim][CH_3SO_4]$	24.69	14.52	26.46 ± 0.53	97.05 ± 0.06
$[C_4mim][C_2H_5SO_4]$	25.71	15.36	29.58 ± 0.79	98.53 ± 0.04
$[C_4mim][OctylSO_4]$	24.98	14.95	2.04 ± 0.41	58.36 ± 3.36
$[C_4mim][N(CN)_2]$	25.00	15.00	20.45 ± 2.08	93.37 ± 0.74
$[C_4mim]Br$	24.96	15.22	23.68 ± 1.51	96.84 ± 0.15
$[C_7mim]Cl$	25.05	15.00	21.94 ± 1.57	98.80 ± 0.08
$[C_8mim]Cl$	25.92	15.23	3.28 ± 0.59	96.45 ± 1.79

[a]standard deviation

Table S41: Experimental weight fraction composition and partition coefficients of gallic acid in ILs + K_2HPO_4/ KH_2PO_4 ABS at 298.15 K.

IL + K_2HPO_4/KH_2PO_4 + water system	Weight fraction composition / wt %		$K_{GA} \pm \sigma^a$	$EE\%_{GA} \pm \sigma^a$
	IL	K_2HPO_4/KH_2PO_4		
$[C_2mim][CF_3SO_3]$	25.06	14.99	0.90 ± 0.06	33.32 ± 1.27
	30.05	14.97	0.84 ± 0.04	40.05 ± 2.01
$[C_4mim][CF_3SO_3]$	25.89	14.85	0.76 ± 0.03	26.30 ± 0.50
	29.93	15.09	1.70 ± 0.07	51.60 ± 1.01
$[C_4mim][CH_3SO_4]$	29.10	16.59	6.43 ± 0.44	94.75 ± 0.35
$[C_4mim][OctylSO_4]$	25.04	15.01	1.18 ± 0.01	44.57 ± 0.19
$[C_4mim][N(CN)_2]$	25.01	15.00	3.19 ± 0.12	72.53 ± 0.65
	29.96	15.03	3.87 ± 0.09	81.20 ± 1.64
$[C_4mim]Br$	29.94	15.41	11.35 ± 0.65	96.93 ± 0.37
$[C_7mim]Cl$	30.00	15.40	5.02 ± 0.40	96.06 ± 0.30
$[C_8mim]Cl$	30.90	15.05	6.98 ± 0.48	96.97 ± 0.60

[a]standard deviation

Table S42: Experimental weight fraction composition and partition coefficients of gallic acid in ILs + K_3PO_4 ABS at 298.15 K.

IL + K_3PO_4 + water system	Weight fraction composition / wt %		$K_{GA} \pm \sigma^a$	$EE\%_{GA} \pm \sigma^a$
	IL	K_3PO_4		
$[C_2mim][CF_3SO_3]$	25.07	14.93	0.58 ± 0.19	14.70 ± 4.19
$[C_4mim][CF_3SO_3]$	25.08	14.96	0.18 ± 0.03	34.66 ± 1.39
$[C_4mim][CH_3SO_4]$	24.97	15.29	1.03 ± 0.09	52.81 ± 0.93
$[C_4mim][OctylSO_4]$	24.98	15.02	0.38 ± 0.09	18.53 ± 3.63
$[C_4mim][N(CN)_2]$	25.02	15.02	0.51 ± 0.08	26.02 ± 1.43
$[C_4mim]Br$	24.82	15.09	0.97 ± 0.20	56.17 ± 0.47
$[C_7mim]Cl$	25.01	15.26	8.16 ± 0.36	89.86 ± 2.76
$[C_8mim]Cl$	25.01	15.08	2.52 ± 0.53	74.22 ± 4.09

[a]standard deviation

Table S43: Weight fraction compositions (wt %) of the top (T) phase, the initial mixture (M), and the bottom (B) phase of the ternary systems composed of ionic liquid + K_3PO_4 + H_2O systems at 298 K.

Ionic liquid	Weight fraction composition / wt %					
	$[IL]_T$	$[K_3PO_4]_T$	$[IL]_M$	$[K_3PO_4]_M$	$[IL]_B$	$[K_3PO_4]_B$
$[C_2mim][CF_3SO_3]$	0.52	29.92	25.07	14.93	74.85	1.47
$[C_4mim][CF_3SO_3]$	1.59	14.96	25.08	1.09	66.42	22.83
$[C_4mim][N(CN)_2]$	59.21	1.96	25.02	15.02	2.95	23.45
$[C_4mim]Br$	45.96	3.51	24.82	15.09	5.48	25.67
$[C_7mim]Cl$	42.33	4.57	25.01	15.26	4.21	28.11
$[C_8mim]Cl$	38.96	6.95	25.01	15.08	7.34	25.37

Table S44: Weight fraction compositions (wt %) of the top (T) phase, the initial mixture (M), and the bottom (B) phase of the ternary systems composed of ionic liquid + K_2HPO_4/KH_2PO_4 + H_2O systems at 298 K.

Ionic liquid	Weight fraction composition / wt %					
	$[IL]_T$	$[K_2HPO_4/KH_2PO_4]_T$	$[IL]_M$	$[K_2HPO_4/KH_2PO_4]_M$	$[IL]_B$	$[K_2HPO_4/KH_2PO_4]_B$
$[C_4mim][CF_3SO_3]$	74.59	1.20	25.89	14.85	0.80	21.88
	80.09	1.00	29.93	15.09	0.47	23.36
$[C_4mim][N(CN)_2]$	49.79	2.10	25.01	15.00	3.75	26.10
	56.86	1.17	29.96	15.03	1.91	29.48
$[C_7mim]Cl$	33.72	11.54	30.00	15.40	11.88	34.18
$[C_8mim]Cl$	47.56	6.09	31.90	15.05	26.66	18.04

Table S45: Weight fraction compositions (wt %) of the top (T) phase, the initial mixture (M), and the bottom (B) phase of the ternary systems composed of ionic liquid + Na_2SO_4 + H_2O systems at 298 K.

Ionic liquid	Weight fraction composition / wt %					
	$[IL]_T$	$[Na_2SO_4]_T$	$[IL]_M$	$[Na_2SO_4]_M$	$[IL]_B$	$[Na_2SO_4]_B$
$[C_2mim][CF_3SO_3]$	71.67	0.80	24.88	15.28	2.22	22.30
$[C_4mim][CF_3SO_3]$	2.15	20.00	24.95	14.97	90.03	0.60
$[C_4mim][CH_3SO_4]$	45.93	4.36	24.69	14.52	11.88	20.64
$[C_4mim][OctylSO_4]$	73.70	1.75	24.98	14.95	0.14	21.68
$[C_4mim][N(CN)_2]$	60.82	0.56	25.00	15.00	0.40	24.92
$[C_4mim]Br$	39.71	5.21	24.96	15.22	12.73	23.52
$[C_7mim]Cl$	63.27	1.66	25.05	15.00	12.88	19.25
$[C_8mim]Cl$	72.69	0.38	25.92	15.23	7.64	21.03

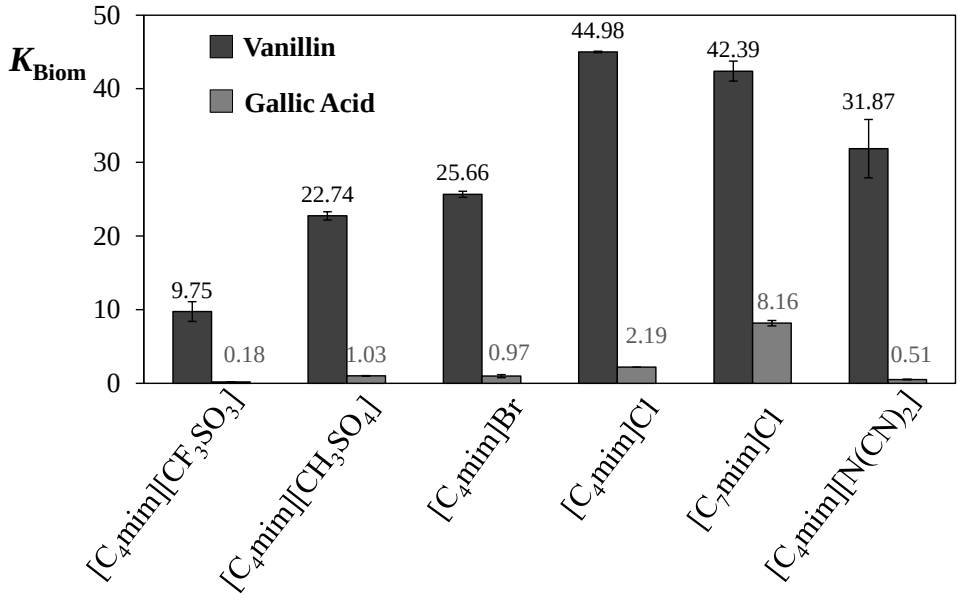

Figure S6: Partition coefficients of vanillin and gallic acid in different ABS composed of 25 wt % of IL + 15 wt % of K_3PO_4 at 298 K.

Table S46: Experimental weight fraction composition and partition coefficients of vanillin in ILs + K_3PO_4 ABS at 298 K.

IL + K_3PO_4 + water system	Weight fraction composition / wt %		$K_{Van} \pm \sigma$[a]
	IL	K_3PO_4	
[C_4mim]Cl	25.00	15.02	44.98 ± 0.10
[C_7mim]Cl	24.61	14.88	42.39 ± 1.35
[C_4mim]Br	24.74	15.55	25.66 ± 0.40
[C_4mim][CF_3SO_3]	24.67	15.16	9.75 ± 1.34
[C_4mim][CH_3SO_4]	25.05	15.16	22.74 ± 0.55
[C4mim][$N(CN)_2$]	24.63	14.77	31.87 ± 3.97

[a]standard deviation

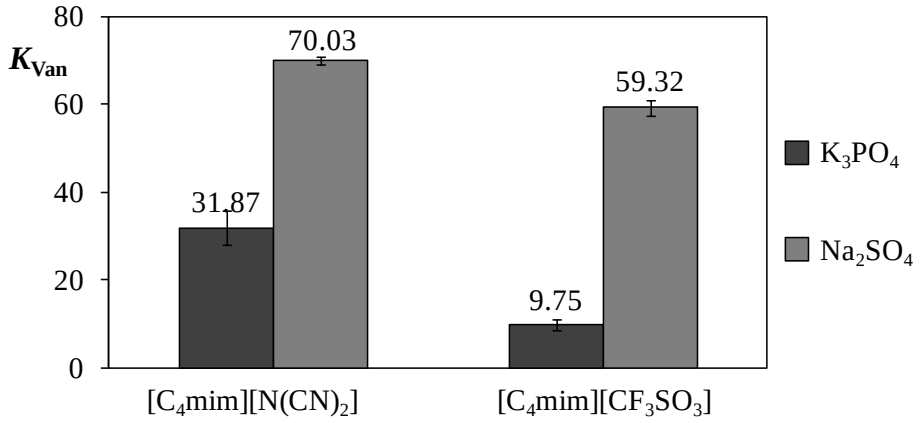

Figure S7: Partition coefficients of vanillin for different ATPS composed of 25 wt % of IL + 15 wt % of inorganic salt at 298 K.

Table S47: Experimental weight fraction composition and partition coefficients of vanillin in ILs + Na_2SO_4 ABS at 298.15 K.

IL + Na_2SO_4 + water system	**Weight fraction composition / wt %**		**K_{Van} ± σ[a]**
	IL	**Na_2SO_4**	
$[C_4mim][CF_3SO_3]$	24.71	14.89	70.03 ± 0.77
$[C_4mim][N(CN)_2]$	24.93	14.97	59.32 ± 1.75

[a]standard deviation

Referring to Chapter 2.7: Development of Back-Extraction and Recyclability Routes for Ionic-Liquid-based Aqueous Biphasic Systems

Table S48: Experimental weight fraction composition and extraction efficiencies of gallic acid and pH of the coexisting phases of ABS composed of ILs + Na_2CO_3 at 298 K.

ionic liquid		% $EE_{Salt \pm}$ σ[a]	Weight fraction composition / (wt%)		pH_{IL}	pH_{salt}
			IL	Salt		
$[C_4C_1im][N(CN)_2]$	20%	85.81 ± 1.04	20.19	10.38	11.39	11.43
	25%	87.97 ± 1.34	24.36	10.41	11.02	11.10
	30%	85.37 ± 2.85	30.02	10.14	11.39	11.47
	35%	80.26 ± 0.90	34.90	10.05	11.64	11.01
$[C_4C_1im]Br$	20%	48.40 ± 0.39	20.42	10.59	11.41	11.39
	25%	45.68 ± 0.34	25.20	9.88	10.99	10.86
	30%	41.65 ± 1.58	29.98	10.07	11.28	11.38
	35%	38.92 ± 3.09	35.06	10.19	10.99	11.07
$[C_4C_1im][CF_3SO_3]$	20%	98.88 ± 0.03	20.08	9.89	11.26	11.28
	30%	95.16 ± 1.74	29.99	10.05	10.59	10.87
$[C_4C_1im][C_2H_5SO_4]$	20%	45.79 ± 0.49	19.76	10.00	10.96	11.06
	30%	42.56 ± 2.36	29.95	10.01	9.93	9.92
$[C_4C_1im][CH_3SO_4]$	20%	53.73 ± 0.12	20.50	10.63	11.19	11.31
	30%	45.94 ± 1.06	29.99	9.98	11.08	11.00

[a] standard deviation

Table S48: Experimental weight fraction composition and extraction efficiencies of gallic acid and pH of the coexisting phases of ABS composed of ILs + Na_2SO_4 at 298 K.

IL + Na_2SO_4 + water system	$EE\%_{GA}$ ± σ[a]	Weight fraction composition / (wt%)		pH_{IL}	pH_{salt}
		IL	Na_2SO_4		
$[C_4C_1im][CF_3SO_3]$	88.90 ± 0.60	24.95	14.97	3.12	3.04
	89.93 ± 1.14	25.00	19.96	3.15	3.08
$[C_4C_1im][CH_3SO_4]$	97.05 ± 0.06	24.69	14.52	1.88	1.57
$[C_4C_1im][C_2H_5SO_4]$	98.53 ± 0.04	25.71	15.36	2.29	1.29
$[C_4C_1im][N(CN)_2]$	93.37 ± 0.74	25.00	15.00	8.54	8.07
	94.56 ± 0.49	25.09	19.20	8.49	8.04
$[C_4C_1im]Br$	96.84 ± 0.15	24.96	15.22	5.43	5.22

[a] standard deviation

Table S49: Fraction data for the system composed of IL (1) + Na_2CO_3 (2) + H_2O (3) at 298 K.

[C_4C_1im]Cl ***Mw* = 174.67**					
100 w_1	**100 w_2**	**100 w_1**	**100 w_2**	**100 w_1**	**100 w_2**
41.57	2.74	20.05	9.47	15.21	12.61
33.81	3.48	19.68	9.65	14.60	13.02
31.60	4.15	19.24	9.87	14.00	13.45
29.73	4.72	18.92	10.10	13.55	13.88
27.92	5.28	18.65	10.34	12.93	14.30
26.45	5.74	18.23	10.60	12.16	14.80
21.64	8.55	17.84	10.90	11.35	15.68
21.46	8.72	17.63	11.14	10.63	16.35
21.20	8.90	17.17	11.44	9.67	17.05
21.08	9.04	16.21	11.85	8.93	17.80
20.33	9.29	15.72	12.21		

Table S50: Experimental binodal curve weight fraction data for the system IL (1) + Na_2CO_3 (2) + H_2O (3) at 298 K.

[C_4C_1im]Br ***Mw* = 219.12**					
100 w_1	**100 w_2**	**100 w_1**	**100 w_2**	**100 w_1**	**100 w_2**
54.22	1.04	27.02	6.83	22.79	8.63
43.53	1.93	26.76	6.91	22.68	8.72
40.74	2.71	26.62	6.79	22.30	8.87
38.91	3.02	26.52	7.00	22.00	9.01
36.71	3.56	26.27	7.09	21.86	9.12
34.62	4.13	26.06	7.17	21.45	9.27
32.80	4.62	25.82	7.27	21.08	9.43
30.70	5.34	25.76	7.34	20.96	9.55
29.68	5.91	25.46	7.44	20.48	9.73
28.94	6.11	25.13	7.56	20.32	9.85
28.85	5.96	25.08	7.63	19.84	10.02
28.69	6.19	24.79	7.75	19.63	10.15
28.53	6.25	24.48	7.86	19.30	10.04
28.27	6.33	24.40	7.94	19.23	10.33
28.15	6.39	24.07	8.05	19.10	10.46
28.00	6.46	23.78	8.17	18.56	10.68
27.95	6.51	23.74	7.99	18.37	10.83
27.77	6.58	23.49	8.30	17.81	11.05
27.46	6.68	23.41	8.39		
27.27	6.75	23.12	8.51		

Table S51: Experimental binodal curve weight fraction data for the system IL (1) + Na2CO3 (2) + H_2O (3) at 298 K

$[C_4C_1im][CF_3SO_3]$		***Mw* = 288.29**	
100 w_1	**100 w_2**	**100 w_1**	**100 w_2**
58.94	0.53	12.36	4.95
46.68	0.94	12.13	5.01
41.19	1.32	11.83	5.04
36.80	1.57	11.53	5.19
33.45	1.81	11.24	5.45
30.38	1.99	11.00	5.58
28.27	2.18	10.75	5.70
26.43	2.32	10.58	5.74
24.77	2.46	10.35	5.85
23.45	2.64	10.11	5.98
22.36	2.75	9.87	6.10
21.69	2.88	9.65	6.20
20.92	3.00	9.40	6.37
20.08	3.13	9.16	6.41
19.15	3.26	8.88	6.63
18.37	3.36	8.50	6.80
17.86	3.51	8.21	7.03
17.47	3.55	7.81	7.22
17.05	3.66	7.42	7.48
16.67	3.74	7.05	7.68
16.28	3.85	6.59	8.08
15.95	3.91	6.19	8.45
15.53	4.06	5.90	8.72
15.16	4.17	5.34	9.34
14.78	4.27	4.96	9.78
14.42	4.33	4.61	10.19
14.08	4.40	4.23	10.53
13.88	4.50	4.05	10.76
13.57	4.60	3.79	11.10
13.31	4.68	3.21	12.17
12.87	4.81	2.31	14.10
12.61	4.89		

Table S52: Experimental binodal curve weight fraction data for the system IL (1) + Na_2CO_3 (2) + H_2O (3) at 298 K.

[C_4C_1im][Tos]		**M_w = 310.41**	
100 w_1	**100 w_2**	**100 w_1**	**100 w_2**
57.37	0.50	17.77	7.93
52.87	1.01	17.11	8.18
50.27	1.47	16.58	8.34
46.83	1.85	16.16	8.47
43.87	2.20	15.87	8.51
41.21	2.54	15.53	8.68
39.56	2.87	15.27	8.71
37.96	3.18	14.86	8.84
36.57	3.44	14.50	8.94
35.25	3.71	14.06	9.11
34.07	3.96	13.78	9.20
32.88	4.21	13.43	9.29
31.75	4.43	13.11	9.39
30.70	4.65	12.81	9.51
29.69	4.83	12.54	9.59
28.72	5.03	12.20	9.73
27.86	5.24	11.92	9.83
27.03	5.41	11.66	9.92
25.86	5.74	11.38	10.02
24.82	6.05	11.12	10.13
24.03	6.25	10.91	10.20
23.51	6.40	10.71	10.27
22.87	6.48	10.49	10.32
21.94	6.80	10.20	10.46
21.38	6.90	9.94	10.58
20.81	6.98	9.75	10.64
19.86	7.35	9.57	10.70
19.15	7.61	9.35	10.80
18.72	7.67	9.13	10.91
18.13	7.86	8.91	11.01

Table S53: Experimental binodal curve weight fraction data for the system IL (1) + Na_2CO_3 (2) + H_2O (3) at 298 K.

[C_4C_1im][$N(CN)_2$] *Mw* = 205.26					
100 w_1	**100 w_2**	**100 w_1**	**100 w_2**	**100 w_1**	**100 w_2**
58.14	0.53	27.13	4.22	6.40	11.37
46.30	1.08	25.96	4.38	6.01	11.71
43.04	1.52	25.24	4.58	5.70	11.91
39.32	1.91	24.11	4.96	5.37	12.17
36.82	2.23	11.64	8.32	5.03	12.48
35.28	2.61	10.96	8.41	4.61	12.96
33.40	2.91	10.39	8.70	4.28	13.32
31.55	3.19	9.95	8.92	4.01	13.61
30.41	3.51	8.68	9.50	3.71	13.94
29.08	3.73	8.27	9.70	3.21	14.63
28.07	3.97	7.04	10.98		

Table S54: Experimental binodal curve weight fraction data for the system IL (1) + Na_2CO_3 (2) + H_2O (3) at 298 K.

[C_4C_1im][CH_3SO_4] *Mw* = 250.31					
100 w_1	**100 w_2**	**100 w_1**	**100 w_2**	**100 w_1**	**100 w_2**
58.39	0.62	24.69	7.65	16.52	11.17
51.80	1.19	24.09	7.68	16.08	11.38
47.28	1.65	23.89	7.94	14.63	12.43
44.59	2.11	23.10	8.25	13.50	13.09
42.20	2.51	22.72	8.51	12.26	13.76
39.44	2.79	21.79	8.84	10.88	14.48
36.75	3.53	21.20	9.15	9.32	15.33
34.29	4.21	20.10	9.53	8.68	15.98
32.18	4.80	20.01	9.51	6.96	16.97
30.28	5.30	19.28	9.91	6.06	17.83
27.16	6.46	18.74	10.23	5.27	18.68
25.39	7.39	17.41	10.72		

Table S55: Experimental binodal curve weight fraction data for the system IL (1) + Na_2CO_3 (2) + H_2O (3) at 298 K.

[C_4C_1im][$N(CN)_2$] *Mw* = 205.26					
100 w_1	**100 w_2**	**100 w_1**	**100 w_2**	**100 w_1**	**100 w_2**
58.14	0.53	27.13	4.22	6.40	11.37
46.30	1.08	25.96	4.38	6.01	11.71
43.04	1.52	25.24	4.58	5.70	11.91
39.32	1.91	24.11	4.96	5.37	12.17
36.82	2.23	11.64	8.32	5.03	12.48
35.28	2.61	10.96	8.41	4.61	12.96
33.40	2.91	10.39	8.70	4.28	13.32
31.55	3.19	9.95	8.92	4.01	13.61
30.41	3.51	8.68	9.50	3.71	13.94
29.08	3.73	8.27	9.70	3.21	14.63
28.07	3.97	7.04	10.98		

Table S56: Experimental binodal curve weight fraction data for the system IL (1) + Na_2CO_3 (2) + H_2O (3) at 298 K.

[C_4C_1im][CH_3SO_4] *Mw* = 250.31					
100 w_1	**100 w_2**	**100 w_1**	**100 w_2**	**100 w_1**	**100 w_2**
58.39	0.62	24.69	7.65	16.52	11.17
51.80	1.19	24.09	7.68	16.08	11.38
47.28	1.65	23.89	7.94	14.63	12.43
44.59	2.11	23.10	8.25	13.50	13.09
42.20	2.51	22.72	8.51	12.26	13.76
39.44	2.79	21.79	8.84	10.88	14.48
36.75	3.53	21.20	9.15	9.32	15.33
34.29	4.21	20.10	9.53	8.68	15.98
32.18	4.80	20.01	9.51	6.96	16.97
30.28	5.30	19.28	9.91	6.06	17.83
27.16	6.46	18.74	10.23	5.27	18.68
25.39	7.39	17.41	10.72		

Table S57: Experimental binodal curve weight fraction data for the system IL (1) + Na_2CO_3 (2) + H_2O (3) at 298 K.

[C_4C_1im][$C_2H_5SO_4$] *Mw* = 264.34					
100 w_1	**100 w_2**	**100 w_1**	**100 w_2**	**100 w_1**	**100 w_2**
56.04	1.33	36.34	3.60	29.13	5.36
46.50	1.83	35.60	3.66	27.44	5.87
42.71	2.27	34.63	3.94	25.06	6.78
42.40	2.35	33.75	4.01	23.03	7.54
40.40	2.74	33.07	4.25	20.91	8.39
39.86	2.84	31.65	4.51	18.63	9.41
38.30	3.17	31.37	4.70	16.60	10.33
37.60	3.29	29.47	5.21	15.09	11.00

Table S58: Experimental binodal curve weight fraction data for the system IL (1) + Na_2CO_3 (2) + H_2O (3) at 298 K.

[C_4C_1im][SCN]		**Mw = 194.28**			
100 w_1	**100 w_2**	**100 w_1**	**100 w_2**	**100 w_1**	**100 w_2**
57.91	0.69	16.67	5.82	10.32	7.50
45.16	1.22	16.15	5.86	10.05	7.60
40.76	1.73	15.81	5.99	9.80	7.72
37.06	2.12	15.38	6.04	9.46	7.87
34.69	2.46	15.07	6.13	9.22	7.96
32.63	2.78	14.77	6.23	9.01	8.03
30.88	3.03	14.39	6.27	8.70	8.15
29.24	3.30	14.14	6.35	8.46	8.28
28.16	3.58	13.88	6.44	8.22	8.42
26.82	3.79	13.64	6.52	7.96	8.50
25.61	3.93	13.29	6.57	7.71	8.68
24.49	4.08	12.99	6.62	7.42	8.78
23.80	4.30	12.57	6.77	7.13	8.97
22.85	4.43	12.16	6.92	6.78	9.09
22.00	4.59	11.98	6.98	3.45	10.65
21.47	4.73	11.65	7.07	2.74	12.30
20.63	4.83	11.48	7.14	2.49	13.23
20.07	5.02	11.32	7.19	2.03	15.07
19.32	5.12	11.12	7.28	1.49	16.50
18.88	5.26	10.89	7.29	1.02	19.68
17.05	5.70	10.59	7.41		

Table S59: Parameters *A*, *B* and *C* of eq. 2.1.1 (and respective standard deviations, σ, and correlation coefficients, R^2) for the $[C_4C_1im]$-based ILs + Na_2CO_3 + H_2O systems at 298 K.

IL + Na_2CO_3 + H_2O	***A* ± σ**	***B* ± σ**	10^5 (***C* ± σ**)	R^2
$[C_4C_1im]Cl$	67.40 ± 1.06	0.372 ± 0.007	8.1±0.4	0.999
$[C_4C_1im]Br$	78.00 ± 0.62	0.39 ± 0.004	10.0±0.3	0.999
$[C_4C_1im][CF_3SO_3]$	126.00 ± 2.57	1026 ± 0.017	40.0±20.0	0.996
$[C_4C_1im][TOS]$	80.05 ± 0.83	0.413 ± 0.007	70.0±1.7	0.998
$[C_4C_1im][N(CN)_2]$	85.99 ± 1.71	0.555 ± 0.013	50.0±3.6	0.996
$[C_4C_1im][CH_3SO_4]$	80.23 ± 0.48	0.408 ± 0.003	10.0±0.4	0.999
$[C_4C_1im][CH_3SO_3]$	86.39 ± 0.80	0.417 ± 0.050	8.1±0.6	0.999
$[C_4C_1im][DMP]$	72.49 ± 2.51	0.346 ± 0.014	9.4±0.9	0.995
$[C_4C_1im][C_2H_5SO_4]$	97.00 ± 3.06	0.521 ± 0.019	6.6±4.3	0.997
$[C_4C_1im][SCN]$	97.71 ± 1.72	0.653 ± 0.012	100.0±5.0	0.997

Table S60: Equilibrium phase compositions for IL + Na_2CO_3 + water ABS at 298 K and respective values of TLL.

IL + Na_2CO_3 + H_2O	Weight fraction composition / (wt%)							
	$[IL]_{IL}$	$[Salt]_{IL}$	$[IL]_M$	$[Salt]_M$	$[IL]_{salt}$	$[Salt]_{salt}$	α	TLL
$[C_4C_1im]Cl$	28.98	5.01	20.23	11.93	2.44	25.98	0.67	33.82
	33.80	3.40	21.12	12.77	2.03	26.88	0.60	39.50
$[C_4C_1im]Br$	27.03	6.92	20.42	10.59	11.48	15.56	0.57	17.79
	36.71	3.68	25.20	9.88	5.79	20.33	0.63	35.12
	39.60	2.99	25.69	10.38	4.68	21.55	0.60	39.54
	42.47	2.41	25.90	11.31	3.23	23.47	0.58	44.53
	45.66	1.88	29.98	10.07	2.68	24.35	0.64	48.49
	47.35	1.63	30.65	10.43	2.08	25.47	0.63	51.16
	52.36	1.04	35.06	10.19	1.05	28.16	0.66	58.04
	54.66	0.83	34.89	11.10	0.89	28.76	0.63	60.59
$[C_4C_1im][CF_3SO_3]$	34.45	1.61	26.93	3.37	4.98	8.51	0.74	30.27
	37.37	1.42	27.11	4.05	3.15	10.19	0.70	35.32
	83.61	0.17	20.08	9.89	1.42	12.75	0.23	83.14
	84.34	0.16	29.90	10.05	0.53	15.38	0.35	85.18
$[C_4C_1im][TOS]$	43.88	2.08	30.06	6.12	2.18	14.29	0.67	43.46
	46.23	1.74	30.16	7.03	0.54	16.77	0.65	48.09
$[C_4C_1im][N(CN)_2]$	43.01	1.55	22.07	7.04	7.07	10.97	0.47	43.09
	52.78	0.77	19.97	9.95	1.83	15.02	0.36	52.90
	55.65	0.61	24.36	10.41	0.47	17.89	0.43	57.83
	58.07	0.50	30.42	9.99	0.10	20.39	0.52	61.28
	58.41	0.48	30.02	10.14	0.11	20.32	0.51	61.59
	61.60	0.36	34.79	9.96	0.02	22.41	0.56	65.40
	61.99	0.35	34.90	10.05	0.02	22.55	0.56	65.82
$[C_4C_1im][CH_3SO_4]$	29.66	5.74	20.50	10.71	9.63	16.61	0.54	22.79
	36.98	3.57	27.82	8.56	4.83	21.09	0.72	36.61
	43.45	2.25	30.10	9.03	3.82	22.35	0.66	44.43
	45.64	1.91	29.88	9.94	2.94	23.65	0.63	47.91
	54.43	0.91	34.81	12.04	0.35	31.60	0.64	62.19
$[C_4C_1im][C_2H_5SO_4]$	32.22	4.42	21.13	10.06	8.83	16.32	0.53	26.24
	38.23	3.17	26.69	9.30	4.88	20.88	0.65	37.76
	46.69	1.96	29.95	10.01	3.76	22.61	0.61	47.64
	47.37	1.89	30.08	10.13	3.70	22.72	0.60	48.39
$[C_4C_1im][CH_3SO_3]$	39.28	3.55	29.96	8.98	3.33	24.51	0.74	41.61
$[C_4C_1im][DMP]$	29.45	6.41	21.96	12.09	1.70	27.46	0.73	34.83
	34.40	4.53	24.02	14.03	0.12	35.90	0.70	47.64
$[C_4C_1im][SCN]$	41.64	1.69	20.53	6.06	6.97	8.86	0.39	35.40
	47.35	1.22	20.44	7.11	3.09	10.90	0.39	45.31

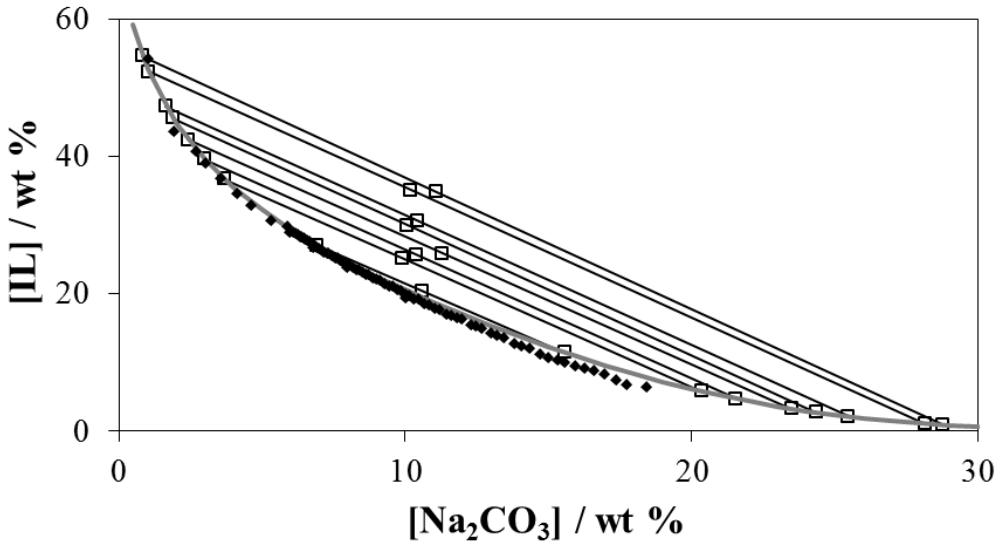

Figure S8: Ternary phase diagram for the ABS composed of $[C_4C_1im]Br$ + Na_2CO_3 + water at 298K: ◆, experimental solubility data; □, TL data, ▬, fitting by equation 2.1.1.

Table S61: Experimental weight fraction composition, extraction efficiencies of gallic acid and pH values in ABS corresponding to the two sequential cycles composed of 25 wt% of IL + 20 wt% of Na_2SO_4 and 20 wt% of IL + 10 wt% of Na_2CO_3 (at 298K).

ionic liquid	extraction	% $EE_{Salt \pm}\sigma^a$	Weight fraction composition / (wt%)		pH_{IL}	pH_{salt}
			IL	Salt		
$[C_4C_1im][N(CN)_2]$	1st to IL -rich phase	94.56 ±0.47	25.09	19.20	7.40	7.69
	1st to Na_2CO_3-rich phase (back extraction)	70.58 ± 0.74	19.94	9.96	11.20	11.34
	2nd to IL-rich phase	50.06 ± 3.69	24.94	19.05	8.86	9.89
	2nd to Na_2CO_3-rich phase (back extraction)	79.39 ± 4.20	19.98	10.01	11.34	11.75
$[C_4C_1im][N(CN)_2]$ adjusted pH	1st to IL -rich phase	93.12 ± 0.17	24.98	19.49	7.54	7.49
	1st to Na_2CO_3-rich phase (back extraction)	72.43 ± 1.22	19.70	9.85	11.72	11.74
	2nd to IL-rich phase	96.70 ± 3.30	24.55	19.14	6.42	6.28
	2nd to Na_2CO_3-rich phase (back extraction)	78.71 ± 1.99	20.05	9.91	11.13	11.33
$[C_4C_1im][CF_3SO_3]$	1st to IL -rich phase	89.93 ± 1.14	25.00	19.96	4.60	4.55
	1st to Na_2CO_3-rich phase (back extraction)	98.67 ± 2.50	20.02	9.96	11.13	11.49
	2nd to IL-rich phase	35.65 ± 4.95	24.95	19.58	8.55	8.45
	2nd to Na_2CO_3-rich phase (back extraction)	91.05 ± 2.050	19.89	9.95	11.35	11.45
$[C_4C_1im][CF_3SO_3]$ adjusted pH	1st to IL -rich phase	93.33 ± 3.67	25.13	19.95	3.97	3.34
	1st to Na_2CO_3-rich phase (back extraction)	98.29 ± 1.71	20.00	9.92	11.12	11.05
	2nd to IL-rich phase	95.49 ± 2.60	24.88	20.39	2.88	2.95
	2nd to Na_2CO_3-rich phase (back extraction)	99.23 ± 0.80	19.61	9.95	11.42	11.34

Table S62: Sodium content in the coexisting phases in sequential ABS composed of 25 wt% of IL + 20 wt% Na_2SO_4 and 20 wt% of IL + 10 wt% Na_2CO_3 at 298K.

ABS	[Sodium] by TL / (wt%)	[Sodium] by ICPOES / (wt%)	Relative deviation / (wt%)
$[C_4C_1im][CF_3SO_3]$ + Na_2CO_3 top phase	12.88	13.86	0.08
$[C_4C_1im][CF_3SO_3]$ + Na_2CO_3 bottom phase	0.17	0.17	-0.02
$[C_4C_1im][CF_3SO_3]$ + Na_2SO_4 bottom phase	27.47	26.70	-0.03
$[C_4C_1im][CF_3SO_3]$ + Na_2SO_4 top phase	0.67	0.68	0.01
$[C_4C_1im][N(CN)_2]$ + Na_2CO_3 bottom phase	15.02	13.95	-0.07
$[C_4C_1im][N(CN)_2]$ + Na_2CO_3 top phase	0.78	0.91	0.17
$[C_4C_1im][N(CN)_2]$ + Na_2SO_4 bottom phase	33.96	33.43	-0.02
$[C_4C_1im][N(CN)_2]$ + Na_2SO_4 top phase	1.16	1.23	0.06

Table S63: IL content in the coexisting phases in sequential ABS composed of 25 wt% of IL + 20 wt% Na_2SO_4 and 20 wt% of IL + 10 wt% Na_2CO_3 at 298 K.

ABS	[IL] by TL / (wt%)	[IL] by UV-Vis / (wt%)	Relative deviation / (wt%)
$[C_4C_1im][CF_3SO_3]$ + Na_2CO_3 top phase	1.36	1.44	0.06
$[C_4C_1im][CF_3SO_3]$ + Na_2CO_3 bottom phase	83.09	81.44	-0.02
$[C_4C_1im][CF_3SO_3]$ + Na_2SO_4 bottom phase	0.79	0.76	-0.04
$[C_4C_1im][CF_3SO_3]$ + Na_2SO_4 top phase	83.17	89.35	0.07
$[C_4C_1im][N(CN)_2]$ + Na_2CO_3 bottom phase	1.83	1.77	-0.04
$[C_4C_1im][N(CN)_2]$ + Na_2CO_3 top phase	52.71	56.24	0.07
$[C_4C_1im][N(CN)_2]$ + Na_2SO_4 bottom phase	0.85	0.79	-0.06
$[C_4C_1im][N(CN)_2]$ + Na_2SO_4 top phase	54.94	57.73	0.05

Table S64: Experimental weight fraction composition and extraction efficiencies of syringic and vanillic acid in sequential ABS composed of 25 wt% of IL + 20 wt% Na_2SO_4) and 20 wt% of IL + 10 wt% Na_2CO_3 at 298 K.

Ionic liquid	Antioxidant	Extraction	% $EE_{Salt \pm}$ σ^a	Weight fraction composition / (wt%)	
				IL	Salt
$[C_4C_1im][CF_3SO_3]$	Syringic acid	1st to IL -rich phase	97.82 ± 0.25	25.00	20.15
		1st to Na_2CO_3-rich phase (back extraction)	97.68 ± 0.28	20.04	9.72
$[C_4C_1im][CF_3SO_3]$	Vanillic acid	1st to IL -rich phase	97.29 ± 0.26	24.99	20.03
		1st to Na_2CO_3-rich phase (back extraction)	97.40 ± 0.25	19.74	9.80

Referring to Chapter 3.1: Enhanced Extraction of Caffeine from Guaraná Seeds using Aqueous Solutions of Ionic Liquids

Table S65: 2^3 factorial planning.

Experiment	χ_1	χ_2	χ_3
1	-1	-1	-1
2	1	-1	-1
3	-1	1	-1
4	1	1	-1
5	-1	-1	1
6	1	-1	1
7	-1	1	1
8	1	1	1
9	-1.68	0	0
10	1.68	0	0
11	0	-1.68	0
12	0	1.68	0
13	0	0	-1.68
14	0	0	1.68
15	0	0	0
16	0	0	0
17	0	0	0
18	0	0	0
19	0	0	0
20	0	0	0

Table S66: Coded levels of independents variables used in the first and second factorial planning.

Independent variables	Coded levels				
	Axial point -1.682	Factorial point (-1)	Central point 0	Factorial point (+1)	Axial point +1.682
Temperature (ºC)	36.4	50.0	70.0	90.0	104.0
Equilibrium time (min)	5.0	15.0	30.0	45.0	55.0
Solid-liquid ratio	0.04	0.07	0.10	0.20	0.27

Table S67: Experimental data and response surface values of the first RSM design using pure water.

Experiment	Temperature / ºC	Solid-liquid ratio	Time / min	Experimental yield of caffeine / wt%	Predicted yield of caffeine / wt%	Relative deviation / %
1	36.0	0.10	30.0	2.74	2.74	0.09
2	50.0	0.20	45.0	2.61	2.70	-3.38
3	50.0	0.20	45.0	2.87	2.72	5.39
4	50.0	0.20	15.0	2.64	2.71	-2.47
5	50.0	0.07	45.0	4.08	3.96	2.91
6	50.0	0.07	45.0	3.91	3.96	-1.26
7	50.0	0.07	15.0	3.82	3.89	-2.00
8	70.0	0.05	30.0	6.06	6.17	-1.83
9	70.0	0.05	30.0	6.31	6.18	1.96
10	70.0	0.10	5.0	3.62	3.45	4.63
11	70.0	0.10	5.0	3.63	3.48	4.17
12	70.0	0.10	55.0	4.24	4.40	-3.90
13	70.0	0.10	30.0	3.82	3.89	-1.73
14	70.0	0.10	30.0	3.90	3.84	1.45
15	70.0	0.10	30.0	3.86	3.86	-0.03
16	90.0	0.07	45.0	5.31	5.17	2.60
17	90.0	0.07	15.0	4.11	4.25	-3.39

Table S68: Regression coefficients of the predicted second-order polynomial model for the caffeine obtained from the first RSM design using pure water.

	Regression coefficients	Standard deviation	t-student (6)	P-value
Interception	**-1.51×10^{1}**	**4.26**	**-3.55**	**0.01**
Temperature	4.94×10^{-1}	0.08	5.85	<0.005
Temperature^2	-2.51×10^{-3}	0.00	-6.54	<0.005
Solid-liquid ratio	1.21×10^{2}	40.78	2.98	0.02
Solid-liquid ratio^2	-8.09×10^{1}	64.42	-1.26	0.26
Time	-2.96×10^{-2}	0.03	-1.08	0.32
Time^2	-2.41×10^{-5}	0.00	-0.10	0.93
Temperature × Solid-liquid ratio	-2.16×10^{0}	0.46	-4.66	<0.005
Solid-liquid ratio × Time	-2.79×10^{-2}	0.08	-0.36	0.73
Temperature × Time	7.04×10^{4}	0.00	2.65	0.04

Table S69: ANOVA data for the extraction of caffeine obtained from the first RSM design using pure water.

	Sum of squares	Degrees of freedom	Mean square	F-value	P-value
Regression	18.01	9	2.00	64.10	2.85×10^{-05}
Residuals	0.19	6	0.03		
Total	18.20				

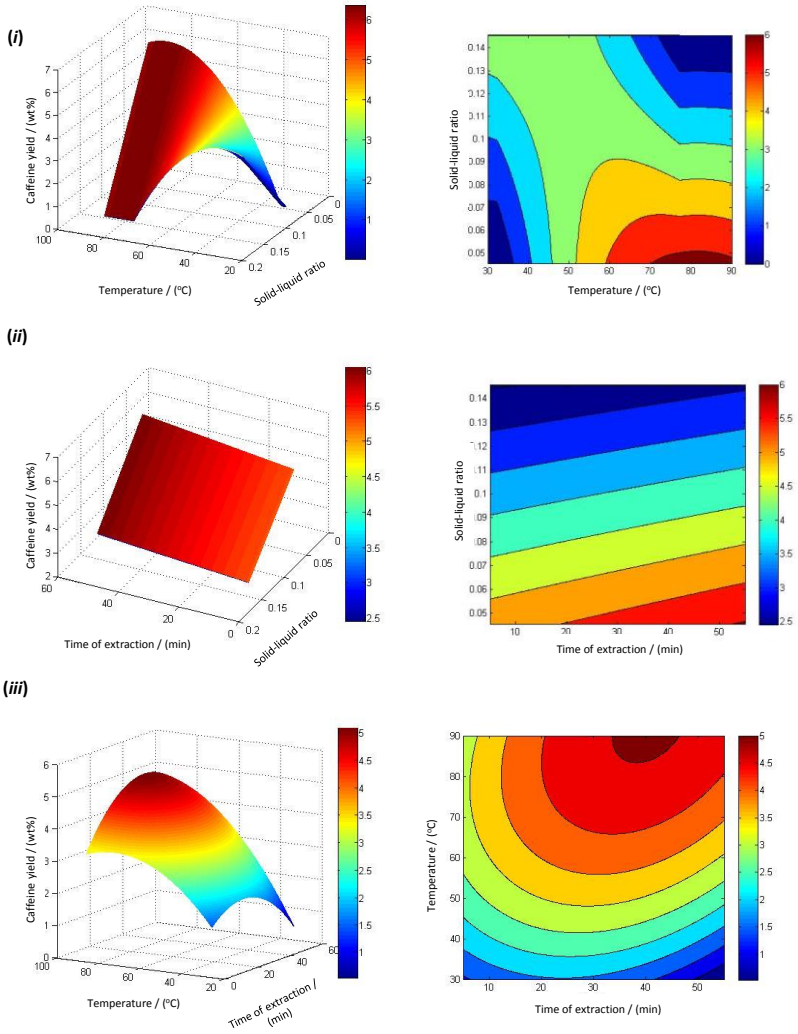

Figure S9: Response surface plots (left) and contour plots (right) on the yield of caffeine with the combined effects of (*i*) temperature and solid-liquid ratio, (*ii*) time and solid-liquid ratio and (*iii*) temperature and time using pure water and guaraná particles with a diameter within 0.4 mm and 1.0 mm.

Table S70: Experimental data and response surface values of the second RSM design using [C_4mim]Cl aqueous solutions.

Experiment	Temperature / ºC	Solid-liquid ratio	Time / min	Experimental yield of caffeine / wt%	Predicted yield of caffeine / wt%	Relative deviation / %
1	36.0	0.10	30.0	3.39	3.39	0.02
2	50.0	0.20	45.0	5.32	5.50	-3.35
3	50.0	0.20	15.0	4.92	4.74	3.60
4	50.0	0.07	45.0	5.34	5.52	-3.39
5	50.0	0.07	15.0	5.16	4,98	3.51
6	70.0	0.04	30.0	8.39	8.39	-0.01
7	70.0	0.10	5.0	4.44	4.87	-9.69
8	70.0	0.10	55.0	7.19	6.76	5.99
9	70.0	0.10	30.0	6.03	6.10	-1.17
10	70.0	0.10	30.0	6.19	6.12	1.16
11	90.0	0.07	45.0	5.33	5.69	-6.73
12	90.0	0.07	15.0	4.43	4.07	8.09

Table S71: Regression coefficients of the predicted second-order polynomial model for the caffeine yield obtained from the second RSM design using [C_4mim]Cl aqueous solutions.

	Regression coefficients	Standard deviation	t-student (2)	P-value
Interception	**-3.76×10^{1}**	**17.74**	**-2.12**	**0.17**
Temperature	1.08×10^{0}	0.36	2.98	0.10
Temperature^2	-6.22×10^{-3}	0.00	-3.74	0.05
Solid-liquid ratio	2.55×10^{2}	168.68	1.51	0.27
Solid-liquid ratio ^{2}	-2.78×10^{2}	262.35	-1.06	0.40
Time	1.70×10^{-3}	0.11	0.02	0.99
Time^2	-5.20×10^{-4}	0.00	-0.53	0.65
Temperature × Solid-liquid ratio	-3.66×10^{0}	1.97	-1.86	0.20
Solid-liquid ratio × Time	4.72×10^{-2}	0.31	0.15	0.89
Temperature × Time	8.93×10^{-4}	0.00	0.88	0.47

Table S72: ANOVA data for the extraction of caffeine obtained from the second RSM design using [C_4mim]Cl aqueous solutions.

	Sum of squares	Degrees of freedom	Mean square	F-value	P-value
Regression	18.43	9	2.05	5.34	0.1675
Residuals	0.77	2	0.38		
Total	19.20				

Table S73: Coded levels of independents variables used in the third RSM design using $[C_4mim]Cl$ aqueous solutions.

Variables	Coded levels				
	Axial point -1.682	Factorial point -1	Central point 0	Axial point -1.682	Factorial point -1
Temperature (ºC)	36.4	50.0	70.0	90.0	103.6
Concentration of ionic liquid (M)	0.66	1.00	1.50	2.00	2.34
Solid-liquid ratio	0.04	0.07	0.10	0.20	0.27

Table S74: Experimental data and response surface values of the third RSM design using $[C_4mim]Cl$ aqueous solutions.

Experiment	Temperature / ºC	Concentration / M	Time / min	Experimental yield of caffeine / wt%	Predicted yield of caffeine / wt%	Relative deviation / %
1	50.0	1.00	0.07	8.13	7.82	3.74
2	90.0	1.00	0.07	7.05	7.13	-1.18
3	50.0	2.00	0.07	9.04	8.59	4.97
4	90.0	2.00	0.07	8.59	8.56	0.29
5	50.0	1.00	0.10	6.28	7.16	-14.07
6	50.0	1.00	0.20	5.04	4.94	1.93
7	90.0	1.00	0.20	1.30	1.42	-9.33
8	50.0	1.00	0.20	8.78	8.72	0.65
9	50.0	1.00	0.10	7.94	8.70	-9.53
10	37.0	1.50	0.10	7.51	7.18	4.46
11	70.0	0.66	0.10	6.47	6.37	1.47
12	70.0	2.34	0.10	9.43	9.49	0.64
13	70.0	1.50	0.05	8.80	9.18	-4.33
14	70.0	1.50	0.10	8.18	8.17	0.02
15	70.0	1.50	0.10	8.37	8.18	2.24
16	70.0	1.50	0.10	8,29	8,19	1.30
17	70.0	1.50	0.10	8.21	8.19	0.27
18	70.0	1.50	0.10	8.34	8.22	1.38
19	70.0	1.00	0.10	7.49	7.16	4.42
20	70.0	0.50	0.10	6.01	5.97	0.60

Table S75: Regression coefficients of the predicted second-order polynomial models for extraction caffeine obtained from the second RSM design using [C_4mim]Cl aqueous solutions.

	Regression coefficients	Standard deviation	t-student (10)	P-value
Interception	**1.14×10^{0}**	**4.14**	**0.28**	**0.79**
Temperature	2.44×10^{-1}	0.07	3.31	0.01
Temperature ^{2}	-1.73×10^{-3}	0.00	-3.75	<0.005
Concentration	-4.91×10^{-1}	2.15	-0.23	0.82
Concentration^2	-3.56×10^{-1}	0.42	-0.85	0.41
Solid-liquid ratio	-1.21×10^{1}	25.59	-0.47	0.65
Solid-liquid ratio^2	-2.08×10^{-1}	58.79	-0.35	0.73
Temperature × Concentration	1.65×10^{-2}	0.02	0.85	0.41
Concentration × Solid-liquid ratio	2.26×10^{-1}	6.61	3.42	0.01
Temperature × Solid-liquid ratio	-5.33×10^{-1}	0.17	-3.22	0.01

Table S76: ANOVA data for the extraction of caffeine obtained from the third RSM design using [C_4mim]Cl aqueous solutions.

	Sum of squares	Degrees of freedom	Mean square	F-value	P-value
Regression	62.04	9	6.89	32.46	3.0797×10^{-06}
Residuals	2.12	10	0.21		
Total	64.16				

Referring to Chapter 3.2: Recovery of caffeine from spent coffee using aqueous ionic liquid solutions.

Table S77: Coded levels of independents variables used in the third RSM design using $[C_4mim]Cl$ aqueous solutions.

Independent variables	Axial point -1.682	Factorial point (-1)	Central point 0	Factorial point (+1)	Axial point +1.682
Temperature (ºC)	44.8	55	70	85	95.2
Equilibrium time (min)	4.48	15	30	45	55.2
Solid-liquid ratio	0.05	0.07	0.1	0.13	0.15

Table S78: Densities, ρ (g·cm^{-3}), viscosities, η (mPa·s), and refractive index, n_D, of the studied PILs as a function of temperature and at atmospheric pressure.

	[EA][CH_3CO_2]			**[DEA][CH_3CO_2]**			**[TEA][CH_3CO_2]**		
T / K	n_D	η /mPa.s	ρ / g.cm^{-3}	n_D	η /mPa.s	ρ / g.cm^{-3}	n_D	η /mPa.s	ρ / g.cm^{-3}
288.15	1.482593			1.481466			1.488035		
298.15	1.480000	2329.20	1.1518	1.478951	3456.80	1.1773	1.485446		
303.15		1532.10	1.1490		2213.70	1.1741			
308.15	1.477414	1037.50	1.1462	1.476391	1460.40	1.1709	1.482774		
313.15		720.63	1.1434		989.07	1.1676		630.24	1.1703
318.15	1.474757	512.12	1.1405	1.473718	684.60	1.1643	1.480029	436.51	1.1666
323.15		371.71	1.1377		483.64	1.1610		310.08	1.1630
328.15	1.472089	274.98	1.1349	1.471056	348.65	1.1577	1.477272	224.73	1.1594
333.15		207.07	1.1321		256.12	1.1544		166.06	1.1558
338.15	1.469410	158.46	1.1294	1.468307	191.38	1.1511	1.474466	125.04	1.1523
343.15		123.06	1.1267		145.77	1.1479		95.63	1.1487
348.15	1.466673	96.94	1.1239	1.465497	112.36	1.1446	1.471649	74.41	1.1451
353.15		77.26	1.1211		87.82	1.1413		58.61	1.1414
358.15	1.463956	62.31	1.1183	1.462714	69.52	1.1380	1.468836	46.75	1.1376
363.15		50.77	1.1155		55.64	1.1346		37.71	1.1338
368.15		41.74	1.1128		45.01	1.1313		30.73	1.1299

Table S79: Experimental data and response surface values of the first RSM design using pure water.

T (ºC) - x_1	T (K) - x_1	T (K) - x_1^2	R - x_2	R - x_2^2	t (min.) - x_3	t (min.) - x_3^2	TR	Rt	Tt	% caf_exp
55	328	107584	0.071	0.0051	15	225	23.4286	1.0714	4920	0.92
55	328	107584	0.125	0.0156	15	225	41.0000	1.8750	4920	0.98
55	328	107584	0.125	0.0156	45	2025	41.0000	5.6250	14760	0.99
85	358	128164	0.071	0.0051	15	225	25.5714	1.0714	5370	1.33
85	358	128164	0.125	0.0156	15	225	44.7500	1.8750	5370	1.16
85	358	128164	0.071	0.0051	45	2025	25.5714	3.2143	16110	1.48
85	358	128164	0.050	0.0025	45	2025	17.9000	2.2500	16110	1.50
70	343	117649	0.050	0.0025	30	900	17.1500	1.5000	10290	1.34
70	343	117649	0.100	0.0100	55	3025	34.3000	5.5000	18865	1.13
70	343	117649	0.100	0.0100	30	900	34.3000	3.0000	10290	1.17
70	343	117649	0.100	0.0100	30	900	34.3000	3.0000	10290	1.20
70	343	117649	0.100	0.0100	30	900	34.3000	3.0000	10290	1.18
70	343	117649	0.100	0.0100	30	900	34.3000	3.0000	10290	1.20
70	343	117649	0.150	0.0225	30	900	51.4500	4.5000	10290	1.13
70	343	117649	0.100	0.0100	5	25	34.3000	0.5000	1715	1.16
70	343	117649	0.100	0.0100	55	3025	34.3000	5.5000	18865	1.27
45	318	101124	0.100	0.0100	30	900	31.8000	3.0000	9540	1.04
90	363	131769	0.100	0.0100	30	900	36.3000	3.0000	10890	1.32
95	368	135424	0.100	0.0100	30	900	36.8000	3.0000	11040	1.31

Table S80: ANOVA data for the extraction of caffeine obtained from the first RSM design using pure water.

	Analysis of Variance; DV: Var1 (Spreadsheet1)				
Effect	Sums of Squares	df	Mean Squares	F	p-value
Regress.	1981,764	1	1981,764	28,5808(	0,000053
Residual	1178,763	17	69,339		
Total	3160,526				

	Regression Summary for Dependent Variable: Var1 (Spreadsheet1) R= ,79185601 R²= ,62703594 Adjusted R²= ,60509688 F(1,17)=28,581 p<,00005 Std.Error of estimate: 8,3270					
N=19	b*	Std.Err. of b*	b	Std.Err. of b	t(17)	p-value
Intercept			-8,08654	15,07238	-0,536514	0,59855
NewVar	0,791856	0,148118	66,57155	12,45235	5,346101	0,000053

	Summary Statistics; DV: Var1 (Spreadsheet1)
Statistic	Value
Multiple R	0,791856009
Multiple R²	0,627035939
Adjusted R²	0,605096877
F(1,17)	28,580799
p	0,000053468891
Std.Err. of Estimate	8,327003

Referring to Chapter 3.3: Ionic liquids as hydrotropes: A study on the enhanced solubility of gallic acid, vanillin and caffeine in water

Table S81: Experimental weight fraction composition and solubility of vanillin and gallic acid using several hydrotropes at 303 K.

hydrotrope	Weight fraction composition / wt %	vanillin	gallic acid	caffeine
		solubility ± σ[a]	solubility ± σ[a]	solubility ± σ[a]
H_2O	0.00	11.12 ± 0.02	14.38 ± 0.41	23.09± 1.36
$[C_4C_1im]Br$	5.02		29.58 ± 0.46	26.36 ± 0.80
	9.98		47.08 ± 1.06	29.52 ± 2.22
	15.03		49.16 ± 2.95	32.20 ± 0.27
	19.97		58.52 ± 1.11	35.88 ± 0.14
$[C_4C_1im][CF_3SO_3]$	5.03		24.98 ± 0.39	32.40 ± 0.44
	10.10		37.17 ± 0.72	43.06 ± 1.65
	15.07		49.38 ± 0.86	49.89 ± 1.17
	20.02		66.07 ± 3.31	61.53 ± 1.99
$[C_4C_1im][CH_3SO_4]$	5.12		28.00 ± 0.85	26.40 ± 0.25
	9.98		39.83 ± 0.64	28.53 ± 1.89
	14.99		50.79 ± 3.28	34.48 ± 1.23
	20.04		82.71 ± 0.51	40.27 ± 2.57
$[C_4C_1im][TOS]$	10.01	48.43 ± 0.47	47.21 ± 0.66	52.56 ± 1.36
	19.96	133.06 ± 5.94	84.52 ± 2.36	71.74 ± 0.88
	50.00	445.60 ± 9.34		
	80.02	402.9 ± 9.38		
	95.01	365.5 ± 10.02		
$[C_4C_1py][N(CN)_2]$	10.07	two-phase	120.59 ± 0.1.08	82.53 ± 2.05
	20.02	two-phase	263.46 ± 1.61	134.36 ± 1.65
$[C_4C_1im][SCN]$	9.94	39.59 ± 0.41	54.63 ± 0.79	50.76 ± 3.38
	20.06	two-phase	93.39 ± 1.83	74.94 ± 5.16
$[C_4C_1im][N(CN)_2]$	5.09		56.46 ± 0.84	36.37 ± 0.88
	10.06	59.40 ± 2.04	96.52 ± 2.74	51.52 ± 2.02
	15.02		115.52 ± 3.83	67.69 ± 0.69
	20.03	two-phase	149.71 ± 0.60	82.96 ± 1.17
	50.04		329.52 ± 7.35	87.87 ± 2.65
	74.99		293.61 ± 118.90	52.69 ± 0.73
	100.00		65.71 ± 6.71	25.99 ± 2.67
$[C_4C_1im]Cl$	4.97		34.71 ± 1.69	24.81 ± 1.36
	9.98	37.03 ± 1.29	64.02 ± 0.32	25.67 ± 1.20
	15.01		91.80 ± 0.85	27.49 ± 0.91
	20.00	89.23 ± 0.92	129.34 ± 5.23	26.28 ± 1.20
	30.00			33.62 ± 0.12
	50			26.65 ± 0.53
	80	374.51 ± 8.17		
	90		59.95 ± 3.28	6.03 ± 0.61
$[C_2C_1im][N(CN)_2]$	5.06	24.52 ± 0.58		

	10.09	49.98 ± 0.97		
	14.94	82.12 ± 2.33		
	20.01	120.7 ± 8.83		
	50.02	394.6 ± 9.50		
	100.00	75.51 ± 3.73		
$[C_2C_1im]Cl$	5.01	17.58 ± 0.21		
	10.03	26.74 ± 0.34		
	15.02	38.89 ± 1.69		
	19.99	45.19 ± 5.61		
$[C_6C_1im]Cl$	10.00	50.02 ± 2.90		
	20.03	152.25 ± 10.00		
$[C_8C_1im]Cl$	10.02	91.37 ± 0.78		
	20.01	202.55 ± 2.44		
$[C_{10}C_1im]Cl$	10.00	83.88 ± 6.29		
	20.03	138.36 ± 2.72		
$[C_{12}C_1im]Cl$	9.99	66.71 ± 0.42		
	19.99	127.06 ± 2.25		
$[C_{14}C_1im]Cl$	10.00	70.95 ± 4.70		
	20.06	100.28 ± 1.94		
$[C_4C_1py]Cl$	9.98	45.97 ± 0.80	69.28 ± 4.46	27.63 ± 2.09
	20.01	115.50 ± 10.84	127.00 ± 0.89	28.51 ± 0.27
$[C_4C_1pyrr]Cl$	10.03		67.00 ± 3.93	21.48 ± 2.53
	20.01		94.68 ± 1.38	19.86 ± 2.53
$[C_4C_1pip]Cl$	10.02		52.88 ± 1.31	19.86 ± 4.27
	20.04		106.78 ± 5.53	19.93 ± 0.97
$[N_{1112}OH]Cl$	10.03		28.08 ± 0.21	15.68 ± 0.40
	20.01		46.92 ± 1.60	11.78 ± 0.96
$[N_{4444}]Cl$	9.98	87.90 ± 0.92	4.44 ± 0.27	26.18 ± 0.62
	20.01	186.55 ± 16.71	3.04± 0.04	41.47 ± 1.42
$[P_{4444}]Cl$	10.02		5.70 ± 0.45	30.74 ± 1.87
	20.01		3.81 ± 0.17	34.07 ± 3.97
sodium citrate	10.00	6.16 ± 0.94	41.69 ± 0.84	9.01 ± 2.07
	19.96	5.07 ± 0.43	39.87 ± 0.90	3.51 ± 0.36
sodium benzoate	5.08	20.83 ± 0.25		
	10.09	31.69 ± 0.66	25.85 ± 2.33	109.78 ± 1.27
	14.97	52.97 ± 1.28		
	20.04	72.96 ± 4.83	33.16 ± 0.89	175.28 ± 1.49
sodium thiocynate	10.08	14.56 ± 0.51	12.59 ± 0.57	79.39 ± 2.60
	20.00	23.17 ± 1.60	12.67 ± 1.20	191.37 ± 6.95
NaCl	9.98	6.19 ± 0.09	10.48 ± 0.02	
	20.01	3.28 ± 0.15	6.61 ± 0.08	
[Na][TOS]	10.01	35.48 ± 0.88	30.85 ± 0.55	
	19.99	84.74 ± 2.09	53.85 ± 0.66	

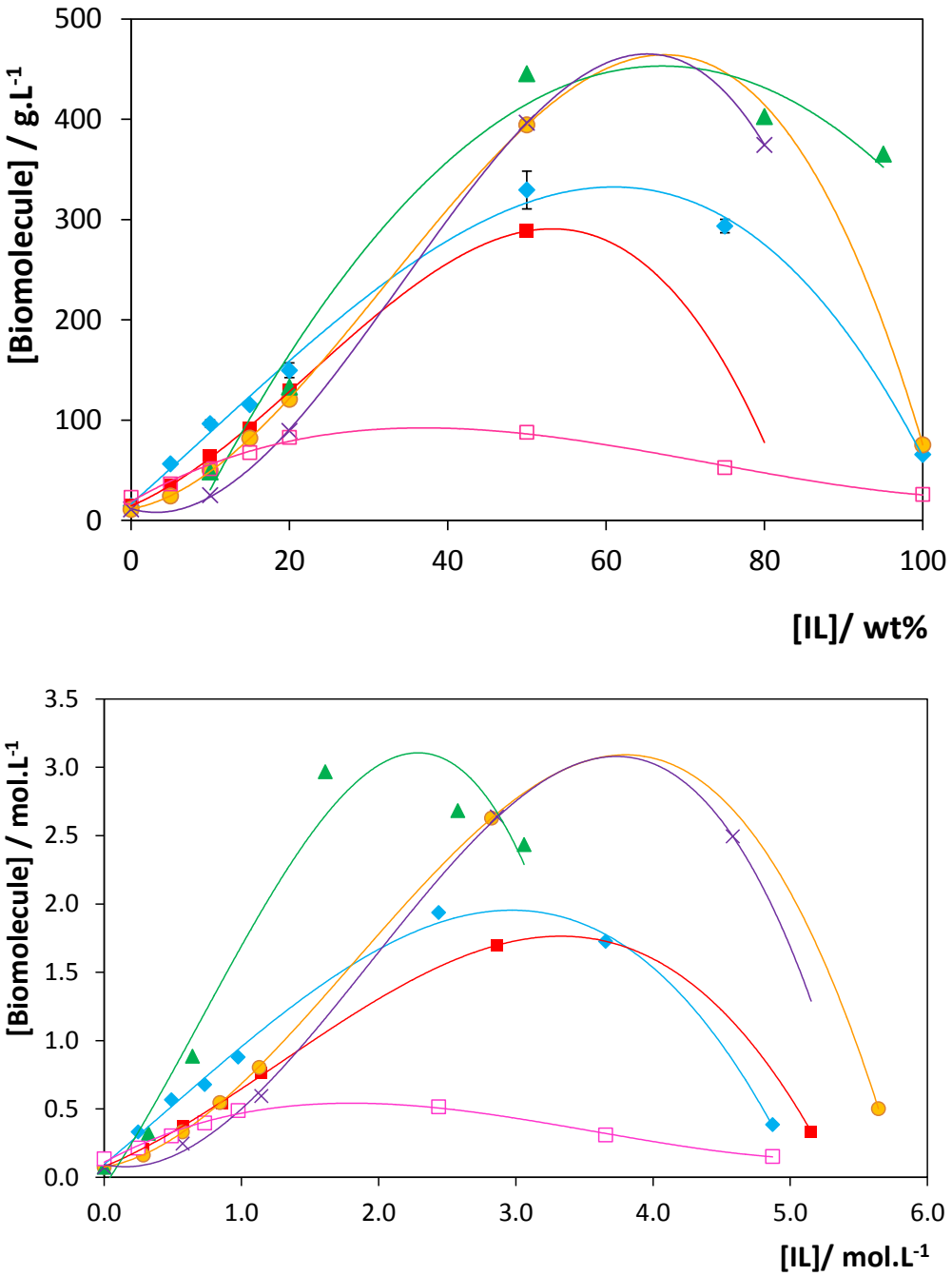

Figure S10: Influence of the concentration of IL in the solubility of gallic acid in aqueous solutions of ◆ $[C_4C_1im][N(CN)_2]$ and ■ $[C_4C_1im]Cl$; vanillin in aqueous solutions of ● $[C_2C_1im][N(CN)_2]$, ▲ $[C_4C_1im][TOS]$, × $[C_4C_1im]Cl$; caffeine in aqueous solutions of □ $[C_4C_1im][N(CN)_2]$ at 303 K. Lines are guides for the eye.

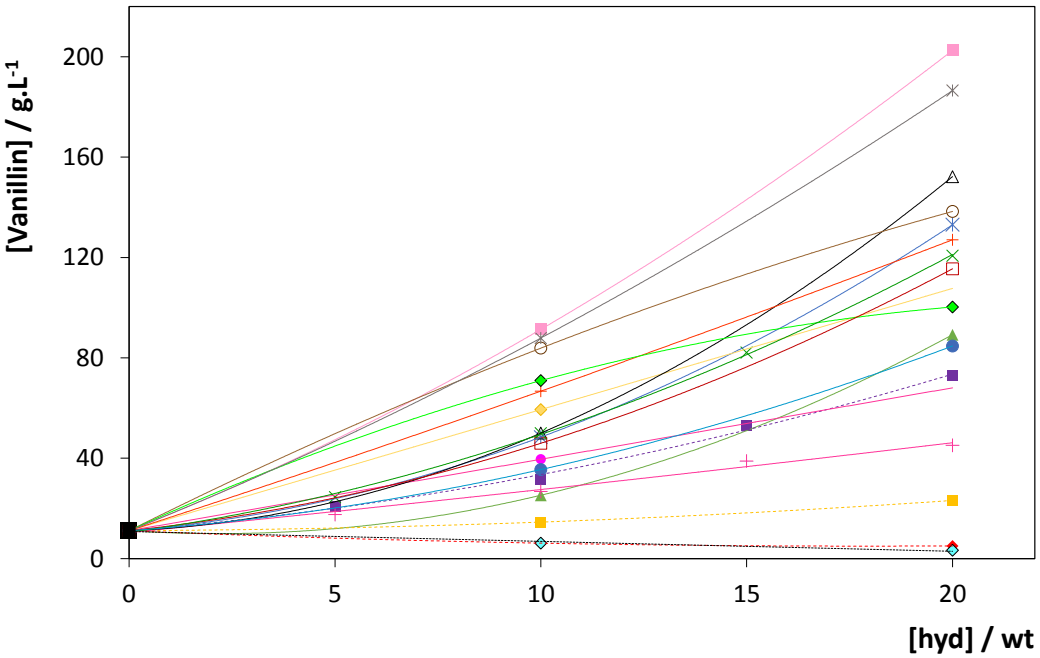

Figure S11: Influence of hydrotropes at different concentrations at 303 K in the vanillin's solubility in ■ water and in aqueous solutions of + [C_2C_1im]Cl, ▲ [C_4C_1im]Cl, △ [C_6C_1im]Cl, ■ [C_8C_1im]Cl, ○ [$C_{10}C_1$im]Cl, + [$C_{12}C_1$im]Cl, ◆ [$C_{14}C_1$im]Cl, × [C_2C_1im][N(CN)2], ◆ [C_4C_1im][N(CN)2]. *[C_4C_1im][TOS], ● [C_4C_1im][SCN], □ [C_4C_1py]Cl, ■ [Na][benzoate], ■ [Na][SCN], ◆ [Na][citrate], ◆ NaCl, ✳ [N_{4444}]Cl, ● NaTOS

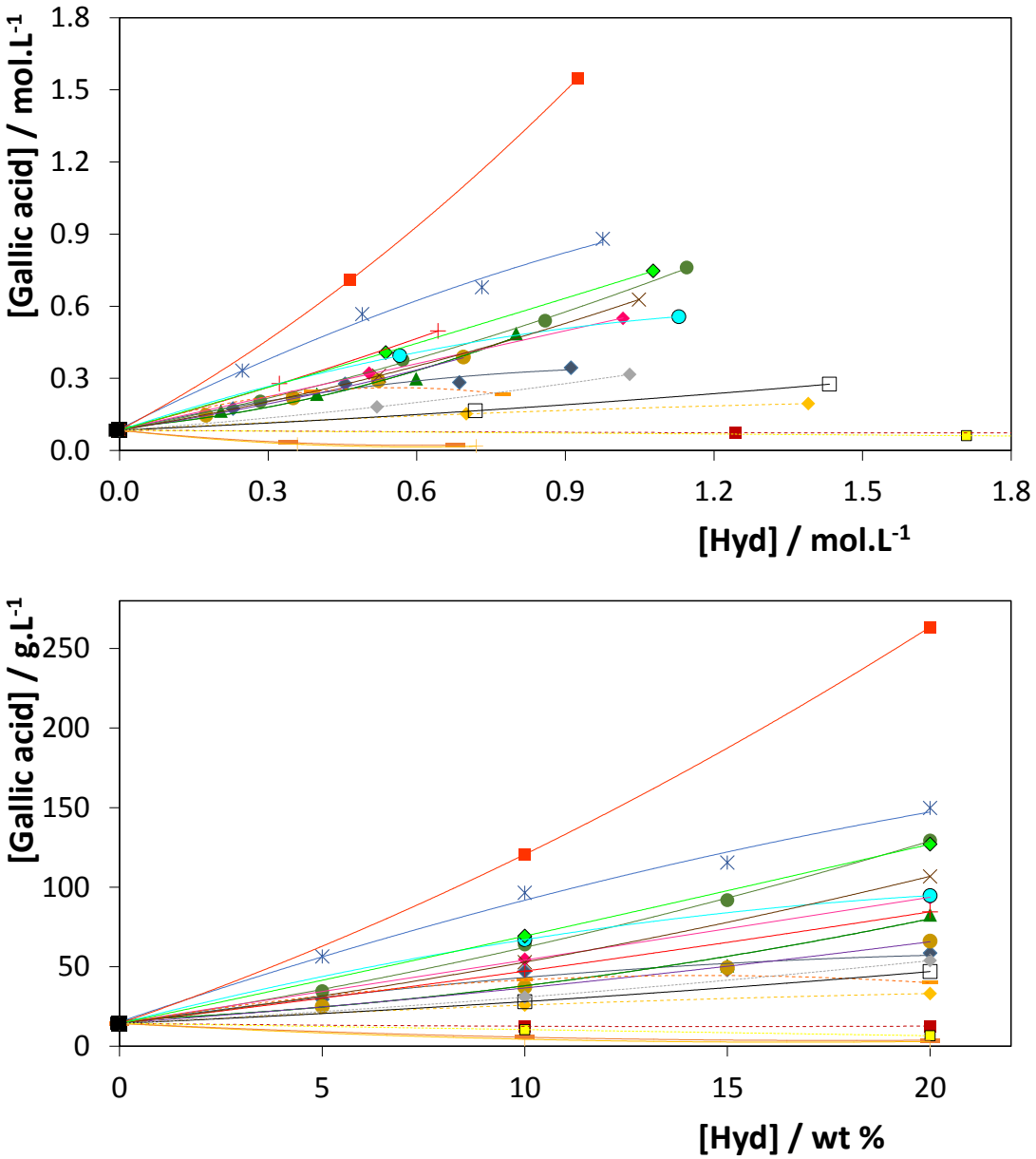

Figure S12: Influence of hydrotropes at different concentrations at 303 K in the gallic acid's solubility in ■ water and in aqueous solutions of ◆ [C_4C_1im]Br, ▲ [C_4C_1im][CH_3SO_4], ● [C_4C_1im][CF_3SO_3], ✕ [C_4C_1im][$N(CN)_2$], ● [C_4C_1im]Cl, + [C_4C_1im][TOS], ◆ [C_4C_1im][SCN], ● [C_4C_1pyrr]Cl, ✕ [C_4C_1pip]Cl, — [P_{4444}]Cl, + [N_{4444}]Cl, ■ [C_4C_1py][$N(CN)_2$], □ [N_{1112}OH]Cl, ◆ [C_4C_1py]Cl, — [Na][citrate], ◆ [Na][benzoate], ■ [Na][SCN], ■, NaCl, ◆ [Na][TOS]

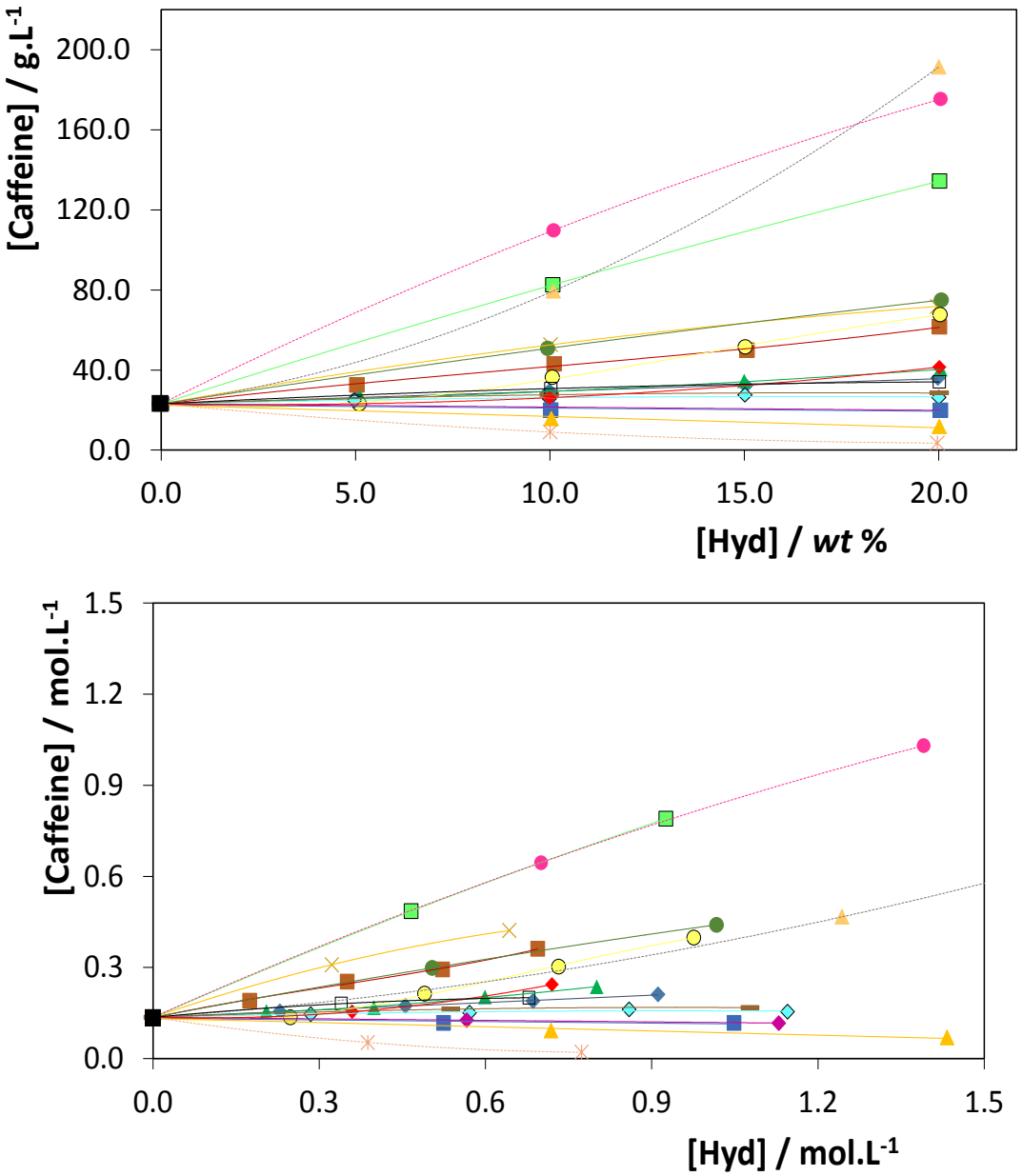

Figure S13: Influence of hydrotropes at different concentrations at 303 K in the caffeine's solubility in ■ water and in aqueous solutions of ◆[C_4C_1im]Br, ▲[C_4C_1im][CH_3SO_4], ■[C_4C_1py][$N(CN)_2$], ●[C_4C_1im][$N(CN)_2$], —[C_4C_1py]Cl, ■[C_4C_1pip]Cl, ◆[N_{4444}]Cl, ●[Na][benzoate], ■[C_4C_1im][CF_3SO_3], × [C_4C_1im][TOS], ●[C_4C_1im][SCN], ◆[C_4C_1im]Cl, ◆[C_4C_1pyrr]Cl, ▲[N_{1112}OH]Cl, *[Na][citrate], ▲[Na][TOS], □[P_{4444}]Cl

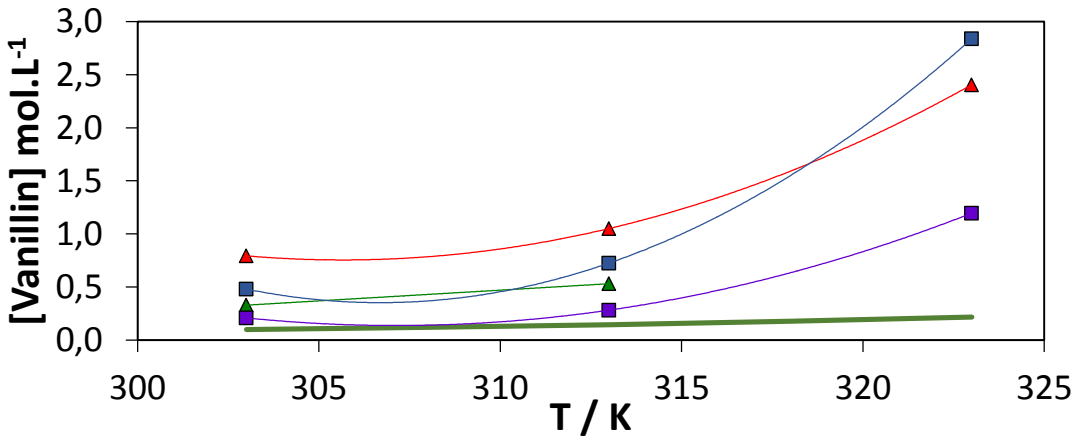

Figure S14: Influence of temperature in the vanillin's solubility in water[40] and in aqueous solutions of 10wt% of sodium benzoate (0.70 mol.L^{-1}), 10wt% of $[C_2C_1im][N(CN)_2]$ (0.57 mol.L^{-1}), 20wt % of sodium benzoate (1.39 mol.L^{-1}),and 20wt% of $[C_2C_1im][N(CN)_2]$ (1.13 mol.L^{-1}).

Table S82: Influence of temperature and hydrotrope concentration in vanillin's solubility.

Hydrotrope	wt % of hydrotrope in aqueous solution	T / K		
		303	313	323
$[C_2C_1im][N(CN)_2]$	10.09	49.98 ± 0.97	80.71 ± 3.32	
	20.01	120.7 ± 8.83	159.83 ± 6.91	366.11 ± 22.90
Sodium benzoate	10.09	31.69 ± 0.66	42.92 ± 0.81	181.90 ± 16.94
	20.04	72.96 ± 4.83	110.32 ± 8.10	432.10 ± 27.82